R83-915540-26

Mass and Momentum Turbulent Transport Experiments With Confined Swirling Coaxial Jets

TABLE OF CONTENTS

Page

ACKNOWLEDGEMENTS i

SUMMARY 1

INTRODUCTION 3

- Background 3
- Outline of Present Study 4

DESCRIPTION OF TEST APPARATUS AND PROCEDURES 7

- Test Apparatus 7
- Flow Visualization 8
- LV and LIF Measurements 9
- Swirler Design Evaluation 11

FLOW VISUALIZATION RESULTS 13

FOREWORD TO PRESENTATION OF RESULTS 16

DISCUSSION OF MEAN AND FLUCTUATING VELOCITY AND CONCENTRATION RESULTS 18

- Velocity Results 18
- Concentration Results 21

DISCUSSION OF TURBULENT TRANSPORT RESULTS 23

- Momentum Transport 23
- Mass Transport 26

DISCUSSION OF SKEWNEWSS AND KURTOSIS RESULTS FOR VELOCITY AND CONCENTRATION PROBABILITY DENSITY FUNCTIONS 29

- Typical Probability Density Functions 29
- Skewness and Kurtosis Distributions 31

DISCUSSION OF SECOND CENTRAL MOMENT, SKEWNESS AND KURTOSIS RESULTS FOR MOMENTUM AND MASS TURBULENT TRANSPORT PROBABILITY DENSITY FUNCTIONS 34

- Typical Turbulent Transport Rate Probability Density Functions 34
- Typical Momentum Turbulent Transport Results 35
- Typical Mass Turbulent Transport Results 36

SUMMARY OF RESULTS 38

REFERENCES 41

APPENDIX I - FLOW VISUALIZATION FOR ALL FLOW CONDITIONS 43

APPENDIX II - SWIRLER EXIT MEASUREMENTS 46

APPENDIX III - DEFINITIONS OF SKEWNESS AND KURTOSIS FOR VELOCITY, CONCENTRATION, AND TRANSPORT PROBABILITY DENSITY FUNCTIONS 50

TABLES 52

FIGURES 125

ACKNOWLEDGEMENTS

The authors gratefully acknowledge the efforts of the following in the acquisition and preparation of data for this report: Dr. John C. Bennett, of the University of Connecticut, for the development of the laser velocimeter optical arrangement used to obtain momentum turbulent transport data in the r-θ plane; Mr. Robert J. Haas for obtaining the fast action photographs and high speed motion pictures used to record the flow visualization; and Ms. Susanne L. Orr for handling the computerized storage, plotting and tabulation of data. The authors also acknowledge Dr. C. J. Marek, the NASA project manager for this program, for his efforts in producing a magnetic tape containing the data used to determine the turbulent transport results presented in this report. Requests for this tape can be made to Dr. Marek.

Mass and Momentum Turbulent Transport Experiments With Confined Swirling Coaxial Jets

R. Roback
B. V. Johnson

SUMMARY

An experimental study of mixing downstream of swirling coaxial jets discharging into an expanded duct was conducted to obtain data for the evaluation and improvement of turbulent transport models currently used in a variety of computational procedures throughout the combustion community. A combination of laser velocimeter (LV) and laser induced fluorescence (LIF) techniques was employed to obtain mean and fluctuating velocity and concentration distributions which were used to derive mass and momentum turbulent transport parameters currently incorporated into various combustor flow models. Flow visualization techniques were also employed to determine qualitatively the time dependent characteristics of the flow and the scale of turbulence. This study was an extension of the mass and momentum turbulent transport experiments with nonswirling coaxial jets which had been conducted in a previous program.

The flow visualization studies indicated that five major shear regions exist in the flow field downstream of the swirling coaxial jets. The first four regions were previously observed in the flow field for nonswirling coaxial streams. They included: (1) a wake region between the inner and annular streams a short distance downstream of the inlet, (2) a large-eddy shear region between the inner and annular streams, (3) an annular recirculation zone adjacent to the inlet plane, and (4) a reattachment region downstream of the annular recirculation zone. A large recirculation region along the centerline was also observed for the swirling coaxial streams.

Simultaneous two component velocity measurements were made in the radial-axial (r-z) plane, the axial-azimuthal (z-θ) plane and the radial-azimuthal (r-θ) plane with the two color LV system. The velocity data pairs were used to determine a momentum transport probability density function (p.d.f.) and average transport rates for each of three measurement planes. A combined LV/LIF system was used to simultaneously measure inner stream fluid concentration and one of the three velocity components. These concentration/velocity data pairs were used to determine the mass transport p.d.f. and average transport rate in the axial, radial, and azimuthal direction. The second central moment (rms fluctuation from the mean), skewness, and kurtosis for each mass and momentum transfer data set p.d.f. were also determined.

The results of these measurements indicated that the largest momentum turbulent transport was in the r-z plane. Peak momentum turbulent transport rates were approximately the same as those for the nonswirling

flow condition. The mass turbulent transport process for swirling flow was complicated. Mixing occurred in several steps of axial and radial mass transport and was coupled with a large radial mean convective flux. Mixing for swirling flow was completed in one-third the length required for nonswirling flow.

INTRODUCTION

Background

Computational procedures used to describe combustion processes are being developed and refined by a number of researchers (e.g., see Ref. 1 through 5). These computational procedures are used to predict the velocity, species concentration, temperature and reaction rate distribution within the combustors which in turn are used to determine combustor liner heat load, engine performance (combustion efficiency), pollution emissions (reaction products) and pattern factor (temperature distribution at turbine inlet). Because turbulent flow exists in most combustors of practical interest, the calculation procedures usually include mathematical models for the turbulent transport of mass (or species), momentum and heat. However, the prediction of combustion processes is very sensitive to the modeling of the mass and momentum transport processes and improper models result in inadequate predictions of combustion efficiency, liner heat load, emissions and exit temperature pattern factor.

The effort in the United States to improve and employ computational procedures for the prediction of aircraft gas turbine combustor processes is continuing in universities, government laboratories and the aircraft gas turbine industry. As part of the NASA program in this technology field, "Aerothermal Modeling" studies were conducted by three U.S. aircraft gas turbine manufacturers (Garrett, General Electric and Pratt & Whitney Aircraft Group) during 1982-1983. These studies were funded through the NASA Hot Section Technology (HOST) program and the results are/will be available in limited distribution reports (e.g., Ref. 6). The present (reported herein) and previous (Ref. 7) experimental studies were conducted as part of NASA's aerothermal modeling program.

The deficiencies in the current computational procedures have been attributed to weaknesses in the mathematical models, including the transport models, and in the numerical methods. One recommendation from a NASA workshop on combustion modeling was that the mathematical models used in the calculation procedures be validated using experiments specifically designed to provide the required input data. (Ref. 1). A first step in this process is the validation of mass and momentum transport models for constant density flows.

The data used to formulate and validate the turbulent transport models have been obtained primarily from velocity and momentum transport measurements because only a limited amount of concentration and mass trasnport data is available. The mass (species) transport data presently available are not sufficient to determine where inadequacies exist in the present models or to formulate improvements for the models. One reason for this situation is that the methods for simultaneously obtaining turbulent mass (species) and momentum transport data often have been indirect, requiring compromising assumptions. To overcome these limitations, techniques have been developed to measure concentration and velocity simultaneously and, therefore obtain mass transport data. This data can be used to evaluate and improve combustion oriented turbulent transport models which include scalars such as concentration of species and temperature.

Several nonintrusive measurement techniques have been used to obtain velocity and concentration simultaneously in recirculating flows (e.g., Ref. 8). Raman scattering, marker nephelometry, and laser induced fluorescence (LIF) of a trace material are three examples of techniques previously used for obtaining the concentration portion of these measurements. In this program, laser induced fluorescence of fluorescein dye as a trace element in water was chosen to study the mixing between constant density fluids. This technique was chosen for the following reasons: (1) the dye and water are relatively inexpensive, (2) the wavelength required to excite the dye is compatible with current LDV equipment, and (3) the fluids are convenient to use. This choice restricts the measurement technique to the acquisition of constant density transport data. Although the combustion process has variable density gases mixing in a reacting environment, the mathematical transport models for combustors are expected to be based on the turbulent transport phenomena found in constant density mixing with modifications for variable density and reacting flows.

A preliminary effort at UTRC was initiated in 1975 to obtain quantitative concentration measurements with fluorescene dye (Paper 28 of Ref. 8). This effort at UTRC was continued in 1978 and made use of improved optics, data handling capabilities and operative procedures. An exploratory study of mixing between confined coaxial jets was reported in Ref. 9. The current NASA sponsored study of mass and momentum turbulent transport experiments with nonswirling and swirling confined coaxial jets was initiated in 1981. The first phase of the study was conducted with nonswirling jets and was reported in Ref. 7. This second phase of the study, reported herein, was conducted with swirling coaxial jets. The current application of the combined LV/LIF measurement techniques along with the available data handling procedures provides an opportunity to obtain data which can be used to evaluate a number of computational methods and turbulent transport models. Results from Ref. 7 and the present study can be used to evaluate (1) the widely used two-equation turbulence model, (2) the Reynolds stress transport model and (3) the probability density function formulation for predicting turbulent transport and concentration fluctuations.

Outline of Present Study

Turbulent mixing of swirling confined coaxial jets is being studied because of its similarity to the combustor situation and thus its value in the mathematical modeling of combustor flow fields. Surveys of previous experimental studies were presented in Refs. 7 and 10. The turbulent mixing characteristics observed in the flow field produced by confined swirling coaxial jets are applicable to the combustion fluid mixing process because similar characteristics are found in gas turbine combustors and furnaces. The coaxial jets provide a method of introducing fuel and air into the combustion chamber. The annular recirculating flow zones associated with swirling and nonswirling coaxial jets expanding in enlarged ducts provide the pilot regions usually required to maintain flame in a combustor over a range of operating conditions.

The Reynolds number ($Re = \rho Vd/\mu$) of fluid flowing through various sections of aircraft gas turbine combustors vary from 10^4 to 10^6 and, therefore, the flows are generally turbulent. The lower Reynolds numbers occur for flow through cooling holes at engine idle conditions. The higher Reynolds numbers occur for flow through swirlers or dilution jets at engine takeoff conditions. The flow conditions selected for the detailed data acquisition in the present study lead to axial Reynolds numbers of 15,900 and 47,500 for the inner and annular streams, respectively. These Reynolds numbers are factors of 5 to 20 greater than the transitional Reynolds number range and are in the range occurring in aircraft gas turbines. Therefore, turbulent transport phenomena measured in the present experiments are expected to be typical of the transport phenomena occurring in gas turbines.

The features which have been previously observed (Refs. 7, 10 and 11) in the flow fields produced by nonswirling and swirling coaxial jets confined in an enlarged duct are presented in Fig. 1. For both the swirling and nonswirling inlet conditions, the flow field contains (1) a wake region downstream of the annular jet/inner jet interface, (2) a shear layer between the inner and annular jets, (3) an annular recirculation cell, and (4) a reattachment region leading to the fully developed duct flow. The swirling flow also contains (5) a centerline recirculation cell. As shown in Fig. 1, the flow fields are relatively complex with interaction between several regions.

The extent of each region pictured in Fig. 1 has been shown to depend upon the dimensions of the coaxial jets and ducts and on the axial and azimuthal velocity distributions. Therefore, the present program was initiated with a flow visualization study to determine the character of the flow and the turbulent transport processes for the experimental configuration chosen for detailed study. The results of the flow visualization study were also used to determine the streamwise locations for obtaining the detailed velocity, concentration and turbulent transport rate data.

The major focus of this study was on the acquisition, reduction and analysis of velocity, concentration, mass turbulent transport rate and momentum turbulent transport rate data at nine axial locations within the duct test section. Single component velocity data and inner jet fluid concentration data were obtained simultaneously to determine the local mass (or scalar) turbulent transport rate. Two velocity components were obtained simultaneously to determine the local momentum turbulent transport rates. As a result, the concentration and velocity distributions were obtained during at least two nonconsecutive data acquisition runs. The data set for each point measurement was analyzed and reduced to obtain the mean and three central moments for each probability density function (p.d.f.), i.e., the mean values, the rms deviation from the mean, the skewness of the p.d.f., and the flatness factor (or kurtosis) of the p.d.f. The mean and central moments were also obtained for the mass and momentum turbulent transport p.d.f.s as well as the velocity and concentration p.d.f.s. The reduced results for each data point set are tabulated and presented in this report. Graphical presentations of representative data are also included to aid in the discussion of the results. The discussion of these results will be related as applicable to each region shown in Fig. 1.

DESCRIPTION OF TEST APPARATUS AND PROCEDURES

Test Apparatus

A schematic of the test facility used in this experimental program is presented in Fig. 2. The principal components of the facility are a water storage tank, a water transfer and metering system, a dye injection system, and a test section. For the laser velocimeter tests, the facility was run in a closed, recirculating loop. Water which was at a temperature of approximately 20C, was circulated by a pump from the storage tank, through metering valves and flow measuring devices to the inner jet and annular jet inlets of the inlet plenum. The water in the annular duct and inner tube entered the test section, mixed and discharged into the exhaust ducts, and was returned to the storage tank.

Whenever fluorescein dye was used as a tracer, such as for the flow visualization tests and the LV/LIF tests, the facility was operated in a single pass mode. The water from the exhaust ducts was discharged into the city sanitary sewer and fresh water replenished the system. For the flow visualization tests, dye was added to either the inner jet fluid or the annular jet fluid several feet upstream of the entrance to the test section to ensure uniform flow of dye into the test section. For the LV/LIF tests, uniform flow of the dye was ensured by adding the dye to a mixing chamber located a short distance from the dye micrometering valve. The 20 to 40 psi pressure drop across the valve was large compared to the other pressure drops in the system, thus ensuring a constant flow of the dye injected into the inner jet flow. The mixing chamber was large enough to ensure adequate mixing and a uniform dye concentration at the entrance of the test section. A magnetic rotating mixer was used in the dye reservoir to keep the dye well stirred and an inline filter was placed in the system to prevent clogging of the dye micrometering valve.

A sketch of the test section along with the inlet and exhaust sections is shown in Fig. 3. The test section was a 122 mm inside diameter by 1 m long, thin-wall glass tube. When flow visualization and optical exeriments are conducted in circular tubes, the water-glass-air interfaces can produce optical distortion. As shown in Fig. 3, the circular duct test section was enclosed in a rectangular, glass-walled optical box filled with water to reduce beam direction distortion as the laser beams passed from air through the glass wall of the duct and into the test section water. A ray tracing program was used to determine that the radial displacement of the probe volume was less than 0.03 mm and the offset of the measurement direction from radial was less than 0.05 deg for radii up to approximately 55 mm.

Water to the test section entered through an annular duct and a smaller inner jet tube. The water then exhausted through the exit duct, up over a weir and flowed to the drain. Since the top end of the exit duct containing the weir was open to the atmosphere, the atmospheric pressure at the weir prevented the test section from becoming overpressurized. The inlet plenum for the annular duct contained three perforated plates to produce uniform flow and a honeycomb section to remove swirl from the flow. The inner jet tube was fed with the same diameter hose for lengths of over 300 cm and included a 60-cm length of straight, nonflexible tubing, containing a perforated plate, positioned immediately upstream of the inlet plenum.

A detail of the inlet to the test section is shown in Fig. 4. The center tube was a 25 mm ID tube with a 7.5 deg half angle flare at the exit of the tube. The 59 mm ID annular duct contained a free-vortex swirler with 30 deg mean angle flow turning blades whose trailing edges were positioned approximately 51 mm from the entrance to the test section. The velocity and coordinate system utilized for the measurements is also shown in Fig. 4.

With this test section, measurements were usually made at a fixed axial location over a range of radial locations. The measured parameters discussed in this report are presented as functions of the radial position r, normalized by the radius of the test section, R_o, i.e., r/R_o. For this representation, the inner jet tube extends from $r/R_o = 0.0$ to $r/R_o = 0.20$ and the annular region containing the swirler extends from $r/R_o = 0.25$ to $r/R_o = 0.48$ (see Fig. 4). The inner and annular regions are separated by a thin wall which extends from $r/R_o = 0.20$ to $r/R_o = 0.25$. The region between $r/R_o = 0.48$ and $r/R_o = 1.0$ is a solid wall which acts like a backward facing step in the flow field.

Flow Visualization

Sketches of the optical arrangements used to obtain flow visualization photographs and motion pictures of the flow pattern in the radial/axial plane (r-z) and radial/azimuthal plane (r-θ) are shown in Figs. 5 and 6 respectively. The light source was an argon ion laser which produced a 1.25 mm diameter beam and was operated either in single line mode (0.4880 μm wavelength) or with all lines operating. The laser beam was passed through a glass or plastic round rod which acted as a cylindrical lens and caused the beam to diverge in one plane while maintaining a beam thickness of approximately 1 mm. The glass rod was positioned perpendicular to the flow axis to illuminate the r-z plane along the center line of the test section and parallel with the flow axis at selected axial locations to illuminate the r-θ plane. Cameras positioned at right angles to the plane being illuminated were used to view the flow. In general, the dye concentration was increased until the fluorescent light level was just high enough for good photographic contrast. When the dye concentration was too high, nonuniform light absorption along the light path occurred.

LV and LIF Measurements

Overview

The laser velocimeter (LV) and laser induced fluorescence (LIF) measurements were obtained using commercially available components. Some electronic components, which were not commercially available when first required at UTRC, were designed and fabricated by the UTRC instrumentation group. The equipment utilized for each measurement will be described as the technique is discussed.

The LV measurement system employed in these experiments is sketched in Fig. 7 and utilized the two-color LV optics system detailed in Fig. 8. The two-color LV concept utilizes the two strong laser lines of an Argon ion laser at 0.4880 μm (blue) and 0.5145 μm (green) wavelengths. These two colored beams are separated in the optical system and subsequently emitted as three beams; a blue beam, a green beam, and a 50-50 mixed blue/green (cyan) beam. The three beams are passed through a lens to produce two sets of orthogonal interference fringe patterns in one common focal volume each having a fringe spacing:

$$d_f = \lambda/(2 \sin(\theta/2)) \tag{1}$$

where λ is the wavelength of the incident light beam, and θ is the intersection angle between the cyan beam and either the blue or green beam. A particle passing through the probe volume will scatter light of both colors, blue and green. The light intensity at the photomultiplier is modulated by a frequency, f_D, corresponding to the particular wavelength and fringe spacing and velocity component. This frequency is related to a particle velocity component through

$$f_D = U_i/d_f \tag{2}$$

where U_i is the velocity component perpendicular to the optical axis and in the plane of one set of intersecting colored beams. More detailed descriptions of the particular two color laser Doppler velocimetry system utilized in this experiment including the frequency shift used to prevent flow direction ambiguity may be found in Ref. 12.

Two Component LV Measurements

For the measurements conducted in this study, the optical system was operated in a direct backscattering mode as shown in Fig. 7. The 0.4880 μm wavelength beam was used to measure the streamwise or axial velocty component, U. The 0.5145 μm wavelength beam was used to measure (a) the azimuthal velocity component, W, when the probe volume was moved horizontally across the stream and (b) the radial velocity component, V, when the probe volume was moved vertically. A Bragg cell was used for both velocity components to eliminate the flow direction ambiguity. This optical subsystem provided signal-to-noise ratios greater than 20 except near the test section walls. For the measurements made in this study, the nominal value of the beam intersection angle, θ, was 9.52 deg. The laser beam diameter was 1.25 mm and the beam separation at the 1.94:1 beam expander output lens was 53.5 mm. A 310 mm focal length achromatic lens was used to focus the beams. With these optical system parameters, the LV probe volume was calculated to have dimensions of 0.08 mm diameter, 1.01 mm length and contained 28 fringes.

Besides the sending and receiving optical subsystem, each LV system contains other components or subsystems which perform specific functions in the flow measurement. These usually include: (1) a scattering particle generator or seeder, (2) a traverse system to position the probe volume, (3) signal processors, and (4) a data handling subsystem. For the experiments performed for this study, the particles naturally occurring in the city water supply proved adequate as LV seeds. As indicated in Fig. 7, the traverse system consisted of a milling machine base having three directions of motion. The range of motion in the streamwise direction was approximately 240 mm while the ranges in the vertical and cross stream directions were greater than the dimension of the test section. The relative traverse position accuracy of this traverse system was approximately 0.1 mm.

Laser Doppler velocimeter (LDV) signal processors amplify and filter the signals from the multiplier tubes, validate the Doppler frequency samples, and finally compute the Doppler period which is the reciprocal of the Doppler frequency. The SCIMETRICS Model 800A signal processors used in this study measured the elapsed time for 8 Doppler cycles and recorded the pulses from a 125 MHz crystal during the 8 cycle period. The processor also measured and recorded pulses for 4 and 5 Doppler cycles, and compared them with the 8 cycle result to ensure that the LDV signal was a valid one-particle signal. The integer number transmitted to the data handling system is the period of the Doppler frequency in nanoseconds. Two signal processors were used in this study (one for each colored light signal).

Once the LDV signals were processed and accepted, a microcomputer data handling system was used to acquire, store and reduce the data. This system consisted of (1) a data handling interface (constructed in-house), (2) a DEC PDP 10/11 minicomputer with a dual disk operating system, (3) a DEC Laboratory Peripheral System (LPS) with an analog to digital (A/D) signal converter, and (4) a DEC writer III teletype printer. The LDV Data Handling Interface was used to accept only those data points for which the two velocity components were obtained within a period of time of 1 msec. This time period was considered appropriate for the probe volume length of approximately 1 mm which was used in this study and for typical velocities of 1 m/sec. Data acquisition rate tests conducted under this criteria indicated that almost all of the sets of two component velocity data were obtained from a single particle moving through the probe volume. A detailed listing of the equipment employed for the two velocity component LV measurements is presented in Table I.

Combined LV/LIF Measurements

The tracer dye used for the LV/LIF measurements was made from fluorescein disodium salt ($C_{20}H_{10}O_5Na_2$). This dye is used extensively for water pollution studies and is availble from chemical supply houses in powder form. Absorption and emission spectra data for fluorescein dye can be obtained from Ref. 13. A liquid dye concentrate was produced by dissolving 2.5 gms of dye powder in 1 liter of water to which was added 1 tablespoon of alcohol in order to stabilize the solution. A dilute solution of dye made by uniformly diluting 1 ml of concentrate with 3.5 liter of water was mixed "inline" with the inner jet fluid in the ratio of 1 part dilute solution to 760 parts water. Any variation in dye concentrations at the inner jet inlet location can be attributed to this last mixing process.

The 0.4880 μm wavelength beam of the argon ion laser was used in the LV/LIF experiment both to induce fluorescence of the fluorescein dye for the LIF measurement and to scatter light from particles for the LV measurements. Fluctuations in the laser beam intensity were monitored in bench tests to determine power fluctuations. The peak to peak power drift over a 20 minute period was less than 0.5 percent. The signal from the photomultiplier was filtered with a 2KHz low pass filter to remove the shot noise associated with photomultiplier tubes. The 2KHz filtering was compatible with the typical velocity of 1 m/sec and probe volume length of 1 mm. The current signal was converted to a voltage, amplified and then processed through an A/D voltage converter each time an acceptable LV signal was obtained. The LV and LIF data were stored as pairs along with the data acquisition time by the Data Handling subsystem. A list of additional equipment used for the LV/LIF measurements is also presented in Table I.

Swirler Design Evaluation

Before conducting the flow visualization tests and the detailed mass and momentum turbulent transport measurements, a short study was conducted to evalute two swirlers designed for use in this program. The eight-bladed swirlers had blade shapes which are typical of that used in gas turbines. The first swirler was designed for a free vortex flow with a 33 deg swirl angle at the mean annulus radius. This swirler produced a flow which appeared to separate at the inner tube wall and was deemed unsatisfactory for this program. The second swirler blade shape was designed to produce a

30 deg-mean-angle, free-vortex tangential velocity distribution with a uniform axial velocity profile. The second swirler produced a swirling annular stream which did not separate from the inner tube wall upstream of the inlet plane. In general, the performance of the second swirler was satisfactory and the resulting flow patterns were the type desired for this study. Therefore, the second swirler was used for the detailed mass and momentum turbulent transport measurements and flow visualization tests. A detailed description of this swirler is presented in Fig. 9.

FLOW VISUALIZATION RESULTS

The present study was conducted to obtain a data base that can be used to evaluate transport models developed for axisymmetric flow computational procedures. Since the transport models are based on time-independent statistics, it is important that the experimental data used to evaluate the models be obtained from statistically steady or stationary flows. Also, good axisymmetric flow characteristics are required because data from the same radial location are obtained at several azimuthal locations. Therefore, flow visualization studies were conducted before data acquisition was initiated to determine if the flow was symmetric and statistically stationary. The results of the flow visualization studies were also used to determine the scale of the turbulent structure of the flow within the test section. The structure and scale of the turbulent eddies was deduced from the interface between regions of high and low dye concentration recorded on high speed motion pictures.

Flow visualization experiments with swirling flow in the annular stream were conducted for the following five flow conditions:

Flow Condition	Mean Axial Velocity, m/s		Flow Rate, gpm	
	Inner Jet, $\overline{U}_i$	Annular Jet, $\overline{U}_a$	Inner Jet	Annular Jet
1	0.52	1.66	6.2	52.8
2	0.27	1.66	3.2	52.8
3	2.08	1.66	24.6	52.8
4	0.94	1.51	11.1	48.0
5	0.94	2.87	11.1	94.8

These flow conditions are identical to those used in the experiments with nonswirling flow in both the inner and annular streams (Ref. 7).

High speed motion pictures, real-time motion pictures, and fast-action (1/1000 sec) 35 mm slides were obtained of the flow at selected locations in the r-z and r-θ planes. One set of flow visualization tests was conducted with a continuous flow of dye added to the inner jet stream. A second set of tests was conducted with a pulsed flow of dye added to the annular stream to determine (1) the nature of the shear layer between the annular stream and the annular recirculation region, and (2) the amount of coupling between the large eddy structure in the inner/annular streams and in the annular stream/annular recirculation shear layers.

General features of the flow field observed for all the flow conditions except Flow Condition 3 are shown in the sketch in Fig. 1. Five distinct flow regions were observed in the flow field. Four of the regions were also observed in the flow field for the nonswirling coaxial streams which is also sketched in Fig. 1. They included: (1) a wake region between the inner and annular streams a short distance downstream of the inlet, (2) a large-eddy shear region between the inner and annular streams, (3) an annular recirculation zone adjacent to the inlet plane, and (4) a reattachment region downstream of the annular recirculation zone. As shown in Fig. 1, a large recirculation region along the centerline was also observed for the swirling coaxial streams. The characteristics of Flow Condition 1, that condition selected for the detailed data acquisition are described in the following paragraphs. This discussion will also be included in Appendix I where the characteristics of the other flow conditions will be described.

Photographs taken for Flow Condition 1 in both the r-z plane and at selected axial locations in the r-θ plane are presented in Fig. 10. The photographs at the top of Fig. 10 are representative of the flow characteristics as seen in the r-z plane when dye is injected both in the inner stream and in the annular stream. The photograph taken when dye is injected into the inner stream (top left) shows that a high inner jet stream concentration persists for an axial distance of approximately 50 mm. In the photograph taken when dye is injected into the annular stream (top right), dye has been entrained near the centerline between an axial distance of approximately 60 mm to 170 mm indicating the presence of a recirculation cell near the centerline. The existence of this recirculation cell became more apparent in the high-speed films and appeared to extend to almost 150 mm. Both photographs show large-scale eddy structure in the shear layer between the jets starting at axial distances of approximately 30 mm and extending downstream to at least 175 mm. The scale of these eddies at z = 50 mm is more than half the inner jet diameter of 30 mm. Although the eddy sizes are large, the eddy structure did not appear to be periodic or symmetric. When dye is injected into the annular stream, the annular recirculation region adjacent to the test section inlet plane and the attachment region downstream of this annular recirculation zone are clearly defined. The length of this annular recirculation cell is approximately 50 mm which is about 1/3 the length observed with nonswirling flow for the same flow condition.

The photographs taken of dye in the r-θ plane at z = 25 mm shows the radial scale (≅ 6 mm) of the eddy structure at the upstream end of the shear region. At z = 51 mm, the scale of the large eddy structure has increased significantly (∿ 15 to 20 mm). The scale does not appear to increase appreciably from z = 100 mm to z = 200 mm. As shown by the photographs in both the r-z and r-θ planes, the large eddy structure is not axisymmetric or azimuthally periodic for z > 50 mm.

Photographs taken at selected axial locations downstream of the test section inlet with dye injected in the annular stream are shown in Fig. 11. These photographs show the structure of the eddies in the r-θ plane. At z = 13 mm, the flow on both the ID and OD of the annular stream show small scale structure with the type of wall eddies expected in an annular duct. At z = 25 mm, the scale of the eddies in the annular jet/inner jet interface increasd to 6 to 20 mm. Within the recirculation cell (38 mm < z < 180 mm) the scale of the eddies varied from 5 to 25 mm or up to 20 percent of the test section duct diameter. Downstream of the recirculation cell (z > 180 mm), the flow initially had large lobes (e.g., z = 203 mm) which evolved into a vortex swirl pattern (z = 406 mm). There was little radial mixing downstream of the recirculation cell.

The high speed motion pictures also provided insight into the mixing process and showed two major mixing regions: (1) at the interface between the inner jet and the centerline recirculation zone (z = 30 to 60 mm) and (2) in the interface between the inner jet/annular jet streams (30 mm < z < 90 mm and $0.3 < r/R_o < 1.0$). The mixing at the inner stream/recirculation cell interface diluted the inner jet concentration and the resulting mixture of fluid from the recirculation cell and the inner jet was entrained by the swirling annular stream.

FOREWORD TO PRESENTATION OF RESULTS

The use of computerized data acquisition, storage, reduction and analysis techniques permitted numerous quantities to be determined from the data obtained in this study in addition to the mean and fluctuating velocity components and concentrations usually obtained. These included (1) parameters which can be used to characterize the probability density functions of the velocity components, the concentrations, the mass transport rates and the momentum transport rates and (2) the various correlation coefficients for the transport processes.

The determination of all possible parameters and correlations obtainable from the experimental data was beyond the scope of this study. However, the most universally used quantities have been calculated and are included in this report. The parameters presented include the mean value and three central moments of the velocity and concentration probability density functions (i.e., rms variation from the mean, skewness and kurtosis or flatness factor), the mean value and three central moments of the mass and momentum turbulent transport rate probability density functions, and the correlation coefficients for the mass and momentum turbulent transport rates.

The data point sets which are presented in this report were obtained for Flow Condition 1, described in the flow visualization section, and consist of single point measurements which were usually made at a fixed axial location over a range of radial locations. A data acquisition run number was assigned to each group of single point measurements. A new run number was assigned to each data point set each time a change in axial location or change in measured parameter was made; i.e., velocity component or concentration. The number of velocity/velocity or velocity/concentration data pairs which were acquired during each single point measurement was either 250, 500, or 1000 depending upon the number of particles traversing the probe volume. During data acquisition, all data was stored on floppy disks. This data was subsequently reduced to obtain the calculated parameters listed in the previous paragraph. The number of data pairs actually used in the data reduction was usually less than the 250, 500 or 1000 data pairs acquired because data pairs were eliminated during data reduction whenever spurious data was encountered. Spurious data was defined as data noncontiguous to and outside of the 3σ region of the probability density functions and was believed to occur when the laser velocimeter signal processor passed "bad" data because multiple or very large particles passed through the probe volume or data was taken in regions of low signal-to-noise ratio.

All the calculated parameters obtained for each data acquisition run are presented in this report in tabular form. Most of the results are also presented in graphical form to aid in the discussion of the results. A listing of the run numbers from which data was utilized for the tables and figures presented in this report is presented in Table II. A listing of numbers assigned to the figures on which results are displayed in this report is presented in Table III. The tabulated parameters for each data point set are tabulated in Tables IV-XX where the term XX denotes the run number.

The results are presented and discussed in the following order. The mean and fluctuating velocity and concentration results are presented first, the turbulent mass and momentum transport rates and correlations second, the higher moments of velocity and concentrations, and the higher moments of the turbulent transport rates are presented in later sections.

DISCUSSION OF MEAN AND FLUCTUATING VELOCITY AND CONCENTRATION RESULTS

Velocity Results

Mean and fluctuating velocity profiles were obtained at nine axial stations as part of both the mass and momentum turbulent transport measurements. Consequently, each velocity profile is comprised of data obtained in two to four radial surveys (two or more runs) through the center of the test section. The coordinate system employed for this study is presented in Fig. 4. The results will be discussed in relation to the shear regions shown in Fig. 1 and will be compared with the results of the study made for nonswirling coaxial jets presented in Ref. 7.

Mean Axial Velocity

The mean axial velocity profile along the centerline of the test section is shown in Fig. 12 and is compared with the profile obtained for the nonswirling flow. As can be seen, the velocity profile for the swirling flow is significantly different from that observed with the nonswirling flow. For the nonswirling flow, the centerline velocity was (1) initially decreased as the inner jet fluid momentum is transported into the wake between the inner and annular streams, (2) increased as the inner jet fluid is accelerated by the annular jet until z = 200 mm, and (3) finally decreased as the duct velocity profile begins to approach that for fully developed duct flow. For the swirling flow, the velocity along the centerline (1) decreased rapidly, (2) passed through zero at z = 40 mm, (3) remained negative until approximately z = 167 mm and (4) gradually increased to the average value for fully developed duct flow. The two stagnation points at z = 40 mm and z = 167 mm mark the extent of a recirculation zone near the centerline of the test section. The length of this zone, 127 mm, agrees with the length observed in the flow visualization tests for this flow condition.

The mean axial velocity profiles are presented in Fig. 13. The velocity profile at the measurement location closest to the inlet, z = 5 mm was similar to that observed with the nonswirling flow for z = 13 mm. For both cases, the peak velocity in the inner jet was approximately one-half the peak velocity in the annular jet and there was a wake region in the vicinity of $r/R_o = 0.25$, the radial location of the thin wall which separates the inner and annular jets.

For the horizontal traverses, the shaded symbols shown in the figure were obtained on the side of the centerline adjacent to the LV optics while the open symbols were obtained on the far side. For the vertical traverses, the open symbols were obtained from the upper half of the traverse and the shaded symbols were obtained from the lower half. The velocity profiles are axisymmetric since data taken on either side of the centerline generally fell on top of one another. However, there is some discrepancy in the annular region for $z = 5$ mm. This discrepancy may be attributed to the swirl vane wakes and the secondary flow which forms adjacent to the swirl vanes and persists in the flow for a short distance downstream from the test section entrance. This behavior will be discussed more fully later (Appendix II) when the results are presented of azimuthal and radial traverses of the flow field a short distance ($z = 5$ mm) downstream of the trailing edge of the swirler.

The changes in the axial velocity profiles from $z = 5$ mm to succesive downstream locations document the development of the various shear and recirculation regions within the test section. The velocity of the inner jet decreased with axial distance and became negative indicating a reversal of flow near the centerline region. Note at $z = 25$ mm, the velocities were negative in the wake region at $0.18 < r/R_o < 0.31$ indicating an "s" shaped path for the fluid in this region. The flow visualization photographs and motion pictures showed significant mixing in this region. A second flow reversal in this region occurred between $z = 152$ mm and $z = 203$ mm after which the velocity gradually increased and flattened out throughout the rest of the duct length.

Negative axial velocities near the peripheral wall were also observed for axial locations up through $z = 51$ mm indicating back flow or a recirculation region near the outside wall. Note that the peak negative velocity near the wall was approximately 0.65 m/s and was measured at an axial location of $z = 51$ mm. This negative velocity is approximately 47 percent of the peak streamwise axial velocity at this location and is almost three times the percentage obtained for the nonswirling case. Also, the downstream end of this outside wall recirculation zone is located between $z = 51$ and $z = 102$ mm whereas the downstream end of the recirculation region for the nonswirling case was located at $z = 254$ mm. Therefore, the recirculating zone near the outside wall is shorter for the swirling case and the recirculating flow within the zone is stronger. One other difference which should be noted is that once reattachment of the annular jet occurred the axial velocity profile tended to flatten with momentum transport from the outside inward for the swirling flow whereas it tended to flatten with momentum transport from the inside outward for the nonswirling flow.

Mean Radial Velocity

The profiles of the mean radial velocity are presented in Fig. 14. These profiles were generally axisymmetric except in the annular region at an axial loction of 5 mm. This behavior has been attributed to swirl vane wakes and/or secondary flows which form adjacent to the swirl vanes and persist in the flow for a short distance downstream of the test section inlet (see Appendix II). The flow showed significant radially outward movement (positive velocities) for $z < 51$ mm. At $z = 51$ mm, the radial velocity is approximately 75 percent of the axial velocity indicating that the flow was moving outward at an angle of approximately 35 degrees. At $z = 25$ mm, there was radially inward movement of the flow near the wall $r/R_o > 0.7$ again indicating the presence of the recirculation zone which was observed in the flow visualization tests and which was also indicated by the negative axial velocities at this location. Between $z = 51$ and $z = 102$ mm, the flow attached to the wall and was directed radially inward as the flow was deflected by the wall. The radial velocity profile flattened out and approached zero as the duct flow became fully developed ($z > 305$ mm).

Mean Azimuthal Velocity

The mean azimuthal velocity profiles are presented in Fig. 15. The azimuthal profiles were generally axisymmetric and well behaved. However, one anomaly occurred in the velocity profile near the inlet ($z = 5$ mm) where the velocity profile on one side of the centerline $0.4 < r/R_o < 0.5$, was greater than on the other side. Similar behavior was also noted in the axial and radial profiles for this location (see Figs. 13 and 14) and has been attributed to swirl vane wakes and/or secondary flows in the vane passage (Appendix II).

The swirling flow azimuthal velocity profile near the entrance to the test section was as expected from the swirler design characteristics. There was no swirl in the inner jet region and the annular profile was essentially that which would be predicted from the swirler design. The azimuthal velocity decreased over the first 51 mm after which an essentially uniform profile was maintained throughout the remaining length of duct.

Fluctuating Velocities

Fluctuating axial, radial, and azimuthal velocity profiles are presented in Figs. 16, 17 and 18 respectively. The profiles for the swirling jets were similar to those observed for the nonswirling jets in that they could be related to the developing shear layers. Near the entrance to the test section ($z = 5$ mm), the peak fluctuating velocities occurred in the wake region separating the inner and annular flows ($r/R_o = 0.25$) and in the shear layer outside the annular jet ($r/R_o = 0.55$). The intensities of the fluctuating velocities increased and decreased with the development of the shear layers (1) between the inner and annular jets, (2) between the annular jet and the recirculation zone near the outside wall and (3) in the reattachment region. The magnitude of the fluctuations were generally greater for the swirling flow than that for the nonswirling flows. For the swirling flow, the more vigorous fluctuations occurred within the first 51 mm while the fluctuations increased to $z = 152$ mm for the nonswirling flows. For the swirling flow, the fluctuations dampened relatively rapidly between 51 mm and 102 mm which might be attributed to the stabilizing effect of the uniform azimuthal velocity profile. The fluctuating radial and azimuthal velocity profiles showed trends similar to the axial profiles but the intensity of the axial velocity fluctuation was generally greater. As the local shear rate decreased ($z > 152$ mm), the ratios of fluctuation, v'/u' and w'/u' tended toward 1.0. However, for those axial locations where the fluctuations were more intense, the axial fluctuations were 1.5 to 2 times greater than either the radial or azimuthal fluctuations indicating nonisotropic turbulence.

Concentration Results

For the concentration measurements, a small amount of fluorescein dye was added to the inner jet fluid. As the dye in the inner stream mixed with the annular stream, the local concentration of inner jet fluid was determined by measuring the intensity of light emitted by the fluorescing dye. The light intensity is proportional to the concentration of dye in the LV probe volume. The local concentration in the fluid, $\bar{f}$, was defined to be the ratio of light emitted locally to the light emitted at the centerline locations at an axial location of 13 mm where $\bar{f} = 1.0$ by definition. The location $z = 13$ mm and $r/R_o = 0$ was chosen as a reference location because: (1) optical interference with the upstream walls occurred in the light collection system at locations closer to test section inlet and (2) the inner jet fluid had not begun to mix at this location. During a particular run, the light intensity at the reference location was measured at the start of the run, after each set of approximately 5 data points had been taken, and again at the end of the run. In this way, any variation in the light emitted at the baseline location could be accounted for during the course of the run. In the discussion of the experimental results which follows, the symbol "$\bar{f}$" and/or the term "concentration" refer to the ratio of the light emitted locally to the light emitted at the baseline location.

Mean Concentration

The axial variation of the concentration along the test section centerline is presented in Fig. 19 along with the variation obtained for the non-swirling flow (Ref. 7). Again, the results presented in this figure point out the significant differences between the swirling and nonswirling flows. For the swirling flow, the mean centerline concentration decreased rapidly from the reference measurement location ($z = 13$ mm) and approached the mass averaged flow concentration level of $\bar{f} = 0.104$ at $z = 100$ mm. For the nonswirling flow, the concentration along the centerline decreased slowly to 75 mm and then fairly rapidly from $z = 100$ mm to $z = 200$ mm and finally approached the mass averaged flow concentration level at $z = 356$ mm. Mixing along the centerline of the test section for swirling flow was therefore completed in one-third the length required for nonswirling flows.

The mean concentration profiles at various axial stations are presented in Fig. 20. At an axial location near the entrance to the test section ($z = 13$ mm), the concentration profile shows the expected large concentration gradient between the inner jet and the annular jet. Note that at $z = 25$ mm and $0.18 < r/R_o < 0.31$, the location where a recirculation zone is indicated by the mean axial velocity profile (Fig. 13), the concentration profile varies from $f = 0.8$ to 0.3. The concentration profile rapidly flattened out with axial distance until $z = 102$ mm where the concentration across the duct became essentially equal to the average duct concentration of $f = 0.104$ for the remaining length of test section. The results shown in Fig. 20 indicate that the concentration profiles were reasonably axisymmetric and repeatable.

Fluctuating Concentrations

The concentration fluctuations, f', are presented in Fig. 21. At an axial location near the entrance to the test section ($z = 13$ mm), the peak concentration fluctuation occurred in the interface region between the inner and annular jets where a large concentration gradient exists. At $z = 25$ mm, the peak concentration fluctuation still occurred in this interface region ($0.15 < r/R_o < 0.35$) but increased activity also occurred along the centerline, $r/R_o = 0.0$. The fluctuations in the centerline region continued to increase between $z = 25$ mm and $z = 51$ mm with peak activity shifting toward the centerline. There was a rapid decrease in activity between $z = 51$ mm and $z = 102$ mm as the fluctuations dampened out from inside to outside. Between $z = 102$ mm and $z = 203$ mm the fluctuation profiles were essentially flat with only slight activity near the outside wall region. The fluctuation for swirling flow were essentially dampened out in approximately one-third the length required for the nonswirling flow.

DISCUSSION OF TURBULENT TRANSPORT RESULTS

Momentum Transport

Profiles of the momentum turbulent transport rates and correlation coefficients obtained for the three measurement planes are presented in Figs. 22 through 27. The discussion of these profiles will be related to the shear regions presented in Fig. 1 and the velocity profiles presented in Fig. 13 through 15.

Radial-Axial Plane (r-z)

The momentum turbulent transport rate distributions obtained in the r-z plane are presented in Fig. 22. This turbulent transport, $\overline{uv}$, is related to the strain rate: $\partial U/\partial r + \partial V/\partial z$. The momentum turbulent transport rates were either positive (outward) or negative (inward) at various locations in the flow and were consistent with the local velocity gradients shown in Figs. 13 and 14. Near the entrance of the test section, z = 5 mm, the momentum turbulent transport was positive for $r/R_o < 0.2$ (the extent of the inner jet region) and remained positive up through an axial location of z = 25 mm. This momentum flux can be attributed to the shear of the inner jet fluid on the wake region downstream of the interface between the inner and annular jets. At z = 5 mm, and for $0.2 < r/R_o < 0.4$, the momentum flux was negative because momentum was being transported from the annular jet fluid into the wake region. Near $r/R_o = 0.5$, the momentum flux was positive which can be attributed to the shear layer which develops between the annular jet and the recirculation zone near the outside wall. At the axial location of z = 25 mm, the momentum turbulent transport rates had approximately doubled.

The flow visualization tests and the axial velocity measurements indicated that a recirculation zone existed near the test section centerline for axial locations 40 mm < z < 167 mm. The results shown in Fig. 22 indicate that there is little momentum transport near the centerline, $r/R_o < 0.4$, for axial locations, z = 51 mm and z = 102 mm, the upstream end of the centerline recirculation cell. There was a weak negative momentum flux for $r/R_o < 0.4$ at z = 152 mm which is close to the downstream edge of the centerline recirculation zone. The momentum turbulent transport rate near the outside wall, $r/R_o > 0.8$ was still positive at z = 51 mm but became essentially zero at z = 102 mm indicating that the end of the recirculation zone near the outside wall is located between z = 51 mm and z = 102 mm which is consistent with the results of the axial and radial velocity measurements and the flow visualization tests. At axial locations, 51 mm < z < 203 mm, the momentum turbulent transport rate was negative (consistent with the axial velocity gradient) and was essentially zero for z > 305 mm. In comparison, the momentum transport in the r-z plane for nonswirling flow was generally positive and significant transport was still observed at an axial location $z = 305$ mm. The peak rates for both swirling and nonswirling flow were of the same order of magnitude (0.6 m^2/s^2) but the peak for the swirling flow occurred at an axial location one-fifth to one-fourth of that observed for the nonswirling flow.

The correlation coefficients, R_{uv}, obtained for the momentum turbulent transport data are presented in Fig. 23. As can be seen from the figure, the correlation coefficients generally followed the same trend as the momentum turbulent transport rate profiles. Peak correlation coefficients occurred at essentially the same locations where the peak transport rates occurred. The absolute values of the peak momentum transport correlation coefficients were between 0.35 and 0.50 which are in the range previously measured for turbulent free shear momentum transport (Ref. 14). Note that the momentum turbulent transport coefficients for $z = 51$ mm and $0.4 < r/R_o < 0.6$ are -0.25 to -0.30 rather than the values of 0.4 to 0.5 measured in other high shear regions. Note also that for $z \geq 305$ mm the correlation coefficients were low and scattered about zero.

Axial-Azimuthal Plane (z-θ)

The axial-azimuthal momentum turbulent transport rates obtained are plotted in Fig. 24. This turbulent transport is related to the strain rate $(1/r)\,\partial U/\partial\theta + \partial W/\partial z$. For axisymmetric flow, $\partial U/\partial\theta$, is zero. The transport rates in this measurement plane were consistent with the trends shown with the corresponding velocity profiles but the peak rates were about half of those observed in the r-z plane. The momentum turbulent transport rate was generally positive for $z < 102$ mm especially in the annular jet region, $0.25 < r/R_o < 0.60$. For $102 \text{ mm} < z < 203$ mm, the momentum transport rate was positive near the centerline region, $r/R_o < 0.4$ and negative near the outside wall, $r/R_o > 0.6$. The momentum turbulent transport rate in the z-θ measurement plane became essentially zero for $z > 305$ mm and $r/R_o > 0.2$. There was a weak negative transport close to the centerline of the test section, $r/R_o < 0.2$.

The momentum transport correlation coefficient, R_{uw}, obtained in this measurement plane is shown in Fig. 25. Again, the correlation coefficient profiles generally followed the same trend as the momentum transport rate profiles. However, the peak values were about half those obtained for the r-z plane. There appears to be more scatter in the R_{uw} correlation coefficients than those for R_{uv}. The flow visualization motion pictures showed more low frequency "wandering" of the flow inside the downstream of the central recirculation zone that may cause this scatter in R_{uw}.

Radial-Azimuthal Plane (r-θ)

The momentum turbulent transport rates in the radial-azimuthal plane were obtained by aligning the laser beams in the test section parallel with the axis of symmetry. For these measurements, the LV laser beams were passed through a 1200 mm focal length lens and entered the test section through a window at the downstream end of the test section. Light from the scattering particles in the probe volume was collected by a set of receiving optics which was aligned perpendicular to the test section axis of symmetry. With this arrangement, data was obtained at three axial locations: $z = 25$ mm (Runs 47, 48 and 49), $z = 50$ mm (Runs 46, 50, 51, 52 and 53) and $z = 102$ mm (Runs 54, 55, 56). Runs 46, 47, 50, 51 and 54 were obtained with the LV optical axis parallel to the test section axis of symmetry. Because of some optical axis constraints with this particular optical orientation, data could only be obtained in the region $r/R_o < 0.5$. In order to obtain data in the region $r/R_o > 0.5$, the optical axis was tilted upward or downward by approximately one degree. This tilted optical orientation allowed data to be obtained closer to the outer wall, Runs 48, 49, 52, 53, 55 and 56. This data should be corrected using the result of the momentum turbulent transport data obtained for the r-z plane. However, since this correction is small (estimated to be within 2 percent of the peak turbulent transport rate measured) and since the details (i.e., higher moments of the vw probability density function would not be available with the correction, uncorrected data is presented herein. It is believed that the uncorrected data provide an adequate representation of the momentum turbulent transport process in the $r-\theta$ plane.

The momentum turbulent transport rates obtained for the $r-\theta$ measurement plane are presented in FIg. 26. This turbulent transport is usually related to the strain rate $(1/r)\ \partial V/\partial\theta + \partial W/\partial r - W/r$. For axisymmetric flow, the azimuthal variation of V is zero. This data was obtained for three axial locations, $z = 25$, 51 and 102 mm. At $z = 25$ mm, there was a negative transport rate in the interface region between the inner and annular jets and a positive transport rate in the shear region between the annular jet and the recirculation zone near the outside wall. The results obtained for the $r-\theta$ plane were similar to those obtained for the r-z and $z-\theta$ planes in that peak momentum transport occurred at an axial location $z = 25$ mm and the rate tended to zero with increasing axial distance. The peak rate observed for the $r-\theta$ plane was approximately equal to the peak obtained for the $z-\theta$ plane ($\sim 0.3\ m^2/s^2$).

The profiles of the correlation coefficient obtained in this plane, R_{wv} are shown in Fig. 27 and generally followed the same trends as the momentum transport rate. The peak correlation coefficient obtained ($R_{wv} = 0.25$) was approximately equal to the correlation coefficient obtained for the $z-\theta$ plane and was about one-half of that obtained for the r-z plane.

Summary Comments

For this flow condition with swirl angles of 25 to 40 degrees in the annular stream, the principal momentum turbulent transport was in the r-z plane, uv, and was caused by the axial velocity gradients. The peak transport rates were approximately the same ($0.06\ m^2/s^2$) as for the nonswirling flow condition but occurred nearer the inlet ($z = 25$ mm) than for the nonswirling flow condition ($z = 150$ and 205 mm). The correlation coefficients for the momentum turbulent transport in the r-z plane were greater than those in the other two planes. This result is compatible with assumptions in the turbulent transport theory regarding the "return to isotropy" for eddy dissipation of energy.

Mass Transport

The mass turbulent transport rate profiles were obtained for the three measurement directions. These transport rates are generally associated with the gradients of the mean concentration profiles (Fig. 20). The discussion of the mass turbulent transport will be related to these concentration profiles, to the shear regions shown in Fig. 1 and to the flow visualization results.

Radial Direction

The radial mass turbulent transport rate profiles, $\overline{vf}$, which are shown in Fig. 28 indicate that radial transport occurred at axial locations $z = 13$, 25 and 50 mm and essentially no mass turbulent transport occurred between $z = 102$ mm through $z = 203$ mm. The peak rates for $z = 13$ mm and 25 mm occurred at the radial location, $r/R_o = 0.25$ which corresponds to the location of the interface between the inner jet and annular jet. At $z = 25$ mm, the peak transport rate occurred for $0.18 < r/R_o < 0.3$ where the axial velocities were negative. At 51 mm, the turbulent transport rate data appear to be scattered about zero especially near the centerline region. According to the flow visualization results and the axial velocity profiles, the axial location of $z = 51$ mm is near the upstream end of the centerline recirculation region where the flow may not be axisymmetric and thus may account for the data scatter. The peak fluctuating radial velocities for swirling flow were approximately 60 percent greater than the peak obtained for nonswirling flow and therefore higher mass turbulent transport rates should be expected for swirling flow. However, the peak radial transport rate of $\overline{vf} = 0.018$ m/s which was obtained at $z = 25$ mm and $r/R_o = 0.26$ is approximtely equal to the peak value obtained for nonswirling flow (Ref. 9). The peak for nonswirling flow also occurred in the interface region ($0.20 < r/R_o < 0.25$) but was obtained much farther downstream (102 mm $< z < 151$ mm). The peak values were relatively low although they occurred at locations where the radial concentration gradients were the highest in the flow field (see Fig. 22). For the swirling flow condition, the mean radial velocities were an appreciable fraction (20 to 70 percent) of the local axial velocity. Thus there was more convection of the inner jet fluid radially outward than occurred for the nonswirling flow condition.

The correlation coefficient, R_{vf}, profiles which are presented in Fig. 29 generally followed the trends of the mass transport rates. The peak correlation coefficient occurred at the same location as the peak mass transport rate ($z = 25$ mm, $r/R_o = 0.26$) but its value of $R_{vf} = 0.31$ is approximately half the correlation coefficients obtained for the nonswirling flow.

Axial Direction

The axial mass turbulent transport rate, $\overline{uf}$, profiles are presented in Fig. 30. The greatest axial mass transport (0.25 m/s $< \overline{uf} < 0.55$ m/s) occurred near the upstream end of the centerline recirculation zone ($r/R_o < 0.3$ and 25 mm $< z < 51$ mm). In this region the mean axial velocity was negative. No appreciable axial mass transport occurred for $z > 102$ mm. There is a significant difference in the axial mass turbulent transport rates between the nonswirling and swirling flows. For nonswirling flow, negative mass turbulent transport rates were obtained in those regions where the inner stream concentration was decreasing with axial location which indicates a counter-gradient mass transfer. For swirling flow, the axial mass turbulent transport rates were positive (gradient mass transfer). The peak axial mass turbulent transfer rate for the swirling flow (0.55 m/s) was higher than the peak obtaned for non-swirling flow (-0.35 m/s). The mass transport in the axial direction for swirling flow was essentially completed within $z = 102$ mm whereas the mass transport for nonswirling flow was not completed until $z = 305$ mm. The axial mass turbulent transport rates were higher than the radial mass transport rates even though the peak radial concentration gradients were approximately seven times greater than the peak axial concentration gradient.

The correlation coefficient R_{uf}, profiles presented in Fig. 31 show the development of the axial mass transfer process more clearly where the mass transport rates are small. At $z = 13$ mm and $z = 25$ mm, the axial mass transport correlation coefficients were generally positive for $r/R_o < 0.40$ which indicates mass transport in the downstream direction. In the shear region between the annular jet and the recirculation zone near the outside wall, $0.45 < r/R_o < 0.8$, the correlation coefficient was negative for $z = 13$ mm and $z = 25$ mm indicating mass transfer upstream. Near the upstream end of the centerline recirculation zone ($z < 51$ mm), the correlation coefficient was positive near the centerline ($r/R_o < 0.4$). At the downstream end of the recirculation zone, (102 mm $< z < 152$ mm), the correlation coefficient was negative. The correlation coefficient is generally positive near the peripheral wall ($r/R_o > 0.8$). Although the peak axial mass turbulent transport rate for swirling flow was greater than that for nonswirling flow, the correlation coefficients for swirling flow were less than that for nonswirling flow.

Azimuthal Direction

The azimuthal mass turbulent transport rate, $\overline{wf}$, and the corresponding correlation coefficient, R_{wf}, profiles are presented in Figs. 32 and 33, respectively. The azimuthal mass turbulent transport rates shown in Fig. 32 were small compared to the rates in the axial and radial direction. At $z = 13$ mm, there was a small negative rate in the interface region between the inner and annular jet streams. This is caused by the preferential turbuent eddy orientation in the interface between the inner and annular streams. The negative value indicates that the inner jet fluid (from the nonswirling inner jet) is rotating at a lower rate than the mean azimuthal velocity. For axial locations, $z = 25$ mm and $z = 51$ mm, there were also variations of the mass transport rate near the centerline region, $r/R_o < 0.4$, which can be attributed to coupling between the mass and swirling momentum transport in those regions. For $z > 102$ mm, the azimuthal mass transport was essentially zero.

The correlation coefficient profiles presented in Fig. 33, essentially showed the same trends as the mass transport profiles. There was scatter in the results in and near the ends of the center recirculation region due to asymmetries and wandering of the center of rotation.

Summary Comments

The mass turbulent transport process for the "simple" swirling coaxial flow configuration utilized in this experiment is very complicated. From the data and the flow visualization high speed motion pictures, it appeared that the turbulent transport and mixing occurred in several steps of axial and radial mass turbulent transport coupled with a large radial or mean convection flux. The turbulent transport rates indicated mass flux across streamlines and the decrease in concentration fluctutaions indicated mixing of the fluid toward the molecular level. These processes appear to begin with high concentration fluid from the inner jet diffusing turbulently into fluid from the recirculation cell near the centerline for $25 \text{ mm} < z < 50$ mm. This diluted inner jet fuid ($\bar{f} \simeq 0.5$) is convected by the negative axial velocities at $z \cong 25$ mm and $0.2 < r/R < 0.3$ to the large eddy shear region at $0.3 < r/R_o < 0.4$ and $25 \text{ mm} < z < 75$ mm. There appeared to be more turbulent transport across the diagonal streamlines ($r/R_o > 0.3$ and < 150 mm) by axial mass turbulent transport than by radial mass turbulent transport. This result may be due to the preferential turbulent structure developed by the shear layer. Additional analysis of the data and comparison with numerical code predictions or results from dimensional analysis (using the equations for turbulent transport) will be required to fully understand this turbulent transport process.

DISCUSSION OF SKEWNESS AND KURTOSIS RESULTS FOR VELOCITY AND CONCENTRATION PROBABILITY DENSITY FUNCTIONS

Although mean and fluctuating velocity and concentration distributions and transport rate distributions are required to evaluate the accuracy of predictions with a given turbulent transport model, they do not provide the insight required to determine where the deficiencies in a turbulent transport model occur. Examination of the probability density function (p.d.f.) for each data set acquired at each location can show if the experimental conditions are compatible with the assumptions in current or proposed models. The experimental techniques and the computer based data acquisition systems employed in this study permitted the examination of these p.d.f.s and the determinations of their skewness and kurtosis parameters used to characterize the degree of asymmetry and flatness respectively of the p.d.f.s. Typical results from this portion of the study are presented in the following sections.

Typical Probability Density Functions

Velocity and concentration p.d.f.s were plotted for data sets obtained at selected radial locations at z = 25 mm from the inlet plane and are presented in Figs. 34 through 37. This axial location was chosen for more detailed analysis of the flow characteristics because the momentum and mass transfer rates are high at this location. These data were obtained as part of the momentum and mass tranfer acquisition; consequently velocity p.d.f.s were comprised of data from two or more different runs. The concentration p.d.f.s are comprised of data from the mass transport rate measurement in three directions. The mean quantity, rms variation from the mean, the skewness and the kurtosis tabulated are averages from the number of runs cited in each figure. The data from the runs was plotted to present a composite picture of the p.d.f. at each location.

Axial Velocity

The axial velocity p.d.f.s presented in Fig. 34 showed significant changes with radial location. The p.d.f. at $r/R_o = 0.0$ was skewed to the lower velocity region which indicated that on the average, flow at this location was being decelerated axially. At $r/R_o = 0.13$, the p.d.f. was approximately symmetric and double peaked. Consequently the kurtosis, $K_u = 2.2$, was lower than the Gaussian value, $K = 3.0$. At $r/R_o = 0.24$, the p.d.f. was skewed toward the higher velocities indicating that on the average, fluid at this radius was being accelerated in the shear layer between the jets. At a radius ratio of 0.36, the p.d.f. was more symmetric and had a kurtosis close to that for Gaussian profiles ($K = 3.0$). At radius ratios of 0.52 and 0.68, the p.d.f.s were again skewed toward lower velocities indicting that the fluid was again being decelerated. The trends indicated by the p.d.f.s are consistent with the axial velocity profiles shown in Fig. 13.

Radial Velocity

Although the radial velocity p.d.f.s presented in Fig. 35 showed less variation with radial location than the axial p.d.f.s, they did have several distinct features. At radial locations $r/R_o = 0.0$ and 0.13, the p.d.f.s were nearly symmetrical, i.e., $S_v = 0.2$ and were sharply peaked near $V = 0$. The p.d.f. at $r/R_o = 0.24$ also peaked about zero but had a negative skewness. The tails on each side of the peak cause the kurtosis to be relatively high, i.e., K_v 5.0. At the radial location $r/R_o = 0.36$, the p.d.f. is skewed toward higher velocities indicating that the fluid in this region was being accelerated. At $r/R_o = 0.52$, the p.d.f. is essentially symmetric which is consistent with the radial velocity profile shown in Fig. 14, i.e., the mean radial velocity at this radial location is at the maximum. At $r/R_o = 0.68$, the radial velocity is close to zero but the p.d.f. is skewed to higher velocities which indicates that some filaments of fluid with relatively high radial velocity occasionally passed through the probe volume.

Azimuthal Velocity

The azimuthal velocity p.d.f.s which are presented in Fig. 36 show that the fluid had essentially zero velocity for radial locations up to $r/R_o = 0.24$ (p.d.f.s peaked near zero). At $r/R_o = 0.36$, the p.d.f. has shifted to higher velocities. However, low velocity fluid occasionally passed through the probe volume since the p.d.f. is skewed toward the lower velocities. The p.d.f. at $r/R_o = 0.52$ where the velocity reaches a maximum is sharply peaked and nearly symmetric ($S_w = 0.06$). At $r/R_o = 0.68$, the p.d.f. is skewed toward lower velocities which is consistent with the fact that the fluid is decelerated in this region.

Concentration

The concentration p.d.f.s are presented in Fig. 37 for the axial location $z = 25$ mm. Each of the profiles show unique and rapidly changing features which were characteristic of specific flow regions. The concentration p.d.f.s at $r/R_o = 0.0$ and 0.52 were obtained from measurements at the inner and outer edges, respectively, of the mean concentration profiles (see Fig. 20). At $r/R_o = 0.0$, the most probable fluid concentration was near 1.0 with the tail of the p.d.f. skewed toward the lower concentrations. The values of the skewness, S_f, and kurtosis, K_f, were -2.91 and 12.4, respectively. At $r/R_o = 0.52$, the most probable fluid concentration was near 0.0 with the p.d.f. skewed toward values up to 0.2. The skewness and kurtosis of the p.d.f. at this location were 3.92 and 27.0 respectively. Note the precipitous slope of the concentration p.d.f. at zero concentration which is the shape expected for an ideal seed and measurement system. The p.d.f.'s at the intermediate radial locations indicate the rapid mixing which is occurring in this region. At r/R_o = 0.13, the concentration fluctuations were increasing (see Fig. 21) and the mean concentration had decreased slightly (see Fig. 20). The p.d.f. at this location is consistent with this trend in that it is skewed to values of lower concentration indicating low concentration fluid was being mixed into the high concentration inner stream. At r/R_o = 0.24, the concentration fluctuations were at the maximum for this axial location and the p.d.f. reflects this result. The p.d.f. is double peaked which indicates that large eddies of high and low concentration existed at this location. The mean concentration value was approximately 0.5 which occurs between the two peaks. At r/R_o = 0.36, the concentration fluctuations have decreased and the mean concentration has decreased further. The p.d.f. at this location has become more symmetric but was still skewed to higher concentrations which indicates that the mean activity had decreased but high concentration fluid was occasionally being carried into the low concentration region. The p.d.f. at r/R_o = 0.68 is essentially symmetric and sharply peaked at a value of approximately 0.05 indicating very little concentration fluctuation. The p.d.f.s at higher values of r/R_o are not shown but were also sharply peaked with the peak near a value of 0.05, the mass flow averaged concentration level within the annular recirculation cell.

Skewness and Kurtosis Distributions

The skewness and kurtosis distributions for the axial, radial and azimuthal velocity p.d.f.s and the mean concentration p.d.f. are presented in Figs. 38 through 45. The skewness, S, is a dimensionless measure of the asymmetry of a p.d.f. If the p.d.f. is symmetric about the origin then the skewness would be zero. A p.d.f. with positive skewness indicates that there are more values of the function in the tail toward the positive side while the negative skewness indicates that there are more values of the function in the tail toward the negative side. The kurtosis, K, is a dimensionless measure of the flatness of the p.d.f. The value of kurtosis is large if the values of the function in the tails of the p.d.f. are relatively large. The kurtosis of a Gaussian p.d.f. profile would be equal to 3.0 while the kurtosis for a square p.d.f. profile would be 1.8.

As will be noted in the discussion which follows, the skewness of the velocity p.d.f.s generally fell within a band of values equal to ± 2. The kurtosis factors were generally greater than 3.0. On the other hand, skewness factors for the concentration p.d.f.s were as high as ± 10 with kurtosis factors approaching 100 in some flow regions. It has been shown (Ref. 15) that utilization of Schwarz's inequality, i.e., $(x^3)^2 < x^4\ x^2$ with the definitions for skewness and kurtosis (see Appendix III) leads to the relation

$$K \geq S^2 \tag{3}$$

Hence, when the skewness is large in magnitude (of either sign), the kurtosis will be large and positive. As will be seen in the discussion which follows, the kurtosis satisfies this inequality.

Axial Velocity

The skewness profiles, S_u, for the axial velocity p.d.f.s are presented in Fig. 38. For axial locations $z \leq 102$ mm, the fluid was accelerated or decelerated in various flow regions, and the skewness of the p.d.f.s were positive or negative, respectively. At axial locations farther downstream where the velocity profiles became uniform, the skewness tended to scatter about zero. Whenever, the skewness deviated from zero, the kurtosis tended to be greater than 3.0, the value for a Gaussian distribution (Fig. 39).

Analysis of the velocity, skewness and kurtosis profiles indicate that the deviation of the skewness and kurtosis from the values for a Gaussian p.d.f. appeared to be correlated to the local curvature of the axial velocity profile. It appeared that $S_u > 0$ whenever $\partial^2U/\partial r^2 > 0$ and $S_u < 0$ whenever $\partial^2U/\partial r^2 < 0$. These results have been explained (Ref. 15) by noting that at a radial location where the mean velocity profile has a local maximum, slower moving fluid will occasionally move by from either side but faster moving fluid would not move by. Similarly, at a radial location where the velocity profile has a local minimum, faster moving fluid will occasionally move by but not slower moving fluid. When the absolute value of the curvature of the velocity profile is high, $K_u > 3.0$. When the curvature passes through zero, the kurtosis decreases and the p.d.f. becomes more Gaussian. The magnitude of the deviations from the values for a Gaussian p.d.f. also appeared to be proportional to the magnitude of $\partial^2U/\partial r^2$.

Radial Velocity

The skewness and kurtosis distributions for the radial velocity p.d.f.s are presented in Figs. 40 and 41. The largest variation in skewness occurred at the axial location closest to the entrance of the test section, z = 5 mm. For increasing axial location, the skewness profiles became flatter and the values tended to scatter about zero. The kurtosis profiles shown, in Fig. 41, were generally higher than the Gaussian value of 3.0. The greatest scatter in the data occurred at z = 102 mm in the upstream end of the centerline recirculation region, $r/R_o < 0.5$.

Azimuthal Velocity

Although the skewness distributions for the azimuthal velocity p.d.f.s shown in Fig. 42 indicated that there was considerable scatter of the data, the average values of the skewness factor, S_w, are generally compatible with the local fluid acceleration or deceleration. The kurtosis profile shown in Fig. 43 also exhibited scatter in the data but except for some isolated radial locations near the entrance of the test section, $z = 5$ mm, and well downstream of the entrance $z > 305$ mm, the kurtosis values generally averaged between 3.0 and 4.0.

Mean Concentration

The skewness and flatness factor profiles obtained for the mean concentration p.d.f.s are presented in Fig. 44 and 45 and behave as expected in most of the flow regions. In the high concentration region ($z = 13$ mm and $0.1 < r/R_o < 0.25$), the skewness, S_f, was negative indicating that eddies of low concentration fluid are occasionally passing through the probe volume. For those regions where the concentration gradients were large ($z = 13$ and 25 mm; $0.2 < r/R_o < 0.4$), the skewness rapidly changed from large negative values to large positive values. Even in the mixed regions, ($r/R_o > 4$; $f = 0.1$), the skewness was greater than zero because some filaments of fluid with relatively high concentration occasionally passed through the probe volume. Farther downstream in the test section, $z > 152$ mm, the skewness leveled out to essentially zero.

The kurtosis profiles presented in Fig. 45 exhibit similar trends. Very large values of kurtosis, $K_f > 100$, occurred in those regions where the concentration gradients are steepest. As the fluid mixing was completed, the kurtosis profile flattened out to an average value of about 4.0.

DISCUSSION OF THE SECOND CENTRAL MOMENT, SKEWNESS AND KURTOSIS RESULTS FOR MOMENTUM AND MASS TURBULENT TRANSPORT PROBABILITY DENSITY FUNCTIONS

Typical Turbulent Transport Rate Probability Density Functions

The probability density functions for the momentum and mass turbulent transport rate data are presented for the axial location, z = 25 mm, which is the same location for which the velocity and concentration p.d.f.s were presented. This location was chosen as typical of the flow region where the mass and momentum turbulent transfer rates are the highest.

Momentum Transport

Typical probability density functions for the momentum transport rates in the r-z, z-θ and r-θ measurement planes are presented in Figs. 46, 47, and 48 respectively. The p.d.f.s are similar in that they all had peaked distributions about the zero momentum turbulent transport rate which is typical of the shape of momentum rate p.d.f.s for turbulent boundary layers (Ref. 16). The p.d.f.s for the r-θ plane were more sharply peaked than those for the r-z and z-θ planes. All three sets of profiles showed essentially the same variation in shape with radial location. The greatest changes in shape occurred at those radial locations where the momentum turbulent transport rates were the highest; i.e., r/R_o = 0.24, 0.36 and 0.68.

Mass Transport

The probability density functions of the radial mass turbulent transport rates which are presented in Fig. 49 indicate that all of the profiles are sharply peaked near zero. However, the p.d.f.s at $0.13 < r/R_o < 0.52$ are broader indicating increased radial mass transport activity in this region. This trend is consistent with the mass transport rate results presented in Fig. 28 which show that the radial mass transport rates are the highest in this region.

Probability density functions of the axial mass turbulent transport are presented in Fig. 50. The p.d.f.s are similar to the radial mass transport p.d.f.s in that they all peaked around zero. In the regions where the axial mass transport rates were highest, $0.13 < r/R_o < 0.52$, the profiles were flatter and the peak values the lowest.

The probability density functions for the azimuthal turbulent mass transport rates are presented in Fig. 51. They are similar to the radial and axial mass transport p d.f.s in that they are also sharply peaked about zero and are flattest where the transport rate is highest.

Typical Momentum Turbulent Transport Results

Radial-Axial Plane (r-z)

The second central moment profiles (or rms fluctuation from the mean) of the momentum turbulent transport in the r-z plane, σ_{uv}, are presented in Fig. 52. This quantity previously was used to analyze and evaluate the turbulent transport process in boundary layers, e.g., Ref. 17. A comparison of the values of σ_{uv} with the corresponding values of the momentum transport rate ($\overline{uv}$) from Fig. 22 show that σ_{uv} was generally at least a factor of two greater than $\overline{uv}$. Ratios of $_{uv}/\overline{uv}$ equal to approximately 3 were previously reported for boundary layers (Ref. 16). The trends shown in Fig. 52 were generally the same as shown in Fig. 22. The σ_{uv} were generally highest were the momentum transport rates, $\overline{uv}$, were highest.

Skewness and kurtosis profiles (S_{uv} and K_{uv}) for the momentum turbu-turbulent transport p.d.f.s obtained in the r-z plane are presented in Fig. 53 and Fig. 54 respectively. The skewness profiles showed the same trends as the momentum turbulent transport rate. The skewness was positive when the momentum transport rate profiles was positive and became negative when the momentum transport rate became negative. For those axial locations where the momentum transport rate became zero, the skewness values tended to scatter about zero.

The kurtosis profiles presented in Fig. 54 showed the trend expected from the skewness profiles. Whenever the skewness was large in magnitude of either sign, the kurtosis was large and positive. However, the low kurtosis values obtained at $z = 5$ mm, $r/R_o = 0.45$ indicate deviations from the processes assumed in the simple transport models such as the joint-Gaussian p.d.f. model.

Axial Azimuthal Plane (z-θ)

The second central moment profiles of the momentum turbulent transport in the z-θ plane, σ_{uw}, are presented in Fig. 55. The σ_{uw} profile generally peaked where the momentum transport rates ($\overline{uw}$) peaked but were 2 to 5 times greater in value. As the momentum transport rate dampened to zero, the values of σ_{uw} also approached zero. The skewness profiles of the p.d.f.s in the z-θ plane which are presented in Figs. 56 generally followed the same trends that were observed for the $\overline{uw}$ profiles. The skewness was generally positive when the turbulent transport rate was negative. However, many of the fluctuations which occurred in the momentum rate were not observed in the skewness profiles. The kurtosis profiles, K_{uw}, presented in Fig. 57 exhibit a large amount of scatter. However, the kurtosis tended to be large whenever the skewness was large in magnitude.

Radial-Azimuthal Plane (r-θ)

The second central moment, skewness and kurtosis profiles for the p.d.f.s obtained in the r-θ plane are shown in Figs. 58, 59 and 60 respectively. The second central moment σ_{wv} was at least twice the momentum transport rate $\overline{wv}$ and generally peaked where the momentum turbulent transport rate peaked. The skewness profiles shown in Fig. 59, did not exhibit the same variations as the momentum rate profiles and the absolute values of skewness were generally less than 4. The kurtosis profiles shown in Fig. 60, followed the same trend as the kurtosis profiles obtained for the p.d.f.s in the r-z and z-θ planes; namely, the kurtosis was large whenever the skewness was large in magnitude of either sign.

Summary Comments

In general, the second central moments of the momentum turbulent transport rate profiles were well behaved. The radial variation and the axial variations are easy to discern. The variations of skewness and kurtosis for the momentum turbulent transport in the r-z plane, i.e, $\overline{uv}$, can also be discerned. However, radial and axial variations for the skewness and kurtosis of the momentum transport in the r-θ and z-θ planes have more scatter especially in the central recirculation region. The result that the ratio of $\sigma_{uw}/\overline{uw}$ and $\sigma_{wv}/\overline{wv}$ were larger than the ratio $\sigma_{uv}/\overline{uv}$ in the high shear regions was probably due to tendency for energy to be transferred from the high intensity u fluctuation to the v and w components.

Typical Mass Turbulent Transport Results

The second central moment, skewness, and kurtosis of the mass turbulent transport p.d.f.s are presented in Figs. 61 through 69. Since the trends observed for each mass transport property was essentially the same for each measurement direction, the discussion of the results for each direction will be presented together.

The second central moment of the turbulent mass transport p.d.f.s are presented in Fig. 61 for the radial direction, in Fig. 64 for the axial direction and in Fig. 67 for the azimuthal direction. The trends shown for all three directions are essentially the same and correspond almost exactly to those observed for the fluctuating concentration profiles (Fig. 21) and generally follow the trends observed in the mass turbulent transport rate profiles. At axial locations z = 13 mm and z = 25 mm, the peak second central moments occurred in the interface region between the inner and annular jets. Increased activity occurred along the centerline, r/R = 0.0, for z = 25 mm and this activity continued to increase for z = 51 mm. The second central moments rapidly decreased for z > 51 mm and became essentially flat for z ≥ 152 mm. The peak values of the second central moments for the radial mass turbulent transfer rates were slightly higher than the peak values for the azimuthal mass transfer rates. The peak second central moment for the axial mass transport is approximately 1.5 times the peak observed for the radial and azimuthal mass transfer. Also, the peak values of the second central moments for all measurement directions were generally higher than the peak mass transport rate for any direction at that measurement location.

The skewness of the mass turbulent transport rate p.d.f.s are shown in Figs. 62, 65 and 68 for the radial, axial and azimuthal directions, respectively. The skewness values deviate from zero where mass transport occurs but no trend consistent with the mass transport profiles is apparent.

The kurtosis profiles of the mass transport p.d.f.s are presented in Fig. 63 for the radial direction, in Fig. 66 for the axial direction and in Fig. 69 for the azimuthal direction. These kurtosis profiles also followed the trends of the kurtosis profiles discussed previously. Whenever the skewness became large in magnitude (of either sign), the kurtosis also became large.

SUMMARY OF RESULTS

Qualitative and quantitative studies were conducted of the flow downstream of swirling coaxial jets discharging into an expanded duct. The ratio of annular jet diameter and duct diameter to the inner jet diameter were approximately 2 and 4, respectively. The inner jet peak axial velocity was approximately one-half the annular jet peak axial velocity and the mean swirl angle in the annular stream was approximately 30 degrees. Results from the studies were related to the five shear regions within the duct: (1) the wake region downstream of the inlet, (2) the shear layer between the jets, (3) the annular recirculation region, (4) the reattachment region, and (5) the centerline recirculation region.

A flow visualization study was conducted using fluorescence dye as a trace material and high-speed motion pictures to record the dye patterns in selected r-z and r- planes. The results of the flow visualization study are summarized with the following observations:

1. The flow was as axisymmetric as could be determined visually.
2. The larger scales of the turbulent structure were observed to grow within the centerline recirculation region. This growth occurred from the width of the wake region downstream of the inner jet tube to a large fraction of the duct diameter.
3. Downstream of the centerline recirculation region, the flow initially had large lobes which evolved into a vortex swirl pattern. There was little radial mixing downstream of the recirculation cell.
4. The high intensity turbulent eddies in the shear layers were not axisymmetric or periodic. The large scale waves and eddies appeared to have a range of wavelengths.
5. Two major mixing regions were observed: (1) at the interface between the inner jet and the centerline recirculation zone, and (2) at the interface between the inner jet and annular jet streams.
6. Mixing at the interface of the inner stream and the recirculation cell diluted the inner jet concentration and the resulting mixture of fluid from the recirculation cell and the inner jet was entrained by the swirling annular stream.

A detailed map of the velocity, concentration, mass turbulent transport rate and momentum turbulent transport rate distributions within the test section was obtained to provide data for the evaluation and improvement of turbulent transport models. Data sets of velocity component pairs were obtained simultaneously to determine the momentum turbulent transport rate and mean velocities. Data sets of velocity and concentration pairs were obtained simultaneously to determine mass turbulent transport rate, concentration and velocity. Probability density functions (p.d.f.s) of all the forementioned parameters were obtained from the data sets. Mean quantities, second central moments, correlation coefficients, skewness and kurtosis were calcualted to characterize each data set. Following are the principal results from this study.

7. The axial, radial and azimuthal velocity profiles described the changes in the shear regions within the duct.

8. The mean and fluctuating concentration profiles described the inner jet fluid distribution within the duct.

9. Mixing for swirling flow was completed in one-third the length required for nonswirling flow.

10. The momentum turbulent transport rate measurements in the r-z, z-θ and r-θ planes described the local momentum fluxes due to turbulent mixing. Correlation coefficients were obtained for each measurement location and data set.

11. The principal momentum turbulent transport was in the r-z plane; i.e., uv, and was attributed to the axial velocity gradients. Peak momentum turbulent transport rates were approximately the same as for the nonswirling flow condition.

12. The axial mass turbulent transport is gradient rather than counter-gradient as occurred for nonswirling flow. The peak axial mass transport rates were greater than the peak radial mass transport rates even though the axial concentration gradients were approximately one-seventh the radial gradients.

13. The mass turbulent transport process for swirling coaxial flow is very complicated. Mixing appears to occur in several steps of axial and radial mass transport coupled with a large radial mean convective flux.

14. The transport process appears to begin with high concentration fluid from the centerline recirculation zone. The diluted inner jet fluid is then convected by the negative axial velocities into the large eddy shear region between the inner and annular streams.

15. Axial mass turbulent transport correlation coefficients as high as 0.5 were measured. These correlation coefficients were less than the

peak mass transport correlation coefficients obtained for nonswirling flow although the axial mass transport rate for swirling flow was greater than that for nonswirling flow.

16. The skewness of the axial velocity, p.d.f.s was related to the curvature of the axial velocity profiles. $S < 0$ was obtained for $\partial^2 U/\partial r^2 < 0$ while $S > 0$ was obtained for $\partial^2 U/\partial r^2 > 0$. The skewness was also proportional to the magnitude of $\partial^2 U/\partial r^2$.

REFERENCES

1. Gerstein, M. (Ed): Fundamentals of Gas Turbine Combustion, NASA Conference Publication 2087, 1979.

2. Hudson, D. A.: Combustion Modeling Needs for the '80s. AIAA Preprint 80-1288.

3. Mellor, A. M.: Turbulent-Combustion Interaction Models for Practical High Intensity Combustors: Seventeenth Symposium on COmbustion, p. 377, Combustion Institute, 1979.

4. Dryburgh, D. and R. B. Edelman: Technical Evalution Report on the Propulsion and Energetics Panel 54th Meeting on Combustion Modeling. AGARD Advisory Report No. 153, March 1980.

5. Mularz, E. J.: New Trends in Combustion Research for Gas Turbine Engines. NASA Technical Memorandum 83338. AVRADCOM Technical Report 83-C-1, June 1983.

6. Sturgess, G. J.: Aerothermal Modeling. Phase I. NASA Contractor Report CR-168202. May 1983.

7. Johnson, B. V. and J. C. Bennett: Mass and Momentum Turbulent Transport Experiments with Confined Coaxial Jets. NASA Contractor Report CR-165574. Also issued as UTRC Report R81-915540-9, November 1981.

8. Application of Non Intrusive Instrumentation in Fluid Flow Research. AGARD Conference Proceedings No. 193. May 1976.

9. Johnson, B. V. and J. C. Bennett: Velocity and Concentration Characteristics and Their Cross Correlations for Coaxial Jets in a Confined Sudden Expansion Part I: Experiments. Proceedings of ASME Fluids Engineering Conference on Fluid Mechanics of Combustion Systems, Boulder, CO, June 1981, p. 145.

10. Habib, M. A. and J. H. Whitelaw: Velocity Characteristics of Confined Coaxial Jets With and Without Swirl. ASME Journal of Fluids Engineering, Vol. 102, pp. 47-53 (1980).

11. Schetz, J. A.: Injection and Mixing in Turbulent Flow, Vol. 68, Progress in Astronautics and Aeronautics, AIAA, 1980.

12. DISA 55X Modulat LDA Optics-Instruction Manual. DISA Information Department; DISA Electronics.

13. -----: Data for Dye Lasers. Kodak Publication No. JJ-169, March 1972.

14. Hinze, J. O.: Turbulence, McGraw-Hill, NY, 1959, Chapter 7.

15. Lumley, J. L.: Cornell University. Private Communication, July 20, 1983.

16. Lu, S. S. and W. W. Willmarth: Measurements of the Structure of the Reynolds Stress in a Turbulent Boundary Layer, J. Fluid Mechanics, Vol. 60, Part 3, pp. 481-511 (1973).

17. Willmarth, W. W.: Structure of Turbulence in Boundary Layers, Advances in Applied Mechanics, Vol. 15, Academic Press, NY, 1975.

18. Tennekes, H. and J. L. Lumley: A First Course in Turbulence, Chapter 6, MIT Press, 1972.

APPENDIX I

FLOW VISUALIZATION FOR ALL FLOW CONDITIONS

Flow visualization studies were conducted prior to the selection of the flow condition for detailed data acquistion to determine the effects of the velocity ratio, U_i/U_a, on the flow characteristics within the test section.

Motion pictures were obtained in the r-z plane with the center of illumination at z = 100 mm and in the r-θ plane at selected axial locations. Motion pictures with a frame speed of 500 per second were obtained for each of the following five flow conditions:

Flow Condition	Mean Axial Velocity, m/s Inner Jet, $\overline{U}_i$	 Annular Jet, $\overline{U}_a$	Flow Rate, gpm Inner Jet	 Annular Jet
1	0.52	1.66	6.2	52.8
2	0.27	1.66	3.2	52.8
3	2.08	1.66	24.6	52.8
4	0.94	1.51	11.1	48.0
5	0.94	2.87	11.1	94.8

In the following paragraphs, the flow visualization photographs for Flow Conditions 2 through 5 presented in Figs. 70 through 73 will be discussed. The discussion of Flow Condition 1 (Fig. 10) will be repeated for reference. Each figure contains two photographs taken in the r-z plane. The photograph at the top left side shows the flow characteristics when dye is injected into the inner stream. The photograph at the top right side is a visualization of the flow field when dye is injected into the annular stream. The four photographs presented at the bottom of each figure show the flow characteristics in the r-θ plane at selected axial locations when dye is injected into the inner stream.

Flow Condition 1

Photographs taken for Flow Condition 1 in both the r-z plane and at selected axial locations in the r-θ plane are presented in Fig. 10. The photographs taken when dye is injected into the inner stream (top left) shows that a high inner jet stream concentration persists for an axial distance of approximately 70 mm. In the photograph taken when dye is injected into the annular stream (top right), dye has been entrained near the centerline between an axial distance of approximately 60 mm to 170 mm indicating the presence of a recirculation cell near the centerline. The existence of this recirculation cell becomes more apparent in the high-speed films and appears to extend to almost 150 mm. Both photographs show large scale eddy structure in the shear layer between the jets starting at an axial distance of approximately 30 mm and extending downstream to at least 175 mm. The scale of these eddies at $z = 50$ mm is more than half the inner jet diameter of 30 mm. Although the eddy sizes are large, the eddy structure did not appear to be periodic or symmetric. When dye is injected into the annular stream, the annular recirculation zone adjacent to the test section inlet plane and the attachment region downstream of this annular recirculation zone are clearly defined. The length of this annular recirculation cell is approximately 50 mm which is about one-third the length observed with nonswirling flow for the same flow condition.

The photographs taken in the $r-\theta$ plane at $z = 25$ mm shows the radial scale (= 6 mm) of the eddy structure at the upstream end of the shear region. At $z = 51$ mm, the scale of the large eddy structure has increased significantly but does not appear to change appreciably from $z = 100$ mm to $z = 200$ mm. As shown by the photographs in both the $r-z$ and $r-\theta$ planes, the large eddy structure is not axisymmetric or azimuthally periodic for $z > 50$ mm.

Flow Condition 2

The inner jet velocity, U_i, for Flow Condition 2 was approximately one-half that of Flow Condition 1. The photographs, (Fig. 70) indicate that the overall flow characteristics are similar to those observed for Flow Condition 1. However, as a result of the reduction in inner jet velocity, the distance over which the high inner jet fluid concentration extends from the test section inlet has been decreased from approximately 70 mm to 35 mm.

Flow Condition 3

The mean inner jet axial velocity for this flow condition was approximately four times that for Flow Condition 1. As a result, the inner jet stream was flowing faster than the annular stream. The ratio of the peak inner jet to the peak annular velocity was estimated to be approximately two. As shown in Fig. 71, the flow field for this flow condition differs from Flow Condition 1 in that the flow becomes asymmetric and the inner jet precesses around the centerline for $z > 70$ mm. The flow appears to be influenced by two forces: (1) the tendency of the inner jet to flow downstream without recirculating and (2) the strong tendency of the swirling annular flow stream to form a centerline recirculation cell. The result appears to be a combination of the two effects in that the inner stream is deflected by the swirling flow in the centerline recirculation cell.

Flow Condition 4

This flow condition has approximately the same total flow as Flow Condition 1, however, the ratio of the inner stream mean velocity to annular stream mean velocity has been increased from 0.32 to 0.64. Based on measurements in Ref. 8, the peak axial velocities in the inner and annular stream are expected to be approximately equal. The photographs (Fig. 72) indicate that the flow field appears to be axisymmetric and stationary. Inner jet velocities 20 to 30 percent greater than that for Flow Condition 4 are required to obtain the precessing center jet characteristics of Flow Condition 3. Compared to Flow Condition 1, the length of the annular recirculation cell is 30 to 50 percent greater and the distance from the inlet plane to the inner recirculation cell is increased by 50 percent. The large scale eddy characteristics also appears approximately the same for Flow Conditions 1 and 4.

Flow Condition 5

The velocity ratios for Flow Conditions 5 and 1 are equal; however, the absolute velocity for Flow Condition 5 is increased by a factor of 1.8 compared to Flow Condition 1. The photographs presented in Fig. 73 indicate that the flow characteristics for Flow Condition 5 were essentially the same as those observed with Flow Condition 1.

The flow visualization study showed (1) an additional flow region; namely, a centerline recirculation region, which occurs when swirl is introduced into the annular stream of confined coaxial jets and (2) the inner jet will precess when the ratio of inner jet velocity to annular stream velocity exceeds a critical value. These characteristics of confined swirling jets have been previously recognized in the literature.

APPENDIX II

SWIRLER EXIT MEASUREMENTS

Laser velocimeter measurement techniques were used to determine the mean and fluctuating velocity distributions approximately 5 mm downstream of the swirler exit face when the trailing edge of the swirler was repositioned at the test section inlet. Data was obtained at various azimuthal and radial locations to define the velocity distribution at the swirler exit. This survey was made because the flow field downstream of the swirl vanes will contain wakes caused by the blade skin friction. Also, the flow field will be influenced by secondary flows which result from the interaction of boundary layers on the vane end walls with the pressure gradient in the vane passage.

Prior to the detailed data acquisition, axial and azimuthal velocity data was obtained at the swirler location $r/R_o = 0.40$ by rotating the swirler and the center duct in 15 deg increments while maintaining the laser velocimeter probe volume at the same location. The azimuthal velocity profiles were to be used to determine the swirler asymmetries and to select an azimuthal location for a more detailed velocity survey. Since the swirler has eight blades, three measurements were obtained downstream of each blade passage. Although the velocity distributions obtained showed some blade-to-blade variation, the variations were only a fraction of the variation across each blade. The blade passage chosen for the detailed measurements was one with a local velocity distribution representative of the entire swirler and was the center passage of three passages which had nearly identical velocity distributions. This blade passage was also the passage in which the detailed measurements presented in the main body of this report were taken.

The flow field 5 mm downstream of the selected vane passage was characterized by making a velocity survey of the axial, radial and azimuthal velocities along radii starting at $r/R_o = 0.225$ (the location of the thin metal tube separating the inner and annular jet streams) and ending at a radial location $r/R_o = 0.6$ which is approximately 7 mm outside the annular passage. Data was obtained at ten azimuthal locations, five (5) deg apart by rotating the center tube and swirler as shown in Fig. 74. The striped blade shown in Fig. 74 is a reference blade chosen for swirler orientation purposes. The detailed measurements reported in the main body of the report were taken with the leading edge of the reference blade set at $\phi = 75$ deg. The LV measurements were made for the axial/azimuthal velocities by traversing horizontally first, along the radius indicated by swirler orientation $\phi = 50$ deg (leading edge of reference blade set at $\phi = 50$ deg). Horizontal traverses were then made along the other radii indicated in Fig. 74 by rotating the reference blade through 5 deg increments. In this way, the flow field downstream of a single swirler vane and vane passage could be characterized. LV measurements were made to determine the axial/radial velocities by first rotating the center tube and swirler 90 degr and then traversing vertically along each radii. The velocity surveys were made first with the trailing edge of the swirler vane positioned at the inlet plane of the test section (Runs 59 through 78); and then repeated with the trailing edge of the swirler vane positioned 51 mm upstream of the inlet plane of the test section (Runs 79 through 98).

As shown in Fig. 74, the velocity measurements made at swirler orientations ϕ = 50, 55, 60 and 95 deg were made in the passage between blades and it would be expected that the axial velocity profile would show no effects of blade wakes. Also, since swirler orientations ϕ = 50 and 95 deg are at the same relative location for two vanes, it would be expected that the velocity distributions for these two locations would be nearly identical. The axial velocity profiles presented in Fig. 75 substantiate these expectations.

As shown in Fig. 75, the velocity distributions at swirler orientation ϕ = 50 and 95 deg are nearly identical and are easily identifiable, when compared to the intermediate orientations, as being periodic profiles. The profiles obtained at ϕ = 55 and 60 deg are similar and show little effect of blade wakes. However, the effect of blade wake on the axial velocity is seen in the profiles obtained for swirler orientations ϕ = 65 through 90 deg. The vane wake produced a dip in the axial velocity profile which occurred at a different radial location for each swirler orientation. Note that the largest dip occurred for a swirler orientation of 80 deg which corresponds to measurements made essentially along the central part of the blade (see Fig. 74).

The mean radial velocity profiles are shown in Fig. 76. The radial velocity downstream of the inner jet increased from a value of zero at the centerline, as expected for axisymmetric flow. Small differences in the profiles occurred for $0.22 < r/R_o < 0.25$ and can be attributed to interaction of the inner jet flow with the flow from the swirler. The distribution of the radial flow inward and outward for $0.25 < r/R_o < 0.5$ is attributed to (1) the formation of corner vortices due to the inviscid conservation of vorticity as the flow through the swirler is turned by the vanes and (2) the radially inward acceleration of low energy flow in the blade wakes. For swirler orientations ϕ = 50, 55, 90 and 95 deg, where the axial velocity profiles were essentially smooth and free of the effects of the blade wakes, the radial velocity profiles are probably being affected by secondary vortices.

The azimuthal velocity profiles presented in Fig. 77 show larger relative velocity changes, due to the blade wakes and secondary flows in the vane passages, than the axial and radial velocity profiles. The variations in the azimuthal velocity profiles due to the blade wakes occurred at the same combinations of swirler orientation and radius as for the axial velocity profile, i.e., $\phi = 60$ deg and $r/R_o = 0.3$ to $\phi = 85$ deg and $r/R_o = 0.45$. Note the azimuthal velocity was slightly greater for $0.5 < r/R_o < 0.6$ than for $r/R_o = 0.48$. In this region, $0.5 < r/R_o < 0.6$, the axial velocities were near zero and the flow was coming from the recirculation cell. This comparison shows that the angular momentum imparted to the flow for $0.45 < r/R_o < 0.50$ was less than that in the outer recirculation cell and hence less than the average angular momentum imparted over the entire blade. This may be due to the leakage around the outer tip of the swirler blades. The blades are soldered to a hub which is fastened to the inner annular wall but they are unattached to the outer annular wall and have approximately 0.1 mm clearance. Some variations in the azimuthal velocity profile, e.g., at $\phi = 75$ deg and $r/R_o = 0.4$, may be caused by the secondary flows developed in the vane passages due to the axial velocity profile at the vane entrance. Another interesting feature of the azimuthal velocity profile is the negative velocity at $\phi = 80$ deg and $r/R_o = 0.47$. The azimuthal velocity profiles also show variations at radial locations where the axial velocity profiles were smooth. With an almost uniform axial velocity profile in the center of the vane passage, the radial and azimuthal velocity profiles should be coupled by any secondary vortex flow.

The axial, radial and azimuthal velocity profiles obtained with the trailing edge of the swirler vane was positioned 51 mm upstream of the test section inlet plane are presented in Figs. 78, 79 and 80, respectively. The axial velocity results presented in Fig. 78 show that the profiles were more nearly uniform but the effects of the blade wakes were still present although the dips in the velocity profiles associated with the wakes were not as pronounced. The radial and azimuthal velocity profiles shown in Figs. 79 and 80 also show the same trend. It appears that even though the swirler is set back 51 mm from the inlet plane of the test section, the velocity profiles a short distance downstream from the inlet to the test section were not axisymmetric because the effects of blade wakes and/or secondary flows still persisted. These asymmetries in the flow were apparent in the velocity profiles obtained at an axial location of 5 mm which were presented in Figs. 13, 14 and 15.

The fluctuating axial, radial and azimuthal velocity profiles obtained when the trailing edge of the swirler was positioned at the inlet plane are shown in Figs. 81, 82 and 83, respectively. Note that the turbulence intensity in the core region was approximately 3 to 4 percent of the axial velocity which is the magnitude expected in the central region of developed tube flow. The fluctuations were highest at the interface between the inner and annular jet ($r/R_o = 0.25$) and between the annular jet and the recirculation zone near the outside wall ($r/R_o = 0.5$). There were also relatively high fluctuations in the blade wake regions.

The fluctuating axial, radial and azimuthal velocity profiles obtained when the trailing edge of the swirler was positioned 51 mm upstream of the inlet plane of the test section are presented in Figs. 84, 85 and 86 respectively. The fluctuations at the interfaces were still present but they have been substantially reduced especially at the interface between the inner jet and the annular jet. The greatest reductions occurred in the fluctuating radial velocity profiles. Substantial reductions in the fluctuation due to the blade wakes also occurred but the fluctuations did not completely disappear.

The momentum turbulent transport rate distributions in the r-z plane, uv, which were obtained for the swirler exit plane at the test section inlet plane are presented in Fig. 87. This transport is related to the strain rate: $\partial U/\partial r + \partial V/\partial z$. For those profiles without blade wakes near the ID of the swirler ($r/R_o = 0.25$) or near the OD of the swirler ($r/R_o = 0.50$), the transport is similar to that shown in Fig. 22. For the swirler orientations where the blade wakes are present, the momentum turbulent transport rates were of the same magnitude as those in the ID or OD region. Note that the turbulent transport rates in the core regions were negligible. The momentum turbulent transport rate distribution, $\overline{uv}$, obtained when the swirler was moved 51 mm upstream of the entrance to the test section are shown in Fig. 88. The profiles have become more uniform and the momentum transport has been substantially reduced in the blade wake regions.

The momentum turbulent transport rates in the z-θ plane, $\overline{uv}$, are shown in Fig. 89. This transport is related to the strain rate: $(1/r)\partial U/\partial \theta + \partial W/\partial z$. The momentum transport was highest at the interface between the inner and annular jets and significant transport also occurred in the blade wake regions. This momentum transport rate was substantially reduced (by a factor or 2 to 3) when the swirler was moved 51 mm upstream of the test section entrance as shown by the distributions presented in Fig. 90. The profiles in Fig. 90 are very similar to the profiles presented in Fig. 24 at the axial location $z = 5$ mm.

The profiles presented in Figs. 75 through 90 show that significant three-dimensional variations can occur in the flow field immediately downstream of a typical combustor like swirler. They also provide insight into initial conditions required for the three-dimensional swirling flows downstream of a swirler inlet. The data was obtained in a simultaneous two velocity component data acquisition mode in the same manner as the turbulent momentum data which was presented in the main body of this report. Therefore, the first four moments of the three velocity components as well as of the local momentum transport in the r-z and z-θ planes were obtained. This data is presented in tabular form in Tables IV-59 through Tables IV-78.

APPENDIX III

DEFINITIONS OF SKEWNESS AND KURTOSIS FOR VELOCITY, CONCENTRATION, AND TRANSPORT PROBABILITY DENSITY FUNCTIONS

Terms in this appendix for the velocity components and concentrations are defined using the notation of Ref. 18 and conventional statistical methods.

$\tilde{u}$	Local instantaneous axial velocity component
$B(\tilde{u})$	Probability density function (p.d.f.) of $\tilde{u}$ with properties $B(\tilde{u}) \geq 0$ and $\int_{-\infty}^{\infty} B(u)\, du = 1.0$
U	Mean value of axial velocity component defined: $U = \int_{-\infty}^{+\infty} \tilde{u}\, B(\tilde{u})\, d\tilde{u}$
u	Local instantaneous axial velocity fluctuation from the mean, defined: $u = \tilde{u} - U$
σ_u or u'	Second central moment of velocity u defined: $\sigma_u^2 = u'^2 = \int_{-\infty}^{-\infty} u^2\, B(\tilde{u})\, d\tilde{u}$ Will also be denoted as rms fluctuation.
$\overline{u^n}$	nth central moment of velocity u defined: $\overline{u^n} = \int_{\infty}^{\infty} u^n\, B(\tilde{u})\, d\tilde{u}$
S_u	Skewness of velocity component, u, p.d.f. defined: $S_u = \overline{u^3}/\sigma_u^3$
K_u	Kurtosis (or flatness factor) of velocity component, u, p.d.f. defined: $K_u = \overline{u^4}/\sigma_u^4$

In like manner, the mean, rms fluctuation, skewness, and kurtosis for the radial velocity, azimuthal velocity and concentration are defined.

The second moments, skewness and kurtosis for the momentum and mass transport rates are defined in a similar manner.

uv	Local instantaneous momentum turbulent transport rate: $(\tilde{u}-U)(\tilde{v}-V)$
$B(uv)$	Probability density function (p.d.f.) of uv with properties $B(uv) > 0$ and $\int_{-\infty}^{+\infty} B(uv)\, d(uv) = 1.0$
$\overline{uv}$	Mean value of turbulent momentum transport rate defined: $uv = \int_{-\infty}^{\infty} (\tilde{u}-U)(\tilde{v}-V)\, b(uv)\, d(uv)$
$(uv)'$	Local instantaneous fluctuation of momentum transport rate from mean, defined: $(uv)' = uv - \overline{uv}$

σ_{uv}	Second central moment of momentum transport rate: $\sigma_{uv} = \int_{-\infty}^{\infty} (uv)'^2 \, B(uv) \, d(uv)$.
$(uv)^n$	nth central moment of momentum transport rate: $(uv)^n = \int_{-\infty}^{\infty} (uv)'^n \, B(uv) \, d(uv)$
S_{uv}	Skewness of momentum transport rate: $S_{uv} = (\overline{uv})^3/\sigma_{uv}^3$
K_{uv}	Kurtosis of momentum transport rate: $K_{uv} = (\overline{uv})^4/\sigma_{uv}^4$.

In a like manner, the mean, second central moment, skewness and kurtosis for the momentum transport in the r-z plane and the mass transport in three directions are defined.

TABLE I

Components Used in LV and LV/LIF Measurement System

I. Laser Light Source

- Argon Ion Laser (Spectra Physics Model 164)
  - TEM_{∞} mode
  - All lines, 1.0 watt power
  - 0.4880 μm wavelength, 0.5 watts power

II. LV Optics

- DISA Type 55x00 Two Color LDV System
  - Polarization rotator
  - Beamsplitter - Module I
  - Bragg Cell, 1 mHz effective frequency offset
  - Beamsplitter - Module II
  - Backscatter Section - 0.4880 μm wavelength filter and photomultiplier tube
  - Backscatter Section - 0.5145 μm wavelength filter and photomultiplier tube
  - Pinhole Section
  - Beam Translator
  - Beam Expander
  - Achromatic lens, 310 mm focal length

III. Electronics

- LV Signal Processor (SCIMETRICS Model 800A)
  - 2 units
  - 0.4 to 2.0 mHz range
  - 3% data window
  - 4/8 and 5/8 comparison for "good signals"
- Oscilloscope (Tektronics Model 465B)
  - 2 units
- LV Data Handling Interface (UTRC design)
  - Clock
  - Coincidence check
- Minicomputer (DEC PDP 11/10)
  - Floppy disk
  - DECwriter III (1200 baud rate)

IV. LIF Electronics

- Low Pass Filter (Kronhite Model 3202)
  - 2KHz
- Voltage Amplifier (Preston 8300 XWB Amplifier - Model A)
  - 1-1000X Amplification
- A/D Converter (DEC LPS11)
  - Computer controlled
- Digital Voltmeter (Hewlett Packard Model 3465A)
- High Voltage Power Supply (Fluke Model 415B)
  - 0-2500 volts

TABLE II

Table of Run Numbers from Which Data was Utilized for Tables and Figures

Measured Parameters	Center-Line	Axial Location, z - mm (in.)								
		5.1(0.2)	12.7(0.5)	25.4(1.0)	50.8(2.0)	101.6(4.0)	152.4(6.0)	203.2(8.0)	304.8(22)	406.4(16)
U, W, uw	13,18	17		3	4	5,6	14	12,40	43	44
U, V, uv		11,16		7	8	9	15	10,41	42	45
U, C, uc	19,39		20,21	22	23	24	25	26		
W, C, wc			29	27	31	33	35	37		
V, C, vc			30	28	32	34	36	38		
V, W, vw				47,48 49	46,50 51,52 53	54,55 56				

TABLE III

Figures on Which Results are Displayed

Quantity	Direction or Plane	Symbol	Figure Number	Quantity	Direction or Plane	Symbol	Figure Number
Axial Velocity	z	U u' S_u K_u	12(C/L), 13 16 38 39	Axial-Azimuthal Momentum Transport	z-θ	$\overline{uw}$ R_{uw} σ_{uw} S_{uw} K_{uw}	24 25 55 56 57
Radial Velocity	r	V v S_v K_v	14 17 40 41	Radial-Azimuthal Momentum Transport	r-θ	$\overline{wv}$ R_{wv} σ_{wv} S_{wv} K_{wv}	26 27 58 59 60
Azimuthal Velocity	θ	W w S_w K_w	15 18 42 53	Axial Mass Transport	z	$\overline{uf}$ R_{uf} σ_{uf} S_{uf} K_{uf}	30 31 64 65 66
Concentration		$\overline{f}$ f' S_f K_f	19(C/L), 20 21 44 45	Radial Mass Transport	r	$\overline{vf}$ R_{vf} σ_{vf} S_{vf} K_{vf}	28 29 61 62 63
Radial-Axial Momentum Transport	r-z	$\overline{uv}$ R_{uv} σ_{uv} S_{uv} K_{uv}	22 23 52 53 54	Azimuthal Mass Transport	θ	$\overline{wf}$ R_{wf} σ_{wf} S_{wf} K_{wf}	32 33 67 68 69

ORIGINAL PAGE IS OF POOR QUALITY

TABLE IV-3

AXIAL AND AZIMUTHAL VELOCITY DATA AND CORRELATIONS

Test Date: 8/11/82 Run No.: 3 Flow Condition: 1 Geometry: 2

Axial Location: 25 mm (1.0 in.) $x/R_o = 0.416$

P_t No.	r mm +(θ=90) -(θ=270)	r/R_o	U m/s	u' m/s	S_u	K_u	W m/s	w' m/s	S_w	K_w	$\overline{uw}$ m^2/s^2	R_{uw}	σ_{uw} m^2/s^2	S_{uw}	K_{uw}	N
1	-35.0	-.574	1.251	.326	-.234	2.74	.498	.263	-.169	2.94	.00670	.079	.086	.20	7.52	987
2	-38.4	-.629	.510	.312	.272	3.10	.451	.258	.105	3.17	.00060	.008	.084	.56	8.79	994
3	-41.8	-.685	.196	.233	-.275	3.21	.413	.197	-.302	4.25	.00040	.010	.052	.46	20.01	996
4	-45.2	-.740	.130	.234	-.307	3.00	.423	.182	-.126	3.01	.00180	.041	.047	.61	10.36	993
5	-31.6	-.518	1.665	.222	-.442	3.49	.635	.143	.040	4.45	.00400	.125	.033	.79	10.21	997
6	-28.2	-.463	1.584	.229	-.535	3.98	.727	.170	-.103	4.41	.01060	.271	.048	1.44	14.94	994
7	-24.8	-.407	1.329	.380	-.733	3.83	.690	.291	-.859	4.64	.02570	.233	.098	.25	7.38	994
8	-21.5	-.352	.609	.433	-.448	2.76	.348	.371	-.244	3.09	.01980	.123	.138	.18	4.91	981
9	-18.1	-.296	-.207	.452	.908	3.52	.193	.360	-.192	3.83	.02920	.179	.138	.30	6.14	244
10	31.6	.518	1.685	.174	-.471	3.59	.664	.118	-.162	4.15	.00180	.088	.023	.03	17.23	990
11	.0	.000	.370	.274	-.880	2.91	-.057	.187	-.043	3.94	.01060	.207	.055	.42	8.47	240
12	-4.5	-.074	.290	.313	-.662	2.58	.086	.192	.059	3.22	-.01500	-.250	.058	-.42	6.85	238
13	-7.9	-.130	.257	.381	-.686	2.35	.073	.185	-.116	3.70	-.00750	-.106	.062	.51	7.05	240
14	-11.3	-.185	.024	.431	.027	1.67	.068	.169	-.254	3.50	.00770	.106	.064	.82	5.95	231
15	28.2	.463	1.615	.196	-.541	3.62	.715	.149	-.152	4.02	.00310	.106	.038	1.45	37.95	990
16	24.8	.407	1.309	.334	-.806	3.54	.744	.255	-.186	3.89	.00300	.035	.090	-.45	10.68	992
17	21.5	.352	.660	.426	-.280	4.05	.322	.370	-.244	3.33	.00180	-.011	.127	-.16	5.55	995
18	18.1	.296	-.029	.467	.532	2.41	.066	.381	.105	3.13	.01320	.074	.148	.04	4.82	492
19	14.7	.241	-.359	.249	.374	3.40	-.019	.230	-.248	3.20	-.00070	-.013	.062	-1.05	12.94	247
20	11.3	.185	-.151	.377	1.267	5.15	.001	.182	.287	3.78	.00010	.001	.069	1.45	16.29	245
21	7.9	.130	.035	.420	.326	2.09	-.002	.197	1.246	7.07	-.00080	-.010	.074	.18	6.13	242
22	35.0	.574	1.360	.316	-.560	3.51	.540	.270	-.300	3.61	.00580	.067	.089	.09	9.15	996
23	38.4	.629	.576	.331	.212	2.97	.480	.290	.284	3.63	-.00430	-.045	.093	-.06	7.62	996
24	41.8	.685	.168	.240	-.260	3.74	.407	.191	.008	4.14	-.00400	-.088	.053	-.23	12.56	995
25	45.2	.740	.065	.245	-.526	3.08	.409	.190	.020	3.60	.00000	-.000	.054	.19	16.49	996
26	48.6	.796	-.031	.271	-.314	2.77	.407	.201	-.372	3.87	.00140	.026	.057	1.06	10.85	498
27	51.9	.851	-.191	.274	-.090	2.78	.391	.206	-.123	4.06	.00640	.113	.055	-.22	10.79	495
28	55.3	.907	-.342	.266	-.060	2.70	.368	.224	-.194	3.05	.01230	.207	.055	.31	5.67	496
29	-48.6	-.796	.015	.301	-.129	2.50	.456	.245	-.491	3.86	.00360	.049	.078	.29	8.68	493
30	-51.9	-.851	-.184	.305	-.087	2.61	.420	.251	-.310	3.00	.01560	.205	.075	.43	5.90	489
31	-55.3	-.907	-.369	.287	.130	2.86	.376	.248	-.095	2.70	.01210	.170	.063	.66	9.52	491
32	-58.7	-.962	-.516	.324	-.006	2.88	.302	.216	.030	2.84	.00950	.135	.069	1.04	9.11	491

ORIGINAL PAGE IS
OF POOR QUALITY

TABLE IV-4

AXIAL AND AZIMUTHAL VELOCITY DATA AND CORRELATIONS

Test Date: 8/13/82 Run No.: 4 Flow Condition: 1 Geometry: 2

Axial Location: 51 mm (2.0 in.) $x/R_o = 0.833$

P_t No.	r mm +(θ=90) -(θ=270)	r/R_o	U m/s	u' m/s	S_u	K_u	W m/s	w' m/s	S_w	K_w	$\overline{uw}$ m^2/s^2	R_{uw}	σ_{uw} m^2/s^2	S_{uw}	K_{uw}	N
1	-58.7	-.962	-.645	.352	1.053	5.94	.384	.392	.070	3.51	.02310	.168	.100	.52	5.90	248
2	-55.3	-.907	-.208	.428	.446	2.87	.334	.337	-.136	2.92	.00860	.060	.128	-.17	5.05	494
3	-51.9	-.851	.358	.460	-.193	2.80	.383	.345	-.163	3.26	-.00730	-.046	.130	.03	4.87	999
4	-48.6	-.796	.766	.413	-.399	3.74	.386	.313	-.125	3.41	-.00220	-.017	.123	.36	9.24	995
5	-45.2	-.740	1.073	.409	-.721	4.78	.405	.288	-.033	3.76	.00110	.009	.119	.83	14.14	991
6	-41.8	-.685	1.257	.436	-1.066	5.36	.407	.299	-.080	3.88	.00170	.013	.145	-.44	12.83	995
7	-38.4	-.629	1.222	.497	-1.018	4.59	.420	.320	-.147	3.39	.00750	.047	.150	.85	9.87	990
8	-35.0	-.574	1.031	.594	-.621	3.03	.381	.369	-.232	3.75	.01480	.067	.208	.60	7.34	998
9	-31.6	-.518	.575	.677	-.116	2.18	.270	.411	-.137	3.33	.04550	.164	.251	.40	5.12	996
10	-28.2	-.463	.037	.482	.628	2.60	.169	.343	.215	3.25	.02520	.153	.177	.68	7.23	490
11	-24.8	-.407	-.275	.362	.909	5.04	.113	.273	.254	3.87	.01700	.173	.129	.19	19.00	497
12	-21.5	-.352	-.306	.232	.820	4.71	.088	.207	.220	4.77	.00390	.081	.056	1.44	17.75	496
13	-18.1	-.296	-.299	.230	.894	5.32	.059	.186	-.518	5.90	.00190	.044	.048	.51	17.41	498
14	-14.7	-.241	-.320	.213	1.136	5.43	.000	.170	-.119	3.48	.00130	.036	.045	1.41	18.58	498
15	-14.7	-.241	-.265	.224	.591	6.07	-.001	.146	-.222	3.18	.00040	.013	.034	.26	13.27	495
16	-38.4	-.629	1.365	.485	-1.386	6.20	.436	.345	-.299	4.16	.01780	.107	.152	.24	10.96	999
17	-38.4	-.629	1.228	.541	-1.224	5.02	.405	.346	-.196	3.68	.01220	.065	.164	-.11	9.24	996
18	-11.3	-.185	-.283	.226	1.137	4.97	-.021	.169	-.862	5.45	.00420	.109	.043	-.10	14.00	249
19	-7.9	-.130	-.283	.225	.738	3.29	-.018	.156	-1.123	6.63	-.00290	-.082	.047	-3.43	28.90	247
20	-4.5	-.074	-.255	.245	.969	3.98	-.044	.184	-.515	5.53	.00200	.045	.042	1.59	17.26	248
21	.0	.000	-.211	.250	.498	4.04	.064	.192	.355	3.20	.00010	.003	.052	1.21	21.57	249
22	55.3	.907	-.205	.487	.702	3.22	.312	.385	-.328	4.63	.01050	.056	.185	-.15	7.61	249
23	51.9	.851	.295	.469	-.183	2.75	.333	.327	-.074	3.04	-.01570	-.103	.162	.20	7.40	249
24	48.6	.796	.760	.371	-.296	3.57	.370	.306	-.375	3.65	.00350	.031	.124	1.37	11.14	499
25	45.2	.740	1.107	.368	-.554	5.32	.380	.295	.212	2.83	-.00740	-.068	.110	-.73	7.25	999
26	41.8	.685	1.320	.338	-.644	4.49	.441	.272	-.097	3.12	.00160	.018	.096	-.92	14.90	997
27	38.4	.629	1.300	.425	-1.052	4.70	.469	.290	-.327	3.85	.00720	.058	.127	.39	12.66	997
28	31.6	.518	.707	.410	-.444	2.63	.300	.425	-.208	3.31	.01970	.076	.236	.48	5.77	499
29	24.8	.407	-.116	.430	1.176	4.16	.136	.303	-.434	4.57	-.00320	-.025	.119	-.79	7.36	248
30	14.7	.241	-.307	.276	2.576	11.63	.066	.136	1.733	8.38	.00120	.033	.041	2.96	31.85	244

ORIGINAL PAGE IS
OF POOR QUALITY

TABLE IV-5

AXIAL AND AZIMUTHAL VELOCITY DATA AND CORRELATIONS

Test Date: 8/17/82 Run No.: 5 Flow Condition: 1 Geometry: 2
Axial Location: 102 mm (4.0 in.) $x/R_o = 1.665$

P_t No.	r mm +(0=90) -(0=270)	r/R_o	U m/s	u' m/s	S_u	K_u	W m/s	w' m/s	S_w	K_w	$\overline{uw}$ m^2/s^2	R_{uw}	σ_{uw} m^2/s^2	S_{uw}	K_{uw}	N
1	.0	.000	-.347	.156	1.046	2.19	-.086	.177	-.718	4.55	-.00430	-.158	.030	-.43	23.05	248
2	-4.5	-.074	-.333	.146	.607	3.66	.150	.192	.010	3.22	.00230	.081	.037	-.74	26.12	249
3	-7.9	-.130	-.343	.169	.874	4.31	.157	.197	.957	3.57	.00390	.118	.041	-.37	16.55	249
4	-11.3	-.185	-.299	.174	.440	2.67	.230	.210	-.006	2.84	.00790	.216	.036	-.12	6.78	246
5	-14.7	-.241	-.297	.154	.444	3.55	.322	.188	-.029	3.23	.00580	.202	.032	1.08	12.21	498
6	-18.1	-.296	-.276	.197	.089	3.83	.334	.206	.055	3.23	.01170	.289	.044	1.05	10.39	497
7	-21.5	-.352	-.204	.223	-.088	2.57	.408	.182	-.190	3.49	.01170	.288	.043	1.19	9.11	498
8	-35.0	-.574	.051	.328	.398	2.90	.355	.288	-.371	2.78	.00120	.012	.097	.51	7.96	496
9	-28.2	-.463	-.157	.241	.553	3.10	.394	.241	-.255	2.66	.01390	.239	.065	.20	9.69	497
10	-41.8	-.685	.412	.330	-.386	3.51	.304	.292	-.128	2.56	-.00750	-.078	.087	.45	7.39	499
11	-48.6	-.796	.778	.270	.196	4.02	.276	.289	.035	2.57	.00050	.007	.084	-1.03	18.66	499
12	-55.3	-.907	1.033	.230	-.154	3.33	.301	.221	.107	2.75	.00350	.069	.050	-.08	6.82	499
13	-57.0	-.935	1.082	.244	-.195	3.12	.250	.248	.538	3.27	.01250	.207	.060	-.19	8.36	499
14	-51.9	-.851	.917	.245	-.253	4.04	.279	.265	.174	2.78	.00090	.014	.059	-.12	5.20	498
15	-55.3	-.907	1.056	.288	-1.138	5.93	.298	.245	.123	2.69	.00570	.080	.076	2.37	30.91	992
16	55.3	.907	.901	.230	-.231	2.85	.309	.238	-.042	2.86	.00150	.028	.058	-.69	9.10	499
17	48.6	.796	.645	.276	-.229	3.48	.353	.264	-.072	2.97	-.01620	-.222	.075	-1.51	11.10	499
18	41.8	.685	.288	.331	.076	2.70	.402	.259	-.469	3.33	-.01090	-.127	.087	.11	6.92	499
19	35.0	.574	-.036	.328	.471	2.32	.421	.255	-.324	2.48	.00150	.018	.091	-.44	5.76	249
20	28.2	.463	-.248	.241	.598	3.10	.392	.223	-.676	3.27	.01110	.206	.055	-.26	8.48	249
21	28.8	.473	-.245	.196	.575	3.29	.365	.213	-.455	3.18	.00480	.116	.049	-1.19	15.97	248
22	28.2	.463	-.224	.213	.935	4.58	.354	.202	-.760	4.55	.00120	.027	.060	-7.51	108.80	499
23	28.2	.463	-.201	.233	.715	3.72	.355	.203	-.269	3.40	.00290	.061	.049	.01	9.86	498
24	21.5	.352	-.295	.177	.467	3.73	.304	.196	-.405	3.95	.00110	.033	.040	-.69	19.94	499
25	14.7	.241	-.337	.162	.292	3.46	.239	.182	-.058	2.89	.00560	.192	.032	1.71	14.20	499
26	7.9	.130	-.368	.151	.302	3.67	.093	.184	.154	3.27	.00100	.036	.031	2.86	36.69	499
27	.0	.000	-.360	.153	.271	3.71	-.042	.161	-.018	4.39	-.00270	-.111	.028	-1.93	26.76	499
28	-7.9	-.130	-.322	.163	.429	3.88	.210	.192	.198	3.17	.00590	.190	.036	1.76	16.41	499
29	-14.7	-.241	-.316	.171	.398	3.46	.290	.211	.189	2.69	.00790	.218	.038	1.05	9.08	499
30	-21.5	-.352	-.268	.191	.777	4.17	.235	.260	.818	2.87	.00750	.152	.055	1.52	12.47	499
31	-48.6	-.796	.774	.249	-.084	3.37	.263	.295	.367	2.34	-.00510	-.070	.079	-1.39	9.59	499
32	-55.3	-.907	1.017	.231	-.178	2.75	.297	.240	.179	2.55	.00400	.071	.055	-.60	5.96	499
33	-41.8	-.685	.433	.303	-.220	2.96	.333	.298	-.184	2.61	-.01100	-.122	.083	.59	6.19	499
34	-28.2	-.463	-.111	.234	.456	3.07	.374	.204	-.060	3.22	.00850	.179	.053	1.12	11.54	499
35	41.8	.685	.290	.296	-.130	2.88	.360	.266	-.425	3.59	-.01350	-.171	.076	-.50	7.53	499
36	41.8	.685	.262	.308	-.059	2.62	.363	.278	-.119	3.06	-.01340	-.157	.081	-.78	9.41	499
37	41.8	.685	.293	.325	-.261	2.74	.358	.283	-.457	3.40	-.01600	-.173	.089	-.73	8.29	499
38	41.8	.685	.285	.306	-.039	2.60	.379	.274	-.488	3.60	-.01400	-.167	.078	.66	7.04	499
39	41.8	.685	.320	.315	-.091	2.93	.365	.258	-.497	3.09	-.01100	-.136	.080	-.64	9.54	499
40	41.8	.685	.310	.311	-.034	2.62	.383	.250	-.372	3.25	-.01460	-.188	.073	.14	8.32	499

TABLE IV-6

AXIAL AND AZIMUTHAL VELOCITY DATA AND CORRELATIONS

Test Date: 8/23/82 Run No.: 6 Flow Condition: 1 Geometry: 2

Axial Location: 102 mm (4.0 in.) x/R_o = 1.665

P_t No.	r mm +(0=90) -(0=270)	r/R_o	U m/s	u' m/s	S_u	K_u	W m/s	w' m/s	S_w	K_w	$\overline{uw}$ m^2/s^2	R_{uw}	σ_{uw} m^2/s^2	S_{uw}	K_{uw}	N
1	41.8	.685	.282	.447	-.761	4.12	.335	.423	-.416	5.82	-.01221	-.064	.144	-1.61	10.79	138
2	41.8	.685	.230	.345	-.356	2.94	.332	.297	-.705	3.72	.01392	.136	.137	2.54	15.62	128
3	.0	.000	-.275	.179	1.392	6.06	-.089	.203	.150	2.84	-.00340	-.094	.048	2.11	15.95	65
4	-7.9	-.130	-.285	.196	.680	3.60	.185	.253	-3.046	16.82	-.00015	-.003	.121	-5.99	46.35	64
5	-14.7	-.241	-.278	.235	-.068	8.73	.276	.251	-2.574	13.61	.00851	.144	.121	-1.02	40.26	129
6	-21.5	-.352	-.233	.217	-.941	7.63	.321	.245	-2.609	17.15	.00513	.096	.081	-5.40	62.39	128
7	-28.2	-.463	-.119	.248	.294	3.63	.349	.205	.073	3.79	.00460	.090	.059	-.14	11.59	128
8	-35.0	-.574	.035	.291	.142	2.45	.304	.308	-1.301	5.80	-.00951	-.106	.101	-1.23	11.77	129
9	-41.8	-.685	.384	.343	-.936	3.87	.357	.280	-.720	4.80	-.00041	-.004	.105	.38	16.11	129
10	-48.6	-.796	.697	.257	-.598	3.68	.324	.317	.095	2.86	.00202	.025	.094	-.09	17.10	129
11	-55.3	-.907	1.018	.299	-1.670	9.82	.275	.224	-.280	3.38	.00003	.000	.079	.50	13.15	128
12	-55.3	-.907	.984	.303	-1.001	7.31	.304	.245	-.036	4.63	.00924	.125	.077	3.51	26.71	254
13	-55.3	-.907	1.024	.295	-.901	4.82	.332	.237	1.219	7.64	-.00066	-.009	.085	-3.39	23.88	129

ORIGINAL PAGE IS OF POOR QUALITY

TABLE IV-7

AXIAL AND RADIAL VELOCITY DATA AND CORRELATIONS

Test Date: 8/23/82 Run No.: 7 Flow Condition: 1 Geometry: 2

Axial Location: 25 mm (1.0 in.) $x/R_o = 0.416$

P_t No.	r mm +(θ=0) −(θ=180)	r/R_o	U m/s	u' m/s	S_u	K_u	V m/s	v' m/s	S_v	K_v	$\overline{uv}$ m^2/s^2	R_{uv}	σ_{uv} m^2/s^2	S_{uv}	K_{uv}	N
1	1.4	.026	.387	.276	-.946	4.22	-.008	.174	.057	3.94	.00474	.098	.060	.01	10.12	249
2	4.1	.070	.304	.295	-.905	3.52	.036	.204	.003	3.14	.01469	.244	.059	.16	10.40	246
3	6.6	.112	.141	.369	-.198	2.21	.016	.183	.173	4.40	.01180	.174	.055	-.04	6.19	249
4	9.2	.154	-.024	.365	-.237	1.83	.038	.191	.004	4.39	.01486	.213	.066	.32	5.17	248
5	11.7	.195	-.189	.327	.686	2.82	.007	.193	-.399	3.95	.01061	.168	.059	.62	6.88	247
6	14.2	.237	-.224	.306	.910	3.51	.017	.242	-.429	3.70	.00833	.113	.072	.25	10.15	498
7	16.8	.278	-.213	.338	.733	3.56	.043	.308	-.271	3.23	-.00321	-.031	.108	-.78	8.30	497
8	19.3	.320	.089	.466	.284	2.56	.059	.367	-.279	3.15	-.04387	-.256	.162	-.68	7.77	499
9	21.9	.362	.633	.461	-.210	3.15	.197	.343	-.005	2.78	-.06230	-.394	.164	-1.11	8.21	499
10	24.4	.403	1.085	.417	-.609	3.19	.370	.284	-.101	3.28	-.04111	-.347	.116	-.97	6.28	499
11	27.0	.445	1.422	.328	-.929	4.20	.539	.237	.190	3.43	-.02425	-.313	.089	-1.03	17.41	995
12	29.5	.487	1.566	.228	-.865	5.57	.626	.197	.233	3.46	-.01522	-.339	.055	-3.59	27.28	998
13	32.0	.528	1.650	.203	-.426	3.85	.628	.190	-.339	3.58	-.00876	-.227	.047	-1.06	14.81	993
14	34.6	.570	1.523	.267	-.405	3.34	.612	.325	-.797	3.87	.02494	.288	.112	3.08	22.32	999
15	37.1	.612	.972	.330	-.027	2.88	.413	.420	-.125	2.48	.05563	.401	.143	1.34	7.93	999
16	39.7	.653	.499	.307	.106	3.46	.188	.417	.468	2.76	.04275	.334	.131	1.47	9.88	999
17	42.2	.695	.248	.255	-.135	3.95	-.046	.315	.842	4.26	.01840	.228	.093	1.09	14.33	499
18	44.7	.736	.161	.255	.201	6.01	-.125	.249	.500	4.09	.01336	.211	.073	-1.12	16.01	249
19	47.3	.778	.138	.274	-.609	3.16	-.160	.221	-.086	3.84	.01815	.299	.068	.12	11.55	249
20	-1.4	-.019	.359	.260	-.808	3.08	.044	.194	-.465	4.15	-.00031	-.006	.060	1.58	19.27	249
21	-6.4	-.102	.308	.332	-.640	4.03	.110	.209	.211	3.72	.00946	.136	.080	1.98	21.64	249
22	-11.5	-.185	-.019	.372	.253	1.96	.087	.191	-.057	3.83	.02905	.408	.068	1.27	8.34	247
23	-16.6	-.269	-.118	.348	.626	3.16	.039	.261	-.538	3.76	.00841	.093	.089	-.89	7.10	249
24	-21.7	-.352	.533	.492	-.372	3.04	.155	.368	.074	2.75	-.05067	-.280	.160	-.34	7.55	499
25	-26.7	-.435	1.430	.305	-.951	4.50	.555	.235	.078	3.45	-.02112	-.294	.082	-2.70	22.56	999
26	-31.8	-.518	1.650	.204	-.195	2.76	.639	.200	-.098	3.49	-.01188	-.292	.041	-1.44	10.42	991
27	-36.9	-.602	1.064	.360	.040	3.38	.513	.392	-.259	2.43	.07011	.496	.144	1.38	7.69	999
28	-42.0	-.685	.229	.254	-.216	3.75	-.028	.296	.529	4.19	.02535	.337	.085	1.26	12.50	994
29	-47.1	-.768	.109	.307	.283	4.65	-.162	.251	.214	2.98	.02494	.324	.079	.84	20.46	995
30	-52.2	-.851	-.056	.414	.903	4.59	-.193	.254	.208	2.76	.02485	.236	.101	.20	7.69	494
31	14.2	.237	-.161	.330	.622	2.99	.038	.247	-.307	3.56	.00915	.112	.082	-.95	14.31	499
32	-14.0	-.227	-.074	.367	.537	2.66	.073	.203	-.257	3.53	.02160	.290	.068	.71	7.64	498

ORIGINAL PAGE IS
OF POOR QUALITY

TABLE IV-8

AXIAL AND RADIAL VELOCITY DATA AND CORRELATIONS

Test Date: 8/25/82 Run No.: 8 Flow Condition: 1 Geometry: 2
Axial Location: 51 mm (2.0 in.) $x/R_o = 0.883$

P_t No.	r mm +(θ=0) −(θ=180)	r/R_o	U m/s	u' m/s	S_u	K_u	V m/s	v' m/s	S_v	K_v	$\overline{uv}$ m^2/s^2	R_{uv}	σ_{uv} m^2/s^2	Suv	Kuv	N
1	.4	.017	-.076	.269	.279	2.40	-.019	.206	-.174	3.62	.00083	.015	.056	1.22	15.67	498
2	4.4	.082	-.119	.271	.208	2.51	.053	.200	-.154	3.14	.00262	.048	.052	.06	6.59	499
3	9.5	.165	-.187	.269	.737	3.40	.060	.178	.323	4.79	-.00022	-.005	.046	-1.69	14.63	498
4	14.5	.249	-.252	.238	.686	3.34	.068	.173	.073	3.47	.00528	.128	.041	.39	13.42	987
5	19.6	.332	-.277	.237	.844	4.43	.057	.204	-.510	5.18	-.00379	-.079	.056	-2.74	27.04	988
6	24.7	.415	-.181	.359	1.313	5.81	.095	.297	-.641	4.55	-.02761	-.259	.136	-2.62	16.15	999
7	29.8	.498	.297	.565	.226	2.35	.177	.360	-.426	3.00	-.06191	-.304	.187	-.21	7.40	999
8	34.9	.582	.857	.552	-.353	2.58	.430	.346	-.263	3.34	-.05634	-.295	.168	-.78	6.97	999
9	39.9	.665	1.162	.446	-.671	3.41	.630	.352	-.382	3.17	-.03610	-.230	.148	-1.10	8.02	999
10	45.0	.748	1.052	.363	-.405	3.25	.724	.392	-.318	2.84	-.01005	-.071	.139	-.34	8.64	999
11	50.[illegible]	.831	.710	.386	-.175	3.96	.540	.436	-.200	2.93	.02400	.143	.162	.71	8.79	499
12	52.6	.873	.552	.582	.602	4.10	.435	.479	-.272	2.85	.04696	.169	.246	.64	5.59	249
13	-1.0	-.005	-.099	.284	.315	2.24	.021	.201	-.095	2.80	-.00205	-.036	.049	.06	4.75	499
14	-6.0	-.089	-.113	.270	.411	2.51	.043	.196	-.192	3.25	-.00310	-.059	.050	.31	8.49	499
15	-11.1	-.172	-.174	.255	.795	3.66	.075	.189	-.059	5.64	.00095	.020	.047	.10	9.72	498
16	-16.2	-.255	-.196	.242	1.109	4.54	.077	.188	-.153	3.73	.00088	.019	.048	-1.59	20.90	493
17	-21.3	-.339	-.266	.216	.834	4.42	.055	.196	-.566	4.02	-.00247	-.058	.047	-.50	20.68	991
18	-26.4	-.422	-.172	.340	1.253	5.12	.075	.286	-.533	4.15	-.01973	-.203	.114	-1.87	16.99	997
19	-31.4	-.505	.305	.576	.266	2.20	.195	.337	-.330	3.21	-.04893	-.252	.179	-.63	6.52	998
20	-36.5	-.588	1.039	.534	-.594	3.14	.456	.388	-.248	2.97	-.02350	-.113	.188	-.17	6.24	999
21	-41.6	-.671	1.175	.435	-.553	3.25	.767	.348	-.370	3.22	-.02068	-.137	.143	-1.01	7.52	499
22	-46.7	-.755	.991	.372	-.243	3.16	.759	.386	-.393	2.75	.01336	.093	.154	.47	9.02	499

ORIGINAL PAGE IS
OF POOR QUALITY

TABLE IV-9

AXIAL AND RADIAL VELOCITY DATA AND CORRELATIONS

Test Date: 8/25/82 Run No.: 9 Flow Condition: 1 Geometry: 2
Axial Location: 102 mm (4.0 in.) $x/R_o = 1.665$

P_t No.	r mm +(θ=0) -(θ=180)	r/R_o	U m/s	u' m/s	S_u	K_u	V m/s	v' m/s	S_v	K_v	$\overline{uv}$ m^2/s^2	R_{uv}	σ_{uv} m^2/s^2	S_{uv}	K_{uv}	N
1	2.1	.054	-.348	.168	.374	3.16	-.049	.193	.063	3.02	-.00225	-.069	.034	-.08	8.29	459
2	4.8	.099	-.370	.150	.988	6.93	-.015	.118	-.004	5.73	-.00122	-.069	.017	-1.62	17.59	498
3	9.9	.182	-.370	.146	.500	4.33	-.009	.090	1.537	13.52	-.00012	-.009	.012	-.27	12.43	496
4	15.0	.265	-.341	.151	.637	3.91	-.015	.093	-.755	12.89	-.00085	-.061	.015	-4.24	43.50	499
5	20.0	.348	-.346	.190	.693	4.43	-.002	.148	-.503	7.74	-.00199	-.071	.032	-2.63	34.41	498
6	25.1	.432	-.297	.216	.418	4.05	-.002	.152	-1.249	10.26	-.00850	-.259	.043	-4.74	37.10	497
7	30.2	.515	-.191	.291	1.024	4.33	-.023	.191	-.757	4.97	-.02453	-.443	.073	-3.69	23.05	495
8	35.3	.598	.060	.343	.332	2.61	-.079	.247	-.904	3.88	-.03656	-.432	.088	-2.07	9.65	497
9	40.4	.682	.296	.347	.205	3.47	-.055	.209	-1.017	4.99	-.02219	-.306	.076	-2.26	19.44	497
10	45.4	.765	.564	.334	.270	4.42	-.115	.259	.101	2.74	-.02422	-.280	.088	-1.18	9.30	499
11	50.5	.848	.817	.376	.215	4.44	-.107	.256	.131	3.27	.00076	.008	.105	-.25	12.86	478
12	53.1	.890	1.077	.486	1.093	4.24	-.008	.254	.458	4.27	.00518	.042	.112	-.69	9.24	249
13	-1.8	-.010	-.337	.192	1.820	10.79	.040	.197	-.159	4.16	.00111	.029	.033	.69	12.81	499
14	-6.9	-.093	-.339	.175	1.452	8.21	.047	.190	-.408	4.03	-.00322	-.097	.035	-1.12	15.37	496
15	-10.8	-.157	-.328	.189	1.562	9.42	.026	.191	-.290	3.65	-.00186	-.052	.041	1.25	42.01	993
16	-13.3	-.199	-.326	.163	.454	3.43	.023	.196	-.131	3.14	-.00452	-.141	.033	-.93	8.56	989
17	-18.4	-.282	-.331	.160	.375	3.25	.049	.205	-.049	3.44	-.00369	-.112	.037	-1.30	14.01	998
18	-23.5	-.365	-.317	.166	.731	4.25	.027	.216	-.512	4.05	-.00737	-.205	.043	-1.74	20.20	993
19	-28.6	-.448	-.236	.237	1.054	4.60	-.003	.253	-.389	3.04	-.02274	-.380	.069	-2.82	18.54	999
20	-33.7	-.532	-.134	.284	.665	2.84	-.014	.260	-.370	3.05	-.02951	-.400	.076	-1.99	14.93	997
21	-38.7	-.615	.115	.401	.697	3.94	-.098	.280	-.094	2.68	-.04593	-.409	.099	-.90	6.84	992
22	-43.8	-.698	.463	.314	-.168	3.72	-.134	.251	.076	3.01	-.02225	-.282	.092	-1.66	10.80	996
23	-48.9	-.781	.745	.334	.928	7.10	-.075	.227	-.081	3.29	-.01323	-.174	.076	-2.22	21.34	988
24	-54.0	-.865	.988	.434	.641	4.71	-.030	.238	-.049	3.31	-.00735	-.071	.102	-.21	9.41	247
25	-56.5	-.906	1.124	.446	.325	4.11	-.028	.211	-.010	2.73	-.00697	-.074	.084	-.13	5.55	247
26	35.3	.598	.073	.342	.332	2.40	-.123	.281	-.571	3.38	-.04209	-.439	.092	-1.70	9.13	498
27	55.6	.931	.817	.591	.227	3.14	-.018	.193	-.152	3.57	-.00107	-.009	.106	.28	7.00	246
28	54.3	.910	1.075	.480	1.308	5.06	-.001	.217	.049	4.60	.00370	.036	.105	2.58	19.70	248
29	56.9	.952	1.049	.430	.785	4.71	-.003	.183	.336	5.13	-.00229	-.029	.078	.87	22.64	248
30	55.6	.931	1.056	.444	1.559	7.32	-.005	.177	.283	5.16	-.00049	-.006	.058	.13	11.23	248
31	55.6	.931	1.142	.552	.757	3.52	.003	.185	.252	5.42	.01047	.103	.099	1.42	15.18	248

TABLE IV-10

AXIAL AND RADIAL VELOCITY DATA AND CORRELATIONS

Test Date: 8/26/82   Run No.: 10   Flow Condition: 1   Geometry: 2
Axial Location: 203 mm (8.0 in.) $x/R_o = 3.331$

P_t No.	r mm +(θ=0) -(θ=180)	r/R_o	U m/s	u' m/s	S_u	K_u	V m/s	v' m/s	S_v	K_v	$\overline{uv}$ m^2/s^2	R_{uv}	σ_{uv} m^2/s^2	S_{uv}	K_{uv}	N
1	1.2	.020	.166	.179	.092	3.24	-.113	.273	.423	2.59	-.00557	-.114	.046	-.51	6.94	499
2	3.9	.065	.163	.186	-.364	4.11	-.118	.269	.166	2.37	-.00074	-.015	.049	-.68	8.69	993
3	9.0	.148	.186	.203	-.089	2.90	-.067	.276	.005	2.94	-.00508	-.091	.054	-.46	6.69	498
4	14.1	.231	.217	.203	-.724	4.37	-.058	.240	-.117	2.85	-.00658	-.135	.048	.39	11.72	498
5	19.2	.314	.279	.198	-.727	4.14	-.063	.236	-.004	3.32	-.00733	-.157	.048	-.39	8.91	496
6	24.3	.398	.297	.251	-1.889	10.87	-.058	.207	.072	3.64	-.01070	-.205	.062	-2.64	30.67	497
7	29.3	.481	.349	.173	-.199	3.88	-.062	.194	-.080	3.31	-.00814	-.242	.032	-1.07	8.37	496
8	34.4	.564	.377	.178	.145	3.30	-.081	.200	.011	2.89	-.01152	-.324	.037	-.72	10.16	498
9	39.5	.647	.415	.187	-.133	3.32	-.078	.186	.083	3.01	-.01142	-.329	.037	-1.22	8.68	498
10	44.6	.731	.462	.181	-.031	3.22	-.064	.160	.072	3.70	-.00689	-.238	.028	-.09	9.95	498
11	47.1	.772	.512	.336	1.171	8.12	-.009	.140	1.846	10.11	-.00107	-.023	.052	3.90	37.93	246
12	-4.0	-.066	.152	.239	-.638	4.08	-.018	.200	-.125	6.51	-.00103	-.021	.053	-.23	19.58	246
13	-9.1	-.149	.218	.181	.319	4.00	.013	.213	.286	4.31	-.00296	-.077	.036	-1.03	9.01	242
14	-14.2	-.233	.239	.182	-.053	2.94	.024	.247	.133	2.93	.00038	.009	.043	.21	7.37	246
15	-19.3	-.316	.264	.169	-.031	3.56	-.029	.238	-.005	3.16	-.00349	-.087	.038	-.38	8.64	497
16	-24.4	-.399	.293	.177	-.328	3.77	-.047	.224	.252	3.10	-.00228	-.058	.038	-.09	8.19	497
17	-29.4	-.483	.334	.176	-.205	3.09	-.063	.183	.164	3.73	-.00366	-.113	.035	-1.22	12.15	496
18	-34.5	-.566	.399	.192	-.277	3.97	-.066	.139	-.705	4.71	-.00695	-.261	.030	-2.50	18.79	493
19	-39.6	-.649	.431	.204	.032	4.09	-.060	.135	-.319	4.41	-.00635	-.231	.028	-1.86	18.06	488
20	-44.7	-.732	.468	.182	-.033	2.93	-.067	.129	-.348	4.03	-.00624	-.265	.025	-1.83	12.97	249
21	-44.7	-.732	.466	.193	.193	3.01	-.061	.143	.111	3.53	-.00645	-.234	.028	-.95	9.02	499
22	-47.2	-.774	.442	.268	-1.353	6.07	-.041	.119	-1.764	11.59	-.00712	-.223	.026	-1.74	8.93	248
23	-49.8	-.816	.363	.370	-.790	4.06	-.012	.126	.312	4.87	-.00489	-.105	.040	.12	10.96	240
24	-49.8	-.816	.446	.297	-1.606	7.02	-.022	.067	-.393	3.87	.00025	.012	.025	4.14	39.83	247
25	-1.5	-.025	.211	.186	-.429	3.82	.013	.155	-.160	8.25	-.00051	-.018	.033	.13	25.80	498
26	1.2	.020	.199	.196	-.348	3.41	-.009	.147	.183	8.42	-.00085	-.030	.032	.28	31.12	491
27	3.9	.065	.183	.192	-.174	3.14	-.034	.218	-.458	4.42	-.00375	-.090	.035	-.41	7.03	492
28	9.0	.148	.190	.190	-.192	3.19	-.042	.205	-.396	4.54	-.00563	-.144	.039	-.63	8.17	490
29	14.1	.231	.244	.196	-.045	2.75	-.056	.222	-.517	4.25	-.00843	-.194	.044	-.59	11.00	491
30	-14.2	-.233	.229	.189	-.615	3.87	-.021	.158	-1.070	6.15	.00149	.050	.028	1.74	20.77	497
31	-49.8	-.816	.514	.206	-.608	4.03	-.018	.082	-.831	4.44	-.00217	-.128	.017	-1.46	13.50	489
32	-54.8	-.899	.617	.394	2.428	10.23	-.023	.113	.167	3.79	.00252	.057	.040	.05	19.61	492
33	-52.3	-.857	.565	.294	1.896	8.35	-.021	.132	.230	4.06	-.00564	-.145	.043	-.96	28.27	496

TABLE IV-11

AXIAL AND RADIAL VELOCITY DATA AND CORRELATIONS

Test Date: 8/26/82 Run No.: 11 Flow Condition: 1 Geometry: 2

Axial Location: 5 mm (0.2 in.) x/R_o = 0.083

P_t No.	r mm +(0=0) -(0=180)	r/R_o	U m/s	u' m/s	S_u	K_u	V m/s	v' m/s	S_v	K_v	$\overline{uv}$ m^2/s^2	R_{uv}	σ_{uv} m^2/s^2	S_{uv}	K_{uv}	N
1	1.3	.025	.754	.068	-.077	2.87	-.001	.066	-.098	3.68	.00068	.151	.005	.51	8.83	244
2	4.1	.069	.747	.070	-.103	2.74	.008	.063	.494	5.60	.00089	.205	.006	-2.82	37.56	238
3	9.1	.152	.606	.202	-2.289	9.70	.052	.090	-1.566	10.58	.00826	.455	.038	7.42	67.03	247
4	14.2	.236	.163	.340	.138	3.49	.006	.240	-.084	4.19	-.01085	-.133	.076	-1.44	11.05	248
5	19.3	.319	1.470	.153	-.423	2.93	.216	.138	.217	3.06	-.00644	-.306	.023	-1.81	11.18	994
6	24.4	.402	1.622	.156	.085	3.10	.145	.213	-.408	2.65	.00031	.009	.034	-.52	9.99	995
7	29.5	.485	1.518	.181	.384	2.67	.102	.121	-.064	3.01	.00132	.060	.021	.50	5.99	994
8	34.5	.569	-.020	.144	-.080	3.06	-.050	.100	-1.149	5.69	.00197	.136	.018	-.76	18.72	242
9	32.0	.527	.180	.232	-.137	3.56	.033	.214	.918	4.50	.01203	.243	.057	.91	9.92	992
10	26.9	.444	1.584	.164	-.130	2.49	.037	.166	.598	3.32	-.00380	-.140	.028	-1.47	14.84	998
11	21.8	.361	1.678	.123	-.062	3.50	.217	.147	-.693	4.62	-.00317	-.176	.021	-1.16	14.12	991
12	30.7	.506	.972	.261	-.072	2.71	.195	.240	-.178	2.84	.02966	.474	.063	1.26	7.16	997
13	16.8	.277	.894	.285	-.449	3.35	.076	.191	.645	4.31	-.01750	-.320	.066	-2.87	2.98	998
14	28.2	.465	1.571	.176	.159	2.52	.064	.142	.517	3.55	-.00280	-.112	.025	-.60	8.14	994
15	25.7	.423	1.541	.154	-.033	2.74	.099	.211	.107	2.36	-.00199	-.061	.032	-.44	6.09	999
16	23.1	.381	1.650	.140	.168	3.57	.204	.179	-.684	3.52	-.00064	-.026	.027	-1.08	18.84	993
17	20.6	.340	1.593	.132	-.242	2.97	.234	.121	-.034	3.28	-.00380	-.238	.018	-1.51	13.21	997
18	15.5	.256	.464	.295	-.213	2.52	-.013	.274	.185	3.34	-.03111	-.385	.086	-.90	7.73	497
19	11.7	.194	.348	.337	-1.020	3.33	.058	.140	-.361	3.72	.01570	.333	.054	.76	10.92	245
20	39.6	.652	-.012	.142	-.340	3.14	-.057	.154	-.503	2.89	.00567	.260	.025	1.12	8.41	247
21	44.7	.735	-.033	.171	-1.190	5.08	-.053	.157	-.487	3.38	.00276	.103	.028	-.08	11.86	245
22	-29.3	-.478	1.535	.138	-.045	3.28	.205	.139	.253	2.86	.00311	.162	.019	.62	6.22	499
23	-28.0	-.457	1.575	.134	-.075	2.56	.176	.156	.176	2.49	.00299	.142	.020	.38	5.49	996
24	-26.8	-.436	1.633	.143	-.036	2.60	.219	.185	-.080	2.33	.00440	.167	.026	.25	6.79	996
25	-24.2	-.395	1.708	.122	.217	3.47	.273	.158	-.755	3.97	-.00001	-.001	.022	-2.06	29.96	994
26	-21.7	-.353	1.674	.123	-.386	3.52	.317	.122	.066	3.65	-.00264	-.176	.017	-1.25	12.59	999
27	-19.2	-.311	1.383	.161	-.425	3.60	.256	.130	.258	3.15	-.00601	-.288	.024	-3.58	37.37	997
28	-16.6	-.270	.721	.282	-.357	3.18	.072	.205	.337	3.21	-.01431	-.248	.064	-1.18	11.17	997
29	-14.1	-.228	.034	.337	.060	2.40	.002	.242	-.266	5.35	.00019	.002	.078	.30	8.18	247
30	-11.5	-.186	.547	.289	-.878	6.41	.081	.090	-.671	4.32	.00819	.314	.033	1.78	22.22	240
31	-9.0	-.145	.700	.110	-1.001	5.89	.078	.080	-1.244	7.86	.00354	.404	.014	9.48	121.80	241
32	-31.9	-.520	.471	.260	.222	3.28	.056	.201	1.073	5.38	.02157	.414	.063	2.48	12.41	990
33	-26.1	-.426	1.619	.153	-.208	2.69	.186	.192	-.097	2.32	.00543	.185	.029	.56	8.15	995
34	-25.5	-.416	1.653	.144	-.186	3.05	.201	.188	-.255	2.51	.00387	.143	.027	.30	9.52	996
35	-24.9	-.405	1.679	.139	-.134	2.90	.215	.190	-.621	3.15	.00332	.126	.030	1.72	15.99	996

ORIGINAL PAGE IS
OF POOR QUALITY

TABLE IV-12

AXIAL AND AZIMUTHAL VELOCITY DATA AND CORRELATIONS

Test Date: 8/27/82 Run No.: 12 Flow Condition: 1 Geometry: 2

Axial Location: 203 mm (8.0 in.) $x/R_o = 3.331$

P_t No.	r mm +(θ=90) −(θ=270)	r/R_o	U m/s	u' m/s	S_u	K_u	W m/s	w' m/s	S_w	K_w	$\overline{uw}$ m^2/s^2	R_{uw}	σ_{uw} m^2/s^2	S_{uw}	K_{uw}	N
1	-.8	-.031	.159	.175	.159	3.24	.111	.258	-.136	2.59	.00608	.134	.044	.54	5.95	498
2	-5.3	-.105	.184	.179	-.074	3.44	.240	.233	-.498	2.85	.00301	.072	.044	-.32	9.67	499
3	-12.1	-.216	.221	.173	.035	3.55	.407	.174	-.335	3.42	.00471	.157	.030	.86	10.11	499
4	-18.9	-.327	.252	.170	-.173	3.77	.441	.146	.053	2.98	.00300	.121	.023	.32	6.89	499
5	-25.6	-.438	.319	.186	.118	3.15	.444	.155	-.241	3.32	.00235	.081	.030	.22	8.39	499
6	-32.4	-.549	.354	.178	.064	2.91	.451	.148	-.026	2.90	.00114	.044	.027	.09	8.31	499
7	-39.2	-.660	.404	.201	-.046	2.47	.416	.151	.062	3.35	-.00296	-.097	.029	-.47	8.07	499
8	-45.9	-.771	.460	.186	-.054	2.91	.407	.158	-.084	3.07	-.00390	-.132	.028	-.52	6.75	499
9	-52.7	-.882	.453	.196	-.376	3.28	.395	.162	.221	3.92	.00086	.027	.029	-.44	6.93	499
10	-56.1	-.938	.413	.180	-.044	2.63	.389	.154	.088	2.98	.00217	.078	.029	.31	9.05	499
11	1.5	.006	.158	.193	-.058	3.33	-.013	.246	.019	3.23	-.00570	-.120	.043	-.26	7.00	498
12	8.2	.117	.179	.192	-.323	4.00	.219	.238	.322	2.40	-.00062	-.014	.046	-.08	7.67	499
13	15.0	.228	.197	.179	.113	3.44	.382	.199	-.479	2.63	-.00486	-.137	.033	-.42	7.73	499
14	21.8	.339	.213	.177	.008	3.57	.446	.177	-.542	4.05	.00054	.017	.034	-.37	16.35	498
15	28.5	.450	.265	.206	.035	3.34	.465	.155	-.335	3.72	-.00083	-.026	.034	.05	12.60	499
16	35.3	.561	.308	.207	.122	2.64	.460	.161	-.482	3.53	-.00382	-.115	.033	-.52	5.90	499
17	42.1	.672	.391	.205	-.410	3.92	.439	.167	-.328	3.14	-.00466	-.136	.031	-.80	8.78	499
18	48.9	.783	.454	.203	-.222	2.70	.420	.171	-.172	3.00	-.01093	-.315	.034	-1.23	7.91	499
19	54.9	.883	.483	.197	-.295	3.07	.413	.189	-.123	3.13	-.00779	-.209	.037	-.76	7.59	496

TABLE IV-14

AXIAL AND AZIMUTHAL VELOCITY DATA AND CORRELATIONS

Test Date: 8/30/82 Run No.: 14 Flow Condition: 1 Geometry: 2
Axial Location: 152 mm (6.0 in.) x/R_o = 2.498

P_t No.	r mm +(0=90) -(0=270)	r/R_o	U m/s	u' m/s	S_u	K_u	W m/s	w' m/s	S_w	K_w	$\overline{uw}$ m^2/s^2	R_{uw}	σ_{uw} m^2/s^2	S_{uw}	K_{uw}	N
1	-2.5	-.032	-.124	.185	.428	3.27	.024	.177	.773	8.13	.00404	.124	.035	3.07	20.48	495
2	3.1	.060	-.134	.180	.284	3.49	.061	.178	1.279	5.14	.00243	.076	.031	.60	14.93	496
3	9.9	.171	-.068	.194	.366	3.02	.243	.250	.496	2.43	.00147	.030	.046	-.54	5.02	249
4	16.7	.282	-.004	.200	.286	2.72	.384	.202	-.215	2.92	.00191	.047	.041	-.32	7.87	248
5	23.5	.393	.059	.216	.106	2.86	.404	.191	-.937	4.26	-.00499	-.121	.045	-1.59	8.55	249
6	30.2	.504	.127	.231	.027	2.48	.404	.210	-.194	2.75	-.00009	-.002	.048	-.01	5.38	249
7	37.0	.615	.254	.248	-.094	2.54	.441	.196	-.240	3.05	-.01145	-.235	.048	-.26	8.01	499
8	43.8	.726	.453	.244	-.498	3.26	.411	.209	-.013	3.17	-.01368	-.268	.044	-.80	5.01	499
9	50.5	.836	.590	.227	-.380	3.19	.371	.213	.158	3.08	-.01074	-.222	.053	-.93	10.34	499
10	53.9	.892	.656	.221	-.530	3.90	.353	.213	.060	3.17	-.00774	-.164	.054	-1.91	14.50	498
11	-10.4	-.162	-.091	.195	.236	3.13	.196	.239	.058	3.28	.00904	.194	.049	1.09	7.77	243
12	-17.2	-.273	-.010	.191	.041	3.21	.380	.194	-.236	3.25	.00377	.102	.037	-.58	9.15	249
13	-24.0	-.384	.046	.199	.099	2.86	.450	.202	-.198	3.44	.00546	.136	.045	1.16	11.70	498
14	-30.7	-.495	.162	.228	.167	2.81	.445	.211	-.181	3.57	.00154	.032	.052	-.29	9.57	499
15	-37.5	-.606	.275	.242	.042	2.55	.430	.221	-.311	3.51	-.00256	-.048	.053	1.05	10.25	499
16	-44.3	-.717	.434	.254	-.168	2.74	.429	.211	-.066	2.96	-.00832	-.155	.052	-.20	10.28	499
17	-51.0	-.828	.600	.230	-.538	3.64	.378	.203	-.066	3.66	-.00597	-.128	.048	-1.05	21.74	495
18	-56.1	-.912	.679	.225	-.235	3.31	.318	.190	.162	3.46	-.00483	-.113	.041	-.06	9.18	499

TABLE IV-15

AXIAL AND RADIAL VELOCITY DATA AND CORRELATIONS

Test Date: 8/30/82 Run No.: 15 Flow Condition: 1 Geometry: 2

Axial Location: 152 mm (6.0 in.) $x/R_o = 2.498$

P_t No.	r mm +(0=0) -(0=180)	r/R_o	U m/s	u' m/s	S_u	K_u	V m/s	v' m/s	S_v	K_v	$\overline{uv}$ m^2/s^2	R_{uv}	σ_{uv} m^2/s^2	S_{uv}	K_{uv}	N
1	1.7	.039	-.090	.186	.321	2.46	-.095	.256	.544	2.71	-.00682	-.144	.049	.12	5.95	246
2	7.0	.125	-.082	.189	.499	2.96	-.124	.249	.051	2.73	-.01152	-.246	.052	-1.00	8.01	249
3	12.0	.208	-.041	.207	.207	2.83	-.129	.241	.200	2.76	-.01419	-.284	.050	-1.00	8.66	498
4	17.1	.291	.032	.217	.112	2.32	-.165	.263	.204	2.56	-.01685	-.295	.057	-.43	7.12	495
5	22.2	.375	.077	.227	-.014	2.51	-.150	.256	.070	2.96	-.02274	-.391	.056	-1.09	7.30	495
6	27.3	.458	.119	.242	-.018	2.57	-.138	.244	.274	2.69	-.02713	-.458	.056	-1.09	6.32	498
7	32.4	.541	.221	.250	-.191	2.87	-.183	.225	.249	2.75	-.02575	-.457	.056	-1.42	6.04	497
8	37.4	.624	.340	.240	-.354	2.73	-.168	.216	.491	2.78	-.02159	-.417	.056	-1.53	8.16	497
9	42.5	.708	.439	.238	-.454	3.09	-.152	.197	.450	3.19	-.02058	-.440	.057	-2.12	10.39	499
10	47.6	.791	.510	.214	-.624	3.48	-.144	.165	.270	3.02	-.00960	-.273	.039	-1.86	10.00	235
11	-3.2	-.042	-.098	.165	.278	3.04	.110	.237	-.033	2.67	.00644	.165	.041	.22	8.40	247
12	-8.3	-.125	-.092	.182	.490	3.32	.088	.269	-.261	2.68	.00213	.043	.052	-.52	11.23	498
13	-13.4	-.208	-.063	.181	.491	2.96	.066	.266	-.094	2.26	-.00406	-.085	.052	-1.44	9.40	241
14	-18.4	-.291	-.025	.216	.324	2.69	.028	.268	.007	2.31	-.01430	-.247	.057	-1.08	6.57	248
15	-23.5	-.375	.030	.214	.200	2.74	.004	.264	.057	2.47	-.01715	-.304	.057	-1.26	8.38	498
16	-28.6	-.458	.139	.236	.080	2.73	-.068	.255	.255	2.36	-.02553	-.424	.057	-1.23	6.64	249
17	-33.7	-.541	.246	.244	.028	2.52	-.070	.215	-.202	3.03	-.02361	-.449	.047	-1.22	5.91	246
18	-38.8	-.624	.342	.260	.090	2.74	-.048	.224	.154	2.59	-.02752	-.471	.065	-1.63	7.34	242
19	-43.6	.708	.461	.224	-.092	3.19	-.087	.220	.235	2.95	-.02186	-.444	.056	-1.89	8.72	248
20	-48.9	.791	.545	.281	-.445	2.95	-.054	.214	.414	3.09	-.01552	-.258	.067	-.28	7.03	243

TABLE IV-16

AXIAL AND RADIAL VELOCITY DATA AND CORRELATIONS

Test Date: 8/31/82 Run No.: 16 Flow Condition: 1 Geometry: 2

Axial Location: 5 mm (0.2 in.) $x/R_o = 0.083$

P_t No.	r mm +(θ=0) −(θ=180)	r/R_o	U m/s	u' m/s	S_u	K_u	V m/s	v' m/s	S_v	K_v	$\overline{uv}$ m^2/s^2	R_{uv}	σ_{uv} m^2/s^2	S_{uv}	K_{uv}	N
1	1.3	.025	.716	.073	−.303	5.50	−.014	.074	−.577	6.40	.00061	.113	.008	8.07	97.86	242
2	6.6	.111	.652	.124	−.986	4.57	.002	.093	−1.448	7.88	.00371	.321	.013	.89	18.23	241
3	11.7	.194	.284	.370	−.745	2.40	.036	.180	−1.114	7.32	.02176	.326	.066	.37	9.65	243
4	16.8	.277	.762	.316	−.457	3.68	.011	.235	.352	3.24	−.01890	−.254	.082	−.66	7.92	499
5	21.8	.361	1.637	.161	−.487	5.43	.225	.140	−.455	5.09	−.00263	−.117	.025	−1.55	16.87	491
6	26.9	.444	1.556	.151	.022	2.56	.089	.176	.386	2.72	−.00313	−.118	.025	−.22	5.49	999
7	32.0	.527	.516	.258	.104	3.39	.095	.219	.589	3.06	.02499	.442	.063	1.93	8.95	498
8	37.1	.610	−.015	.146	−.222	3.78	−.048	.094	−1.006	7.06	.00273	.198	.014	2.04	15.23	248

TABLE IV-17

AXIAL AND AZIMUTHAL VELOCITY DATA AND CORRELATIONS

Test Date: 8/31/82 Run No.: 17 Flow Condition: 1 Geometry: 2

Axial Location: 5 mm (0.2 in.) x/R_o = 0.083

P_t No.	r mm +(0=90) -(0=270)	r/R_o	U m/s	u' m/s	S_u	K_u	W m/s	w' m/s	S_w	K_w	$\overline{uw}$ m^2/s^2	R_{uw}	σ_{uw} m^2/s^2	S_{uw}	K_{uw}	N
1	-1.5	-.025	.718	.072	-.364	3.54	.012	.094	-2.254	25.01	-.00037	-.055	.006	-.33	11.12	242
2	4.1	.067	.672	.112	-1.858	10.04	-.007	.094	-.384	4.44	.00105	.099	.020	.89	41.52	241
3	10.9	.178	.211	.401	-.534	2.11	.017	.161	-.268	6.39	-.00387	-.060	.064	1.09	12.69	247
4	17.6	.289	.926	.289	-.443	2.92	.807	.226	-.387	3.63	.01292	.198	.073	2.02	19.15	249
5	24.4	.400	1.547	.137	.029	2.95	.807	.141	-.262	3.07	.00202	.105	.020	.52	6.93	499
6	31.2	.511	.937	.296	-.190	2.87	.557	.270	.114	3.65	.00416	.052	.078	.07	8.28	499
7	37.9	.622	-.008	.115	-.229	3.45	.431	.123	-.314	3.46	-.00190	-.134	.017	-1.27	21.08	249
8	44.7	.733	-.061	.145	-.996	4.13	.417	.115	-.104	2.99	.00107	.065	.021	2.62	29.12	249
9	51.5	.844	-.085	.181	-1.056	4.14	.430	.132	-.154	4.37	.00113	.048	.027	2.08	29.37	248
10	-9.4	-.155	.635	.146	-1.109	6.14	.018	.098	.612	6.48	-.00391	-.273	.023	-4.99	42.71	238
11	-16.2	-.266	.497	.269	-.024	2.94	.487	.320	.082	4.43	.01315	.153	.075	.75	5.96	248
12	-23.0	-.377	1.672	.127	-.699	4.17	.910	.095	-.080	3.48	.00127	.105	.014	3.38	31.26	499
13	-29.8	-.488	1.639	.162	-1.029	5.90	.782	.139	-.490	4.88	.00700	.310	.035	7.07	78.79	249
14	-36.5	-.599	.006	.135	-.003	3.20	.449	.169	-.223	4.01	-.00133	-.058	.026	-.83	9.48	249
15	-43.3	-.710	-.025	.139	-.565	3.47	.404	.175	-.961	5.50	.00105	.076	.029	1.14	11.93	247
16	-50.1	-.821	-.020	.160	-.730	4.32	.429	.135	.233	3.50	-.00109	-.050	.025	-.55	9.74	249
17	-56.8	-.932	-.001	.158	-1.274	5.39	.414	.114	.102	3.76	.00081	.045	.025	.42	17.68	249
18	7.5	.123	.615	.137	-1.148	5.09	.010	.096	.411	5.54	.00122	.093	.024	-1.11	42.96	231
19	14.2	.234	.155	.317	-.264	2.96	.224	.260	-.370	4.09	.00948	.115	.087	1.28	6.59	249
20	21.0	.345	1.557	.149	-.170	3.41	1.010	.122	.047	3.57	.00169	.093	.019	.11	10.17	499
21	27.8	.456	1.558	.174	.158	2.46	.633	.144	.226	3.12	-.00442	-.176	.023	-.40	6.60	499
22	34.6	.567	-.016	.156	-.217	3.24	.458	.129	-.162	3.90	-.00246	-.121	.023	-.19	13.09	499
23	-12.8	-.210	.310	.365	-1.059	3.48	.042	.171	.862	4.26	-.00953	-.153	.071	-.98	12.26	245
24	-19.6	-.321	1.399	.188	-.809	4.43	1.016	.152	-.093	3.67	.00334	.117	.030	.28	11.53	248
25	-26.4	-.432	1.772	.109	-.343	3.87	.792	.105	-1.097	6.27	.00167	.146	.012	1.12	11.75	249
26	-33.2	-.543	.024	.153	-.475	4.36	.444	.141	-.030	3.26	.00056	.026	.024	.30	11.37	248
27	22.7	.372	1.628	.144	.064	3.20	.924	.134	-.254	3.53	.00142	.074	.023	.10	11.63	994
28	26.1	.428	1.519	.157	-.109	2.75	.697	.150	.136	3.18	-.00013	-.005	.025	-.22	12.69	998
29	-28.1	-.460	1.756	.108	-.402	3.07	.776	.127	-.824	4.25	.00209	.151	.017	1.56	17.79	997
30	-24.7	-.405	1.730	.122	-.144	3.82	.849	.094	-.599	4.84	.00027	.023	.014	1.16	21.97	994
31	29.5	.483	1.507	.197	-.052	2.92	.603	.178	.237	3.84	-.00533	-.152	.034	-1.34	24.36	998
32	25.3	.414	1.531	.158	-.004	3.23	.750	.151	-.009	3.05	.00026	.011	.024	-.89	10.05	996
33	-33.2	-.543	1.342	.303	.572	3.58	.565	.284	.050	3.58	.00295	.034	.090	-1.06	16.00	999
34	12.6	.206	.031	.368	.314	3.60	.127	.264	.340	5.62	.00166	.017	.089	1.67	10.66	248

TABLE IV-20

AXIAL VELOCITY, CONCENTRATION AND MASS TRANSPORT DATA AND CORRELATIONS

Test Date: 9/20/82 Run No.: 20 Flow Condition: 1 Geometry: 2

Axial Location: 13 mm (0.5 in.) $x/R_o = 0.208$

P_t No.	r mm +(θ=90) -(θ=270)	r/R_o	U m/s	u' m/s	$S_{u'}$	$K_{u'}$	f	f'	S_f	K_f	$\overline{uf}$ m/s	R_{uf}	σ_{uf} m/s	S_{uf}	K_{uf}	N
2	.0	.000	.704	.085	-.422	4.34	1.000	.027	-7.437	129.50	-.00019	-.083	.003	-16.95	402.80	928
3	5.6	.092	.671	.109	-.667	4.26	.959	.042	-6.762	60.62	.00040	.085	.006	4.61	99.01	970
4	12.4	.203	.403	.338	-.858	4.31	.899	.175	-2.164	7.38	.02045	.346	.078	4.30	29.26	986
5	19.2	.314	.919	.345	-.330	3.00	.170	.103	1.339	5.38	-.00280	-.079	.037	-1.77	20.39	997
6	25.9	.425	1.716	.159	-.704	3.71	.010	.004	1.221	8.92	-.00001	-.014	.001	-.13	12.98	994
7	32.7	.536	1.191	.365	-.509	3.48	.021	.008	.562	3.66	-.00020	-.072	.003	-.24	11.37	998
8	.0	.000	.700	.090	-.170	3.96	1.000	.022	-4.912	65.73	-.00007	-.035	.002	-8.71	129.50	990
9	39.5	.647	.007	.157	-.310	3.38	.051	.010	.450	3.41	-.00024	-.157	.002	-1.85	14.37	992
10	46.2	.758	-.036	.190	-.242	4.10	.053	.010	.611	4.02	-.00013	-.066	.002	-.14	19.97	985
11	53.0	.869	-.117	.221	-.477	3.09	.058	.013	1.250	7.05	.00008	.029	.003	-3.94	65.84	997
12	56.4	.925	-.140	.248	-.893	3.19	.061	.012	1.143	6.35	.00003	.010	.003	-.74	11.35	983
14	-4.9	-.081	.692	.185	-1.049	12.28	.823	.037	-8.285	112.50	.00020	.029	.006	-2.32	148.40	986
15	-9.0	-.148	.591	.263	-1.615	7.25	.865	.082	-4.799	29.75	.00406	.189	.038	10.93	152.20	993
16	-15.8	-.259	.323	.375	.382	3.31	.417	.175	-.122	2.24	.00344	.053	.066	-.67	10.98	998
17	-22.5	-.370	1.619	.167	-.503	3.72	.010	.024	4.261	26.66	-.00021	-.051	.005	-4.52	73.24	999
18	-29.3	-.481	1.765	.149	-.473	3.73	.000	.003	.500	5.62	-.00002	-.044	.000	.18	13.77	991
19	-36.1	-.592	-.002	.154	.026	4.57	.032	.010	8.483	163.20	-.00004	-.027	.001	-5.62	109.90	993
20	-42.9	-.703	-.018	.164	-.628	4.06	.031	.007	.774	4.11	-.00011	-.092	.001	-1.49	13.79	989
21	-49.6	-.814	-.045	.202	-.730	4.21	.031	.008	.486	3.23	.00009	.054	.002	.53	13.09	991
22	-56.4	-.925	-.027	.211	-1.053	4.15	.031	.008	.765	4.87	.00012	.075	.002	.47	13.42	998
23	34.4	.564	.248	.298	.718	3.67	.034	.009	.478	3.50	-.00017	-.067	.003	-.81	9.04	997
24	-31.0	-.508	1.265	.311	-1.041	4.39	.007	.005	.797	4.36	-.00015	-.077	.002	-.66	9.66	995
25	-27.6	-.453	1.809	.135	-.675	4.80	-.000	.002	.428	5.63	-.00001	-.031	.000	.00	.00	966
26	24.2	.397	1.639	.159	-.167	3.08	.014	.010	8.439	141.30	.00006	.036	.002	-3.38	137.10	985
28	-14.1	-.231	.153	.368	.133	3.34	.708	.237	-.786	2.60	.02460	.282	.088	.35	7.92	993
29	-54.7	-.897	-.006	.261	.530	7.42	.034	.009	1.363	9.35	.00003	.012	.002	-1.40	18.77	992
30	.0	.000	.689	.083	-.233	4.00	1.001	.036	-8.832	105.30	-.00016	-.053	.005	-7.04	180.60	992

TABLE IV-21

AXIAL VELOCITY, CONCENTRATION AND MASS TRANSPORT DATA AND CORRELATIONS

Test Date: 9/22/82 Run No.: 21 Flow Condition: 1 Geometry: 2

Axial Location: 13 mm (0.5 in.) x/R_o = 0.208

P_t No.	r mm +(θ=90) -(θ=270)	r/R_o	U m/s	u' m/s	$S_{u'}$	$K_{u'}$	f	f'	S_f	K_f	$\overline{uf}$ m/s	R_{uf}	σ_{uf} m/s	S_{uf}	K_{uf}	N
1	.0	.000	.729	.088	-.165	4.32	1.000	.038	-5.895	72.92	.00012	.035	.004	5.92	95.97	982
2	5.6	.092	.662	.160	-2.302	10.76	1.046	.037	-5.038	59.00	.00012	.020	.010	15.47	325.00	995
3	12.4	.203	1.361	.388	-.497	3.30	1.011	.169	-2.345	8.41	.02162	.330	.087	3.03	29.84	995
4	19.2	.314	.909	.357	-.464	3.05	.455	.160	.517	2.87	-.00138	-.024	.055	-.04	6.77	999
5	.0	.000	.734	.086	-.554	5.14	1.001	.027	-7.974	138.20	-.00002	-.007	.002	-.85	26.24	947
6	-2.2	-.037	.711	.148	-2.663	15.92	1.044	.033	-5.014	43.94	.00030	.061	.006	10.89	203.10	994
7	-9.0	-.148	.602	.256	-1.518	5.47	1.010	.118	-3.223	15.75	.00484	.160	.041	7.31	89.92	970
8	-15.8	-.259	.263	.346	.335	2.62	.330	.186	.638	2.89	.00711	.110	.063	.96	8.49	995
9	.0	.000	.600	.248	-1.454	3.53	1.000	.030	-5.574	61.05	-.00035	-.039	.007	-.43	57.34	995
10	.0	.000	.703	.131	-3.284	18.75	1.000	.055	-1.319	18.12	.00019	.026	.013	6.76	157.40	995
12	32.7	.536	1.182	.347	-.319	2.70	.026	.008	.241	3.66	-.00013	-.044	.003	-.21	7.45	998
13	39.5	.647	-.003	.146	-.152	4.36	.044	.010	.409	3.29	-.00006	-.043	.001	-1.52	16.66	993
14	.0	.000	.723	.085	-.192	5.39	.999	.031	-2.748	18.83	-.00009	-.033	.003	-1.84	51.98	990
15	-22.5	-.370	1.616	.171	-.241	3.15	-.001	.009	11.140	187.20	.00006	.041	.000	.00	.00	998
16	-29.3	-.481	1.770	.155	-.780	4.40	.006	.006	.543	4.01	-.00008	-.079	.001	-1.55	14.83	999
17	-36.1	-.592	.002	.110	-.278	10.36	.033	.010	.535	5.23	-.00007	-.059	.001	-1.41	25.01	982
18	.0	.000	.723	.091	-.808	6.19	1.000	.051	-6.968	74.86	-.00029	-.062	.008	-8.08	267.80	945
19	.0	.000	.725	.088	.487	6.86	1.000	.033	-.732	4.61	-.00002	-.009	.003	-1.78	39.27	972
20	46.2	.758	-.047	.164	-2.215	8.57	.070	.011	.746	4.44	-.00006	-.034	.002	-.80	20.59	984
21	53.0	.869	-.113	.214	-.629	3.23	.071	.012	1.016	6.26	.00014	.057	.003	1.31	36.67	999
22	56.4	.925	-.114	.234	-.732	3.17	.072	.012	.773	4.09	.00004	.013	.003	-.18	8.43	999
23	.0	.000	.741	.087	-.380	3.39	1.000	.021	-3.168	53.16	.00004	.021	.002	6.97	151.40	911
24	-42.9	-.703	.022	.213	2.245	14.59	.051	.009	.534	4.49	-.00006	-.031	.002	3.17	132.00	998
25	-49.6	-.814	-.058	.189	-.741	3.78	.047	.010	1.615	11.73	.00002	.010	.002	-.31	19.12	996
26	-56.4	-.925	-.032	.212	-1.177	4.20	.046	.007	.459	3.68	-.00001	-.010	.001	-.91	15.74	994
27	.0	.000	.684	.202	-2.449	10.13	1.001	.036	-7.391	96.31	.00017	.023	.009	15.74	402.80	994
28	14.1	.231	.194	.359	-.127	2.62	.976	.181	-1.647	5.27	.02373	.366	.073	1.98	13.36	993
29	34.4	.564	.394	.347	.411	3.01	.041	.010	.498	3.61	-.00016	-.048	.003	-.00	11.74	997
30	-19.2	-.314	1.168	.319	-.629	3.43	.061	.060	2.232	9.22	-.00121	-.064	.021	-3.59	38.92	999
31	.0	.000	.735	.094	.053	5.75	1.000	.027	-8.716	171.00	-.00008	-.033	.002	-3.52	84.56	933

ORIGINAL PAGE IS
OF POOR QUALITY

TABLE IV-22

AXIAL VELOCITY, CONCENTRATION AND MASS TRANSPORT DATA AND CORRELATIONS

Test Date: 9/22/82   Run No.: 22   Flow Condition: 1   Geometry: 2

Axial Location: 25 mm (1.0 in.) x/R_o = 0.416

P_t No.	r mm +(0=90) -(0=270)	r/R_o	U m/s	u' m/s	$S_{u'}$	$K_{u'}$	f	f'	S_f	K_f	$\overline{uf}$ m/s	R_{uf}	σ_{uf} m/s	S_{uf}	K_{uf}	N
3	.0	.000	.516	.186	-1.619	7.64	.977	.118	-3.003	13.47	.00516	.236	.039	9.17	110.60	987
4	5.6	.092	.464	.254	-1.229	6.33	.974	.164	-2.603	9.61	.01420	.341	.075	3.51	32.48	992
5	12.4	.203	.209	.421	.122	3.60	.862	.269	-.981	2.74	.05449	.482	.115	.65	9.52	995
6	-2.2	-.037	.533	.213	-.477	7.25	.964	.128	-2.890	11.67	.00400	.147	.040	3.35	71.41	988
7	-9.0	-.148	.419	.321	-.604	4.32	.934	.214	-1.839	5.77	.01372	.200	.089	1.13	21.70	988
8	19.2	.314	.145	.452	.225	2.97	.425	.213	.889	3.02	.01779	.184	.093	.93	9.93	996
9	25.9	.425	1.400	.320	-1.147	5.10	.140	.089	1.515	5.56	.00009	.003	.028	.10	23.84	999
10	32.7	.536	1.676	.193	-.425	3.64	.038	.014	4.232	33.63	.00001	.005	.003	6.30	137.70	996
11	39.5	.647	.454	.333	.352	3.35	.050	.012	.380	3.24	-.00059	-.150	.004	-.26	8.83	999
12	46.2	.758	.067	.244	-.118	3.42	.059	.012	1.485	9.41	-.00026	-.090	.003	-1.01	24.52	996
13	53.0	.869	-.177	.296	.315	3.96	.058	.013	1.139	6.05	.00012	.032	.004	1.95	32.49	998
14	56.4	.925	-.335	.316	-.270	2.27	.062	.014	1.941	11.96	.00045	.100	.005	1.15	24.71	999
18	-22.5	-.370	1.032	.431	-.534	3.35	.165	.109	.842	3.86	-.00204	-.044	.045	-.38	6.61	997
19	-29.3	-.481	1.656	.193	-.225	3.33	.018	.021	7.457	73.80	.00007	.018	.006	7.21	165.20	997
20	-36.1	-.592	.807	.364	.114	2.80	.033	.009	.542	3.46	-.00051	-.148	.004	-.71	9.33	999
21	-42.9	-.703	.074	.217	.729	6.06	.050	.011	.973	4.89	-.00029	-.116	.002	-1.57	16.57	997
22	-49.6	-.814	-.037	.253	.038	5.37	.046	.011	.838	4.41	.00011	.041	.003	.24	10.70	998
23	-56.4	-.925	-.359	.347	-.272	2.12	.046	.013	1.633	8.16	.00036	.080	.004	.30	8.82	999
25	34.4	.564	1.583	.253	-.723	4.15	.027	.013	5.249	65.15	-.00013	-.040	.004	6.45	235.50	999
26	41.2	.675	.246	.260	.074	3.87	.051	.013	.486	4.91	-.00048	-.144	.003	-1.65	18.44	999
27	44.6	.730	.109	.242	-.199	4.01	.057	.011	.566	4.35	-.00025	-.092	.003	-1.41	22.44	996
28	14.1	.231	-.163	.359	.774	3.78	.572	.286	.275	1.94	.03180	.310	.105	.82	6.88	998
29	15.8	.259	-.139	.372	.680	3.64	.516	.265	.417	2.03	.02800	.284	.104	1.04	7.62	995
30	17.5	.286	-.095	.382	.670	4.17	.442	.237	.605	2.44	.01935	.214	.089	.82	9.49	996

ORIGINAL PAGE IS
OF POOR QUALITY

TABLE IV-23

AXIAL VELOCITY, CONCENTRATION AND MASS TRANSPORT DATA AND CORRELATIONS

Test Date: 9/23/82 Run No.: 23 Flow Condition: 1 Geometry: 2

Axial Location: 51 mm (2.0 in.) $x/R_o = 0.833$

P_t No.	r mm +(θ=90) -(θ=270)	r/R_o	U m/s	u' m/s	$S_{u'}$	$K_{u'}$	f	f'	S_f	K_f	$\overline{uf}$ m/s	R_{uf}	σ_{uf} m/s	S_{uf}	K_{uf}	N
2	.0	.000	-.043	.282	.195	2.98	.503	.308	.111	1.62	.02776	.319	.085	.20	4.51	993
3	5.6	.092	-.106	.293	.551	3.18	.445	.296	.421	1.84	.02986	.345	.091	.81	6.54	992
4	12.4	.203	-.190	.264	.876	3.65	.363	.278	.878	2.56	.02284	.311	.076	1.26	8.91	999
5	19.2	.314	-.251	.255	.767	4.51	.312	.238	1.275	3.67	.01269	.209	.061	1.34	12.99	996
6	25.9	.425	-.034	.441	.868	3.73	.210	.140	2.074	8.27	.00442	.071	.055	2.06	22.47	999
7	32.7	.536	.821	.582	-.326	2.48	.158	.109	1.319	5.63	.00411	.065	.061	.16	10.79	999
10	46.2	.758	.972	.369	-.209	3.53	.042	.037	3.279	18.25	.00081	.060	.013	1.04	23.56	999
11	53.0	.869	.152	.447	-.163	2.73	.042	.025	4.047	37.92	-.00019	-.017	.011	1.87	31.44	998
12	56.4	.925	-.353	.396	.457	3.16	.050	.025	2.365	13.78	-.00023	-.023	.011	1.07	46.41	999
13	-2.2	-.037	-.037	.324	.748	4.63	.508	.322	.183	1.56	.03144	.301	.109	-.77	9.28	994
14	-9.0	-.148	-.018	.382	1.107	5.53	.467	.328	.348	1.62	.03177	.253	.132	1.33	12.21	988
15	-15.8	-.259	-.122	.343	.896	3.80	.389	.308	.699	2.02	.03383	.319	.109	.90	7.03	991
16	-22.5	-.370	-.156	.340	.937	4.16	.277	.238	1.362	3.79	.02357	.292	.099	2.85	18.28	998
18	-29.3	-.481	.332	.554	.295	2.73	.186	.133	2.095	9.02	.00703	.095	.069	1.21	18.35	999
19	-36.1	-.592	1.150	.525	-.610	3.25	.121	.103	1.743	9.04	.00397	.073	.048	.45	10.96	999
20	-42.9	-.703	1.190	.371	-.441	3.54	.060	.071	2.517	11.25	.00148	.056	.026	.89	22.23	999
21	-49.6	-.814	.564	.414	-.212	3.05	.041	.039	4.576	32.00	.00046	.029	.016	1.76	44.92	999
23	-56.4	-.925	-.423	.388	.744	4.22	.041	.031	4.851	44.81	-.00064	-.053	.011	.65	70.37	999
24	41.2	.675	1.297	.354	-.545	3.68	.047	.049	4.443	36.62	-.00033	-.019	.016	-.32	24.18	999
25	9.0	.148	-.066	.354	1.285	5.71	.419	.284	.503	1.85	.02740	.272	.095	.13	6.52	996
26	22.5	.370	-.159	.380	1.396	5.51	.241	.184	1.859	6.22	.00555	.080	.071	3.26	35.46	977
27	10.7	.175	-.109	.330	1.130	5.01	.419	.288	.618	2.08	.03190	.336	.099	1.40	11.49	984
28	5.6	.092	-.044	.326	1.022	6.00	.495	.305	.193	1.64	.03304	.333	.099	.28	10.57	999

ORIGINAL PAGE IS
OF POOR QUALITY

TABLE IV-24

AXIAL VELOCITY, CONCENTRATION AND MASS TRANSPORT DATA AND CORRELATIONS

Test Date: 9/23/82 Run No.: 24 Flow Condition: 1 Geometry: 2

Axial Location: 102 mm (4.0 in.) $x/R_o = 1.665$

P_t No.	r mm +(0=90) -(0=270)	r/R_o	U m/s	u' m/s	$S_{u'}$	$K_{u'}$	f	f'	S_f	K_f	$\overline{uf}$ m/s	R_{uf}	σ_{uf} m/s	S_{uf}	K_{uf}	N
3	.0	.000	-.332	.178	1.047	5.95	.111	.016	.701	5.49	-.00006	-.021	.003	.10	13.09	986
4	5.6	.092	-.343	.190	1.336	7.70	.113	.016	.874	5.95	.00006	.019	.003	1.03	26.03	991
5	12.4	.203	-.330	.171	.499	3.51	.119	.022	5.162	74.83	-.00014	-.037	.004	7.38	140.80	972
6	19.2	.314	-.296	.186	.598	3.70	.124	.021	1.418	8.63	-.00017	-.044	.004	2.71	52.28	980
7	25.9	.425	-.227	.221	.817	4.61	.124	.023	.800	5.15	-.00011	-.022	.005	-.25	15.05	990
8	32.7	.536	-.116	.270	.697	3.63	.128	.031	2.132	17.57	-.00062	-.075	.009	-2.53	43.59	995
9	39.5	.647	.151	.322	.363	3.27	.129	.035	.985	4.60	-.00141	-.125	.011	-.03	11.40	997
10	46.2	.758	.481	.326	-.202	2.71	.123	.041	1.020	4.51	-.00087	-.064	.013	-.94	10.64	995
12	53.0	.869	.834	.269	-.017	3.39	.124	.046	1.382	6.67	.00024	.020	.013	.30	17.86	999
13	56.4	.925	.956	.249	-.121	2.92	.131	.045	1.152	4.93	.00079	.071	.011	.41	7.92	999
14	-2.2	-.037	-.344	.160	.505	4.00	.109	.019	4.796	67.42	-.00001	-.005	.003	4.29	92.79	999
15	-9.0	-.148	-.307	.166	.604	4.16	.110	.016	1.012	7.50	-.00015	-.055	.003	-1.25	16.38	997
16	-15.8	-.259	-.276	.171	.550	3.74	.104	.016	.241	3.90	-.00019	-.069	.003	-.74	9.57	995
17	-22.5	-.370	-.233	.198	.188	2.90	.103	.020	1.596	13.14	-.00004	-.011	.004	4.71	86.26	998
18	-29.3	-.481	-.105	.256	.521	3.71	.109	.024	1.005	6.46	-.00071	-.114	.007	-1.49	16.73	995
19	-36.1	-.592	.105	.306	.453	3.42	.111	.033	1.542	8.58	-.00090	-.090	.010	-.91	16.20	999
20	-42.9	-.703	.483	.330	-.028	3.28	.107	.038	1.788	10.03	-.00046	-.037	.013	-.44	22.77	996
21	-49.6	-.814	.811	.271	-.019	3.23	.106	.044	1.515	7.12	.00071	.060	.012	.89	14.66	998
22	-56.4	-.925	1.101	.258	-.162	2.80	.093	.036	1.190	5.65	.00017	.018	.009	.40	10.21	999

ORIGINAL PAGE IS
OF POOR QUALITY

TABLE IV-25

AXIAL VELOCITY, CONCENTRATION AND MASS TRANSPORT DATA AND CORRELATIONS

Test Date: 9/24/82 Run No.: 25 Flow Condition: 1 Geometry: 2

Axial Location: 152 mm (6.0 in.) $x/R_o = 2.498$

P_t No.	r mm +(θ=90) -(θ=270)	r/R_o	U m/s	u' m/s	S_u'	K_u'	f	f'	S_f	K_f	$\overline{uf}$ m/s	R_{uf}	σ_{uf} m/s	S_{uf}	K_{uf}	N
3	.0	.000	-.082	.205	.615	4.04	.101	.014	-.001	3.55	-.00016	-.059	.003	-1.58	17.28	968
4	5.6	.092	-.095	.193	.523	3.71	.095	.014	.659	5.29	-.00002	-.009	.002	.79	11.08	959
5	17.4	.203	-.066	.198	.539	4.36	.104	.016	.801	5.65	-.00021	-.064	.003	-.12	14.46	963
6	19.2	.314	-.020	.202	.762	5.24	.107	.020	.778	4.08	-.00006	-.015	.004	.21	12.42	985
7	25.9	.425	.044	.229	.435	4.04	.102	.020	.719	4.50	-.00005	-.010	.004	.34	13.12	986
8	32.7	.536	.124	.259	.710	4.15	.105	.022	.613	3.82	-.00009	-.015	.006	2.49	37.22	987
9	39.5	.647	.242	.301	.534	3.85	.109	.028	1.045	5.19	-.00043	-.051	.008	-.10	14.74	988
10	46.2	.758	.451	.288	.110	4.24	.109	.028	.591	3.94	.00012	.015	.009	1.66	38.94	992
12	53.0	.869	.630	.240	-.375	3.04	.111	.033	.849	3.97	.00082	.104	.008	.69	8.47	998
13	56.4	.925	.683	.224	-.535	3.71	.113	.032	.940	4.35	.00049	.069	.007	.55	9.79	998
14	-56.4	-.925	.704	.250	-.512	4.69	.087	.027	1.061	5.22	.00040	.060	.007	-.16	23.09	992
17	-56.4	-.925	.660	.327	-1.374	6.01	.083	.028	.978	4.14	.00090	.100	.009	.27	15.64	982
18	-49.6	-.814	.612	.322	-.422	5.21	.089	.028	1.067	4.98	.00047	.052	.009	.02	16.64	995
19	-42.9	-.703	.434	.316	-.195	3.33	.093	.025	.939	4.87	.00027	.035	.007	.42	7.91	995
20	-36.1	-.592	.295	.289	.532	4.56	.097	.023	.718	3.96	-.00004	-.006	.006	1.47	23.42	993
21	-29.3	-.481	.170	.247	.477	3.28	.094	.019	.551	4.69	-.00037	-.077	.005	-.18	8.71	968
22	-22.5	-.370	.076	.241	1.033	5.50	.092	.018	.698	4.44	.00002	.004	.004	1.29	18.17	991
23	-15.8	-.259	.018	.206	.685	4.30	.088	.015	.496	4.32	-.00034	-.109	.003	-.89	11.53	948
27	-9.0	-.148	-.057	.185	.352	3.59	.101	.015	.373	4.13	-.00005	-.017	.003	-.31	10.55	929
28	-2.2	-.037	-.080	.186	.274	3.84	.099	.015	.373	5.08	-.00008	-.028	.003	-.78	15.19	977
29	15.8	.259	-.037	.202	.442	4.51	.109	.018	.676	5.05	-.00006	-.018	.004	.00	18.04	973

ORIGINAL PAGE IS
OF POOR QUALITY

TABLE IV-26

AXIAL VELOCITY, CONCENTRATION AND MASS TRANSPORT DATA AND CORRELATIONS

Test Date: 9/24/82 Run No.: 26 Flow Condition: 1 Geometry: 2

Axial Location: 203 mm (8.0 in.) $x/R_o = 3.331$

P_t No.	r mm +(θ=90) −(θ=270)	r/R_o	U m/s	u' m/s	$S_{u'}$	$K_{u'}$	f	f'	S_f	K_f	$\overline{uf}$ m/s	R_{uf}	σ_{uf} m/s	S_{uf}	K_{uf}	N
1	.0	.000	.151	.180	.330	3.82	.095	.013	.154	3.82	.00006	.026	.002	.06	14.79	973
2	5.6	.092	.158	.216	.966	5.65	.093	.012	.158	3.62	.00026	.100	.003	-2.24	57.05	989
3	12.4	.203	.168	.265	1.893	9.57	.101	.015	.421	4.10	.00011	.027	.004	2.21	28.23	994
4	19.2	.314	.192	.211	1.105	5.56	.103	.016	.774	4.00	-.00011	-.032	.003	.01	12.67	988
5	25.9	.425	.232	.208	.774	4.52	.108	.021	.913	5.57	.00005	.012	.004	-.65	12.65	979
7	32.7	.536	.302	.206	.411	3.65	.109	.022	.605	3.56	.00003	.006	.005	1.05	13.25	998
8	39.5	.647	.365	.220	.438	4.20	.112	.023	.475	3.78	-.00003	-.006	.005	-.72	20.81	998
9	46.2	.758	.431	.240	.672	5.69	.109	.026	1.117	6.89	-.00006	-.009	.006	.78	13.68	999
10	53.0	.869	.475	.236	.063	3.76	.112	.027	.970	5.29	-.00007	-.012	.007	-.55	13.30	986
11	56.4	.925	.459	.241	-.703	4.57	.112	.025	.761	3.91	.00027	.044	.006	-.00	10.07	994
12	-56.4	-.925	.403	.243	-.668	4.50	.087	.020	.603	3.65	.00016	.032	.005	-.00	8.55	994
15	-49.6	-.814	.497	.220	-.268	3.28	.086	.022	.964	5.52	.00035	.074	.005	1.42	24.86	985
16	-42.9	-.703	.456	.219	.190	3.89	.088	.020	.745	4.24	.00010	.022	.005	1.92	20.72	996
17	-36.1	-.592	.400	.245	.643	5.50	.087	.020	.725	4.69	-.00002	-.004	.005	1.13	18.67	990
18	-29.3	-.481	.316	.212	.472	4.32	.085	.016	.714	4.94	-.00010	-.028	.004	1.37	27.78	988
19	-22.5	-.370	.278	.195	.235	3.74	.089	.015	.082	3.25	-.00013	-.046	.003	.32	10.73	996
20	-15.0	-.246	.255	.206	1.066	6.00	.088	.013	.137	3.61	.00010	.035	.003	.35	16.50	986

TABLE IV-27

AZIMUTHAL VELOCITY, CONCENTRATION AND MASS TRANSPORT DATA AND CORRELATIONS

Test Date: 10/7/82   Run No.: 27   Flow Condition: 1   Geometry: 2

Axial Location: 25 mm (1.0 in.) $x/R_o = 0.416$

P_t No.	r mm +(θ=90) −(θ=270)	r/R_o	W m/s	w' m/s	S_w	K_w	f	f'	S_f	K_f	$\overline{wf}$ m/s	R_{wf}	σ_{wf} m/s	S_{wf}	K_{wf}	N
2	.0	.000	-.019	.122	-.143	4.86	.950	.120	-2.847	12.27	-.00122	-.083	.018	-1.38	28.79	490
3	4.3	.070	-.013	.122	1.016	6.23	.937	.143	-3.037	13.04	-.00264	-.151	.028	-6.58	70.01	492
4	11.0	.181	-.005	.117	.932	5.93	.833	.245	-1.441	3.81	-.00660	-.231	.030	-2.22	13.81	484
5	-7.7	-.125	.013	.118	.108	4.82	.843	.148	-2.531	9.05	.00020	.011	.018	1.62	32.79	486
6	-14.4	-.236	.010	.218	-.772	7.46	.591	.251	-.480	1.90	.00040	.007	.056	.87	15.04	982
7	-21.2	-.347	.331	.411	-.696	4.30	.252	.166	.973	3.53	.00409	.060	.068	-.57	12.71	987
8	17.8	.292	.045	.225	.391	4.09	.453	.239	.559	2.17	-.00364	-.067	.050	.04	7.14	970
10	24.6	.403	.569	.363	-.202	3.42	.161	.104	1.404	5.64	.00117	.031	.036	1.42	15.41	996
11	31.3	.514	.644	.157	.084	5.70	.027	.019	2.583	17.94	-.00004	-.013	.003	.13	22.33	990
12	38.1	.625	.524	.347	.401	4.07	.027	.013	.345	3.11	-.00005	-.010	.005	-.36	11.35	989
13	44.9	.736	.414	.244	.369	3.88	.036	.012	.771	4.26	-.00010	-.033	.003	-.30	12.12	977
14	51.7	.847	.400	.229	-.073	2.93	.039	.016	2.407	15.30	.00022	.057	.004	2.54	43.73	499
15	58.4	.958	.344	.232	.017	3.17	.043	.018	1.352	7.60	.00001	.003	.004	-.46	12.13	499
17	-28.0	-.458	.724	.200	-1.197	7.60	.032	.068	2.222	9.50	.00068	.050	.012	.21	16.87	988
18	-34.7	-.569	.470	.312	-.412	3.68	-.008	.006	1.574	11.52	-.00013	-.068	.000	.00	.00	985
22	-48.3	-.791	.391	.229	-.395	3.51	.037	.013	1.079	5.41	-.00005	-.015	.003	-.26	12.00	999
24	-28.0	-.458	.739	.161	-.497	5.95	.074	.069	1.660	5.83	-.00005	-.004	.012	-1.17	36.81	998
26	-41.5	-.680	.397	.221	-.280	4.18	.050	.010	.391	3.80	-.00008	-.036	.002	-1.22	18.84	991
27	31.3	.514	.647	.151	.285	4.73	.056	.017	2.034	15.23	.00007	.028	.003	.32	19.90	997
28	38.1	.625	.479	.311	.138	3.21	.057	.012	.262	3.57	-.00009	-.024	.004	-.46	10.74	959
29	44.9	.736	.414	.212	-.111	3.44	.065	.012	.775	4.40	-.00008	-.034	.002	.03	9.35	995
30	24.6	.403	.600	.345	-.403	4.23	.172	.086	1.462	5.62	-.00087	-.029	.031	.63	30.37	997
31	-14.4	-.236	.039	.199	-.302	6.50	.727	.249	-.782	2.21	-.00713	-.144	.047	.26	9.34	497

ORIGINAL PAGE IS
OF POOR QUALITY

TABLE IV-28

RADIAL VELOCITY, CONCENTRATION AND MASS TRANSPORT DATA AND CORRELATIONS

Test Date: 10/7/82 Run No.: 28 Flow Condition: 1 Geometry: 2

Axial Location: 25 mm (1.0 in.) $x/R_o = 0.416$

P_t No.	r mm +(θ=0) -(θ=180)	r/R_o	V m/s	v' m/s	S_v	K_v	f	f'	S_f	K_f	$\overline{vf}$ m/s	R_{vf}	σ_{vf} m/s	S_{vf}	K_{vf}	N
1	.0	.000	-.019	.118	.870	6.25	.977	.107	-2.880	11.39	-.00012	-.010	.022	-1.56	42.16	488
2	2.9	.047	.015	.110	.028	7.45	.988	.133	-3.010	13.86	.00201	.137	.026	1.10	54.69	491
3	7.9	.130	.059	.132	.222	4.42	.837	.196	-1.461	4.38	.00220	.085	.028	-1.30	18.22	487
4	-5.4	-.089	.073	.133	-.413	8.33	1.005	.128	-2.682	10.75	.00233	.137	.020	-.65	30.73	496
6	-5.4	-.089	.066	.134	-.588	7.75	1.012	.133	-2.731	10.92	.00280	.157	.021	4.82	40.52	494
7	-5.4	-.089	.059	.131	-.312	5.97	.993	.135	-2.596	10.47	.00315	.178	.027	3.98	63.24	981
8	-10.5	-.177	.096	.155	-.654	5.18	.886	.216	-1.588	4.60	.00934	.278	.038	2.12	16.64	992
9	-15.6	-.255	.089	.226	-1.202	6.46	.704	.267	-.539	1.95	.01873	.310	.057	1.39	15.03	995
10	-20.7	-.339	.101	.344	-.309	4.07	.365	.192	.810	3.09	.00667	.101	.064	1.27	8.91	997
11	-25.7	-.422	.473	.267	-.572	4.41	.132	.117	1.361	5.53	-.00263	-.084	.035	.83	49.13	991
12	-30.8	-.505	.633	.198	.169	3.83	.009	.029	4.961	29.58	.00028	.048	.006	3.76	75.05	998
13	-35.9	-.588	.562	.383	-.520	3.73	.015	.009	.556	3.25	-.00028	-.078	.004	-.65	13.20	999
14	-41.0	-.671	.040	.277	.297	5.07	.036	.010	-.098	3.94	-.00027	-.099	.003	-2.78	30.23	994
15	-46.1	-.755	-.103	.238	-.723	4.27	.046	.010	1.068	6.68	-.00014	-.061	.002	.64	22.17	998
16	-51.1	-.838	-.159	.256	-.540	3.69	.027	.009	.967	4.63	-.00020	-.092	.002	-.41	7.38	496
17	-56.2	-.921	-.045	.126	-2.045	7.77	.011	.007	1.851	11.75	.00002	.018	.001	.16	24.91	439
18	18.1	.297	.117	.309	.580	6.73	.476	.244	.416	2.07	.00525	.070	.070	-.51	8.44	498
19	23.2	.380	.279	.337	.342	3.30	.202	.119	1.163	5.11	-.00048	-.012	.041	.76	12.76	998
22	28.3	.463	.576	.223	.119	3.63	.027	.052	2.716	11.84	-.00107	-.093	.017	-11.11	257.40	998
23	33.3	.547	.582	.274	-.915	4.87	.003	.008	4.835	57.61	-.00013	-.058	.002	-1.50	17.91	998
24	38.4	.630	.293	.429	.405	3.06	.016	.009	.367	3.20	-.00052	-.130	.004	-.61	8.33	999
25	43.5	.713	-.073	.289	.941	5.49	.017	.008	.597	4.35	-.00007	-.029	.002	1.40	30.06	991
26	48.6	.796	-.194	.243	.392	4.10	.052	.010	.364	3.39	-.00020	-.086	.002	-.30	11.50	492
27	53.7	.880	.054	.494	1.306	3.98	.018	.008	1.152	6.20	.00024	.060	.004	1.33	13.10	452
28	58.7	.963	-.001	.169	1.206	6.82	-.005	.005	-1.043	19.05	-.00012	-.133	.000	.00	.00	424
29	58.7	.963	.105	.372	1.676	5.01	-.004	.005	1.459	7.92	.00005	.025	.000	.00	.00	473
30	13.0	.214	.117	.253	1.317	6.28	.656	.268	-.409	1.95	-.00062	-.009	.079	-1.37	14.42	441
32	13.0	.214	.068	.167	.002	3.40	.653	.259	-.243	1.79	.01114	.258	.039	-.45	7.19	469

ORIGINAL PAGE IS OF POOR QUALITY

TABLE IV-29

AZIMUTHAL VELOCITY, CONCENTRATION AND MASS TRANSPORT DATA AND CORRELATIONS

Test Date: 10/7/82 Run No.: 29 Flow Condition: 1 Geometry: 2

Axial Location: 13 mm (0.5 in.) $x/R_o = 0.208$

P_t No.	r mm +(θ=90) -(θ=270)	r/R_o	W m/s	w' m/s	S_w	K_w	f	f'	S_f	K_f	$\overline{wf}$ m/s	R_{wf}	σ_{wf} m/s	S_{wf}	K_{wf}	N
2	4.3	.070	-.029	.100	.653	6.23	1.031	.035	-6.843	67.43	-.00010	-.030	.005	6.38	173.50	968
3	11.0	.181	.005	.123	.711	5.24	.961	.126	-2.939	12.31	-.00271	-.175	.023	-2.19	53.01	969
4	17.8	.292	.365	.394	1.219	5.93	.298	.114	.923	4.10	-.00234	-.052	.042	.35	16.38	984
5	-7.7	-.125	.030	.096	.259	4.68	.917	.043	-5.923	56.45	-.00095	-.229	.007	-10.22	143.70	957
6	-14.4	-.236	.123	.253	-.038	5.19	.650	.199	-1.052	3.16	-.00391	-.078	.057	.19	16.07	487
7	-21.2	-.347	.998	.151	-.110	4.06	.109	.090	1.186	4.32	.00063	.046	.013	.17	12.20	994
8	-28.0	-.456	.803	.109	-.790	5.17	.002	.004	1.638	20.43	.00001	.013	.000	2.35	49.14	995
10	24.6	.403	.829	.136	-.251	3.67	.069	.017	.967	5.78	.00002	.008	.002	.33	13.14	998
11	31.3	.514	.730	.182	-.399	3.76	.037	.009	.110	4.12	.00003	.017	.002	.17	9.30	997
12	38.1	.625	.431	.148	-.042	3.92	.051	.010	.454	3.92	.00002	.011	.001	.65	12.89	999
13	21.2	.347	.367	.222	-.240	3.98	.132	.042	1.876	10.45	.00025	.027	.010	1.02	24.09	999
14	44.9	.736	.431	.150	.288	3.28	.049	.011	.572	3.43	-.00016	-.099	.002	-.73	8.54	479
15	51.7	.847	.416	.186	-.038	4.80	.048	.012	.735	4.19	-.00017	-.071	.002	-.73	12.44	490
16	58.4	.958	.394	.174	-.279	3.69	.106	.011	.727	4.96	-.00003	-.017	.002	-.13	10.47	495
18	-41.5	-.680	.400	.152	-.271	3.99	.038	.009	.761	4.62	-.00005	-.036	.001	-.38	9.48	494
20	-48.3	-.791	.363	.175	-.439	3.44	.041	.010	.319	4.04	-.00005	-.029	.002	.12	7.39	473
22	-55.1	-.902	.389	.150	-.184	3.38	.028	.007	.813	4.76	-.00002	-.021	.001	.67	15.29	498
23	-48.3	-.791	.387	.156	-.116	3.84	.027	.008	.923	5.72	-.00005	-.041	.001	.35	26.07	498
24	44.9	.736	.413	.146	-.038	3.15	.056	.011	.460	3.33	-.00009	-.055	.002	-.36	6.66	499
25	33.1	.542	.607	.309	-.176	3.07	.053	.010	.210	3.18	.00005	.016	.003	.18	6.25	999
26	-21.2	-.347	.992	.147	.225	3.89	.115	.090	1.138	4.37	.00045	.034	.015	1.95	32.13	991

TABLE IV-30

RADIAL VELOCITY, CONCENTRATION AND MASS TRANSPORT DATA AND CORRELATIONS

Test Date: 10/11/82 Run No.: 30 Flow Condition: 1 Geometry: 2

Axial Location: 13 mm (0.5 in.) $x/R_o = 0.208$

P_t No.	r mm +(θ=0) -(θ=180)	r/R_o	V m/s	v' m/s	S_v	K_v	f	f'	S_f	K_f	$\overline{vf}$ m/s	R_{vf}	σ_{vf} m/s	S_{vf}	K_{vf}	N
1	.0	.000	-.022	.097	.252	3.38	.999	.035	-5.567	48.55	-.00042	-.122	.006	-7.31	147.00	491
3	12.2	.200	.087	.175	1.304	14.65	.853	.710	-1.632	4.72	.00190	.052	.044	-2.08	32.63	495
4	18.3	.300	.116	.281	.230	2.94	.249	.120	.710	3.47	.00081	.024	.034	-.60	11.03	986
5	-3.0	-.050	.044	.098	-.437	3.96	.989	.038	-5.585	46.15	.00010	.026	.004	5.73	87.26	493
6	-9.1	-.150	.098	.108	-.627	5.10	.912	.082	-3.820	20.34	.00071	.080	.011	3.95	51.28	487
7	-15.2	-.250	.074	.244	-1.028	4.61	.666	.234	-.720	2.48	.01113	.195	.063	2.14	14.48	489
8	-21.4	-.350	.437	.177	.063	3.28	.037	.059	2.513	10.54	-.00008	-.008	.010	-.58	19.49	997
9	-27.5	-.451	.564	.121	-.105	4.46	-.001	.003	-.065	4.47	-.00001	-.026	.000	.00	.00	999
10	-33.6	-.550	.227	.334	.265	2.72	.023	.009	.722	4.93	-.00018	-.057	.003	-.20	8.66	999
11	.0	.000	-.038	.093	-.124	3.71	.999	.029	-2.880	21.85	.00041	.151	.003	1.16	64.29	483
12	24.4	.400	.406	.149	.033	3.77	.000	.004	2.511	21.92	-.00000	-.008	.001	-4.56	71.17	998
13	30.5	.500	.400	.184	-.605	4.69	.002	.005	1.293	6.94	-.00005	-.052	.001	-2.18	27.89	998
14	36.6	.600	-.103	.168	-.041	3.90	.034	.008	.393	4.07	-.00001	-.004	.001	-.11	7.04	493
15	42.7	.699	-.146	.184	.480	5.55	.032	.008	.366	3.11	.00005	.037	.001	.41	10.00	499
16	48.8	.799	-.032	.114	-1.519	9.84	.037	.008	.298	3.06	.00007	.068	.001	.71	16.25	487
17	54.9	.899	-.047	.136	-.715	5.29	.012	.005	.868	5.97	.00001	.010	.001	-.75	27.90	465
18	-24.4	-.400	.542	.152	-.384	5.18	.001	.007	7.611	86.83	.00002	.018	.001	-5.48	143.80	998
19	-30.5	-.500	.532	.146	-.780	5.44	.001	.004	.387	4.27	-.00003	-.056	.001	.07	11.36	994
20	.0	.000	-.029	.085	-.372	3.67	1.001	.034	-4.551	40.44	.00028	.098	.005	7.79	175.30	476
22	.0	.000	-.024	.091	.136	3.55	1.000	.036	-9.856	130.20	.00023	.071	.003	9.74	165.20	432
23	-27.5	-.451	.570	.111	.176	3.83	.025	.003	5.933	109.50	-.00000	-.009	.000	5.00	81.38	979
24	-39.7	-.650	-.147	.247	-1.560	5.97	.051	.007	.495	3.71	.00013	.074	.002	-.45	16.19	470
25	-45.8	-.751	-.216	.270	-1.203	4.88	.058	.007	.669	3.75	.00003	.014	.002	.03	6.88	484
26	-51.9	-.851	-.039	.109	-.851	4.12	.030	.005	.673	3.79	.00004	.086	.000	1.42	7.96	180
27	18.3	.300	.111	.304	1.160	4.94	.246	.116	.739	3.43	.00097	.028	.032	.03	8.35	994
28	24.4	.400	.408	.182	.040	3.87	.018	.006	13.040	243.00	-.00002	-.015	.001	-9.14	198.20	977
29	30.5	.500	.412	.239	.706	5.56	.020	.003	1.438	8.03	-.00006	-.077	.001	-.73	21.77	993
30	21.3	.350	.319	.262	1.600	8.20	.051	.055	2.386	9.36	-.00035	-.024	.014	2.45	39.49	997
31	27.4	.450	.391	.232	.597	5.93	.017	.002	.059	4.22	.00002	.042	.000	-.09	11.70	995
33	33.5	.550	.199	.352	.241	2.77	.032	.007	.493	3.24	-.00007	-.030	.002	-.60	6.58	999
34	42.7	.699	-.093	.162	-.761	3.90	.047	.007	.961	6.39	.00005	.045	.001	.67	9.23	482
35	48.8	.799	-.107	.180	.010	4.08	.042	.006	.699	4.58	-.00003	-.023	.001	1.14	26.89	481
36	54.9	.899	-.041	.142	-.206	5.00	.023	.009	-.898	3.15	.00000	.004	.001	.20	10.60	456
37	9.7	-.650	-.119	.178	-.488	3.18	.020	.019	1.251	2.97	-.00007	-.020	.004	-.73	10.47	481
38	-45.8	-.751	-.160	.222	-.963	4.63	.051	.010	.691	3.44	.00016	.071	.002	-.40	22.80	488

TABLE IV-31

AZIMUTHAL VELOCITY, CONCENTRATION AND MASS TRANSPORT DATA AND CORRELATIONS

Test Date: 10/11/82 Run No.: 31 Flow Condition: 1 Geometry: 2

Axial Location: 51 mm (2.0 in.) $x/R_o = 0.833$

P_t No.	r mm +(θ=90) -(θ=270)	r/R_o	W m/s	w' m/s	S_w	K_w	f	f'	S_f	K_f	$\overline{wf}$ m/s	R_{wf}	σ_{wf} m/s	S_{wf}	K_{wf}	N
2	.0	.000	.033	.221	.939	7.79	.641	.281	-.281	1.74	-.00660	-.106	.063	-.81	14.88	496
3	6.1	.100	.036	.160	.073	4.64	.588	.288	-.013	1.58	.00322	.070	.043	.45	4.85	488
4	12.2	.200	.058	.155	.235	3.74	.473	.278	.588	1.97	-.00199	-.046	.042	-.01	8.81	488
5	-9.1	-.150	-.022	.153	.069	4.54	.545	.298	.080	1.55	.00257	.059	.045	.26	7.52	475
6	-3.0	-.050	.001	.166	.027	4.95	.630	.297	-.352	1.67	.00120	.024	.048	-.03	7.65	486
7	-15.2	-.250	-.020	.180	-1.391	7.45	.457	.266	.460	1.89	-.00629	-.132	.049	-2.25	23.40	489
9	-21.3	-.350	.041	.195	.060	3.98	.329	.213	1.157	3.30	-.00312	-.075	.043	-.98	14.89	484
10	-27.5	-.450	.118	.358	-.304	4.08	.264	.161	1.594	5.00	.00105	.018	.055	.43	17.58	993
11	-33.6	-.550	.331	.405	-.542	3.95	.207	.106	1.690	7.21	-.00009	-.002	.041	-1.66	30.11	991
12	-39.7	-.650	.408	.283	-.200	3.55	.139	.076	1.857	9.39	-.00075	-.035	.021	-1.17	23.71	991
13	48.8	.800	.344	.341	.315	3.58	.099	.032	3.128	18.55	.00010	.009	.012	3.89	64.32	992
14	42.7	.700	.427	.298	.051	3.65	.114	.054	3.201	19.40	.00007	.004	.014	1.27	33.43	998
15	36.6	.600	.440	.349	.018	4.38	.169	.087	1.567	6.29	-.00128	-.042	.028	-.67	10.30	996
16	30.5	.500	.194	.378	.427	4.06	.266	.133	1.843	7.97	-.00033	-.007	.050	1.35	18.89	996
18	24.4	.400	.106	.210	.575	5.94	.327	.194	1.421	4.44	.00000	.000	.039	.37	16.40	486
19	18.3	.300	.065	.154	.570	5.33	.395	.249	.994	2.80	-.00173	-.045	.041	.57	14.54	483
20	54.9	.900	.288	.303	-.048	3.01	.093	.027	2.542	14.76	-.00015	-.015	.008	-.15	9.46	499
21	-45.7	-.750	.337	.324	-.330	4.01	.092	.053	2.546	12.58	-.00013	-.008	.016	-.31	19.69	996
22	-51.8	-.850	.323	.307	-.422	3.47	.081	.027	3.176	17.91	-.00024	-.025	.011	-3.93	86.53	496
25	-9.1	-.150	-.026	.205	-.699	6.76	.539	.291	.041	1.65	-.00001	-.000	.056	-.55	11.81	494
25	12.2	.200	.040	.167	.751	6.62	.581	.319	.292	1.71	-.00048	-.009	.052	.73	13.44	497
27	39.7	.650	.446	.302	.025	3.96	.129	.305	-12.330	306.70	-.00113	-.036	.019	-1.01	12.75	998
28	39.7	.650	.452	.297	-.169	3.82	.115	.069	1.996	8.17	-.00005	-.002	.020	-.96	17.90	999
29	56.7	.930	.198	.389	.550	3.32	.082	.026	2.178	10.41	-.00057	-.057	.009	1.27	22.37	499

ORIGINAL PAGE IS
OF POOR QUALITY

TABLE IV-32

RADIAL VELOCITY, CONCENTRATION AND MASS TRANSPORT DATA AND CORRELATIONS

Test Date: 10/12/82 Run No.: 32 Flow Condition: 1 Geometry: 2

Axial Location: 51 mm (2.0 in.) $x/R_o = 0.833$

P_t No.	r mm +(θ=0) -(θ=180)	r/R_o	V m/s	v' m/s	S_v	K_v	f	f'	S_f	K_f	$\overline{vf}$ m/s	R_{vf}	σ_{vf} m/s	S_{vf}	K_{vf}	N
2	.0	.000	.027	.174	-.047	3.55	.612	.286	-.270	1.77	-.00398	-.080	.048	-.48	4.89	482
3	6.1	.100	.077	.185	-.020	3.37	.435	.255	.186	1.70	-.00762	-.162	.046	-.50	5.00	488
4	12.2	.200	.076	.173	.295	4.37	.389	.260	.647	2.12	-.00328	-.073	.045	.07	8.83	491
5	18.3	.300	.080	.184	-.026	4.52	.278	.205	1.130	3.20	-.00098	-.026	.034	-.11	10.25	491
6	-3.0	-.050	-.018	.201	-.507	5.32	.571	.265	-.257	1.78	.00453	.085	.054	.38	9.64	492
7	-9.1	-.150	.044	.184	-.095	4.94	.538	.270	-.126	1.70	.00318	.064	.045	.08	7.49	493
8	-15.2	-.250	.042	.179	-.435	4.84	.446	.251	.241	1.81	.00204	.045	.042	-.29	5.34	489
9	-21.4	-.350	.043	.182	-.321	4.63	.345	.236	.838	2.47	.00409	.095	.041	-.24	12.13	493
10	-27.5	-.451	.031	.301	-.530	4.06	.178	.126	1.702	5.72	-.00037	-.010	.035	-.60	12.13	989
11	-33.6	-.550	.281	.364	-.262	3.53	.171	.100	1.609	6.56	-.00173	-.047	.033	-.59	9.56	997
12	-39.7	-.650	.640	.356	-.529	3.70	.075	.059	1.081	4.43	-.00186	-.089	.022	-1.91	27.37	996
14	-45.8	-.751	.624	.481	-1.121	5.82	.068	.047	2.063	8.28	.00076	.034	.020	.12	10.50	992
15	-51.9	-.851	.416	.568	-1.247	5.48	.025	.025	3.183	17.06	.00009	.007	.016	-4.60	67.19	984
16	24.4	.400	.058	.297	-.630	3.54	.180	.118	1.710	6.10	.00116	.033	.036	-.25	13.29	496
17	30.5	.500	.207	.355	-.391	2.94	.133	.074	1.273	5.17	.00159	.060	.028	1.01	11.26	496
18	36.6	.600	.485	.357	-.242	3.56	.080	.065	1.499	6.50	.00042	.018	.022	.22	19.66	999
19	42.7	.699	.691	.376	-.353	3.22	.027	.036	2.486	11.10	.00009	.006	.013	-1.79	23.83	999
20	48.8	.799	.598	.439	-.071	2.84	.045	.019	2.758	14.33	.00017	.020	.008	.28	18.48	999
22	.0	.000	.047	.233	.698	6.11	.587	.291	-.145	1.72	-.00209	-.031	.068	-.55	10.51	494
26	.0	.000	.028	.197	.010	2.93	.625	.300	-.352	1.73	-.00699	-.119	.058	-.26	4.70	495
27	6.1	.100	.058	.203	.162	5.11	.444	.238	.087	1.70	-.00358	-.074	.048	.06	7.08	499
28	12.2	.200	.088	.201	.508	5.54	.406	.260	.348	1.68	.00131	.025	.051	1.33	15.80	993
29	18.3	.300	.082	.186	-.118	3.56	.294	.206	.842	2.52	.00150	.039	.041	-.36	12.96	992
30	-45.8	-.751	.785	.377	-.410	2.75	.075	.054	2.280	10.54	.00098	.048	.019	.09	13.08	999
31	-48.8	-.801	.686	.435	-.494	3.35	.032	.033	3.814	24.65	.00024	.017	.017	-7.25	133.70	999
32	-51.9	-.851	.634	.437	-.485	3.69	.023	.025	2.649	11.82	-.00109	-.100	.011	-.29	24.55	499
33	-54.9	-.900	.485	.433	-.465	3.32	.014	.019	2.507	11.53	.00058	.071	.007	2.27	17.27	499
34	-58.0	-.951	.132	.456	-.653	5.68	.006	.012	2.662	16.94	.00035	.063	.004	.11	10.56	499

ORIGINAL PAGE IS
OF POOR QUALITY

TABLE IV-33

AZIMUTHAL VELOCITY, CONCENTRATION AND MASS TRANSPORT DATA AND CORRELATIONS

Test Date: 10/12/82 Run No.: 33 Flow Condition: 1 Geometry: 2

Axial Location: 102 mm (4.0 in.) $x/R_o = 1.665$

P_t No.	r mm +(θ=90) -(θ=270)	r/R_o	W m/s	w' m/s	S_w	K_w	f	f'	S_f	K_f	$\overline{wf}$ m/s	R_{wf}	σ_{wf} m/s	S_{wf}	K_{wf}	N
3	.0	.000	-.018	.205	.489	4.35	.115	.014	.007	3.43	-.00014	-.050	.003	.19	10.60	493
4	6.1	.100	.142	.217	.190	4.07	.116	.017	2.699	25.39	-.00011	-.030	.003	-1.11	14.21	992
5	12.2	.200	.201	.175	-.204	3.40	.117	.015	1.024	8.21	-.00006	-.025	.002	-1.00	12.97	991
6	18.3	.300	.281	.185	.118	4.50	.119	.019	3.452	41.16	-.00005	-.014	.004	-.02	15.48	998
7	-3.0	-.050	.077	.215	-.410	4.02	.116	.013	.369	4.58	-.00005	-.018	.003	-.32	7.27	499
8	-9.1	-.150	.192	.196	-.212	3.59	.119	.017	2.129	20.14	.00014	.041	.003	.33	21.79	995
9	-15.2	-.250	.255	.192	-.343	4.11	.112	.016	.666	5.18	-.00002	-.006	.003	.06	14.22	988
10	-21.3	-.350	.298	.183	-.421	4.24	.107	.017	.724	4.99	-.00008	-.027	.004	-1.69	38.49	991
12	-27.5	-.450	.319	.207	-.202	3.69	.114	.021	.716	4.48	.00013	.029	.004	.64	12.41	987
13	-33.5	-.550	.335	.260	-.596	4.33	.118	.027	1.070	5.69	-.00037	-.051	.008	-.80	16.93	994
14	-39.7	-.650	.325	.278	-.385	3.28	.118	.034	1.534	9.26	-.00047	-.050	.009	-1.86	20.42	998
16	-51.8	-.850	.316	.233	-.089	3.24	.109	.034	1.040	4.78	-.00046	-.058	.007	-.46	8.34	496
17	54.9	.900	.294	.237	-.001	2.79	.122	.040	1.188	5.83	.00099	.010	.009	1.42	12.04	499
18	57.9	.950	.289	.233	.005	2.96	.139	.042	.918	4.31	-.00030	-.031	.010	-.90	13.82	499
19	48.8	.800	.274	.302	-.078	2.83	.136	.039	.893	4.20	-.00026	-.021	.012	-.60	10.00	498
20	42.7	.700	.321	.281	-.150	2.98	.126	.035	.938	4.50	-.00056	-.056	.010	-.88	9.80	999
21	36.6	.600	.365	.246	-.280	3.84	.128	.031	1.264	8.37	.00025	.033	.008	3.14	54.35	999
23	30.5	.500	.345	.209	-.361	4.35	.116	.022	.793	4.41	-.00017	-.037	.004	-.83	12.13	988
24	24.4	.400	.317	.195	-.073	3.68	.121	.020	1.309	7.53	.00001	.001	.004	.22	11.58	997

ORIGINAL PAGE IS
OF POOR QUALITY

TABLE IV-34

RADIAL VELOCITY, CONCENTRATION AND MASS TRANSPORT DATA AND CORRELATIONS

Test Date: 10/12/82 Run No.: 34 Flow Condition: 1 Geometry: 2

Axial Location: 102 mm (4.0 in.) $x/R_o = 1.665$

P_r No.	r mm +(θ=0) -(θ=180)	r/R_o	V m/s	v' m/s	S_v	K_v	f	f'	S_f	K_f	$\overline{vf}$ m/s	R_{vf}	σ_{vf} m/s	S_{vf}	K_{vf}	N
2	.0	.000	-.010	.188	.155	3.25	.123	.022	7.423	105.70	.00010	.024	.004	6.86	125.80	985
3	6.1	.100	-.016	.213	.567	4.67	.103	.012	.442	4.25	-.00007	-.028	.003	-.73	13.05	992
4	12.2	.200	-.009	.217	.869	7.93	.108	.017	4.508	68.34	.00009	.023	.003	3.62	50.01	995
5	-3.0	-.050	.024	.187	-.193	4.01	.112	.016	6.768	101.80	-.00004	-.015	.002	.02	11.00	992
6	-9.1	-.150	.001	.217	-.593	4.48	.105	.014	.506	5.42	-.00001	-.004	.003	.64	10.99	998
7	18.3	.300	-.031	.221	.185	4.02	.096	.014	.603	4.70	.00012	.039	.003	.21	12.42	991
8	24.4	.400	-.039	.232	.098	3.94	.083	.015	.557	4.16	.00013	.038	.004	.35	11.31	992
9	30.5	.500	-.064	.271	.425	4.91	.079	.017	1.095	7.00	.00017	.038	.004	-.27	13.45	996
10	36.6	.600	-.085	.293	.654	5.05	.082	.020	.932	4.78	.00001	.001	.006	-.21	10.18	997
11	42.7	.699	-.095	.294	.425	4.02	.063	.019	1.307	7.50	.00009	.017	.006	2.60	55.21	996
12	48.8	.799	-.024	.293	.849	5.02	.073	.020	.910	4.27	-.00003	-.005	.006	-.09	12.74	992
15	-51.9	-.851	-.052	.250	-.450	4.66	.075	.029	1.277	5.70	.00032	.045	.007	-.65	17.52	989
16	-45.8	-.751	-.097	.265	-.183	4.21	.127	.036	1.470	8.70	-.00014	-.015	.010	-.29	23.84	998
17	-39.7	-.650	-.145	.296	-.783	5.46	.084	.024	1.832	13.59	.00012	.017	.007	.26	11.05	998
18	-33.6	-.550	-.077	.261	-.385	3.29	.107	.023	1.140	8.54	.00020	.033	.006	-.27	11.76	996
19	-27.5	-.451	-.026	.234	-.623	3.53	.092	.018	1.839	14.93	.00014	.033	.005	3.69	66.76	993
20	-21.4	-.350	-.010	.226	-.688	4.84	.105	.018	2.060	17.72	.00012	.029	.004	.67	38.21	997
21	-15.2	-.250	.009	.198	-.212	3.07	.107	.015	1.108	9.21	.00003	.009	.003	-.59	10.99	995
22	-39.7	-.650	-.126	.274	-.138	3.16	.083	.024	1.023	4.93	.00043	.066	.007	.43	16.80	995
24	48.8	.799	-.054	.258	.359	4.11	.077	.019	.821	3.83	.00012	.025	.005	.54	16.63	994
26	54.9	.899	.001	.290	1.170	6.03	.042	.015	.826	3.73	-.00003	-.007	.004	-.44	11.48	480
27	-58.0	-.951	-.053	.221	-.430	2.93	.038	.014	.844	3.19	.00046	.154	.003	-1.06	13.48	132

ORIGINAL PAGE IS
OF POOR QUALITY

TABLE IV-35

AZIMUTHAL VELOCITY, CONCENTRATION AND MASS TRANSPORT DATA AND CORRELATIONS

Test Date: 10/13/82 Run No.: 35 Flow Condition: 1 Geometry: 2

Axial Location: 152 mm (6.0 in.) $x/R_o = 2.498$

Pt No.	r mm +(θ=90) -(θ=270)	r/R_o	W m/s	w' m/s	S_w	K_w	f	f'	S_f	K_f	$\overline{wf}$ m/s	R_{wf}	σ_{wf} m/s	S_{wf}	K_{wf}	N
2	.0	.000	-.043	.268	.373	3.61	.120	.013	-.112	3.28	.00011	.033	.004	1.71	22.52	995
3	6.1	.100	.172	.251	-.327	2.97	.123	.013	.061	3.66	-.00010	-.029	.003	-.12	9.88	988
4	12.2	.200	.289	.221	-.078	4.31	.124	.014	.275	3.66	.00012	.039	.003	1.39	15.87	998
5	-3.0	-.050	.140	.247	-.370	3.09	.121	.013	.199	3.62	.00024	.074	.003	.54	8.16	995
6	-9.1	-.150	.279	.218	-.744	4.30	.120	.014	.425	4.54	.00011	.036	.003	1.21	15.78	987
7	-15.2	-.250	.361	.190	-.345	3.76	.105	.016	.321	3.70	-.00002	-.007	.003	-.39	12.16	988
8	-21.3	-.350	.365	.213	-.680	4.55	.100	.018	.598	4.99	.00002	.004	.004	-2.82	35.57	990
9	-27.5	-.450	.371	.205	-.669	4.67	.101	.019	.697	4.58	-.00007	-.019	.004	.16	11.93	991
10	-33.6	-.550	.391	.200	-.487	4.43	.101	.022	.796	4.16	.00002	.004	.004	.62	10.29	992
11	-39.7	-.650	.382	.229	-.505	4.13	.105	.027	1.190	5.60	.00013	.021	.006	-.68	21.53	993
12	-45.7	-.750	.362	.221	-.642	4.69	.100	.028	1.059	4.56	-.00014	-.023	.006	.13	11.38	987
13	-51.8	-.850	.328	.189	-.183	3.74	.097	.026	1.163	5.68	.00006	.012	.005	-.91	9.84	984
14	-56.7	-.929	.300	.192	-.087	3.07	.099	.021	.997	5.27	.00033	.081	.004	1.50	17.57	249
15	-56.7	-.929	.295	.176	.092	3.38	.098	.022	.881	3.95	-.00034	-.087	.004	-.78	15.72	999
16	54.9	.900	.337	.194	.287	3.47	.125	.035	.979	4.25	-.00028	-.042	.006	.04	9.41	998
17	48.8	.800	.375	.208	-.058	2.95	.118	.028	.745	4.24	-.00017	-.030	.006	.09	10.28	999
18	42.7	.700	.408	.213	-.140	3.19	.125	.032	.958	5.08	-.00013	-.020	.007	-.74	16.93	997
19	36.6	.600	.399	.208	-.018	3.30	.116	.026	.788	4.49	.00006	.011	.006	-1.05	23.55	996
20	30.5	.500	.416	.194	-.172	3.20	.112	.020	.878	5.46	-.00030	-.077	.004	-1.39	14.35	996
21	24.4	.400	.398	.203	.069	3.62	.110	.019	.936	5.61	.00002	.005	.004	.84	13.64	996
22	18.3	.300	.349	.212	-.264	3.50	.112	.017	.780	6.20	-.00005	-.015	.004	.49	19.74	996

ORIGINAL PAGE IS
OF POOR QUALITY

TABLE IV-36

RADIAL VELOCITY, CONCENTRATION AND MASS TRANSPORT DATA AND CORRELATIONS

Test Date: 10/13/82 Run No.: 36 Flow Condition: 1 Geometry: 2
Axial Location: 152 mm (6.0in.) $x/R_o = 2.498$

P_t No.	r mm +(θ=0) -(θ=180)	r/R_o	V m/s	v' m/s	S_v	K_v	f	f'	S_f	K_f	$\overline{vf}$ m/s	R_{vf}	σ_{vf} m/s	S_{vf}	K_{vf}	N
1	.0	.000	-.030	.110	.919	5.48	1.000	.029	-3.587	27.22	.00014	.044	.006	-13.62	261.30	492
2	.0	.000	-.050	.265	.264	2.53	.106	.014	.041	3.51	.00021	.056	.004	.49	7.62	998
3	6.1	.100	-.059	.257	.485	4.45	.096	.012	.582	4.57	-.00019	-.060	.003	-1.45	22.57	497
4	12.2	.200	-.060	.278	.565	3.74	.094	.014	.441	4.06	.00009	.073	.004	-.23	11.54	989
5	18.3	.300	-.078	.273	.705	4.60	.086	.015	.421	4.06	.00016	.039	.004	.26	8.08	996
6	-3.0	-.050	.001	.262	-.286	3.39	.094	.012	.206	4.17	-.00008	-.024	.003	-.30	12.90	495
7	-9.1	-.150	.014	.257	-.015	2.68	.100	.016	.936	5.96	-.00036	-.090	.004	-1.01	11.69	496
8	-15.2	-.250	-.039	.276	-.234	3.36	.104	.016	.512	4.12	.00012	.027	.005	-.01	10.69	997
9	-21.4	-.350	-.064	.267	-.107	2.94	.101	.019	.671	4.45	.00003	.007	.005	-.47	10.69	995
10	-27.5	-.451	-.110	.253	-.106	3.34	.090	.020	.762	4.48	.00014	.027	.006	1.26	15.64	994
11	24.4	.400	-.061	.300	.775	4.58	.075	.015	.373	4.09	.00028	.062	.004	.45	12.73	981
12	30.5	.500	-.082	.285	.388	3.69	.070	.016	.517	4.06	.00014	.030	.005	.61	9.42	984
13	36.6	.600	-.114	.243	.726	4.22	.066	.017	.522	3.58	.00025	.060	.004	.67	12.85	984
14	42.7	.699	-.116	.231	.936	5.00	.046	.015	.520	3.57	.00020	.056	.003	.01	10.71	991
15	48.8	.799	-.095	.189	.556	3.84	.040	.013	.617	3.36	.00012	.051	.002	-.20	9.48	972
16	54.9	.899	-.059	.171	.808	4.41	.006	.009	.619	3.38	-.00010	-.066	.002	-.64	9.89	364
17	-33.6	-.550	-.160	.284	-.467	4.71	.086	.022	.721	4.18	.00036	.059	.006	1.17	19.11	982
18	-39.7	-.650	-.165	.262	-.698	5.44	.070	.023	1.038	4.78	-.00003	-.005	.006	-.56	20.92	984
19	-45.8	-.751	-.127	.219	-.555	5.23	.090	.027	.864	3.94	-.00007	-.012	.006	-.75	15.05	975
20	-51.9	-.851	-.088	.186	-.474	4.72	.060	.020	.759	4.25	.00010	.027	.004	-.18	11.84	975
21	-55.0	-.901	-.056	.162	-.385	4.54	.038	.018	1.125	4.67	.00001	.003	.003	.37	9.20	932
22	51.8	.849	-.063	.208	.832	4.69	.015	.011	.832	4.12	-.00015	-.067	.002	-.49	10.46	884
23	.0	.000	-.045	.090	.289	5.13	1.074	.022	-1.976	7.93	.00015	.075	.002	-3.32	38.67	485
24	.0	.000	-.039	.086	-.246	3.13	-.000	.003	.943	9.39	-.00001	-.021	.000	.00	.00	488

ORIGINAL PAGE IS
OF POOR QUALITY

TABLE IV-37

AZIMUTHAL VELOCITY, CONCENTRATION AND MASS TRANSPORT DATA AND CORRELATIONS

Test Date: 10/14/82 Run No.: 37 Flow Condition: 1 Geometry: 2

Axial Location: 203mm (8.0 in.) $x/R_o = 3.331$

P_t No.	r mm +(θ=90) -(θ=270)	r/R_o	W m/s	w' m/s	S_w	K_w	f	f'	S_f	K_f	$\overline{wf}$ m/s	R_{wf}	σ_{wf} m/s	S_{wf}	K_{wf}	N
2	.0	.000	-.051	.245	.689	4.02	.105	.012	.444	4.20	-.00009	-.027	.003	-.37	9.39	988
3	6.1	.100	.180	.262	.147	4.57	.106	.012	.638	4.59	-.00004	-.013	.003	.36	13.37	989
4	-3.0	-.050	.165	.246	-.603	3.46	.101	.012	.055	3.87	.00002	.006	.003	-.04	14.39	976
5	-9.1	-.150	.308	.250	-1.849	9.59	.105	.014	.174	3.42	-.00033	-.093	.004	-1.74	22.96	984
6	-15.2	-.250	.395	.162	-.383	3.89	.103	.014	.363	4.06	-.00001	-.006	.002	-.19	15.16	976
7	-21.3	-.350	.411	.154	-.061	3.32	.098	.016	.262	3.43	-.00016	-.062	.002	-.33	9.03	956
8	-27.5	-.450	.399	.178	-1.059	5.35	.097	.018	.796	4.67	-.00006	-.019	.003	-1.30	23.07	971
9	-33.6	-.550	.410	.161	-.255	3.36	.094	.020	.906	5.42	.00004	.013	.003	-.15	9.92	946
10	-39.7	-.650	.401	.157	-.344	3.68	.092	.020	.540	3.40	.00023	.073	.003	.74	7.82	962
11	-45.7	-.750	.382	.164	-.334	3.69	.093	.022	.842	5.00	.00016	.044	.004	.14	14.08	920
12	-51.8	-.850	.377	.163	-.322	4.26	.089	.019	.674	3.99	.00005	.017	.003	.52	9.62	975
13	-45.7	-.750	.355	.248	-2.171	10.79	.094	.020	.564	3.58	-.00009	-.018	.006	-4.55	86.23	981
16	.0	.000	-.026	.326	1.341	7.11	.107	.012	.318	3.93	-.00010	-.027	.004	1.23	29.68	996
17	6.1	.100	.172	.271	.342	4.66	.107	.013	.501	4.18	.00018	.049	.004	.52	13.41	987
19	18.3	.300	.438	.253	1.740	9.76	.105	.015	.837	5.23	-.00003	-.007	.003	.98	19.44	993
20	24.4	.400	.420	.163	-.032	3.24	.104	.017	.680	4.15	-.00007	-.024	.003	.28	8.92	989
21	30.5	.500	.442	.158	.049	2.91	.105	.021	4.888	77.45	-.00006	-.018	.003	-1.19	20.91	986
22	36.6	.600	.437	.177	.868	6.46	.108	.021	.690	3.84	-.00002	-.007	.003	.28	13.67	998
24	42.7	.700	.419	.162	.007	4.20	.106	.027	3.023	35.12	.00004	.010	.004	.98	16.42	998
25	48.8	.800	.419	.167	.032	3.32	.107	.024	.422	3.10	.00024	.058	.004	.59	6.94	992
26	54.9	.900	.363	.188	-.092	3.10	.104	.024	.523	3.35	.00020	.044	.004	.34	5.94	997
27	-21.3	-.350	.431	.162	-.375	3.62	.089	.015	.529	4.13	-.00009	-.034	.003	-.47	13.89	984
28	-27.5	-.450	.400	.191	-1.142	7.16	.089	.019	.646	4.67	.00003	.009	.004	-.80	26.94	987
29	-33.6	-.550	.402	.189	-1.461	8.97	.086	.019	.903	5.36	-.00000	-.000	.004	-5.15	86.55	981
30	-39.7	-.650	.401	.152	-.155	3.22	.085	.020	1.044	6.53	-.00003	-.009	.003	-2.19	29.83	987
31	-45.7	-.750	.402	.148	-.124	3.28	.088	.021	.744	3.94	.00025	.082	.003	1.67	17.47	994

ORIGINAL PAGE IS OF POOR QUALITY

TABLE IV-38

RADIAL VELOCITY, CONCENTRATION AND MASS TRANSPORT DATA AND CORRELATIONS

Test Date: 10/14/82   Run No.: 38   Flow Condition: 1   Geometry: 2

Axial Location: 203 mm (8.0 in.) x/R_o = 3.331

P_t No.	r mm +(θ=0) -(θ=180)	r/R_o	V m/s	v' m/s	S_v	K_v	f	f'	S_f	K_f	$\overline{vf}$ m/s	R_{vf}	σ_{vf} m/s	S_{vf}	K_{vf}	N
2	.1	.001	-.036	.339	1.271	6.57	.107	.012	.420	4.19	-.00002	-.006	.003	.07	8.26	995
3	6.1	.100	-.101	.297	-.093	3.63	.092	.012	.553	4.97	-.00006	-.018	.004	.27	12.06	490
4	12.2	.200	-.074	.281	1.084	5.55	.096	.013	.058	3.38	.00002	.004	.004	-.01	14.56	497
5	18.3	.300	-.073	.256	.781	5.27	.086	.013	.447	4.25	.00011	.033	.003	1.65	18.50	499
6	24.4	.400	-.060	.277	.656	5.91	.080	.014	.253	3.27	.00000	.000	.004	1.06	13.63	495
7	30.5	.500	-.067	.250	.922	5.37	.069	.014	.563	3.69	.00012	.036	.003	.20	9.95	986
8	-3.0	-.050	.033	.288	-.618	3.77	.092	.011	.229	3.48	.00011	.034	.003	.52	11.11	497
9	-9.1	-.150	.020	.276	-.564	4.15	.096	.012	.225	3.35	-.00034	-.107	.003	.25	8.45	498
10	-15.2	-.250	.006	.250	-.422	3.81	.098	.015	.120	3.25	.00010	.026	.004	.09	10.25	498
11	-21.4	-.350	-.007	.224	.133	2.74	.095	.015	.633	4.88	.00016	.046	.004	-.48	13.67	496
12	-27.5	-.451	-.057	.253	-.747	5.98	.090	.017	.444	3.81	.00020	.045	.004	.66	20.97	496
15	.0	.000	-.042	.099	.269	4.84	1.000	.035	-7.786	89.55	.00004	.012	.005	-5.44	151.70	481
16	-33.6	-.550	-.071	.248	-1.138	7.14	.098	.022	1.147	5.48	.00033	.060	.005	1.19	13.14	494
17	-39.7	-.650	-.079	.182	-.043	3.97	.076	.018	.617	4.06	.00021	.064	.003	2.38	22.90	480
18	-45.8	-.751	-.071	.203	-.839	6.47	.094	.023	.764	3.67	-.00042	-.090	.005	-2.37	31.83	486
19	-51.9	-.851	-.037	.148	.163	3.16	.060	.017	.566	3.12	.00016	.066	.002	.57	8.68	474
20	-54.4	-.892	-.017	.143	-.893	6.43	.046	.016	.835	3.88	.00008	.034	.002	.13	10.17	462
21	36.6	.600	-.054	.253	1.404	6.68	.060	.015	.582	3.81	.00009	.024	.004	-.28	20.50	485
22	42.7	.699	-.051	.239	1.506	7.09	.049	.014	.508	3.23	-.00014	-.042	.003	1.51	23.65	496
23	48.8	.799	-.046	.172	.774	4.45	.033	.012	.445	3.12	.00001	.004	.002	-.04	9.52	468
25	45.7	.749	-.056	.195	.995	5.20	.043	.012	.622	3.40	-.00003	-.011	.003	.65	18.64	441
26	39.6	.649	-.089	.205	.306	3.44	.054	.014	.608	3.84	.00002	-.008	.003	.82	12.20	491
27	33.5	.550	-.093	.228	.600	3.52	.065	.015	.391	3.47	-.00012	-.036	.003	-.47	11.59	487
28	-48.8	-.801	-.066	.208	-2.131	13.91	.058	.017	.756	3.78	-.00017	-.049	.004	-7.15	103.50	498
29	-42.7	-.701	-.081	.239	-1.363	7.37	.088	.021	.587	3.28	-.00024	-.049	.005	-.90	12.23	495
30	-36.6	-.600	-.086	.205	-.551	5.17	.079	.019	.877	4.22	.00019	.047	.004	.88	9.46	495

TABLE IV-40

AXIAL AND AZIMUTHAL VELOCITY DATA AND CORRELATIONS

Test Date: 11/2/82 Run No.: 40 Flow Condition: 1 Geometry: 2

Axial Location: 203 mm (8.0 in.) $x/R_o = 3.331$

P_t No.	r mm +(θ=90) −(θ=270)	r/R_o	U m/s	u' m/s	S_u	K_u	W m/s	w' m/s	S_w	K_w	$\overline{uw}$ m^2/s^2	R_{uw}	σ_{uw} m^2/s^2	S_{uw}	K_{uw}	N
1	1.8	.030	.145	.195	-.106	4.01	.137	.274	-.138	2.86	.00026	.005	.058	1.39	19.63	495
2	18.8	.307	.212	.198	-.901	6.02	.448	.169	-.399	3.83	.00079	.023	.035	-1.73	15.33	494
3	35.7	.585	.330	.227	-.735	4.82	.448	.170	-.173	3.70	-.00540	-.141	.039	-.30	11.19	493
4	-15.1	-.248	.200	.167	.129	3.57	.387	.187	-.330	3.44	.00262	.084	.032	.69	10.55	495
5	-32.0	-.525	.291	.183	.035	2.62	.425	.158	-.081	3.60	.00201	.070	.030	.25	11.45	499
6	-49.0	-.803	.438	.191	-.075	2.56	.388	.155	.075	3.09	-.00181	-.061	.029	-.69	6.51	496
7	52.6	.862	.490	.190	-.246	2.75	.390	.165	.003	3.04	-.00235	-.075	.029	-.23	5.43	499
8	44.2	.724	.434	.202	-.289	3.14	.406	.165	-.077	3.21	-.00590	-.177	.033	-1.33	10.11	498
9	27.2	.446	.287	.184	-.080	3.07	.439	.158	-.039	3.61	.00203	.070	.027	-.50	7.33	499
10	10.3	.169	.177	.174	-.191	3.10	.338	.199	-.607	4.00	.00300	.087	.033	.39	9.09	499
11	-6.6	-.109	.173	.160	-.277	3.12	.247	.216	-.455	3.25	.00192	.056	.039	3.23	39.15	499
12	-23.6	-.386	.262	.164	-.044	3.21	.451	.153	-.030	2.84	.00738	.294	.028	2.34	15.51	497
13	-40.5	-.664	.374	.181	-.176	3.12	.416	.163	-.113	3.21	-.00138	-.047	.028	-.77	9.07	499

ORIGINAL PAGE IS
OF POOR QUALITY

TABLE IV-41

AXIAL AND RADIAL VELOCITY DATA AND CORRELATIONS

Test Date: 11/3/82 Run No.: 41 Flow Condition: 1 Geometry: 2

Axial Location: 203 mm (8.0 in.) $x/R_o = 3.331$

P_t No.	r mm +(θ=0) -(θ=180)	r/R_o	U m/s	u' m/s	S_u	K_u	V m/s	v' m/s	S_v	K_v	$\overline{uv}$ m^2/s^2	R_{uv}	σ_{uv} m^2/s^2	S_{uv}	K_{uv}	N
1	.0	.000	.149	.162	.172	3.00	-.034	.267	.115	2.57	-.00011	-.003	.044	-.05	8.46	499
2	12.7	.208	.201	.193	-.281	3.87	-.089	.252	.313	2.95	-.00041	-.008	.048	-.21	7.70	493
4	-12.7	-.208	.211	.203	-.521	4.76	-.012	.255	-.372	2.88	.00028	.005	.058	1.29	15.54	491
5	-25.4	-.416	.294	.197	-.867	5.27	-.031	.243	-.307	3.03	-.00748	-.156	.049	.70	12.51	492
6	-38.1	-.624	.396	.260	.162	4.70	.021	.306	1.246	5.71	-.00966	-.121	.069	1.53	14.80	483
7	11.0	.180	.481	.270	-.844	5.08	.048	.162	.548	5.31	.00901	.206	.043	1.41	16.55	491
8	99.9	1.637	.361	.210	-.253	3.50	-.083	.197	.549	3.02	-.01224	-.296	.041	-1.57	11.51	498
9	112.6	1.845	.483	.200	-.763	4.56	-.039	.147	.389	2.88	-.00613	-.209	.035	-3.86	43.68	249

ORIGINAL PAGE IS
OF POOR QUALITY

TABLE IV-42

AXIAL AND RADIAL VELOCITY DATA AND CORRELATIONS

Test Date: 11/4/82 Run No.: 42 Flow Condition: 1 Geometry: 2

Axial Location: 305 mm (12.0 in.) $x/R_o = 4.996$

P_t No.	r mm +(θ=0) -(θ=180)	r/R_o	U m/s	u' m/s	S_u	K_u	V m/s	v' m/s	S_v	K_v	$\overline{uv}$ m^2/s^2	R_{uv}	σ_{uv} m^2/s^2	S_{uv}	K_{uv}	N
1	.0	.000	.349	.153	-.088	5.13	.091	.275	-.457	2.18	-.00333	-.079	.042	.21	8.32	497
2	.0	.000	.344	.166	-.047	5.20	.108	.254	-.499	2.32	-.00131	-.031	.044	-.07	13.41	495
3	12.2	.200	.334	.168	.159	5.50	.046	.208	-.518	3.68	.00084	.024	.035	2.28	23.70	491
4	24.4	.400	.343	.125	.057	3.96	.016	.148	-.638	3.66	-.00031	-.017	.019	-.38	12.31	478
5	36.6	.600	.377	.124	.151	5.98	.005	.120	-.338	4.41	-.00159	-.106	.015	-2.07	20.50	484
6	48.8	.799	.434	.202	-.214	3.09	-.007	.103	.110	3.10	.00046	.022	.019	.35	4.85	151
7	-6.1	-.100	.315	.157	.149	4.14	-.129	.231	.547	2.68	.00234	.065	.036	-1.11	13.17	495
8	-12.1	-.198	.330	.149	.454	5.24	-.103	.187	.242	2.62	.00108	.040	.029	-.78	15.66	487
9	-18.3	-.300	.343	.132	-.357	4.30	-.064	.146	-.081	2.72	.00078	.040	.018	.48	6.27	495
10	-29.0	-.475	.358	.128	-.319	5.90	-.027	.116	-.172	3.04	.00059	.040	.017	.98	23.97	493
11	-42.7	-.700	.353	.110	-.015	3.18	-.020	.097	.021	3.60	.00047	.044	.011	.44	12.76	483
12	-54.9	-.900	.299	.167	-.049	4.81	.009	.084	.803	6.43	.00085	.060	.013	.80	15.67	217
13	12.2	.200	.322	.127	.608	4.16	.055	.183	-.472	3.00	-.00188	-.081	.023	-.33	7.78	498
14	6.1	.100	.306	.157	-.096	4.53	.060	.234	-.502	2.54	.00245	.067	.041	.43	14.60	499
15	48.8	.799	.369	.167	-.030	4.81	.004	.098	.264	3.31	.00068	.041	.017	-2.27	22.82	236
16	.0	.000	.328	.154	.102	3.94	.001	.251	-.072	2.00	-.00156	-.040	.038	.15	7.63	498
17	6.1	.100	.327	.147	.039	3.82	.015	.225	-.197	2.43	-.00105	-.032	.033	.55	8.76	498
18	12.2	.200	.332	.126	.035	3.45	.026	.178	-.427	2.93	-.00092	-.041	.023	-.28	8.70	494
19	18.3	.300	.336	.143	.671	4.79	-.001	.158	-.266	3.43	-.00204	-.091	.024	.25	13.35	490
20	-6.1	-.100	.339	.150	-.074	3.70	-.033	.235	.203	2.30	-.00088	-.025	.035	-.13	8.28	490
21	-12.1	-.198	.334	.136	.400	3.91	-.043	.188	.058	2.73	-.00012	-.005	.027	-.92	11.66	490
22	-18.3	-.300	.344	.120	-.008	3.43	-.034	.151	-.016	2.83	.00088	.049	.019	.82	9.45	496
23	-24.4	-.400	.370	.138	.593	5.45	-.025	.127	-.051	2.70	.00085	.049	.016	.20	6.52	495
24	.0	.000	.340	.158	.135	3.91	.032	.255	-.074	1.93	.00126	.031	.041	.47	8.73	497
25	-6.1	-.100	.327	.150	.033	4.16	-.026	.221	.076	2.48	.00065	.020	.032	-.85	8.68	497

TABLE IV-43

AXIAL AND AZIMUTHAL VELOCITY DATA AND CORRELATIONS

Test Date: 11/4/82 Run No.: 43 Flow Condition: 1 Geometry: 2

Axial Location: 305 mm (12.0 in.) $x/R_o = 4.996$

P_t No.	r mm +(θ=90) −(θ=270)	r/R_o	U m/s	u' m/s	S_u	K_u	W m/s	w' m/s	S_w	K_w	$\overline{uw}$ m^2/s^2	R_{uw}	σ_{uw} m^2/s^2	S_{uw}	K_{uw}	N
1	.0	.000	.330	.150	-.616	3.42	.062	.249	-.317	2.24	-.00180	-.048	.037	.31	8.72	492
2	24.4	.400	.341	.112	.081	3.38	.438	.099	.084	3.67	.00054	.047	.012	.14	12.91	496
3	12.2	.200	.322	.121	.403	3.53	.381	.128	-.694	4.67	-.00176	-.113	.018	-1.42	12.56	497
4	36.6	.599	.366	.106	-.160	3.33	.412	.097	.004	2.95	.00020	.021	.010	.45	7.43	499
5	48.8	.799	.359	.114	.104	3.53	.399	.090	.094	3.01	-.00009	-.009	.011	-.97	11.96	499
6	54.8	.899	.342	.108	.388	3.40	.384	.090	.220	3.90	-.00014	-.014	.010	-.25	10.21	498
7	42.7	.699	.367	.107	.201	4.03	.393	.087	.225	3.15	-.00030	-.032	.011	-1.74	16.34	498
8	30.5	.499	.357	.113	.159	3.27	.412	.093	-.063	3.16	-.00060	-.057	.010	-1.05	8.62	497
9	18.3	.300	.316	.112	.103	2.87	.412	.103	-.199	3.74	-.00067	-.058	.012	-.30	16.82	499
10	6.1	.100	.327	.129	.105	3.25	.266	.185	-.834	3.99	-.00349	-.146	.023	-.73	9.39	498
11	-6.1	-.100	.320	.139	-.128	3.49	.219	.227	-.569	2.66	-.00624	-.197	.033	.21	10.37	497
12	-12.2	-.200	.314	.127	-.069	3.12	.377	.135	-.621	4.23	-.00104	-.061	.020	-1.76	18.08	496
13	-18.3	-.300	.336	.127	-.053	2.75	.421	.108	-.146	3.42	-.00060	-.044	.015	-1.32	12.99	496
14	-33.5	-.549	.358	.113	.202	3.53	.423	.096	.135	3.17	.00030	.027	.011	.60	11.89	496
15	-51.8	-.849	.327	.103	.189	3.93	.414	.087	.592	4.27	.00019	.021	.010	.87	17.92	494
16	57.9	.949	.329	.119	.159	3.16	.379	.093	.326	3.67	.00004	.004	.012	1.43	18.55	498
17	-3.0	-.050	.307	.147	.053	4.12	.090	.261	-.242	2.02	.00037	.010	.039	.40	9.53	496
18	3.0	.050	.313	.148	-.080	3.05	.170	.234	-.659	2.91	-.00402	-.116	.035	-.20	8.16	496

TABLE IV-44

AXIAL AND AZIMUTHAL VELOCITY DATA AND CORRELATIONS

Test Date: 11/4/82 Run No.: 44 Flow Condition: 1 Geometry: 2

Axial Location: 406 mm (16.0 in.) $x/R_o = 6.661$

P_t No.	r mm +(θ=90) -(θ=270)	r/R_o	U m/s	u' m/s	S_u	K_u	W m/s	w' m/s	S_w	K_w	$\overline{uw}$ m^2/s^2	R_{uw}	σ_{uw} m^2/s^2	S_{uw}	K_{uw}	N
1	.0	.000	.361	.150	-.337	4.68	.364	.237	-.438	2.23	-.00058	-.016	.033	.53	7.16	494
2	12.2	.200	.330	.096	.005	3.18	.376	.096	-.862	5.19	-.00221	-.239	.012	-3.01	27.02	493
3	24.4	.400	.336	.079	.005	2.91	.409	.067	-.118	3.22	-.00083	-.156	.005	-.82	7.22	496
4	36.6	.599	.344	.072	.087	3.36	.386	.063	.022	3.30	-.00100	-.217	.005	-.83	8.27	497
5	48.8	.799	.326	.087	1.082	7.76	.375	.055	.157	2.95	-.00043	-.091	.005	-1.02	10.40	494
6	54.8	.899	.308	.040	.017	3.00	.376	.059	.512	3.98	-.00050	-.105	.005	-.41	8.44	495
7	57.9	.949	.297	.082	.161	3.26	.369	.058	.343	3.10	-.00060	-.126	.005	.38	11.23	499
8	6.1	.100	.350	.118	.072	4.64	.273	.154	-1.070	4.23	-.00526	-.290	.019	-2.16	14.53	495
9	-3.0	-.050	.364	.159	-.790	6.73	.107	.217	-.428	2.40	-.00332	-.096	.033	1.73	15.74	495
10	-18.3	-.300	.316	.087	-.139	3.16	.418	.071	-.013	3.32	-.00108	-.174	.006	-1.43	12.55	494
11	-9.1	-.150	.329	.122	.641	4.02	.319	.149	-1.441	5.55	-.00565	-.312	.024	-2.37	33.95	495
12	-30.5	-.499	.336	.078	.086	2.91	.413	.062	.204	3.02	-.00021	-.044	.005	-.61	7.88	490
13	-42.7	-.699	.348	.076	.248	3.18	.391	.059	.047	3.41	-.00027	-.060	.005	-.39	9.34	497

ORIGINAL PAGE IS
OF POOR QUALITY

TABLE IV-45

AXIAL AND RADIAL VELOCITY DATA AND COI :LATIONS

Test Date: 11/4/82 Run No.: 45 Flow Condition: 1 Geometry: 2

Axial Location: 406 mm (16.0 in.) $x/R_o = 6.661$

P_t No.	r mm +(θ=0) -(θ=180)	r/R_o	U m/s	u' m/s	S_u	K_u	V m/s	v' m/s	S_v	K_v	$\overline{uv}$ m^2/s^2	R_{uv}	σ_{uv} m^2/s^2	S_{uv}	K_{uv}	N
1	.0	.000	.371	.136	.078	3.95	.035	.229	-.193	2.28	-.00231	-.074	.030	-.05	9.68	494
2	12.2	.200	.337	.094	.021	4.15	.012	.142	.158	3.26	-.00093	-.070	.015	-1.91	17.82	489
3	24.4	.400	.341	.108	-.400	4.77	.014	.085	.095	3.79	-.00072	-.078	.009	-1.00	12.24	469
4	36.6	.600	.344	.113	-1.252	7.56	-.009	.071	-.174	3.41	-.00038	-.047	.007	-.57	8.56	492
5	48.8	.799	.368	.079	.563	3.32	-.013	.074	-1.043	5.71	.00024	.041	.007	-.06	13.59	201
6	-6.1	-.100	.348	.132	.108	3.53	-.024	.231	.108	2.08	.00088	.029	.029	.17	6.78	495
7	-18.3	-.300	.311	.090	.093	3.98	-.001	.126	.155	3.38	.00024	.021	.012	1.04	16.33	493
8	-30.5	-.500	.334	.081	.136	4.48	.006	.078	-.194	3.02	-.00016	-.025	.007	-2.09	23.60	492
9	-42.7	-.699	.347	.073	.124	3.31	.008	.062	-.184	3.07	.00042	.093	.005	1.21	9.69	492
10	-54.9	-.899	.318	.148	-.816	4.60	.002	.058	-.123	3.77	.00064	.075	.008	.49	9.44	216
11	-48.8	-.799	.332	.130	-.284	5.27	.004	.061	.164	4.03	-.00011	-.013	.007	-.64	9.52	227
12	-24.4	-.400	.321	.097	-.506	4.51	-.001	.092	-.190	3.67	-.00024	-.027	.009	-.62	17.09	487
13	-12.2	-.200	.325	.119	.336	4.83	-.011	.175	.116	2.48	.00016	.008	.020	-.01	8.76	487

ORIGINAL PAGE IS
OF POOR QUALITY

TABLE IV-46

AZIMUTHAL AND RADIAL VELOCITY DATA AND CORRELATIONS

Test Date: 12/1/82 Run No.: 46 Flow Condition: 1 Geometry: 2

Axial Location: 51 mm (2.0 in.) x/R_o = 0.833

P_t No.	r mm +(θ=0) -(θ=180)	r/R_o	W m/s	w' m/s	S_w	K_w	V m/s	v' m/s	S_v	K_v	$\overline{wv}$ m^2/s^2	R_{wv}	σ_{wv} m^2/s^2	S_{wv}	K_{wv}	N
1	.0	.000	-.002	.220	-.117	3.44	.022	.197	.086	2.65	.00224	.052	.048	1.45	12.44	248
2	5.1	.083	.017	.210	.420	3.35	.029	.168	-.307	4.79	.00056	.016	.039	-.25	9.64	246
3	10.2	.167	.023	.201	.107	2.83	.033	.176	.126	3.73	-.00210	-.059	.037	-.50	8.66	249
4	15.2	.250	.074	.204	-.388	4.07	.064	.179	.052	3.98	-.00188	-.052	.043	-2.12	22.86	249
5	20.3	.333	.116	.197	.045	3.48	.048	.210	-1.462	7.57	-.00435	-.105	.043	-2.13	17.32	249
6	25.4	.416	.150	.280	-.073	3.88	.051	.305	-.605	4.37	-.00474	-.058	.115	-1.30	13.93	249
7	30.5	.500	.195	.350	.044	3.81	.175	.338	-.138	3.65	-.00296	-.025	.130	.37	12.61	499
8	35.6	.583	.339	.358	-.239	3.58	.431	.363	-.326	3.17	-.00108	-.008	.142	.61	10.66	498
9	40.6	.666	.400	.337	-.425	4.05	.645	.360	-.184	2.86	-.00422	-.035	.123	.56	10.94	497
10	.0	.000	-.004	.223	.170	3.60	.028	.193	-.037	2.69	.00231	.054	.049	-.83	14.07	248
11	-5.1	-.083	.025	.230	.614	6.97	-.001	.207	.422	4.70	.00421	.088	.041	.19	9.42	248
12	-10.2	-.167	-.006	.218	.108	3.54	.025	.200	-.140	3.62	.00126	.029	.043	-.05	6.91	249
14	-15.2	-.250	.015	.190	.285	3.78	.021	.182	-.181	3.38	.00630	.182	.039	2.45	20.82	248
15	-15.2	-.250	.020	.349	-4.224	31.38	.037	.221	-.012	3.10	.00620	.080	.047	.64	5.77	248
16	-15.2	-.250	.023	.219	.042	3.59	.049	.218	.209	3.62	.00759	.158	.053	.41	9.21	247
17	-20.3	-.333	.063	.209	.115	3.13	.096	.209	.543	6.55	.00454	.104	.041	.64	8.09	247
18	-17.8	-.291	.025	.206	.018	3.88	.051	.197	.097	4.20	.00150	.037	.038	.85	10.31	246
19	43.2	.708	.291	.312	.227	3.18	.718	.462	-.505	2.25	-.00275	-.017	.145	-.43	6.06	495
20	38.1	.624	.369	.351	.018	3.37	.528	.450	-.307	2.31	-.00221	-.014	.155	-.53	6.21	499
21	33.0	.541	.239	.355	-.027	3.60	.258	.404	.029	3.14	.00539	.038	.143	.36	8.46	498
22	27.9	.458	.094	.282	-.086	5.45	.086	.353	-.327	4.75	.00042	.004	.097	1.18	18.52	497
23	22.9	.375	.068	.180	-.459	5.01	.032	.225	-.495	4.06	.01126	.278	.040	1.50	9.46	245
24	17.8	.291	.063	.194	.977	14.46	.039	.221	-1.065	5.32	-.00279	-.065	.065	-6.92	77.29	249
25	12.7	.208	.006	.158	-.301	6.30	.044	.182	-.672	4.12	.00012	.004	.027	-2.29	23.14	247

C-2

TABLE IV-47

AZIMUTHAL AND RADIAL VELOCITY DATA AND CORRELATIONS

Test Date: 12/7/82 Run No.: 47 Flow Condition: 1 Geometry: 2

Axial Location: 25 mm (1.0 in.) $x/R_o = 0.416$

P_t No.	r mm +(θ=0) -(θ=180)	r/R_o	W m/s	w' m/s	S_w	K_w	V m/s	v' m/s	S_v	K_v	$\overline{wv}$ m^2/s^2	R_{wv}	σ_{wv} m^2/s^2	S_{wv}	K_{wv}	N
1	2.1	.035	.010	.148	.130	5.40	.031	.156	-.070	4.27	.00233	.101	.028	1.02	15.84	477
2	7.2	.118	-.006	.166	-.229	4.00	.035	.154	-.210	3.38	.00386	.151	.034	1.45	12.51	478
3	12.3	.202	-.004	.169	.182	4.52	.070	.177	-.403	4.45	.00021	.007	.042	-.76	24.15	479
4	17.4	.285	.036	.237	.062	3.70	.030	.299	-.450	3.12	-.00068	-.010	.078	.17	8.73	497
5	22.5	.368	.327	.344	-.043	3.25	.176	.318	.028	2.93	-.00529	-.048	.110	.52	9.14	496
6	27.5	.451	.702	.224	-.181	4.07	.500	.233	-.056	2.77	.00117	.022	.054	-.14	10.03	495
7	32.6	.535	.616	.175	-.653	4.89	.556	.211	-.253	3.68	.00350	.095	.046	.09	19.35	475
8	2.1	.035	.009	.111	.998	7.09	.030	.141	.247	4.50	.00090	.058	.019	.13	17.10	495
9	-2.9	-.048	-.003	.112	.197	5.80	.011	.149	-.221	4.36	.00076	.046	.020	.37	15.85	491
10	-5.5	-.090	.001	.123	.779	7.44	.031	.145	-.174	4.26	.00241	.136	.021	2.53	27.98	499
11	-10.6	-.173	-.013	.135	.016	4.81	.061	.174	.016	3.27	.00100	.043	.029	.28	15.99	498
12	-15.6	-.256	-.014	.159	-.818	7.34	.019	.236	-.444	4.32	-.00019	-.005	.043	.79	27.25	495
14	-20.7	-.340	.096	.330	.512	4.50	.105	.353	.177	2.86	-.01300	-.111	.115	-.51	9.99	990
15	-25.8	-.423	.580	.403	-.276	2.19	.488	.302	-.141	2.90	-.00028	-.002	.124	.08	6.25	995
16	-28.3	-.465	.648	.331	-.739	2.97	.652	.278	-.129	3.03	.00053	.006	.093	-.73	8.95	493

ORIGINAL PAGE IS
OF POOR QUALITY

TABLE IV-48

AZIMUTHAL AND RADIAL VELOCITY DATA AND CORRELATIONS

Test Date: 12/7/82   Run No.: 48   Flow Condition: 1   Geometry: 2

Axial Location: 25 mm (1.0 in.) $x/R_o = 0.416$

P_t No.	r mm +(θ=0) -(θ=180)	r/R_o	W m/s	w' m/s	S_w	K_w	V m/s	v' m/s	S_v	K_v	$\overline{wv}$ m^2/s^2	R_{wv}	σ_{wv} m^2/s^2	S_{wv}	K_{wv}	N
1	.5	.084	-.005	.060	-2.590	23.07	.073	.095	1.029	7.66	-.00016	-.028	.006	-4.09	50.13	245
2	10.7	.251	.011	.141	.778	6.88	.043	.156	-.271	3.78	-.00062	-.028	.020	1.45	19.87	248
3	20.9	.417	.394	.367	-.232	2.63	.224	.283	.387	3.40	-.01120	-.108	.100	-.81	8.11	494
4	25.9	.500	.721	.229	-1.372	6.72	.559	.196	.198	3.57	.00673	.150	.046	1.51	13.98	492
	31.0	.584	.662	.155	-.453	4.06	.576	.209	-.748	4.55	-.00051	-.016	.037	.48	15.99	492
6	36.1	.667	.470	.357	-.185	3.20	.282	.397	.067	2.34	.02448	.173	.139	.68	8.69	496
7	41.2	.750	.346	.244	-.744	4.31	-.098	.192	.071	3.50	.01155	.247	.057	3.04	22.53	494
8	46.3	.833	.305	.249	-.355	4.04	-.167	.183	.020	2.63	.00997	.218	.051	2.44	23.15	499
9	51.3	.917	.258	.249	.423	4.78	-.162	.174	-.310	3.47	.00883	.204	.046	1.64	17.87	496

TABLE IV-49

AZIMUTHAL AND RADIAL VELOCITY DATA AND CORRELATIONS

Test Date: 12/7/82 Run No.: 49 Flow Condition: 1 Geometry: 2

Axial Location: 25 mm (1.0 in.) $x/R_o = 0.416$

F_t No.	r mm +(θ=0) -(θ=180)	r/R_o	W m/s	w' m/s	S_w	K_w	V m/s	v' m/s	S_v	K_v	$\overline{wv}$ m^2/s^2	R_{wv}	σ_{wv} m^2/s^2	S_{wv}	K_{wv}	N
1	.0	.000	-.030	.148	-.093	4.14	.021	.143	.357	4.34	.00229	.108	.023	1.55	13.80	247
2	-10.2	-.167	.007	.161	-.039	4.74	.062	.164	-.107	3.19	.00300	.113	.029	2.52	17.15	248
3	-20.3	-.333	.200	.376	.706	3.15	.172	.333	.231	2.63	-.02153	-.172	.120	-.16	6.36	492
4	-25.4	-.416	.503	.497	.092	1.43	.523	.242	.039	2.97	.00567	.047	.122	.19	4.11	496
5	-30.5	-.500	-.026	.048	-.141	3.28	.055	.210	-.065	4.69	.00015	.015	.010	-.49	10.13	434
6	-30.5	-.500	.740	.219	-1.776	7.99	.646	.205	-.185	3.37	.00128	.028	.051	2.20	28.78	498
7	-35.6	-.583	.457	.415	.235	1.97	.473	.416	.032	1.97	.03311	.192	.158	-.12	3.78	498
8	-40.6	-.666	.424	.298	-.177	3.04	-.045	.260	.543	5.69	.01416	.183	.094	2.53	19.18	496
9	-45.7	-.749	.431	.277	-.056	2.56	-.177	.243	-.554	2.74	.01779	.264	.066	.78	6.29	498
10	-38.1	-.624	.508	.303	.005	2.79	.136	.371	.949	3.77	.01342	.119	.126	.31	8.87	495

TABLE IV-50

AZIMUTHAL AND RADIAL VELOCITY DATA AND CORRELATIONS

Test Date: 12/10/82 Run No.: 50 Flow Condition: 1 Geometry: 2

Axial Location: 51 mm (2.0 in.) $x/R_o = 0.833$

P_t No.	r mm +(θ=0) -(θ=180)	r/R_o	W m/s	w' m/s	S_w	K_w	V m/s	v' m/s	S_v	K_v	$\overline{wv}$ m^2/s^2	R_{wv}	σ_{wv} m^2/s^2	S_{wv}	K_{wv}	N
1	.0	.000	.054	.158	1.157	6.19	.009	.197	-.236	3.16	.00106	.034	.035	-.57	13.57	491
2	2.5	.042	.055	.150	.401	5.66	.027	.193	-.182	3.12	.00305	.100	.030	-.11	13.96	492
3	5.1	.083	.069	.158	.717	4.77	.036	.180	-.505	3.30	.00270	.095	.031	1.54	14.73	496
4	10.2	.167	.064	.127	.774	5.13	.067	.167	-.033	3.10	.00119	.056	.024	.15	15.75	493
5	15.2	.250	.094	.149	1.319	5.57	.055	.173	-.702	4.06	-.00096	-.037	.032	-3.51	40.45	495
6	20.3	.333	.102	.148	.960	4.69	.071	.191	-.362	3.35	.00144	.051	.031	-.49	11.16	492
7	25.4	.416	.123	.217	.680	5.09	.063	.274	-.536	3.45	.00073	.012	.075	-.38	19.95	497
8	30.5	.500	.162	.301	1.159	4.89	.177	.313	-.556	3.38	-.00972	-.103	.106	-1.33	13.01	487
9	.0	.000	.065	.160	1.249	5.65	.008	.193	-.446	3.34	-.00023	-.008	.030	.36	9.05	494
10	-2.5	-.042	-.040	.128	-.777	5.12	.017	.186	.016	3.07	.00173	.073	.024	.20	10.30	495
11	-5.1	-.083	-.048	.142	-.887	6.00	.004	.175	.160	3.29	-.00200	-.081	.025	-.74	10.15	492
12	-10.2	-.167	-.027	.129	-1.246	7.38	.057	.168	.059	3.42	.00153	.071	.024	2.18	21.70	496
14	-15.2	-.250	.001	.127	-.826	8.86	.075	.168	.203	3.93	.00111	.052	.022	.72	12.82	498
15	-20.3	-.333	.054	.120	.111	3.78	.098	.151	-.140	3.19	.00092	.051	.018	.16	10.04	496
16	-25.4	-.416	.086	.148	.536	4.23	.073	.191	-.454	3.97	.00134	.047	.033	-.68	16.59	487
17	-30.5	-.500	.047	.221	-.653	5.71	.060	.283	-.857	3.76	.00697	.111	.082	-.54	15.69	490

ORIGINAL PAGE IS
OF POOR QUALITY

TABLE IV-51

AZIMUTHAL AND RADIAL VELOCITY DATA AND CORRELATIONS

Test Date: 12/10/82 Run No.: 51 Flow Condition: 1 Geometry: 2

Axial Location: 51 mm (2.0 in.) $x/R_o = 0.833$

P_t No.	r mm +(θ=0) -(θ=180)	r/R_o	W m/s	w' m/s	S_w	K_w	V m/s	v' m/s	S_v	K_v	$\overline{wv}$ m^2/s^2	R_{wv}	σ_{wv} m^2/s^2	S_{wv}	K_{wv}	N
1	.0	.000	.075	.173	.563	5.22	.013	.186	-.274	3.25	.00190	.059	.036	1.52	11.97	494
2	15.2	.250	.097	.166	.907	5.64	.077	.171	-.424	4.16	.00145	.051	.031	.74	13.34	494
3	30.5	.500	.156	.278	-.056	3.65	.081	.284	-.459	3.06	.01529	.194	.093	.63	11.31	492
4	-15.2	-.250	.019	.171	-1.025	7.83	.083	.172	-.047	3.36	.00532	.180	.037	2.66	24.56	498
5	-15.2	-.250	.015	.161	-.663	5.34	.068	.153	-.034	3.30	.00471	.191	.030	.70	13.16	492
6	-25.4	-.416	.073	.205	-.719	4.90	.073	.234	-.794	4.27	.01040	.217	.060	1.67	18.45	490
7	-20.3	-.333	.093	.157	-.027	4.29	.095	.167	-.117	3.46	.00182	.070	.032	.56	12.07	494
8	-15.2	-.250	.025	.154	-.421	5.85	.080	.173	-.395	4.24	.00487	.184	.032	2.78	21.18	499
9	-10.2	-.167	-.006	.154	-.147	4.83	.059	.176	.202	3.31	.00491	.181	.032	1.83	19.73	496
10	-5.1	-.083	-.039	.155	-.167	4.77	.052	.170	-.008	3.12	.00539	.205	.032	1.32	18.32	497
11	5.1	.083	.055	.170	-.200	4.15	.016	.191	-.431	3.22	.00696	.215	.039	.86	13.03	497
12	10.2	.167	.100	.165	-.255	3.91	.065	.168	-.316	3.55	.00279	.101	.034	1.80	16.49	498
14	20.3	.333	.128	.163	-.056	4.54	.061	.185	-.514	4.13	.00304	.100	.043	-1.78	30.42	498
15	25.4	.416	.143	.200	-.056	3.68	.077	.200	-.424	3.74	.00097	.024	.052	-.53	13.26	491
16	30.5	.500	.163	.292	-.073	3.74	.108	.293	-.619	3.54	.00690	.081	.102	1.64	13.87	497
17	.0	.000	.063	.180	.277	3.90	.009	.176	-.206	3.00	.00325	.103	.033	1.26	8.08	493

TABLE IV-52

AZIMUTHAL AND RADIAL VELOCITY DATA AND CORRELATIONS

Test Date: 12/13/82 Run No.: 52 Flow Condition: 1 Geometry: 2

Axial Location: 51 mm (2.0 in.) $x/R_o = 0.833$

P_t No.	r mm +(θ=0) -(θ=180)	r/R_o	W m/s	w' m/s	S_w	K_w	V m/s	v' m/s	S_v	K_v	$\overline{wv}$ m^2/s^2	R_{wv}	σ_{wv} m^2/s^2	S_{wv}	K_{wv}	N
1	.0	.000	.064	.190	-.075	3.11	.016	.188	-.080	3.21	-.00338	-.095	.038	-.17	9.08	493
2	5.1	.033	.081	.197	-.089	2.92	.023	.189	-.380	2.97	.00192	.052	.039	.16	7.27	493
3	10.2	.167	.086	.178	.115	2.99	.056	.168	-.369	3.19	.00094	.032	.033	-.58	11.57	498
4	15.2	.250	.092	.164	.197	3.72	.073	.171	-.166	3.08	.00043	.015	.027	.23	8.25	497
5	20.3	.333	.119	.179	-.028	3.64	.044	.182	-.540	3.56	.00112	.034	.040	-1.21	22.12	492
6	25.4	.416	.135	.240	-.407	3.94	.033	.245	-.746	3.72	.00401	.068	.060	.14	15.10	495
7	30.5	.500	.152	.334	-.281	3.53	.110	.298	-.464	3.39	-.00130	-.013	.106	-.41	9.72	496
8	50.8	.833	.264	.354	-.205	2.96	.295	.343	-.274	2.88	-.00341	-.028	.129	-.21	7.72	493
9	40.6	.666	.370	.340	-.127	3.50	.528	.367	-.422	3.18	-.01646	-.132	.128	-.28	10.99	498
10	45.7	.749	.367	.293	.179	3.18	.650	.349	-.445	2.79	.00246	.024	.103	-1.27	12.05	498
11	50.8	.833	.330	.317	-.012	3.18	.564	.360	-.198	2.55	.00640	.056	.121	1.46	9.21	491
12	.0	.000	.050	.192	-.165	2.92	-.020	.179	-.014	3.10	.00057	.016	.033	.11	6.13	498
14	-5.1	-.083	-.033	.188	.400	2.94	.050	.190	-.342	3.37	-.00030	-.008	.039	-.18	9.34	499
15	.0	.000	.058	.224	-.122	3.09	-.006	.188	-.050	2.94	-.00417	-.099	.044	-.54	8.67	498

ORIGINAL PAGE IS
OF POOR QUALITY

TABLE IV-53

AZIMUTHAL AND RADIAL VELOCITY DATA AND CORRELATIONS

Test Date: 12/13/82 Run No.: 53 Flow Condition: 1 Geometry: 2

Axial Location: 51 mm (2.0 in.) $x/R_o = 0.833$

P_t No.	r mm +(θ=0) −(θ=180)	r/R_o	W m/s	w' m/s	S_w	K_w	V m/s	v' m/s	S_v	K_v	$\overline{wv}$ m^2/s^2	R_{wv}	σ_{wv} m^2/s^2	S_{wv}	K_{wv}	N
1	-21.2	-.250	.120	.217	-.203	4.61	.078	.232	-.969	4.79	.00660	.131	.067	2.53	24.60	460
2	-26.3	-.334	.139	.267	-.053	4.13	.118	.255	-.672	4.00	.00069	.010	.083	.49	15.29	492
3	-31.3	-.417	.143	.387	.095	3.54	.175	.321	-.492	3.11	-.00646	-.052	.123	-.78	8.83	498
4	-36.4	-.500	.198	.380	.506	3.72	.350	.368	-.494	3.09	.00304	.022	.133	.70	9.36	494
5	-41.5	-.583	.359	.343	-.122	3.28	.536	.409	-.362	3.19	.00477	.034	.136	.64	7.20	495
6	-21.2	-.250	.133	.213	.244	4.23	.086	.211	-.656	3.79	.00529	.118	.058	-.23	22.40	473
7	-16.1	-.167	.086	.181	.159	4.39	.107	.154	-.086	2.91	.00069	.025	.026	.80	11.67	471
8	-11.0	-.084	.059	.169	.511	4.38	.087	.167	-.175	3.04	-.00099	-.035	.029	-.50	10.33	490
9	-5.9	-.001	.006	.178	.060	3.35	.080	.174	-.199	3.01	-.00069	-.022	.034	-.50	8.85	483
10	-.9	.083	.044	.175	-.240	4.02	-.033	.163	.123	3.11	-.00000	-.000	.032	-.73	8.73	245
11	4.2	.166	.054	.207	-.703	4.88	.015	.172	.009	3.53	-.00393	-.110	.043	-.94	15.81	245

ORIGINAL PAGE IS
OF POOR QUALITY

TABLE IV-54

AZIMUTHAL AND RADIAL VELOCITY DATA AND CORRELATIONS

Test Date: 12/15/82   Run No.: 54   Flow Condition: 1   Geometry: 2

Axial Location: 102 mm (4.0 in.) x/R_o = 1.665

P_t No.	r mm +(θ=0) −(θ=180)	r/R_o	W m/s	w m/s	S_w	K_w	V m/s	v' m/s	S_v	K_v	$\overline{wv}$ m^2/s^2	R_{wv}	σ_{wv} m^2/s^2	S_{wv}	K_{wv}	N
1	2.1	.083	.078	.198	−.353	3.82	−.076	.206	.104	3.18	−.00027	−.007	.044	−.20	7.92	484
2	7.2	.166	.177	.204	−.409	3.69	−.056	.208	−.023	2.74	.00433	.102	.045	1.94	21.21	494
3	12.3	.250	.261	.188	−.283	4.13	−.068	.199	−.200	3.09	.00478	.128	.043	3.44	38.30	490
4	17.3	.333	.295	.181	−.067	3.67	−.060	.207	−.014	2.74	.00591	.158	.039	.60	7.58	495
5	22.4	.416	.356	.197	−.902	6.31	−.084	.176	.135	2.86	.00699	.181	.037	.81	7.65	497
6	27.5	.499	.359	.195	−.243	4.09	−.066	.208	−.195	2.73	.00611	.150	.042	1.05	10.08	496
7	32.6	.583	.351	.206	−.360	3.89	−.095	.229	−.006	2.39	.00584	.124	.048	1.12	9.31	498
8	35.1	.624	.345	.208	−.401	3.82	−.117	.212	−.020	2.74	.01063	.241	.048	1.48	18.64	496
9	2.1	.083	.100	.194	−.343	3.23	−.083	.203	.154	2.53	.00131	.033	.043	.42	8.79	482
10	−.4	.041	.003	.222	−.343	2.97	−.053	.206	.005	2.30	−.00225	−.049	.046	.60	7.67	490
11	−5.5	−.042	.072	.205	.428	3.37	.044	.220	−.106	2.65	−.00065	−.014	.048	.85	8.20	483
12	−10.6	−.125	.191	.233	.400	4.00	.009	.242	−.019	2.80	.00145	.026	.061	.28	13.72	485
14	−15.7	−.208	.288	.223	−.325	3.63	.031	.232	−.128	2.56	.00215	.042	.052	1.35	12.21	494
15	−20.7	−.292	.332	.230	−.007	3.66	−.045	.232	.019	2.62	.00521	.098	.053	.09	7.44	494
16	−25.3	−.375	.339	.253	.010	3.42	−.059	.243	.211	2.47	.01292	.211	.061	1.25	8.40	490
17	−28.4	−.417	.341	.215	−.310	3.19	−.037	.245	−.095	2.33	.00581	.111	.049	.32	5.11	243

TABLE IV-55

AZIMUTHAL AND RADIAL VELOCITY DATA AND CORRELATIONS

Test Date: 12/15/82 Run No.: 55 Flow Condition: 1 Geometry: 2

Axial Location: 102 mm (4.0 in.) x/R_o = 1.665

P_t No.	r mm +(θ=0) -(θ=180)	r/R_o	W m/s	w' m/s	S_w	K_w	V m/s	v' m/s	S_v	K_v	$\overline{wv}$ m^2/s^2	R_{wv}	σ_{wv} m^2/s^2	S_{wv}	K_{wv}	N
1	.0	.000	.010	.211	.001	2.87	-.022	.212	-.183	2.75	-.00317	-.071	.045	-.71	8.80	496
2	5.1	.083	.107	.196	-.306	3.60	-.054	.208	-.084	2.91	.00354	.087	.044	1.74	14.71	499
3	10.2	.167	.213	.192	-.174	3.56	-.046	.205	.014	2.43	.00272	.069	.040	.29	5.97	498
4	15.2	.250	.270	.184	.023	3.58	-.048	.206	-.264	2.94	.00063	.017	.036	.72	11.34	494
5	20.3	.333	.310	.181	-.231	3.68	-.062	.210	-.245	2.90	.00566	.149	.042	1.56	10.68	498
6	25.4	.416	.361	.187	-.133	3.21	-.066	.216	-.308	2.87	.01008	.250	.044	1.40	12.33	498
7	30.5	.500	.333	.206	-.608	4.30	-.106	.220	-.013	2.58	.01267	.279	.046	1.64	10.38	498
8	35.6	.583	.331	.236	-.441	3.83	-.096	.229	-.094	2.76	.00748	.139	.057	.37	8.24	499
9	40.6	.666	.339	.241	-.162	3.29	-.106	.246	-.001	2.61	.01178	.199	.058	1.03	8.42	498
10	45.7	.749	.320	.251	-.196	2.83	-.095	.235	-.050	2.54	.00750	.127	.057	.43	6.61	497
11	50.8	.833	.322	.255	-.179	2.97	-.054	.234	-.123	2.87	.00609	.102	.060	2.25	20.73	495
12	.0	.000	-.000	.205	-.078	3.15	-.023	.198	-.156	2.82	-.00018	-.004	.044	.25	8.79	497
13	-5.1	-.083	.091	.205	.013	2.59	.017	.210	.089	2.88	-.00426	-.099	.043	-.68	8.16	493
14	-10.2	-.167	.183	.205	-.034	2.92	-.027	.220	.278	3.20	-.00160	-.036	.048	.18	8.36	487

TABLE IV-56

AZIMUTHAL AND RADIAL VELOCITY DATA AND CORRELATIONS

Test Date: 12/15/82 Run No.: 56 Flow Condition: 1 Geometry: 2

Axial Location: 102 mm (4.0 in.) $x/R_o = 1.665$

P_t No.	r mm +(θ=0) -(θ=180)	r/R_o	W m/s	w' m/s	S_w	K_w	V m/s	v' m/s	S_v	K_v	$\overline{wv}$ m^2/s^2	R_{wv}	σ_{wv} m^2/s^2	S_{wv}	K_{wv}	N
1	.0	.000	.048	.223	-.413	3.79	-.015	.238	-.128	2.79	.00002	.000	.054	-.37	7.44	491
2	-25.4	-.416	.315	.229	.068	4.66	-.063	.241	.024	2.91	.01068	.193	.052	1.42	8.28	490
3	-30.5	-.500	.341	.255	.015	4.60	-.112	.241	-.012	2.66	.00813	.132	.064	.34	11.49	481
4	-35.6	-.583	.358	.266	.157	3.45	-.140	.241	.029	2.72	.01412	.220	.057	.53	6.92	495
5	-40.6	-.666	.331	.291	.300	3.68	-.151	.247	.356	2.91	.00488	.068	.070	-.45	10.43	488
6	-45.7	-.749	.312	.325	.025	3.21	-.114	.249	.275	2.77	.00475	.059	.078	-.21	8.73	490
7	-50.8	-.833	.330	.293	.300	3.86	-.068	.256	.526	3.25	.00346	.046	.071	.35	8.21	491
8	-20.3	-.333	.321	.207	-.029	4.11	-.077	.216	-.181	3.08	.01008	.225	.047	2.07	12.14	493
9	-15.2	-.250	.281	.215	-.083	3.58	-.046	.193	.076	3.05	.00413	.099	.042	.20	11.12	482
10	-10.2	-.167	.167	.247	.826	5.67	-.047	.221	.149	3.64	.00393	.072	.057	2.78	28.90	495

TABLE IV-59

AXIAL AND AZIMUTHAL VELOCITY DATA AND CORRELATIONS

Test Date: 2/28/83 Run No.: 59 Flow Condition: 1 Geometry: 3

Axial Location: 5 mm (0.2 in.) x/R_o = 0.083 Swirler Orientation, ϕ = 75 deg

P_t No.	r mm +(θ=90) -(θ=270)	r/R_o	U m/s	u' m/s	S_u	K_u	W m/s	w' m/s	S_w	K_w	$\overline{uw}$ m^2/s^2	R_{uw}	σ_{uw} m^2/s^2	S_{uw}	K_{uw}	N
1	15.2	.250	.284	.483	.114	2.71	.064	.395	-.122	3.25	.05605	.294	.191	.63	6.14	498
2	18.3	.300	1.602	.117	-.684	3.39	1.061	.085	-.492	3.50	.00205	.206	.011	1.31	12.55	999
3	21.3	.350	1.609	.085	-.773	4.89	.936	.062	-.424	3.47	.00056	.107	.006	2.01	19.60	999
4	24.4	.400	1.600	.082	-.125	8.09	1.002	.067	.466	5.16	.00092	.168	.008	7.29	149.50	995
5	27.4	.449	1.337	.377	-.778	3.31	.788	.248	-.215	3.28	.00373	.040	.101	.48	9.64	998
6	30.5	.499	1.371	.417	-.645	3.47	.343	.323	-.186	3.13	-.01381	-.103	.133	-.94	9.97	999
7	33.5	.549	-.007	.130	-.481	3.92	.596	.145	-.287	3.44	-.00243	-.128	.022	2.92	43.57	999
8	36.6	.599	.006	.113	-.103	4.35	.578	.134	-.152	3.09	-.00056	-.037	.017	-1.92	29.34	996
9	35.0	.574	-.001	.110	-.156	3.25	.582	.130	-.067	3.11	-.00129	-.090	.014	-.20	8.74	994
10	32.0	.524	.097	.276	.833	4.85	.585	.222	-.029	3.77	-.01157	-.188	.079	-1.12	15.84	992
11	29.0	.475	1.484	.317	-.638	3.41	.517	.223	-.351	4.16	.01102	.156	.082	.51	17.22	999
12	31.2	.512	.680	.509	.294	2.38	.452	.357	-.254	3.24	-.06849	-.377	.170	-.88	6.20	997
13	29.7	.487	1.555	.787	-.307	3.84	.466	.254	-.612	3.71	.00684	.094	.078	.53	13.18	996
14	28.2	.462	1.340	.369	-.627	3.33	.594	.242	-.065	3.39	.00186	.021	.090	-.31	10.51	995
15	25.9	.424	1.580	.207	-1.350	5.53	1.002	.151	.426	5.75	-.00218	-.070	.047	[illegible]	24.62	982
16	22.8	.375	1.684	.074	-.418	6.68	.956	.053	-.514	3.93	.00035	.088	.004	1.33	12.72	998
17	19.8	.325	1.639	.104	-.677	4.22	.979	.080	-.519	2.88	.00140	.168	.009	1.48	13.63	998
18	16.8	.275	1.370	.317	-1.053	4.16	1.102	.248	-1.251	5.50	.02624	.334	.108	2.00	17.44	989

ORIGINAL PAGE IS
OF POOR QUALITY

TABLE IV-60

AXIAL AND AZIMUTHAL VELOCITY DATA AND CORRELATIONS

Test Date: 3/1/83 Run No.: 60 Flow Condition: 1 Geometry: 3

Axial Location: 5 mm (0.2 in.) x/R_O = 0.082 Swirler Orientation, ϕ = 80 deg

P_E No.	r mm +(θ=90) −(θ=270)	r/R_O	U m/s	u' m/s	S_u	K_u	W m/s	w' m/s	S_w	K_w	$\overline{uw}$ m^2/s^2	R_{uw}	σ_{uw} m^2/s^2	S_{uw}	K_{uw}	N
1	15.2	.250	.745	.480	.085	2.46	.686	.402	-.094	2.66	.04282	.222	.192	-.08	6.88	247
2	18.3	.300	1.578	.089	-.734	5.46	1.081	.076	-1.813	13.56	.00004	.006	.308	-.44	30.65	985
3	21.3	.350	1.743	.079	-.217	2.71	.920	.056	-.103	2.53	-.00042	-.095	.005	.83	13.06	975
4	24.4	.400	1.740	.162	-1.162	7.89	.876	.122	-.156	9.66	.00170	.086	.033	.28	41.83	996
5	27.4	.449	.768	.324	-.107	3.29	.660	.398	-.121	2.88	.02819	.219	.133	1.31	11.14	994
6	30.5	.499	.720	.492	.375	2.59	.199	.369	-.223	2.75	-.07313	-.403	.170	-.65	5.38	998
7	33.5	.549	.043	.105	.046	3.26	.580	.143	-.069	2.94	-.00118	-.079	.017	-1.81	17.50	995
8	36.6	.599	.025	.109	.024	3.39	.583	.129	-.017	3.16	-.00014	-.010	.015	.09	8.87	991
9	32.0	.524	.081	.139	-.473	4.26	.563	.164	.150	3.22	-.00331	-.145	.024	-.48	10.54	996
10	29.0	.475	1.371	.363	-.246	2.73	-.085	.295	.463	4.24	.00134	.013	.111	-.23	12.08	997
11	25.9	.424	1.128	.358	-.084	2.64	.861	.263	-.128	3.41	.00355	.038	.094	.19	7.52	999
12	22.8	.375	1.763	.072	-.068	2.21	.893	.047	.049	2.52	-.00026	-.075	.003	-1.19	11.63	996
13	19.8	.325	1.709	.074	-.394	7.22	.991	.063	-.352	3.62	-.00076	-.163	.005	.66	14.02	993
14	16.8	.275	1.545	.214	-1.534	6.82	1.150	.139	-.400	5.08	.00365	.123	.043	5.51	54.79	991
15	-3.4	-.055	.842	.078	.778	8.65	.008	.086	-.741	11.06	-.00068	-.102	.007	-1.46	21.96	979
16	-.3	-.006	.840	.094	.862	11.08	.011	.081	.609	8.45	.00020	.026	.008	3.53	47.04	980
17	2.7	.044	.810	.111	-.606	8.02	-.003	.087	.271	8.20	.00026	.026	.012	.00	60.33	963
18	5.8	.094	.753	.195	.618	13.21	.007	.096	.369	7.07	.00003	.002	.023	-1.10	52.47	981
19	8.8	.144	.551	.281	-1.897	7.62	.037	.145	.829	6.80	-.00502	-.123	.059	-6.20	85.44	945
20	10.3	.169	.437	.414	-.143	3.84	.002	.553	-1.797	7.66	-.02480	-.108	.182	-.69	11.24	986
21	11.9	.194	.359	.512	.777	3.57	.782	.437	-1.006	4.84	.00284	.013	.193	.64	6.41	976
22	10.8	.176	.264	.421	.128	3.43	.180	.499	-.846	5.12	-.03214	-.153	.190	-.51	9.68	951
23	11.3	.186	.293	.522	1.300	5.30	.484	.518	-.912	4.90	-.00689	-.025	.208	.10	6.76	972

ORIGINAL PAGE IS
OF POOR QUALITY

TABLE IV-61

AXIAL AND AZIMUTHAL VELOCITY DATA AND CORRELATIONS

Test Date: 3/1/83 Run No.: 61 Flow Condition: 1 Geometry: 3

Axial Location: 5 mm (0.2 in.) $x/R_o = 0.083$ Swirler Orientation, $\phi = 85$ deg

P_t No.	r mm +(θ=90) -(θ=270)	r/R_o	U m/s	u' m/s	S_u	K_u	W m/s	w' m/s	S_w	K_w	$\overline{uw}$ m^2/s^2	R_{uw}	σ_{uw} m^2/s^2	S_{uw}	K_{uw}	N
1	15.2	.250	.707	.473	-.058	2.30	.806	.394	-.201	2.88	.06891	.369	.171	.81	5.97	498
2	13.5	.222	.177	.413	-.310	2.31	.090	.223	.727	4.41	-.02488	-.270	.079	-.70	5.92	245
3	16.8	.275	1.613	.131	-.567	3.56	1.140	.097	.173	3.43	-.00082	-.064	.014	.09	11.93	991
4	18.3	.300	1.688	.077	-.369	8.13	1.055	.061	-.250	2.59	-.00098	-.209	.005	-.02	11.64	988
5	19.8	.325	1.725	.069	-.291	7.08	.956	.060	-.050	3.00	-.00084	-.205	.005	-.93	14.05	994
6	21.3	.350	1.768	.068	-.380	4.34	.856	.055	.134	2.35	-.00075	-.200	.004	-1.03	11.22	993
7	22.8	.375	1.805	.070	-.164	2.03	.766	.054	.197	3.72	-.00074	-.198	.004	-.95	11.87	996
8	24.4	.400	1.858	.112	.216	3.60	.632	.103	-1.219	6.25	.00144	.124	.015	2.17	23.10	973
9	25.9	.424	1.623	.327	-.525	3.18	.462	.277	-.558	3.86	.01939	.214	.098	1.33	11.73	998
10	27.4	.449	1.405	.296	-.177	3.11	.503	.309	-.690	3.34	.01254	.137	.095	-.06	9.67	998
11	29.0	.475	1.366	.302	-.348	3.21	.327	.333	-.847	3.58	.01254	.125	.108	.05	8.66	998
12	30.5	.499	.547	.373	.643	2.61	.472	.249	-.412	3.87	-.01410	-.152	.100	-1.44	15.97	999
13	32.0	.524	.115	.122	-.367	3.39	.595	.158	-.139	3.18	-.00353	-.183	.020	-.87	9.75	991
14	33.5	.549	.070	.111	-.039	3.71	.611	.154	-.031	2.93	-.00163	-.096	.018	-.32	12.91	998
15	36.6	.599	.037	.127	-.168	3.23	.594	.139	-.201	3.48	.00044	.026	.018	-.19	7.99	498
16	28.2	.462	1.445	.266	-.219	3.31	.430	.329	-.854	3.57	.02216	.254	.094	.66	10.18	996
17	25.1	.412	1.805	.230	-.766	4.34	.530	.205	-1.248	5.42	.00880	.187	.067	1.44	21.92	992

TABLE IV-62

AXIAL AND AZIMUTHAL VELOCITY DATA AND CORRELATIONS

Test Date: 3/1/83 Run No.: 62 Flow Condition: 1 Geometry: 3

Axial Location: 5 mm (0.2 in.) $x/R_o = 0.083$ Swirler Orientation, $\phi = 90$ deg

P_t No.	r mm +(θ=90) -(θ=270)	r/R_o	U m/s	u' m/s	S_u	K_u	W m/s	w' m/s	S_w	K_w	$\overline{uw}$ m^2/s^2	R_{uw}	σ_{uw} m^2/s^2	S_{uw}	K_{uw}	N
1	13.5	.222	.795	.496	-.529	2.73	.099	.229	.443	4.82	-.01899	-.209	.091	-1.69	14.67	238
2	15.2	.250	.846	.499	-.198	2.68	.832	.356	-.315	2.81	.05126	.289	.169	.80	6.28	999
3	16.8	.275	1.625	.138	-.665	3.86	1.126	.103	.068	4.15	-.00102	-.072	.018	1.09	37.07	991
4	18.3	.300	1.687	.079	-.591	6.68	1.036	.071	-.063	3.42	-.00122	-.219	.006	-.92	15.80	992
5	19.8	.325	1.727	.069	-.143	6.04	.924	.064	-.054	2.31	-.00121	-.273	.005	-1.18	9.50	993
6	21.3	.350	1.777	.069	-.227	3.65	.816	.061	.179	2.41	-.00135	-.319	.005	-1.21	9.06	990
7	22.8	.375	1.814	.063	-.150	-2.93	.717	.057	.466	3.86	-.00100	-.278	.004	-2.71	26.69	997
8	24.4	.400	1.875	.066	-.369	8.96	.598	.057	.043	3.35	-.00078	-.207	.004	-2.95	31.35	993
9	25.9	.424	1.900	.089	-.695	5.44	.524	.077	-.245	3.82	-.00117	-.170	.008	-1.54	16.54	993
10	27.4	.449	1.852	.118	-.291	3.03	.502	.090	-.267	4.26	-.00142	-.134	.012	-2.28	24.07	993
11	29.0	.475	1.724	.145	-.509	3.76	.491	.110	-.051	3.28	-.00060	-.038	.017	-.99	15.18	997
12	30.5	.499	.753	.494	.350	1.98	.558	.217	.167	3.42	.00444	.041	.097	-.51	6.30	997
13	32.0	.524	.130	.123	-.364	3.64	.611	.160	.015	2.93	-.00401	-.204	.021	-1.25	12.54	995
14	33.5	.549	.083	.110	-.278	3.22	.619	.141	.109	2.95	-.00120	-.078	.017	-.33	10.57	992
15	36.6	.599	.050	.113	-.364	3.82	.601	.137	-.047	3.74	-.00133	-.086	.017	-.23	9.49	498

ORIGINAL PAGE IS
OF POOR QUALITY

TABLE IV-63

AXIAL AND AZIMUTHAL VELOCITY DATA AND CORRELATIONS

Test Date: 3/1/83 Run No.: 63 Flow Condition: 1 Geometry: 3

Axial Location: 5 mm (0.2 in.) $x/R_o = 0.083$ Swirler Orientation, ϕ = 95 deg

P_t No.	r mm +(θ=90) -(θ=270)	r/R_o	U m/s	u' m/s	S_u	K_u	W m/s	w' m/s	S_w	K_w	$\overline{uw}$ m^2/s^2	R_{uw}	σ_{uw} m^2/s^2	S_{uw}	K_{uw}	N
1	13.5	.222	.165	.600	-.551	3.96	-1.366	1.097	.201	1.60	-.01751	-.024	.410	.01	2.64	244
2	15.2	.250	.470	.500	.189	2.69	.510	.312	-.183	3.22	.04498	.288	.161	.54	8.55	979
3	16.8	.275	1.339	.387	-.581	2.89	.925	.257	-.267	3.48	.01527	.153	.104	.72	8.69	995
4	18.3	.300	1.655	.104	-.138	4.69	1.036	.065	.591	4.40	-.00009	-.010	.011	-1.31	40.30	981
5	19.8	.325	1.705	.070	-.066	6.81	.913	.060	.019	2.57	-.00081	-.192	.005	-.60	9.90	993
6	21.3	.350	1.759	.068	-.061	4.98	.803	.060	.135	2.88	-.00130	-.321	.004	-1.33	10.69	993
7	22.8	.375	1.800	.069	-.195	-.17	.705	.061	.396	3.55	-.00146	-.348	.005	-1.50	16.99	985
8	24.4	.400	1.851	.071	-.448	2.29	.610	.059	.230	3.34	-.00112	-.272	.005	-3.35	33.01	992
9	25.9	.424	1.887	.081	-.603	2.55	.537	.062	.142	3.91	-.00109	-.216	.006	-1.49	20.57	983
10	27.4	.449	1.859	.112	-.606	3.15	.485	.073	.036	3.44	-.00171	-.210	.009	-1.08	25.38	990
11	29.0	.475	1.770	.133	-.751	2.62	.489	.092	.001	2.91	-.00138	-.112	.013	-.16	11.01	985
12	30.5	.499	.916	.517	-.094	1.84	.558	.200	.024	3.54	-.00316	-.031	.093	-.46	6.05	997
13	32.0	.524	.127	.129	-.288	3.34	.642	.160	-.022	3.13	-.00252	-.122	.022	-.89	11.61	988
14	33.5	.549	.082	.113	-.194	3.39	.644	.142	-.222	2.92	-.00147	-.091	.018	-.82	14.43	988
15	36.6	.599	.028	.113	-.004	3.62	.626	.141	-.048	2.81	.00161	.101	.017	1.25	10.67	491

ORIGINAL PAGE IS
OF POOR QUALITY

TABLE IV-64

AXIAL AND AZIMUTHAL VELOCITY DATA AND CORRELATIONS

Test Date: 3/2/83 Run No.: 64 Flow Condition: 1 Geometry: 3

Axial Location: 5 mm (0.2 in.) $x/R_o = 0.083$ Swirler Orientation, $\phi = 70$ deg

P_t No.	r mm +(θ=90) -(θ=270)	r/R_o	U m/s	u' m/s	S_u	K_u	W m/s	w' m/s	S_w	K_w	$\overline{uw}$ m^2/s^2	R_{uw}	σ_{uw} m^2/s^2	S_{uw}	K_{uw}	N
1	13.5	.222	.235	.491	-.822	3.42	-.050	.306	-1.710	6.73	-.01505	-.100	.128	-.18	8.48	210
2	15.2	.250	.208	.440	.577	3.26	.587	.386	-.311	3.14	.04598	.271	.180	1.16	7.74	469
3	16.8	.275	1.284	.365	-.967	4.40	1.069	.262	-1.518	7.10	.03106	.324	.106	3.02	19.18	987
4	18.3	.300	1.501	.193	-1.996	11.09	1.002	.119	-.980	6.27	.00478	.207	.029	6.62	101.00	989
5	19.8	.325	1.563	.135	-.526	4.96	.898	.093	-.362	3.29	.00296	.236	.012	.99	15.10	988
6	21.3	.350	1.613	.111	-.357	4.06	.880	.082	-.620	3.27	.00220	.242	.010	3.41	40.88	991
7	22.8	.375	1.600	.104	-.312	5.24	.926	.090	-.799	4.79	.00210	.224	.012	1.72	24.52	987
8	24.4	.400	1.583	.136	-.338	3.76	.889	.182	-1.704	8.55	.00658	.266	.035	5.13	52.03	994
9	25.9	.424	1.448	.235	-.333	3.62	.748	.369	-.678	2.72	.01336	.154	.090	.55	9.47	996
10	27.4	.449	1.397	.302	-.418	3.29	.542	.425	.204	1.98	-.05007	-.389	.113	-.83	9.20	997
11	29.0	.475	1.749	.283	-.584	3.41	.544	.243	1.099	5.09	-.02049	-.299	.076	-1.68	11.60	998
12	30.5	.499	1.479	.474	-.900	3.50	.456	.284	-.825	5.52	.00851	.063	.141	.21	12.95	997
13	32.0	.524	.075	.227	.356	5.16	.703	.217	.358	3.72	-.00821	-.166	.066	-1.37	22.88	990
14	33.5	.549	-.007	.124	-.461	3.77	.643	.152	-.045	2.87	-.00347	-.183	.021	-1.41	13.02	994
15	36.6	.599	-.002	.115	-.310	3.57	.588	.129	-.183	2.93	-.00026	-.017	.015	-.19	10.73	989
16	31.2	.512	.539	.462	.500	2.59	.546	.353	-.436	3.79	-.03955	-.243	.162	-.81	9.32	994
17	29.7	.487	1.862	.183	-.432	3.64	.538	.133	.932	5.07	-.00016	-.007	.031	-2.55	32.70	982
18	28.2	.462	1.542	.311	-.216	2.70	.554	.343	.492	2.59	-.04063	-.381	.096	-.46	5.10	996
19	26.7	.437	1.368	.274	-.263	3.14	.573	.422	-.015	1.79	-.03036	-.262	.105	-.12	5.15	997
20	25.1	.412	1.486	.204	-.615	4.27	.851	.272	-1.044	3.93	.01690	.305	.067	2.75	21.14	988

ORIGINAL PAGE IS
OF POOR QUALITY

TABLE IV-65

AXIAL AND AZIMUTHAL VELOCITY DATA AND CORRELATIONS

Test Date: 3/2/83 Run No.: 65 Flow Condition: 1 Geometry: 3

Axial Location: 5 mm (0.2 in.) x/R_o = 0.083 Swirler Orientation, ϕ = 65 deg

P_t No.	r mm +(θ=90) -(θ=270)	r/R_o	U m/s	u' m/s	S_u	K_u	W m/s	w' m/s	S_w	K_w	$\overline{uw}$ m^2/s^2	R_{uw}	σ_{uw} m^2/s^2	S_{uw}	K_{uw}	N
1	15.2	.250	.041	.376	.464	2.61	.354	.399	.111	2.51	.04891	.327	.158	1.03	6.40	245
2	16.8	.275	1.108	.305	-1.024	3.78	1.011	.315	-1.248	5.14	.04954	.388	.150	2.74	15.04	977
3	18.3	.300	1.329	.163	-.520	3.52	.879	.159	-.727	4.24	.00795	.305	.031	2.38	18.61	968
4	19.8	.325	1.085	.242	-.407	2.83	.585	.260	-.646	3.31	.03059	.485	.069	2.28	14.09	992
5	21.3	.350	.858	.273	-.150	3.11	.405	.348	.132	2.43	.01987	.210	.098	-.12	7.76	999
6	22.8	.375	1.151	.378	-.088	2.41	.516	.362	.309	2.87	-.03896	-.285	.125	-.80	6.35	993
7	24.4	.400	1.591	.340	-.756	3.72	.678	.254	.956	4.43	-.02066	-.240	.098	-.86	14.21	990
8	25.9	.424	1.770	.137	-.563	5.08	.683	.114	1.011	4.91	-.00061	-.039	.021	-3.42	38.06	994
9	27.4	.449	1.828	.066	-.197	3.38	.623	.057	.416	3.72	-.00022	-.058	.004	.11	7.48	995
10	29.0	.475	1.865	.077	-.705	4.94	.564	.055	-.288	4.56	-.00034	-.079	.006	3.39	62.57	996
11	30.5	.499	1.424	.513	-.968	3.02	.540	.191	-.830	5.90	.01394	.142	.105	1.47	12.36	996
12	32.0	.524	.160	.141	.077	4.35	.623	.171	.179	3.50	.00076	.032	.026	.78	15.70	993
13	33.5	.549	.040	.119	-.279	3.08	.653	.147	.073	2.87	-.00204	-.117	.019	-.65	11.37	995
14	36.6	.599	-.006	.117	-.144	3.34	.613	.137	.009	3.47	-.00178	-.111	.017	-1.31	11.65	999
15	22.1	.362	.971	.301	-.027	2.71	.503	.354	.028	2.62	-.00911	-.085	.105	-1.04	9.98	998
16	20.6	.337	.932	.252	-.170	2.93	.354	.299	-.125	2.73	.02632	.350	.075	.85	7.79	996
17	19.0	.312	1.270	.193	-.750	3.99	.766	.182	-.715	3.54	.01494	.427	.040	2.27	12.78	987
18	.0	.000	.845	.076	.125	5.17	-.019	.085	-1.009	8.20	.00068	.106	.010	6.47	115.90	972
19	3.0	.050	.843	.085	.936	7.67	-.006	.085	.733	9.53	.00008	.011	.008	-2.46	36.29	976
20	6.1	.100	.802	.103	.115	5.94	-.004	.079	.595	6.91	-.00037	-.046	.010	-4.01	50.90	965
21	9.1	.150	.737	.143	-1.727	10.32	.005	.092	.441	7.44	-.00033	-.025	.017	-3.83	80.56	970
22	12.2	.200	.522	.327	-.989	6.55	.001	.151	-.992	9.18	-.00368	-.074	.055	-2.49	47.33	980
23	13.7	.225	.252	.405	-.051	3.12	.025	.262	-.670	7.40	-.00883	-.083	.117	-.61	14.79	974
24	15.2	.250	.157	.428	.921	4.18	.514	.491	-.687	4.48	-.00183	-.009	.184	.24	6.72	979
25	14.5	.237	.162	.470	1.339	6.47	.157	.394	-.710	6.05	-.00932	-.050	.145	.40	8.83	974
26	14.9	.244	.078	.397	.977	4.88	.336	.479	-.510	4.69	-.00791	-.042	.172	-.24	8.87	966

ORIGINAL PAGE IS
OF POOR QUALITY

TABLE IV-66

AXIAL AND AZIMUTHAL VELOCITY DATA AND CORRELATIONS

Test Date: 3/2/83 Run No.: 66 Flow Condition: 1 Geometry: 3

Axial Location: 5 mm (0.2 in.) $x/R_o = 0.083$ Swirler Orientation, $\phi = 60$ deg

P_t No.	r mm +(θ=90) -(θ=270)	r/R_o	U m/s	u' m/s	S_u	K_u	W m/s	w' m/s	S_w	K_w	$\overline{uw}$ m^2/s^2	R_{uw}	σ_{uw} m^2/s^2	S_{uw}	K_{uw}	N
1	15.2	.250	-.013	.369	.667	3.10	.148	.398	.091	2.99	.03895	.252	.151	1.60	8.96	238
2	16.6	.275	.344	.435	-.115	2.72	.056	.422	-.376	2.91	.04715	.257	.179	.64	6.62	995
3	18.3	.300	.925	.271	-.415	3.37	.684	.333	-.675	3.31	.02359	.262	.102	1.38	13.45	997
4	19.6	.325	1.149	.327	-.033	2.73	.524	.284	.009	3.13	-.00689	-.074	.091	.33	8.09	996
5	21.3	.350	1.698	.201	-1.205	6.28	.763	.150	.419	4.70	-.00082	-.027	.035	.68	21.32	994
6	22.8	.375	1.758	.079	-.713	3.65	.779	.077	.792	4.67	-.00057	-.100	.007	-3.54	45.94	987
7	24.4	.400	1.807	.055	-.109	.63	.723	.044	.151	4.46	-.00023	-.094	.003	.36	16.36	987
8	25.9	.424	1.848	.048	.059	-9.14	.648	.040	.172	4.51	-.00033	-.170	.002	.02	10.77	975
9	27.4	.449	1.887	.054	-.712	.45	.589	.043	-.310	3.68	-.00026	-.114	.003	.17	18.51	989
10	29.0	.475	1.874	.097	-1.183	5.45	.543	.068	-.208	4.82	-.00012	-.018	.009	1.67	35.43	994
11	30.5	.499	1.203	.549	-.556	2.10	.574	.170	-.026	4.02	.00916	.098	.088	-.34	7.68	990
12	32.0	.524	.146	.121	-.235	3.59	.625	.149	-.197	2.94	.00038	.021	.020	.35	13.03	988
13	33.5	.549	.071	.117	-.404	3.46	.633	.148	.027	3.02	.00012	.007	.019	.01	11.05	984
14	36.6	.599	.009	.116	-.147	3.16	.610	.135	-.024	2.90	-.00048	-.031	.017	.38	9.65	983
15	19.0	.312	.917	.281	-.155	3.17	.522	.312	-.383	2.89	.00327	.037	.096	-.70	12.10	994
16	20.6	.337	1.495	.320	-.460	3.15	.647	.243	.179	3.64	-.00579	-.074	.085	-1.66	15.99	998

TABLE IV-67

AXIAL AND AZIMUTHAL VELOCITY DATA AND CORRELATIONS

Test Date: 3/2/83 Run No.: 67 Flow Condition: 1 Geometry: 3

Axial Location: 5 mm (0.2 in.) $x/R_o = 0.083$ Swirler Orientation, ϕ = 55 deg

P_t No.	r mm +(θ=90) -(θ=270)	r/R_o	U m/s	u' m/s	S_u	K_u	W m/s	w' m/s	S_w	K_w	$\overline{uw}$ m^2/s^2	R_{uw}	σ_{uw} m^2/s^2	S_{uw}	K_{uw}	N
1	15.2	.250	.078	.442	.593	2.91	.151	.335	.037	3.08	.00908	.061	.155	-.83	9.17	231
2	16.8	.275	.641	.466	.225	3.25	.495	.345	-.158	2.79	-.01185	-.074	.153	-.26	6.75	491
3	18.3	.300	1.313	.368	-.537	3.21	.753	.298	-.190	3.76	-.00604	-.055	.116	.12	13.30	990
4	19.8	.325	1.662	.142	-.935	5.41	.875	.102	.555	4.24	-.00062	-.043	.018	-3.14	38.63	977
5	21.3	.350	1.750	.074	-.509	7.42	.789	.059	-.106	3.00	-.00039	-.091	.004	-.46	10.82	987
6	22.8	.375	1.785	.063	-.383	4.63	.740	.047	.243	4.41	-.00041	-.138	.004	-1.56	22.20	994
7	24.4	.400	1.836	.056	.189	-6.01	.668	.042	-.030	4.36	-.00050	-.211	.003	-1.10	14.88	991
8	25.9	.424	1.876	.053	-.221	-5.70	.592	.046	-.132	3.98	-.00042	-.175	.003	-2.03	22.95	992
9	27.4	.449	1.880	.078	-1.035	4.43	.531	.051	.028	3.43	-.00029	-.072	.005	-.88	19.40	987
10	29.0	.475	1.824	.136	-1.276	6.30	.506	.080	.301	4.65	-.00127	-.117	.013	-2.17	36.34	996
11	30.5	.499	1.083	.540	-.392	1.92	.558	.172	.047	3.36	.00684	.074	.087	-.30	5.73	993
12	32.0	.524	.125	.124	-.218	3.61	.605	.150	-.004	3.37	-.00001	-.001	.020	1.29	15.31	990
13	33.5	.549	.083	.113	-.285	3.88	.602	.137	-.137	2.93	-.00033	-.022	.015	.12	9.56	990
14	36.0	.599	.026	.120	-.042	3.21	.590	.133	-.122	3.46	-.00014	-.009	.017	-.76	13.17	980

TABLE IV-68

AXIAL AND AZIMUTHAL VELOCITY DATA AND CORRELATIONS

Test Date: 3/3/83 Run No.: 68 Flow Condition: 1 Geometry: 3

Axial Location: 5 mm (0.2 in.) $x/R_o = 0.083$ Swirler Orientation, ϕ = 50 deg

P_t No.	r mm +(θ=90) -(θ=270)	r/R_o	U m/s	u' m/s	S_u	K_u	W m/s	w' m/s	S_w	K_w	$\overline{uw}$ m^2/s^2	R_{uw}	σ_{uw} m^2/s^2	S_{uw}	K_{uw}	N
1	14.4	.236	.198	.501	.743	3.70	.213	.361	.014	2.21	-.00562	-.031	.162	.44	5.66	231
2	15.2	.250	.734	.593	.002	2.57	.539	.389	-.758	3.96	.04418	.191	.212	.17	5.99	493
3	18.3	.300	1.662	.132	-.338	3.37	.975	.097	.151	3.45	-.00062	-.048	.014	-1.40	17.99	988
4	19.8	.325	1.858	.064	-.241	3.97	.705	.042	.033	4.90	-.00027	-.101	.003	.68	19.61	982
5	21.3	.350	1.806	.075	-.349	.92	.792	.049	-.115	3.41	-.00067	-.184	.004	-3.36	39.48	994
6	22.8	.375	1.848	.066	.564	2.68	.725	.044	-.036	4.60	-.00033	-.116	.003	-.78	9.26	989
7	24.4	.400	1.888	.060	.079	.29	.651	.046	-.534	5.22	-.00022	-.079	.003	-.94	14.87	992
8	25.9	.424	1.923	.064	.022	2.25	.568	.050	-.373	3.71	-.00030	-.093	.004	-.95	19.62	988
9	27.4	.449	1.902	.096	-.866	3.50	.534	.063	-.151	4.11	-.00040	-.066	.008	-.96	27.09	989
10	29.0	.475	1.821	.145	-.599	3.07	.510	.096	-.128	3.88	.00026	.019	.015	-.17	12.24	981
11	30.5	.499	.827	.528	.260	1.90	.555	.189	-.230	3.36	.01041	.105	.089	-.61	7.86	992
12	32.0	.524	.108	.122	-.213	3.21	.613	.159	-.002	3.26	-.00178	-.092	.020	-1.35	12.40	984
13	33.5	.549	.065	.113	-.185	3.62	.615	.146	-.086	3.13	-.00107	-.065	.018	-1.27	16.67	973
14	19.8	.325	1.743	.095	-.533	3.93	.874	.069	.057	3.39	-.00099	-.151	.007	-1.31	13.25	993
15	36.6	.599	.036	.123	.241	4.33	.602	.127	-.097	3.13	.00026	.017	.016	.02	11.29	974
16	16.8	.275	1.513	.304	-1.027	4.19	.927	.230	-.897	4.93	.01139	.163	.087	1.78	21.12	990
17	.0	.000	.853	.098	.130	8.76	-.019	.074	-.040	5.87	-.00014	-.019	.007	-.49	16.79	960
18	3.0	.050	.845	.096	.177	6.05	-.007	.082	.043	8.56	-.00024	-.031	.010	-5.59	86.01	976
19	6.1	.100	.818	.107	.629	7.39	-.008	.083	-.358	6.55	-.00081	-.092	.011	-2.87	54.61	975
20	9.1	.150	.740	.148	-1.455	8.85	-.001	.094	.241	6.54	-.00088	-.063	.015	-1.62	38.51	977
21	12.2	.200	.545	.315	-.635	5.86	.013	.155	.240	5.21	-.00510	-.105	.054	-.68	23.91	970
22	13.7	.225	.242	.429	.444	4.06	.237	.385	-.070	4.32	-.01485	-.090	.148	-.49	7.50	978
23	15.2	.250	.742	.513	-.012	2.55	.830	.296	-.929	4.27	.00369	.024	.145	-.00	7.90	987
24	14.5	.237	.258	.501	1.004	4.81	.544	.367	-.400	2.88	.00913	.050	.176	.28	8.90	989
25	13.0	.212	.393	.409	-.274	4.01	.022	.239	-.642	9.74	-.00964	-.099	.090	-.50	16.50	988

ORIGINAL PAGE IS
OF POOR QUALITY

TABLE IV-69

AXIAL AND RADIAL VELOCITY DATA AND CORRELATIONS

Test Date: 3/10/83 Run No.: 69 Flow Condition: 1 Geometry: 3

Axial Location: 5 mm (0.2 in.) $x/R_o = 0.083$ Swirler Orientation, $\phi = 50$ deg

P_t No.	r mm +(θ=0) -(θ=180)	r/R_o	U m/s	u' m/s	S_u	K_u	V m/s	v' m/s	S_v	K_v	$\overline{uv}$ m^2/s^2	R_{uv}	σ_{uv} m^2/s^2	S_{uv}	K_{uv}	N
1	15.2	.250	.412	.399	-.236	2.60	-.229	.397	-.437	2.77	-.04605	-.290	.159	-.50	7.95	244
2	12.2	.200	.581	.160	-.616	3.93	.129	.087	-.394	5.19	.00340	.244	.016	1.94	13.91	228
3	9.1	.150	.698	.120	-.993	5.91	.080	.072	-1.230	6.96	.00340	.395	.017	6.10	53.29	264
4	6.1	.100	.760	.089	-.346	3.33	.039	.082	-.586	6.39	.00304	.414	.010	5.40	48.60	245
5	3.0	.050	.797	.073	-.223	3.29	.001	.072	.613	5.21	.00145	.276	.006	2.70	14.22	244
6	.0	.000	.810	.071	.057	3.46	.009	.074	.256	4.08	.00035	.067	.005	1.02	11.89	246
7	-3.0	-.050	.822	.080	-.956	6.20	.029	.084	-1.372	7.30	.00190	.284	.012	6.46	54.74	234
8	-6.1	-.100	.777	.152	-1.620	8.15	.061	.115	-1.109	6.03	.00567	.325	.025	4.65	45.23	241
9	-9.1	-.150	.687	.159	-1.479	5.94	.115	.096	-.622	6.67	.00520	.340	.023	2.58	23.52	223
10	-12.2	-.200	.342	.443	-1.077	3.08	.144	.148	-.406	4.46	.01748	.267	.083	1.21	12.64	242
11	-15.2	-.250	.019	.430	.158	2.04	-.030	.296	-.255	3.16	-.01865	-.146	.123	-.24	5.00	243
12	-18.3	-.300	1.371	.325	-.883	3.95	.024	.199	.663	4.12	-.02052	-.317	.085	-3.71	27.33	492
13	18.3	.300	1.598	.135	-.397	3.65	-.101	.105	.752	4.91	-.00333	-.234	.017	-1.56	19.84	991
14	16.8	.275	1.303	.357	-.718	3.73	-.222	.250	.634	3.90	-.01990	-.223	.100	-2.37	21.45	997
15	13.7	.225	.270	.354	-.837	2.93	.114	.140	-.863	5.04	.01771	.358	.055	2.75	16.10	490
16	21.6	.354	1.762	.072	-.714	3.38	.001	.057	.284	3.62	-.00053	-.129	.005	-2.74	35.29	999
17	24.1	.396	1.846	.057	.775	-6.29	.049	.050	.124	3.40	.00002	.005	.003	-.62	22.97	995
18	27.2	.446	1.888	.080	-.874	5.24	.097	.059	-.517	3.86	.00143	.303	.007	4.37	35.72	996
19	27.2	.446	1.867	.083	-.919	5.40	.110	.062	-.814	5.79	.00200	.388	.007	4.34	32.31	996
20	30.5	.500	1.276	.298	-.675	3.25	.117	.173	-.355	3.57	.02719	.527	.061	2.16	14.85	996
21	33.5	.550	.134	.140	-.389	3.29	-.199	.296	-2.745	11.65	.00397	.095	.038	1.20	27.72	480
22	36.6	.600	.069	.136	.421	4.44	-.585	.619	-1.177	3.28	-.00078	-.009	.085	1.49	17.24	229
23	32.0	.525	.219	.145	-.567	4.28	-.571	.694	-1.358	3.65	-.00136	-.014	.100	-.10	15.98	230
24	16.0	.262	.997	.396	-.343	2.77	-.291	.333	.260	2.78	-.01965	-.149	.136	-1.38	9.10	494
25	-.8	-.012	.862	.094	.096	7.62	-.009	.098	-1.781	14.64	-.00039	-.042	.010	-2.29	78.00	965
26	2.3	.037	.839	.088	.079	8.17	.030	.079	.249	4.04	.00121	.176	.007	2.45	26.15	977
27	5.3	.087	.805	.122	-2.841	20.19	.052	.078	.764	10.94	.00177	.187	.011	5.06	62.62	989
28	8.4	.137	.755	.151	-1.247	10.27	.080	.078	-.931	7.67	.00256	.218	.016	2.25	44.47	986
29	11.4	.187	.579	.262	-1.887	7.65	.116	.105	-.949	6.07	.00305	.111	.043	1.41	43.30	970
30	13.0	.212	.383	.367	-.767	3.91	.133	.143	-.723	6.58	.00452	.086	.064	-1.43	35.14	982
31	14.5	.237	.191	.420	.574	4.29	-.050	.305	-.878	4.20	.00230	.018	.120	.47	10.56	996
32	14.0	.229	.157	.404	.311	3.77	.079	.206	-.881	6.05	.00602	.072	.083	.37	17.59	983
33	13.5	.221	.281	.386	-.056	3.41	.120	.152	-.457	4.10	.00972	.166	.065	.24	12.98	975

TABLE IV-70

AXIAL AND RADIAL VELOCITY DATA AND CORRELATIONS

Test Date: 3/11/83 Run No.: 70 Flow Condition: 1 Geometry: 3

Axial Location: 5 mm (0.2 in.) $x/R_o = 0.083$ Swirler Orientation, $\phi = 55$ deg

P_t No.	r mm +(θ=0) -(θ=180)	r/R_o	U m/s	u' m/s	S_u	K_u	V m/s	v' m/s	S_v	K_v	$\overline{uv}$ m^2/s^2	R_{uv}	σ_{uv} m^2/s^2	S_{uv}	K_{uv}	N
1	12.2	.200	.451	.357	-1.354	4.25	-.092	.451	-1.347	3.27	.01097	.068	.162	1.48	11.70	189
2	13.7	.225	.163	.428	.002	2.30	.117	.184	-.655	3.65	.01776	.226	.077	.15	6.54	197
3	15.2	.250	.195	.451	.343	2.47	-.232	.380	-.402	2.93	-.04809	-.281	.160	-1.09	7.40	491
4	14.5	.237	-.093	.331	.465	2.52	-.040	.294	-1.165	4.22	-.01013	-.104	.101	-1.82	13.78	240
5	16.8	.275	.972	.458	-.348	2.97	-.333	.340	.175	2.86	-.00630	-.040	.157	-.22	7.74	978
6	18.3	.300	1.412	.335	-.882	3.94	-.134	.238	.585	3.94	-.02827	-.354	.098	-2.40	18.41	990
7	20.3	.333	1.693	.106	-.551	4.57	-.006	.084	.348	4.22	-.00162	-.182	.011	-3.12	35.44	983
8	24.4	.400	1.828	.061	.026	.85	.078	.084	-6.431	72.52	-.00043	-.084	.004	-3.92	48.52	994
9	27.4	.450	1.877	.067	-.782	2.44	.151	.058	-.548	4.01	.00077	.196	.005	4.94	52.91	995
10	30.5	.500	1.518	.237	-.906	4.11	.155	.155	-.854	5.26	.01589	.432	.048	3.41	23.83	995
11	22.7	.373	1.777	.070	-.837	3.88	.041	.054	.087	3.38	-.00076	-.200	.004	-1.81	13.94	986
12	29.0	.475	1.832	.110	-.671	3.07	.169	.074	-.375	3.97	.00199	.245	.009	2.41	15.01	990
13	32.0	.525	.221	.155	-.708	4.18	-.073	.113	.014	3.16	.00548	.312	.020	2.19	11.88	235
14	33.5	.550	.121	.134	-.060	3.86	-.144	.117	-.117	3.04	.00127	.080	.015	1.30	8.79	239
15	35.1	.575	.059	.131	-.093	2.54	-.146	.124	-.025	2.63	.00039	.024	.017	-.15	5.99	241
16	36.6	.600	.013	.148	-.080	2.84	-.184	.133	.179	2.91	.00019	.010	.019	.22	5.40	237
17	9.1	.150	.715	.147	-.774	5.90	.086	.076	-.606	4.61	.00511	.458	.015	3.83	24.06	218

ORIGINAL PAGE IS
OF POOR QUALITY

TABLE IV-71

AXIAL AND RADIAL VELOCITY DATA AND CORRELATIONS

Test Date: 3/14/83 Run No.: 71 Flow Condition: 1 Geometry: 3

Axial Location: 5 mm (0.2 in.) x/R_O = 0.083 Swirler Orientation, ϕ = 60 deg

P_t No.	r mm +(θ=0) -(θ=180)	r/R_o	U m/s	u' m/s	S_u	K_u	V m/s	v' m/s	S_v	K_v	$\overline{uv}$ m^2/s^2	R_{uv}	σ_{uv} m^2/s^2	S_{uv}	K_{uv}	N
1	9.1	.150	.678	.193	-1.792	7.06	.053	.195	-3.637	18.16	.00533	.142	.031	.99	25.30	226
2	12.2	.200	.269	.456	-.666	2.17	.119	.136	-.276	4.64	.01912	.309	.067	2.26	17.23	227
3	13.7	.225	.006	.402	.146	2.82	.126	.188	.116	3.77	.00213	.028	.072	-1.64	12.17	228
4	15.2	.250	-.097	.305	.395	2.87	.003	.295	-.912	3.75	-.01711	-.190	.107	-1.12	10.20	240
5	16.8	.275	.625	.397	-.116	3.07	.035	.406	-.564	4.13	-.02395	-.148	.151	-.02	6.57	484
6	18.3	.300	.999	.277	-.441	3.49	.206	.269	-.285	3.72	.00376	.051	.085	-.34	17.20	996
7	21.3	.350	1.672	.188	-.947	5.61	.029	.241	.962	5.38	-.00498	-.110	.052	-2.47	24.70	995
8	24.4	.400	1.783	.068	-.899	6.06	.154	.062	.638	5.02	-.00013	-.030	.004	-.51	18.70	993
9	27.4	.450	1.874	.054	-.517	4.00	.237	.053	-.013	3.44	.00012	.041	.003	-1.23	22.52	995
10	30.5	.500	1.655	.203	-.927	4.53	.242	.138	-.373	3.56	.00636	.226	.033	2.16	17.40	995
11	30.5	.500	1.651	.189	-.395	3.28	.225	.137	-.400	3.95	.00535	.207	.028	1.88	15.78	991
12	29.0	.475	1.869	.088	-.757	3.88	.250	.066	-.693	4.70	.00097	.166	.007	4.07	47.71	995
13	19.8	.325	1.302	.347	-.329	2.66	.126	.332	-.002	2.53	-.01724	-.150	.116	-.75	8.64	991
14	32.0	.525	.207	.134	-.642	5.29	-.083	.112	-.173	3.70	.00307	.205	.021	2.19	33.67	977
15	33.5	.550	.229	.372	2.120	7.29	-.147	.127	-.704	4.70	.00472	.100	.058	-3.10	37.62	197
16	33.5	.550	.111	.134	.248	4.10	-.129	.118	.475	3.99	.00028	.018	.016	-.30	10.60	237
17	35.1	.575	.058	.136	.002	3.23	-.155	.138	.071	2.77	.00314	.168	.019	.61	7.34	235
18	36.6	.600	.008	.155	.039	4.42	-.157	.149	.030	3.55	.00066	.029	.025	-1.38	18.15	238
19	10.7	.175	.609	.259	-2.629	11.38	.098	.196	-1.554	7.63	.01060	.385	.060	7.13	64.81	217
20	16.0	.262	.209	.409	.272	2.64	-.033	.366	-.366	2.78	-.00130	-.410	.150	-1.28	9.54	484
21	13.7	.225	.122	.396	.092	2.29	.090	.221	-1.506	6.37	.00933	.107	.076	.11	6.97	218
22	22.9	.375	1.744	.091	-.639	5.68	.059	.090	-.199	8.79	.00003	.003	.009	2.63	42.82	994

ORIGINAL PAGE IS
OF POOR QUALITY

TABLE IV-72

AXIAL AND RADIAL VELOCITY DATA AND CORRELATIONS

Test Date: 3/14/83 Run No.: 72 Flow Condition: 1 Geometry: 3

Axial Location: 5 mm (0.2 in.) $x/R_o = 0.083$ Swirler Orientation, ϕ = 65 deg

P_t No.	r mm +(θ=0) -(θ=180)	r/R_o	U m/s	u' m/s	S_u	K_u	V m/s	v' m/s	S_v	K_v	$\overline{uv}$ m^2/s^2	R_{uv}	σ_{uv} m^2/s^2	S_{uv}	K_{uv}	N
1	30.5	.500	.913	.294	.011	2.60	.169	.293	-.035	2.78	.03741	.434	.085	.70	10.66	996
2	27.4	.450	1.833	.054	-.006	-8.81	.257	.057	.092	3.59	.00009	.031	.003	1.26	16.18	996
3	29.0	.475	1.852	.076	-.665	3.66	.286	.063	-.261	4.74	.00105	.218	.006	3.34	24.84	998
4	23.0	.376	1.666	.249	-.725	3.68	.118	.206	.356	5.82	-.01778	-.347	.073	-1.75	20.03	994
5	21.3	.350	1.029	.332	.044	2.76	.117	.336	-.215	2.54	-.01625	-.146	.108	-.37	6.81	993
6	22.9	.375	1.425	.363	-.457	2.86	.081	.309	.379	3.31	-.04382	-.390	.116	-1.24	9.46	993
7	19.8	.325	.973	.273	-.148	3.25	.234	.236	-.677	4.56	.01919	.297	.067	1.17	12.42	990
8	18.3	.300	1.232	.212	-.634	4.53	.238	.187	-.485	5.12	.00809	.204	.053	4.82	57.79	992
9	19.0	.312	1.125	.259	-.463	3.51	.241	.195	-.695	4.85	.01681	.334	.063	3.51	36.44	993
10	20.6	.337	.937	.305	.154	2.94	.187	.312	-.615	3.32	.00850	.090	.098	-1.16	17.86	989
11	22.1	.362	1.247	.361	-.137	2.70	.099	.338	.080	2.71	-.03128	-.256	.118	-.31	7.08	994
12	16.8	.275	1.050	.405	-.589	3.15	.146	.290	-.036	3.06	-.02260	-.193	.134	-1.60	12.28	963
13	15.2	.250	.040	.417	1.183	4.60	.055	.300	-.414	3.27	-.01266	-.101	.130	-.64	14.58	243
14	13.7	.225	.151	.484	.686	3.19	-.048	.419	-1.464	4.23	.01543	.076	.179	.37	7.49	192
15	13.7	.225	-.051	.398	.267	2.06	.148	.156	-.238	4.22	.00879	.141	.059	-.75	9.20	237
16	12.2	.200	.349	.437	-.700	3.20	.123	.126	-.539	3.59	.01128	.206	.062	1.08	12.03	222
17	32.0	.525	.251	.132	.069	4.33	-.137	.134	-.530	4.82	.00184	.104	.024	2.78	28.69	238
18	33.5	.550	.103	.144	-.719	5.61	-.184	.137	-.208	3.62	.00692	.349	.027	3.78	22.40	238
19	36.6	.600	-.038	.126	.031	2.94	-.170	.126	.185	3.14	.00149	.094	.015	.74	7.46	240
20	-.8	-.012	.864	.111	.651	12.30	-.012	.087	.952	10.46	-.00057	-.060	.010	-.84	44.28	960
21	2.3	.037	.863	.095	1.396	11.62	.033	.075	.229	4.81	.00100	.140	.008	-.15	34.76	971
22	5.3	.087	.849	.092	.540	5.97	.057	.085	-1.428	13.74	.00169	.217	.008	2.07	13.23	973
23	8.4	.137	.768	.133	-1.834	11.97	.084	.079	1.082	9.42	.00211	.200	.011	-2.41	60.88	963
24	11.4	.187	.629	.250	-1.947	9.13	.127	.111	-1.696	11.76	.00421	.152	.030	1.81	35.16	975
25	13.0	.212	.436	.356	-.099	5.58	.154	.130	-.298	4.70	.00365	.079	.049	-.94	27.71	982
26	14.5	.237	.131	.458	1.881	9.05	.141	.199	-.740	5.11	.00160	.018	.085	-.56	16.37	990
27	14.0	.229	.190	.383	.202	3.42	.146	.187	-.910	8.12	-.00156	-.022	.076	-1.41	14.58	986
28	15.2	.250	.191	.425	1.074	5.02	.092	.326	-.538	3.47	-.00525	-.038	.133	-.46	9.12	984

ORIGINAL PAGE IS
OF POOR QUALITY

TABLE IV-73

AXIAL AND RADIAL VELOCITY DATA AND CORRELATIONS

Test Date: 3/14/83 Run No.: 73 Flow Condition: 1 Geometry: 3

Axial Location: 5 mm (0.2 in.) x/R_o = 0.083 Swirler Orientation, ϕ = 70 deg

P_t No.	r mm +(θ=0) -(θ=180)	r/R_o	U m/s	u' m/s	S_u	K_u	V m/s	v' m/s	S_v	K_v	$\overline{uv}$ m^2/s^2	R_{uv}	σ_{uv} m^2/s^2	S_{uv}	K_{uv}	N
1	30.5	.500	1.350	.318	-.127	2.60	.333	.387	-.231	2.58	.04510	.366	.123	.91	6.20	996
2	29.0	.475	1.680	.321	-.484	3.22	.304	.254	.474	3.62	-.02365	-.291	.090	-1.19	12.34	996
3	27.4	.450	1.433	.306	-.223	7.64	.366	.284	-.062	2.51	-.02517	-.291	.080	-.24	7.37	996
4	25.9	.425	1.546	.206	-.775	4.53	.382	.178	-.984	4.83	-.00730	-.063	.040	1.25	20.99	996
5	29.7	.487	1.832	.244	-.840	4.69	.377	.214	.787	5.06	-.01004	-.193	.075	-1.06	29.24	996
6	24.4	.400	1.598	.125	-.550	5.36	.362	.089	-.310	5.03	-.00137	-.124	.013	-.85	26.25	998
7	28.2	.462	1.518	.324	-.161	2.64	.279	.296	.137	3.15	-.03057	-.319	.096	-.79	9.01	996
8	26.7	.437	1.158	.263	-.340	3.00	.374	.255	-.299	2.76	-.01536	-.228	.073	-.46	12.15	997
9	22.9	.375	1.595	.093	-.321	3.81	.351	.080	.418	4.61	-.00138	-.186	.009	-1.63	21.31	980
10	21.3	.350	1.590	.103	-.577	4.35	.329	.071	-.110	4.07	-.00093	-.127	.008	-.99	8.80	999
11	19.8	.325	1.570	.119	-.305	3.18	.279	.081	.266	3.39	-.00095	-.099	.011	-.42	12.23	999
12	18.3	.300	1.494	.174	-.684	3.91	.246	.134	.628	4.28	-.00463	-.198	.029	-2.90	31.71	992
13	16.8	.275	1.399	.273	-.864	3.97	.199	.203	.248	3.54	-.01037	-.187	.067	-1.44	15.78	991
14	15.2	.250	.054	.347	.493	3.02	.047	.387	-.481	2.88	-.03841	-.286	.136	-.87	7.48	240
15	13.7	.225	-.024	.425	.293	2.43	.065	.317	-1.884	7.18	-.00437	-.033	.108	-.37	7.67	201
16	32.0	.525	.223	.238	.023	3.76	-.118	.252	-.055	3.63	.00183	.031	.077	-1.48	17.68	234
17	33.5	.550	-.245	.176	-.309	3.27	-.132	.124	-.020	3.14	-.00108	-.049	.024	-2.12	21.37	238
18	36.6	.600	-.042	.135	-.011	2.96	-.104	.159	.041	2.75	.00128	.063	.020	.26	7.44	240
19	35.1	.575	-.030	.132	-.023	3.03	-.111	.144	-.013	2.95	-.00127	-.067	.018	.35	5.94	240

ORIGINAL PAGE IS
OF POOR QUALITY

TABLE IV-74

AXIAL AND RADIAL VELOCITY DATA AND CORRELATIONS

Test Date: 3/15/83 Run No.: 74 Flow Condition: 1 Geometry: 3

Axial Location: 5 mm (0.2 in.) $x/R_o = 0.083$ Swirler Orientation, ϕ = 75 deg

P_t No.	r mm +(0=0) -(0=180)	r/R_o	U m/s	u' m/s	S_u	K_u	V m/s	v' m/s	S_v	K_v	$\overline{uv}$ m^2/s^2	R_{uv}	σ_{uv} m^2/s^2	S_{uv}	K_{uv}	N
1	30.5	.500	1.104	.388	.065	3.03	.240	.424	.000	2.49	.05946	.362	.173	1.19	7.51	994
2	29.0	.475	1.649	.218	-.880	4.84	.496	.211	-1.481	7.56	.00572	.124	.063	1.74	31.05	997
3	27.4	.450	1.518	.265	-1.324	5.15	.654	.157	.359	3.85	-.00499	-.120	.052	-1.55	17.62	977
4	25.9	.425	1.578	.163	-1.777	6.90	.401	.131	-1.856	10.35	.00384	.179	.036	4.05	43.10	998
5	24.4	.400	1.645	.078	-.188	5.49	.230	.086	-.631	5.99	.00094	.140	.008	5.66	88.16	997
6	29.7	.487	1.574	.280	-.452	3.42	.135	.483	-.928	5.27	-.00238	-.022	.103	-1.33	13.13	989
7	28.2	.462	1.607	.236	-1.085	5.09	.587	.229	-2.632	18.41	.00065	.012	.064	1.11	33.91	987
8	26.7	.437	1.561	.207	-1.433	5.81	.524	.149	-.587	5.36	.00204	.066	.040	1.03	21.92	995
9	22.9	.375	1.662	.077	-.049	7.20	.199	.084	.140	3.17	-.00014	-.021	.007	-.11	11.33	995
10	21.3	.350	1.673	.082	-.597	6.81	.208	.071	.197	3.23	-.00078	-.135	.006	-.96	14.66	996
11	19.8	.325	1.661	.095	-.507	5.06	.195	.071	.401	3.63	-.00111	-.163	.008	-2.69	21.99	999
12	18.3	.300	1.625	.107	-.780	4.13	.172	.077	.543	4.88	-.00144	-.174	.010	-2.26	18.00	997
13	16.8	.275	1.504	.213	-.996	4.80	.156	.171	.384	3.68	-.00836	-.229	.050	-3.60	30.16	993
14	15.2	.250	.182	.385	.043	2.47	.059	.399	-.315	2.77	-.05551	-.361	.153	-1.29	7.64	492
15	13.7	.225	.029	.474	.694	3.20	.123	.217	-1.065	6.14	.00492	.048	.083	.38	10.22	236
16	12.2	.200	.314	.449	-.821	2.63	.110	.147	-.726	4.49	.00682	.103	.065	-.09	6.37	224
17	23.6	.387	1.657	.075	-.066	6.86	.197	.075	.048	3.53	-.00063	-.111	.006	-.62	12.05	991
18	32.0	.525	.114	.293	.017	2.99	.082	.373	.503	2.92	.01773	.162	.114	.72	7.67	246
19	33.5	.550	-.007	.149	-.035	2.65	-.069	.135	.171	2.50	-.00453	-.225	.019	-.32	5.04	245
20	35.1	.575	.008	.134	.360	4.61	-.109	.155	-.204	3.11	.00000	.000	.028	3.76	42.08	243
21	36.6	.600	-.028	.127	-.382	3.17	-.141	.148	.301	2.78	-.00091	-.048	.020	.52	7.10	245
22	31.2	.512	.936	.413	.251	2.78	.223	.448	.115	2.41	.06442	.348	.186	1.17	4.94	244
23	9.1	.150	.668	.272	-2.092	9.00	.076	.107	-.439	5.82	.00677	.233	.057	-1.17	36.08	220
24	6.1	.100	.862	.334	1.655	7.32	.033	.098	-1.585	10.33	.00439	.079	.031	1.67	23.18	224
25	3.0	.050	.819	.139	-2.113	16.85	.006	.109	-2.071	13.34	.00553	.363	.036	10.08	117.40	217
26	.0	.000	.849	.104	1.297	6.49	-.014	.085	-.166	3.82	.00038	.043	.009	-1.19	13.93	162

ORIGINAL PAGE IS
OF POOR QUALITY

TABLE IV-75

AXIAL AND RADIAL VELOCITY DATA AND CORRELATIONS

Test Date: 3/15/83   Run No.: 75   Flow Condition: 1   Geometry: 3

Axial Location: 5 mm (0.2 in.) $x/R_o = 0.083$ Swirler Orientation, ϕ = 80 deg

P_t No.	r mm +(0=C) -(0=180)	r/R_o	U m/s	u' m/s	S_u	K_u	V m/s	v' m/s	S_v	K_v	$\overline{uv}$ m^2/s^2	R_{uv}	σ_{uv} m^2/s^2	S_{uv}	K_{uv}	N
1	30.5	.500	1.090	.467	-.214	2.61	-.020	.362	.249	2.71	.00746	.044	.170	.11	5.92	993
2	29.0	.475	1.615	.319	-.511	3.41	-.450	.408	.290	2.71	.00176	.013	.131	.25	6.88	995
3	27.4	.450	.694	.384	.010	3.35	-.291	.510	-.084	2.74	-.01011	-.052	.194	-.23	6.71	998
4	25.9	.425	1.193	.311	-.254	3.12	-.297	.438	-.046	2.30	.00199	.015	.129	-.12	5.12	998
5	24.4	.400	1.621	.103	-.661	7.76	-.091	.116	-.324	3.90	.00110	.092	.012	1.62	16.31	993
6	22.9	.375	1.674	.068	-.090	10.72	.035	.080	.364	3.41	-.00039	-.072	.006	-.92	9.92	996
9	26.7	.437	.900	.347	-.187	3.11	-.224	.481	-.007	2.71	.04389	.263	.165	.44	7.25	997
10	25.2	.412	1.496	.212	-.945	4.96	-.094	.245	-1.362	5.87	.01835	.353	.073	3.33	24.26	997
11	21.3	.350	1.688	.071	-.105	5.12	.084	.071	.194	3.15	-.00089	-.174	.005	-.44	10.49	998
12	19.8	.325	1.680	.080	-.582	7.58	.109	.070	.221	3.22	-.00109	-.197	.007	-2.88	29.84	999
13	18.3	.300	1.662	.084	-.629	6.40	.097	.073	.303	3.53	-.00067	-.110	.007	-.87	18.65	998
14	16.8	.275	1.595	.152	-.736	3.90	.080	.122	.573	3.65	-.00291	-.158	.021	-.78	18.40	997
15	15.2	.250	.478	.370	-.211	2.88	-.048	.397	.072	2.42	-.03915	-.267	.149	-.93	6.39	997
16	13.7	.225	-.043	.418	.219	2.25	.148	.246	-1.684	7.58	-.00244	-.024	.103	-.33	14.75	236
17	12.2	.200	.364	.471	-.585	3.15	.134	.129	.087	4.21	.00794	.131	.071	-.55	10.86	237
18	32.0	.525	.139	.219	.952	7.29	-.043	.203	.504	6.89	-.00346	-.078	.062	2.63	48.75	488
19	33.5	.550	.107	.208	2.218	11.03	-.140	.148	.227	3.45	-.00067	-.022	.031	4.51	47.67	244
21	36.6	.600	.024	.193	2.399	13.87	-.212	.159	.094	3.19	.00124	.040	.031	-.95	32.91	243
22	-.8	-.012	.849	.085	-.004	3.76	-.005	.098	.360	8.64	-.00058	-.069	.009	-2.09	25.70	912
23	2.3	.037	.847	.083	-.010	4.34	.020	.082	-.129	3.72	.00090	.131	.007	1.14	12.78	935
24	5.3	.087	.621	.108	-.476	6.57	.047	.096	-1.696	11.22	.00279	.271	.015	4.22	56.20	961
25	8.4	.137	.761	.138	-.980	7.39	.081	.088	-1.349	8.92	.00214	.176	.015	.42	65.48	942
26	11.4	.187	.566	.342	-.633	7.46	.112	.130	-1.699	10.91	.00118	.027	.054	-.48	28.83	963
27	13.0	.212	.318	.426	-.013	4.41	.128	.191	-2.070	11.68	.00610	.075	.074	1.67	17.75	973
28	14.5	.237	.203	.459	1.638	7.68	.007	.379	-.771	3.90	.00205	.012	.159	.32	10.19	987
29	13.7	.225	.136	.400	.467	4.09	.112	.240	-1.406	7.51	.00379	.039	.092	.95	18.71	980
30	16.0	.262	1.468	.232	-.819	4.08	.127	.152	.646	4.97	-.00223	-.063	.034	-.18	11.95	996

ORIGINAL PAGE IS
OF POOR QUALITY

TABLE IV-76

AXIAL AND RADIAL VELOCITY DATA AND CORRELATIONS

Test Date: 3/16/83 Run No.: 76 Flow Condition: 1 Geometry: 3

Axial Location: 5 mm (0.2 in.) $x/R_o = 0.083$ Swirler Orientation, $\phi = 85$ deg

P_t No.	r mm +(θ=0) -(θ=180)	r/R_o	U m/s	u' m/s	S_u	K_u	V m/s	v' m/s	S_v	K_v	$\overline{uv}$ m^2/s^2	R_{uv}	σ_{uv} m^2/s^2	S_{uv}	K_{uv}	N
1	30.5	.500	.256	.178	.601	6.37	-.176	.185	.708	5.46	.01020	.346	.042	3.56	31.91	976
2	29.0	.475	1.262	.335	-.299	3.39	-.411	.312	.136	3.02	.02236	.214	.108	.98	9.33	997
3	27.4	.450	1.199	.374	-.063	3.15	-.704	.508	.530	2.58	.00364	.019	.200	.54	8.15	996
4	25.9	.425	1.515	.336	-.274	3.20	-.367	.345	-.772	3.33	.01430	.123	.114	.12	8.14	994
5	24.4	.400	1.726	.213	-3.956	23.97	-.180	.106	-.390	3.79	-.00074	-.033	.022	-3.69	43.97	991
6	29.7	.487	1.053	.397	.109	2.77	-.188	.239	-.333	3.44	.03538	.373	.091	1.31	7.35	996
7	28.2	.462	1.137	.299	-.439	2.86	-.653	.453	.653	2.81	-.00067	-.049	.134	-.17	7.19	918
8	26.7	.437	1.255	.357	-.156	3.35	-.574	.466	.293	2.23	.01488	.089	.160	.57	6.84	997
9	22.9	.375	1.754	.096	-.078	6.42	-.057	.078	.379	4.18	-.00055	-.074	.008	-3.17	42.87	983
10	21.3	.350	1.725	.136	-3.383	23.46	.014	.076	.104	3.34	-.00111	-.108	.009	-.78	17.31	988
11	19.8	.325	1.687	.153	-3.283	20.39	.041	.078	.247	3.44	-.00107	-.089	.012	1.02	44.32	984
12	18.3	.300	1.682	.103	-.991	7.41	.032	.074	.424	3.33	-.00104	-.136	.008	-2.28	26.71	978
13	16.8	.275	1.628	.132	-.457	3.59	.017	.105	.629	4.68	-.00157	-.113	.016	-2.77	26.89	987
14	15.2	.250	.695	.387	-.232	3.06	-.090	.407	.099	2.53	-.07003	-.445	.160	-1.17	6.79	990
15	13.7	.225	.015	.473	.663	3.08	.048	.281	-.699	3.64	.00268	.020	.117	-1.11	11.43	235
16	32.0	.525	.181	.132	-.155	4.64	-.180	.118	.051	3.10	-.00116	-.075	.017	-1.69	16.30	235
17	33.5	.550	.125	.128	.348	4.28	-.214	.137	.291	3.48	-.00142	-.081	.019	.02	7.08	225
18	35.1	.575	.082	.141	-.152	3.08	-.211	.144	.181	3.15	.00213	.105	.020	.49	5.35	232
19	36.6	.600	.016	.140	-.240	3.16	-.234	.142	.186	3.44	.00239	.120	.021	1.38	13.34	245
20	16.0	.262	1.404	.266	-.870	4.59	-.035	.247	.634	4.36	-.02175	-.330	.094	-4.11	30.13	994
21	14.5	.237	.225	.570	.855	3.45	-.061	.393	-.294	2.41	-.03569	-.159	.201	-.38	5.46	232

TABLE IV-77

AXIAL AND RADIAL VELOCITY DATA AND CORRELATIONS

Test Date: 3/16/83 Run No.: 77 Flow Condition: 1 Geometry: 3

Axial Location: 5 mm (0.2 in.) $x/R_o = 0.083$ Swirler Orientation, $\phi = 90$ deg

P_t No.	r mm +(0=0) -(0=180)	r/R_o	U m/s	u' m/s	S_u	K_u	V m/s	v' m/s	S_v	K_v	$\overline{uv}$ m^2/s^2	R_{uv}	σ_{uv} m^2/s^2	S_{uv}	K_{uv}	N
1	30.5	.500	.970	.348	-.033	2.46	.025	.210	-.299	2.80	.04220	.578	.073	1.23	6.25	988
2	29.0	.475	1.686	.215	-2.261	13.19	.065	.118	.237	4.31	.00472	.186	.025	2.01	21.55	990
3	27.4	.450	1.799	.163	-.066	4.09	.073	.092	-.101	4.12	.00255	.169	.018	1.13	17.44	979
4	25.9	.425	1.806	.195	-2.826	17.08	-.050	.084	-.116	3.27	.00042	.026	.017	-2.41	32.74	990
5	24.4	.400	1.778	.193	-3.608	19.96	-.059	.075	-.112	3.87	-.00073	-.050	.015	-3.28	63.32	992
6	22.9	.375	1.760	.161	-3.779	23.05	-.039	.071	.050	3.27	-.00132	-.115	.011	-4.33	35.85	984
7	21.3	.350	1.718	.202	-3.757	22.97	-.003	.070	.055	3.75	-.00019	-.013	.020	7.79	215.10	993
8	19.8	.325	1.673	.227	-3.639	22.23	.013	.069	.139	3.56	-.00110	-.070	.021	.81	117.00	996
10	16.8	.275	1.598	.276	-3.195	19.25	-.017	.108	.717	4.89	-.00140	-.058	.032	-5.06	108.70	992
11	15.2	.250	.795	.407	-.685	3.73	-.252	.396	.321	2.66	-.04450	-.276	.156	-.72	8.39	490
12	28.2	.462	1.757	.205	-1.910	12.92	.129	.112	.202	4.47	.00301	.132	.026	1.50	35.13	999
13	26.7	.437	1.835	.153	-.765	5.68	.000	.088	-.708	5.18	.00084	.062	.018	1.96	82.80	980
14	25.2	.412	1.822	.172	-2.456	15.63	-.063	.082	-.299	3.67	-.00004	-.003	.014	-2.03	31.03	984
15	23.6	.387	1.777	.188	-3.895	22.56	-.056	.071	.262	3.22	-.00145	-.108	.013	-3.53	33.42	991
16	22.1	.362	1.734	.204	-3.815	20.68	-.008	.073	.291	3.24	-.00144	-.097	.017	-3.95	42.60	990
17	13.7	.225	-.118	.582	1.194	3.91	-.084	.491	-2.363	8.58	-.01492	-.052	.200	-.50	12.22	237
18	32.0	.525	.199	.153	-.570	4.21	-.176	.117	-.184	2.67	-.00198	-.110	.021	-1.50	9.82	215
19	33.5	.550	.136	.168	.057	4.10	-.197	.129	-.224	3.22	.00153	.071	.023	.23	7.38	228
20	35.1	.575	.115	.256	2.239	8.86	-.220	.135	-.150	3.35	.00319	.092	.041	3.32	27.11	231

ORIGINAL PAGE IS
OF POOR QUALITY

TABLE IV-78

AXIAL AND RADIAL VELOCITY DATA AND CORRELATIONS

Test Date: 3/17/83 Run No.: 78 Flow Condition: 1 Geometry: 3

Axial Location: 5 mm (0.2 in.) $x/R_o = 0.083$ Swirler Orientation, ϕ = 95 deg

P_t No.	r mm +(θ=0) -(θ=180)	r/R_o	U m/s	u' m/s	S_u	K_u	V m/s	v' m/s	S_v	K_v	$\overline{uv}$ m^2/s^2	R_{uv}	σ_{uv} m^2/s^2	S_{uv}	K_{uv}	N
1	36.6	.600	-.001	.167	.685	4.23	-.185	.158	-.002	3.54	.00145	.055	.027	1.48	9.55	226
2	35.1	.575	.052	.170	.764	3.96	-.169	.149	.140	3.23	.00132	.052	.031	2.96	21.59	221
3	33.5	.550	.167	.265	1.144	4.75	-.168	.145	-.274	4.89	-.00088	-.023	.053	-6.43	67.40	209
4	32.0	.525	.176	.195	-1.027	4.89	-.108	.126	-.034	3.48	.00087	.035	.023	.19	7.68	223
5	30.5	.500	1.224	.305	-.456	2.81	.133	.178	-.445	3.87	.03137	.578	.064	2.81	15.78	999
6	29.0	.475	1.790	.136	-.402	3.72	.123	.086	-.174	3.06	.00361	.308	.011	1.06	9.97	995
7	27.4	.450	1.870	.120	-.511	3.20	.107	.078	-.254	3.57	.00265	.282	.011	2.61	17.64	988
8	25.9	.425	1.862	.147	-3.724	24.37	.084	.066	-.551	4.13	.00042	.043	.011	-1.25	45.80	991
9	24.4	.400	1.855	.082	-.197	2.13	.061	.064	.008	3.08	.00039	.075	.006	.79	13.25	990
10	22.9	.375	1.804	.075	-.098	2.96	.050	.063	.714	3.56	-.00021	-.044	.005	-.31	10.78	992
11	21.3	.350	1.768	.091	-1.527	15.20	.054	.064	.048	2.95	-.00052	-.089	.006	-1.43	53.91	991
12	19.8	.325	1.715	.083	-.931	9.17	.056	.065	.185	3.23	-.00045	-.084	.006	-1.47	16.57	996
13	18.3	.300	1.675	.092	-.368	5.32	.041	.084	.317	2.99	-.00097	-.125	.009	-1.28	11.63	987
14	16.8	.275	1.540	.277	-1.362	6.20	-.061	.191	.870	5.24	-.01498	-.284	.085	-3.16	36.23	996
15	15.2	.250	.657	.496	-.479	2.87	-.393	.354	.220	2.69	-.03132	-.178	.171	-1.06	7.84	495
17	16.8	.275	1.564	.255	-1.265	5.63	-.064	.180	.731	4.74	-.01187	-.258	.061	-2.56	19.60	996
18	15.2	.250	.701	.468	-.289	2.75	-.405	.381	.135	2.80	-.03247	-.182	.185	-.88	8.18	493
19	13.7	.225	-.127	.374	.641	2.71	-.024	.271	-.890	3.98	-.00089	-.009	.107	-.38	10.98	242
20	13.7	.225	.151	.501	.520	3.01	.009	.251	-1.427	5.90	-.00348	-.028	.126	.23	9.89	219
21	18.3	.300	1.680	.093	-.409	7.25	.081	.110	.852	5.82	-.00024	-.024	.009	-.46	16.56	972
23	15.2	.250	.588	.472	-.062	2.85	-.262	.369	-.124	2.58	.00173	.010	.178	-.36	6.74	495
25	12.2	.200	.598	.539	.120	3.67	.125	.100	-.037	3.30	.00497	.092	.046	.83	7.61	214
26	12.2	.200	.485	.388	-.802	4.44	.148	.095	-.224	4.96	.00200	.054	.034	-.51	10.15	211
27	10.7	.175	.618	.368	-.432	5.94	.108	.083	-1.090	6.94	.00000	.000	.029	-.61	21.71	218
28	9.1	.150	.703	.177	-1.289	5.76	.091	.078	-1.051	7.38	-.00047	-.034	.011	-.16	13.15	209
30	6.1	.100	.794	.115	.265	5.15	.057	.070	-.487	3.76	.00027	.033	.008	-.05	10.24	186
31	4.6	.075	.839	.115	1.249	5.56	.048	.067	.063	8.85	-.00020	-.026	.005	-.49	8.97	196
32	.0	.000	.835	.143	.601	5.45	.027	.064	-.265	3.46	-.00107	-.116	.009	-1.19	9.77	163
33	.0	.000	.825	.120	-.865	5.71	-.002	.077	-.162	3.70	-.00028	-.030	.007	.37	6.10	183
36	9.1	.150	.850	.309	.015	3.36	.062	.102	-.905	4.50	.00146	.046	.034	-.32	7.92	114

ORIGINAL PAGE IS
OF POOR QUALITY

FIG. 1

SHEAR REGIONS WITH CONFINED, EXPANDING COAXIAL JETS

a) SWIRLING FLOW

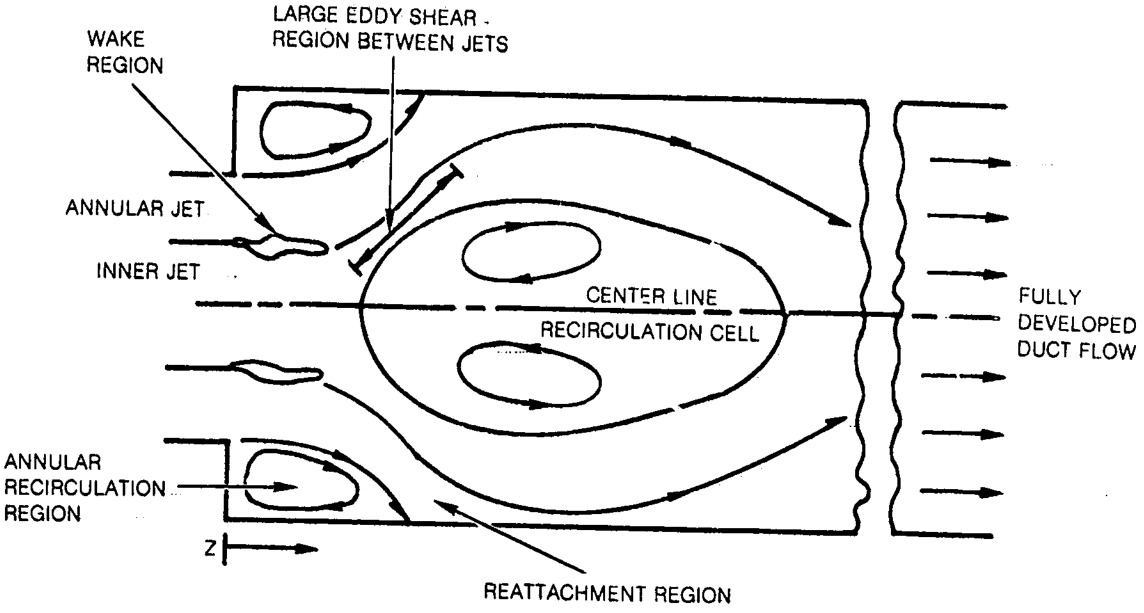
LARGE EDDY SHEAR REGION BETWEEN JETS
WAKE REGION
ANNULAR JET
INNER JET
CENTER LINE
RECIRCULATION CELL
FULLY DEVELOPED DUCT FLOW
ANNULAR RECIRCULATION REGION
Z
REATTACHMENT REGION

b) NONSWIRLING FLOW

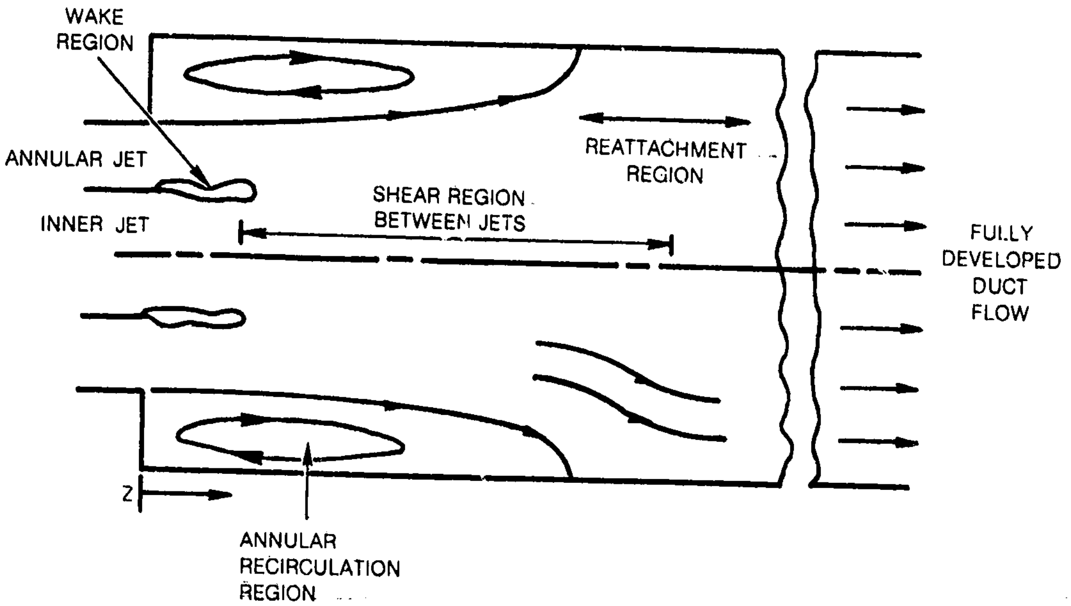
WAKE REGION
ANNULAR JET
REATTACHMENT REGION
SHEAR REGION BETWEEN JETS
INNER JET
FULLY DEVELOPED DUCT FLOW
Z
ANNULAR RECIRCULATION REGION

83-7-19-1

FIG. 2

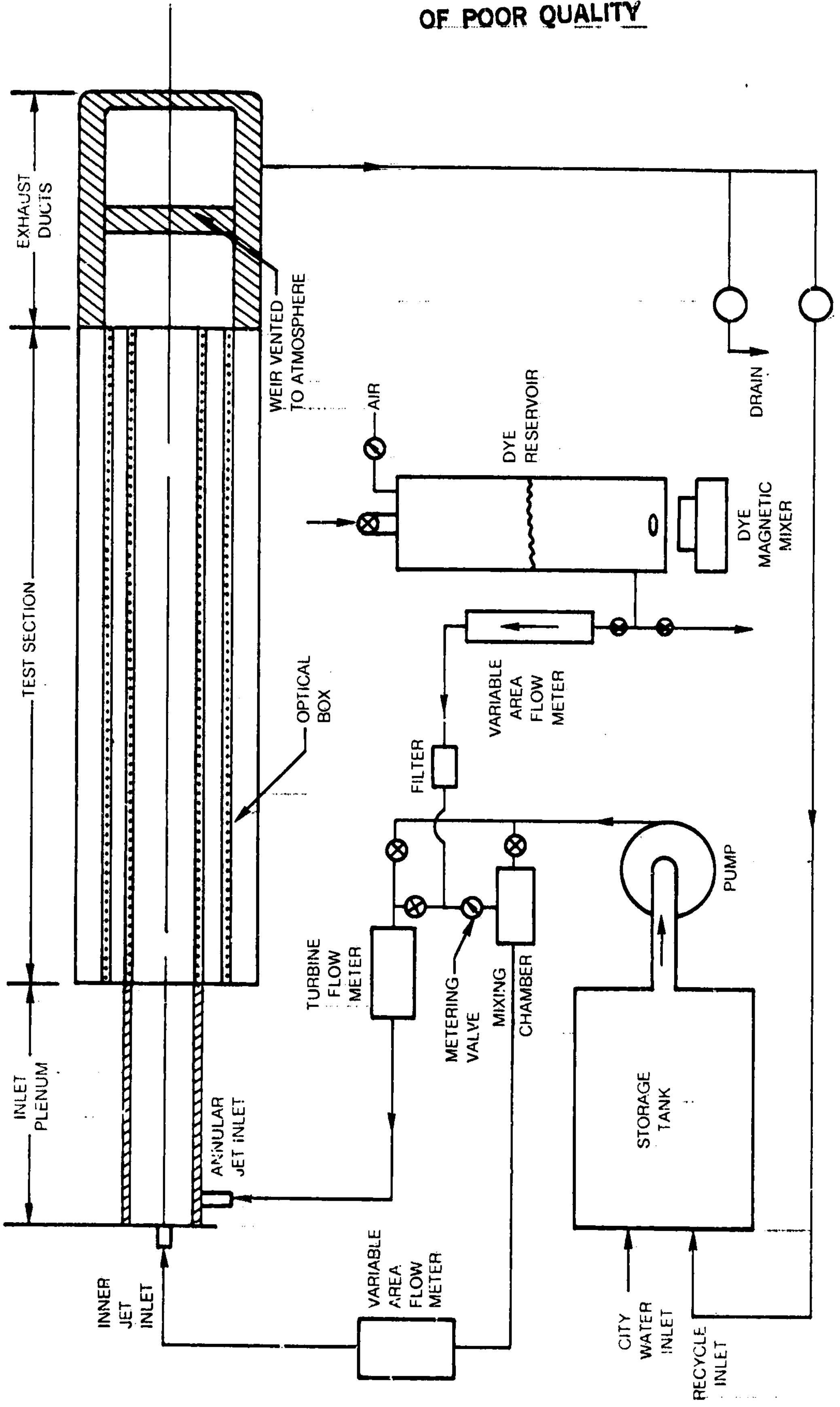
EXHAUST DUCTS
WEIR VENTED TO ATMOSPHERE
TEST SECTION
OPTICAL BOX
INLET PLENUM
ANNULAR JET INLET
INNER JET INLET
VARIABLE AREA FLOW METER
TURBINE FLOW METER
METERING VALVE
MIXING CHAMBER
FILTER
VARIABLE AREA FLOW METER
AIR
DYE RESERVOIR
DYE MAGNETIC MIXER
DRAIN
PUMP
STORAGE TANK
CITY WATER INLET
RECYCLE INLET
81-12-38-4

SCHEMATIC OF TEST FACILITY

FIG. 3

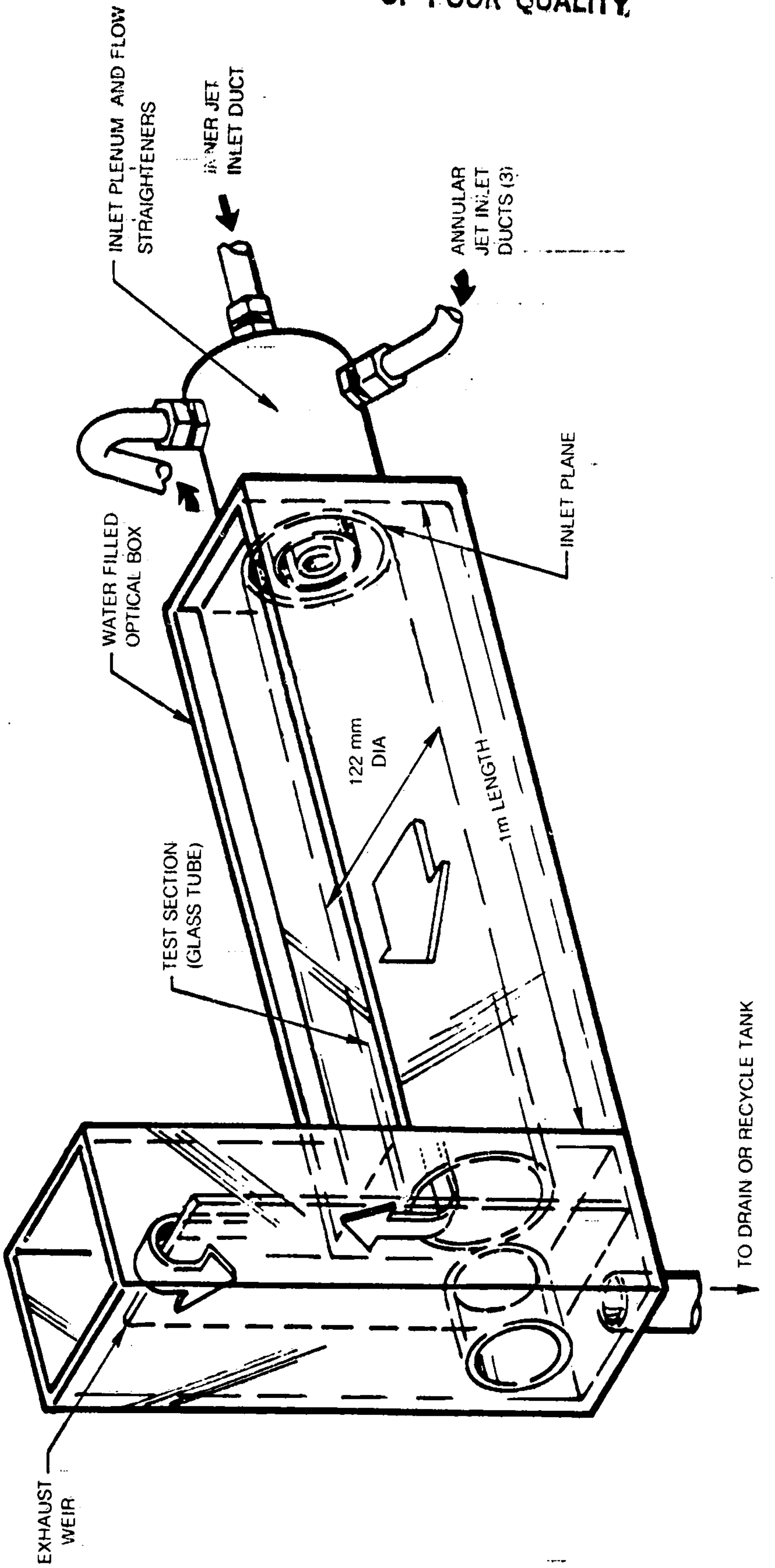
INLET PLENUM AND FLOW STRAIGHTENERS
INNER JET INLET DUCT
ANNULAR JET INLET DUCTS (3)
INLET PLANE
WATER FILLED OPTICAL BOX
122 mm DIA
1m LENGTH
TEST SECTION (GLASS TUBE)
TO DRAIN OR RECYCLE TANK
EXHAUST WEIR

SKETCH OF TEST SECTION

SKETCHES OF TEST SECTION INLET REGION WITH VELOCITY AND COORDINATE SYSTEM

30 DEG MEAN ANGLE SWIRLER IN ANNULAR INLET DUCT

DIMENSION	R_{i1}	R_{i2}	R_a	R_o	S	L
LENGTH (mm)	12.5	15.3	29.5	61.0	51	1016
LENGTH (in.)	0.492	0.601	1.162	2.402	2.0	40
RADIUS RATIO, r/R_o	0.205	0.251	0.484	1.0	–	–

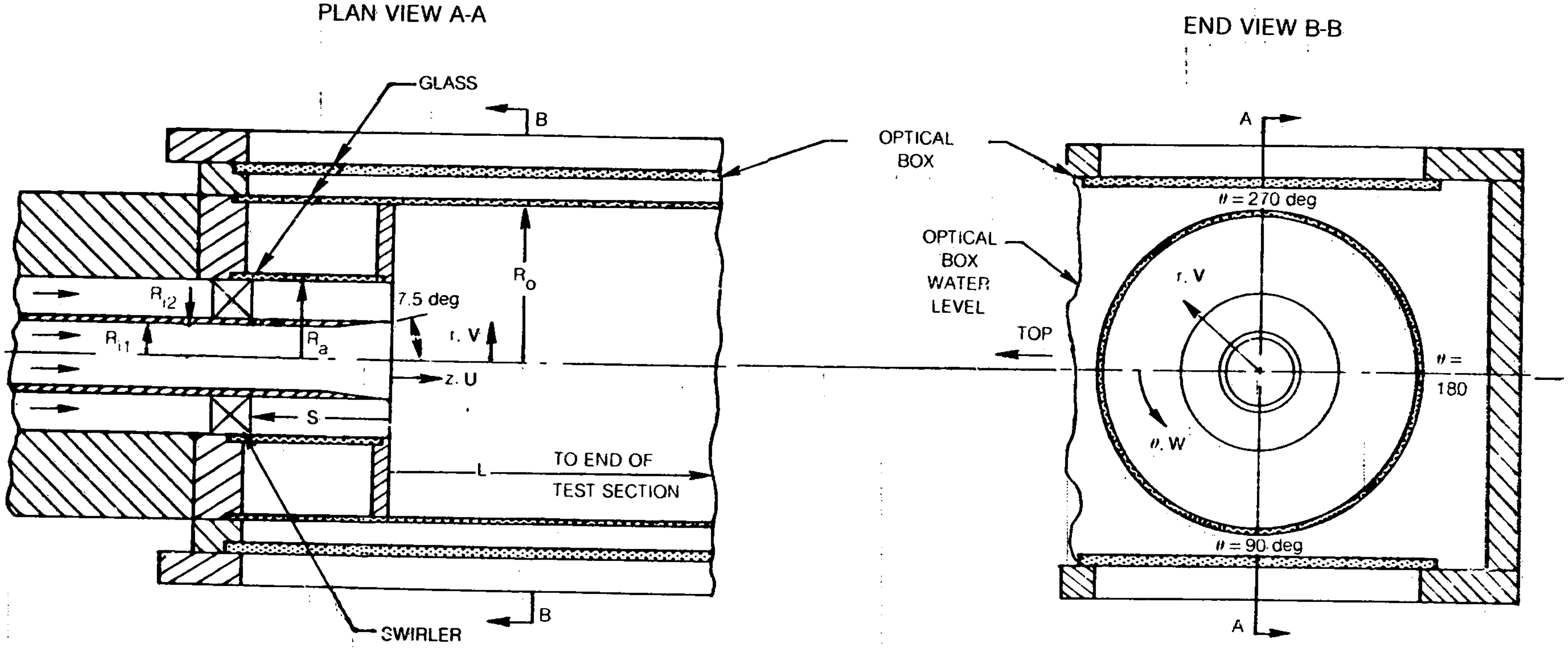
PLAN VIEW A-A
GLASS
B
R_{i2}
R_{i1}
R_a
7.5 deg
r, V
R_o
z, U
S
L
TO END OF
TEST SECTION
B
SWIRLER
OPTICAL
BOX
OPTICAL
BOX
WATER
LEVEL
TOP
END VIEW B-B
A
A
θ = 270 deg
r, V
θ, W
θ =
180
θ = 90 deg

FIG. 4

ORIGINAL PAGE IS
OF POOR QUALITY

FIG. 5

OPTICAL ARRANGEMENT FOR FLOW VISUALIZATION PHOTOGRAPHS AND MOTION PICTURES IN r-z PLANE

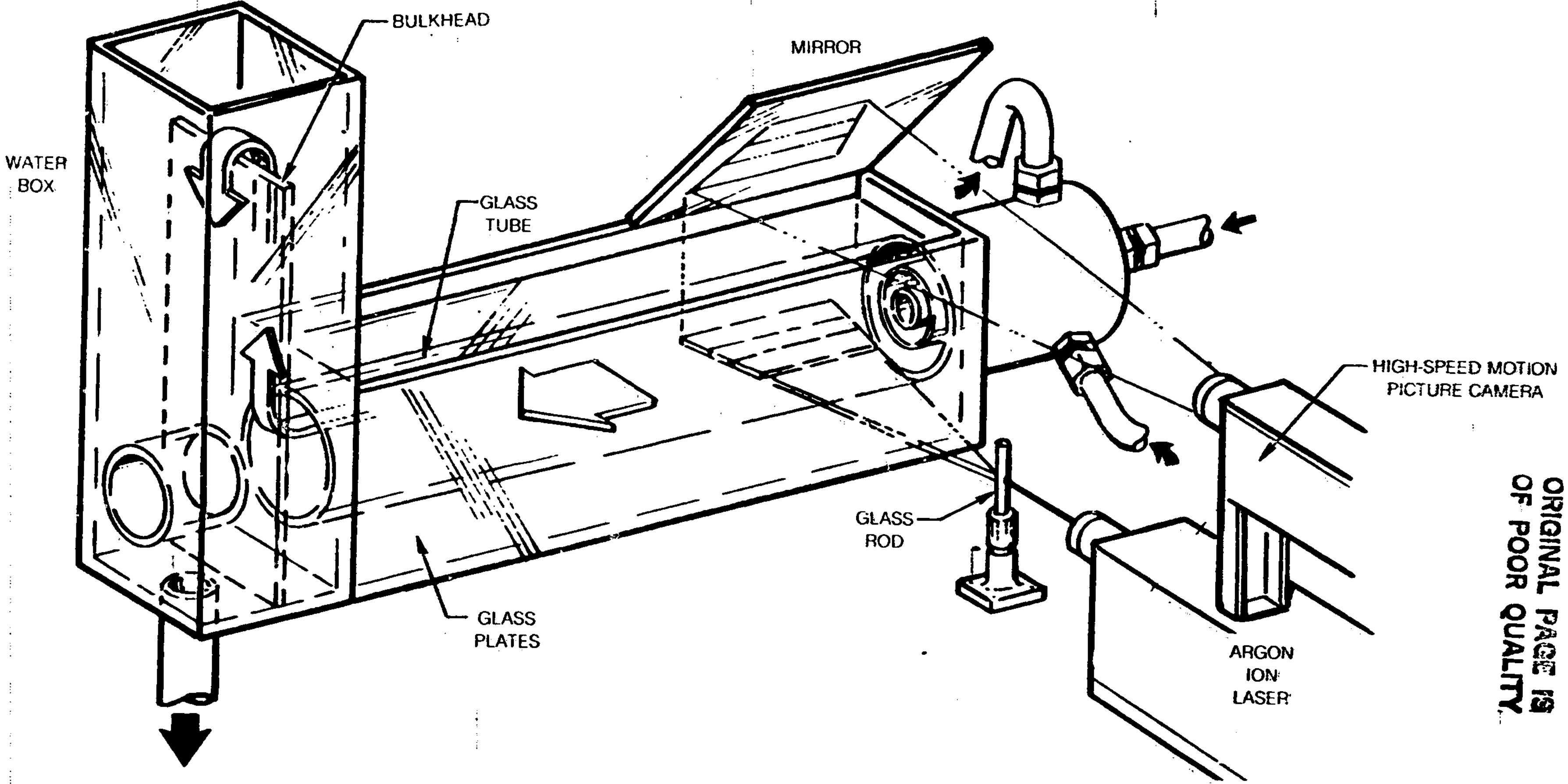
BULKHEAD
MIRROR
WATER BOX
GLASS TUBE
HIGH-SPEED MOTION PICTURE CAMERA
GLASS ROD
GLASS PLATES
ARGON ION LASER

81-12-38-5

ORIGINAL PAGE IS
OF POOR QUALITY

FIG. 6

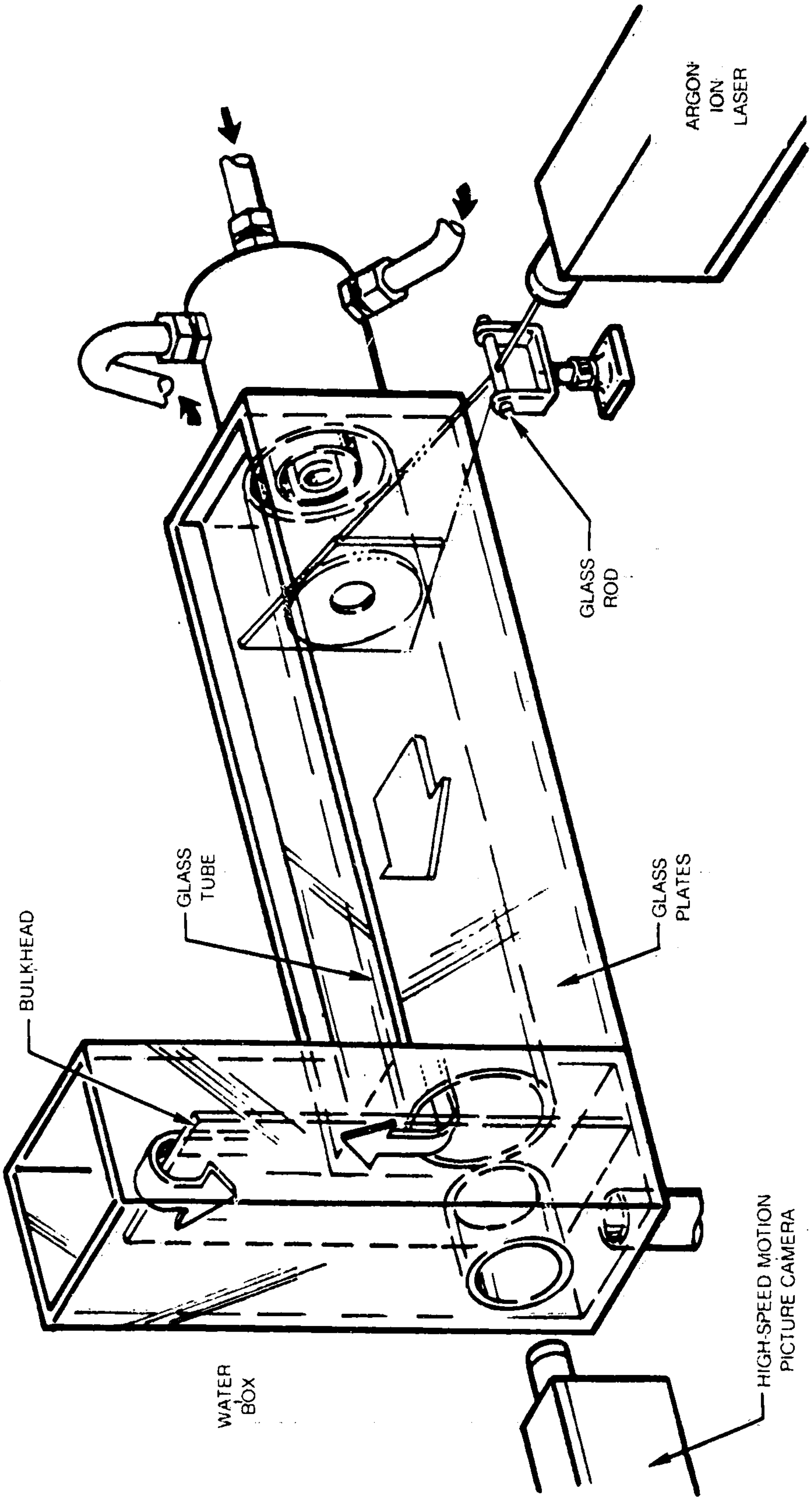
ARGON ION LASER
GLASS ROD
GLASS TUBE
GLASS PLATES
BULKHEAD
WATER BOX
HIGH-SPEED MOTION PICTURE CAMERA

OPTICAL ARRANGEMENT FOR FLOW VISUALIZATION PHOTOGRAPHS AND MOTION PICTURES IN r-θ PLANE

81-12-38-6

FIG. 7

ORIGINAL PAGE IS
OF POOR QUALITY

OPTICAL ARRANGEMENT FOR TWO COMPONENT LV MEASUREMENTS

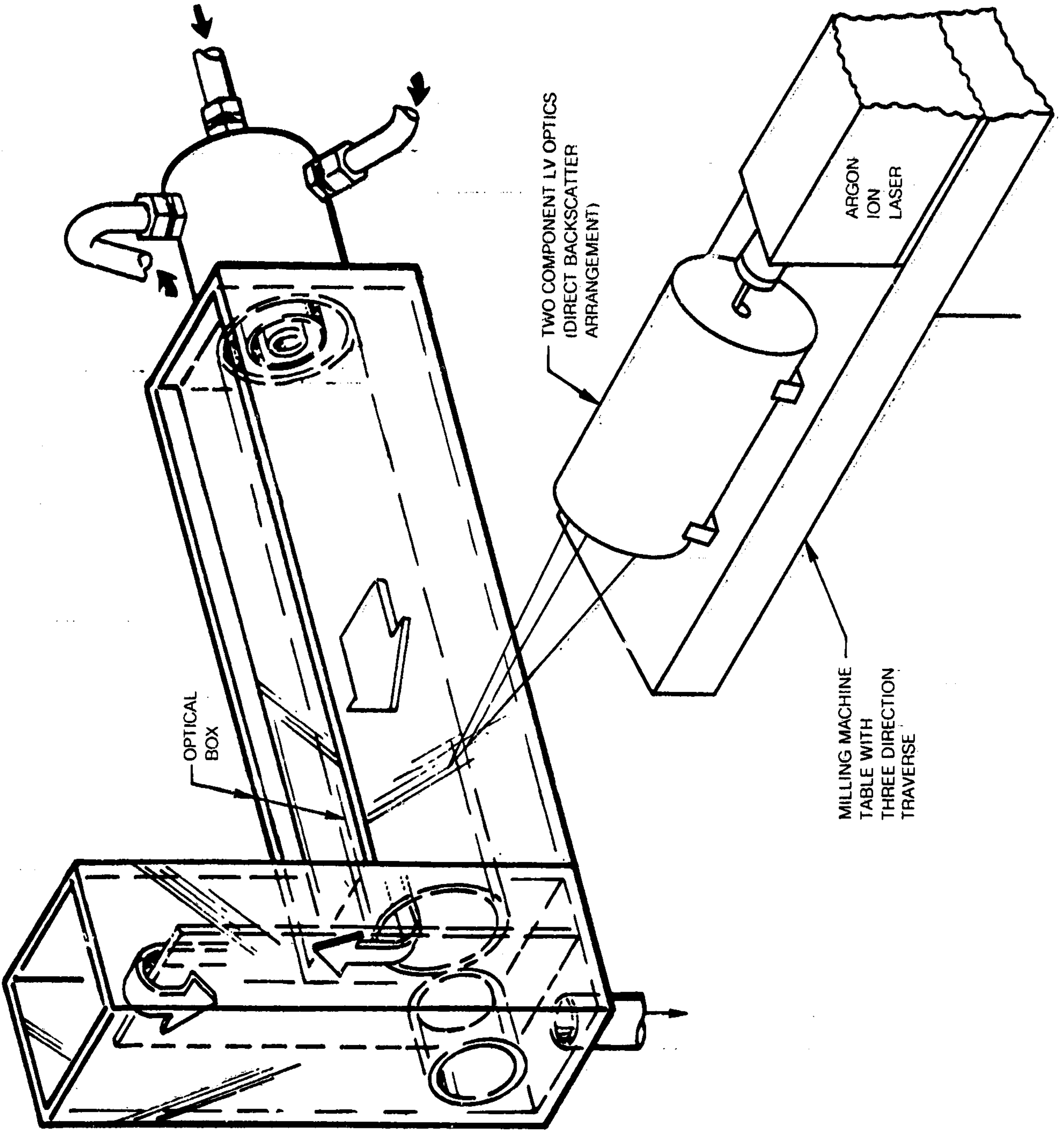
TWO COMPONENT LV OPTICS
(DIRECT BACKSCATTER
ARRANGEMENT)
ARGON
ION
LASER
OPTICAL
BOX
MILLING MACHINE
TABLE WITH
THREE DIRECTION
TRAVERSE

81-12-38-7

FIG. 8

SKETCH OF OPTICAL COMPONENTS AND BEAM PATHS USED FOR TWO COMPONENT VELOCITY MEASUREMENTS

DISA 55 x 00 OPTIC COMPONENTS

02 — BACKCOVER PLATE WITH POLARIZATION ROTATOR
03 — BEAM SPLITTER MODULE, TYPE I
04 — BRAGG CELL SECTION
05 — BEAM SPLITTER MODULE, TYPE II
06 — BACKSCATTER SECTION WITH GREEN LASER LINE FILTER
07 — BACKSCATTER SECTION WITH BLUE LASER LINE FILTER
08 — PHOTOMULTIPLIER TUBE
09 — LENS MOUNTING RING
10 — PINHOLE SECTION
11 — BEAM TRANSLATOR
12 — BEAM EXPANDER
13 — FRONT LENS

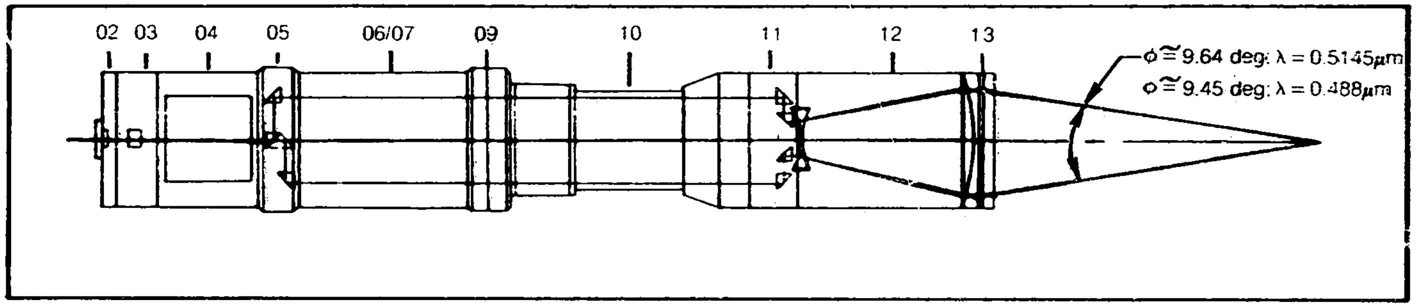
02
03
04
05
06/07
09
10
11
12
13
$\phi \cong 9.64$ deg; $\lambda = 0.5145 \mu m$
$\phi \cong 9.45$ deg; $\lambda = 0.488 \mu m$

TRANSMITTER BEAM PATH

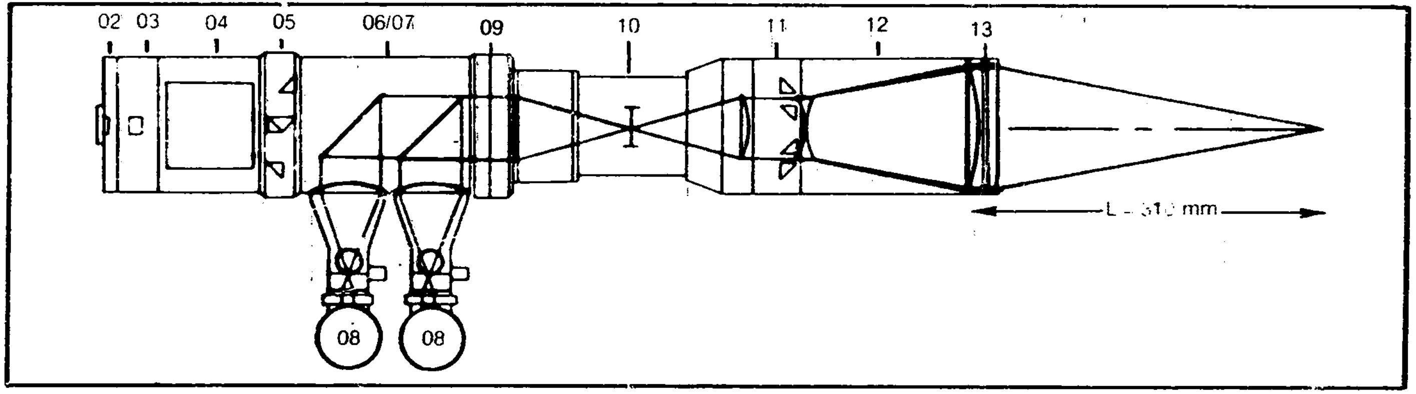
02
03
04
05
06/07
09
10
11
12
13
08
08
L = 310 mm

RECEIVER BEAM PATH

ORIGINAL PAGE IS
OF POOR QUALITY

FIG. 9

30 DEG FREE VORTEX SWIRLER DESIGN CHARACTERISTICS

ALL DIMENSIONS IN MM

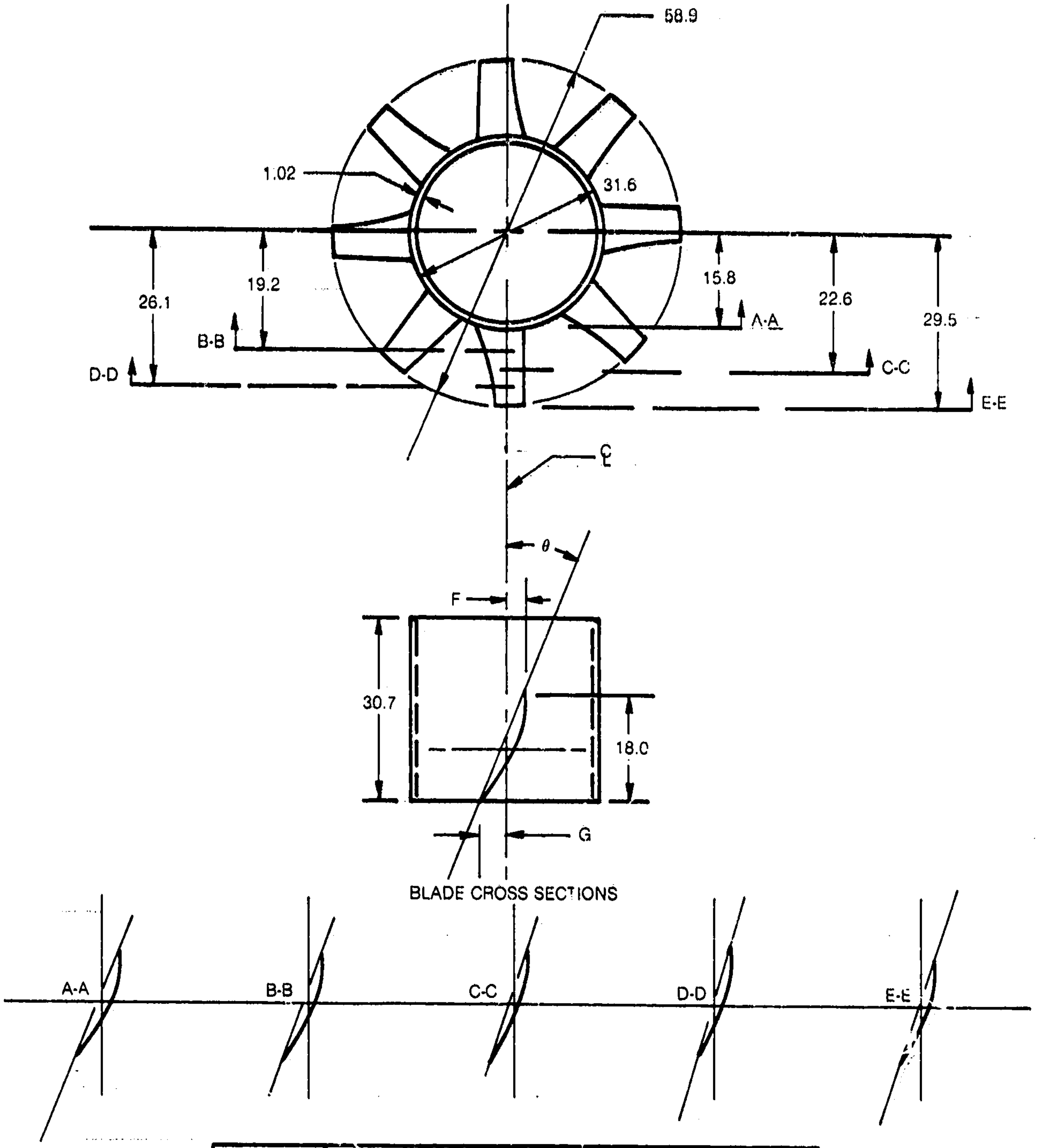
58.9
1.02
31.6
26.1
19.2
15.8
22.6
29.5
B-B
A-A
C-C
D-D
E-E
℄
θ
F
30.7
18.0
G
BLADE CROSS SECTIONS
A-A
B-B
C-C
D-D
E-E

SECTION	POSITION	ANGLE θ, deg	F	G
A-A	HUB	22.14	2.08	5.23
B-B	25%	19.38	2.11	4.22
C-C	MID	18.07	2.16	3.71
D-D	75%	17.26	2.18	3.40
E-E	TIP	18.14	2.24	3.18

83-9-92-1

ORIGINAL PAGE IS
OF POOR QUALITY

FIG. 10

VISUALIZATION OF FLOW CONDITION 1 WITH SWIRL IN ANNULAR STREAM

$U_i = 0.52$ m/s $\quad U_a = 1.66$ m/s

$Q_i = 6.2$ gpm $\quad Q_a = 52.8$ gpm

r-z PLANE

$0 < z < 230$ mm

+ \+

→| 25.4mm |←

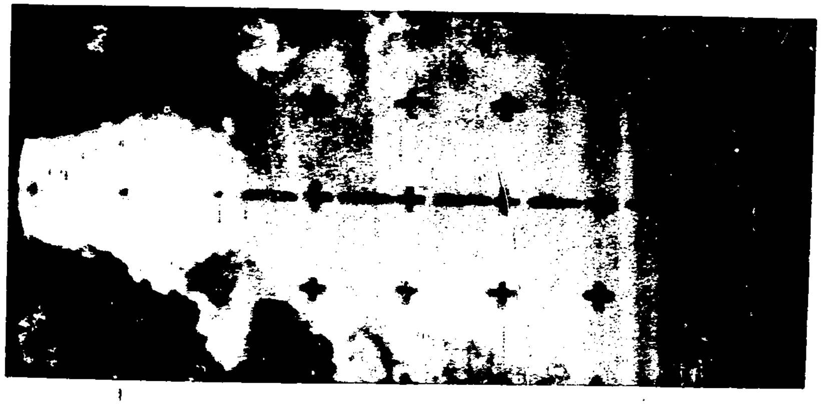

DYE ADDED TO INNER STREAM

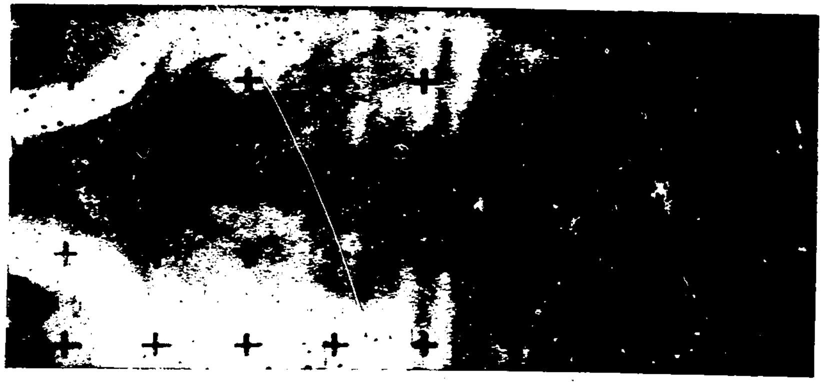

DYE ADDED TO ANNULAR STREAM

r-θ PLANE

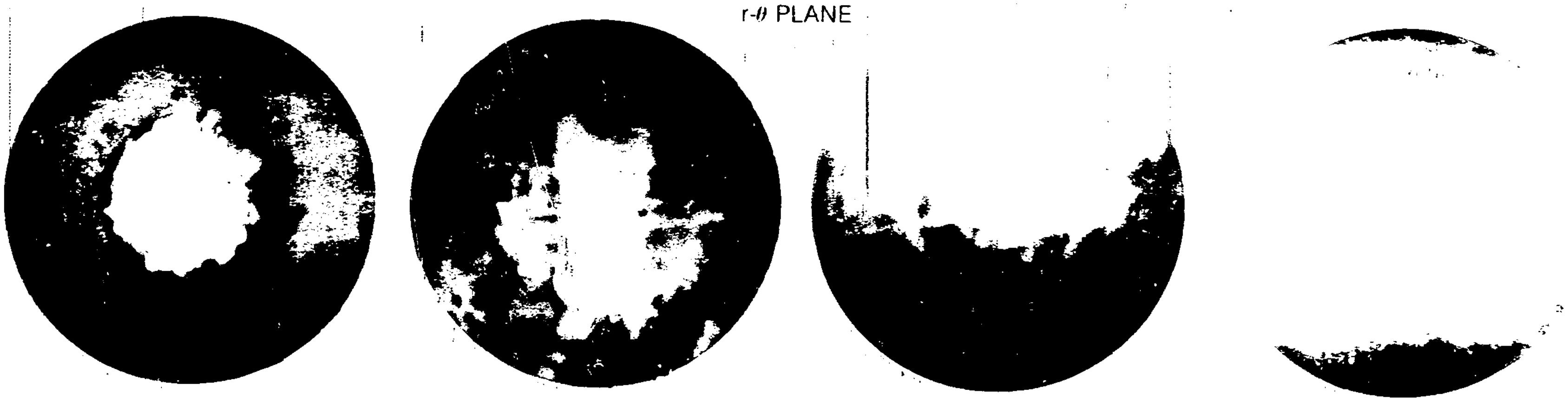

z = 25 mm

z = 51 mm

z = 102 mm

z = 203 mm

DYE ADDED TO INNER STREAM

ORIGINAL PAGE IS
OF POOR QUALITY

FIG. 11

VISUALIZATION OF FLOW CONDITION 1 WITH SWIRL IN ANNULAR STREAM

$U_i = 0.52$ m/s $U_a = 1.66$ m/s
$Q_i = 6.2$ gpm $Q_a = 52.8$ gpm
DYE ADDED TO ANNULAR STREAM
r-θ PLANE

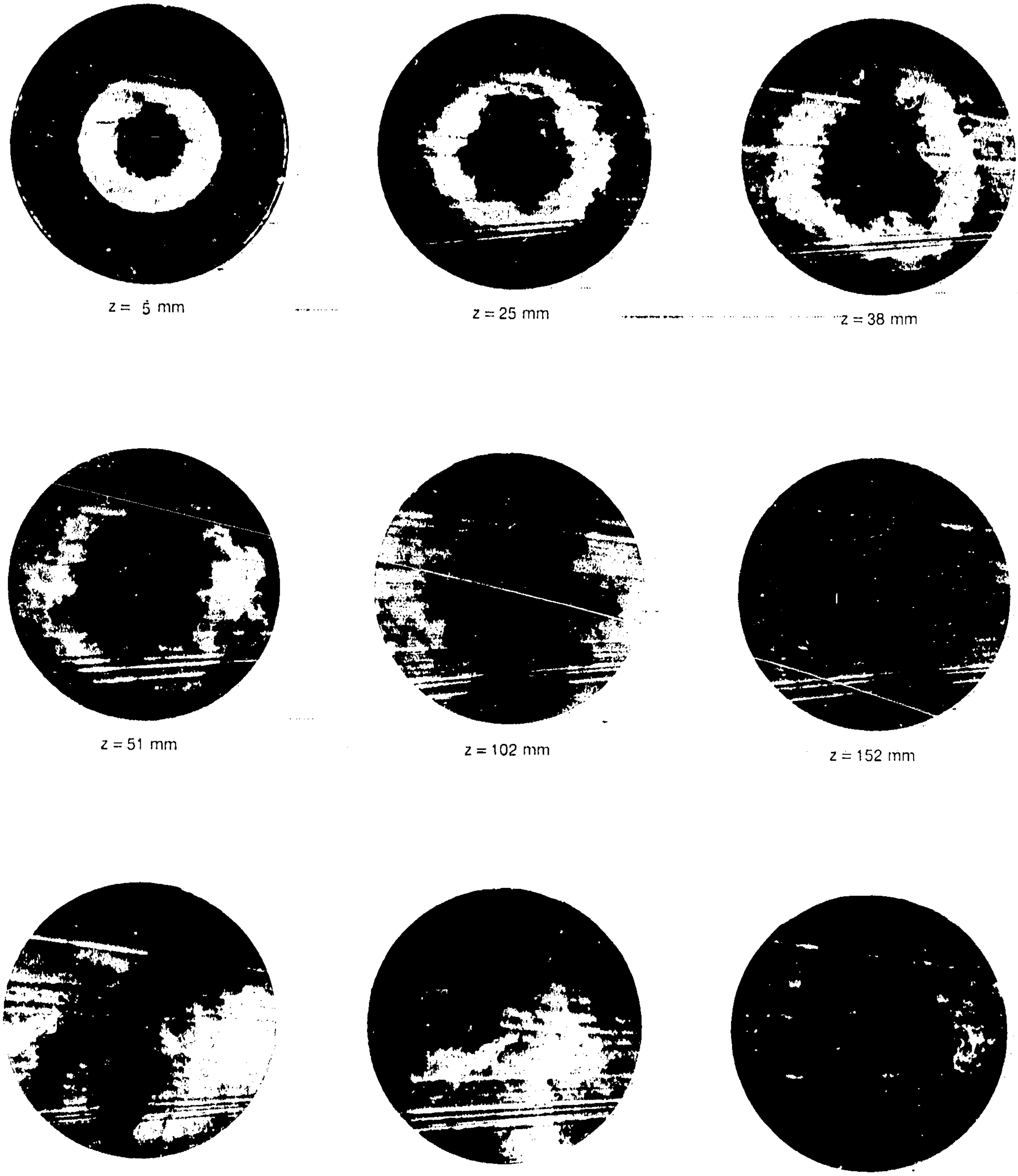

z = 5 mm

z = 25 mm

z = 38 mm

z = 51 mm

z = 102 mm

z = 152 mm

z = 203 mm

z = 305 mm

z = 406 mm

83-7-19-31

ORIGINAL PAGE IS
OF POOR QUALITY

FIG. 12

MEAN AXIAL VELOCITY ALONG TEST SECTION CENTERLINE

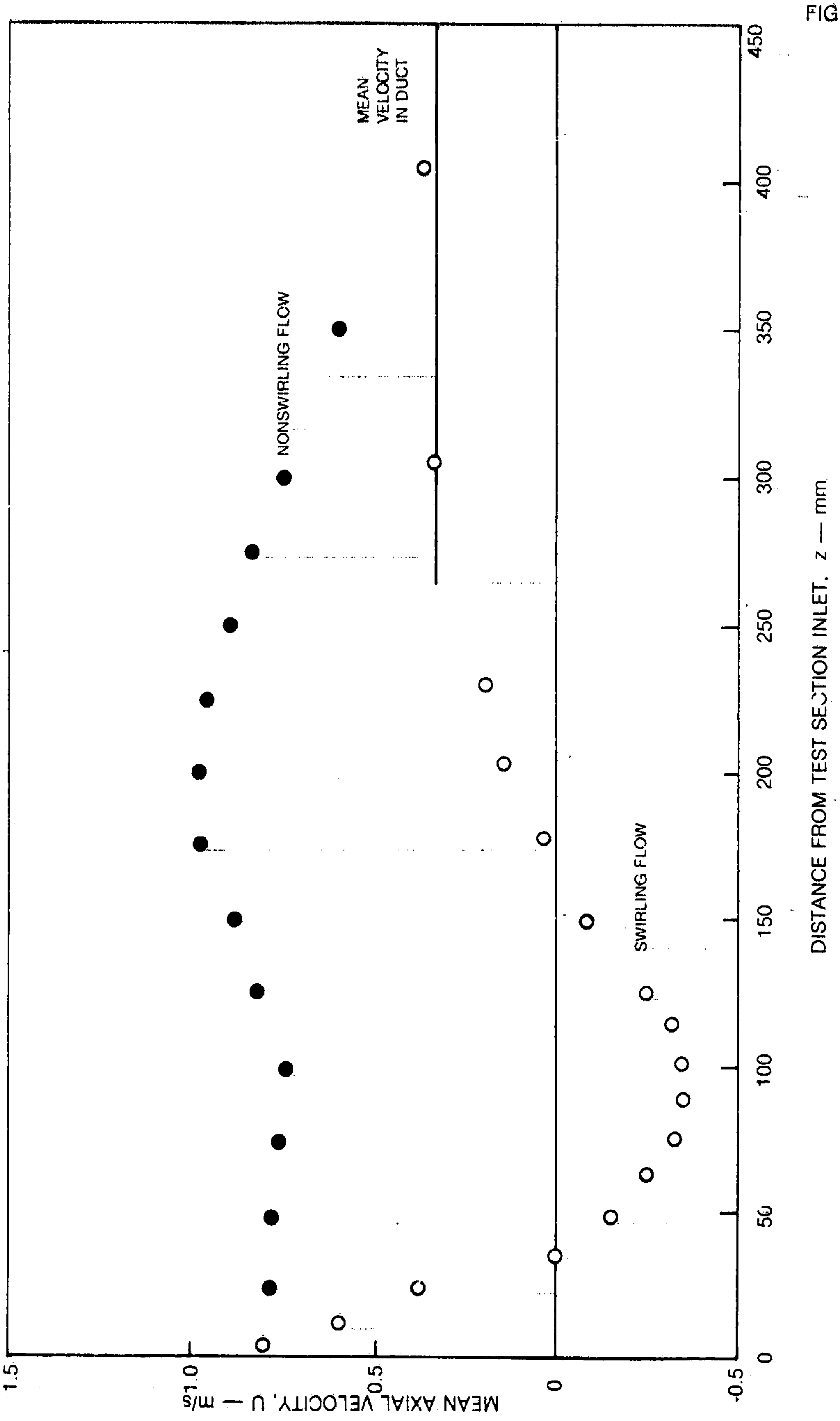

83-7-19-32

ORIGINAL PAGE IS
OF POOR QUALITY

FIG. 13

MEAN AXIAL VELOCITY PROFILES

	HORIZONTAL TRAVERSE	VERTICAL TRAVERSE
OPEN SYMBOLS:	$\theta = 90°$	$\theta = 0°$
SOLID SYMBOLS:	$\theta = 270°$	$\theta = 180°$

SYMBOL	○	●	□	■	△	▲	◇	◆
RUN NOS.	11, 3, 4, 5		16, 7, 8, 6		17, 22, 23, 9		24	

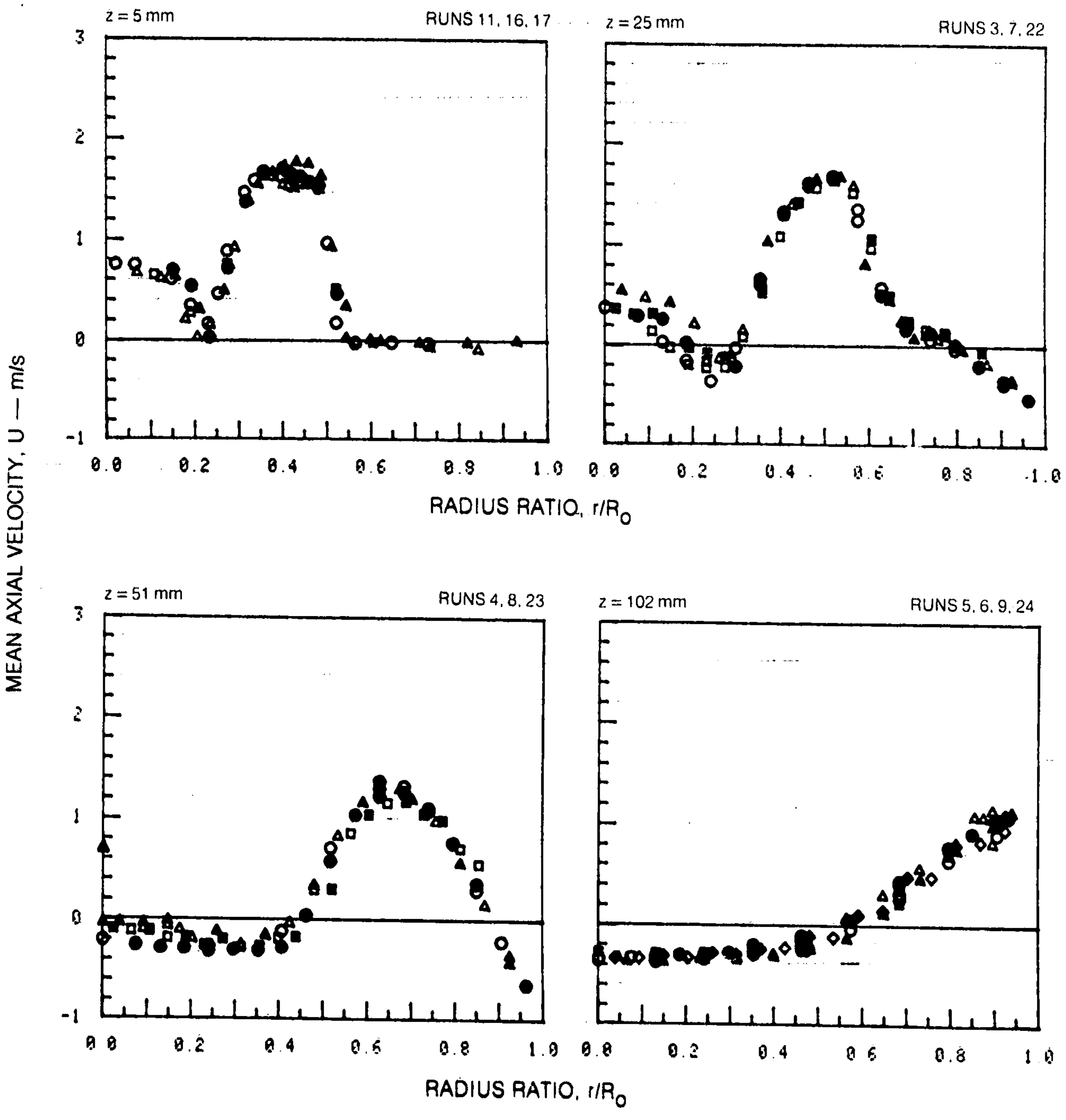

FIG. 13 (CONT.)

MEAN AXIAL VELOCITY PROFILES (CONT)

	HORIZONTAL TRAVERSE	VERTICAL TRAVERSE
OPEN SYMBOLS	θ = 90°	θ = 0°
SOLID SYMBOLS	θ = 270°	θ = 180°

SYMBOL	○	●	□	■	△	▲	◇	◆	▽	▼
RUN NOS	14, 10, 42, 44		15, 12, 43, 45		25, 26		40		41	

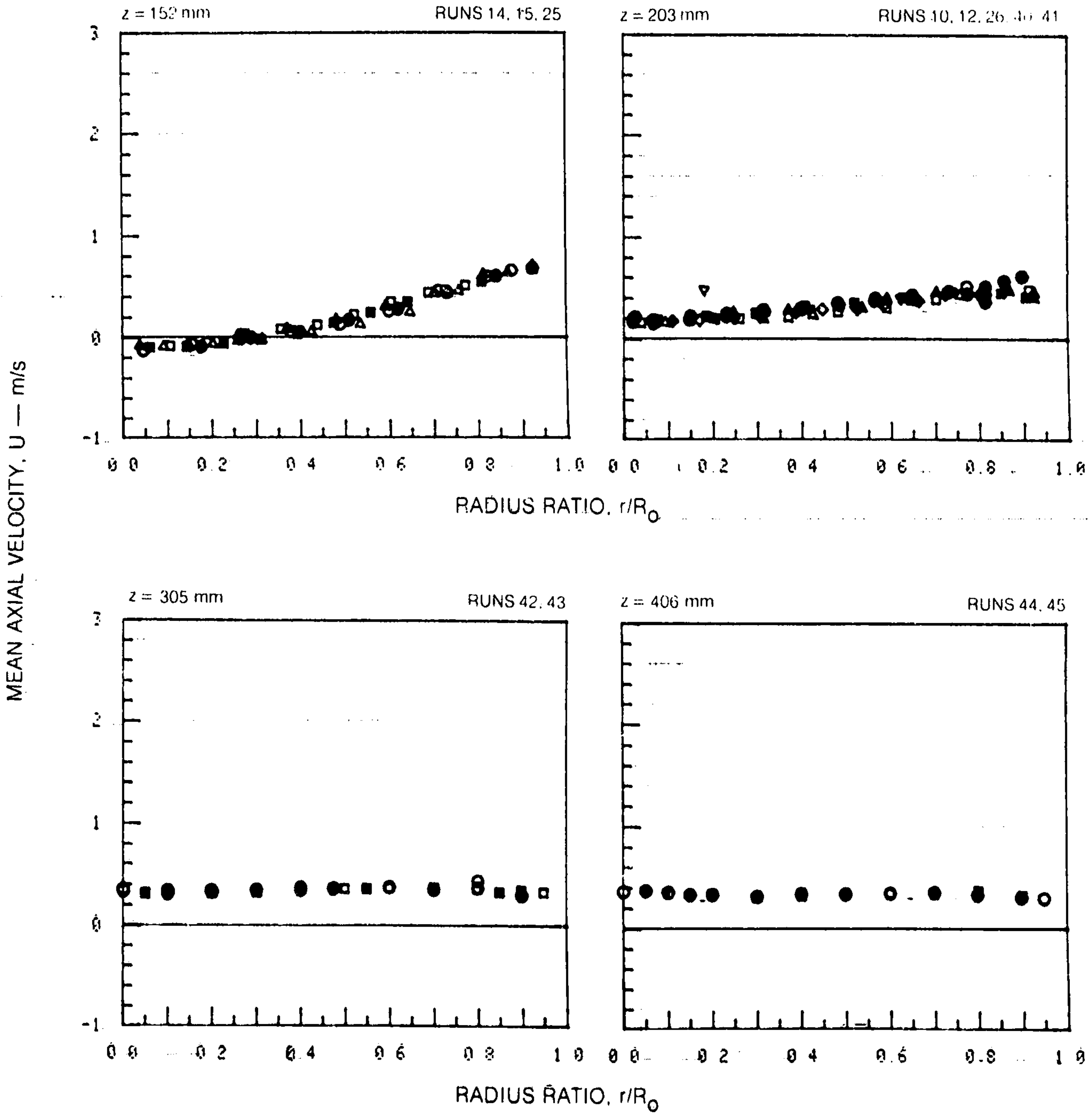

83-3-76-29

ORIGINAL PAGE IS
OF POOR QUALITY

FIG. 14

MEAN RADIAL VELOCITY PROFILES

	HORIZONTAL TRAVERSE	VERTICAL TRAVERSE
OPEN SYMBOLS:	$\theta = 90°$	$\theta = 0°$
SOLID SYMBOLS:	$\theta = 270°$	$\theta = 180°$

SYMBOL	○	●	□	■	△	▲	◇	◆	▽	▼
RUN NOS.	11, 7, 8, 9		16, 28, 32, 34		47, 46, 54		50		51	

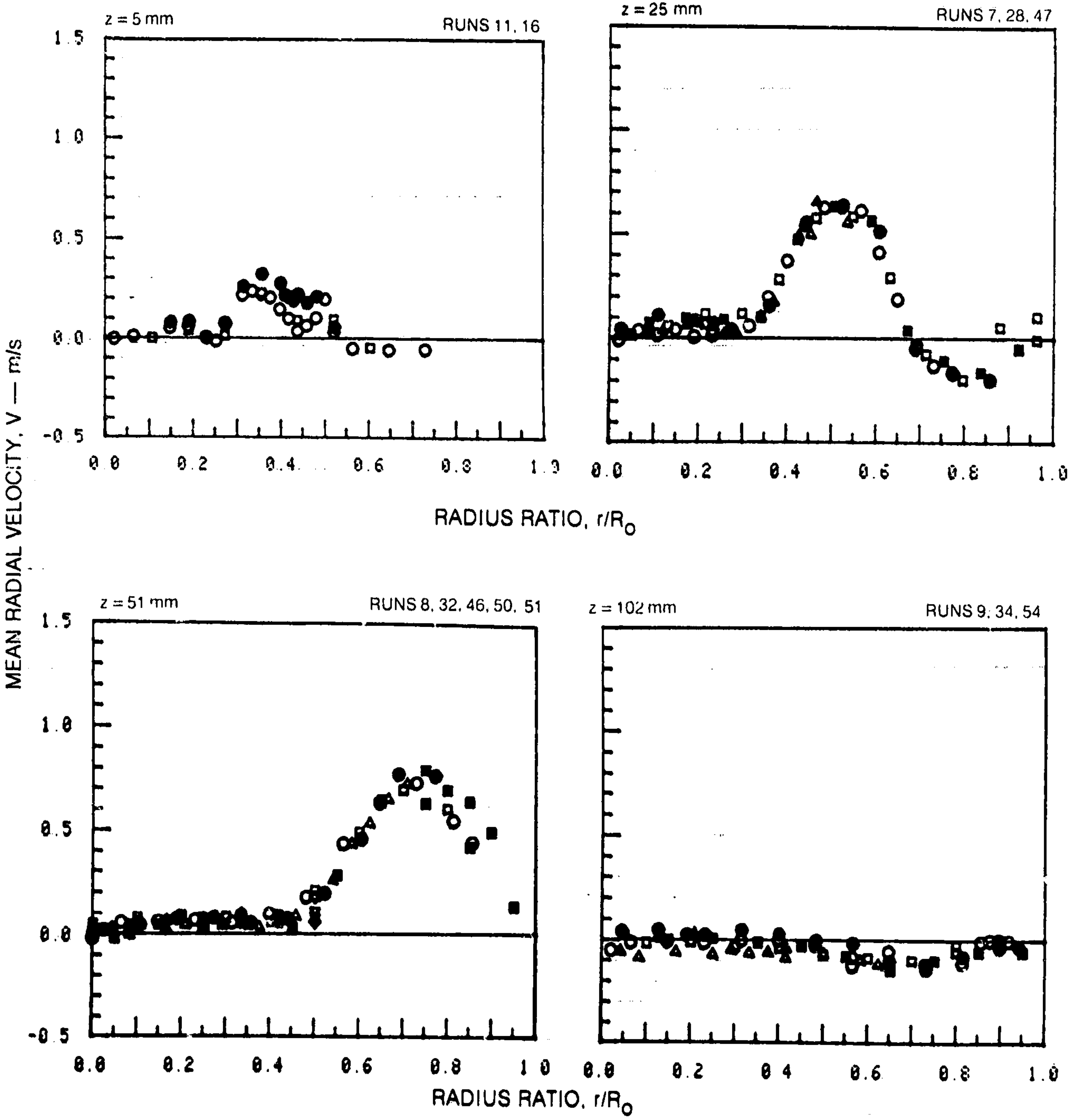

83-3-76-28

FIG.14 (CONT.)

MEAN RADIAL VELOCITY PROFILES (CONT)

	HORIZONTAL TRAVERSE	VERTICAL TRAVERSE
OPEN SYMBOLS:	θ = 90°	θ = 0°
SOLID SYMBOLS:	θ = 270°	θ = 180°

SYMBOL	○	●	□	■	△	▲
RUN NOS.	15, 10, 42, 45		36, 38		41	

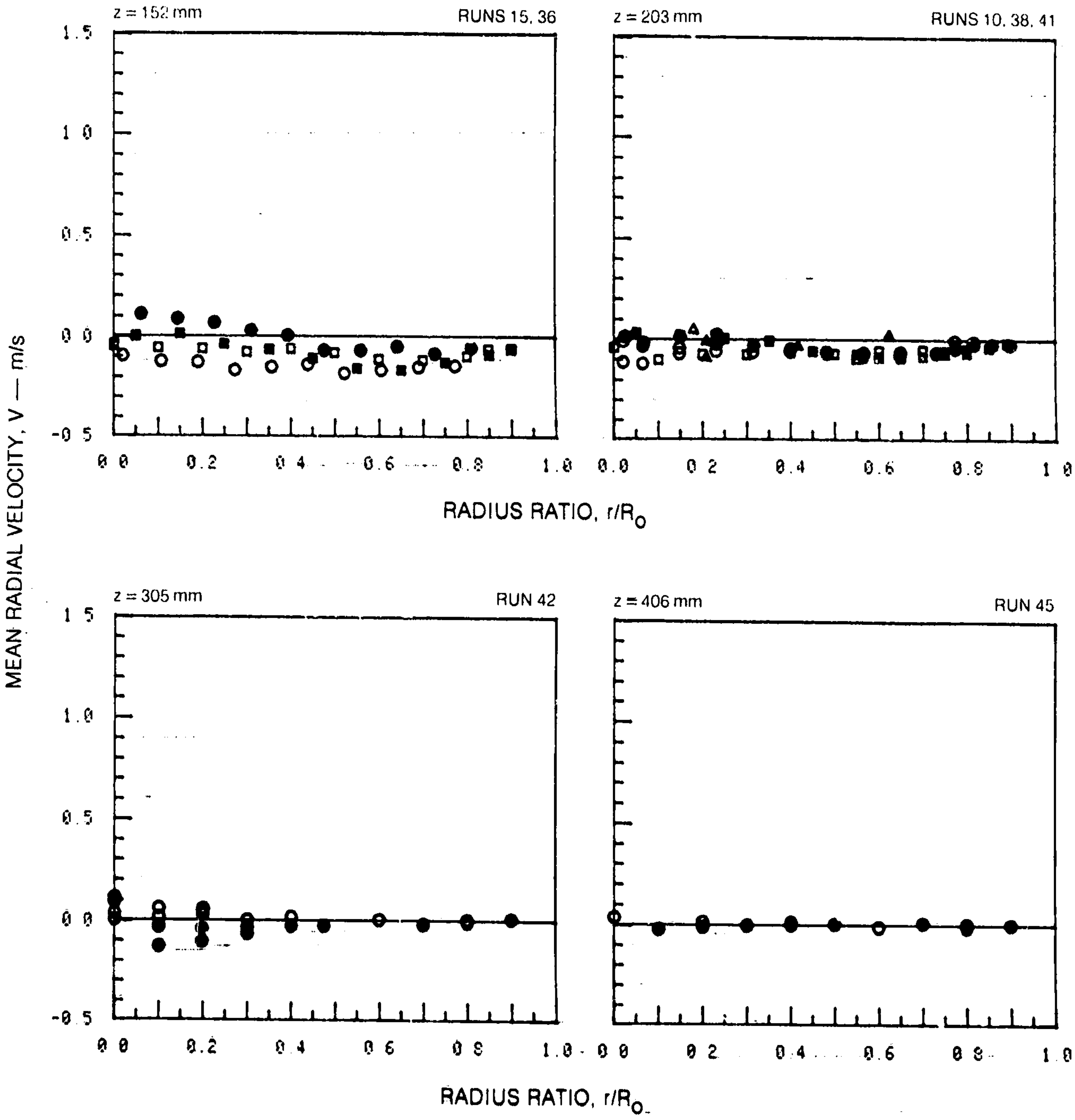

83-3-76-27

ORIGINAL PAGE IS
OF POOR QUALITY

FIG. 15

MEAN AZIMUTHAL VELOCITY PROFILES

	HORIZONTAL TRAVERSE	VERTICAL TRAVERSE
OPEN SYMBOLS:	θ = 90°	θ = 0°
SOLID SYMBOLS:	θ = 270°	θ = 180°

SYMBOL	○	●	□	■	△	▲	◇	◆	▽	▼
RUN NOS.	17, 3, 4, 5		27, 31, 6		47, 46, 33		50, 54		51	

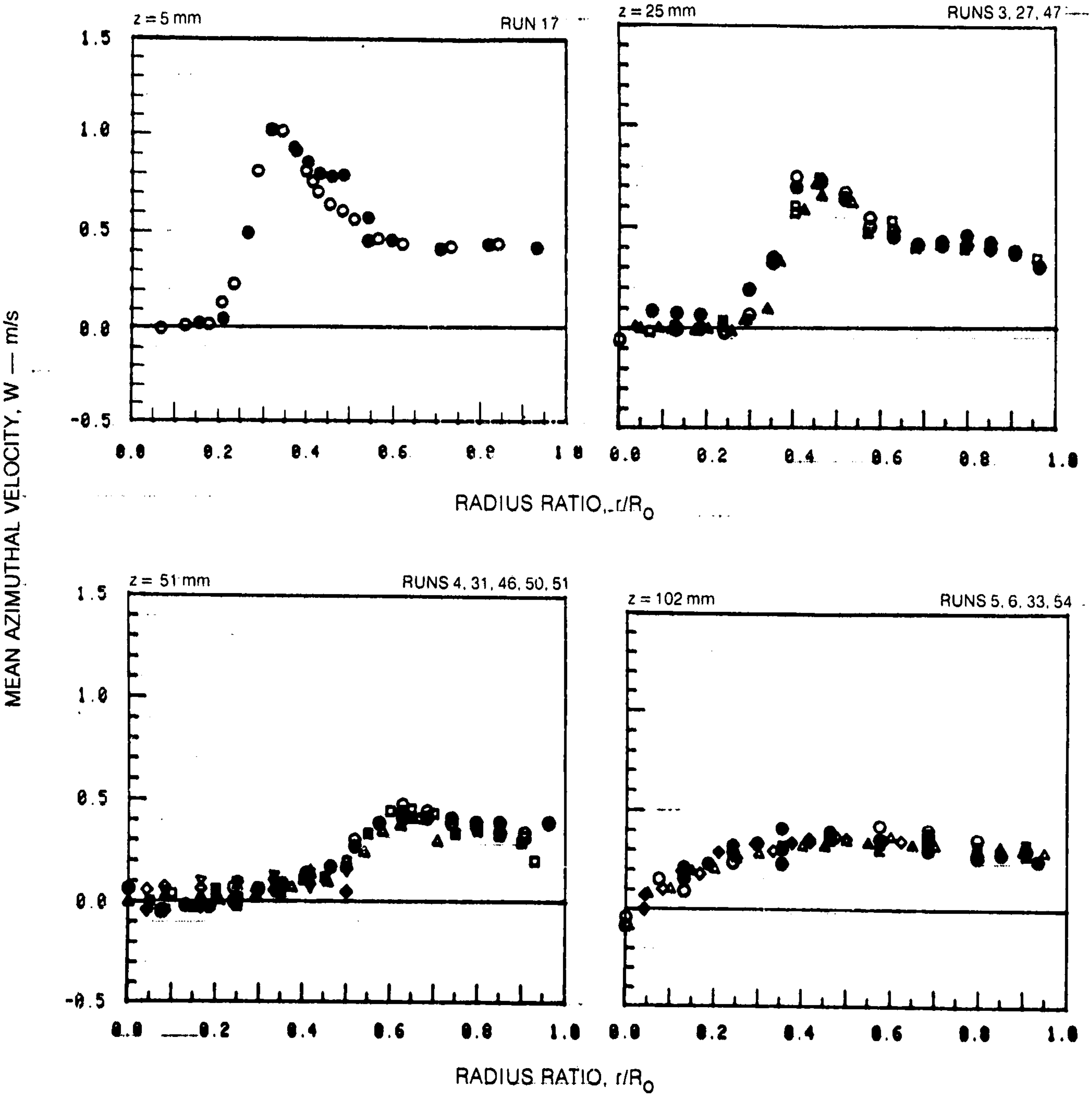

83–3–76–23

ORIGINAL PAGE IS
OF POOR QUALITY

FIG. 15 (CONT)

MEAN AZIMUTHAL VELOCITY PROFILES (CONT)

	HORIZONTAL TRAVERSE	VERTICAL TRAVERSE
OPEN SYMBOLS:	θ = 90°	θ ≐ 0°
SOLID SYMBOLS:	θ = 270°	θ = 180°

SYMBOL	○	●	□	■	△	▲
RUN NOS.	14, 12, 43, 44		35, 37		40	

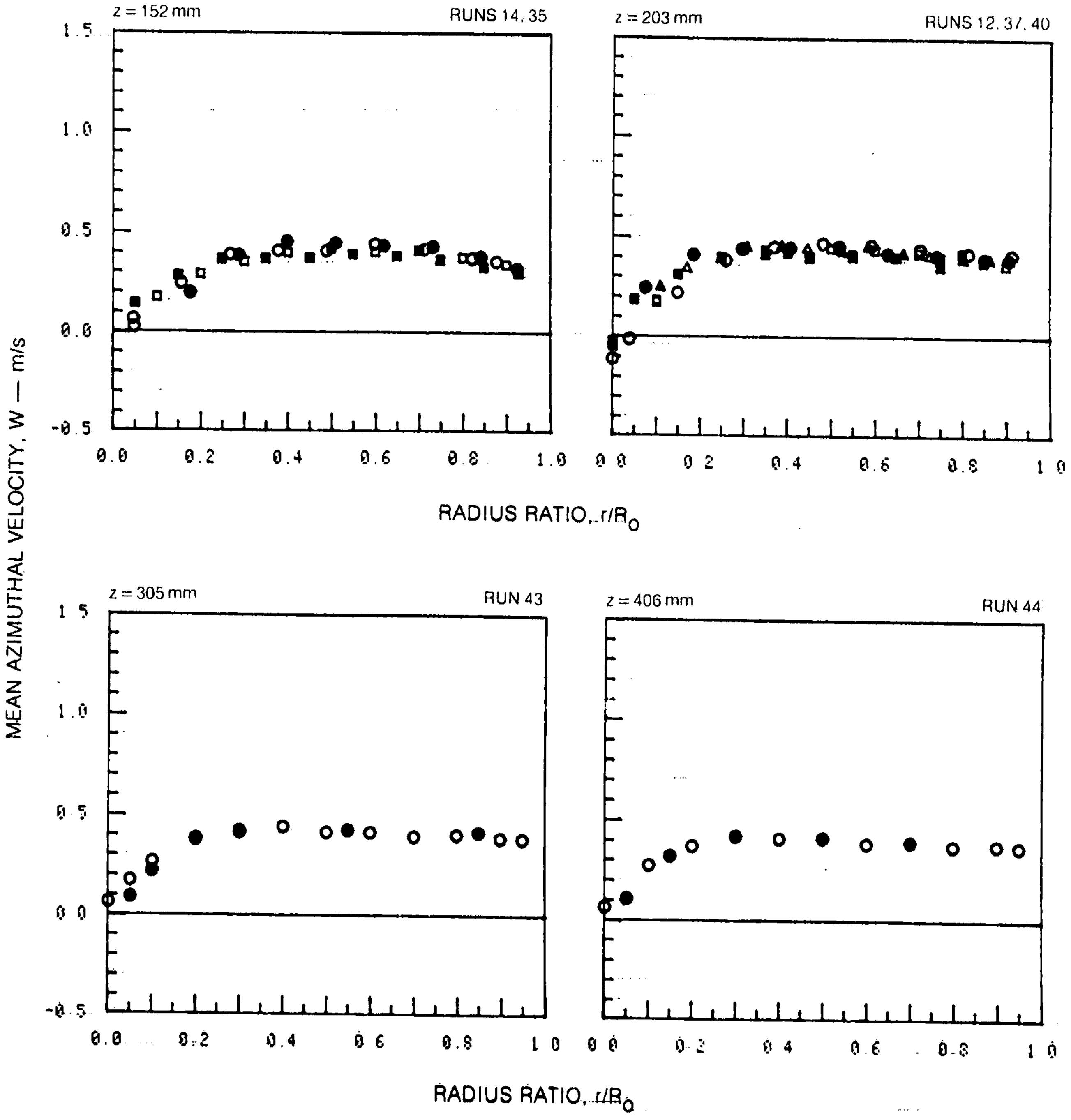

FIG. 16

FLUCTUATING AXIAL VELOCITY PROFILES

	HORIZONTAL TRAVERSE	VERTICAL TRAVERSE
OPEN SYMBOLS:	θ = 90°	θ = 0°
SOLID SYMBOLS:	θ = 270°	θ = 180°

SYMBOL	○	●	□	■	△	▲	◇	◆
RUN NOS.	11, 3, 4, 5		16, 7, 8, 6		17, 22, 23, 9		24	

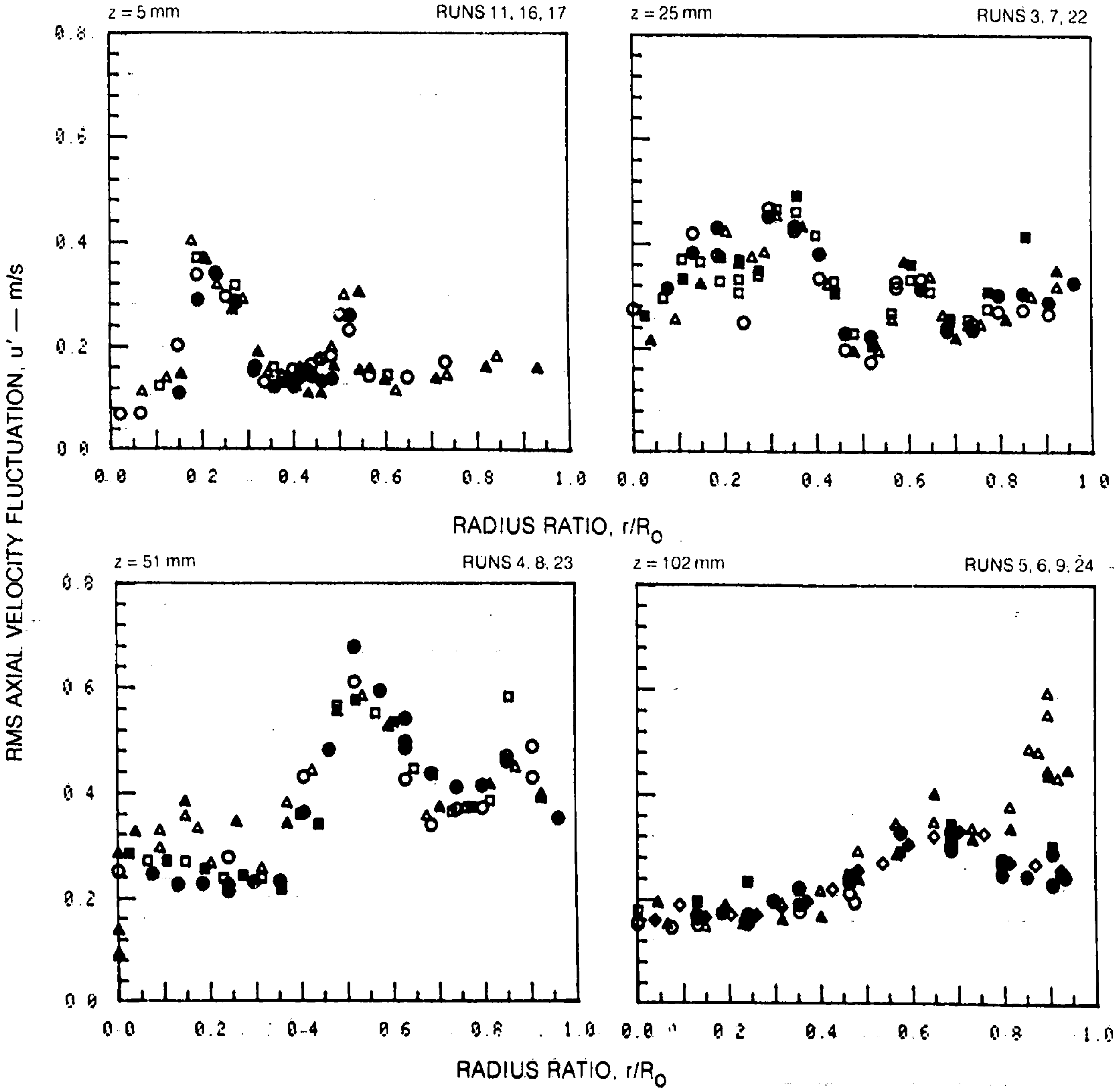

83-3-76-25

ORIGINAL PAGE IS
OF POOR QUALITY

FIG. 16 (CONT)

FLUCTUATING AXIAL VELOCITY PROFILES (CONT)

	HORIZONTAL TRAVERSE	VERTICAL TRAVERSE
OPEN SYMBOLS:	θ = 90°	θ = 0°
SOLID SYMBOLS:	θ = 270°	θ = 180°

SYMBOL	○	●	□	■	△	▲	◇	◆	▽	▼
RUN NOS.	14, 10, 42, 44		15, 12, 43, 45		25, 26		40		41	

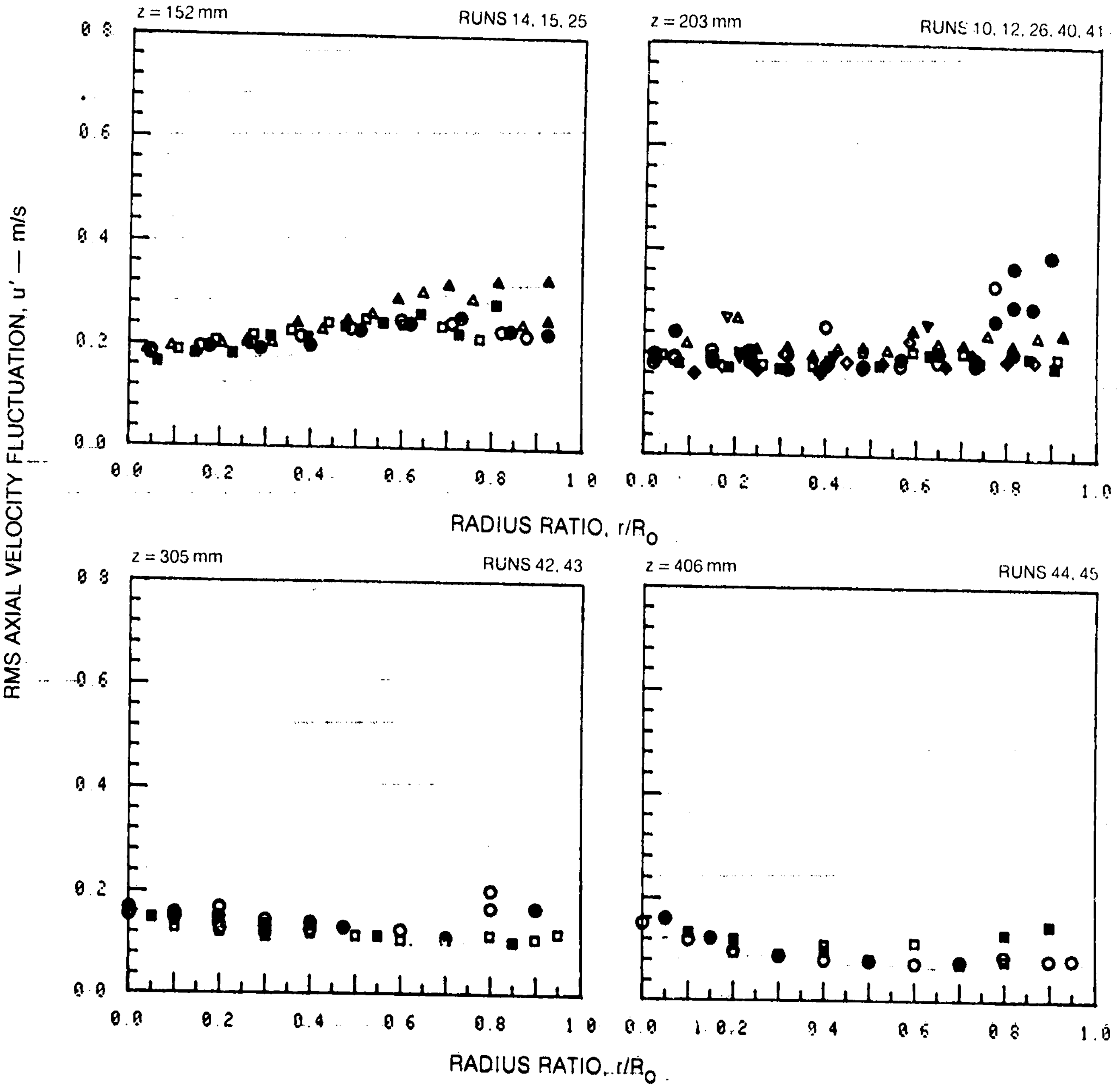

83–3–76–24

FIG. 17

FLUCTUATING RADIAL VELOCITY PROFILES

	HORIZONTAL TRAVERSE	VERTICAL TRAVERSE
OPEN SYMBOLS.	θ = 90°	θ = 0°
SOLID SYMBOLS:	θ = 270°	θ = 180°

SYMBOL	○	●	□	■	△	▲	◇	◆	▽	▼
RUN NOS.	11, 7, 8, 9		16, 28, 32, 34		47, 46, 54		50		51	

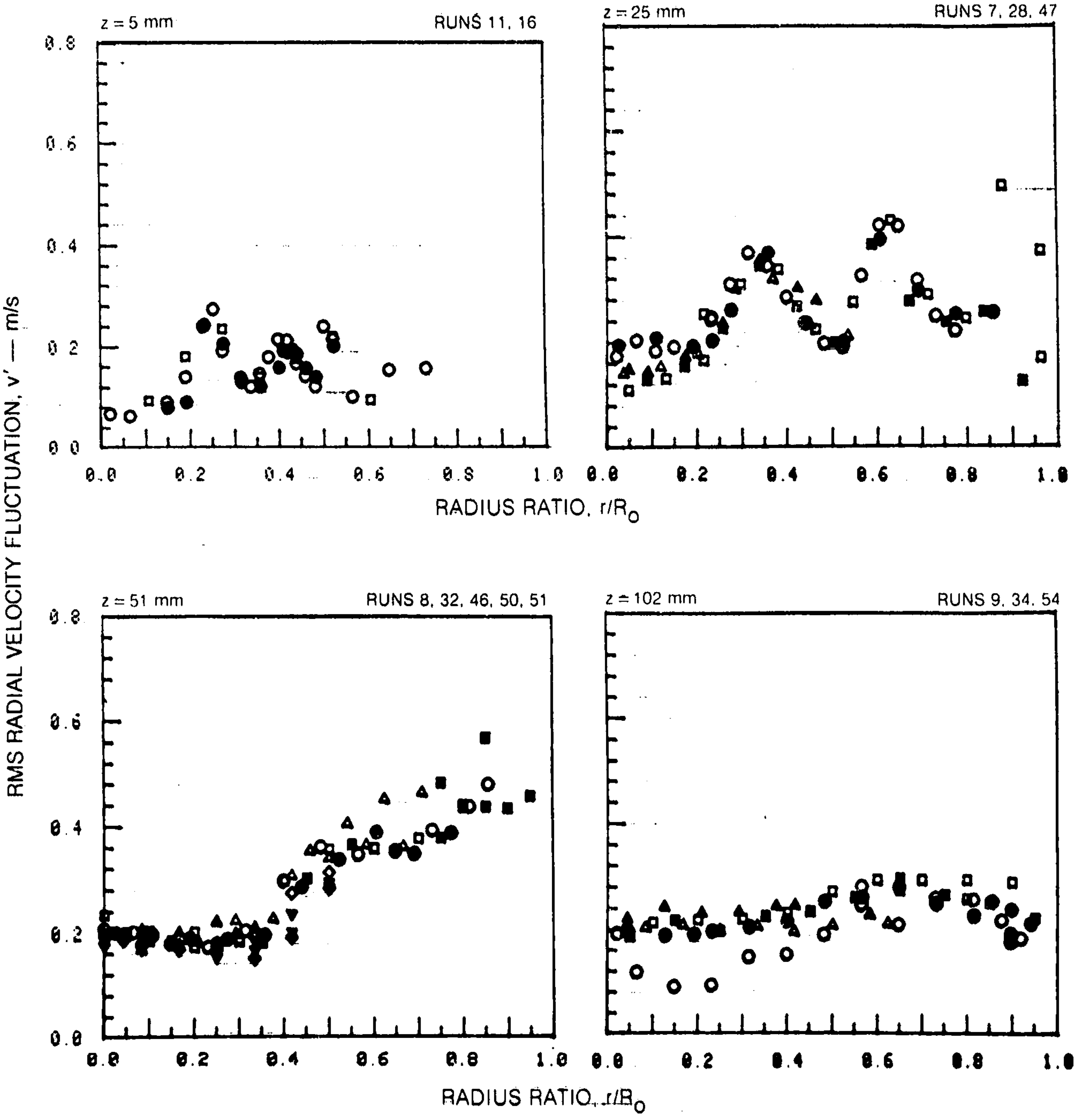

ORIGINAL PAGE IS
OF POOR QUALITY

FIG. 17 (CONT.)

FLUCTUATING RADIAL VELOCITY PROFILES (CONT.)

	HORIZONTAL TRAVERSE	VERTICAL TRAVERSE
OPEN SYMBOLS	θ = 90°	θ = 0°
SOLID SYMBOLS	θ = 270°	θ = 180°

SYMBOL	○	●	□	■	△	▲
RUN NOS	15, 10, 42, 45		36, 38		41	

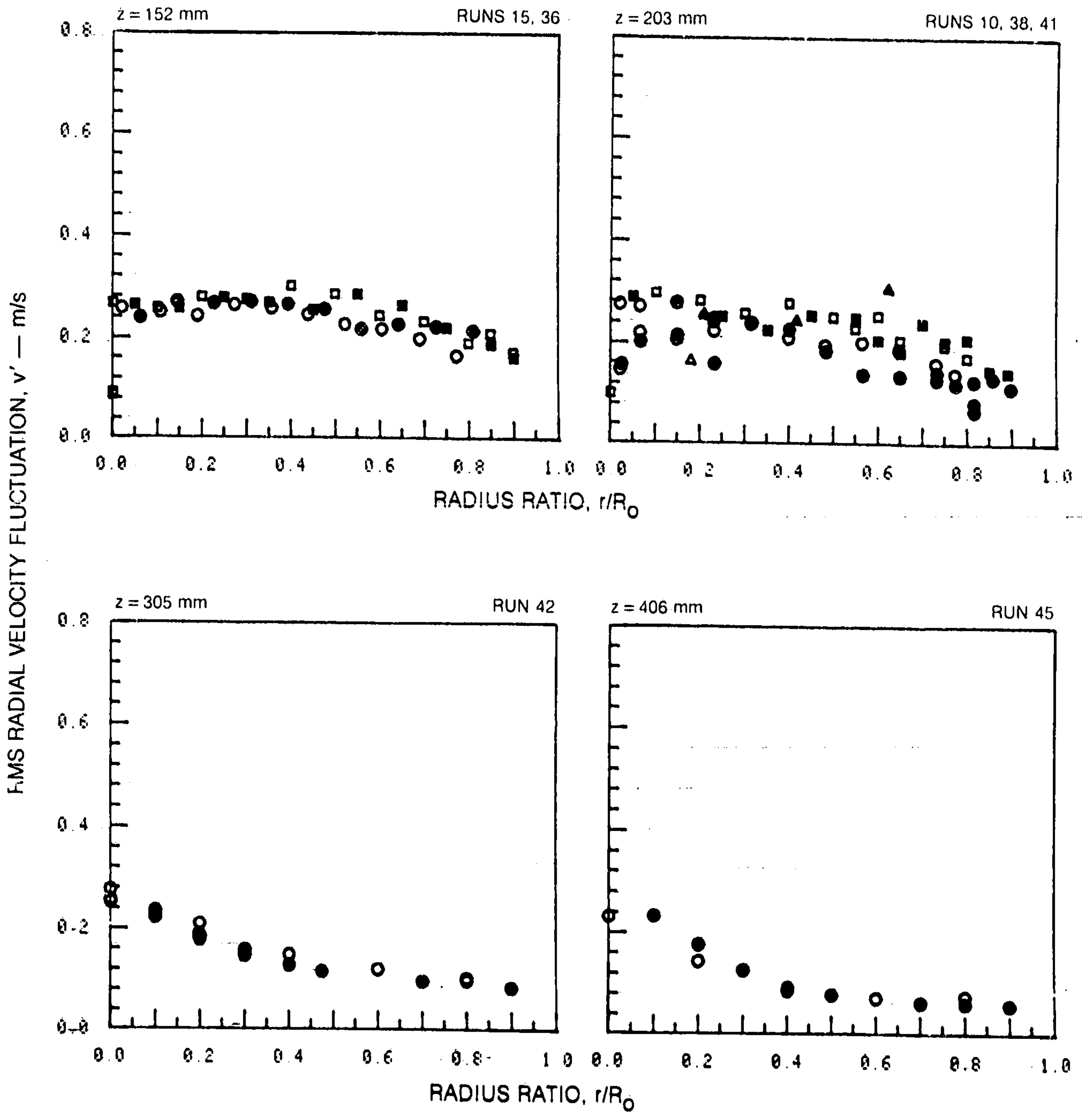

83-3-76-21

FIG. 18

FLUCTUATING AZIMUTHAL VELOCITY PROFILES

	HORIZONTAL TRAVERSE	VERTICAL TRAVERSE
OPEN SYMBOLS:	θ = 90°	θ = 0°
SOLID SYMBOLS	θ = 270°	θ = 180°

SYMBOL	○	●	□	■	△	▲	◇	◆	▽	▼
RUN NOS	17, 3, 4, 5		27, 31, 6		47, 46, 53		50, 54		51	

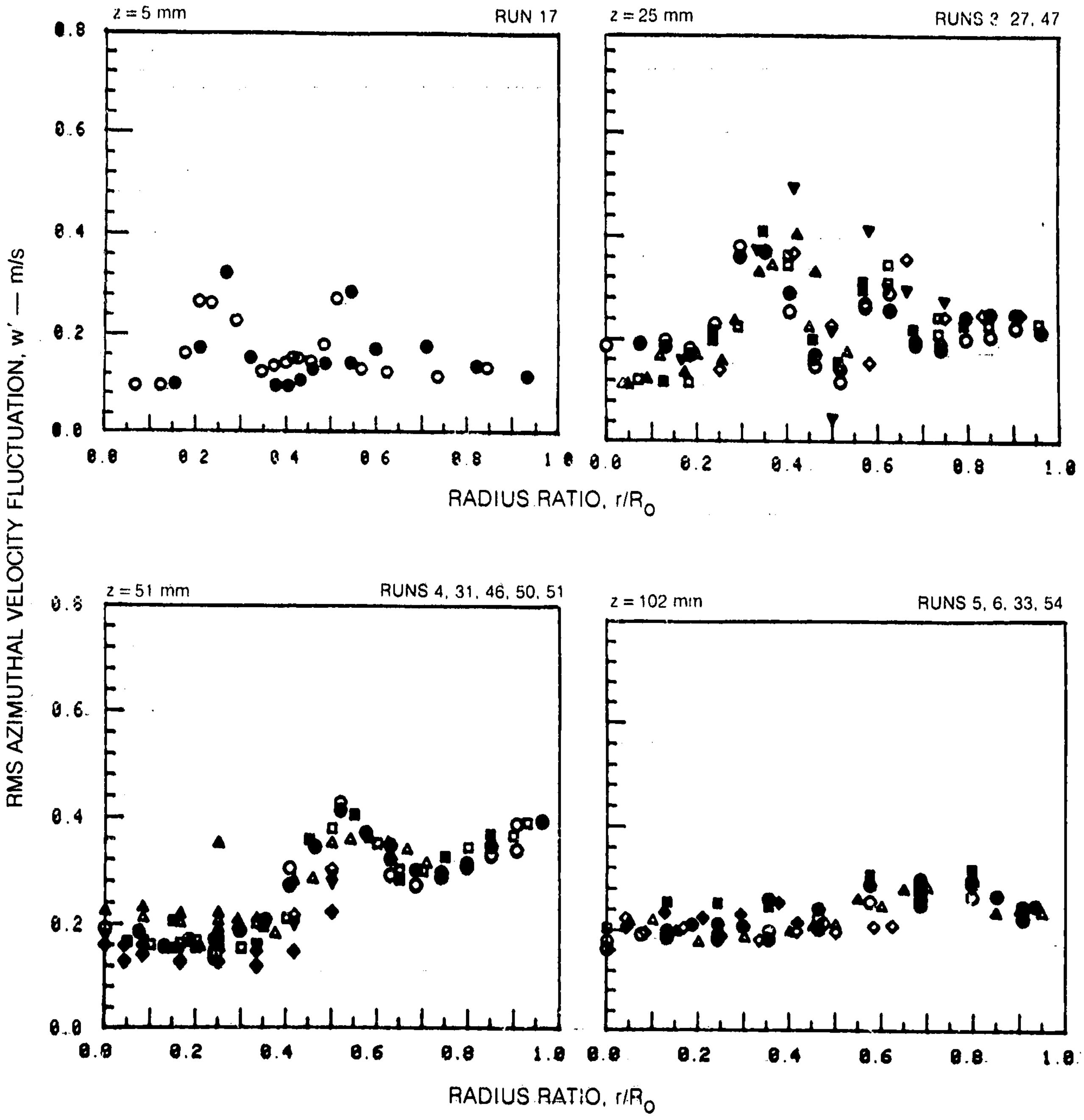

83-3-76-20

ORIGINAL PAGE IS
OF POOR QUALITY

FIG. 18 (CONT.)

FLUCTUATING AZIMUTHAL VELOCITY PROFILES (CONT.)

	HORIZONTAL TRAVERSE	VERTICAL TRAVERSE
OPEN SYMBOLS	θ = 90°	θ = 0°
SOLID SYMBOLS	θ = 270°	θ = 180°

SYMBOL	○	●	□	■	△	▲
RUN NOS.	14, 12, 43, 44		35, 37		40	

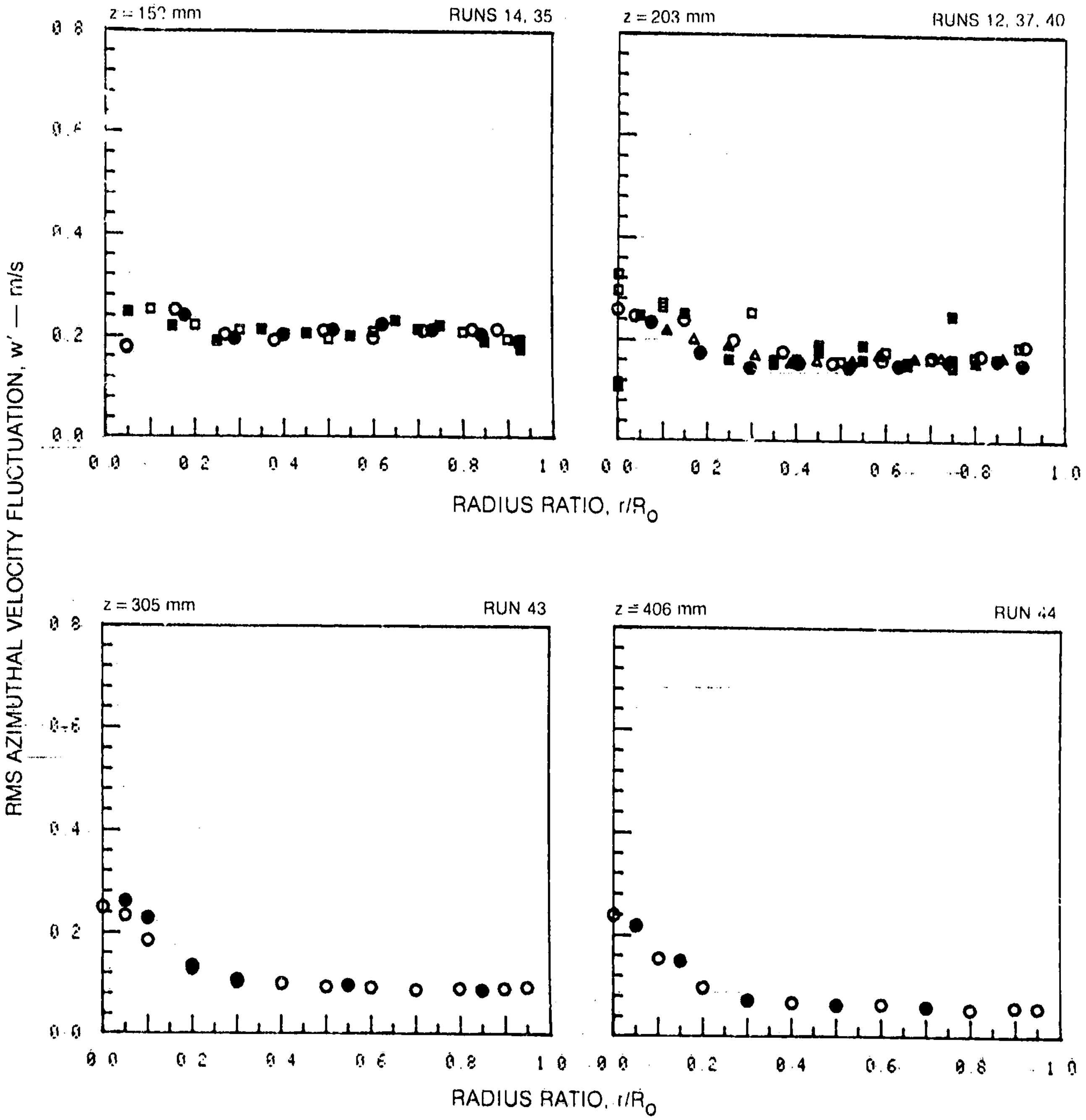

83-3-76-19

ORIGINAL PAGE IS
OF POOR QUALITY

FIG. 19

MEAN INNER JET FLUID CONCENTRATION ALONG TEST SECTION CENTERLINE

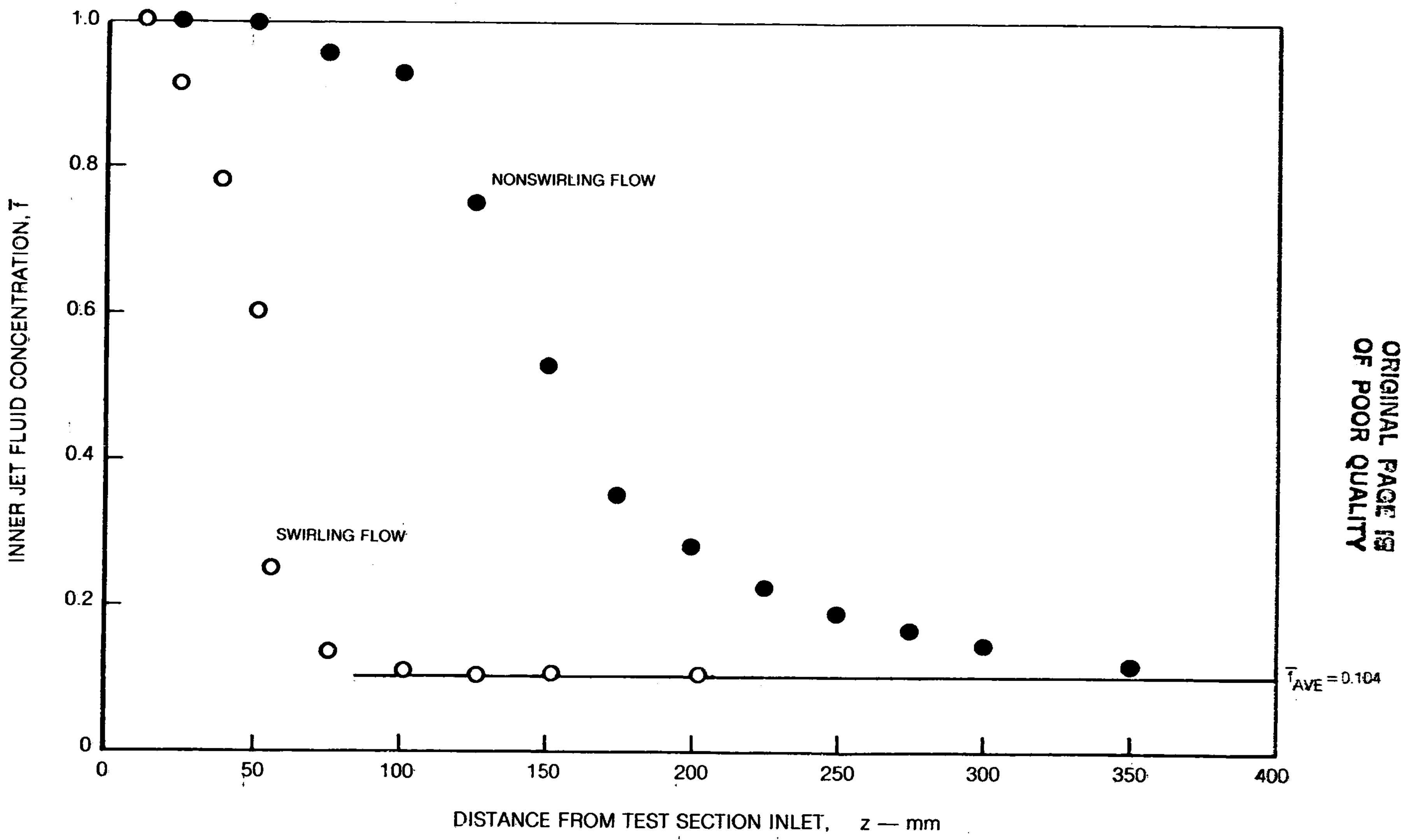

83-7-19-33

FIG. 20

MEAN INNER JET FLUID CONCENTRATION PROFILES

	HORIZONTAL TRAVERSE	VERTICAL TRAVERSE
OPEN SYMBOLS:	θ = 90°	θ = 0°
SOLID SYMBOLS:	θ = 270°	θ = 180°

SYMBOL	○	●	□	■	△	▲	◇	◆
RUN NOS.	20, 22, 23, 24		21, 27, 31, 33		29, 28, 32, 34		30	

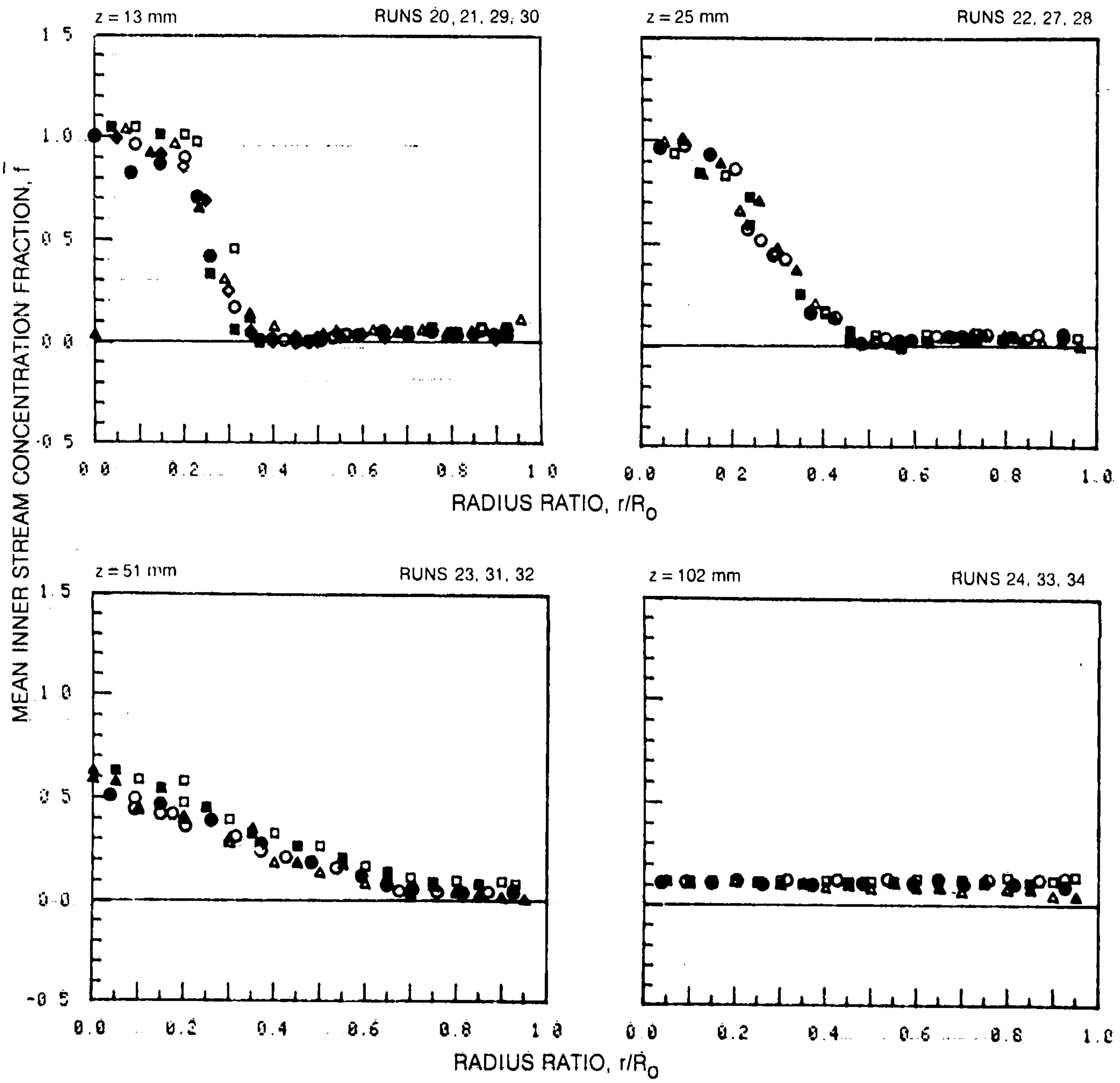

FIG. 20 (CONT)

ORIGINAL PAGE IS
OF POOR QUALITY

MEAN INNER JET FLUID CONCENTRATION PROFILES (CONT)

	HORIZONTAL TRAVERSE	VERTICAL TRAVERSE
OPEN SYMBOLS:	$\theta = 90°$	$\theta = 0°$
SOLID SYMBOLS:	$\theta = 270°$	$\theta = 180°$

SYMBOL	○	●	□	■	△	▲
RUN NOS.	25, 26		35, 37		36, 38	

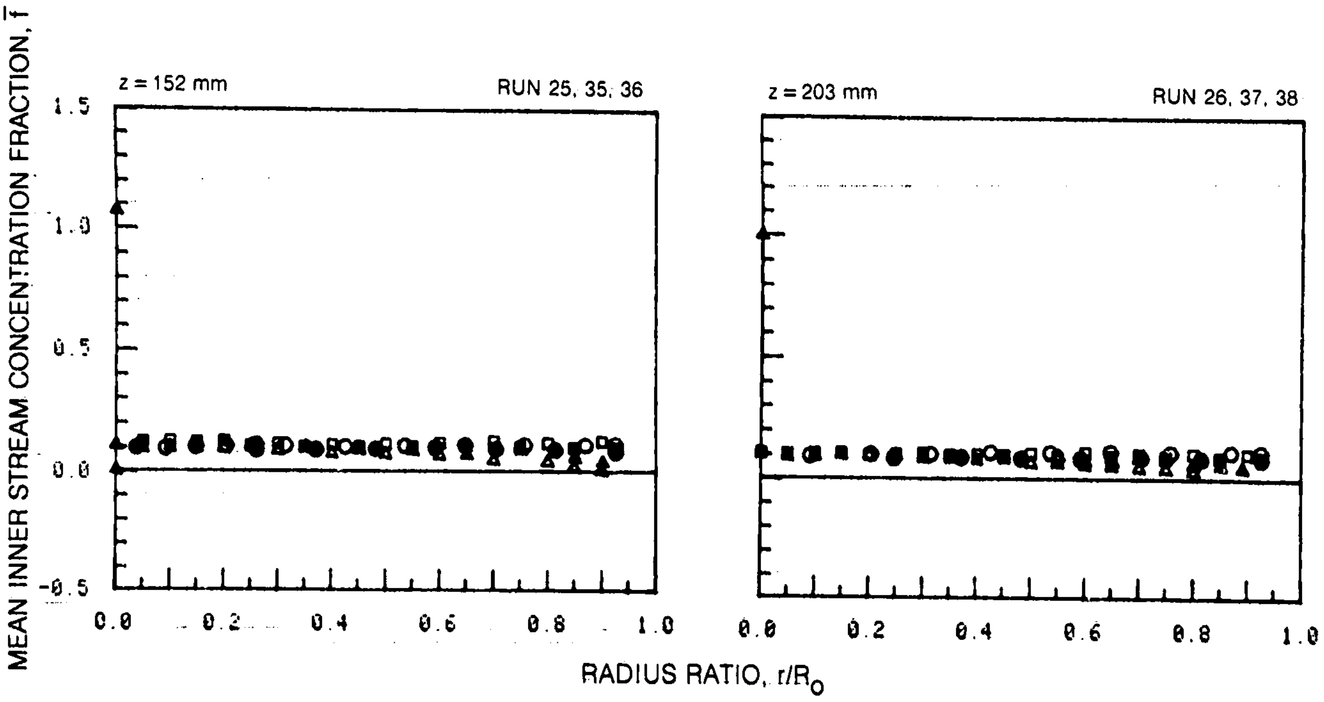

82–11–36–4

ORIGINAL PAGE IS
OF POOR QUALITY

FLUCTUATING INNER JET FLUID CONCENTRATION PROFILES

	HORIZONTAL TRAVERSE	VERTICAL TRAVERSE
OPEN SYMBOLS:	$\theta = 90°$	$\theta = 0°$
SOLID SYMBOLS:	$\theta = 270°$	$\theta = 180°$

SYMBOL	○	●	□	■	△	▲	◇	◆
RUN NOS.	20, 22, 23, 24		21, 27, 31, 33		29, 28, 32, 34		30	

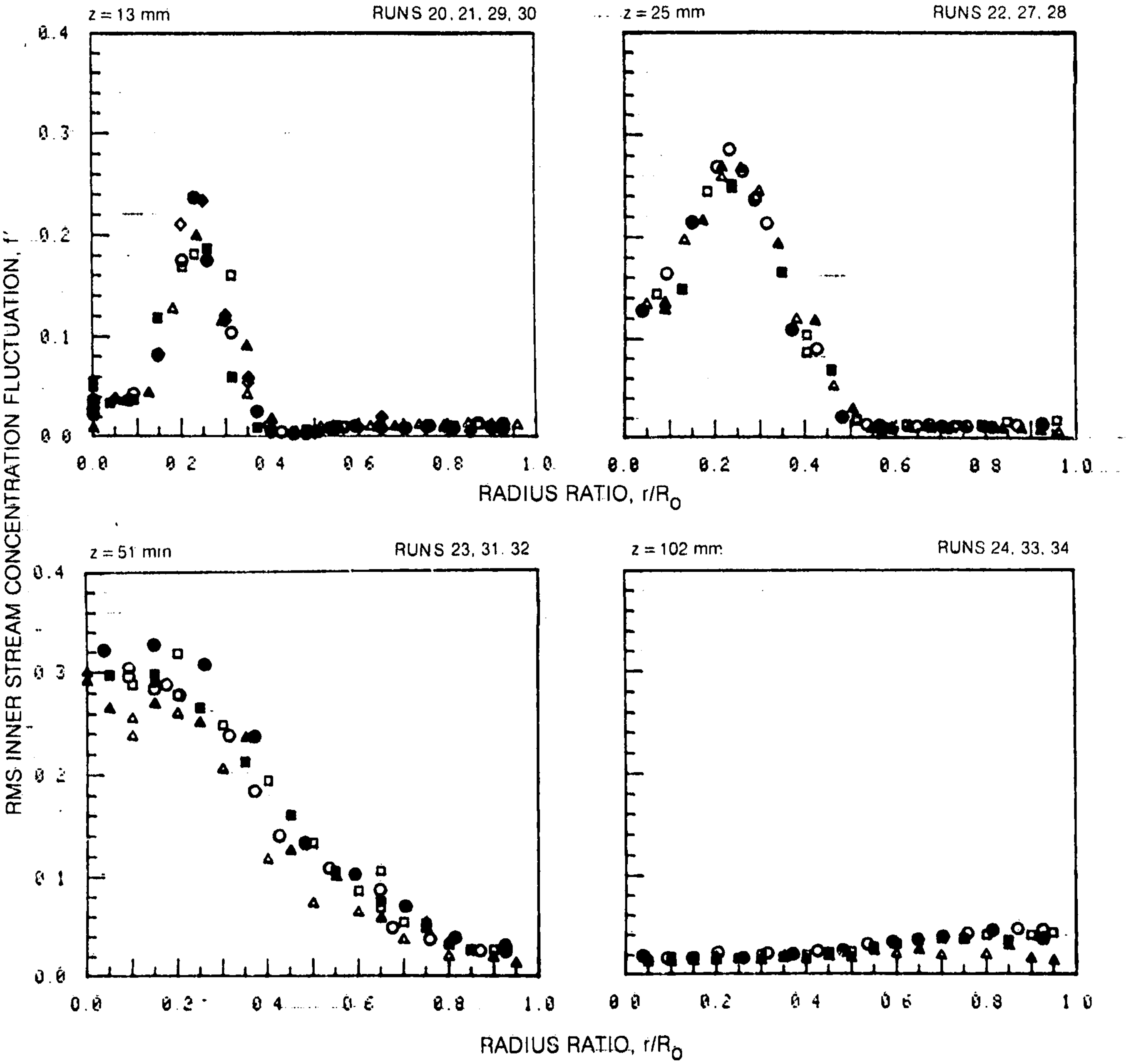

FIG. 21 (CONT)

FLUCTUATING INNER JET FLUID CONCENTRATION PROFILES (CONT)

	HORIZONTAL TRAVERSE	VERTICAL TRAVERSE
OPEN SYMBOLS:	θ = 90°	θ = 0°
SOLID SYMBOLS:	θ = 270°	θ = 180°

SYMBOL	○	●	□	■	△	▲
RUN NOS.	25, 26		35, 37		36, 38	

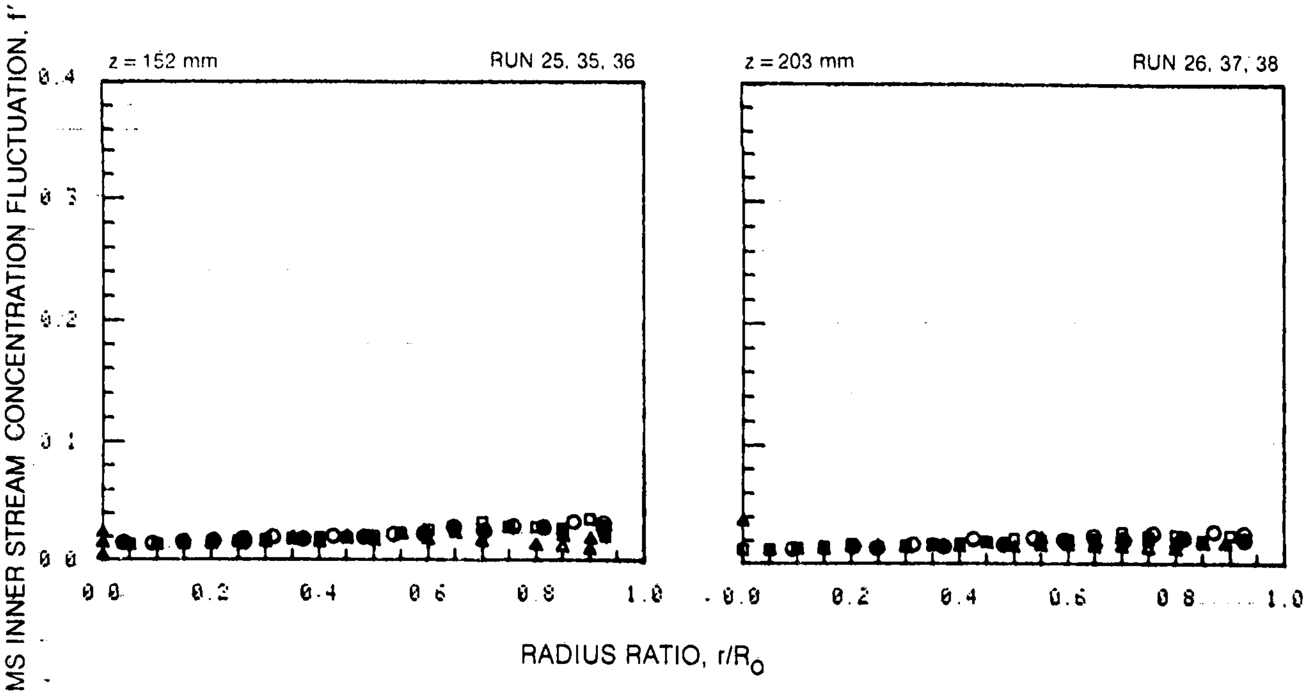

82-11-36-2

FIG. 22

MOMENTUM TRANSPORT RATE, $\overline{uv}$, PROFILES

	HORIZONTAL TRAVERSE	VERTICAL TRAVERSE
OPEN SYMBOLS	θ = 90°	θ = 0°
SOLID SYMBOLS	θ = 270°	θ = 180°

SEE TABLE I FOR TRAVERSE DIRECTION

SYMBOL	○	●	□	■
RUN NOS.	11, 7, 8, 9		16	

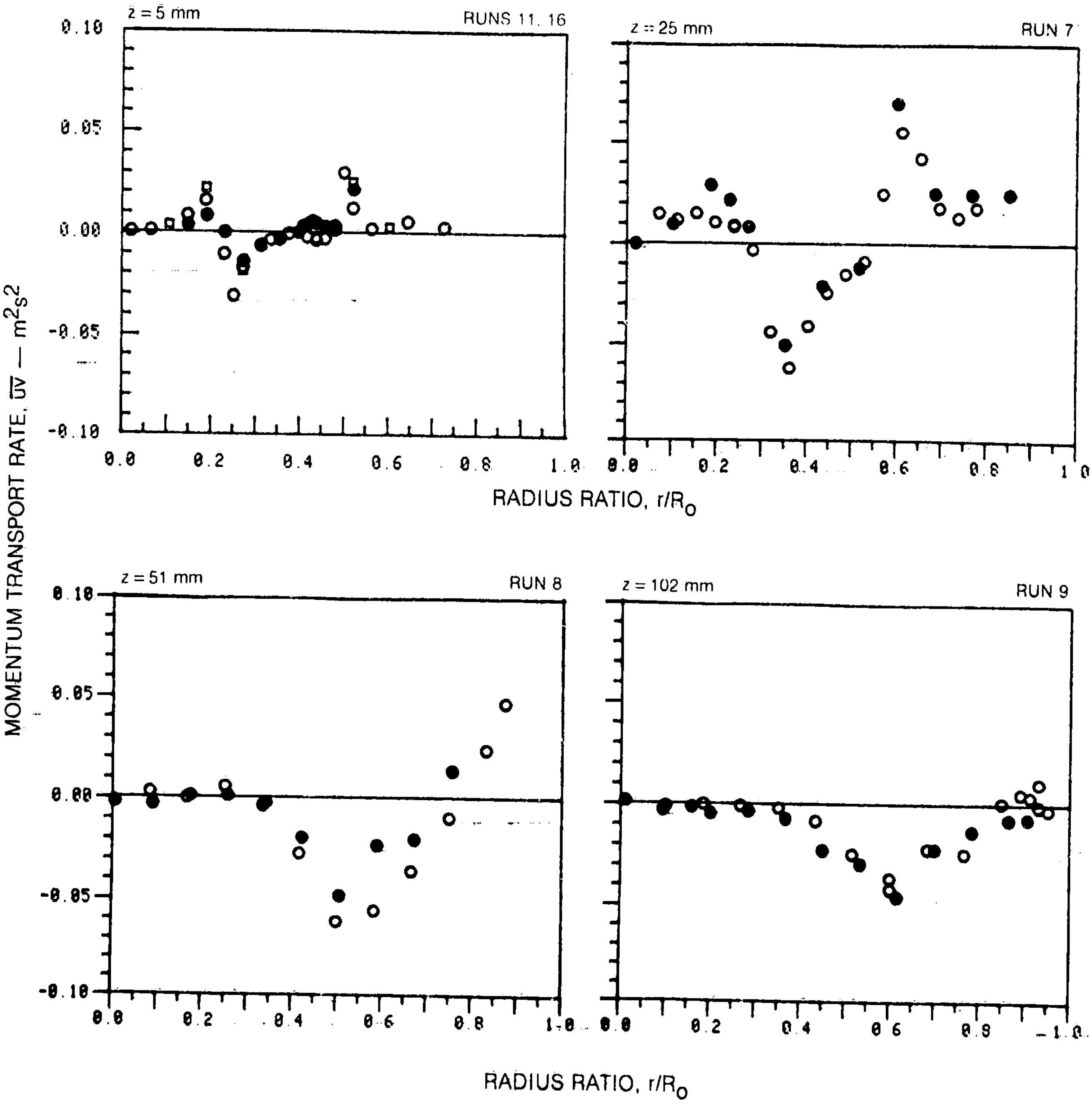

82-10-33-13

ORIGINAL PAGE IS
OF POOR QUALITY

FIG. 22 (CONT.)

MOMENTUM TRANSPORT RATE, $\overline{uv}$, PROFILES (CONT.)

	HORIZONTAL TRAVERSE	VERTICAL TRAVERSE
OPEN SYMBOLS:	$\theta = 90°$	$\theta = 0°$
SOLID SYMBOLS:	$\theta = 270°$	$\theta = 180°$

SYMBOL	○	●	□	■
RUN NOS.	15, 10, 42, 45		41	

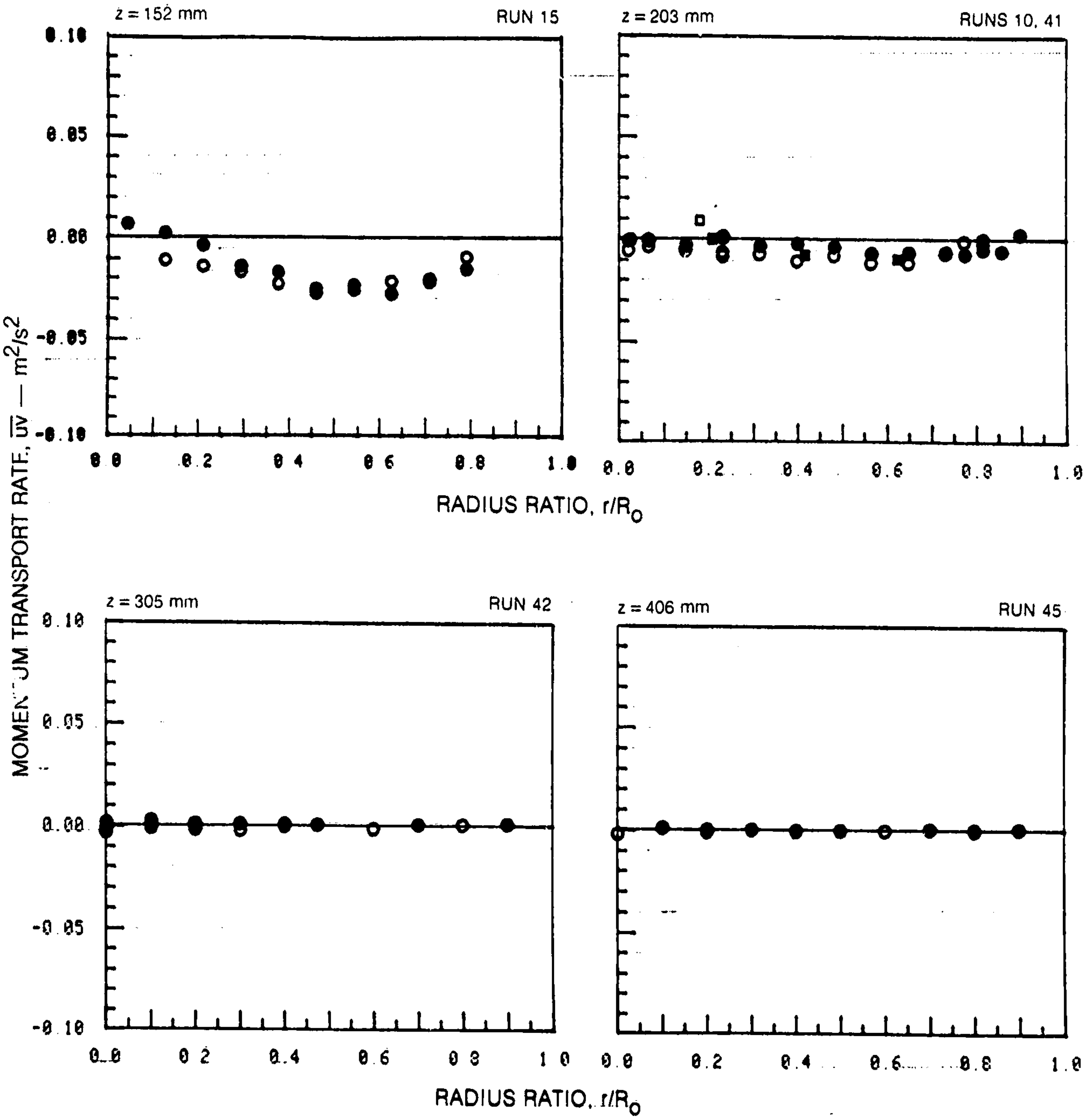

83-3-76-18

FIG. 23

MOMENTUM TRANSPORT CORRELATION COEFFICIENT, R_{uv}, PROFILES

	HORIZONTAL TRAVERSE	VERTICAL TRAVERSE
OPEN SYMBOLS	$\theta = 90°$	$\theta = 0°$
SOLID SYMBOLS	$\theta = 270°$	$\theta = 180°$

SYMBOL	○	●	□	■
RUN NOS	11, 7, 8, 9		16	

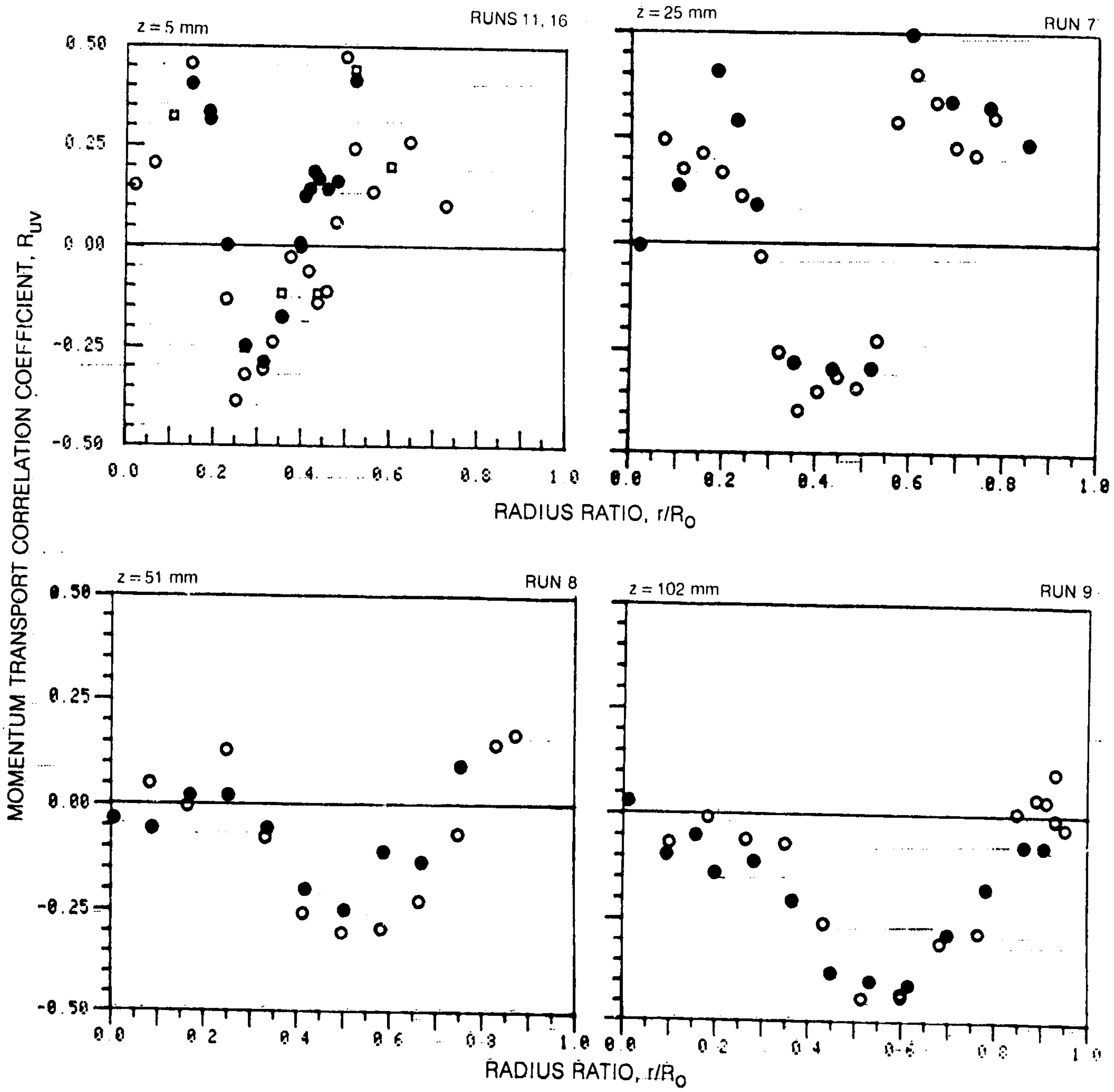

FIG. 23 (CONT.)

MOMENTUM TRANSPORT CORRELATION COEFFICIENT, R_{uv}, PROFILES (CONT.)

	HORIZONTAL TRAVERSE	VERTICAL TRAVERSE
OPEN SYMBOLS:	θ = 90°	θ = 0°
SOLID SYMBOLS:	θ = 270°	θ = 180°

SYMBOL	○	●	□	■
RUN NOS.	15, 10, 42, 45		41	

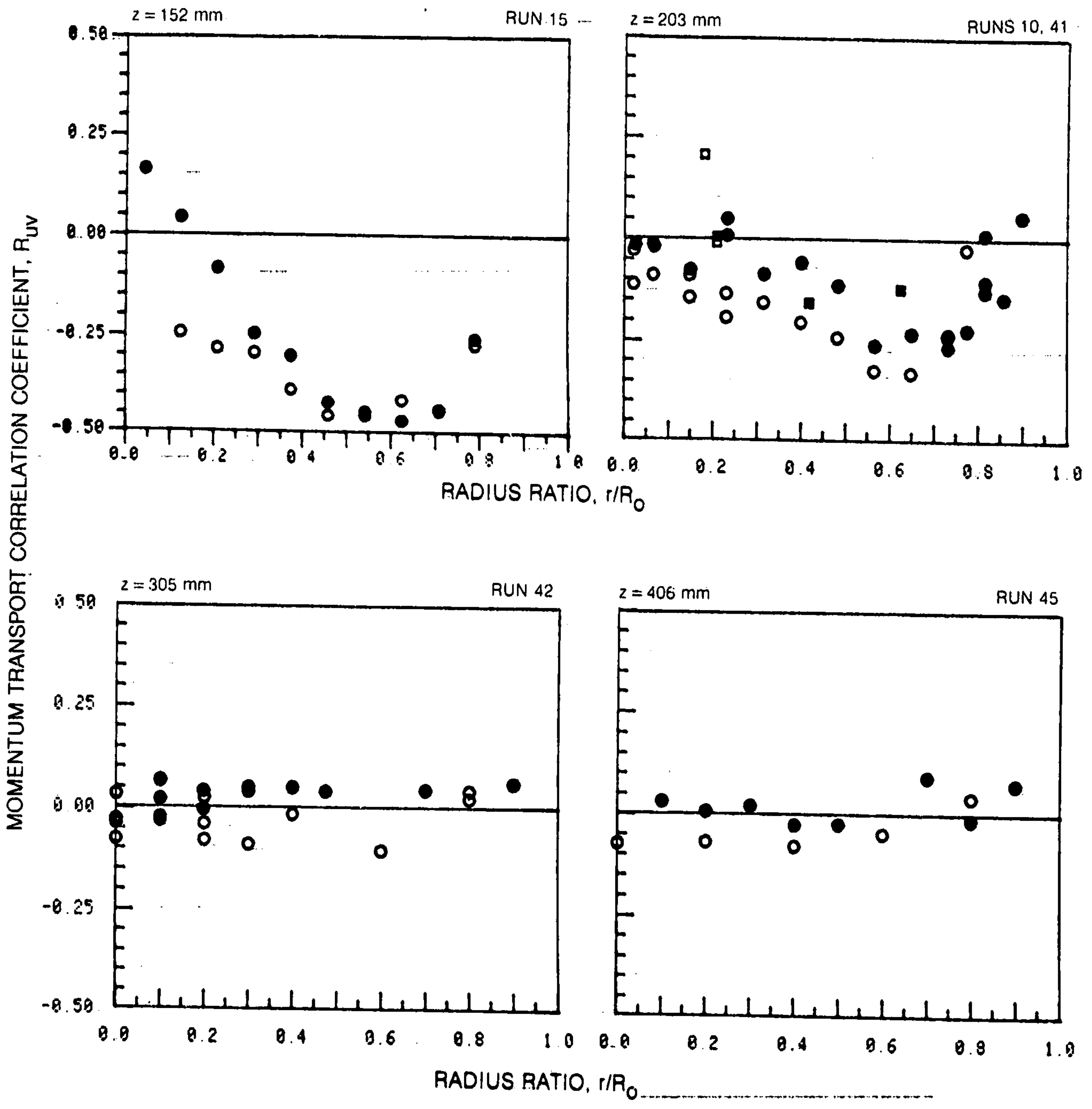

83-3-76-15

ORIGINAL PAGE IS
OF POOR QUALITY

MOMENTUM TRANSPORT RATE, $\overline{uw}$, PROFILES

	HORIZONTAL TRAVERSE	VERTICAL TRAVERSE
OPEN SYMBOLS:	$\theta = 90°$	$\theta = 0°$
SOLID SYMBOLS:	$= 270°$	$\theta = 180°$

SYMBOL	○	●	□	■
RUN NOS.	17, 3, 4, 5		6	

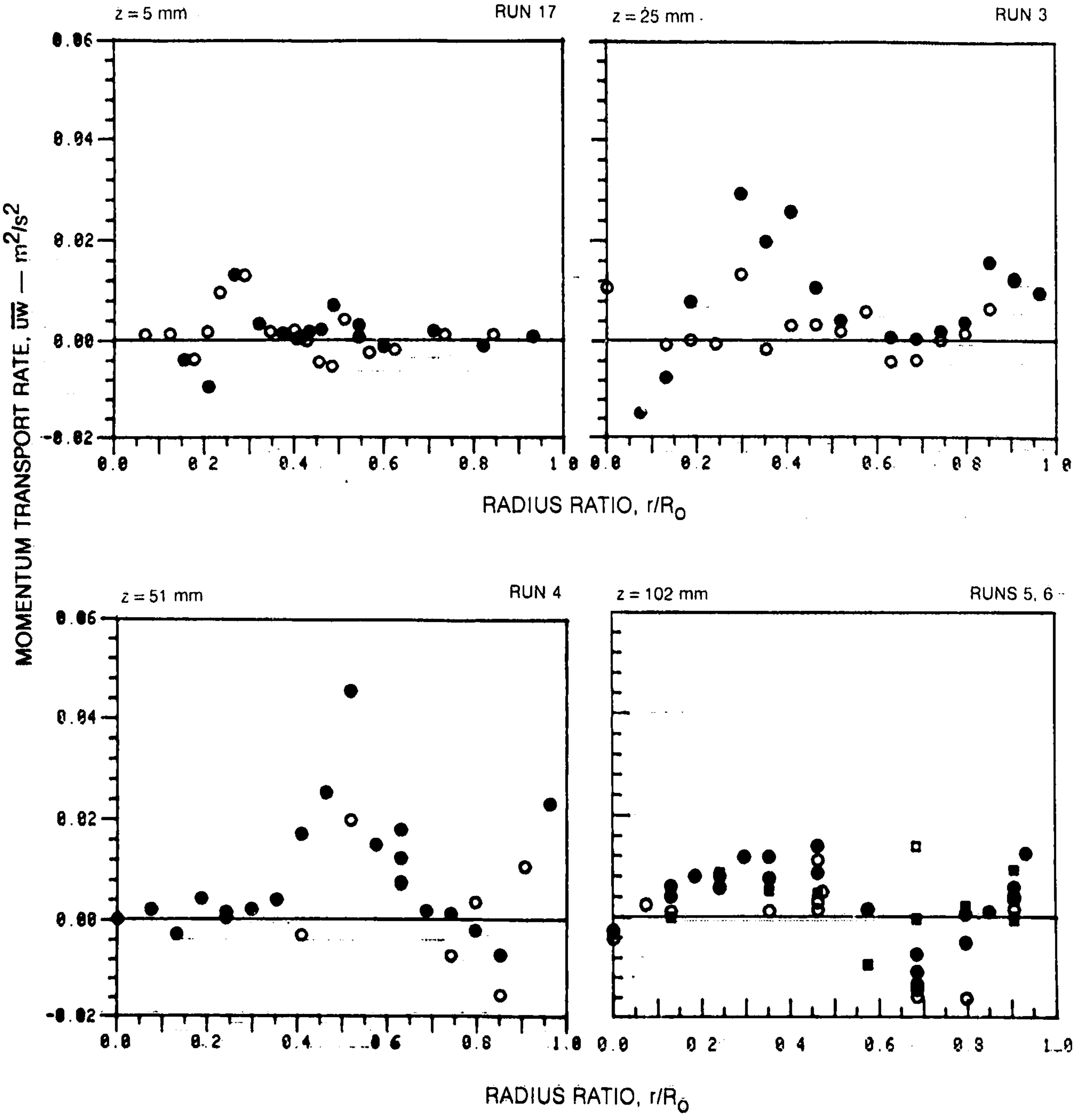

ORIGINAL PAGE IS
OF POOR QUALITY

FIG. 24 (CONT.)

MOMENTUM TRANSPORT RATE, $\overline{uw}$, PROFILES (CONT.)

	HORIZONTAL TRAVERSE	VERTICAL TRAVERSE
OPEN SYMBOLS	$\theta = 90°$	$\theta = 0°$
SOLID SYMBOLS	$\theta = 270°$	$\theta = 180°$

SYMBOL	○	●	□	■
RUN NOS.	14, 12, 43, 44		40	

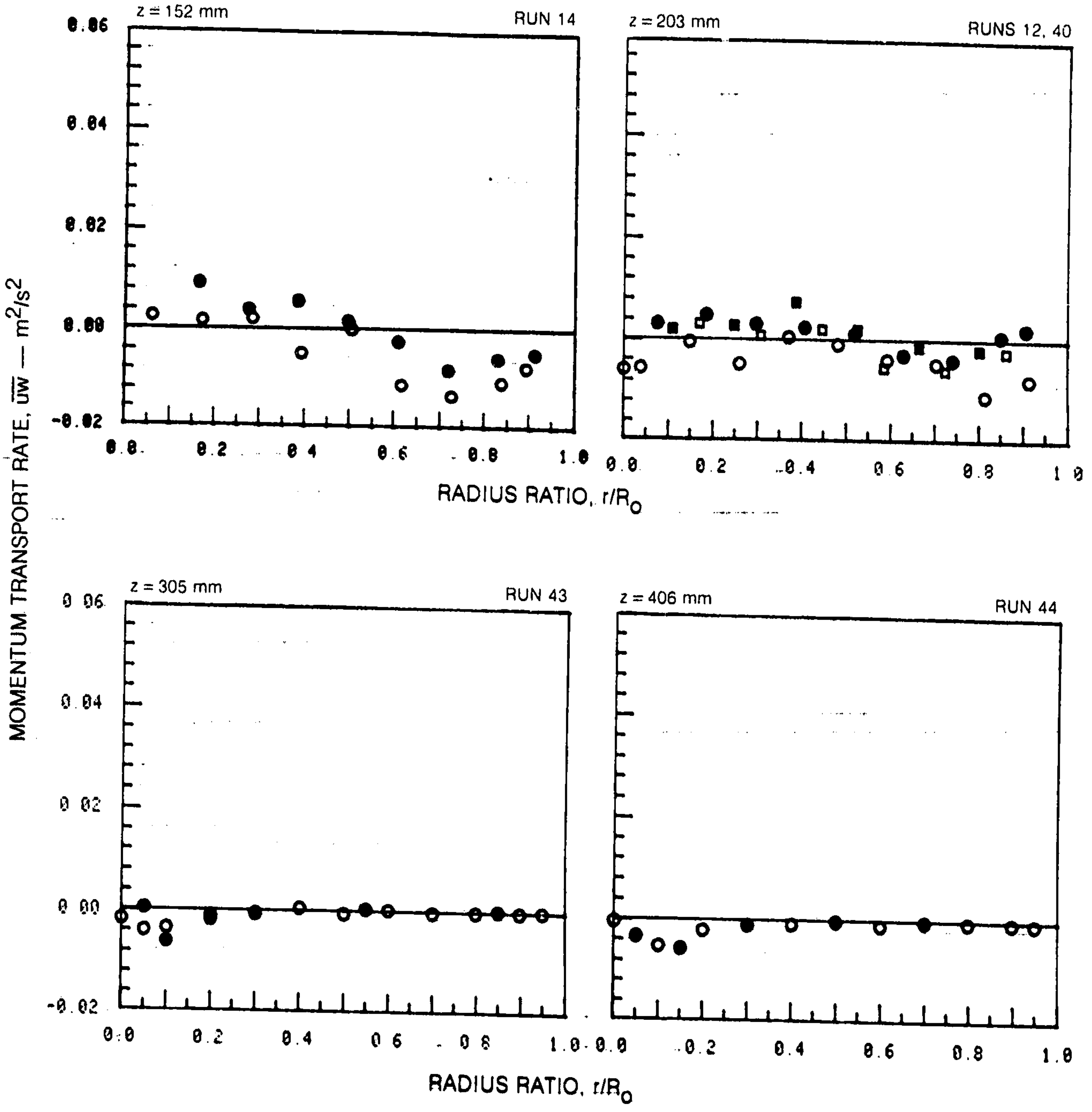

83-3-76-17

FIG. 25

MOMENTUM TRANSPORT CORRELATION COEFFICIENT, R_{uw}, PROFILES

	HORIZONTAL TRAVERSE	VERTICAL TRAVERSE
OPEN SYMBOLS	$\theta = 90°$	$\theta = 0°$
SOLID SYMBOLS	$\theta = 270°$	$\theta = 180°$

SYMBOL	○	●	□	■
RUN NOS.	17, 3, 4, 5		6	

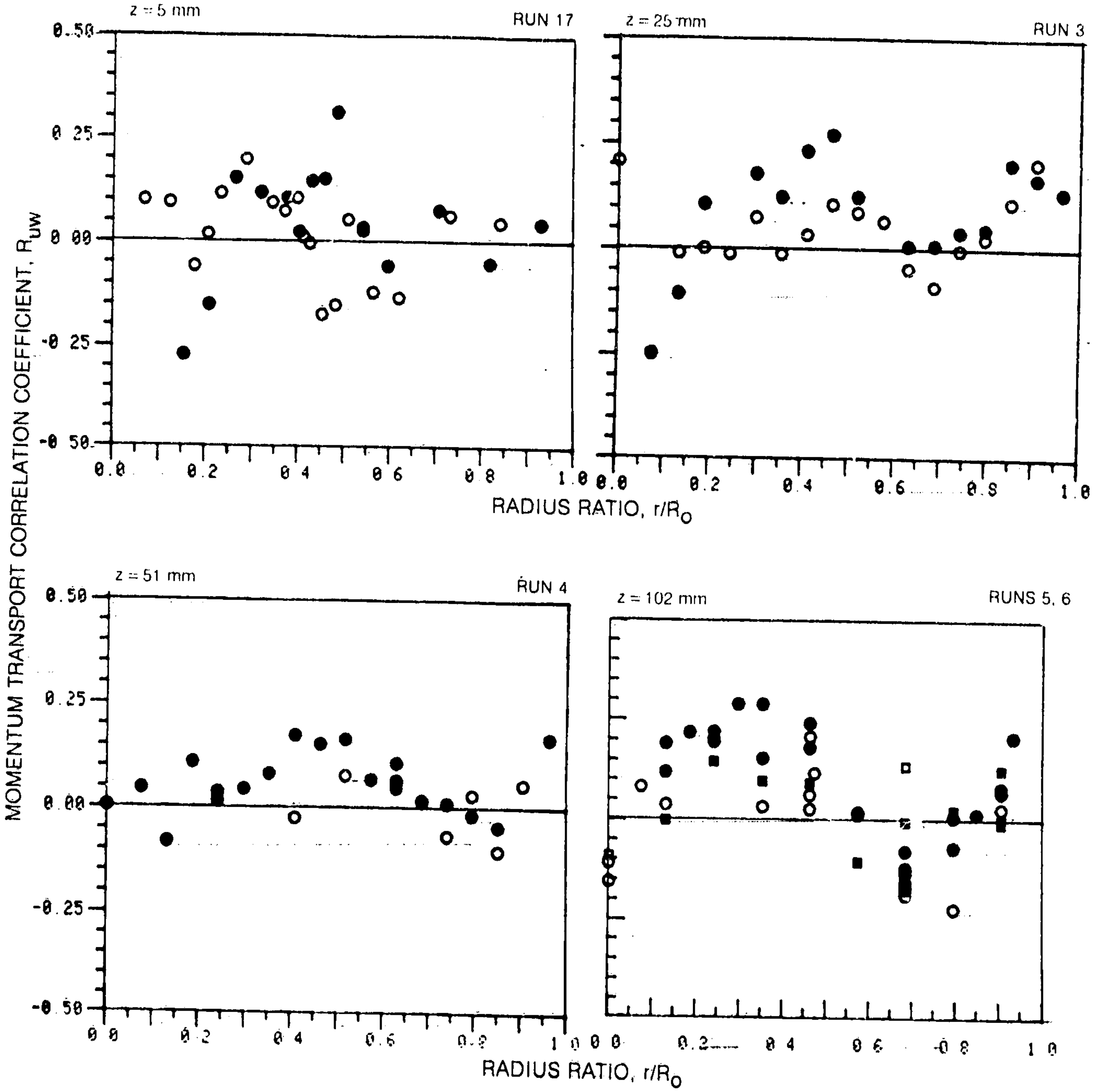

ORIGINAL PAGE IS
OF POOR QUALITY

FIG. 25 (CONT.)

MOMENTUM TRANSPORT CORRELATION COEFFICIENT, R_{uw}, PROFILES (CONT.)

	HORIZONTAL TRAVERSE	VERTICAL TRAVERSE
OPEN SYMBOLS:	$\theta = 90°$	$\theta = 0°$
SOLID SYMBOLS:	$\theta = 270°$	$\theta = 180°$

SYMBOL	○	●	□	■
RUN NOS.	14, 12, 43, 44		40	

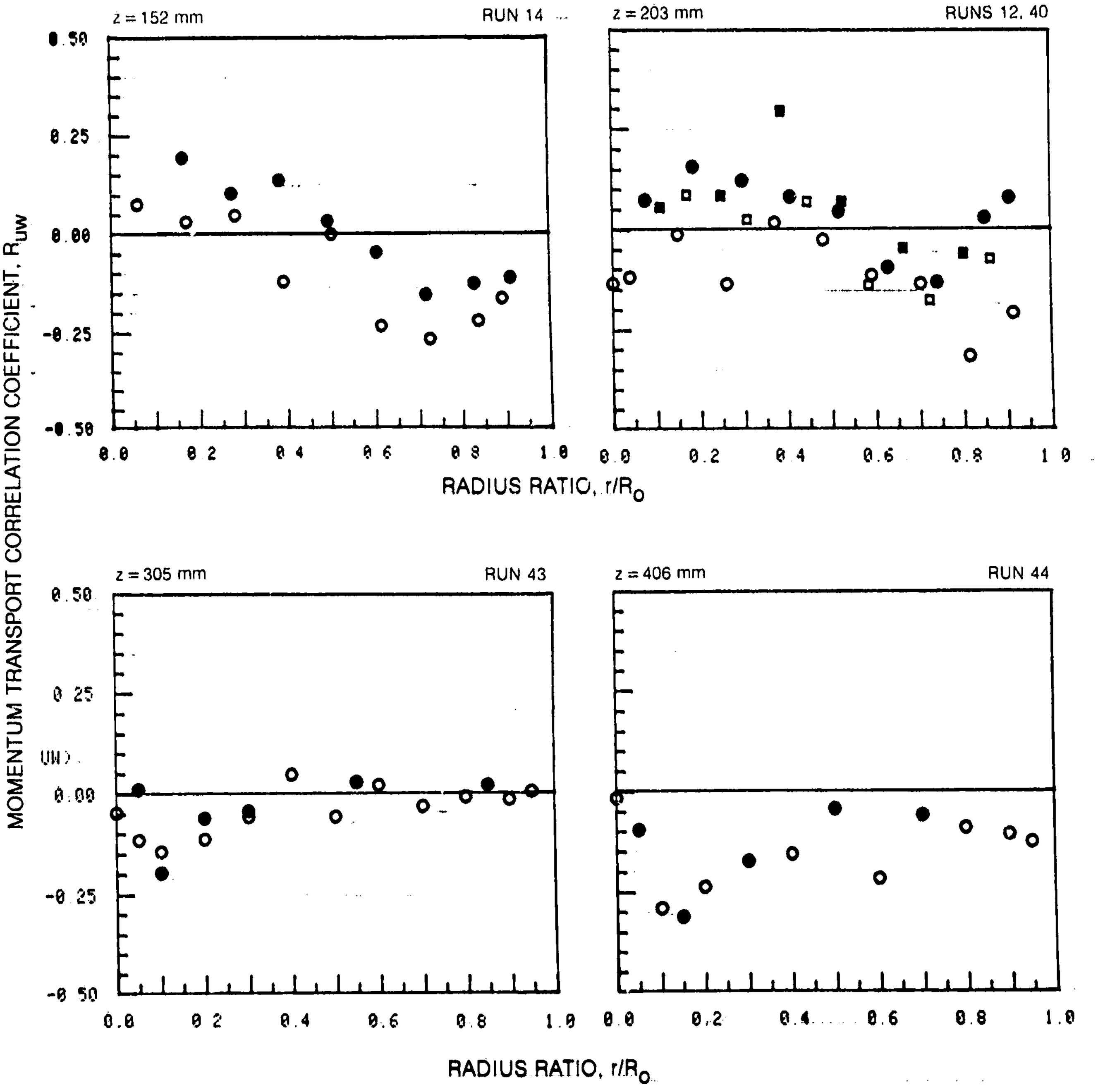

83-3-76-14

MOMENTUM TRANSPORT RATE, $\overline{wv}$, PROFILES

	HORIZONTAL TRAVERSE	VERTICAL TRAVERSE
OPEN SYMBOLS	θ = 90°	θ = 0°
SOLID SYMBOLS	θ = 270°	θ = 180°

SYMBOL	○	●	□	■	△	▲	◊	◆	▽	▼
RUN NOS	47, 46, 54		48*, 50, 55*		49*, 51, 56*		52*		53*	

* DATA OBTAINED WITH OPTICAL AXIS ± 1 DEG FROM TEST SECTION CENTERLINE

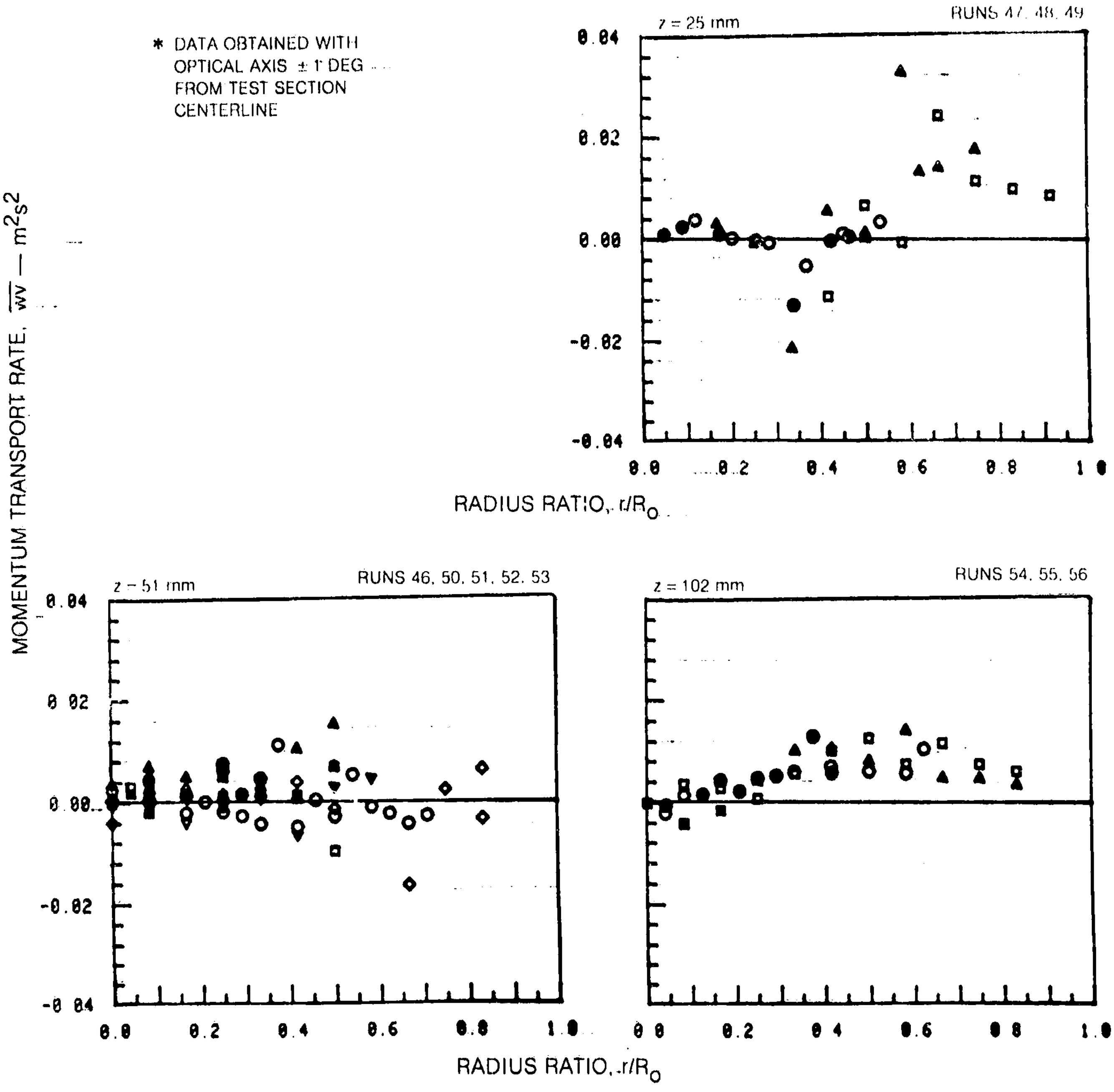

ORIGINAL PAGE IS
OF POOR QUALITY

FIG. 27

MOMENTUM TRANSPORT CORRELATION COEFFICIENT, R_{wv}, PROFILES

	HORIZONTAL TRAVERSE	VERTICAL TRAVERSE
OPEN SYMBOLS:	$\theta = 90°$	$\theta = 0°$
SOLID SYMBOLS:	$\theta = 270°$	$\theta = 180°$

SYMBOL	○	●	□	■	△	▲	◇	◆	▽	▼
RUN NOS.	47, 46, 54		48,* 50, 55*		49,* 51, 56*		52*		53*	

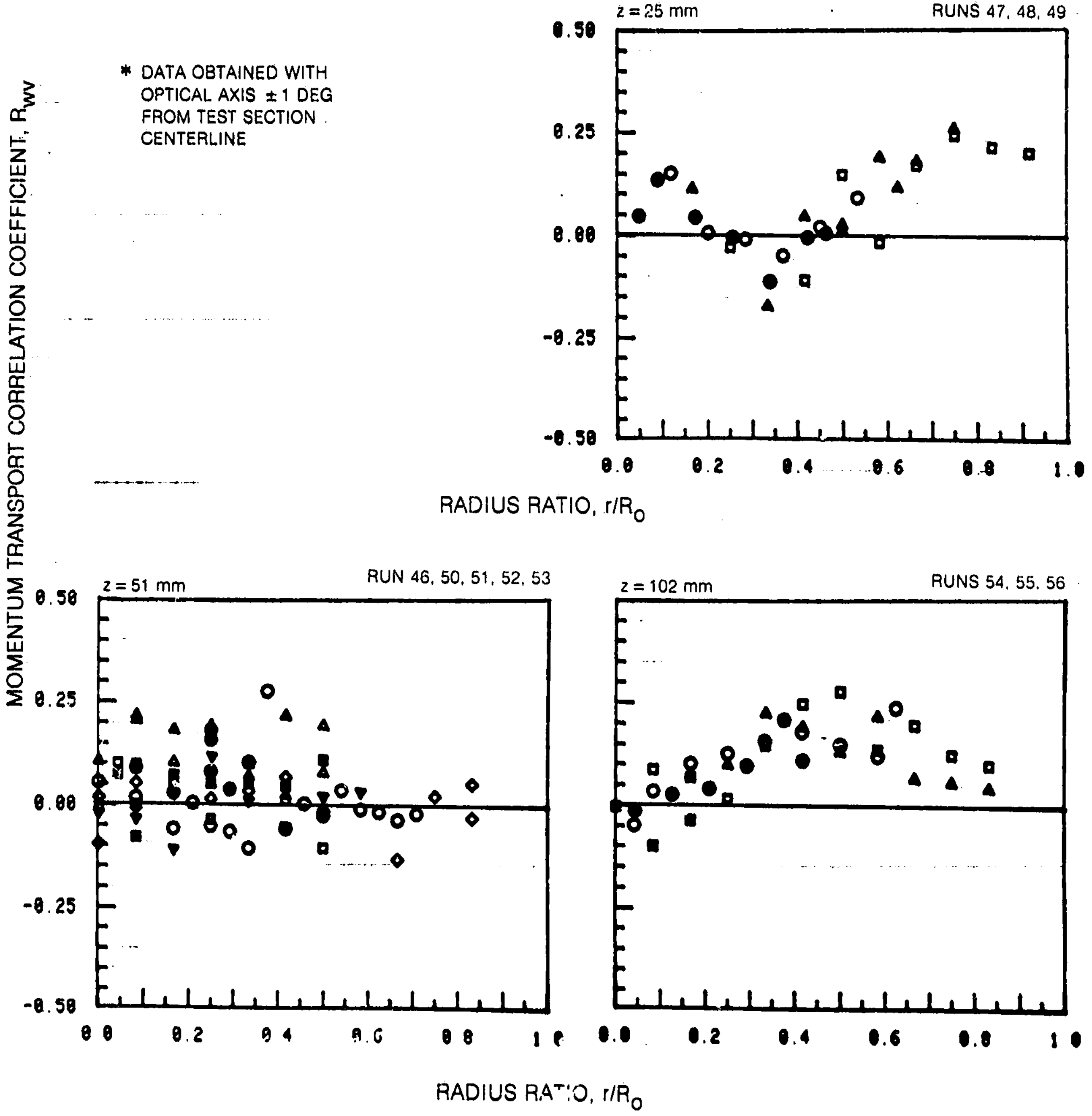

* DATA OBTAINED WITH OPTICAL AXIS ± 1 DEG FROM TEST SECTION CENTERLINE

ORIGINAL PAGE IS
OF POOR QUALITY

FIG. 28

RADIAL MASS TRANSPORT RATE, $\overline{vf}$, PROFILES

	HORIZONTAL TRAVERSE	VERTICAL TRAVERSE
OPEN SYMBOLS:	$\theta = 90°$	$\theta = 0°$
SOLID SYMBOLS:	$\theta = 270°$	$\theta = 180°$

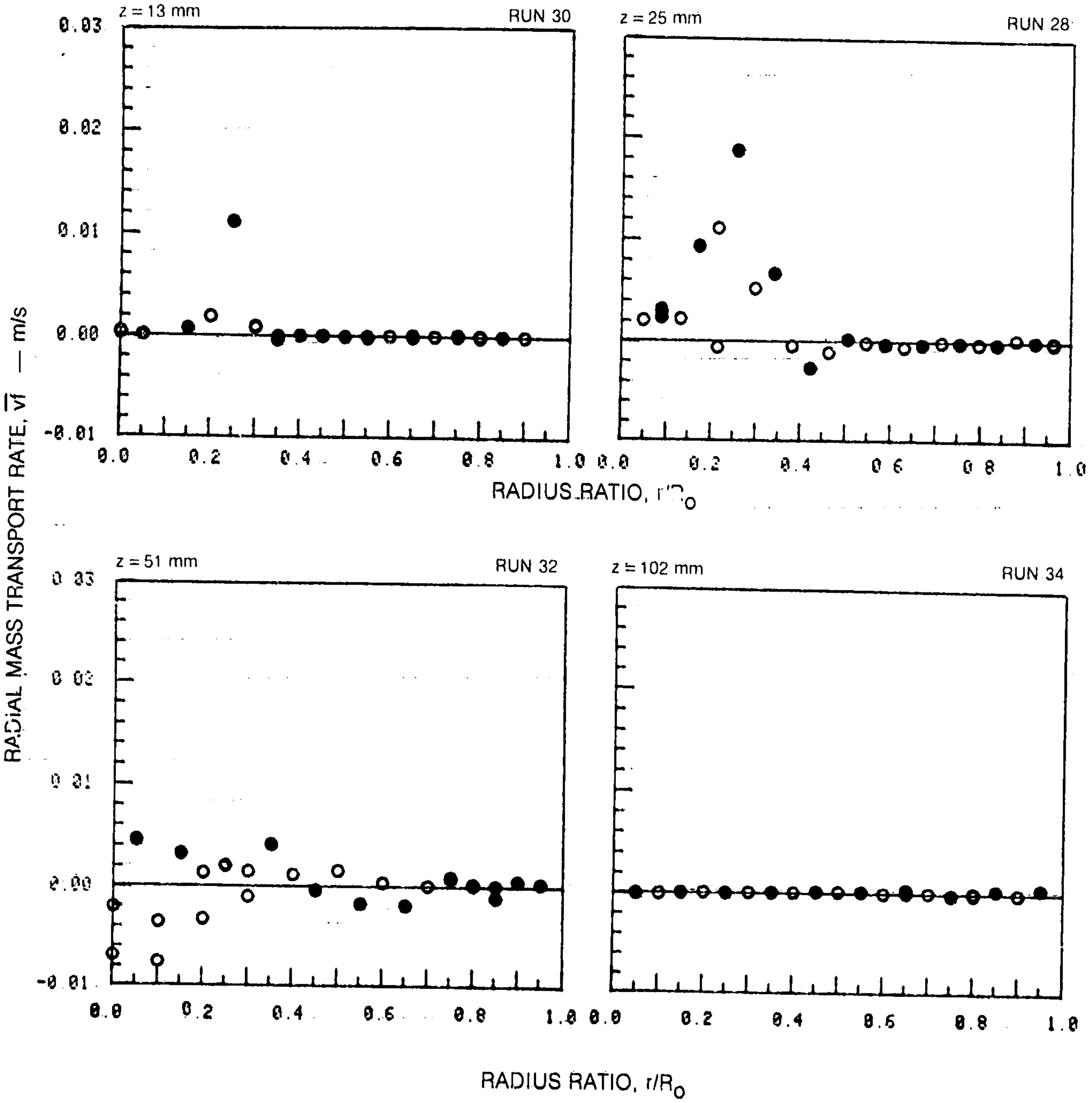

FIG. 28 (CONT.)

RADIAL MASS TRANSPORT RATE, $\overline{vf}$, PROFILES (CONT.)

	HORIZONTAL TRAVERSE	VERTICAL TRAVERSE
OPEN SYMBOLS:	θ = 90°	θ = 0°
SOLID SYMBOLS:	θ = 270°	θ = 180°

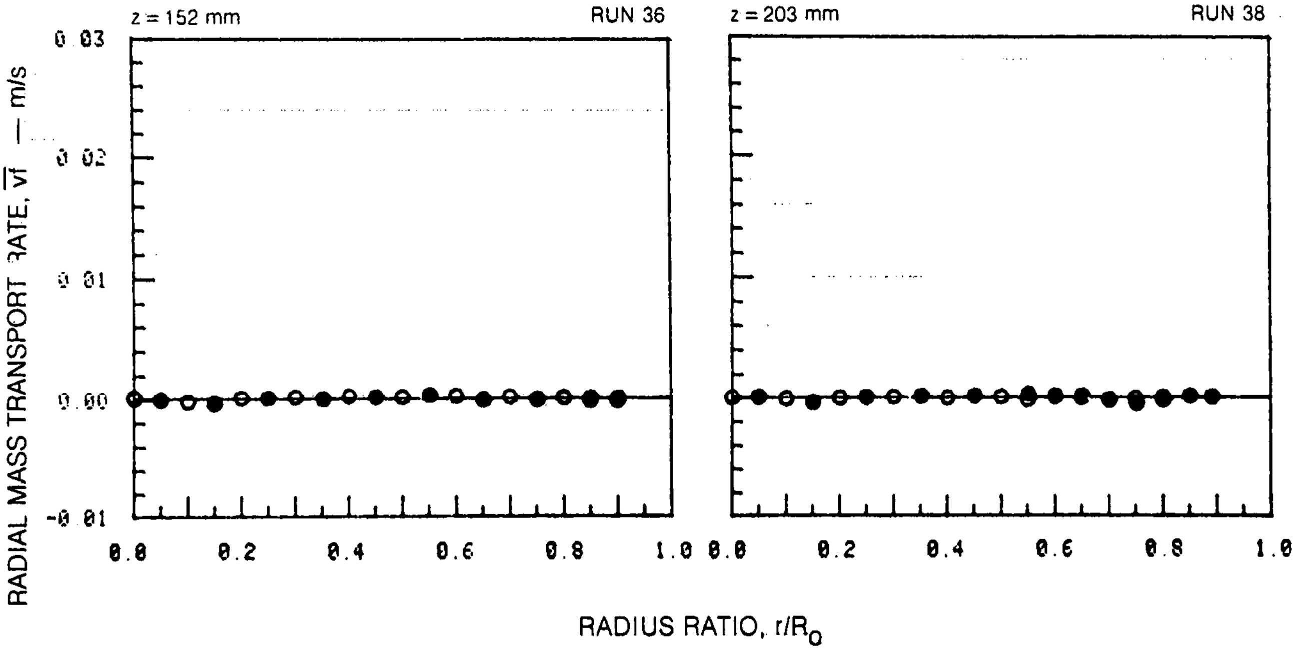

83-2-55-10B

ORIGINAL PAGE IS
OF POOR QUALITY

FIG. 29

RADIAL MASS TRANSPORT CORRELATION COEFFICIENT, R_{vf}, PROFILES

	HORIZONTAL TRAVERSE	VERTICAL TRAVERSE
OPEN SYMBOLS:	$\theta = 90°$	$\theta = 0°$
SOLID SYMBOLS:	$\theta = 270°$	$\theta = 180°$

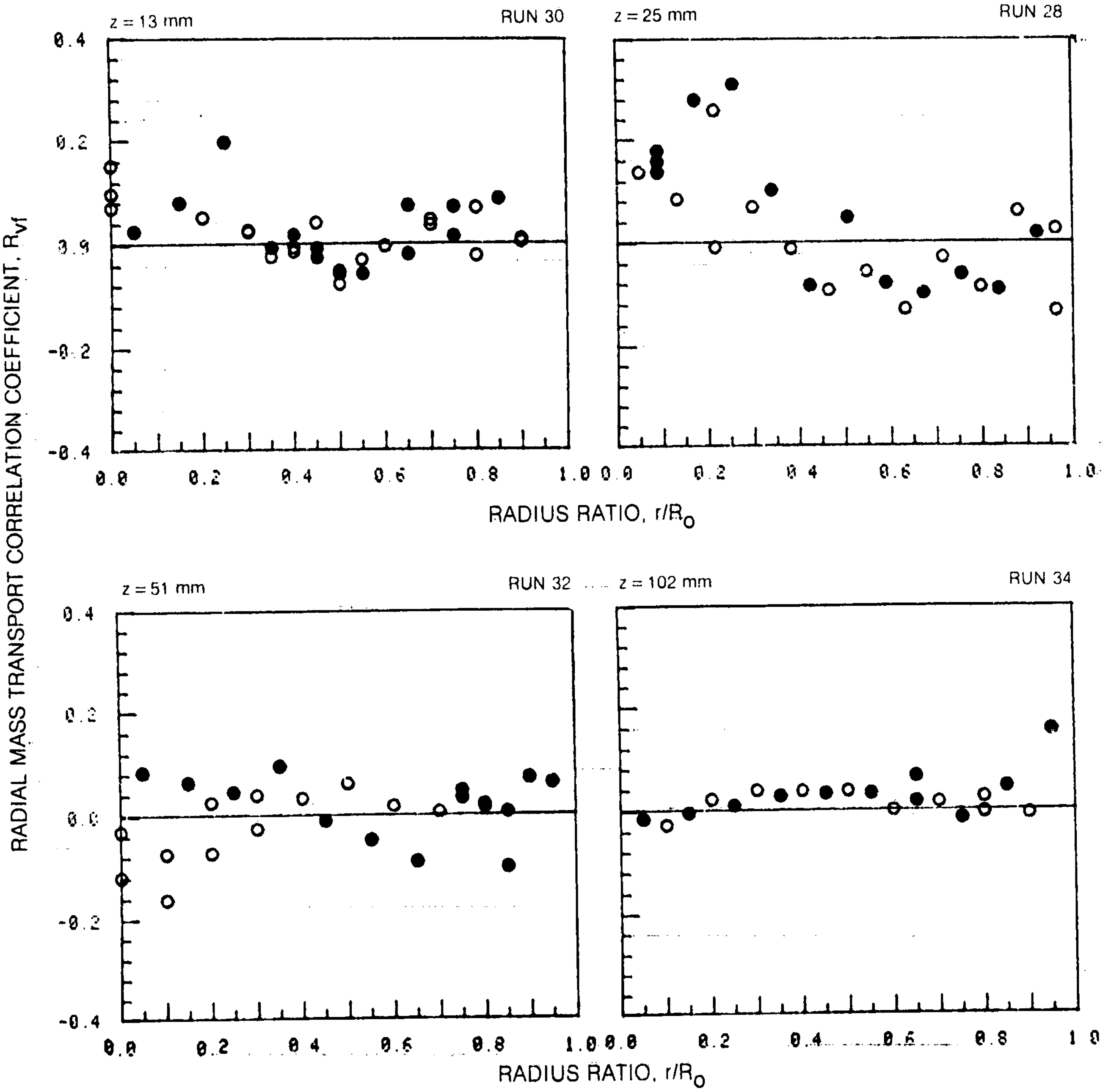

RADIAL MASS TRANSPORT CORRELATION COEFFICIENT, R_{vf}, PROFILES (CONT.)

	HORIZONTAL TRAVERSE	VERTICAL TRAVERSE
OPEN SYMBOLS:	θ = 90°	θ = 0°
SOLID SYMBOLS:	θ = 270°	θ = 180°

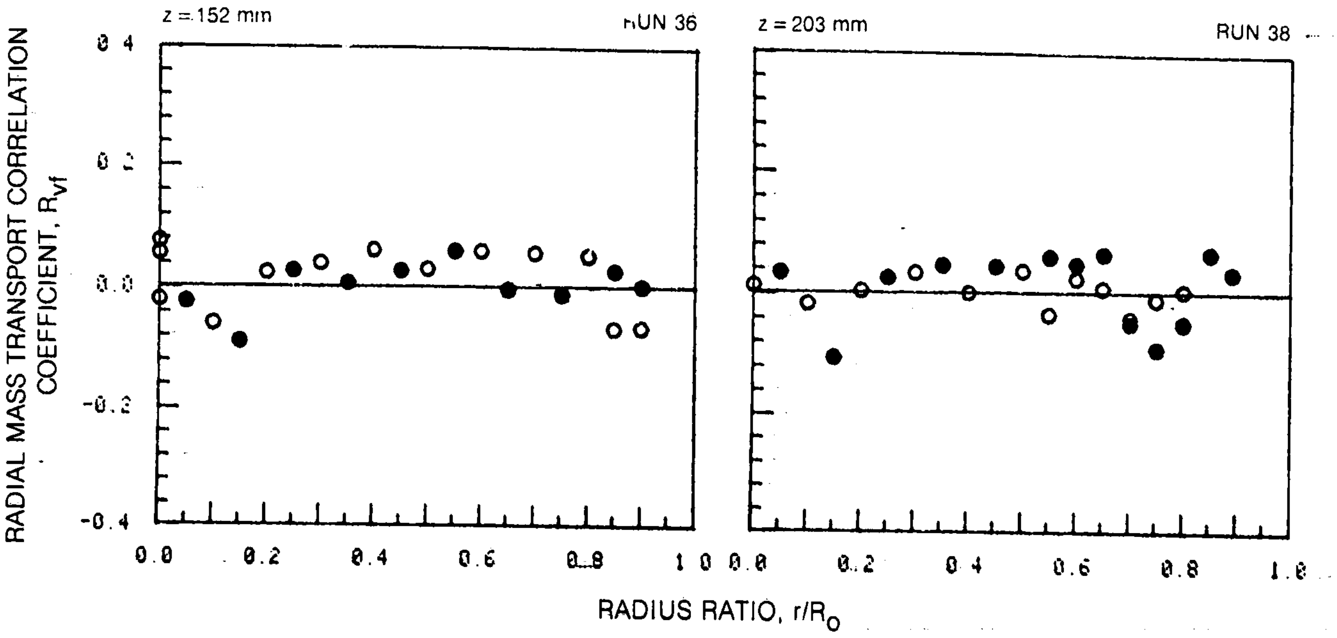

AXIAL MASS TRANSPORT RATE, $\overline{uf}$, PROFILES

	HORIZONTAL TRAVERSE	VERTICAL TRAVERSE
OPEN SYMBOLS.	$\theta = 90°$	$\theta = 0°$
SOLID SYMBOLS.	$\theta = 270°$	$\theta = 180°$

SYMBOL	○	●	□	■
RUN NOS.	20, 22		21	

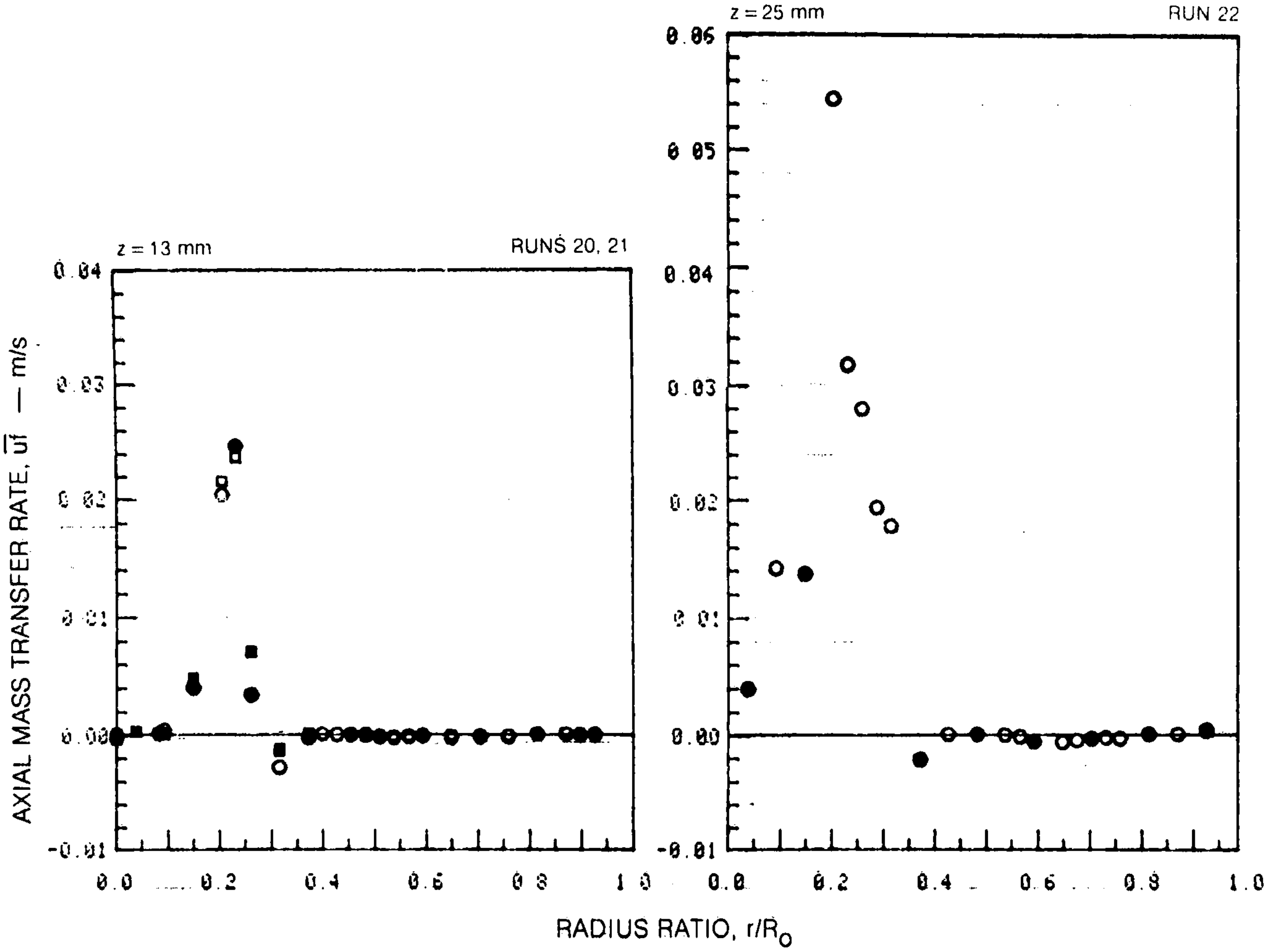

ORIGINAL PAGE IS
OF POOR QUALITY

FIG. 30 (CONT.)

AXIAL MASS TRANSPORT RATE, $\overline{uf}$, PROFILES (CONT.)

	HORIZONTAL TRAVERSE	VERTICAL TRAVERSE
OPEN SYMBOLS.	θ = 90°	θ = 0°
SOLID SYMBOLS:	θ = 270°	θ = 180°

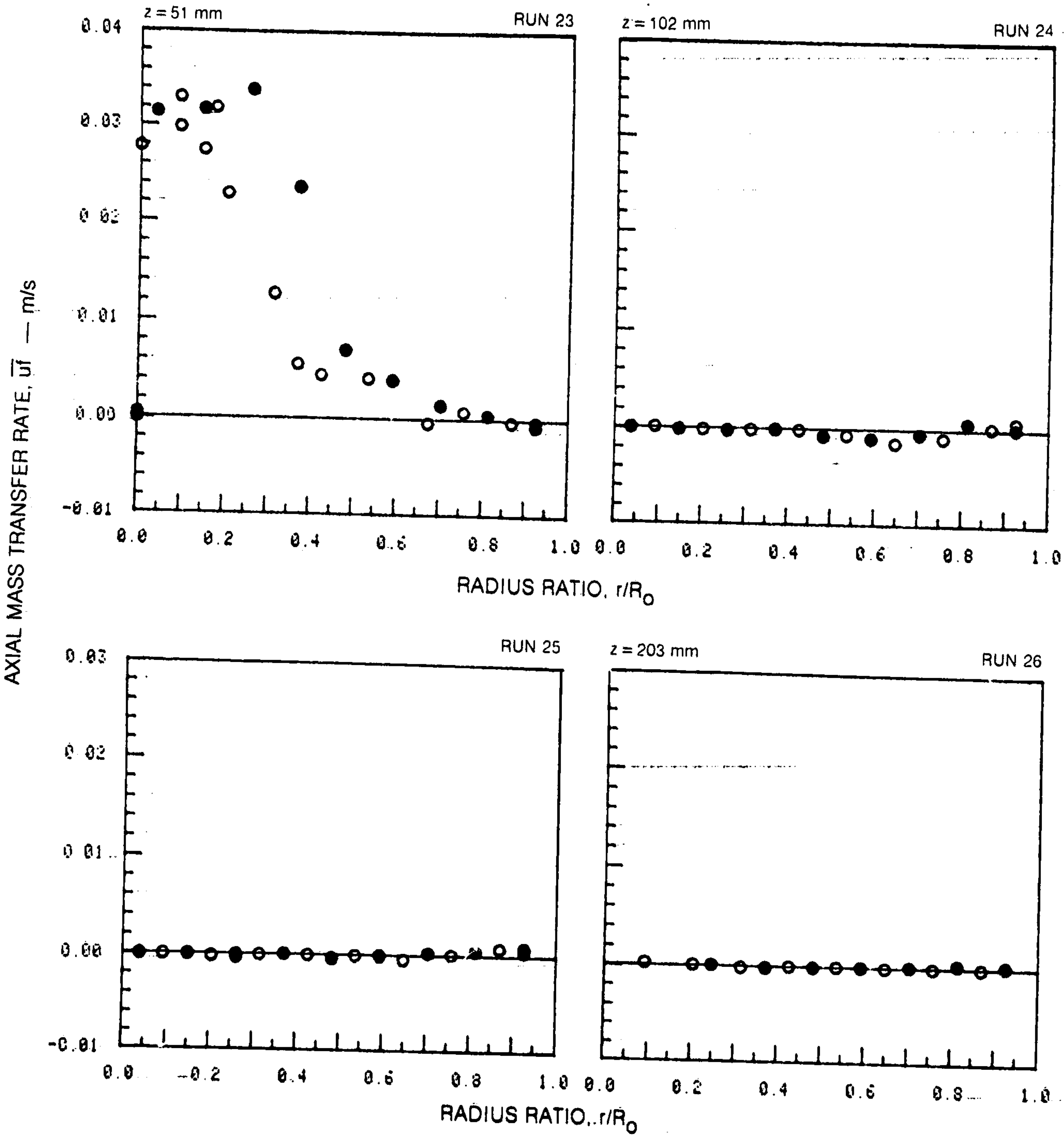

ORIGINAL PAGE IS
OF POOR QUALITY

FIG. 31

AXIAL MASS TRANSPORT CORRELATION COEFFICIENT, R_{uf}, PROFILES

	HORIZONTAL TRAVERSE	VERTICAL TRAVERSE
OPEN SYMBOLS:	$\theta = 90°$	$\theta = 0°$
SOLID SYMBOLS:	$\theta = 270°$	$\theta = 180°$

SYMBOL	○	●	□	■
RUN NOS.	20 22, 23, 24		21	

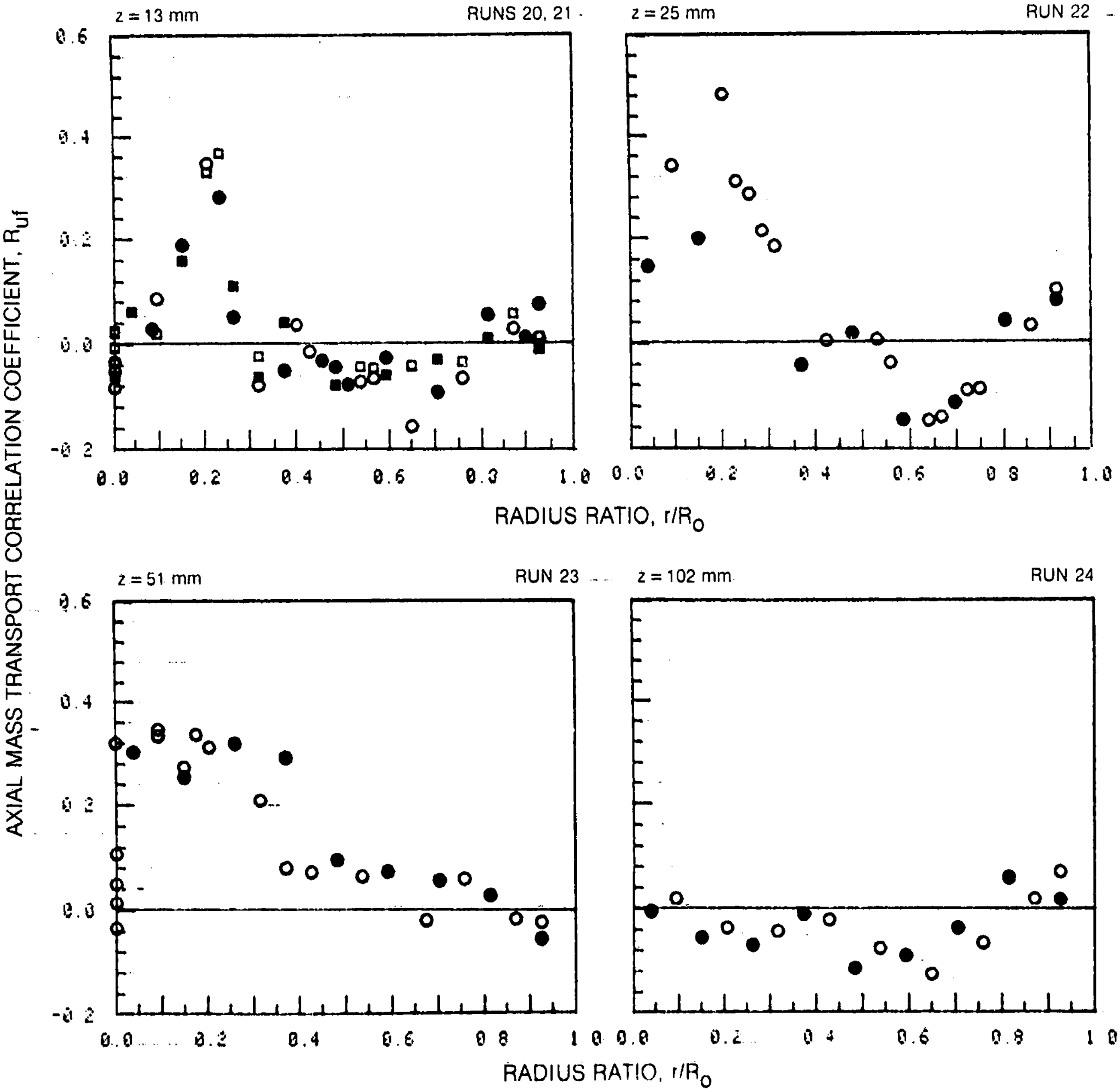

83-2-55-11A

FIG. 31 (CONT.)

AXIAL MASS TRANSPORT CORRELATION COEFFICIENT, R_{uf}, PROFILES (CONT.)

	HORIZONTAL TRAVERSE	VERTICAL TRAVERSE
OPEN SYMBOLS:	θ = 90°	θ = 0°
SOLID SYMBOLS:	θ = 270°	θ = 180°

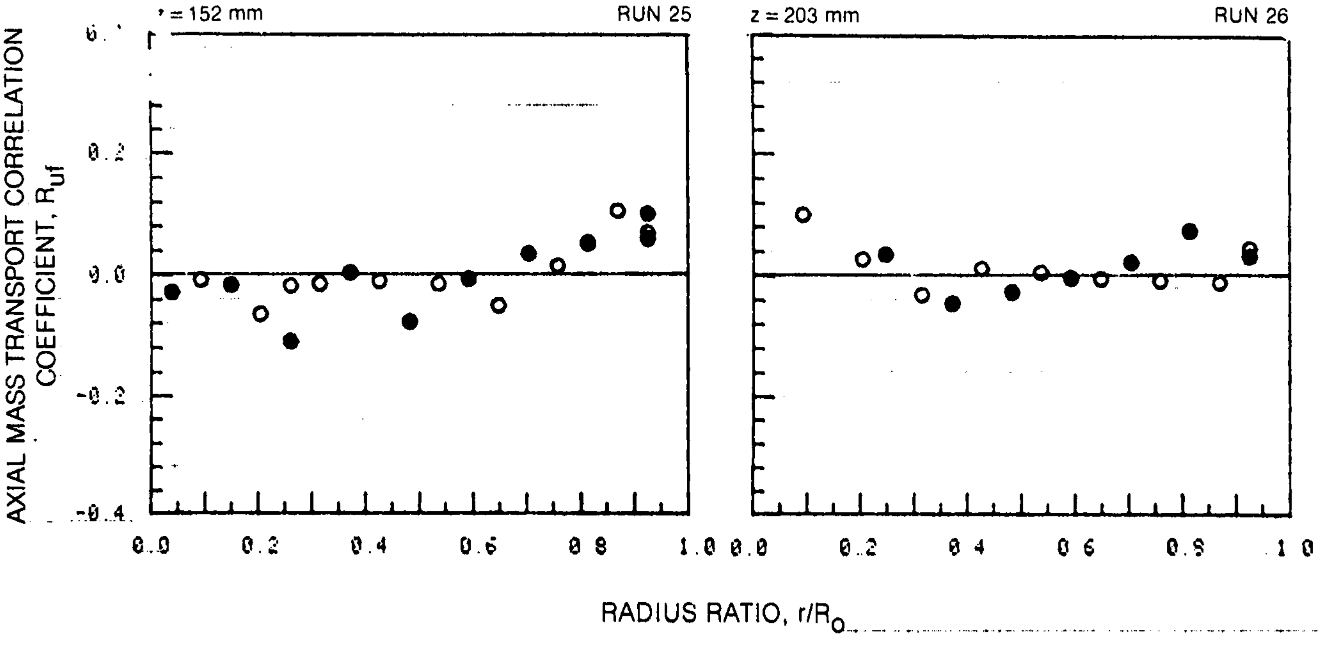

ORIGINAL PAGE IS
OF POOR QUALITY

FIG. 32

AZIMUTHAL MASS TRANSPORT RATE, $\overline{wf}$, PROFILES

	HORIZONTAL TRAVERSE	VERTICAL TRAVERSE
OPEN SYMBOLS:	$\theta = 90°$	$\theta = 0°$
SOLID SYMBOLS:	$\theta = 270°$	$\theta = 180°$

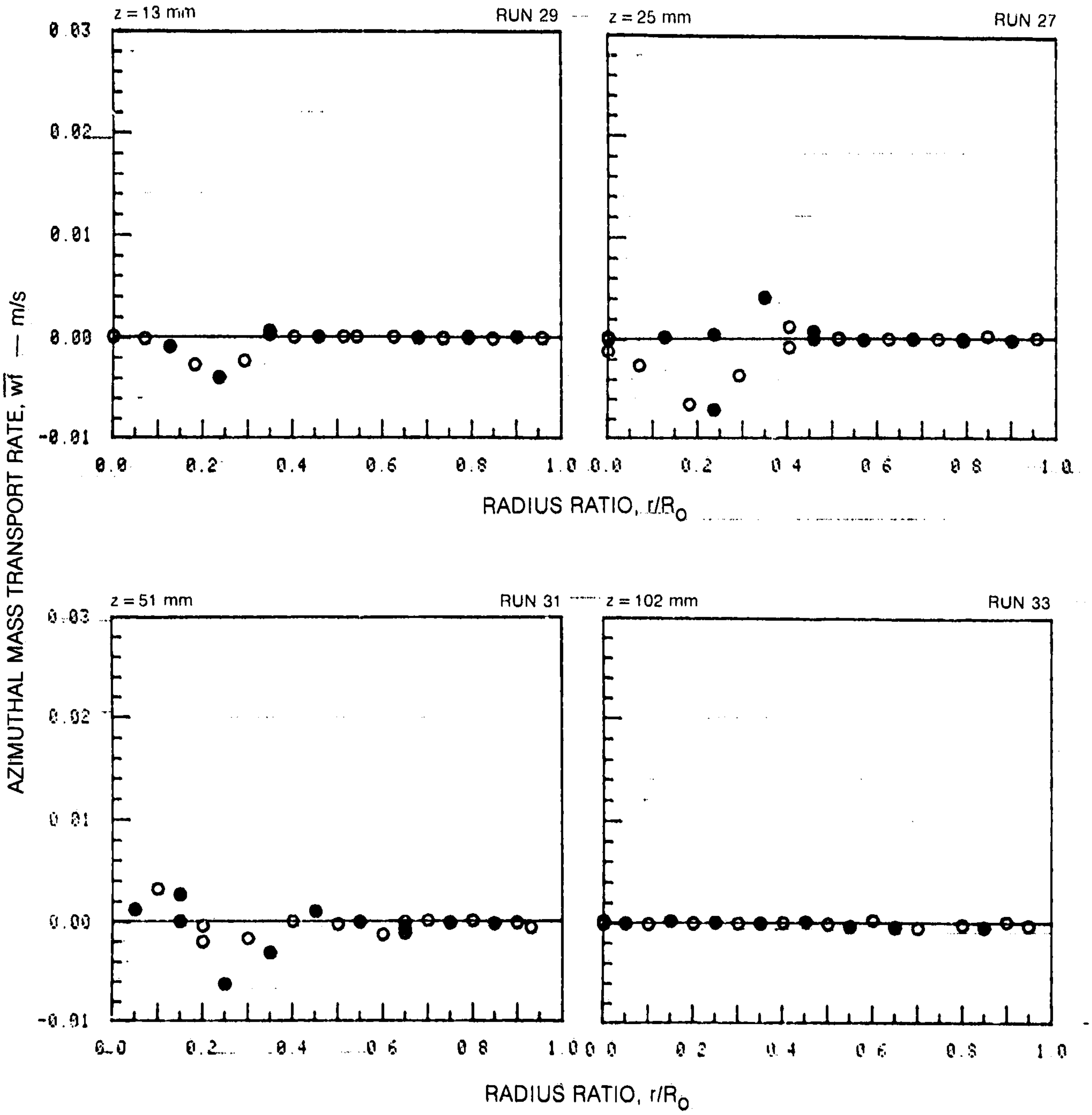

83-2-55-23A

AZIMUTHAL MASS TRANSPORT RATE, $\overline{wf}$, PROFILES (CONT.)

	HORIZONTAL TRAVERSE	VERTICAL TRAVERSE
OPEN SYMBOLS:	$\theta = 90°$	$\theta = 0°$
SOLID SYMBOLS:	$\theta = 270°$	$\theta = 180°$

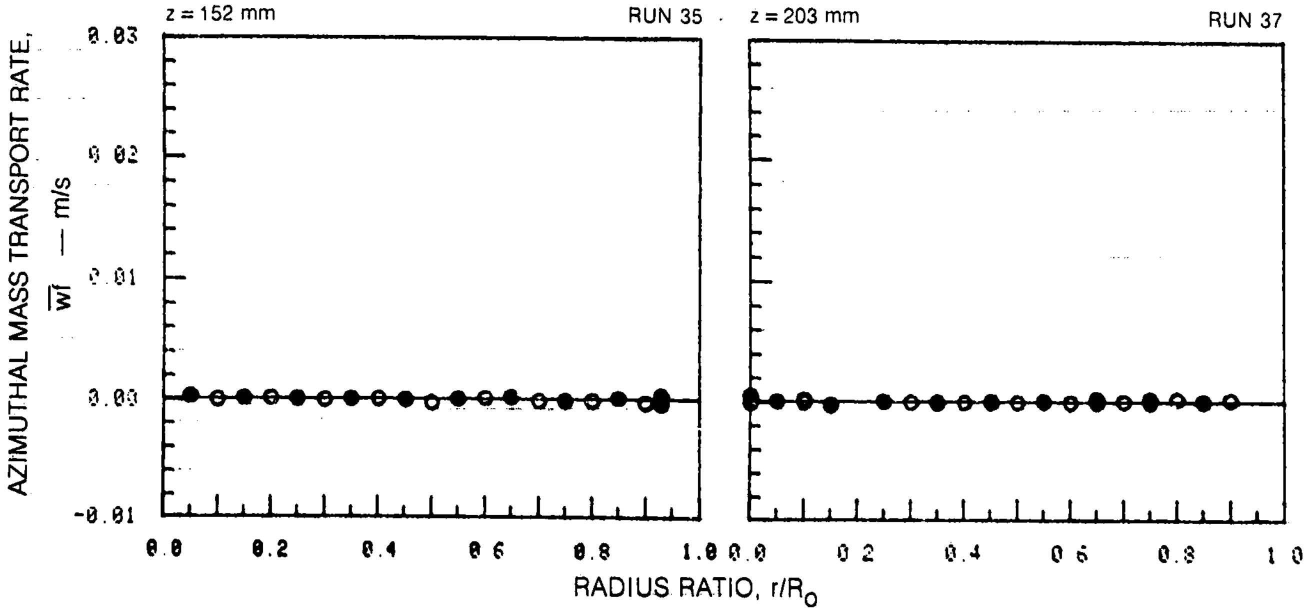

ORIGINAL PAGE IS
OF POOR QUALITY

FIG. 33

AZIMUTHAL MASS TRANSPORT CORRELATION COEFFICIENT, R_{wf}, PROFILES

	HORIZONTAL TRAVERSE	VERTICAL TRAVERSE
OPEN SYMBOLS:	$\theta = 90°$	$\theta = 0°$
SOLID SYMBOLS:	$\theta = 270°$	$\theta = 180°$

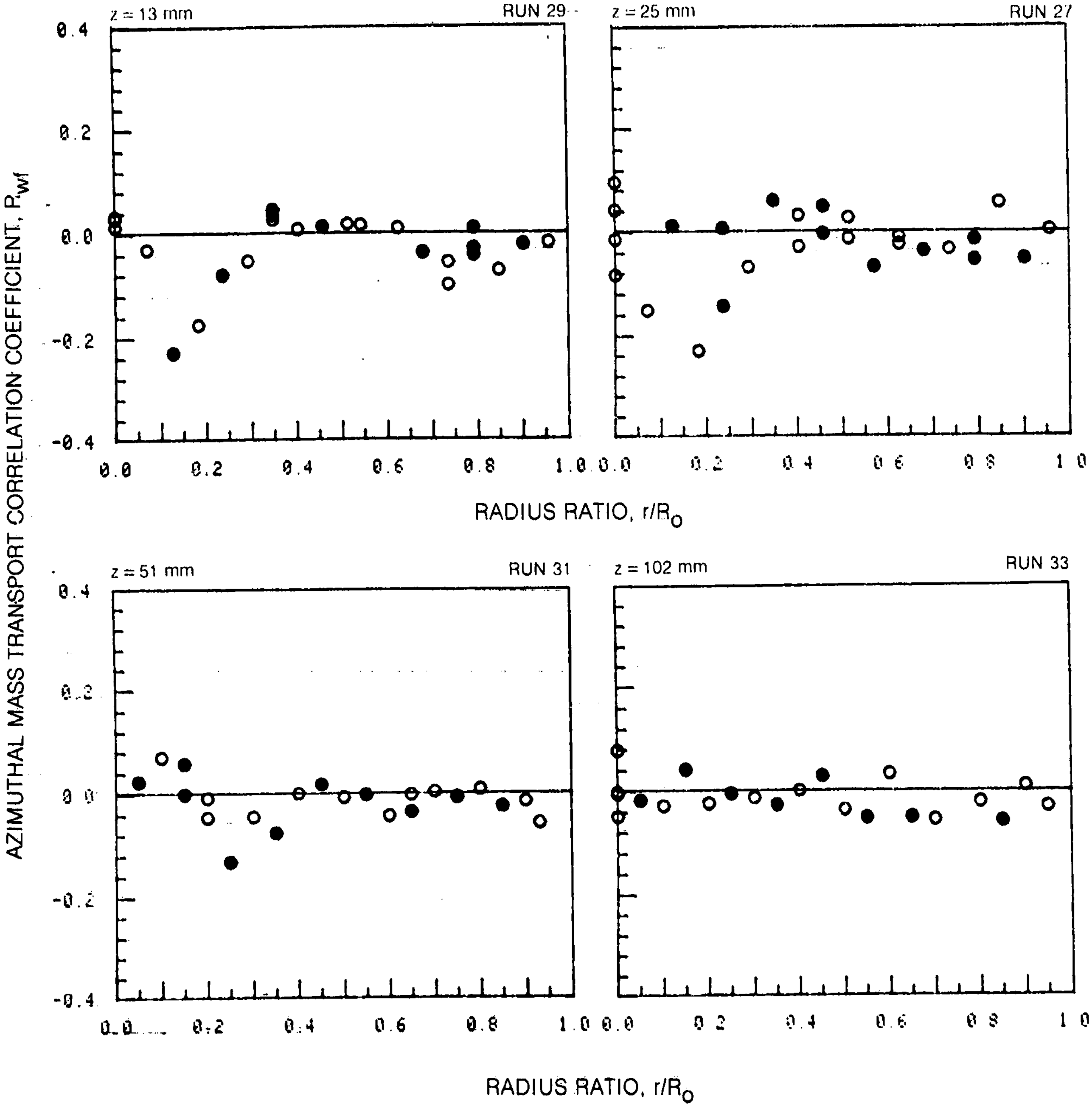

ORIGINAL PAGE IS
OF POOR QUALITY

AZIMUTHAL MASS TRANSPORT CORRELATION COEFFICIENT, R_{wf}, PROFILES (CONT.)

	HORIZONTAL TRAVERSE	VERTICAL TRAVERSE
OPEN SYMBOLS:	θ = 90°	θ = 0°
SOLID SYMBOLS:	θ = 270°	θ = 180°

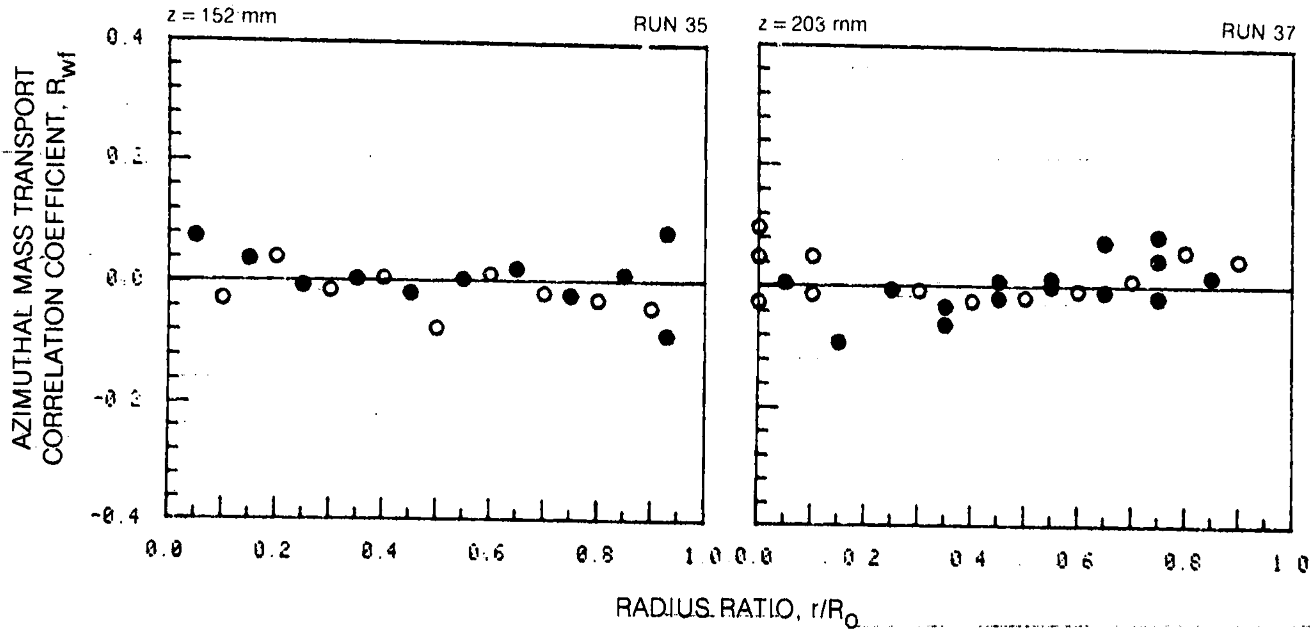

ORIGINAL PAGE IS
OF POOR QUALITY

AXIAL VELOCITY PROBABILITY DENSITY FUNCTIONS

AXIAL LOCATION: 25 mm

AVERAGES OF DATA FROM RUNS 3 (△) AND 7 (○)

r/R_o	$\tilde{u}$	u'	S_u	K_u
0.00	0.36	0.27	-0.84	3.0
0.13	0.09	0.39	0.06	2.2
0.24	-0.29	0.28	0.64	3.5
0.36	0.65	0.44	0.24	3.1
0.52	1.66	0.21	-0.32	3.1
0.68	0.21	0.24	-0.24	3.5

$\Delta\tilde{u} = 0.1$ m/s

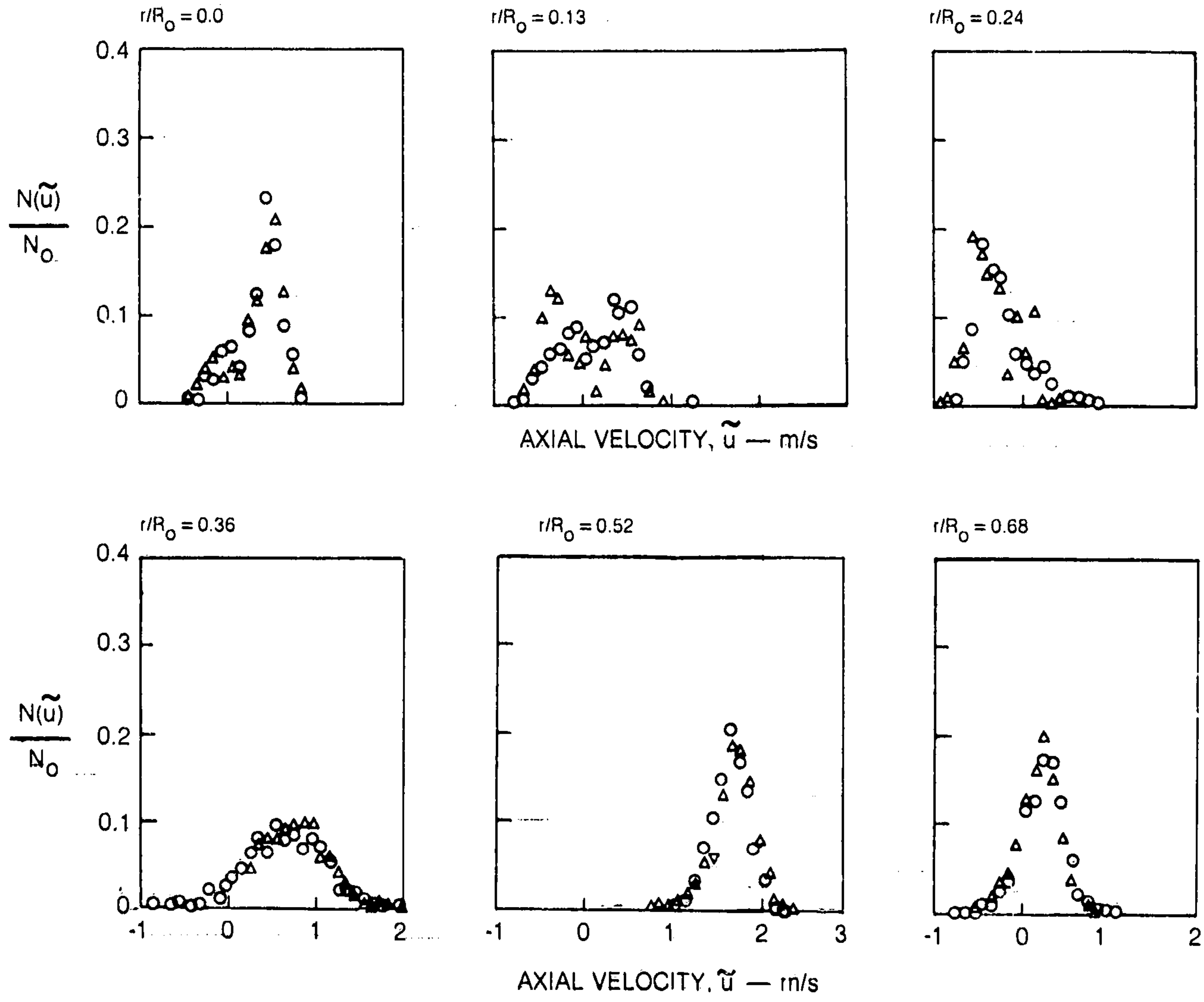

83-7-19-10

ORIGINAL PAGE IS
OF POOR QUALITY

FIG. 35

RADIAL VELOCITY PROBABILITY DENSITY FUNCTIONS

AXIAL LOCATION: 25 mm

AVERAGES OF DATA FROM RUNS 7 (○) AND 28 (□)

r/R_o	$\tilde{v}$	v'	S_v	K_v
0.00	0.01	0.16	0.20	5.2
0.13	0.04	0.16	0.20	4.4
0.24	0.05	0.23	-0.82	5.1
0.36	0.24	0.34	0.17	3.0
0.52	0.64	0.20	0.04	3.7
0.68	0.01	0.29	0.41	4.6

$\Delta\tilde{v} = 0.1$ m/s

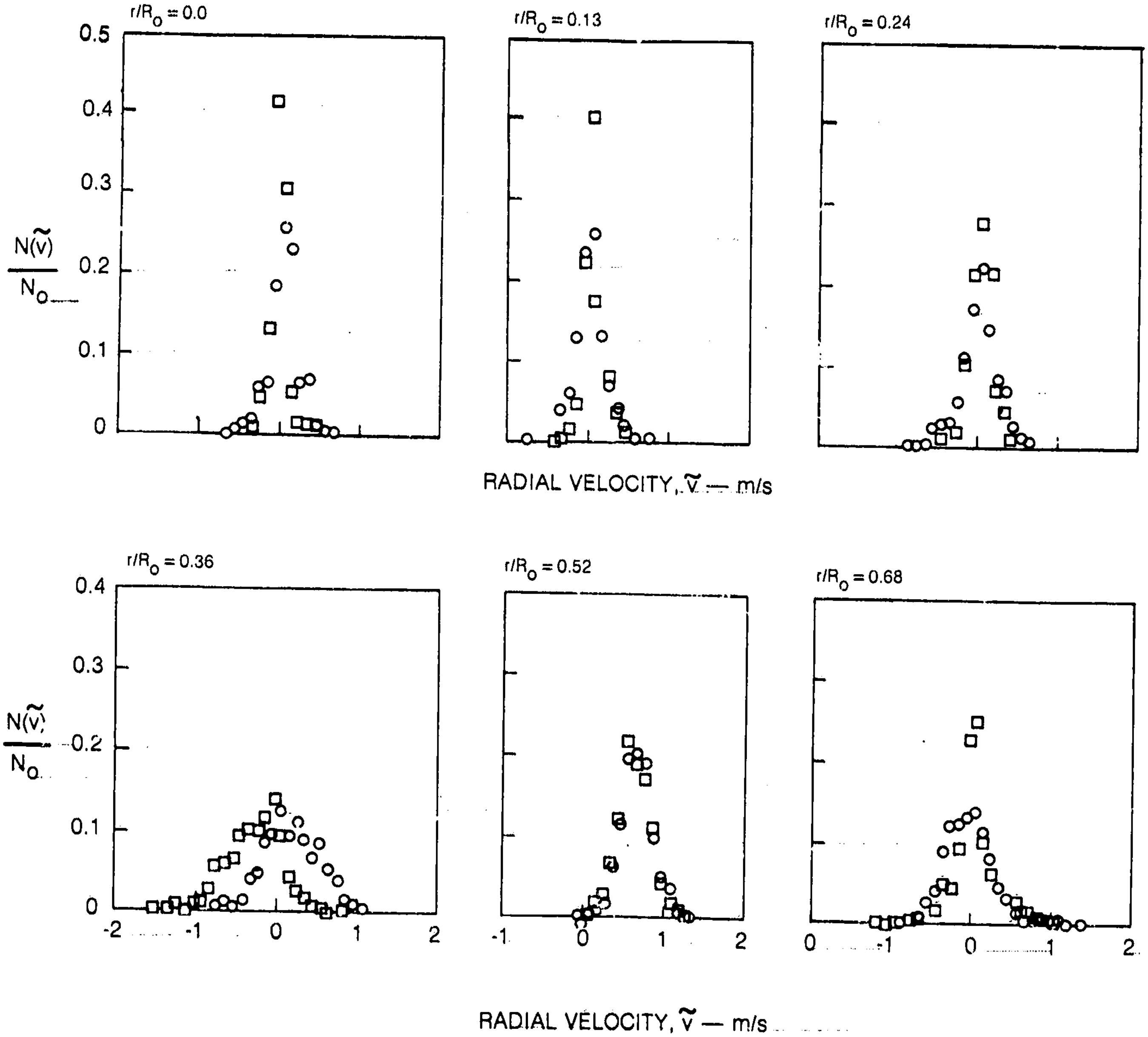

83-7-19-9

ORIGINAL PAGE IS
OF POOR QUALITY

FIG. 36

AZIMUTHAL VELOCITY PROBABILITY DENSITY FUNCTIONS

AXIAL LOCATION: 25 mm

AVERAGES OF DATA FROM RUNS 3(○) AND 27(△)

r/R_0	$\tilde{w}$	w'	S_w	K_w
0.00	-0.04	0.15	-0.09	4.4
0.13	0.01	0.16	0.68	5.9
0.24	-0.01	0.22	-0.51	5.3
0.36	0.33	0.39	-0.47	3.8
0.52	0.64	0.15	0.06	5.1
0.68	0.41	0.21	-0.29	4.2

$\Delta\tilde{w} = 0.1$ m/s

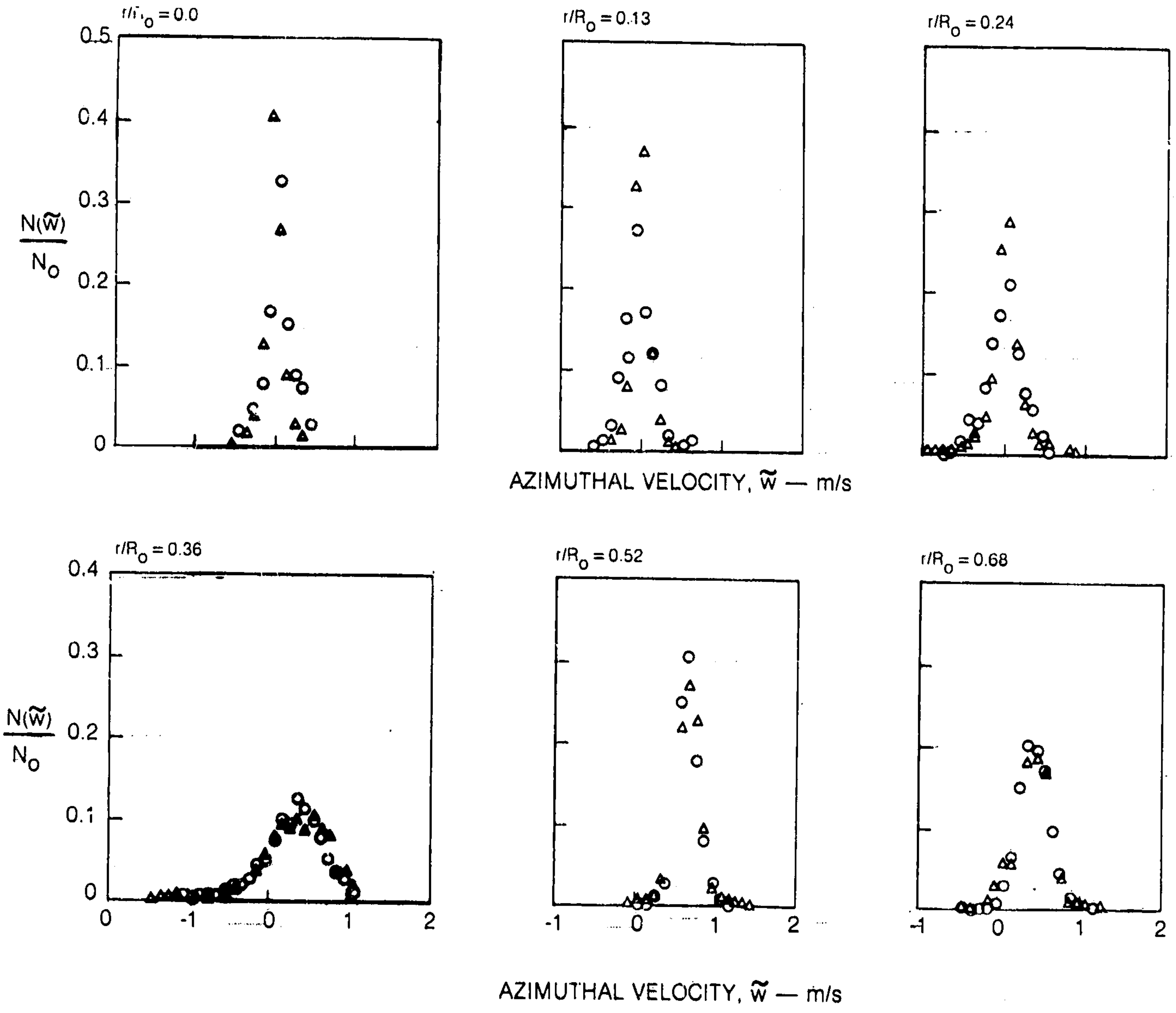

83-7-19-8

ORIGINAL PAGE IS
OF POOR QUALITY

CONCENTRATION PROBABILITY DENSITY FUNCTIONS

AXIAL LOCATION: 25 mm

AVERAGES OF DATA FROM RUNS 22 (○), 27 (△) AND 28 (□)

r/R_o	$\bar{f}$	f'	S_f	K_f
0.00	0.97	0.12	-2.91	12.4
0.13	0.86	0.18	-1.94	6.4
0.24	0.63	0.27	-0.25	1.9
0.36	0.21	0.13	0.99	4.2
0.52	0.03	0.02	3.93	27.5
0.68	0.05	0.01	0.26	4.2

$\Delta f = 0.02$

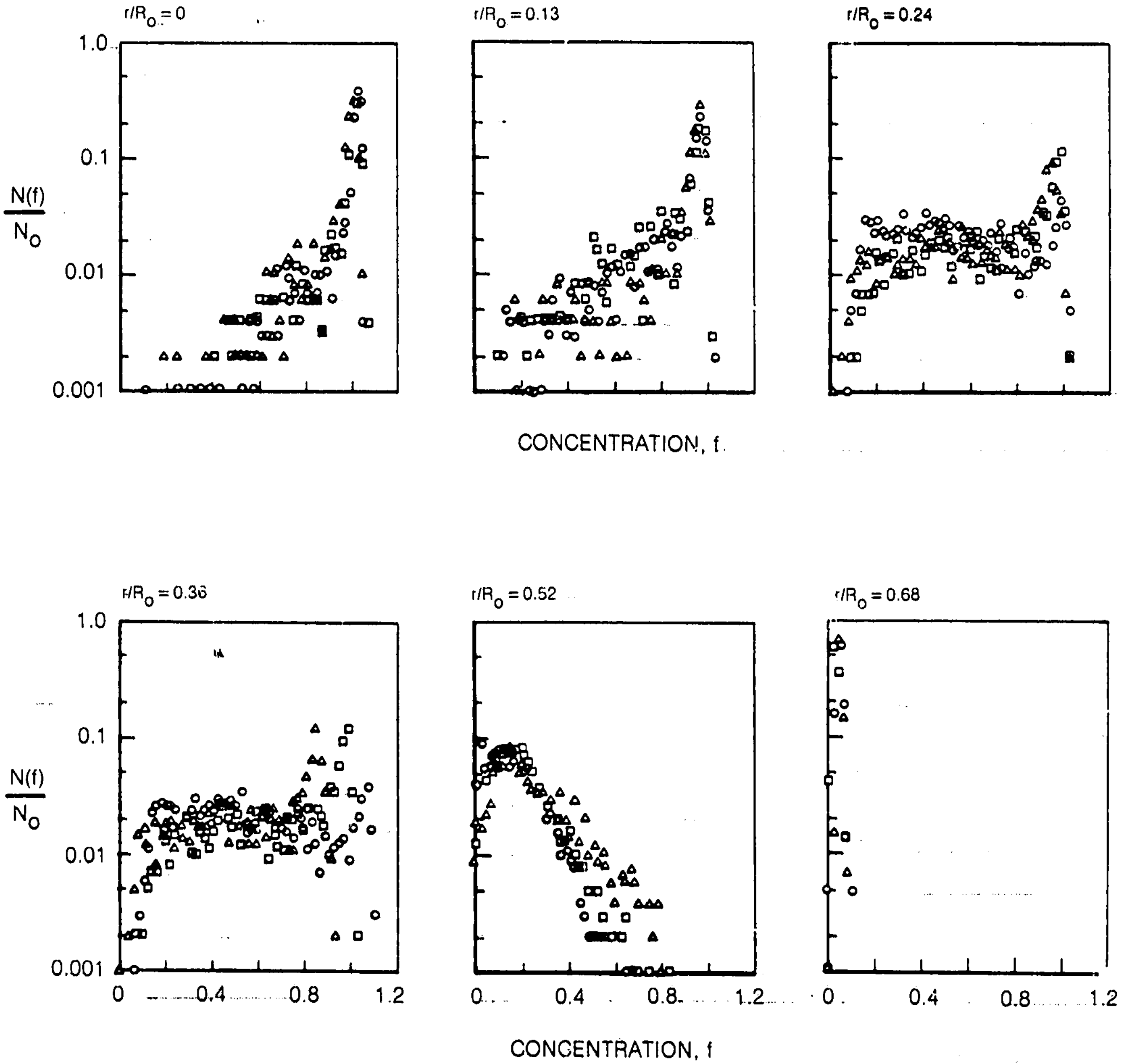

83-7-19-24

FIG. 38

SKEWNESS OF AXIAL VELOCITIES PROFILES

	HORIZONTAL TRAVERSE	VERTICAL TRAVERSE
OPEN SYMBOLS	θ = 90°	θ = 0°
SOLID SYMBOLS	θ = 270°	θ = 180°

SYMBOL	○	●	□	■	△	▲	◇	◆
RUN NOS	11, 3, 4, 5		16, 7, 8, 6		17, 22, 23, 9		24	

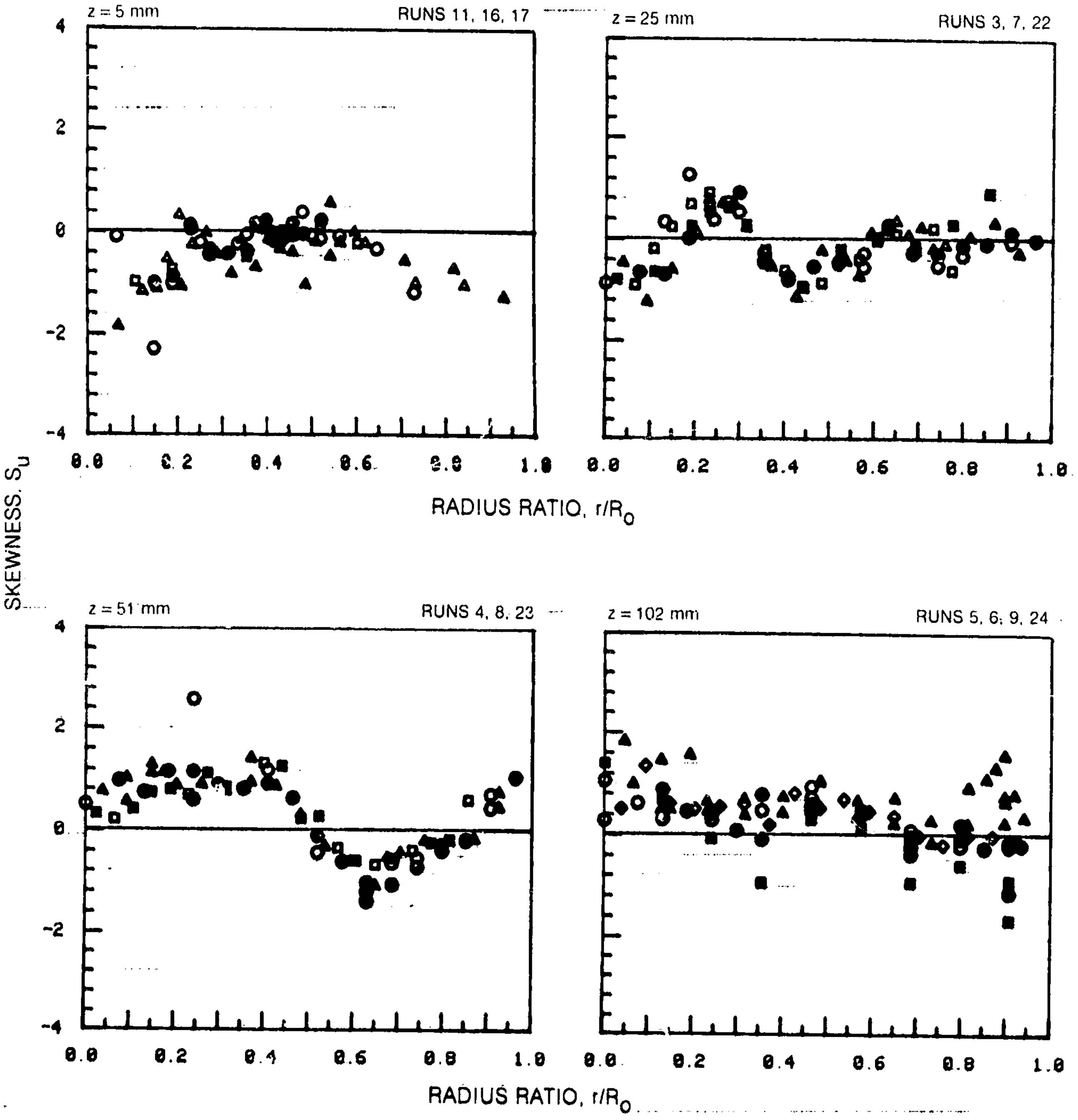

83-3-76-11

FIG. 38 (CONT.)

SKEWNESS OF AXIAL VELOCITIES PROFILES (CONT.)

	HORIZONTAL TRAVERSE	VERTICAL TRAVERSE
OPEN SYMBOLS	θ = 90°	θ = 0°
SOLID SYMBOLS	θ = 270°	θ = 180°

SYMBOL	○	●	□	■	△	▲	◇	◆	▽	▼
RUN NOS	14, 10, 42, 44		15, 12, 43, 45		25, 26		40		41	

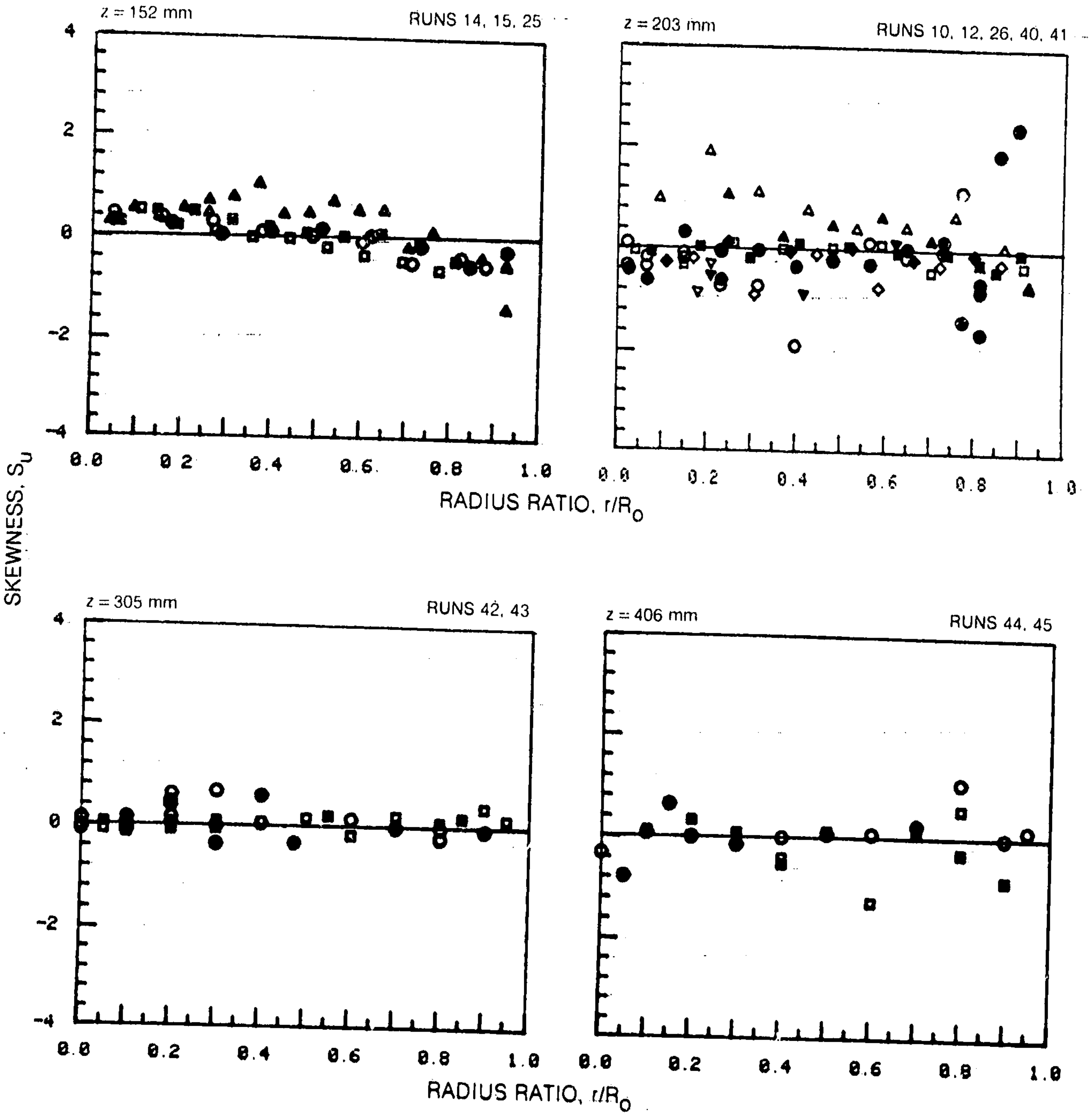

83-3-76-11A

ORIGINAL PAGE IS
OF POOR QUALITY

FIG. 39

KURTOSIS OF AXIAL VELOCITIES PROFILES

	HORIZONTAL TRAVERSE	VERTICAL TRAVERSE
OPEN SYMBOLS	θ = 90°	θ = 0°
SOLID SYMBOLS	θ = 270°	θ = 180°

SYMBOL	○	●	□	■	△	▲	◇	◆
RUN NOS	11, 3, 4, 5		16, 7, 8, 6		17, 22, 23, 9		24	

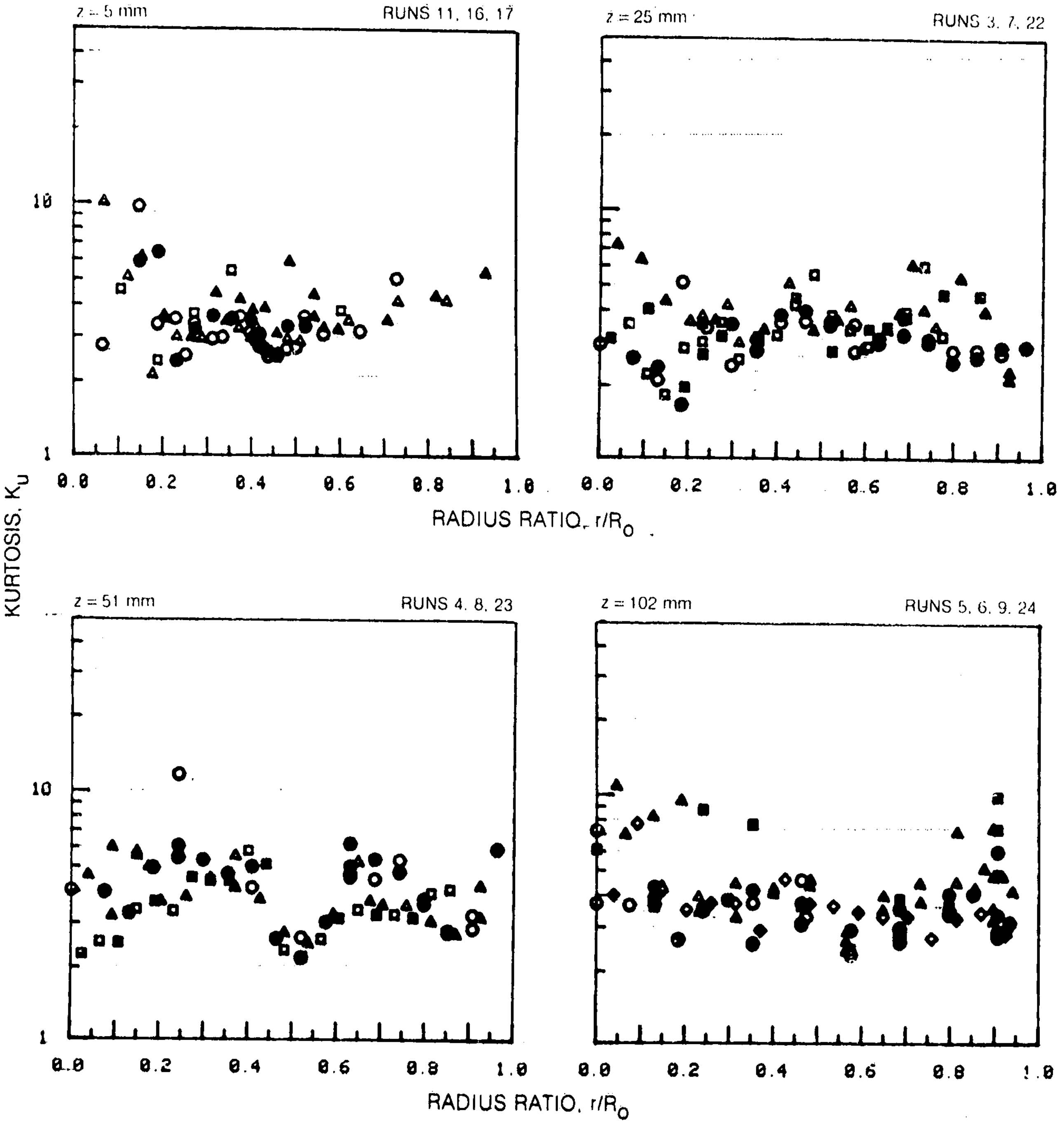

83-3-76 12

ORIGINAL PAGE IS
OF POOR QUALITY

KURTOSIS OF AXIAL VELOCITIES PROFILES (CONT.)

	HORIZONTAL TRAVERSE	VERTICAL TRAVERSE
OPEN SYMBOLS	θ = 90°	θ = 0°
SOLID SYMBOLS	θ = 270°	θ = 180°

SYMBOL	○	●	□	■	△	▲	◇	◆	▽	▼
RUN NOS	14, 10, 42, 44		15, 12, 43, 45		25, 26		40		41	

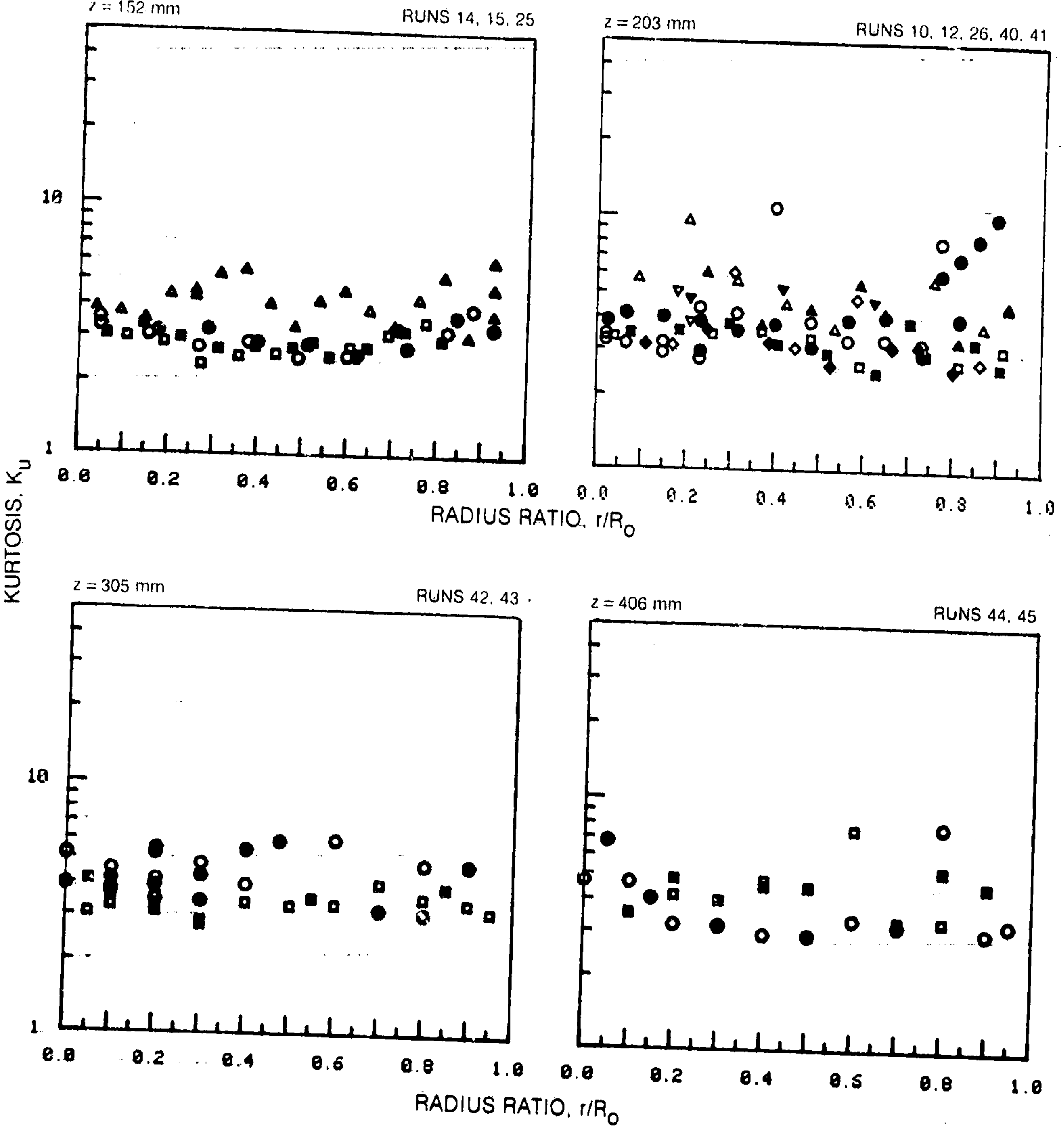

83-3-76-12A

ORIGINAL PAGE IS
OF POOR QUALITY

FIG. 40

SKEWNESS OF RADIAL VELOCITIES PROFILES

	HORIZONTAL TRAVERSE	VERTICAL TRAVERSE
OPEN SYMBOLS	θ = 90°	θ = 0°
SOLID SYMBOLS	θ = 270°	θ = 180°

SYMBOL	○	●	□	■	△	▲	◇	◆	▽	▼
RUN NOS	11, 7, 8, 9		16, 28, 32, 34		47, 46, 54		50		51	

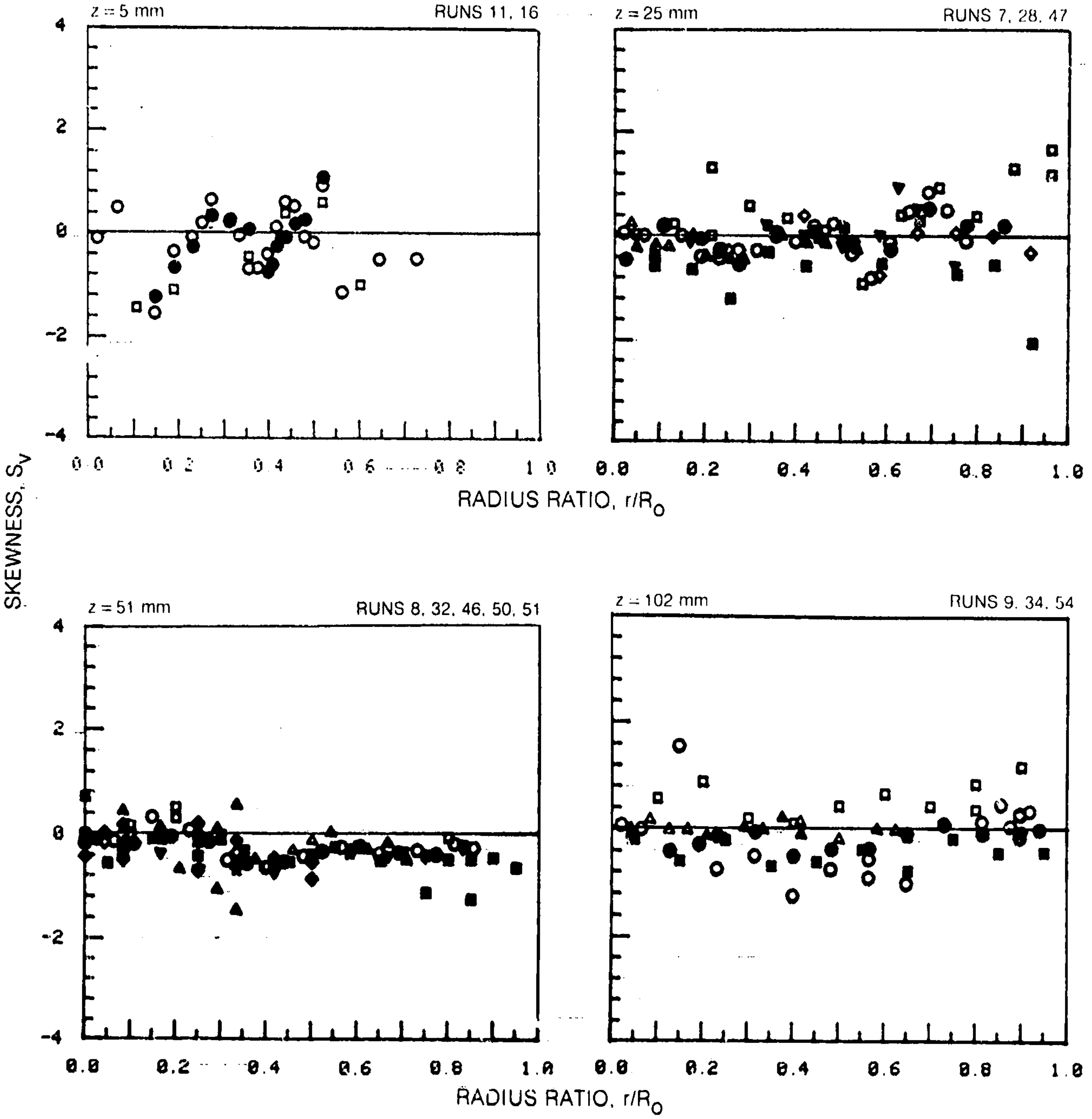

83-3-76-10

FIG. 40 (CONT.)

SKEWNESS OF RADIAL VELOCITIES PROFILES (CONT.)

	HORIZONTAL TRAVERSE	VERTICAL TRAVERSE
OPEN SYMBOLS	θ = 90°	θ = 0°
SOLID SYMBOLS	θ = 270°	θ = 180°

SYMBOL	○	●	□	■	△	▲
RUN NOS	15, 10, 42		36, 38, 45		41	

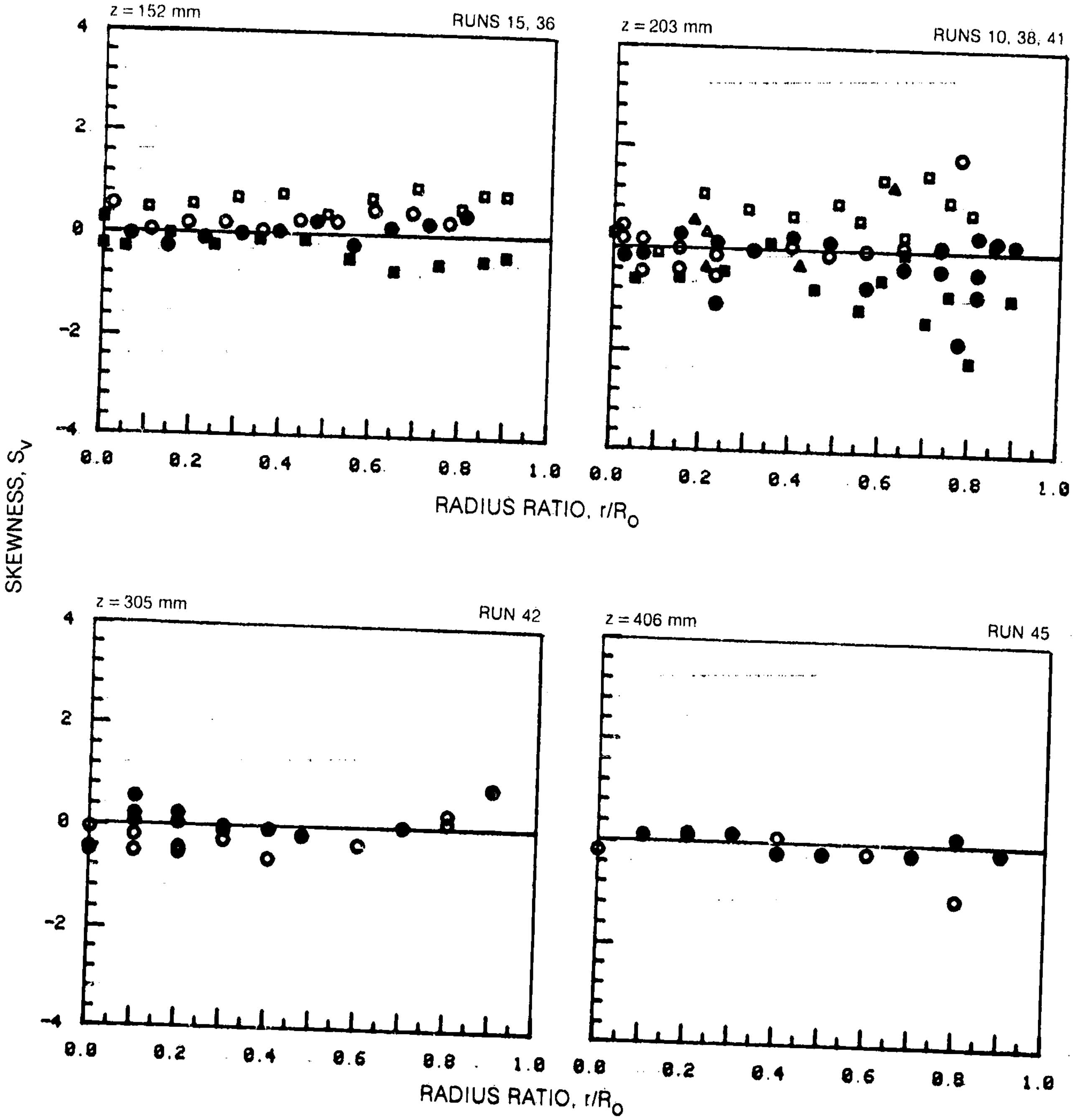

83-3-76-10A

ORIGINAL PAGE IS
OF POOR QUALITY

FIG. 41

KURTOSIS OF RADIAL VELOCITIES PROFILES

	HORIZONTAL TRAVERSE	VERTICAL TRAVERSE
OPEN SYMBOLS	θ = 90°	θ = 0°
SOLID SYMBOLS	θ = 270°	θ = 180°

SYMBOL	○	●	□	■	△	▲	◇	◆	▽	▼
RUN NOS.	11, 7, 8, 9		16, 28, 32, 34		47, 46, 54		50		51	

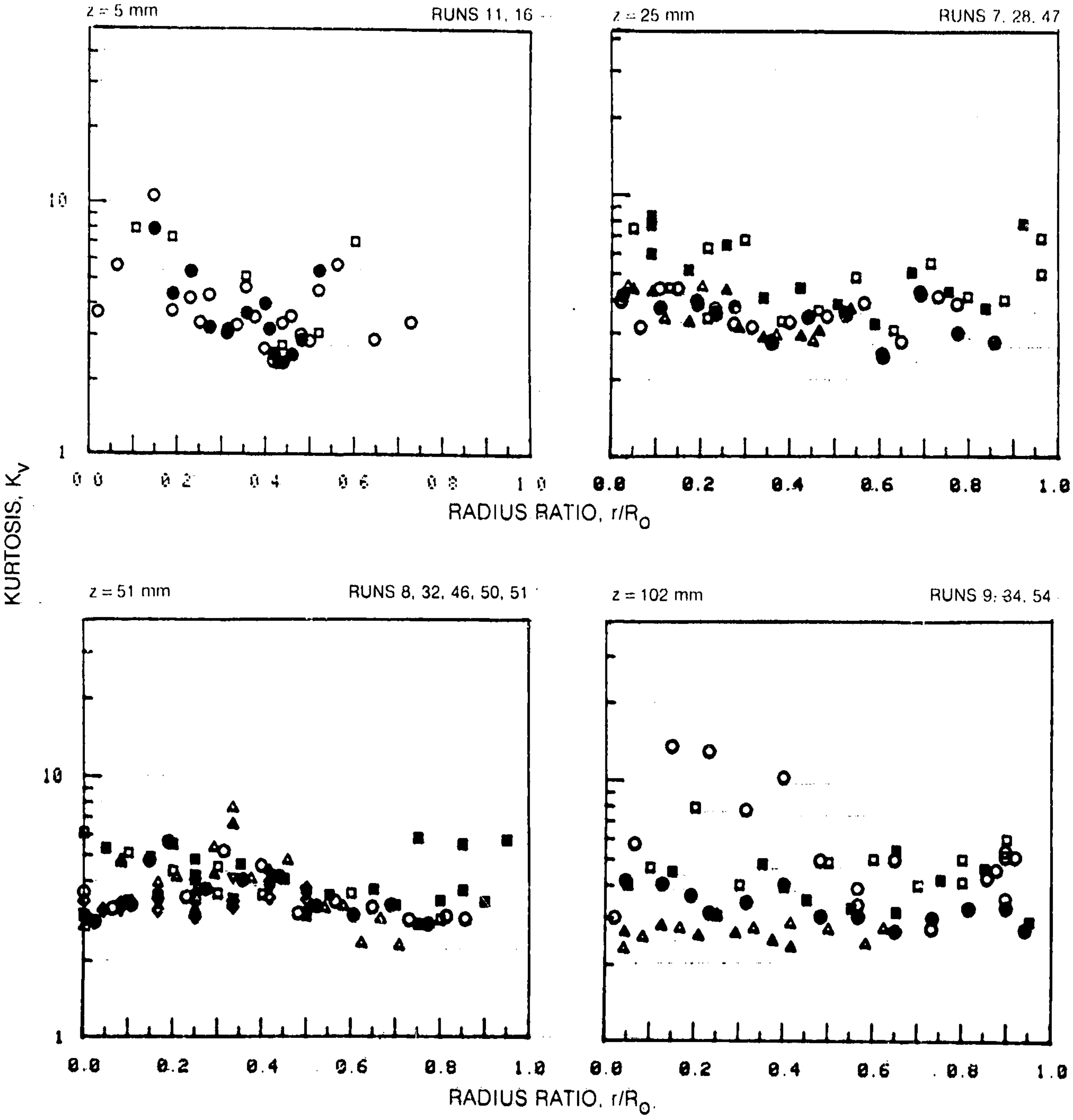

ORIGINAL PAGE IS
OF POOR QUALITY

FIG. 41 (CONT.)

KURTOSIS OF RADIAL VELOCITIES PROFILES (CONT.)

	HORIZONTAL TRAVERSE	VERTICAL TRAVERSE
OPEN SYMBOLS.	θ = 90°	θ = 0°
SOLID SYMBOLS.	θ = 270°	θ = 180°

SYMBOL	○	●	□	■	△	▲
RUN NOS	15, 10, 42		36, 38, 45		41	

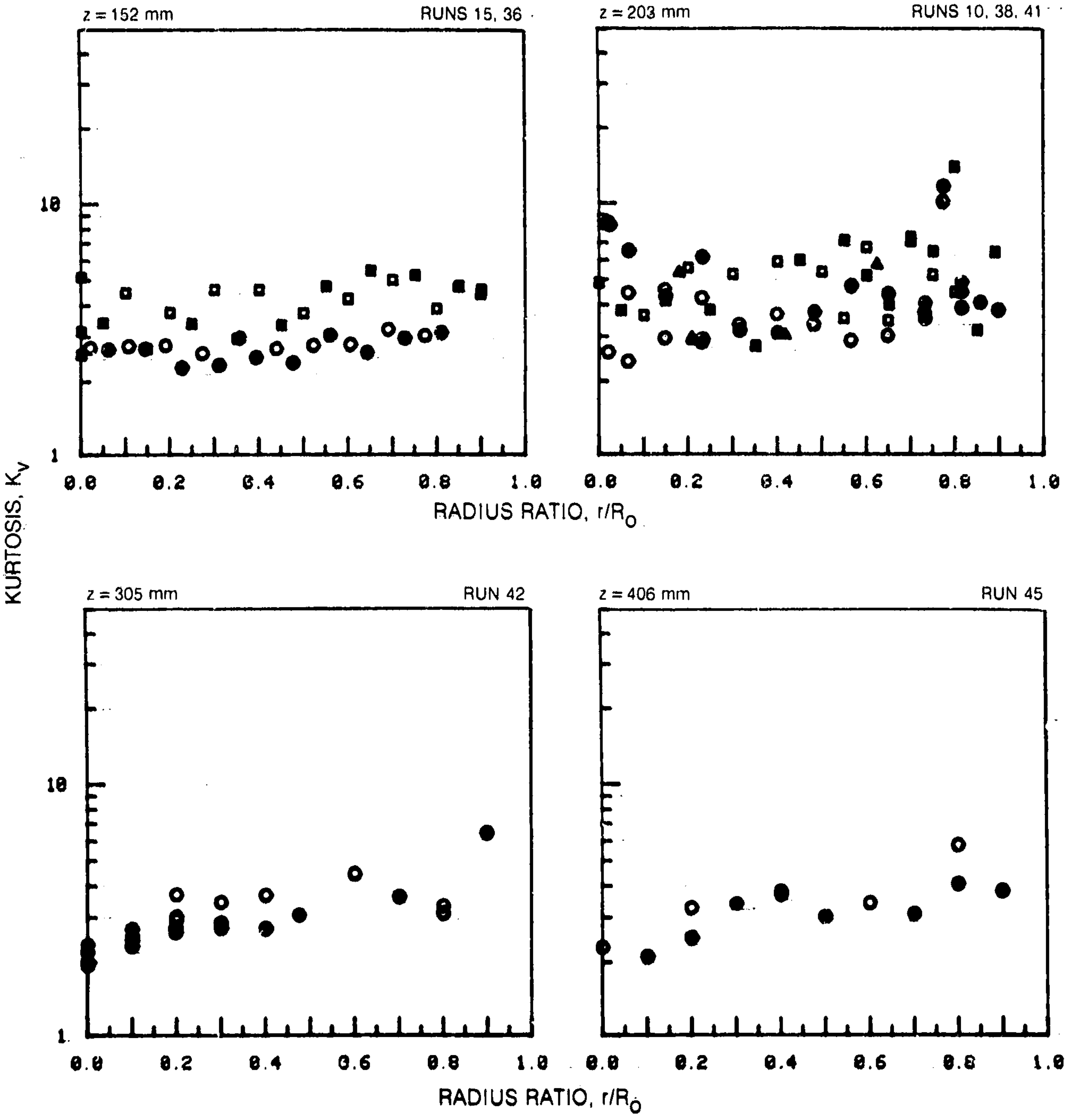

83-3-76-9A

FIG. 42

SKEWNESS OF AZIMUTHAL VELOCITIES PROFILES

	HORIZONTAL TRAVERSE	VERTICAL TRAVERSE
OPEN SYMBOLS	θ = 90°	θ = 0°
SOLID SYMBOLS	θ = 270°	θ = 180°

SYMBOL	○	●	□	■	△	▲	◇	◆	▽	▼
RUN NOS	17, 3, 4, 5		27, 31, 6		47, 46, 33		50, 54		51	

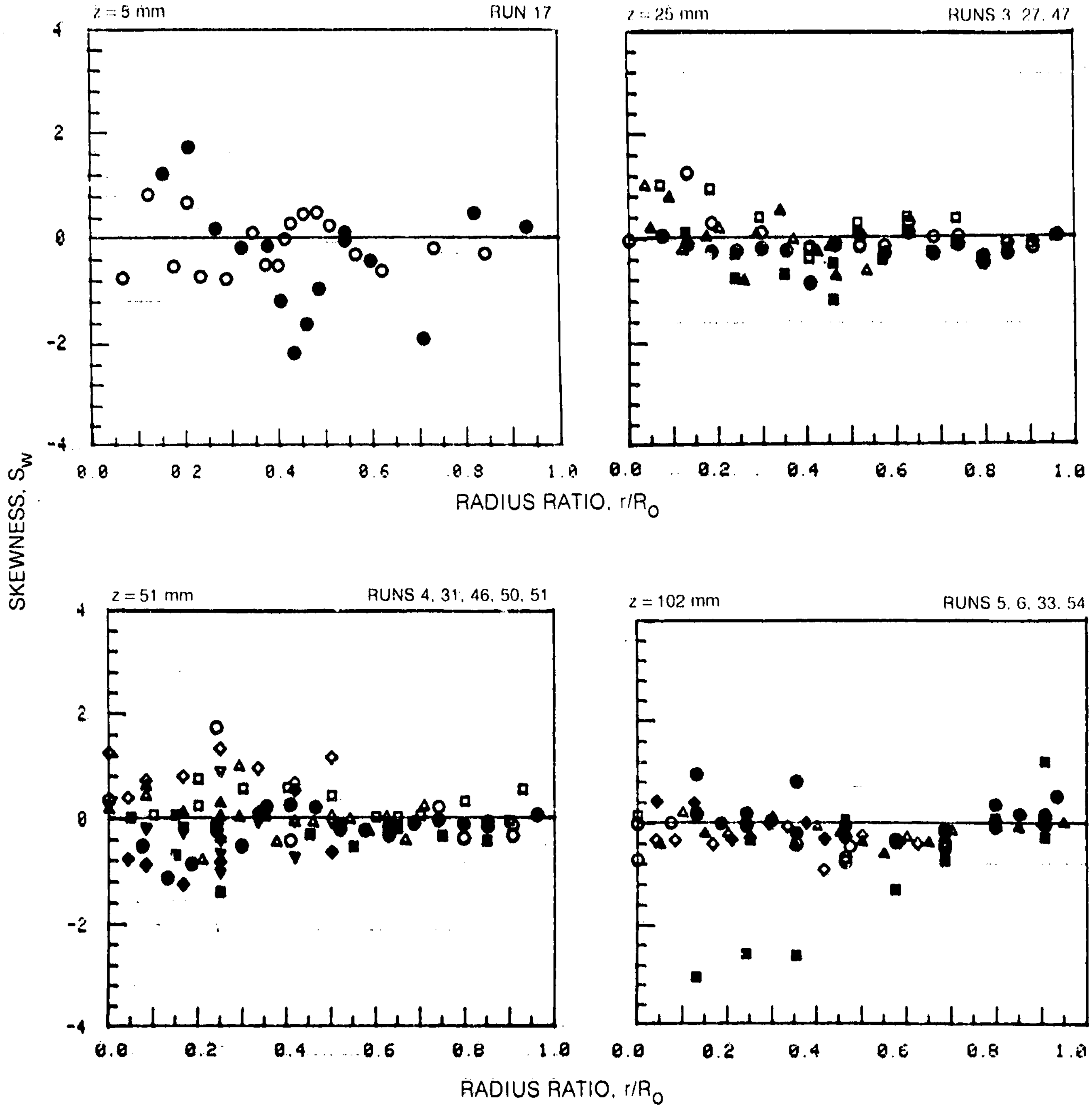

ORIGINAL PAGE IS
OF POOR QUALITY

FIG. 42 (CONT.)

SKEWNESS OF AZIMUTHAL VELOCITIES PROFILES (CONT.)

	HORIZONTAL TRAVERSE	VERTICAL TRAVERSE
OPEN SYMBOLS	θ = 90°	θ = 0°
SOLID SYMBOLS	θ = 270°	θ = 180°

SYMBOL	○	●	□	■	△	▲
RUN NOS.	14, 12, 43, 44		35, 37		40	

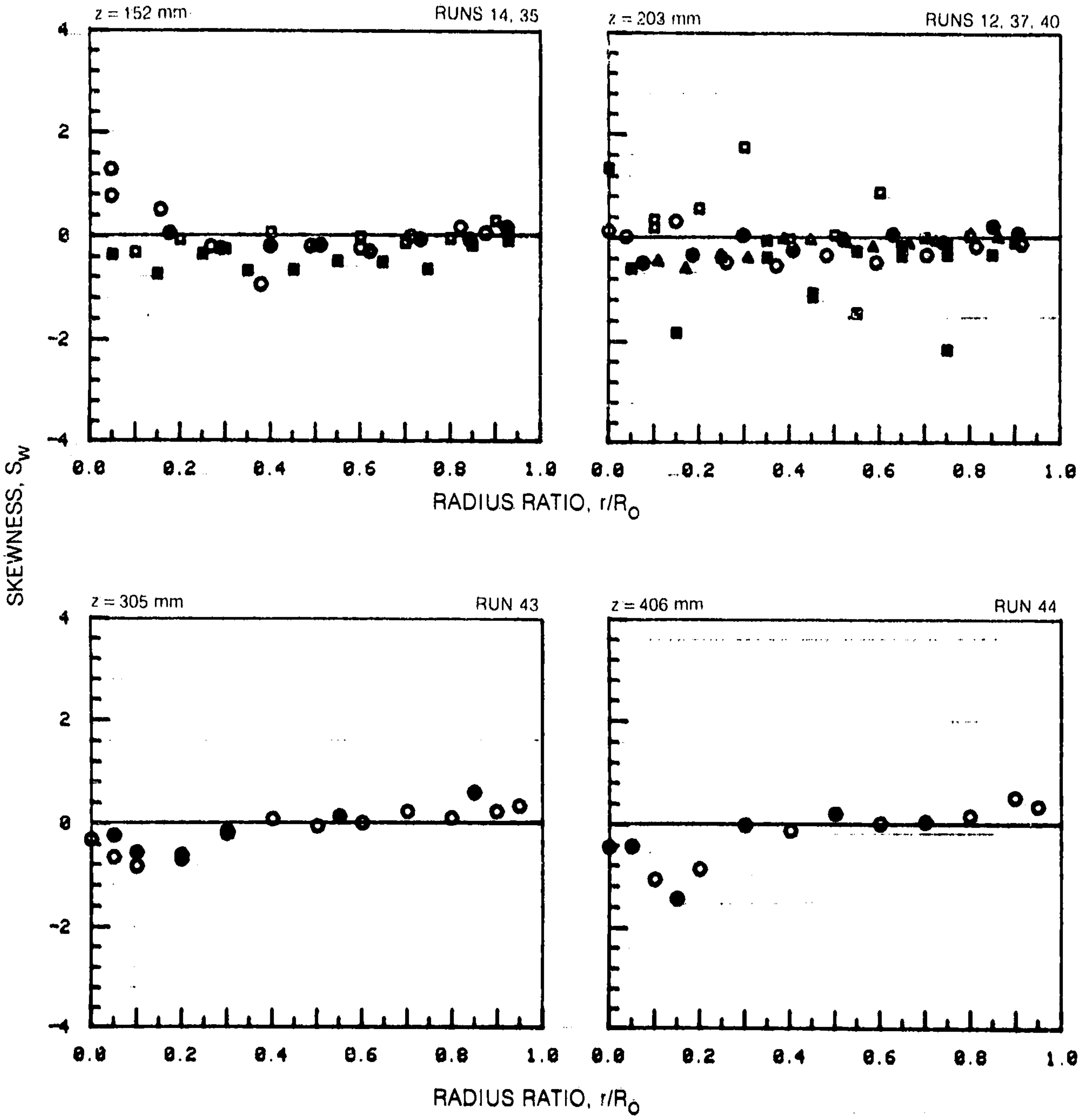

83-3-76-8A

ORIGINAL PAGE IS
OF POOR QUALITY

FIG. 43

KURTOSIS OF AZIMUTHAL VELOCITIES PROFILES

	HORIZONTAL TRAVERSE	VERTICAL TRAVERSE
OPEN SYMBOLS	θ = 90°	θ = 0°
SOLID SYMBOLS	θ = 270°	θ = 180°

SYMBOL	○	●	□	■	△	▲	◇	◆	▽	▼
RUN NOS	17, 3, 4, 5		27, 31, 6		47, 46, 33		50, 54		51	

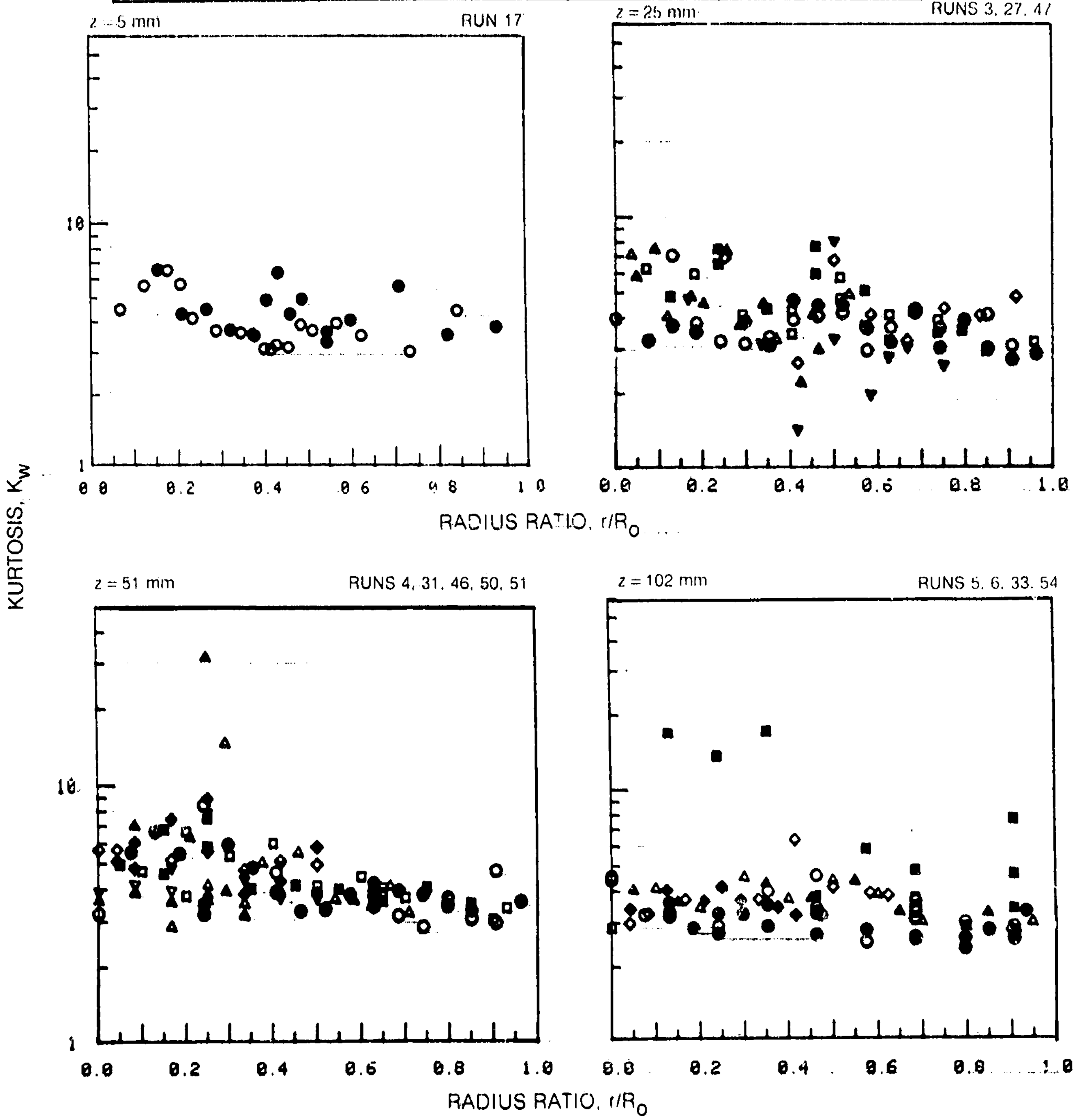

83-3-76-7

ORIGINAL PAGE IS
OF POOR QUALITY

KURTOSIS OF AZIMUTHAL VELOCITIES PROFILES (CONT.)

	HORIZONTAL TRAVERSE	VERTICAL TRAVERSE
OPEN SYMBOLS	$\theta = 90°$	$\theta = 0°$
SOLID SYMBOLS	$\theta = 270°$	$\theta = 180°$

SYMBOL	○	●	□	■	△	▲
RUN NOS	14, 12, 43, 44		35, 37		40	

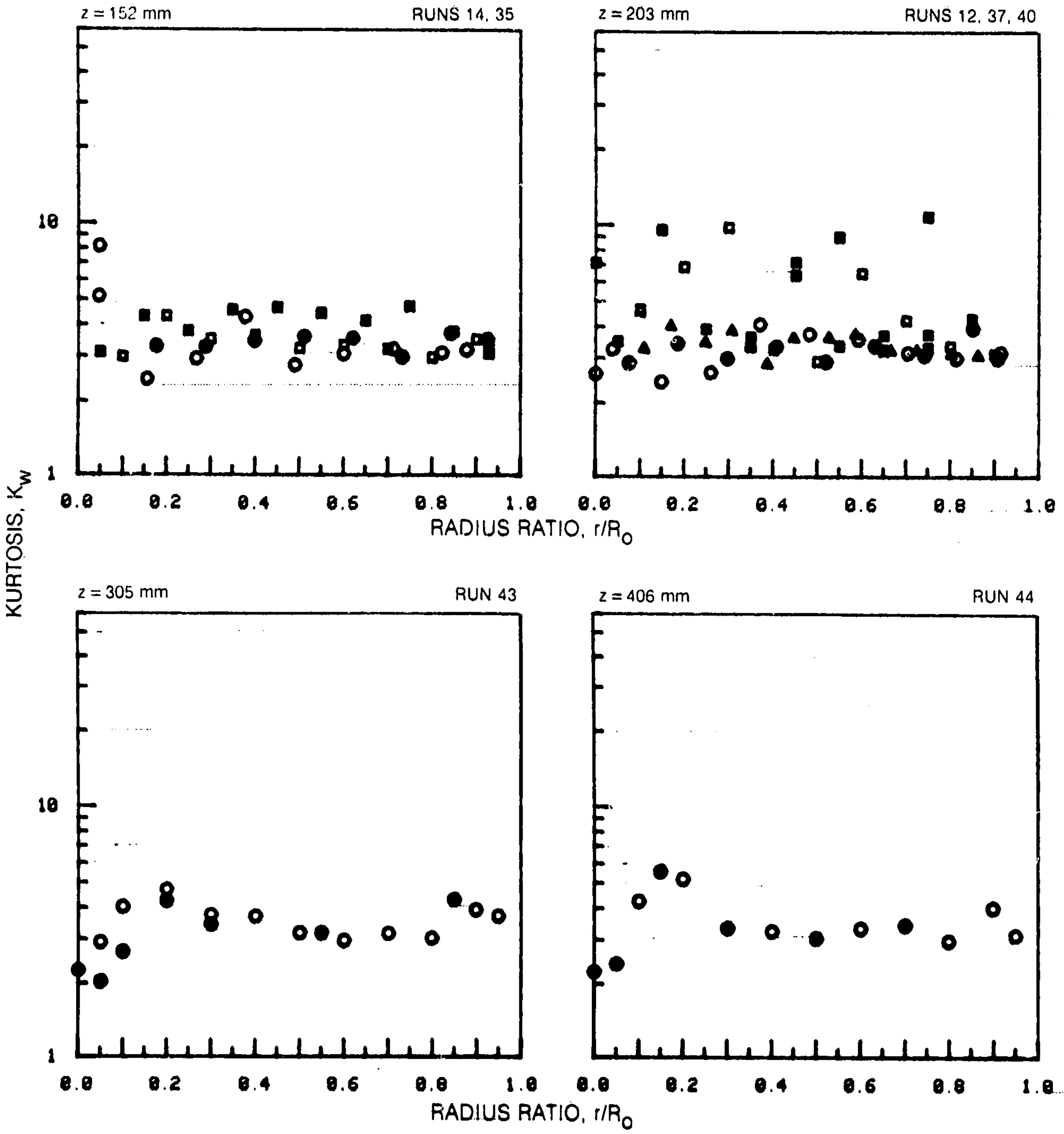

83-3-76-7A

C-3

FIG. 44

SKEWNESS OF INNER JET FLUID CONCENTRATION PROFILES

	HORIZONTAL TRAVERSE	VERTICAL TRAVERSE
OPEN SYMBOLS:	θ = 90°	θ = 0°
SOLID SYMBOLS	θ = 270°	θ = 180°

SYMBOL	○	●	□	■	△	▲	◇	◆
RUN NOS	20, 22, 23, 24		21, 27, 31, 33		29, 28, 32, 34		30	

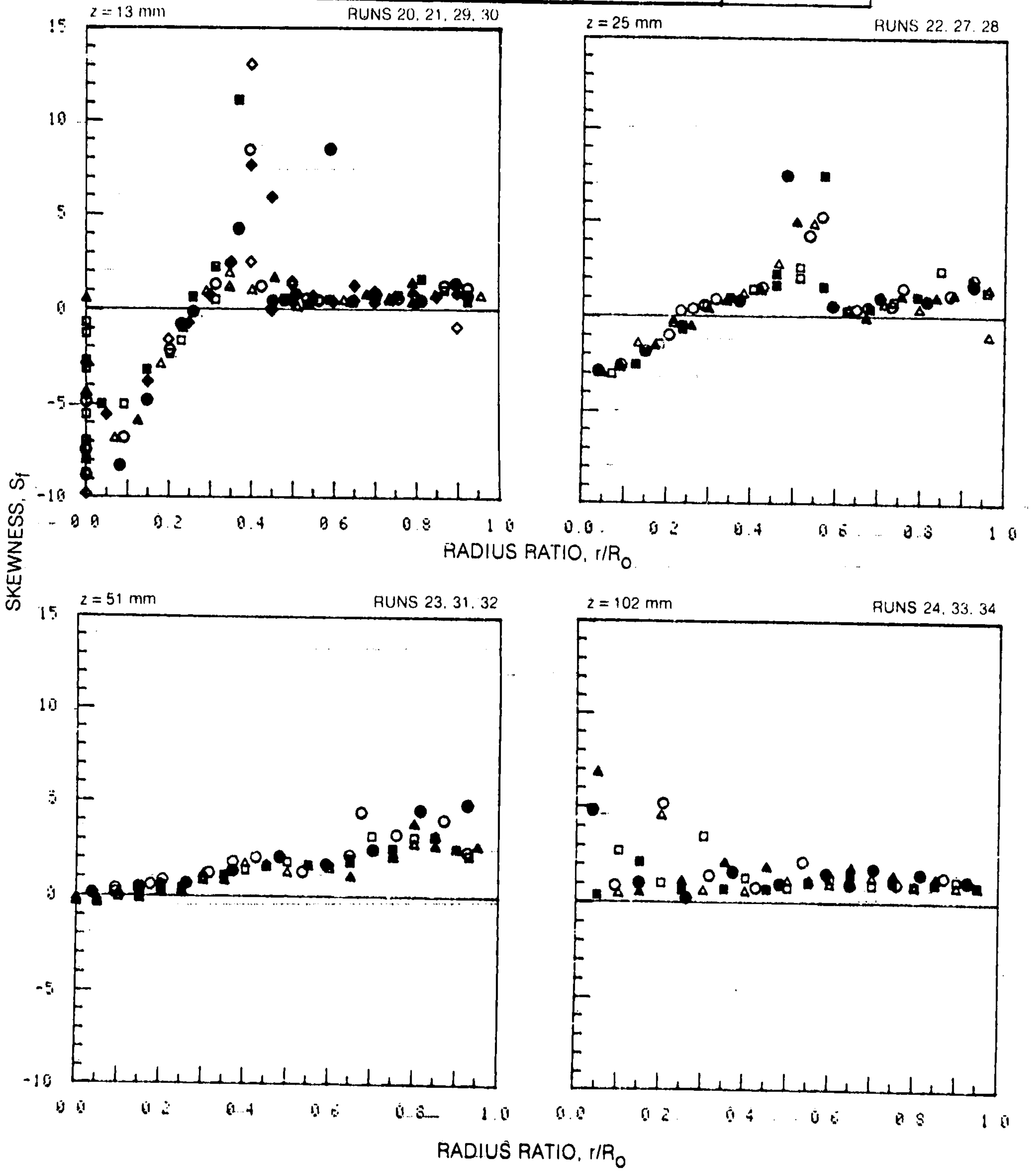

FIG. 44 (CONT.)

ORIGINAL PAGE IS
OF POOR QUALITY

SKEWNESS OF INNER JET FLUID CONCENTRATION PROFILES (CONT)

	HORIZONTAL TRAVERSE	VERTICAL TRAVERSE
OPEN SYMBOLS:	$\theta = 90°$	$\theta = 0°$
SOLID SYMBOLS:	$\theta = 270°$	$\theta = 180°$

SYMBOL	○	●	□	■	△	▲
RUN NOS.	25, 26		35, 37		36, 38	

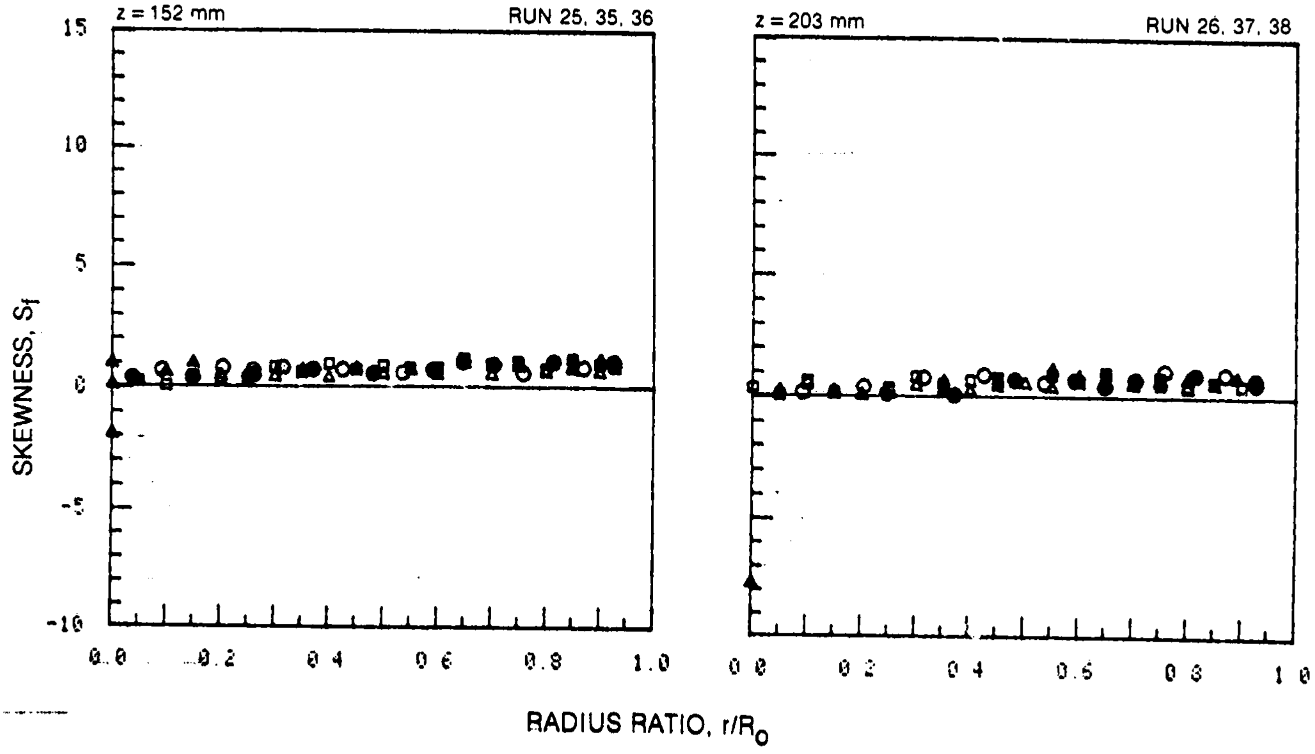

82-11-36-8

FIG. 45

KURTOSIS OF INNER JET FLUID CONCENTRATION PROFILES

	HORIZONTAL TRAVERSE	VERTICAL TRAVERSE
OPEN SYMBOLS:	θ = 90°	θ = 0°
SOLID SYMBOLS	θ = 270°	θ = 180°

SYMBOL	○	●	□	■	△	▲	◇	◆
RUN NOS	20, 22, 23, 24		21, 27, 31, 33		29, 28, 32, 34		30	

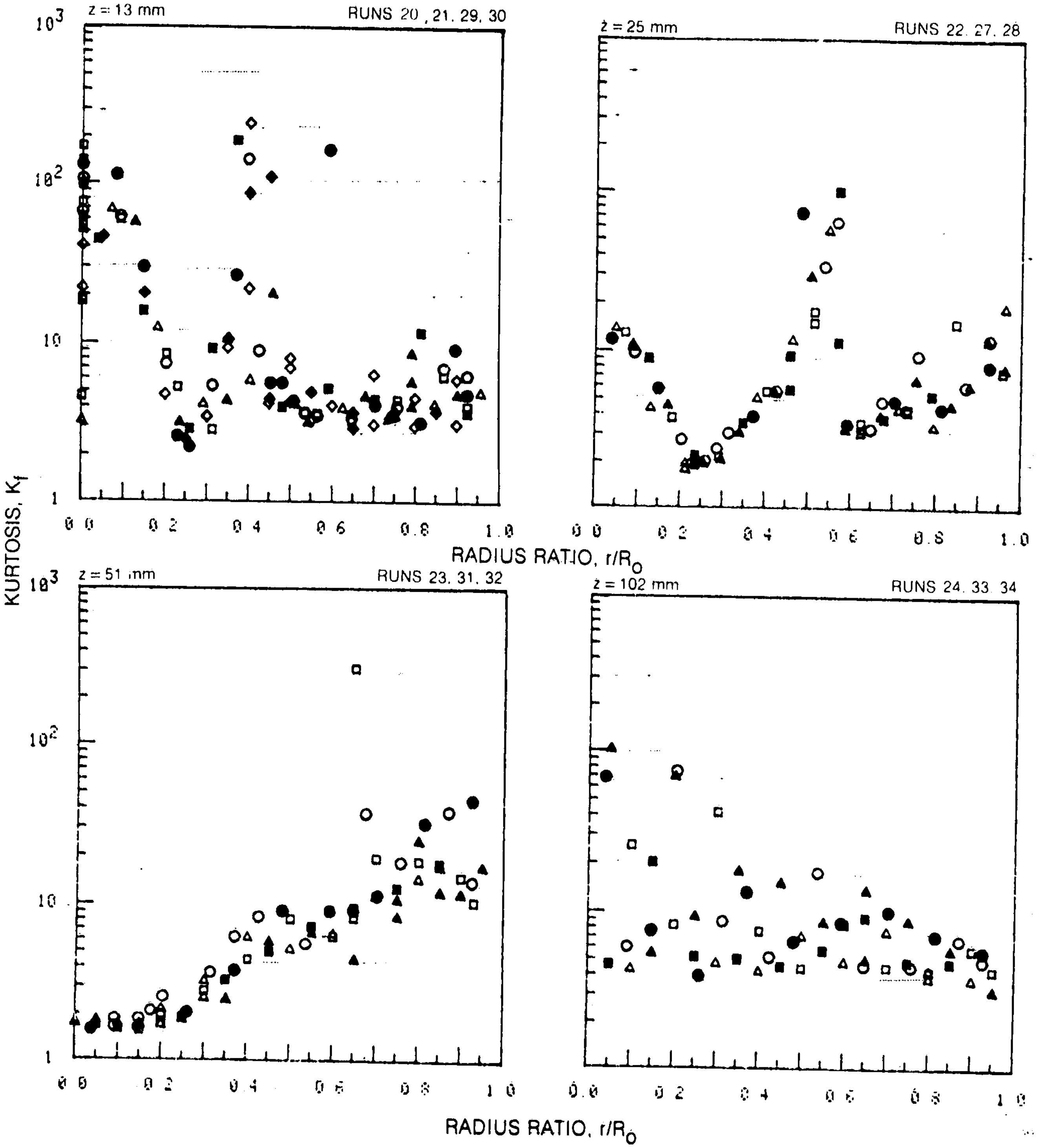

FIG. 45 (CONT.)

KURTOSIS OF INNER JET FLUID CONCENTRATION PROFILES (CONT)

	HORIZONTAL TRAVERSE	VERTICAL TRAVERSE
OPEN SYMBOLS:	$\theta = 90°$	$\theta = 0°$
SOLID SYMBOLS:	$\theta = 270°$	$\theta = 180°$

SYMBOL	○	●	□	■	△	▲
RUN NOS	25, 26		35, 37		36, 38	

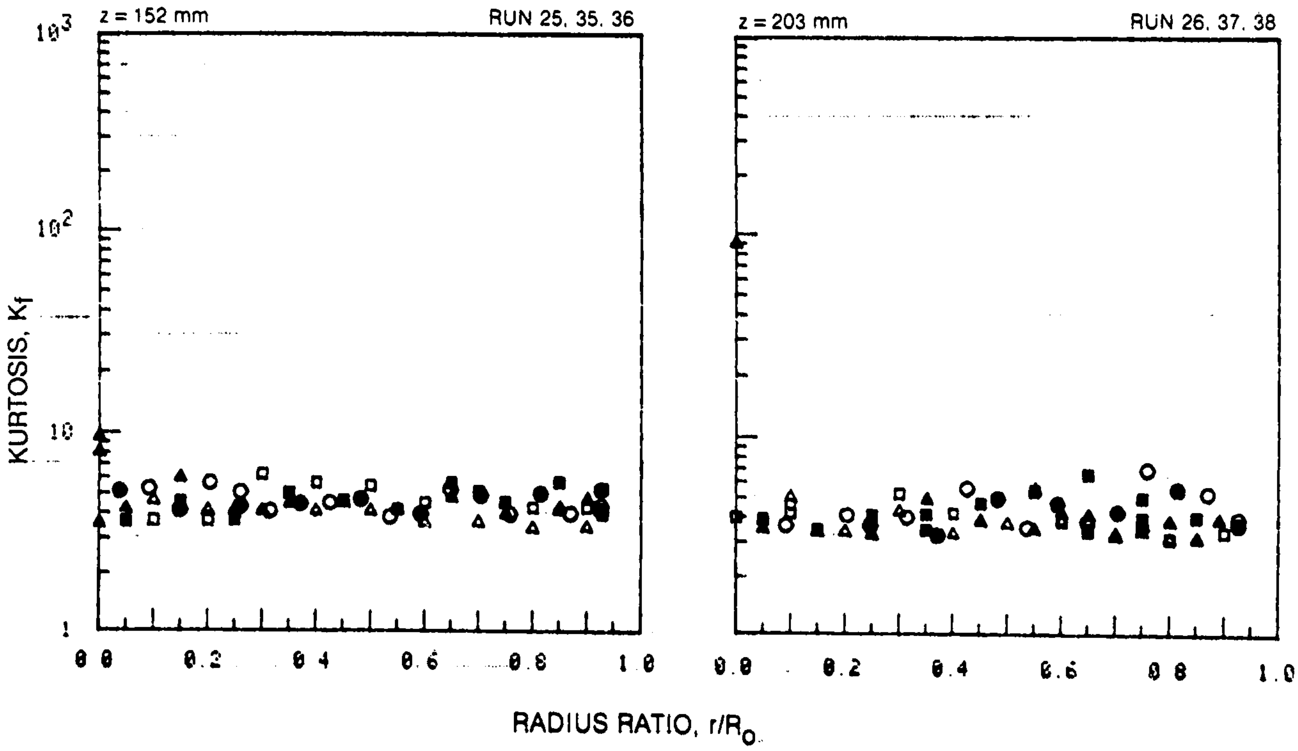

82-11-36-6

TURBULENT MOMENTUM TRANSPORT RATE, $\overline{uv}$, PROBABILITY DENSITY FUNCTIONS

AXIAL LOCATION: 25 mm

DATA FROM RUN 7

r/R_o	uv	σ_{uv}	S_{uv}	K_{uv}
0.00	-0.0003	0.060	1.58	19.27
0.13	0.0118	0.055	-0.04	6.19
0.24	0.0083	0.072	0.25	10.15
0.36	-0.0623	0.164	-1.11	8.21
0.52	-0.0119	0.041	-1.44	10.42
0.68	0.0254	0.085	1.26	12.50

$\Delta(uv) = 0.02\ m^2/s^2$

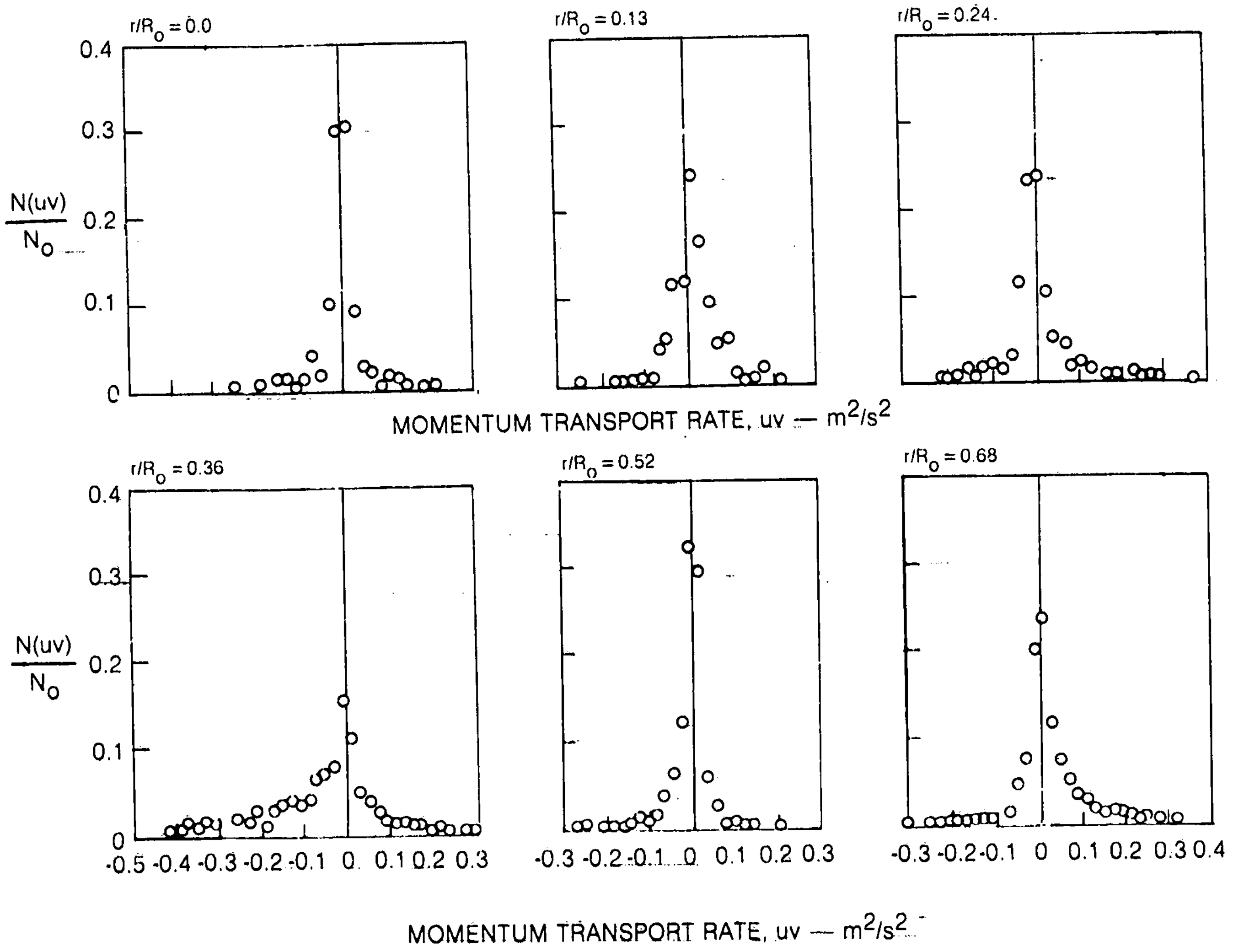

ORIGINAL PAGE IS
OF POOR QUALITY

FIG. 47

TURBULENT MOMENTUM TRANSPORT RATE, $\overline{uw}$, PROBABILITY DENSITY FUNCTIONS

AXIAL LOCATION: 25 mm

DATA FROM RUN 3

r/R_o	uw	σ_{uw}	S_{uw}	K_{uw}
0.00	0.0106	0.055	0.42	8.47
0.13	-0.0008	0.074	0.18	6.13
0.24	-0.0007	0.062	-1.05	12.94
0.36	-0.0018	0.127	-0.16	5.55
0.52	0.0040	0.033	0.79	10.21
0.68	0.0004	0.052	0.46	20.01

$\Delta(uw) = 0.02\ m^2/s^2$

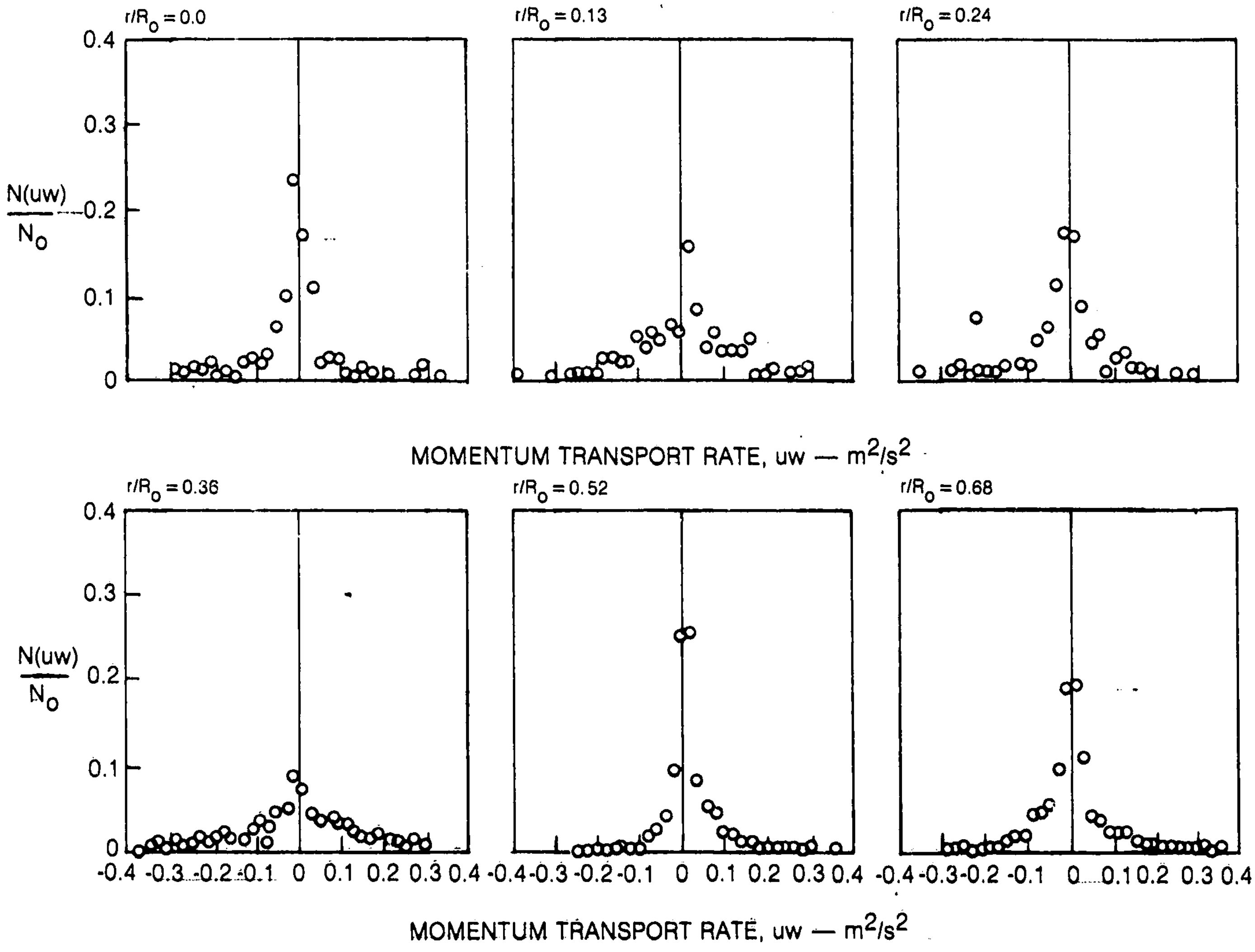

83-7-19-6

ORIGINAL PAGE IS
OF POOR QUALITY

FIG. 48

TURBULENT MOMENTUM TRANSPORT RATE, $\overline{wv}$, PROBABILITY DENSITY FUNCTIONS

AXIAL LOCATION: 25 mm

AVERAGES OF DATA FROM RUNS 47(○), 48(□) AND 49(△)

r/R_o	wv	σ_{wv}	S_{wv}	K_{wv}
0.00	0.0023	0.026	1.28	14.8
0.13	0.0039	0.034	1.45	12.5
0.24	-0.0004	0.032	1.12	23.4
0.36	-0.0134	0.120	-0.15	7.9
0.52	0.0035	0.034	0.37	14.5
0.68	0.0193	0.117	1.64	13.9

$\Delta(wv) = 0.1\ m^2/s^2$

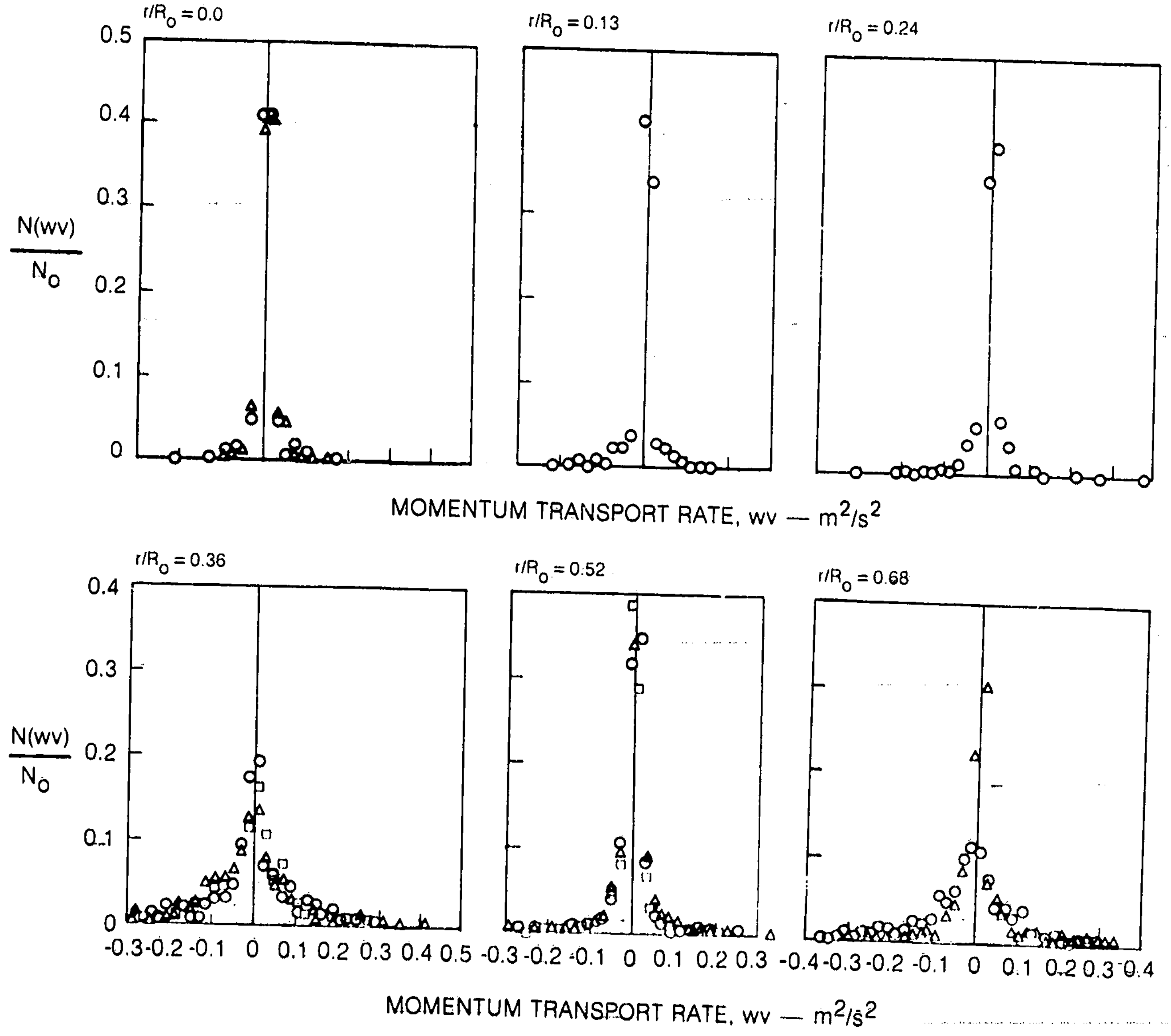

FIG. 49

TURBULENT RADIAL MASS TRANSPORT RATE, $\overline{vf}$, PROBABILITY DENSITY FUNCTIONS

AXIAL LOCATION: 25 mm

DATA FROM RUN 28

r/R_0	$\overline{vf}$	σ_{vf}	S_{vf}	K_{vf}
0.00	-0.0001	0.018	-1.38	28.8
0.13	0.0002	0.018	1.62	32.8
0.24	0.0004	0.056	0.87	15.0
0.36	0.0041	0.068	0.57	12.7
0.52	-0.0004	0.003	0.13	22.3
0.68	-0.0001	0.002	-1.22	18.8

$\Delta(vf) = 0.04$ m/s

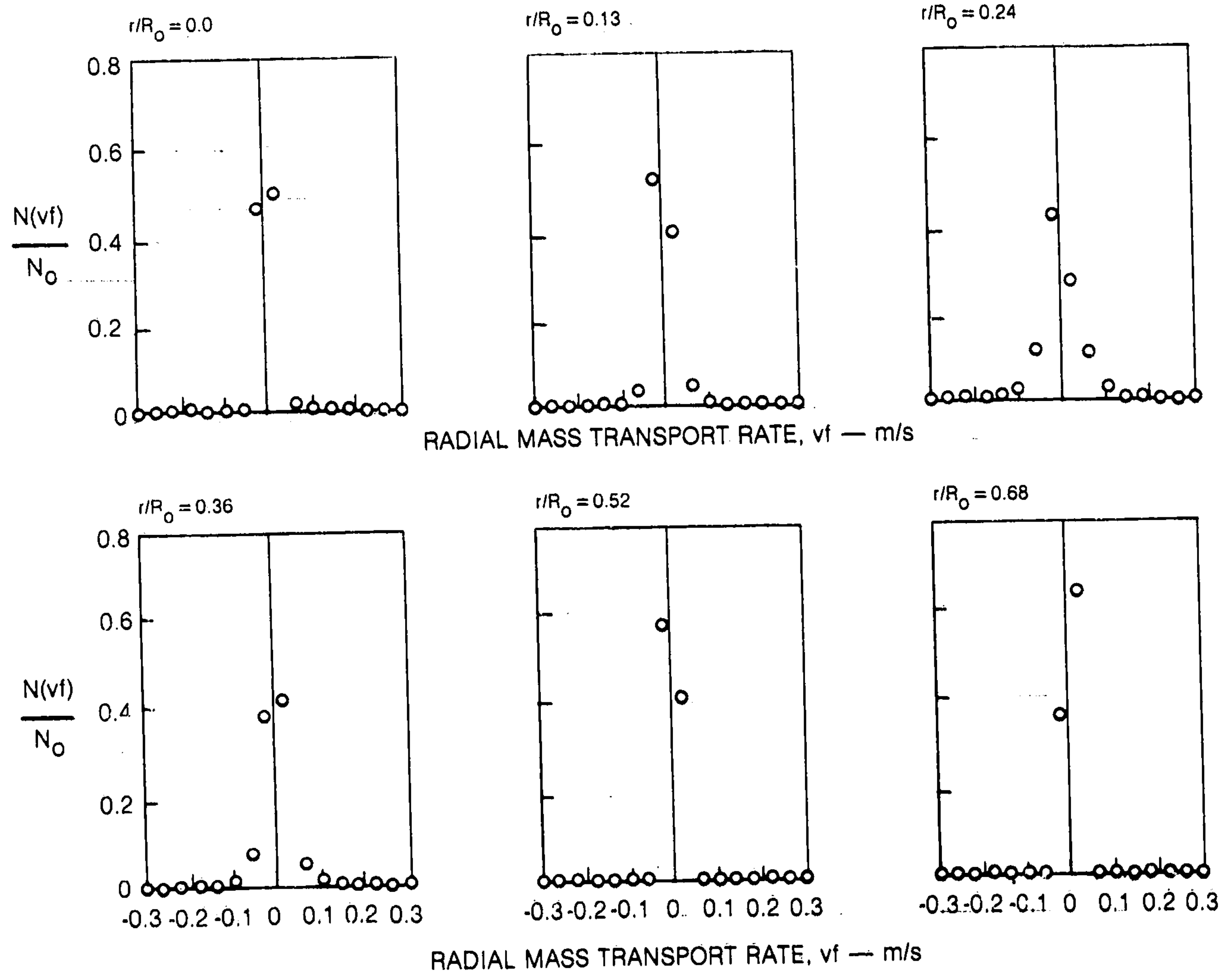

83–7–19–4

ORIGINAL PAGE IS
OF POOR QUALITY

FIG. 50

TURBULENT AXIAL MASS TRANSPORT RATE, $\overline{uf}$, PROBABILITY DENSITY FUNCTIONS

AXIAL LOCATION: 25 mm

DATA FROM RUN 22

r/R_o	uf	σ_{uf}	S_{uf}	K_{uf}
0.00	0.0052	0.039	9.17	110.6
0.13	0.0137	0.089	1.13	21.7
0.24	0.0318	0.105	0.82	6.9
0.36	-0.0020	0.045	-0.38	6.6
0.52	0.0001	0.003	6.30	137.7
0.68	-0.0005	0.003	-1.65	18.4

$\Delta(uf) = 0.04$ m/s

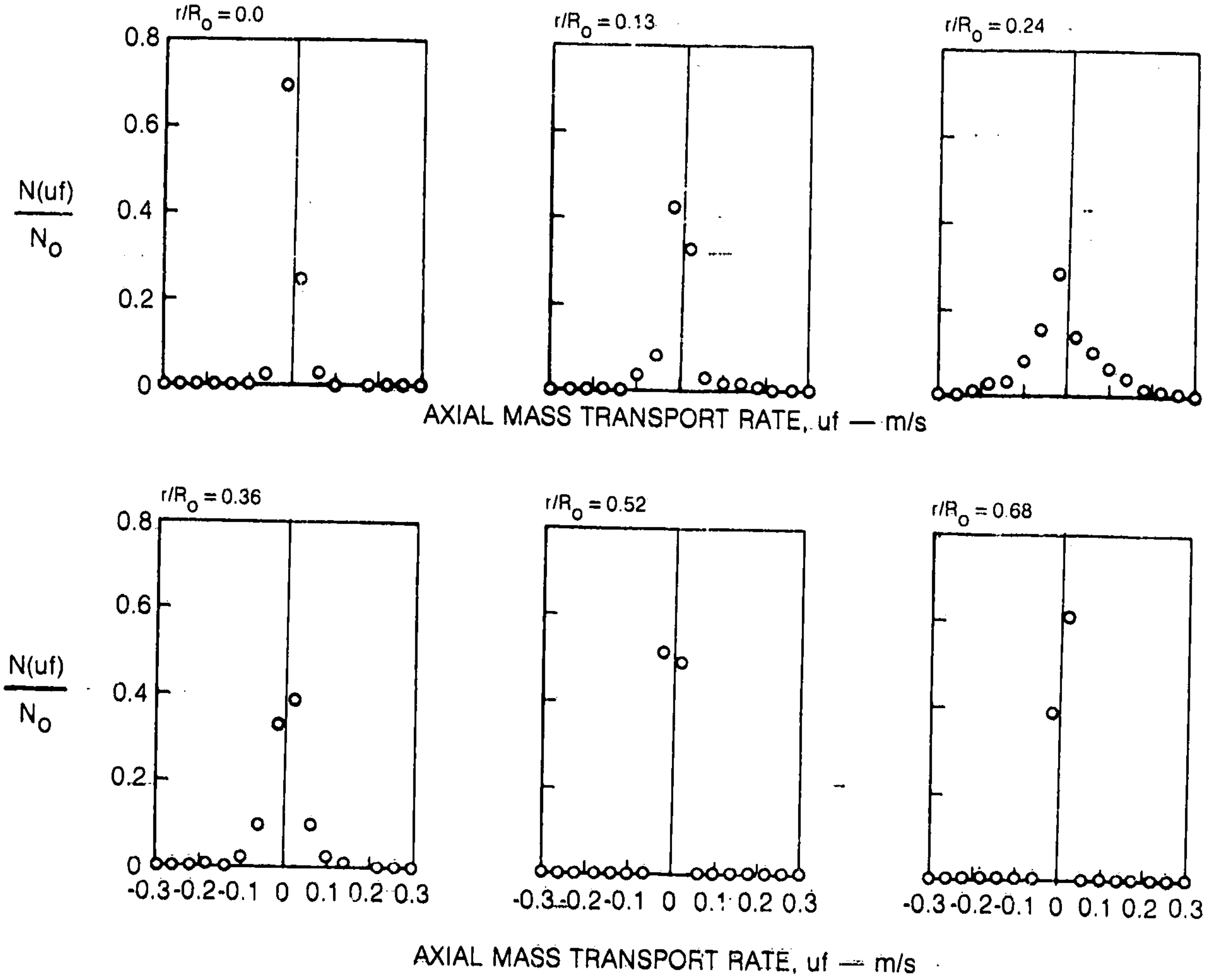

ORIGINAL PAGE IS
OF POOR QUALITY

FIG. 51

TURBULENT AZIMUTHAL MASS TRANSPORT RATE, $\overline{wf}$, PROBABILITY DENSITY FUNCTIONS

AXIAL LOCATION: 25 mm

DATA FROM RUN 27

r/R_o	$\overline{wf}$	σ_{wf}	S_{wf}	K_{wf}
0.0	-0.0001	0.022	-1.56	42.2
0.13	0.0002	0.028	-1.30	18.2
0.24	0.0187	0.057	1.39	15.0
0.36	-0.0005	0.041	0.76	12.8
0.52	0.0003	0.006	3.76	75.1
0.68	0.0003	0.003	-2.78	30.2

$\Delta(wf) = 0.04$ m/s

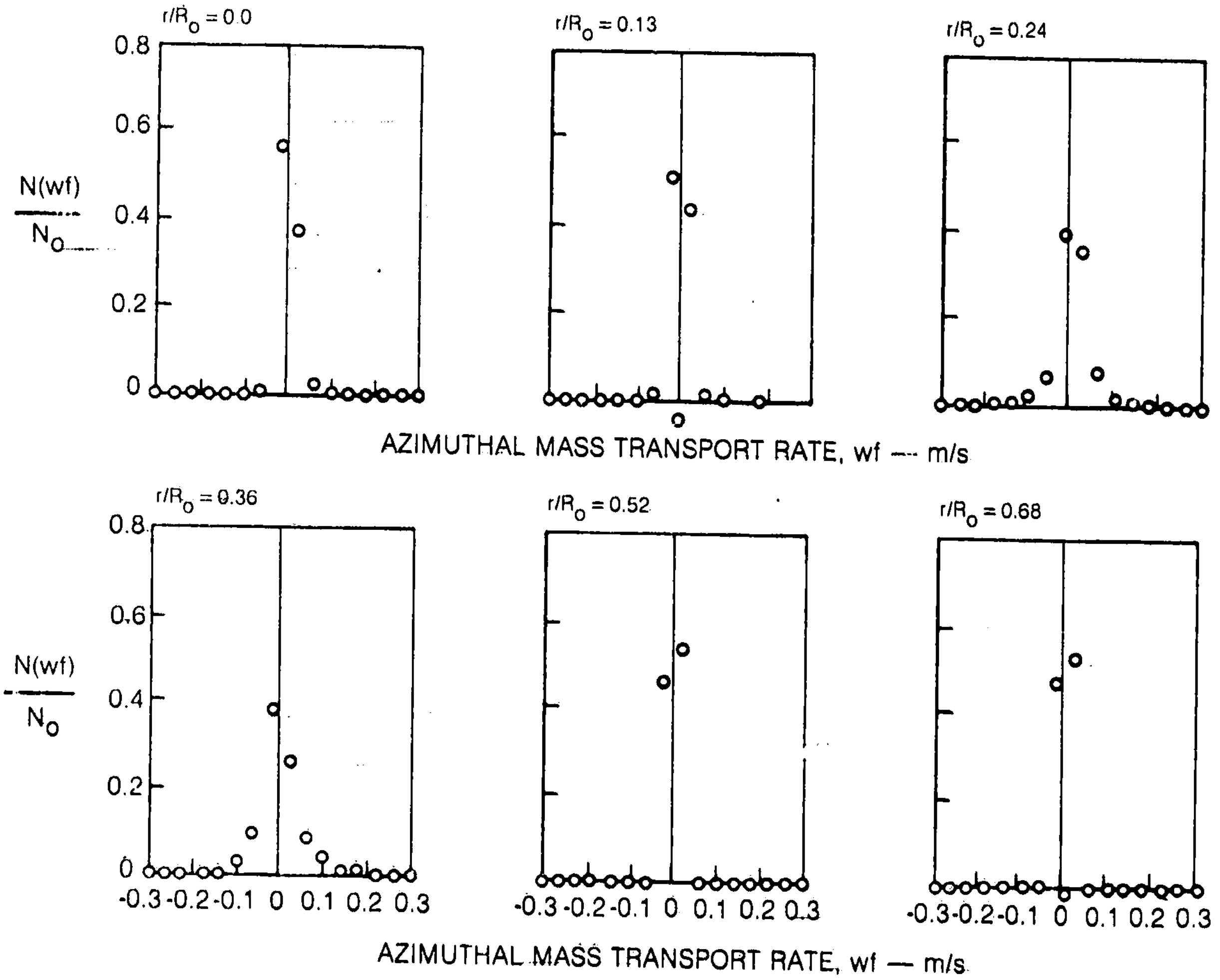

ORIGINAL PAGE IS
OF POOR QUALITY

FIG. 52

SECOND CENTRAL MOMENT OF $\overline{uv}$ TURBULENT TRANSPORT RATE PROFILES

	HORIZONTAL TRAVERSE	VERTICAL TRAVERSE
OPEN SYMBOLS	θ = 90°	θ = 0°
SOLID SYMBOLS	θ = 270°	θ = 180°

SYMBOL	○	●	◇	◆
RUN NOS.	11, 7, 8, 9		16	

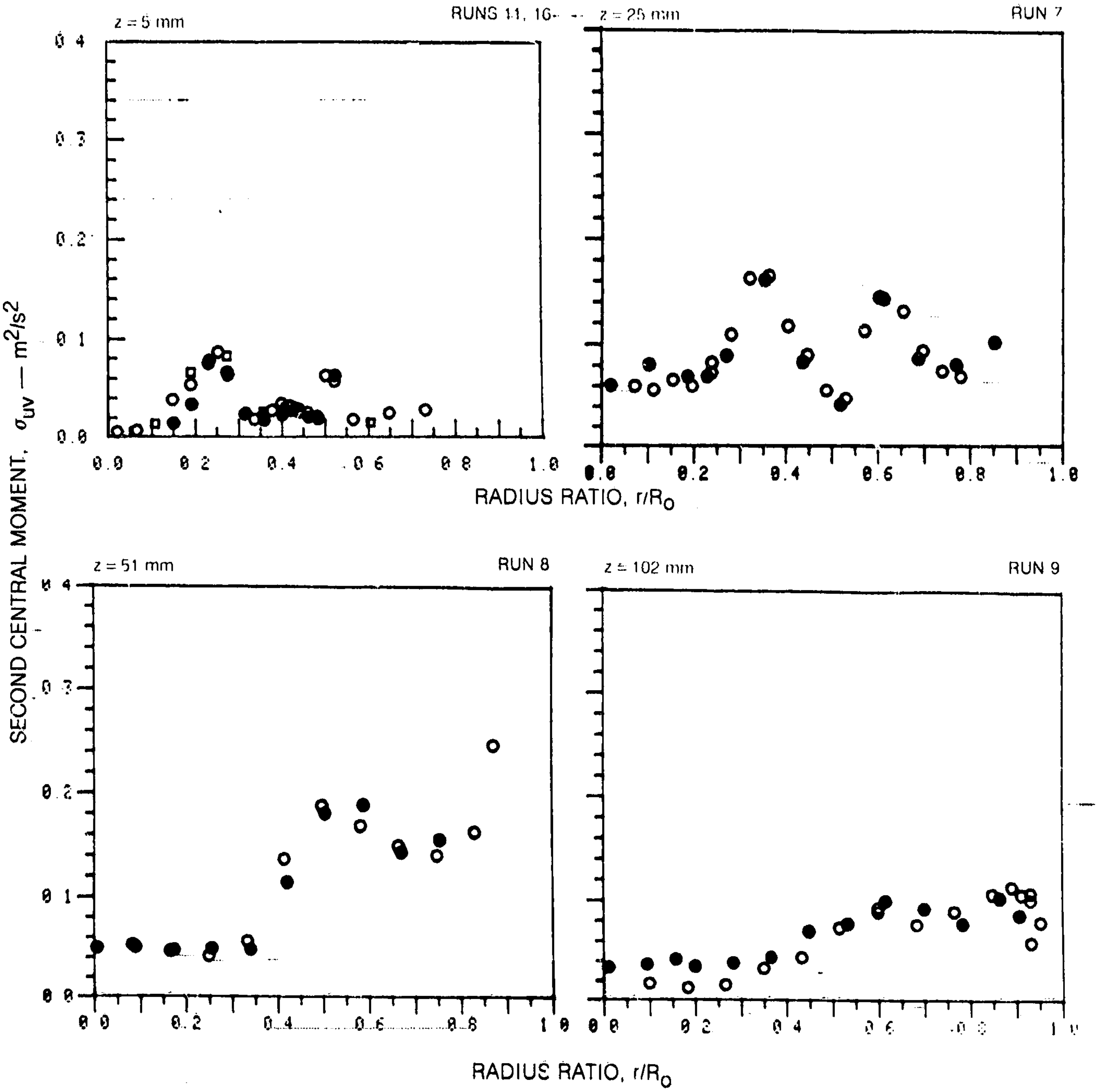

ORIGINAL PAGE IS
OF POOR QUALITY

FIG. 52 (CONT.)

SECOND CENTRAL MOMENT OF $\overline{uv}$ TURBULENT TRANSPORT RATE PROFILES (CONT.)

	HORIZONTAL TRAVERSE	VERTICAL TRAVERSE
OPEN SYMBOLS	θ = 90°	θ = 0°
SOLID SYMBOLS	θ = 270°	θ = 180°

SYMBOL	○	●	□	■
RUN NOS	15, 10, 42, 45		41	

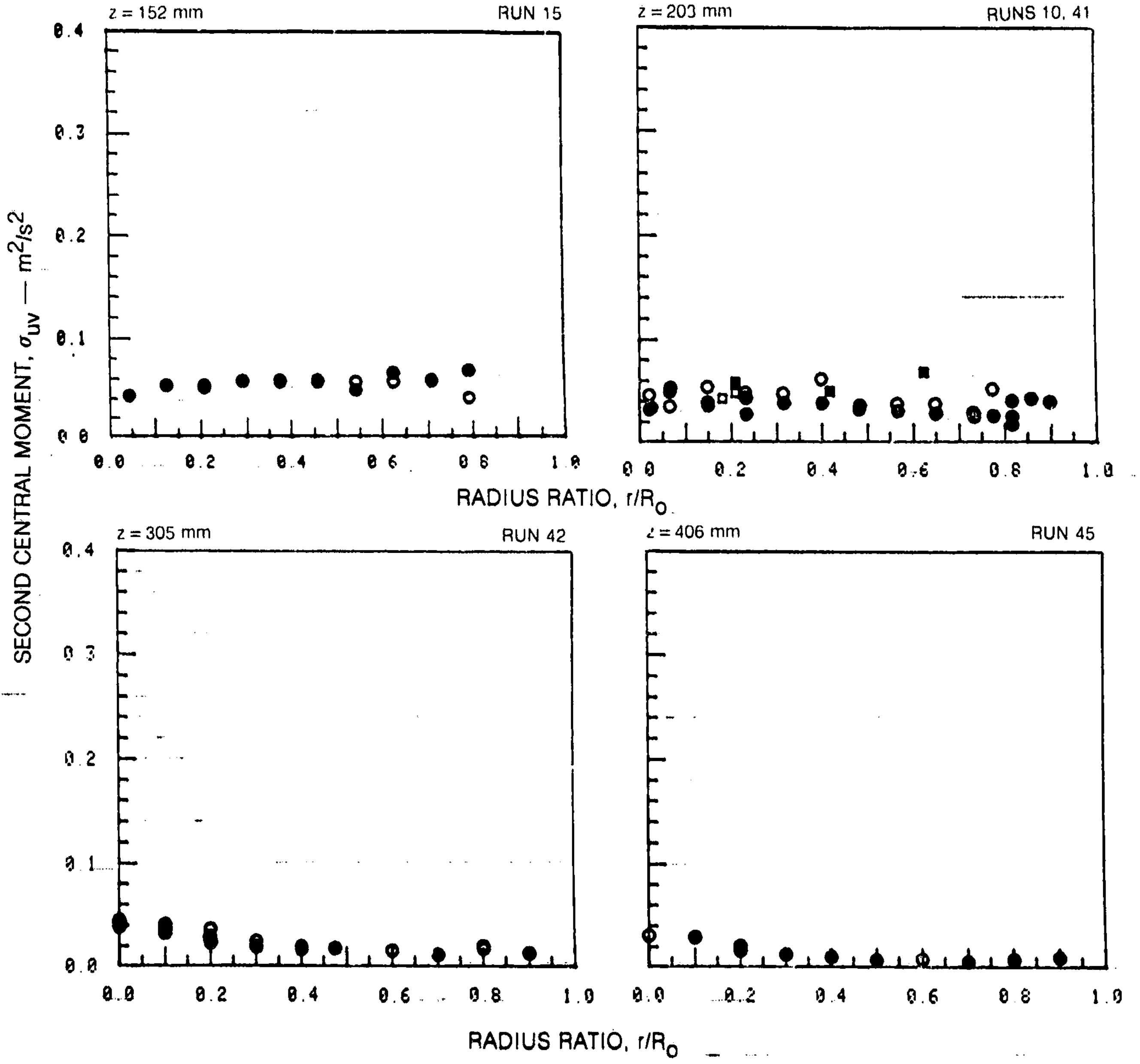

83-3-76-13

SKEWNESS OF $\overline{uv}$ TURBULENT MOMENTUM TRANSPORT RATE PROFILES

	HORIZONTAL TRAVERSE	VERTICAL TRAVERSE
OPEN SYMBOLS	θ = 90°	θ = 0°
SOLID SYMBOLS	θ = 270°	θ = 180°

SYMBOL	○	●	□	■
RUN NOS	11, 7, 8, 9		16	

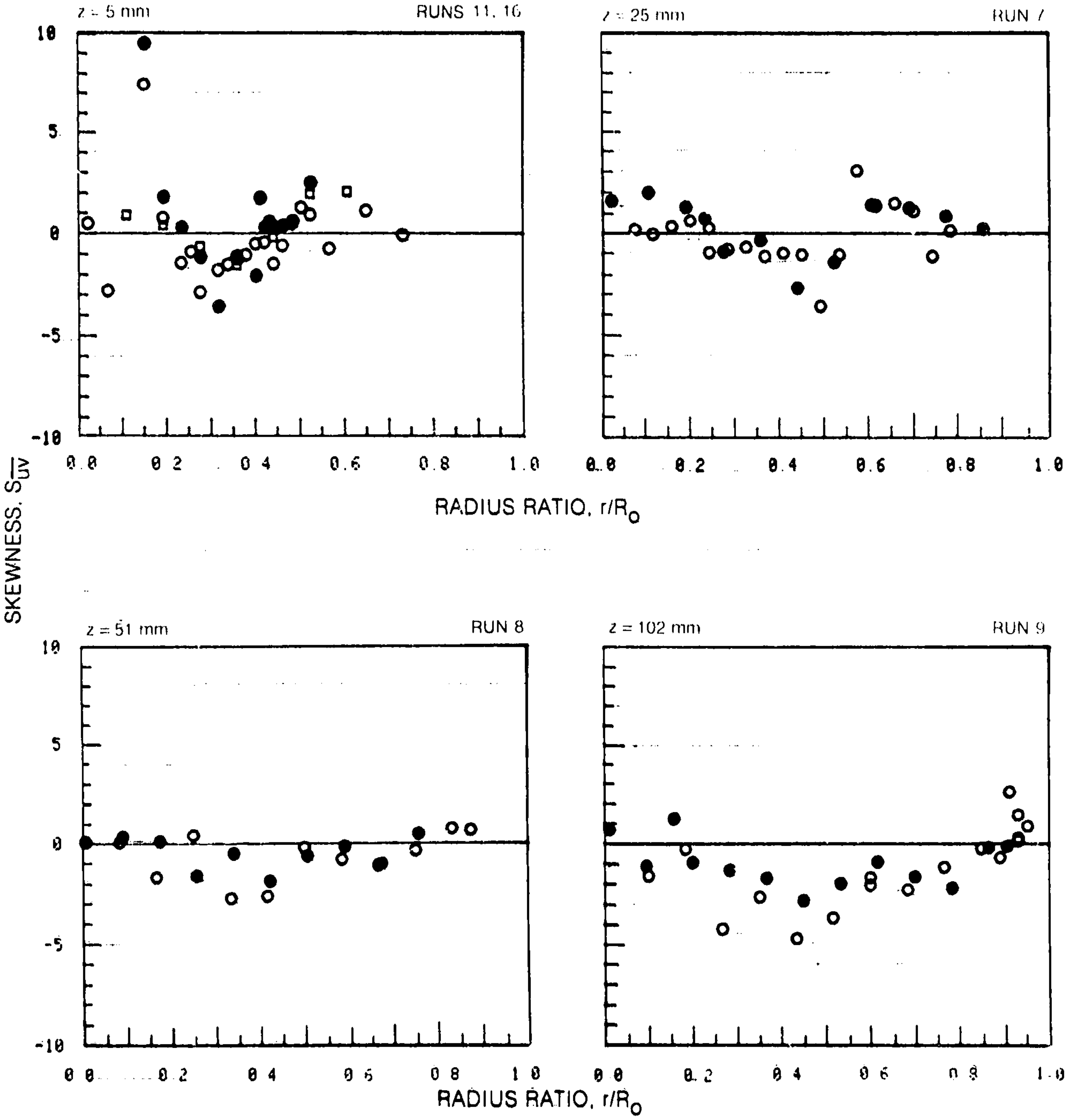

83-3-76-6

FIG. 53 (CONT.)

SKEWNESS OF $\overline{uv}$ TURBULENT MOMENTUM TRANSPORT RATE PROFILES (CONT.)

	HORIZONTAL TRAVERSE	VERTICAL TRAVERSE
OPEN SYMBOLS	θ = 90°	θ = 0°
SOLID SYMBOLS	θ = 270°	θ = 180°

SYMBOL	○	●	□	■
RUN NOS	15, 10, 42, 45		41	

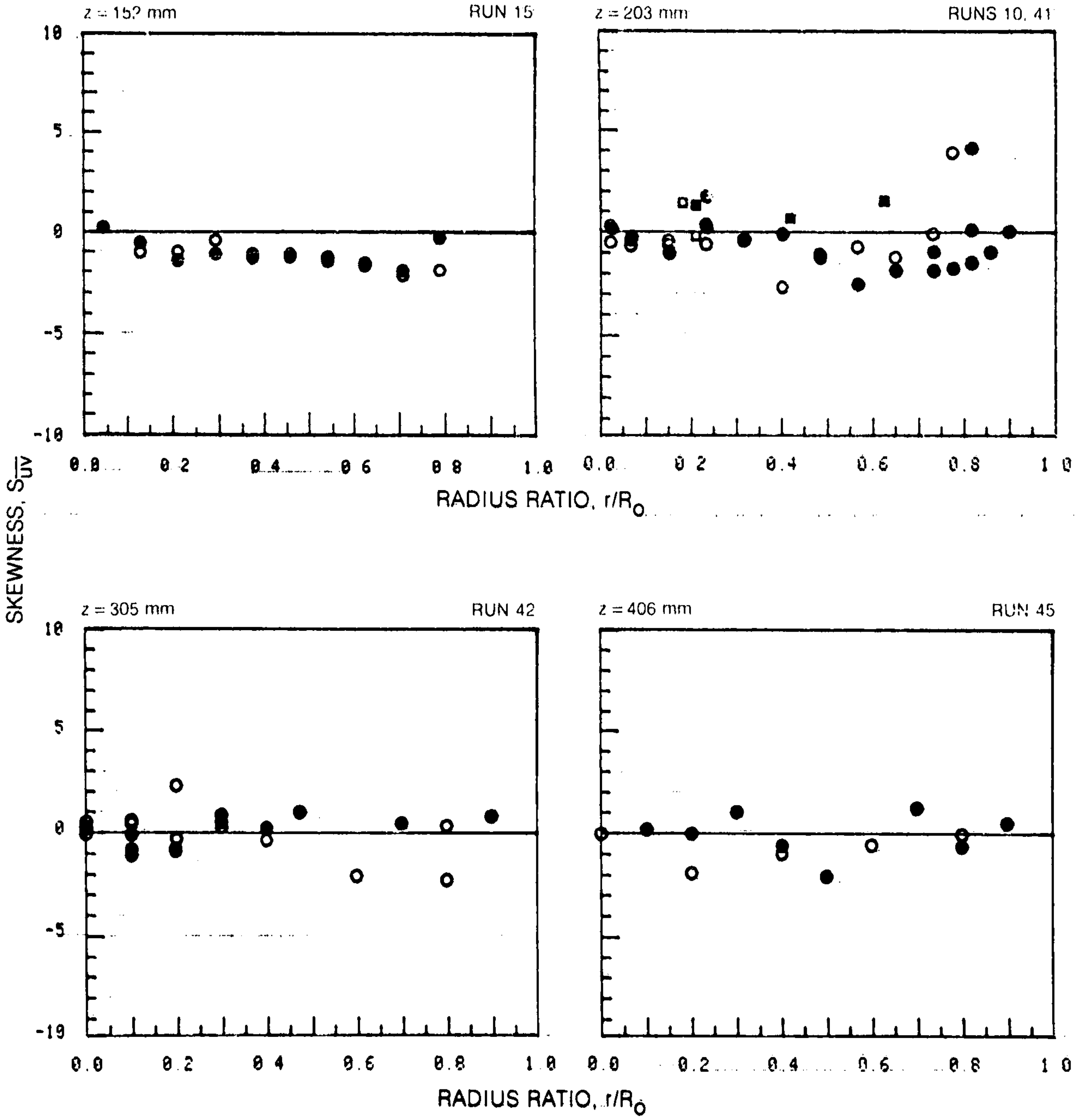

83-3-76-6A

ORIGINAL PAGE IS
OF POOR QUALITY

FIG. 54

KURTOSIS OF $\overline{uv}$ TURBULENT MOMENTUM TRANSPORT RATE PROFILES

	HORIZONTAL TRAVERSE	VERTICAL TRAVERSE
OPEN SYMBOLS	θ = 90°	θ = 0°
SOLID SYMBOLS	θ = 270°	θ = 180°

SYMBOL	○	●	□	■
RUN NOS	11, 7, 8, 9		16	

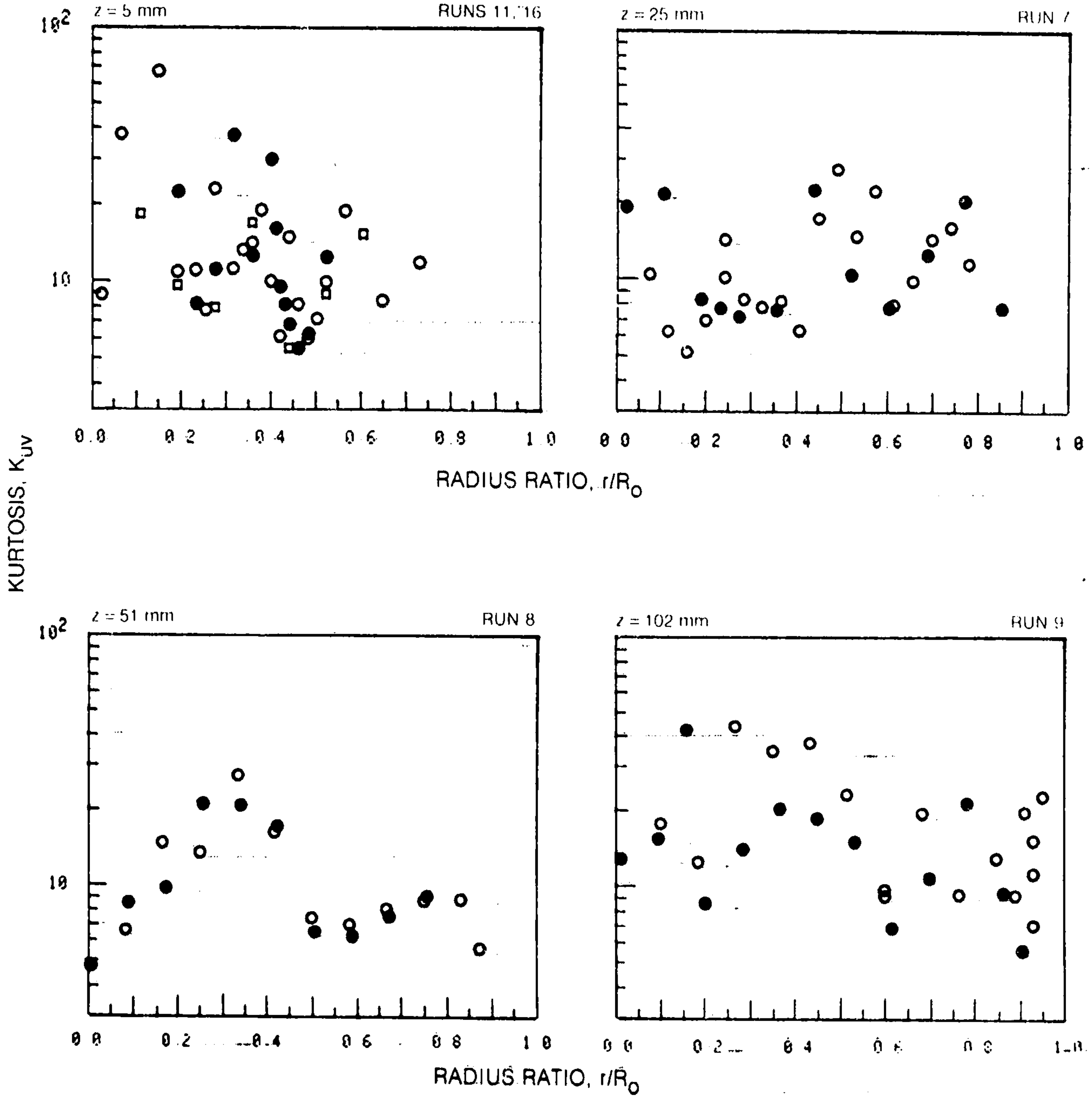

83-3-76-5

ORIGINAL PAGE IS
OF POOR QUALITY

FIG. 54 (CONT.)

KURTOSIS OF $\overline{uv}$ TURBULENT MOMENTUM TRANSPORT RATE PROFILES (CONT.)

	HORIZONTAL TRAVERSE	VERTICAL TRAVERSE
OPEN SYMBOLS.	$\theta = 90°$	$\theta = 0°$
SOLID SYMBOLS:	$\theta = 270°$	$\theta = 180°$

SYMBOL	○	●	□	■
RUN NOS	15, 10, 42, 45		41	

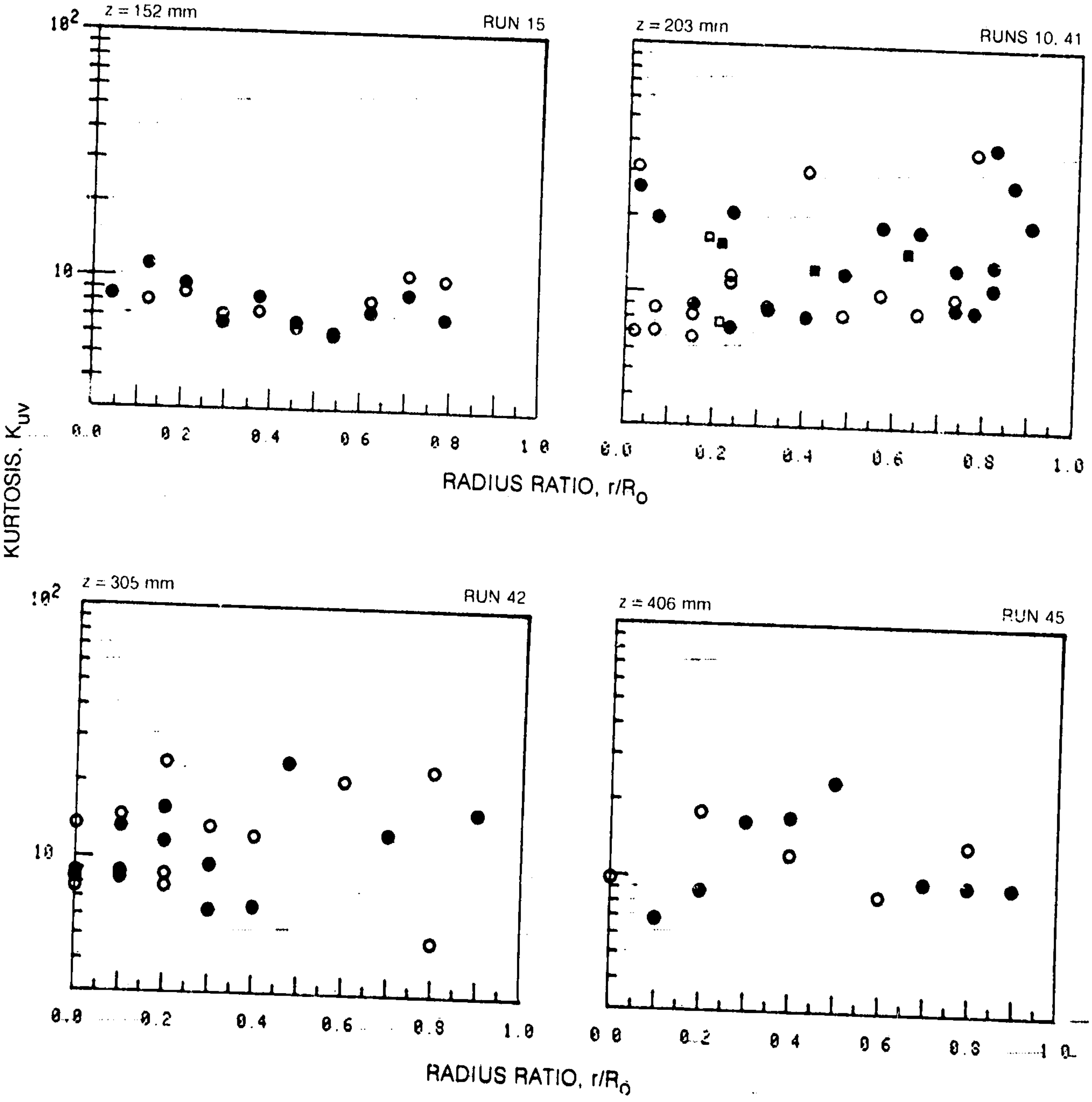

83-3-76-5A

FIG. 55

SECOND CENTRAL MOMENT OF $\overline{uw}$ TURBULENT TRANSPORT RATE PROFILES

	HORIZONTAL TRAVERSE	VERTICAL TRAVERSE
OPEN SYMBOLS:	θ = 90°	θ = 0°
SOLID SYMBOLS	θ = 270°	θ = 180°

SYMBOL	○	●	□	■
RUN NOS.	17, 3, 4, 5		6	

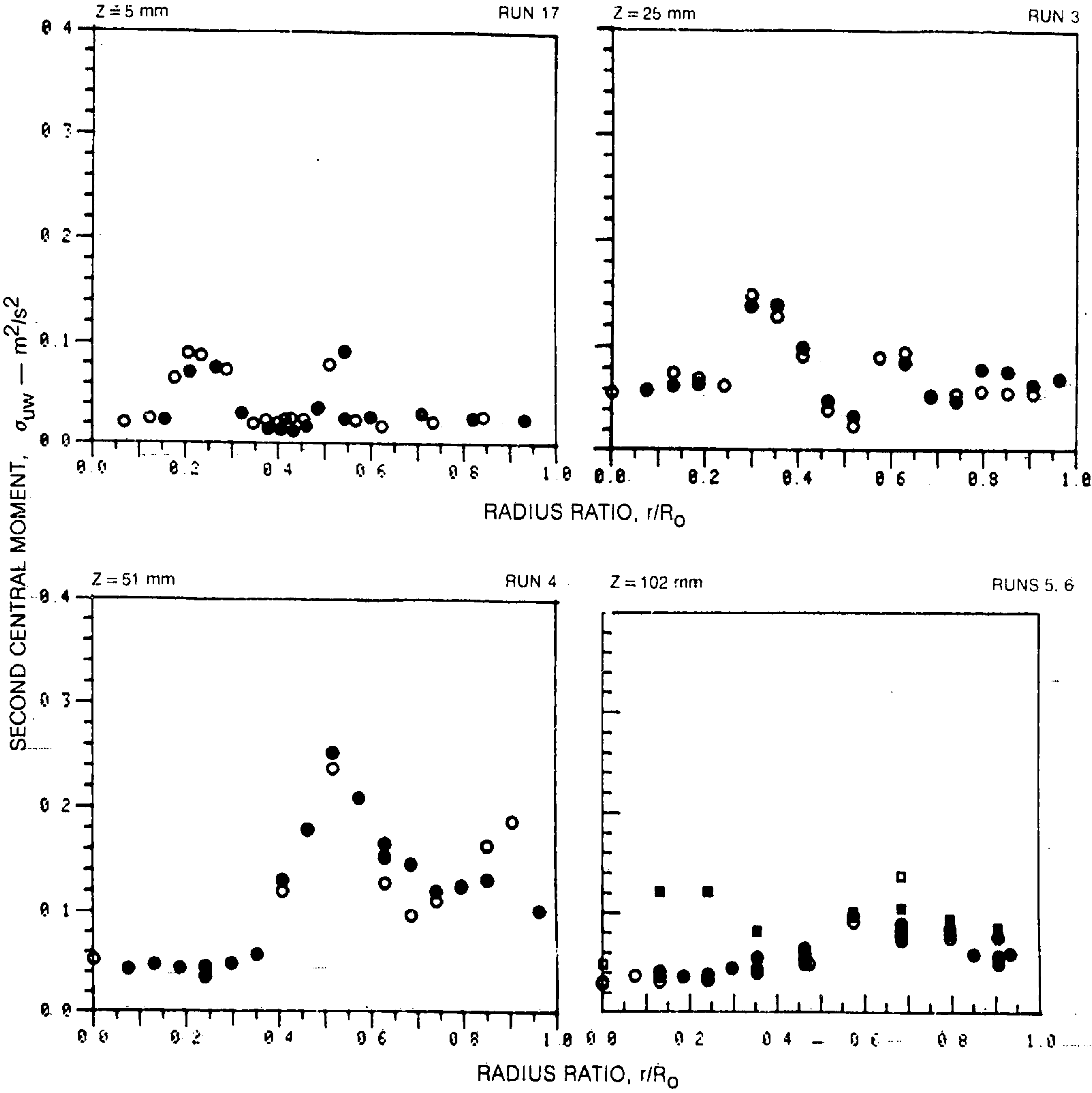

82 10 33-17

FIG. 55 (CONT.)

SECOND CENTRAL MOMENT OF $\overline{uw}$ TURBULENT TRANSPORT RATE PROFILES (CONT.)

	HORIZONTAL TRAVERSE	VERTICAL TRAVERSE
OPEN SYMBOLS.	$\theta = 90°$	$\theta = 0°$
SOLID SYMBOLS.	$\theta = 270°$	$\theta = 180°$

SYMBOL	○	●	□	■
RUN NOS.	14, 12, 43, 44		40	

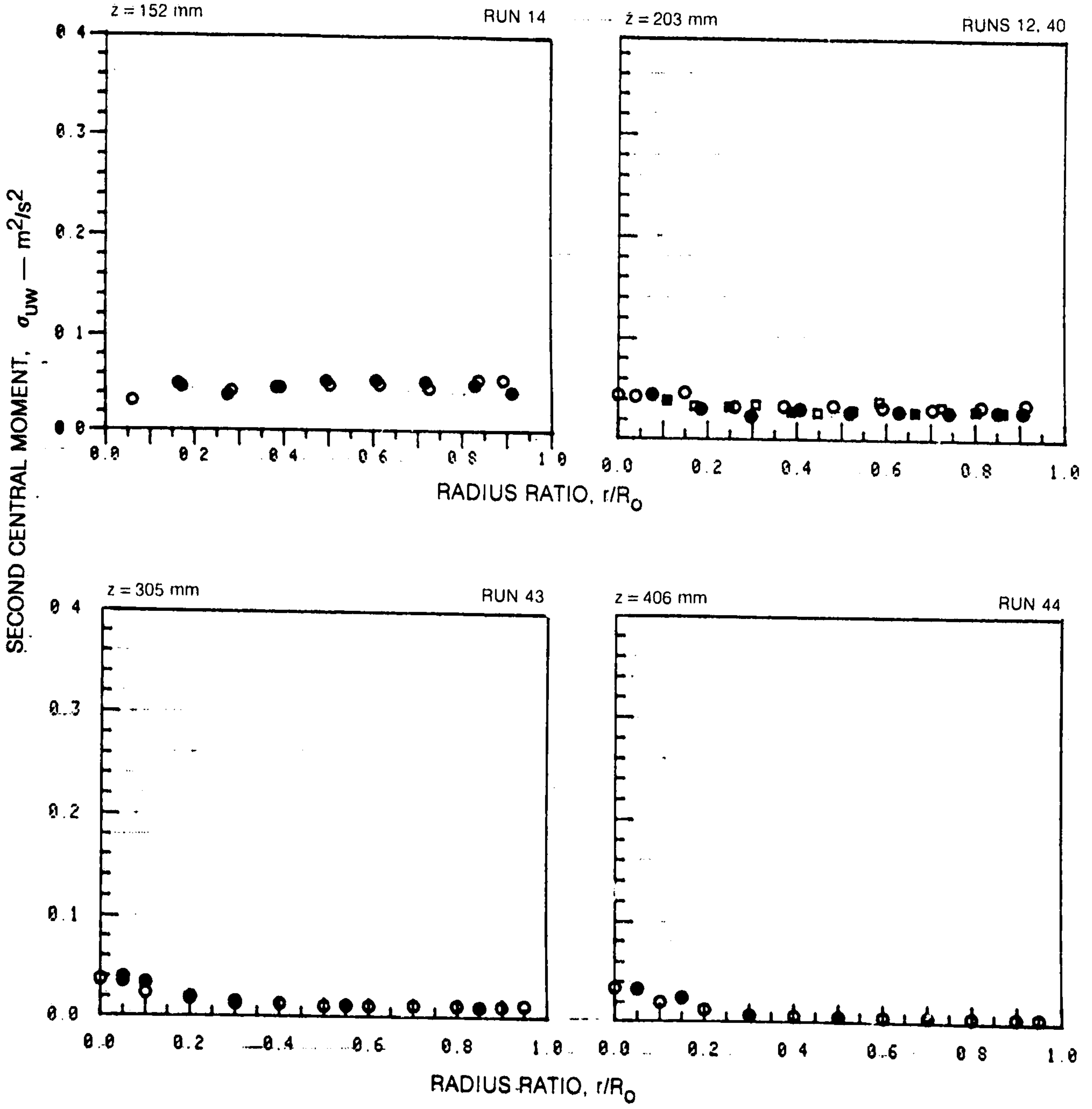

83-3-76-16

ORIGINAL PAGE IS
OF POOR QUALITY

FIG. 56

SKEWNESS OF $\overline{uw}$ TURBULENT MOMENTUM TRANSPORT RATE PROFILES

	HORIZONTAL TRAVERSE	VERTICAL TRAVERSE
OPEN SYMBOLS	θ = 90°	θ = 0°
SOLID SYMBOLS	θ = 270°	θ = 180°

SYMBOL	○	●	□	■
RUN NOS.	17, 3, 4, 5		6	

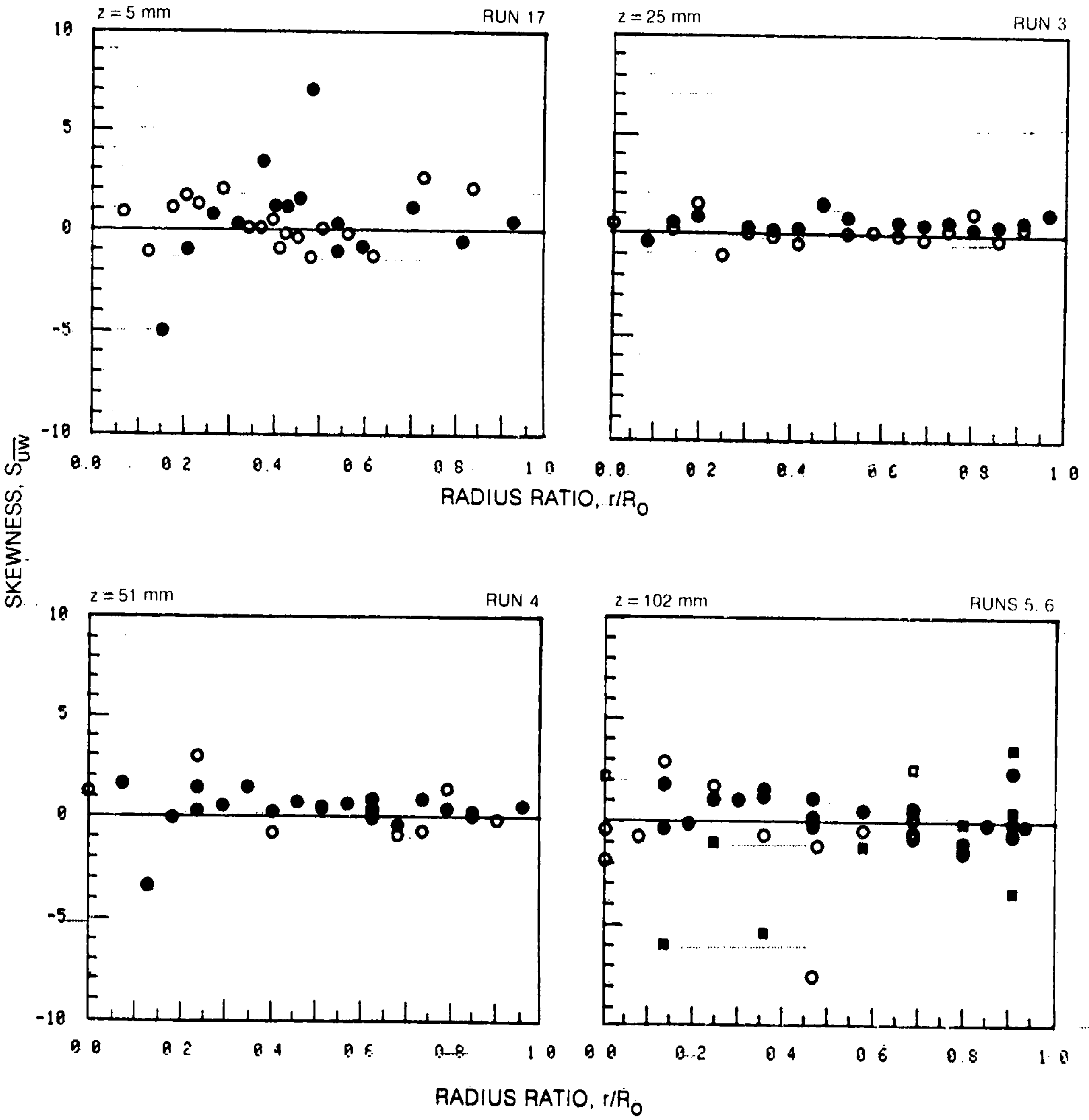

83-3-76-4

FIG. 56 (CONT.)

SKEWNESS OF $\overline{uw}$ TURBULENT MOMENTUM TRANSPORT RATE PROFILES (CONT.)

	HORIZONTAL TRAVERSE	VERTICAL TRAVERSE
OPEN SYMBOLS	$\theta = 90°$	$\theta = 0°$
SOLID SYMBOLS	$\theta = 270°$	$\theta = 180°$

SYMBOL	○	●	□	■
RUN NOS	14, 12, 43, 44		40	

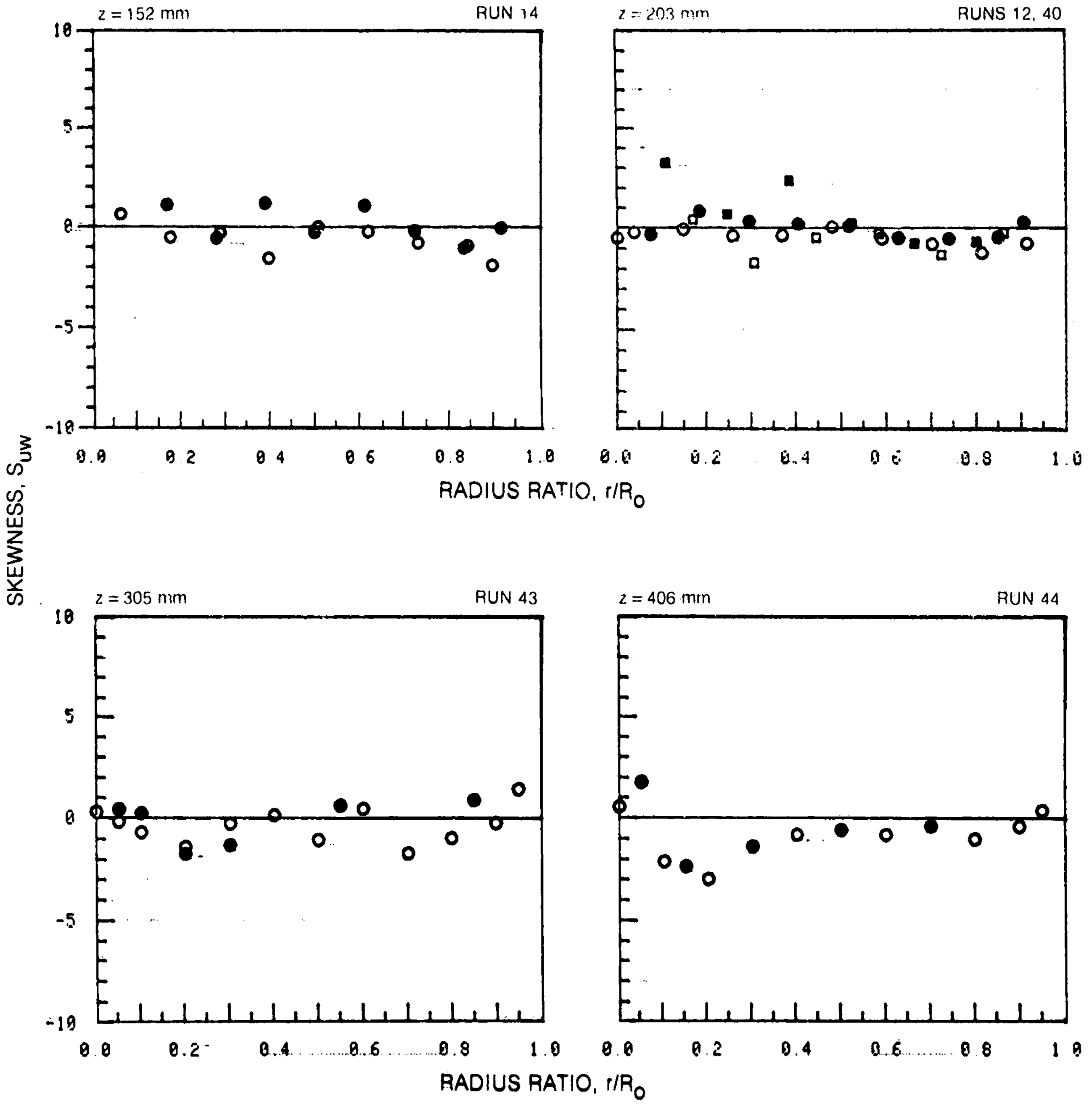

83-3-76-4A

ORIGINAL PAGE IS
OF POOR QUALITY

FIG. 57

KURTOSIS OF $\overline{uw}$ TURBULENT MOMENTUM TRANSPORT RATE PROFILES

	HORIZONTAL TRAVERSE	VERTICAL TRAVERSE
OPEN SYMBOLS	$\theta = 90°$	$\theta = 0°$
SOLID SYMBOLS	$\theta = 270°$	$\theta = 180°$

SYMBOL	○	●	□	■
RUN NOS	17, 3, 4, 5		6	

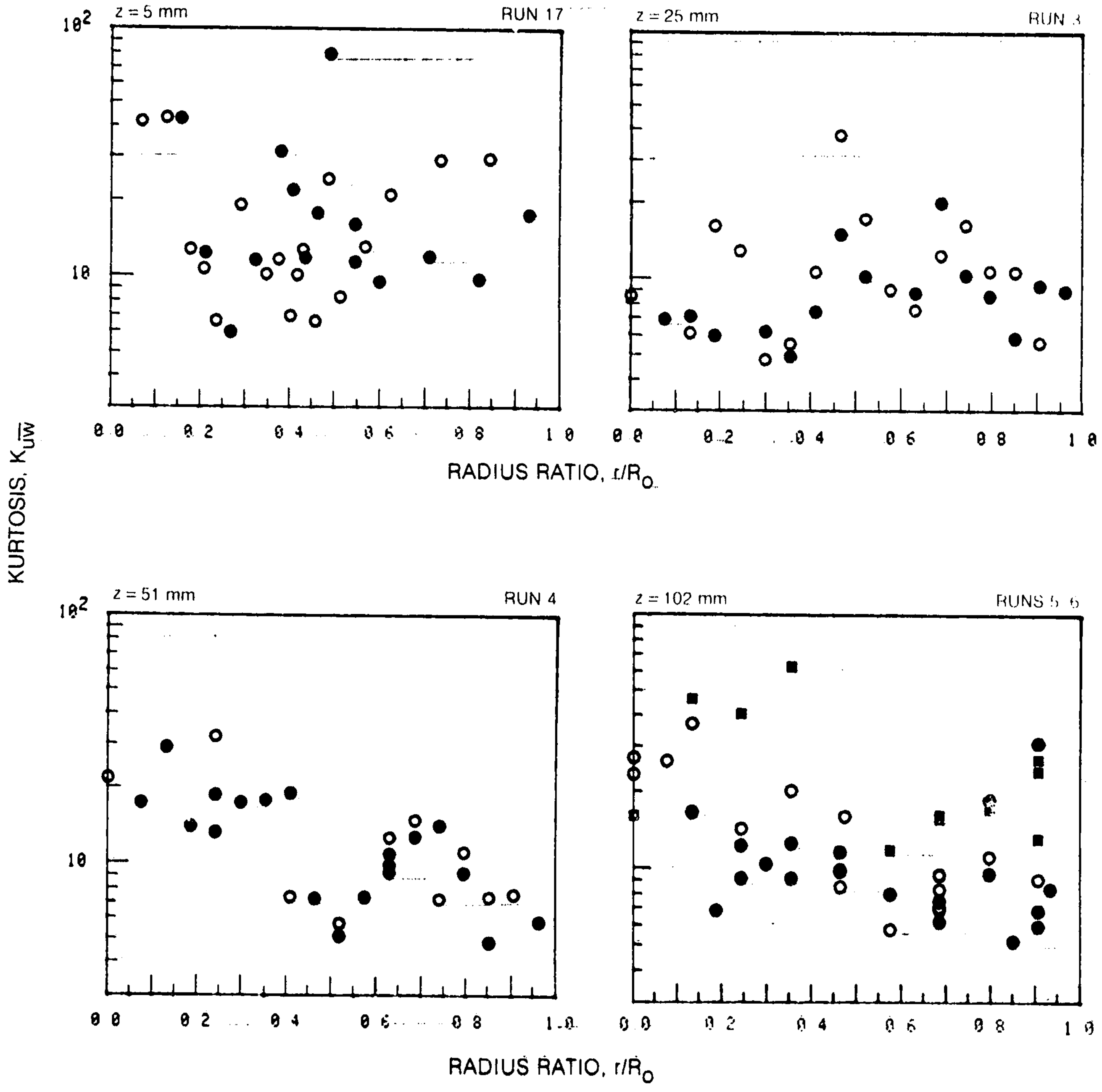

FIG. 58

SECOND CENTRAL MOMENT OF $\overline{wv}$ TURBULENT TRANSPORT RATE PROFILES

	HORIZONTAL TRAVERSE	VERTICAL TRAVERSE
OPEN SYMBOLS:	$\theta = 90°$	$\theta = 0°$
SOLID SYMBOLS:	$\theta = 270°$	$\theta = 180°$

SYMBOL	○	●	□	■	△	▲	◇	◆	▽	▼
RUN NOS.	47, 46, 54		48, 50, 55		49, 51, 56		52		53	

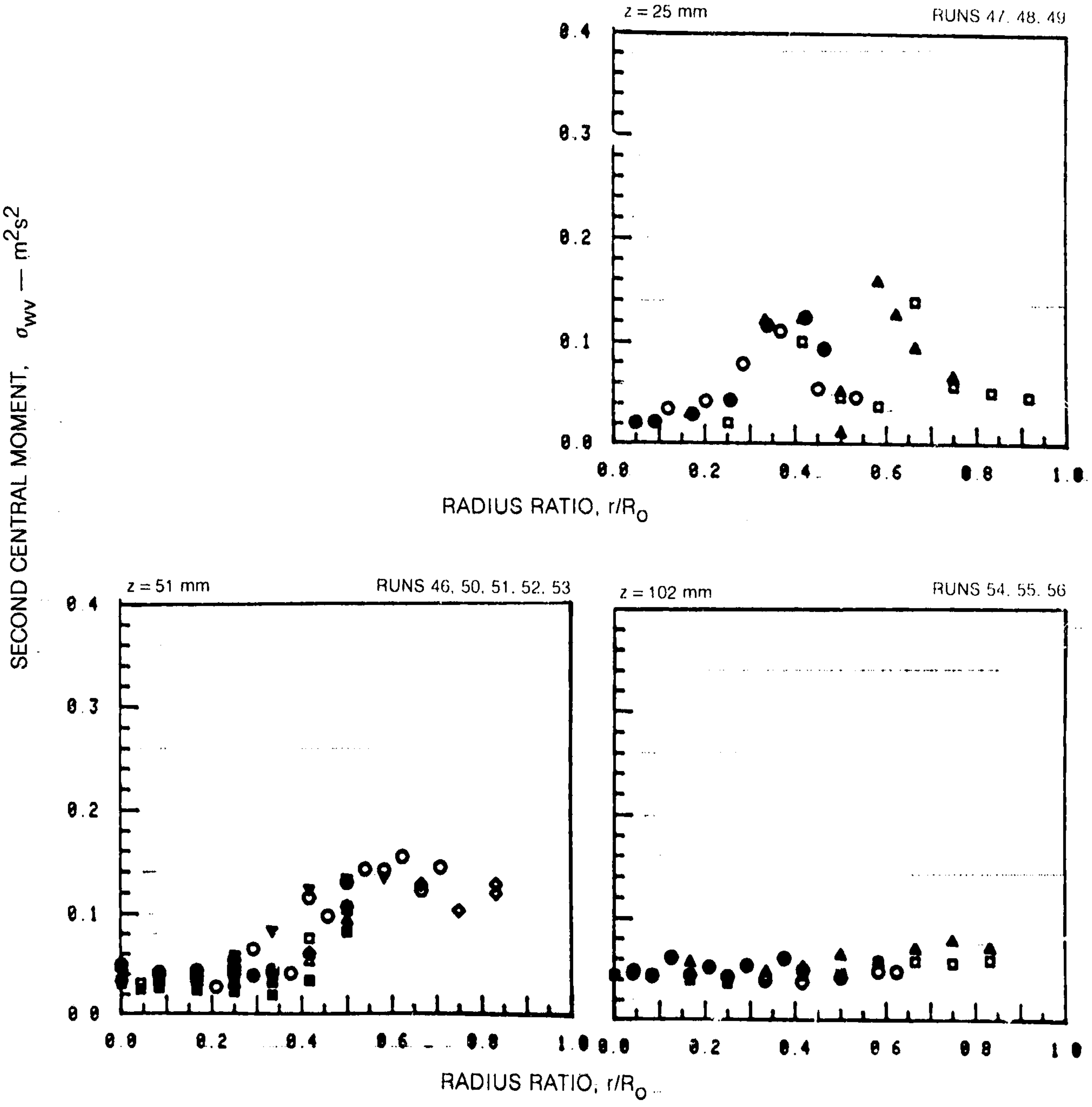

PRECEDING PAGE BLANK NOT FILMED

83-1-58-3

FIG. 59

SKEWNESS OF $\overline{wv}$ TURBULENT MOMENTUM TRANSPORT RATE PROFILES

	HORIZONTAL TRAVERSE	VERTICAL TRAVERSE
OPEN SYMBOLS	θ = 90°	θ = 0°
SOLID SYMBOLS	θ = 270°	θ = 180°

SYMBOL	○	●	□	■	△	▲	◇	◆	▽	▼
RUN NOS	47, 46, 54		48, 50, 55		49, 51, 56		52		53	

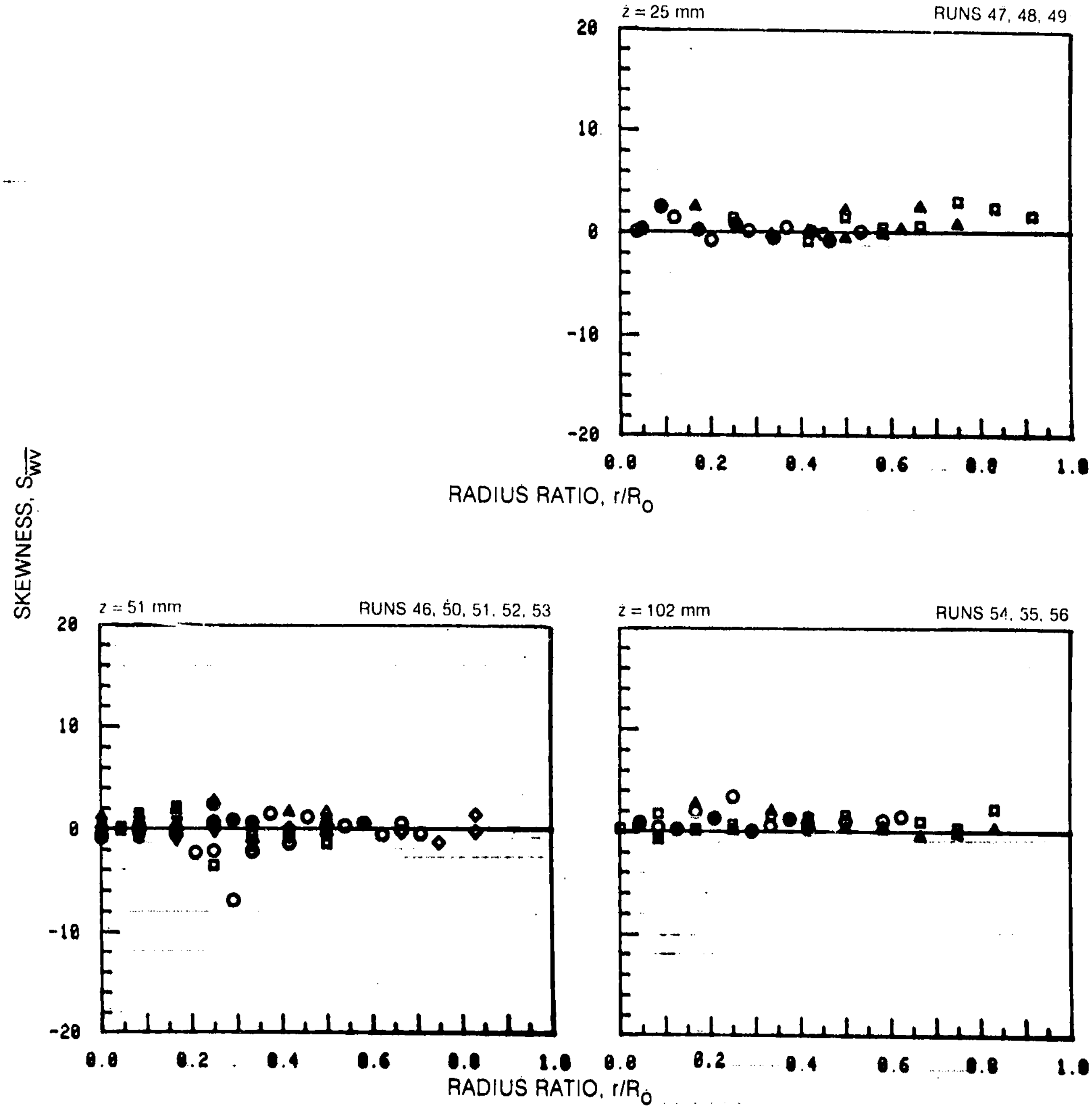

83-3-76-2

ORIGINAL PAGE IS
OF POOR QUALITY

FIG. 60

KURTOSIS OF $\overline{wv}$ TURBULENT MOMENTUM TRANSPORT RATE PROFILES

	HORIZONTAL TRAVERSE	VERTICAL TRAVERSE
OPEN SYMBOLS	θ = 90°	θ = 0°
SOLID SYMBOLS	θ = 270°	θ = 180°

SYMBOL	○	●	□	■	△	▲	◇	◆	▽	▼
RUN NOS	47, 46, 54		48, 50, 55		49, 51, 56		52		53	

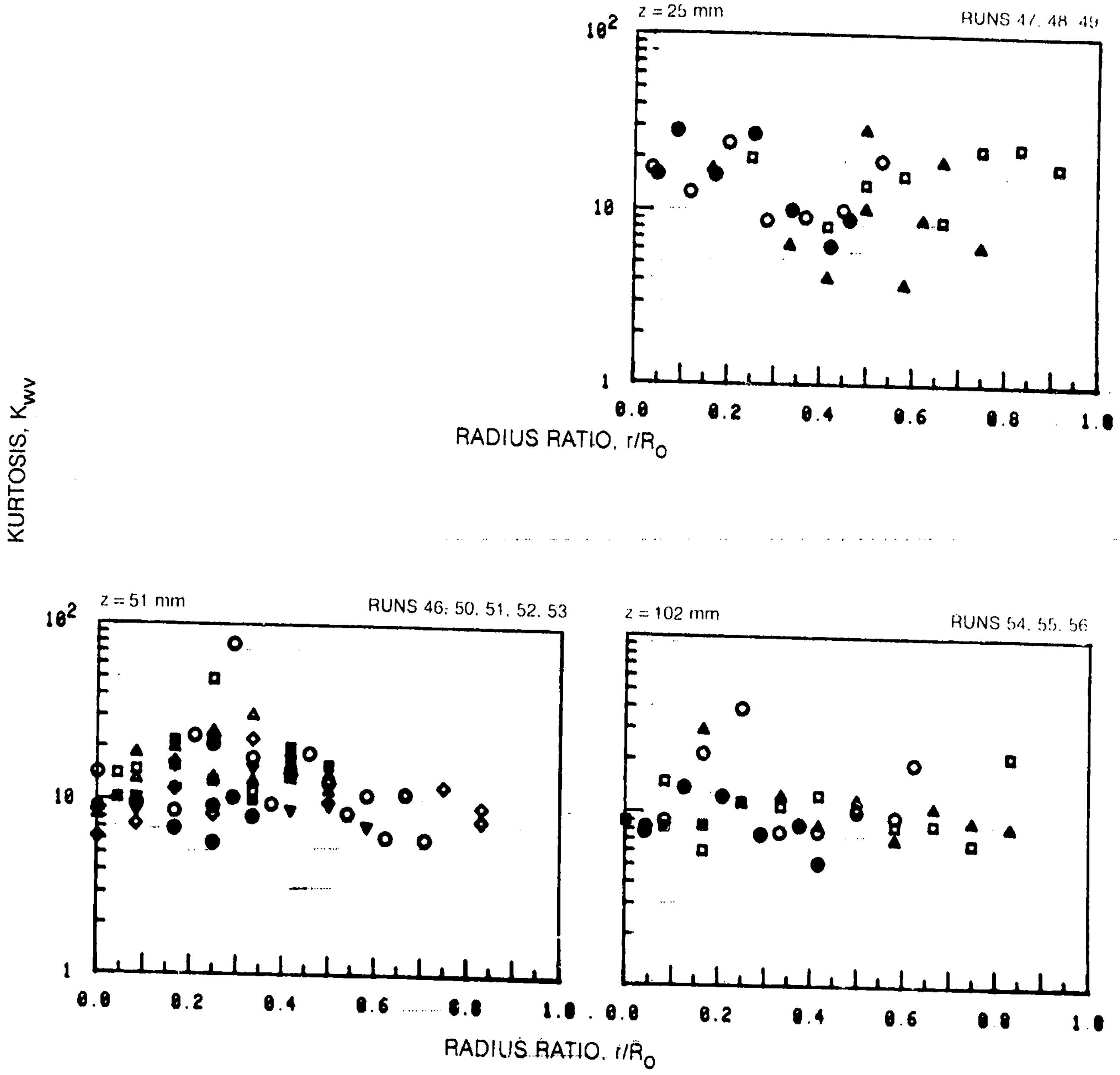

83-3-76-1

FIG. 61

SECOND CENTRAL MOMENT OF TURBULENT RADIAL MASS TRANSPORT RATE PROFILES

	HORIZONTAL TRAVERSE	VERTICAL TRAVERSE
OPEN SYMBOLS:	θ = 90°	θ = 0°
SOLID SYMBOLS:	θ = 270°	θ = 180°

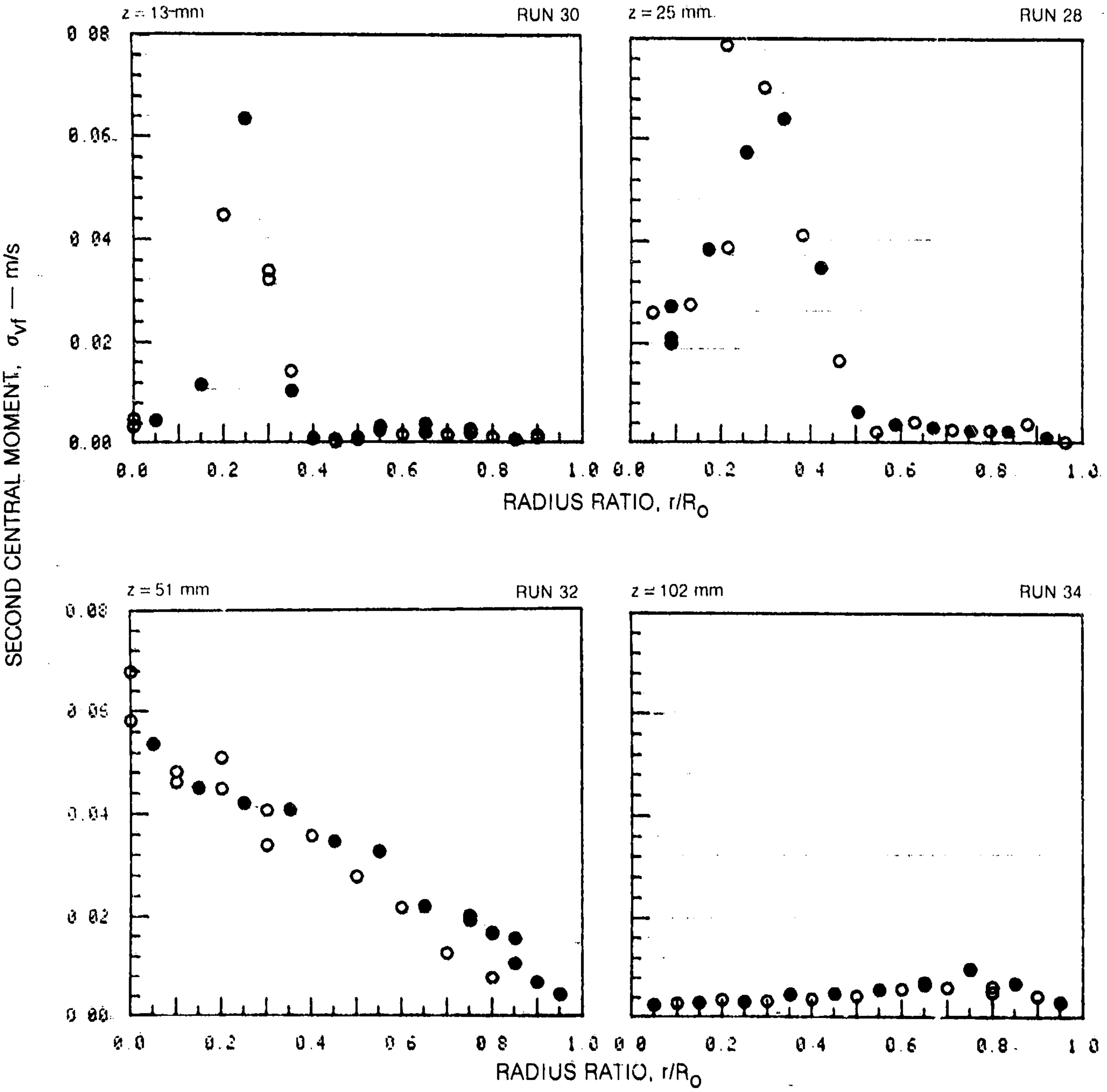

83-2-55-15A

SECOND CENTRAL MOMENT OF TURBULENT RADIAL MASS TRANSPORT RATE PROFILES (CONT.)

	HORIZONTAL TRAVERSE	VERTICAL TRAVERSE
OPEN SYMBOLS:	$\theta = 90°$	$\theta = 0°$
SOLID SYMBOLS:	$\theta = 270°$	$\theta = 180°$

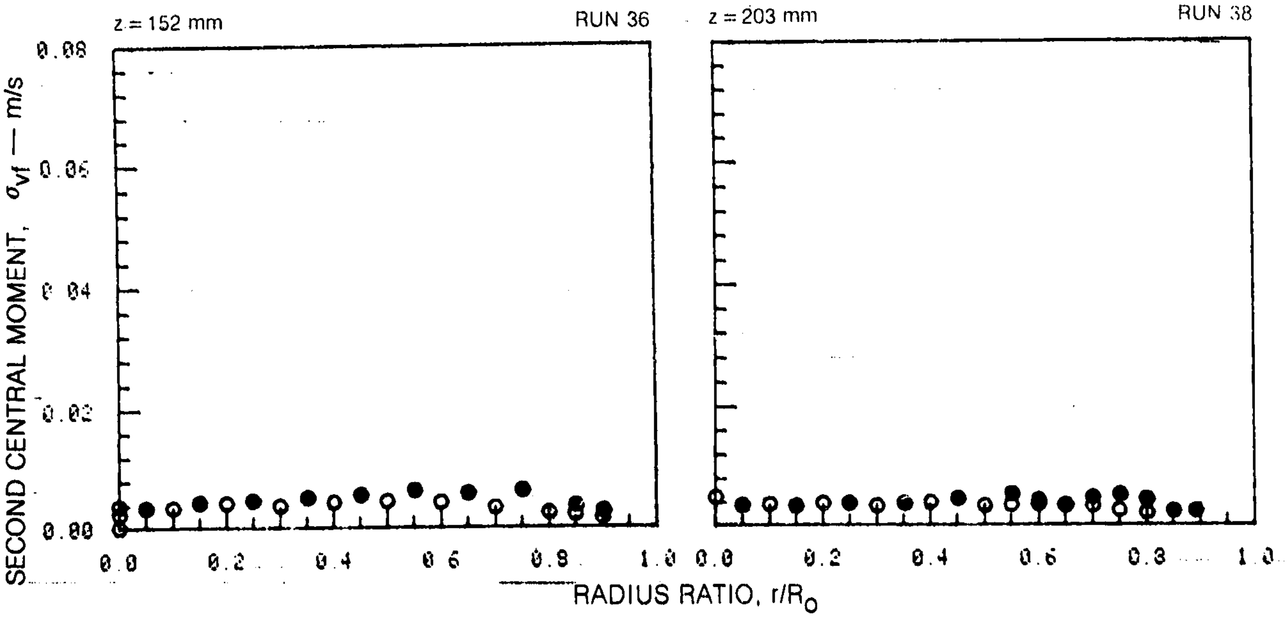

ORIGINAL PAGE IS
OF POOR QUALITY

FIG. 62

SKEWNESS OF TURBULENT RADIAL MASS TRANSPORT RATE PROFILES

	HORIZONTAL TRAVERSE	VERTICAL TRAVERSE
OPEN SYMBOLS:	θ = 90°	θ = 0°
SOLID SYMBOLS:	θ = 270°	θ = 180°

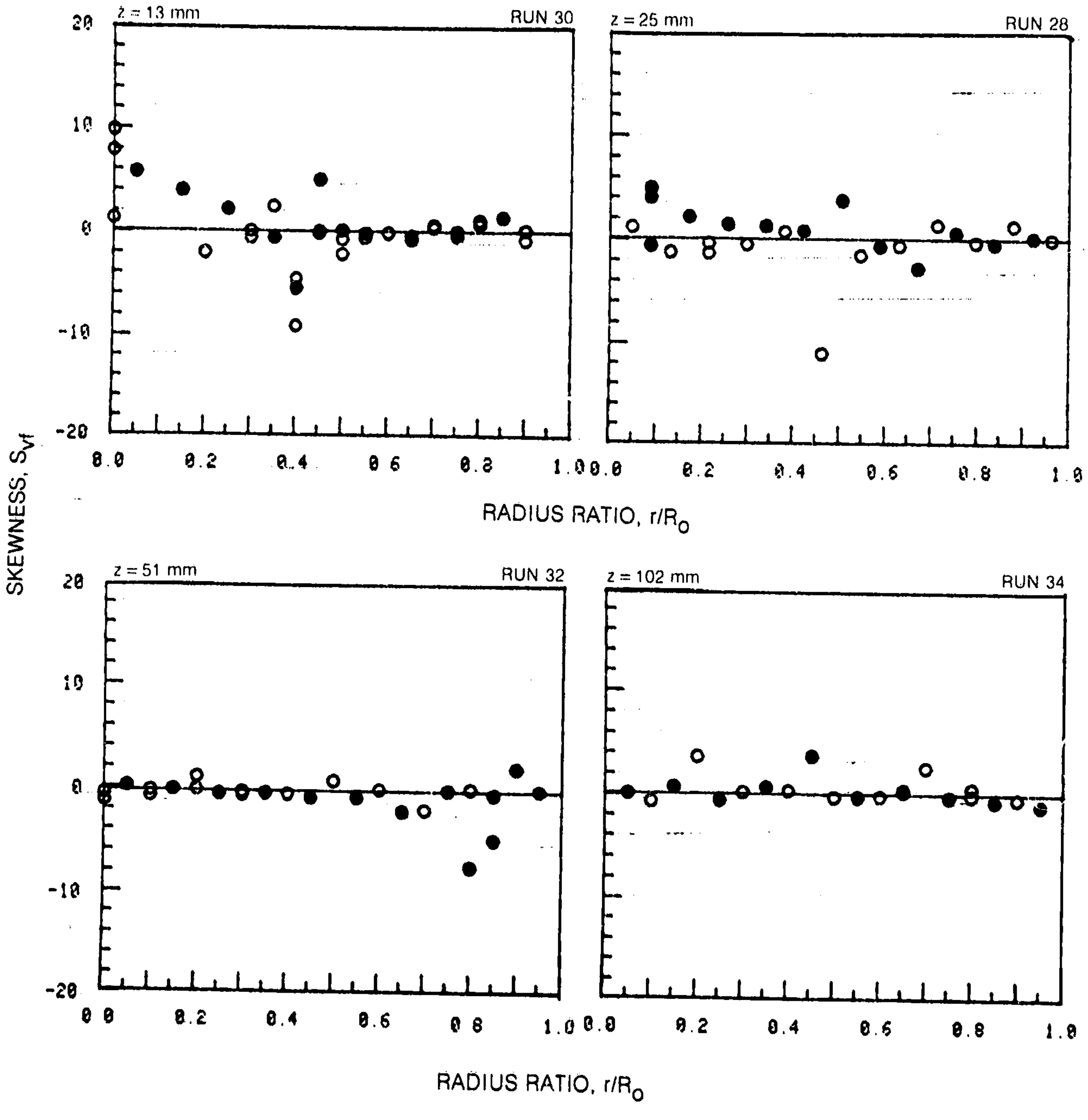

83-2-55-18A

SKEWNESS OF TURBULENT RADIAL MASS TRANSPORT RATE PROFILES (CONT.)

	HORIZONTAL TRAVERSE	VERTICAL TRAVERSE
OPEN SYMBOLS	θ = 90°	θ = 0°
SOLID SYMBOLS	θ = 270°	θ = 180°

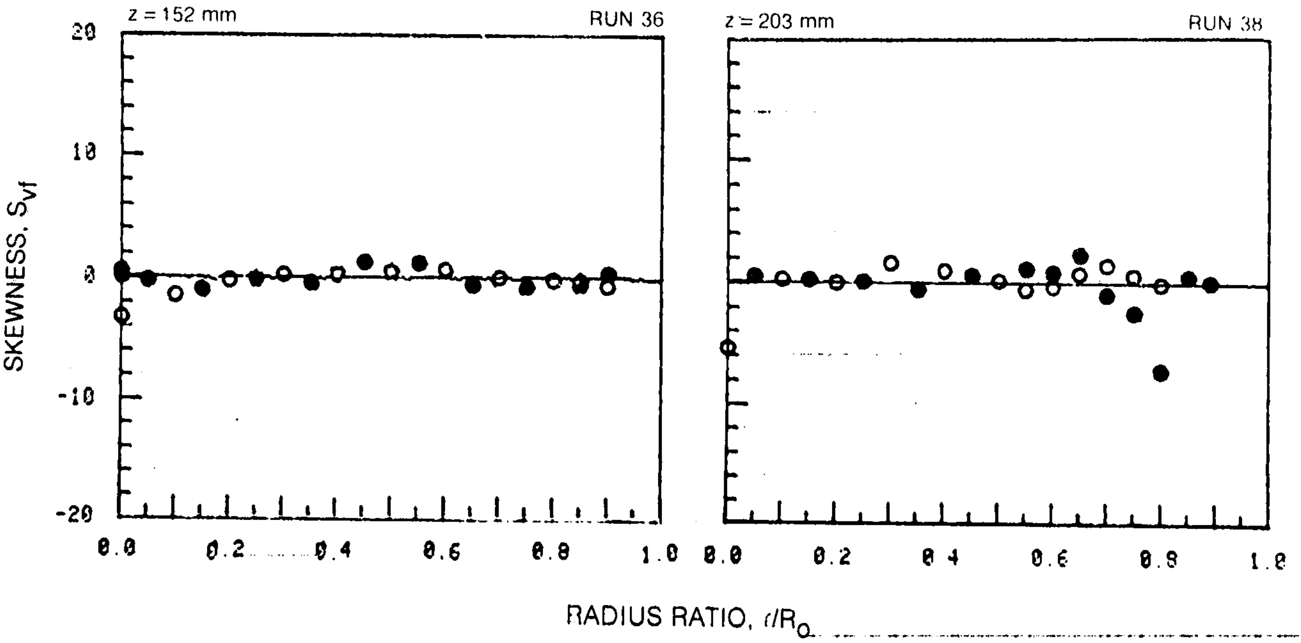

FIG. 63

KURTOSIS OF TURBULENT RADIAL MASS TRANSPORT RATE PROFILES

	HORIZONTAL TRAVERSE	VERTICAL TRAVERSE
OPEN SYMBOLS:	θ = 90°	θ = 0°
SOLID SYMBOLS:	θ = 270°	θ = 180°

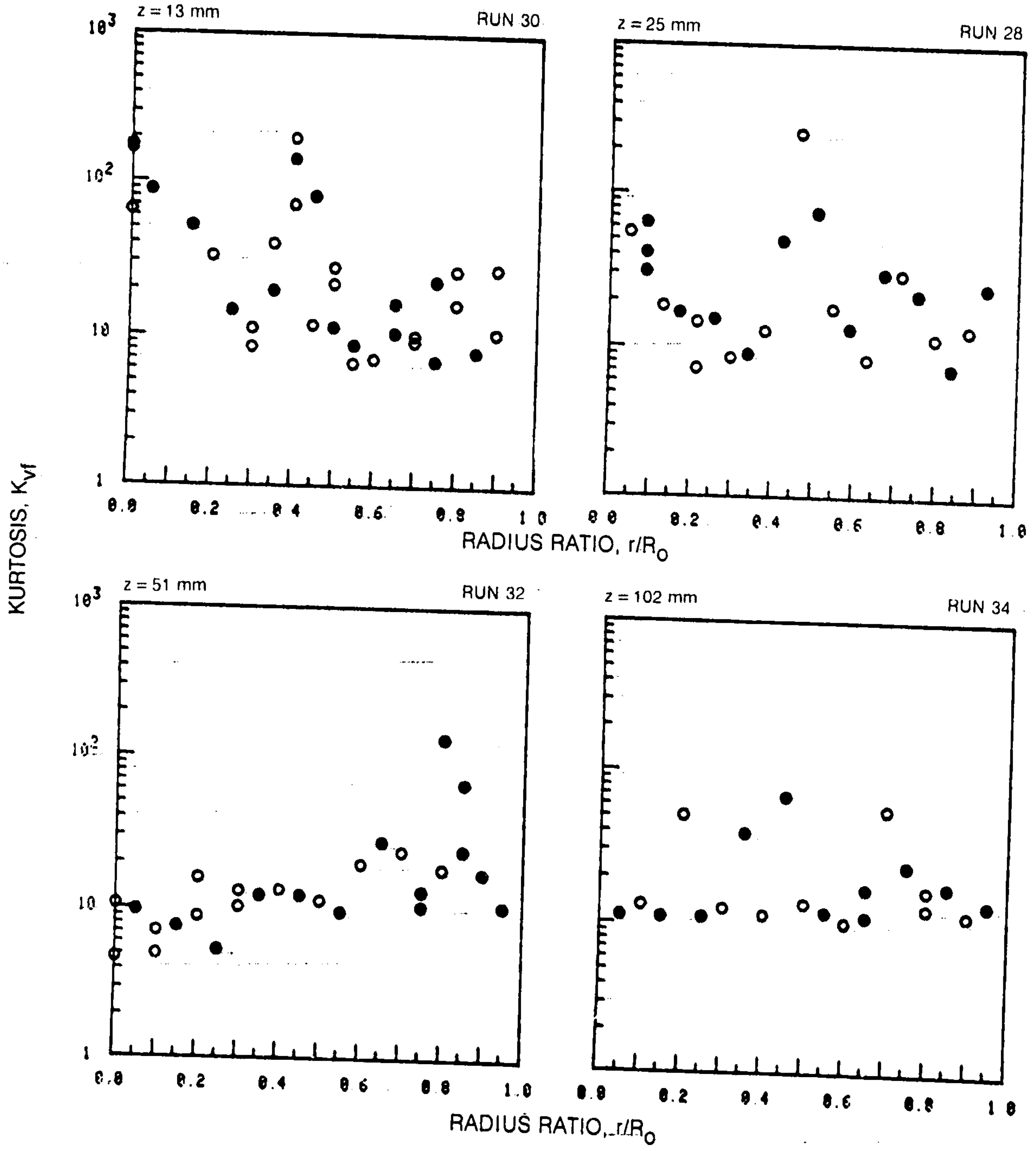

83-2-55-21A

KURTOSIS OF TURBULENT RADIAL MASS TRANSPORT RATE PROFILES (CONT.)

	HORIZONTAL TRAVERSE	VERTICAL TRAVERSE
OPEN SYMBOLS:	$\theta = 90°$	$\theta = 0°$
SOLID SYMBOLS:	$\theta = 270°$	$\theta = 180°$

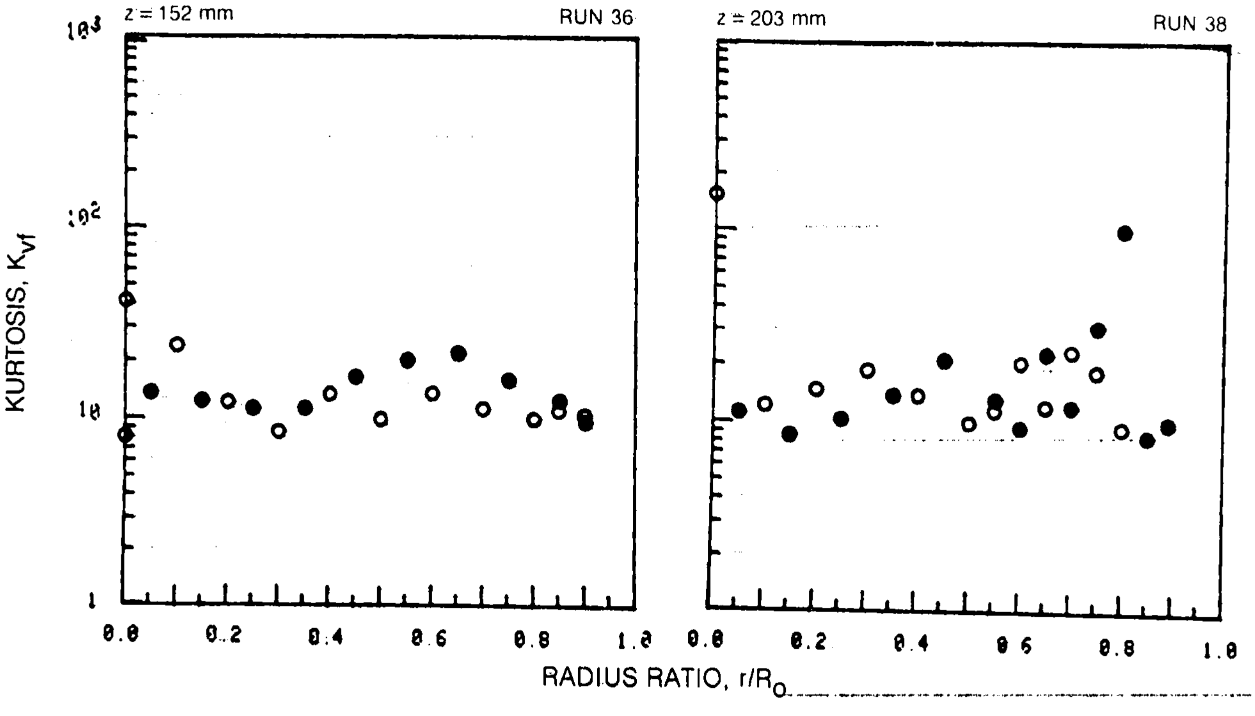

ORIGINAL PAGE IS
OF POOR QUALITY

FIG. 64a

SECOND CENTRAL MOMENT OF TURBULENT AXIAL MASS TRANSPORT RATE PROFILES

	HORIZONTAL TRAVERSE	VERTICAL TRAVERSE
OPEN SYMBOLS:	θ = 90°	θ = 0°
SOLID SYMBOLS:	θ = 270°	θ = 180°

SYMBOL	○	●	□	■
RUN NOS.	20, 22		21	

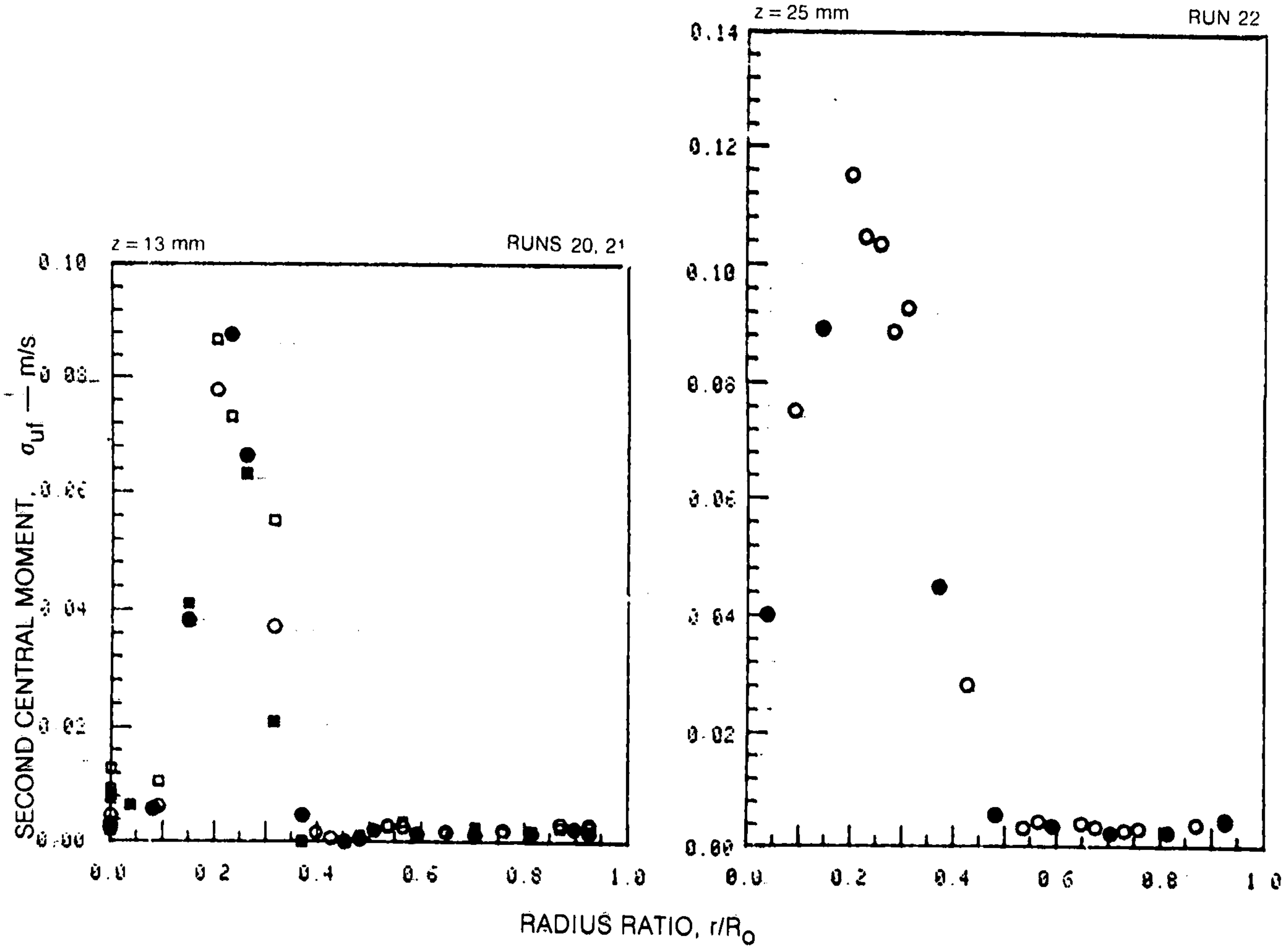

83-2-55-14A

ORIGINAL PAGE IS
OF POOR QUALITY

SECOND CENTRAL MOMENT OF TURBULENT AXIAL MASS TRANSPORT RATE PROFILES (CONT.)

	HORIZONTAL TRAVERSE	VERTICAL TRAVERSE
OPEN SYMBOLS:	θ = 90°	θ = 0°
SOLID SYMBOLS:	θ = 270°	θ = 180°

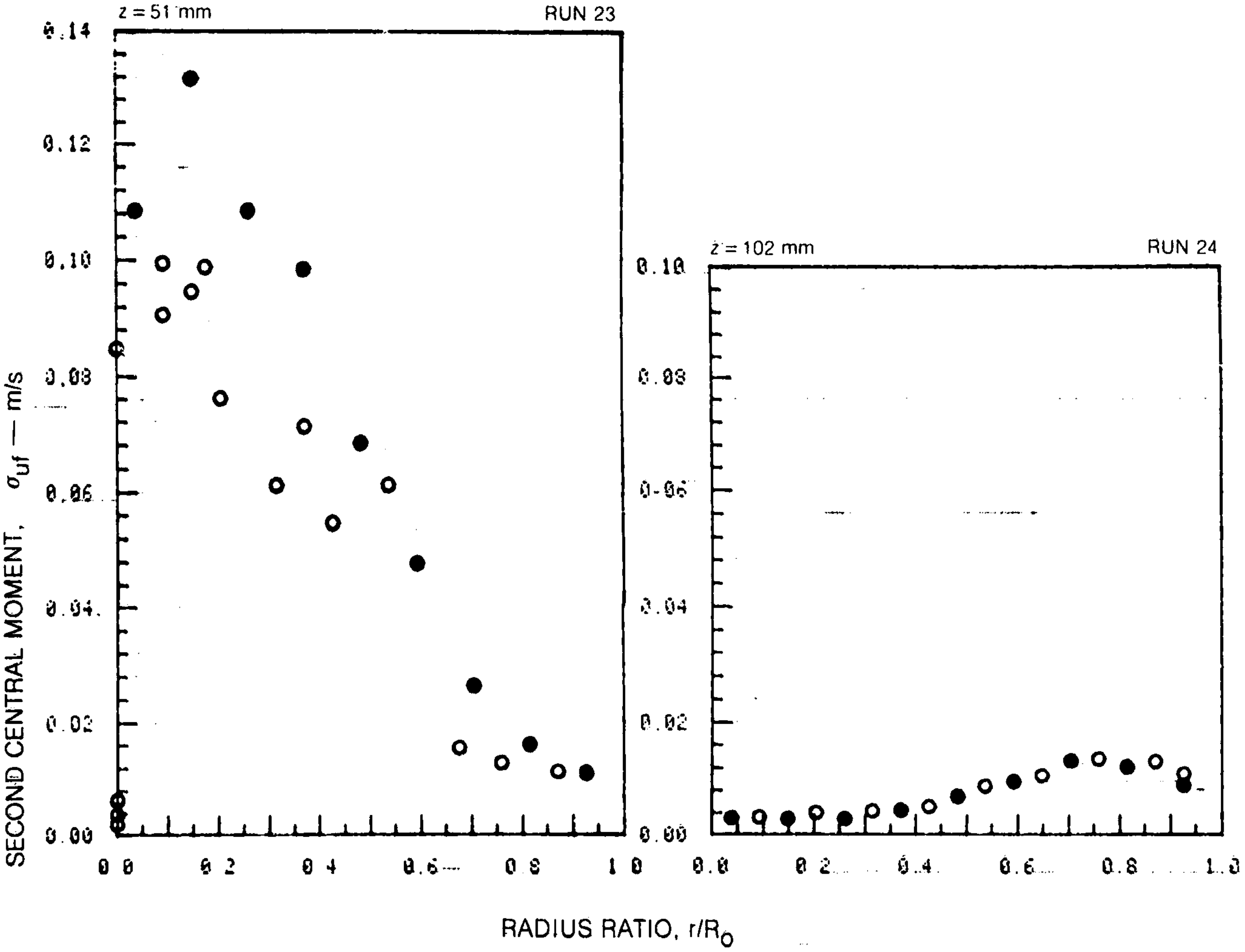

ORIGINAL PAGE IS
OF POOR QUALITY

SECOND CENTRAL MOMENT OF TURBULENT AXIAL MASS TRANSPORT RATE PROFILES (CONT.)

	HORIZONTAL TRAVERSE	VERTICAL TRAVERSE
OPEN SYMBOLS:	$\theta = 90°$	$\theta = 0°$
SOLID SYMBOLS:	$\theta = 270°$	$\theta = 180°$

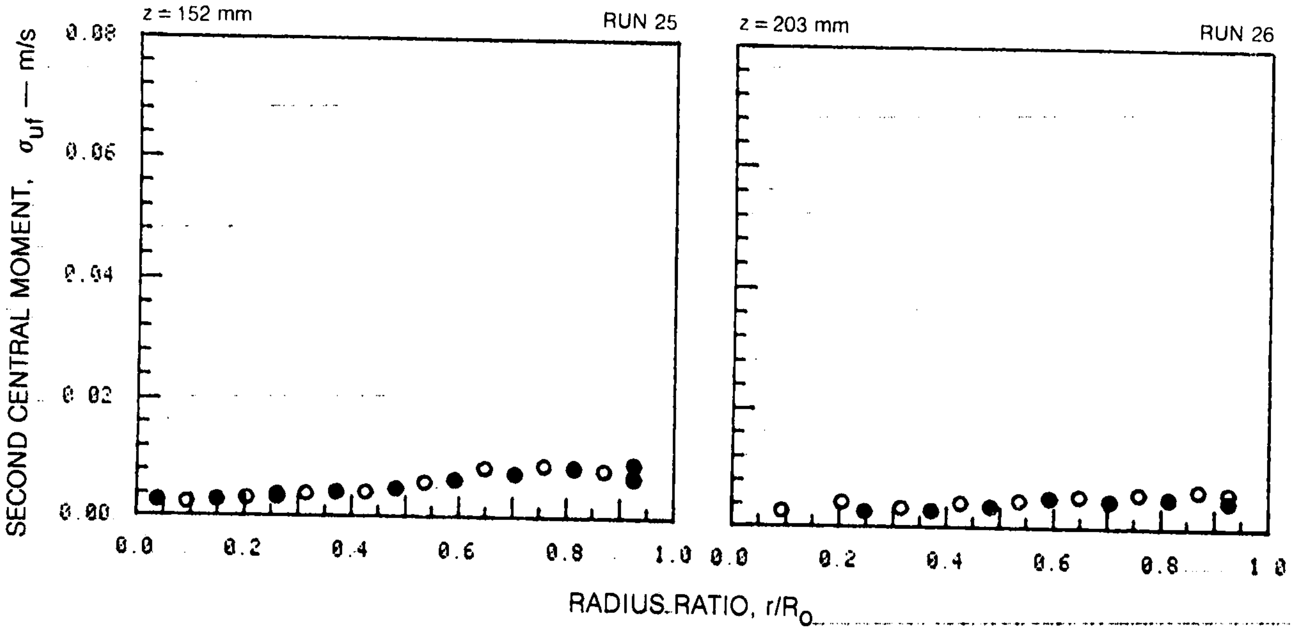

ORIGINAL PAGE IS
OF POOR QUALITY

FIG. 65

SKEWNESS OF TURBULENT AXIAL MASS TRANSPORT RATE PROFILES

	HORIZONTAL TRAVERSE	VERTICAL TRAVERSE
OPEN SYMBOLS:	$\theta = 90°$	$\theta = 0°$
SOLID SYMBOLS:	$\theta = 270°$	$\theta = 180°$

SYMBOL	○	●	□	■
RUN NOS.	20, 22, 23, 24		21	

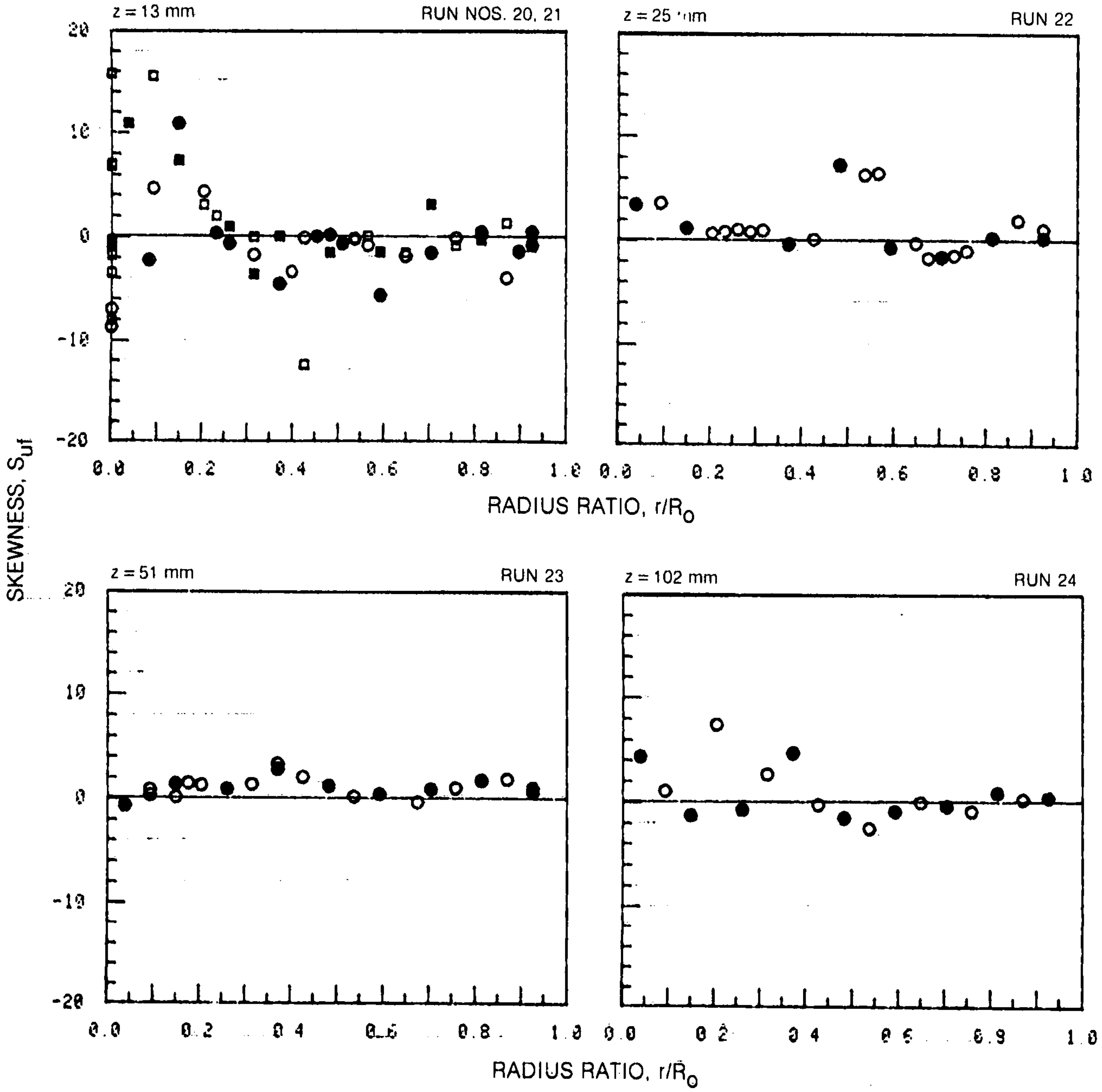

83-2-55-17A

FIG. 65 (CONT.)

ORIGINAL PAGE IS
OF POOR QUALITY

SKEWNESS OF TURBULENT AXIAL MASS TRANSPORT RATE PROFILES (CONT.)

	HORIZONTAL TRAVERSE	VERTICAL TRAVERSE
OPEN SYMBOLS:	θ = 90°	θ = 0°
SOLID SYMBOLS:	θ = 270°	θ = 180°

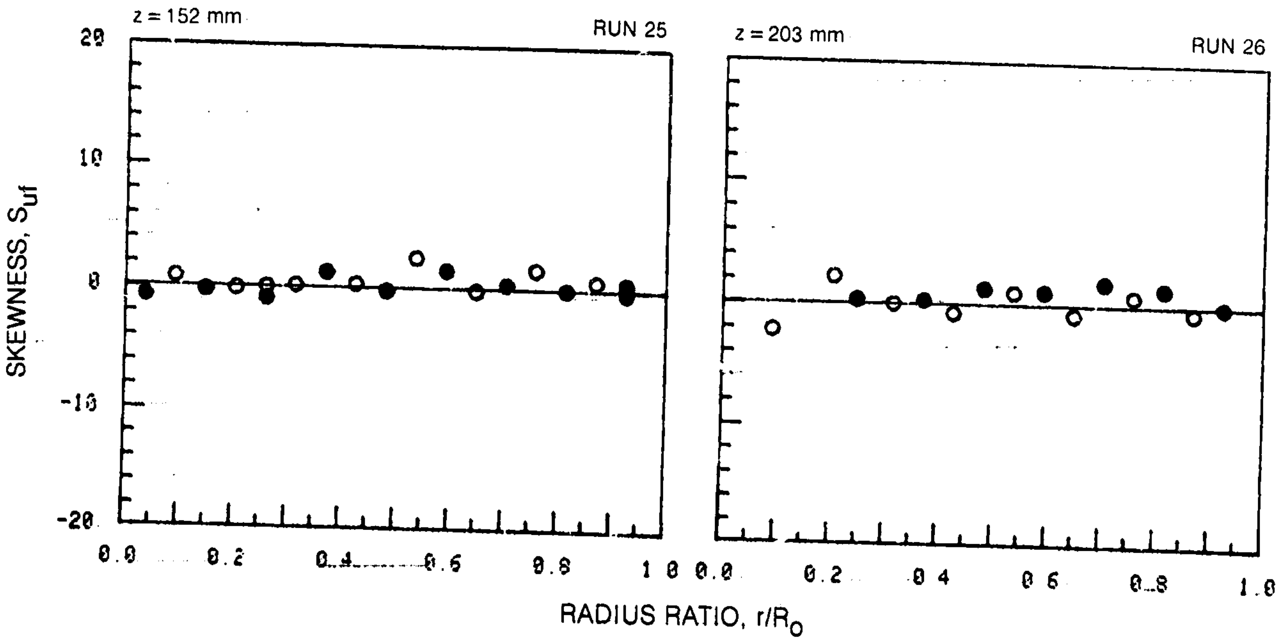

83-2-55-17B

FIG. 66

KURTOSIS OF TURBULENT AXIAL MASS TRANSPORT RATE PROFILES

	HORIZONTAL TRAVERSE	VERTICAL TRAVERSE
OPEN SYMBOLS:	θ = 90°	θ = 0°
SOLID SYMBOLS:	θ = 270°	θ = 180°

SYMBOL	○	●	□	■
RUN NOS.	20, 22, 23, 24		21	

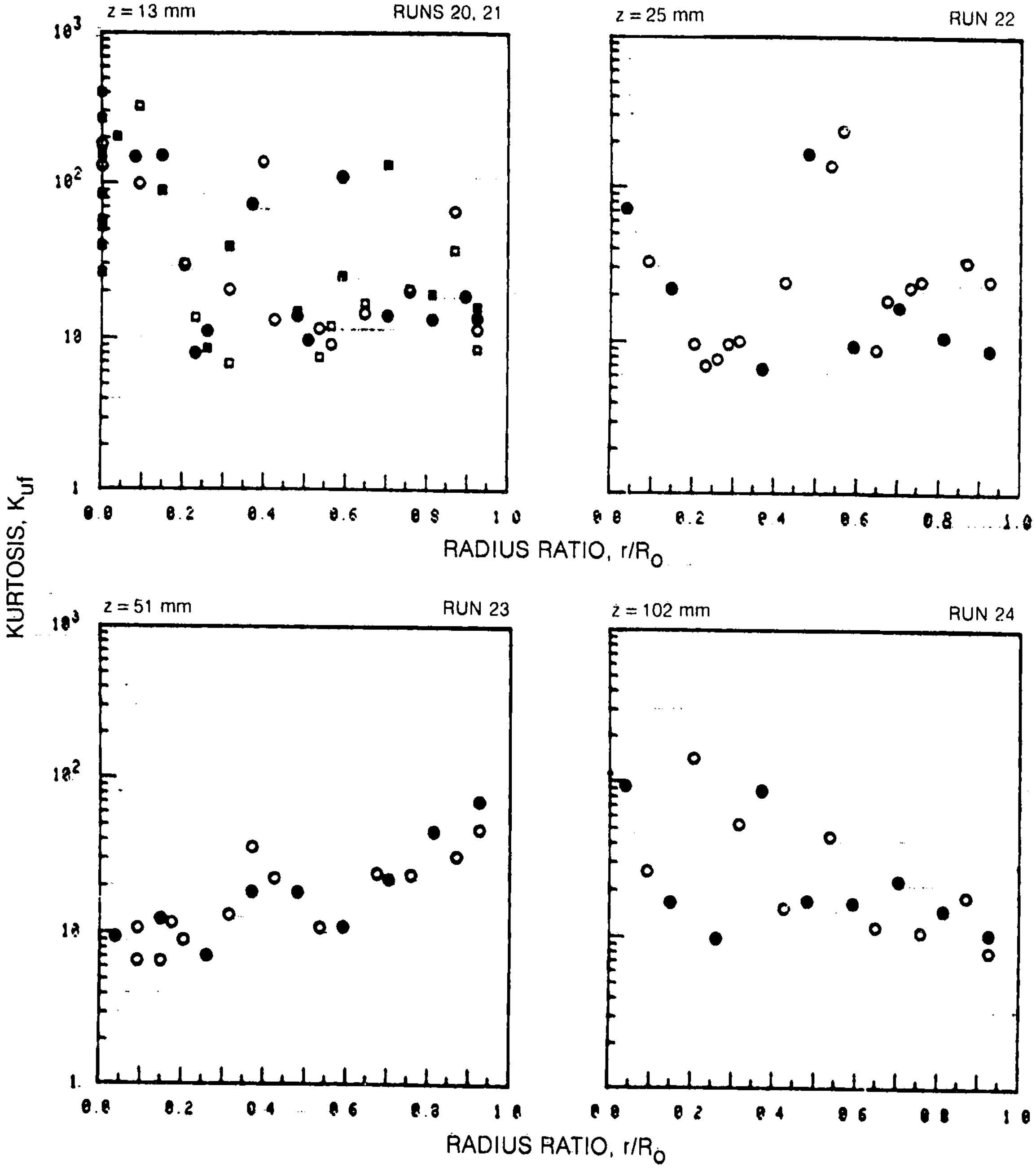

83–2–55–20A

ORIGINAL PAGE IS
OF POOR QUALITY

KURTOSIS OF TURBULENT AXIAL MASS TRANSPORT RATE PROFILES (CONT.)

	HORIZONTAL TRAVERSE	VERTICAL TRAVERSE
OPEN SYMBOLS:	$\theta = 90°$	$\theta = 0°$
SOLID SYMBOLS:	$\theta = 270°$	$\theta = 180°$

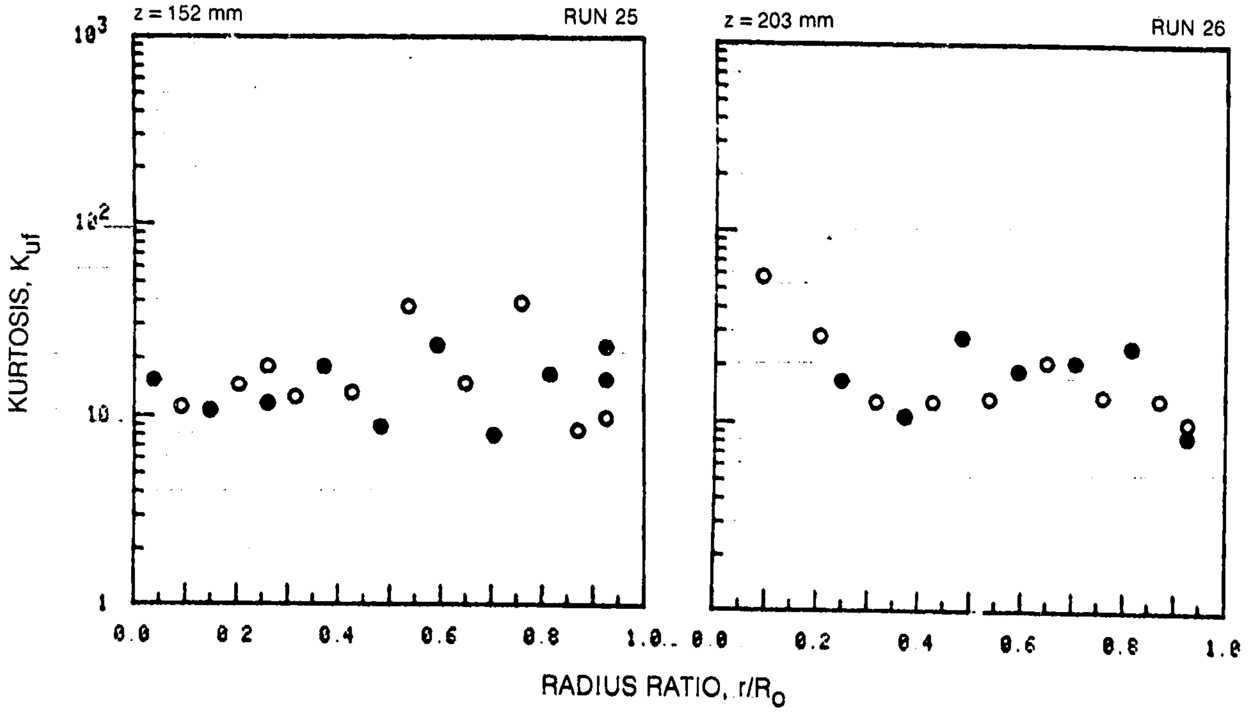

83-2-55-20B

**ORIGINAL PAGE IS
OF POOR QUALITY**

FIG. 67

SECOND CENTRAL MOMENT OF TURBULENT AZIMUTHAL MASS TRANSPORT RATE PROFILES

	HORIZONTAL TRAVERSE	VERTICAL TRAVERSE
OPEN SYMBOLS	$\theta = 90°$	$\theta = 0°$
SOLID SYMBOLS	$\theta = 270°$	$\theta = 180°$

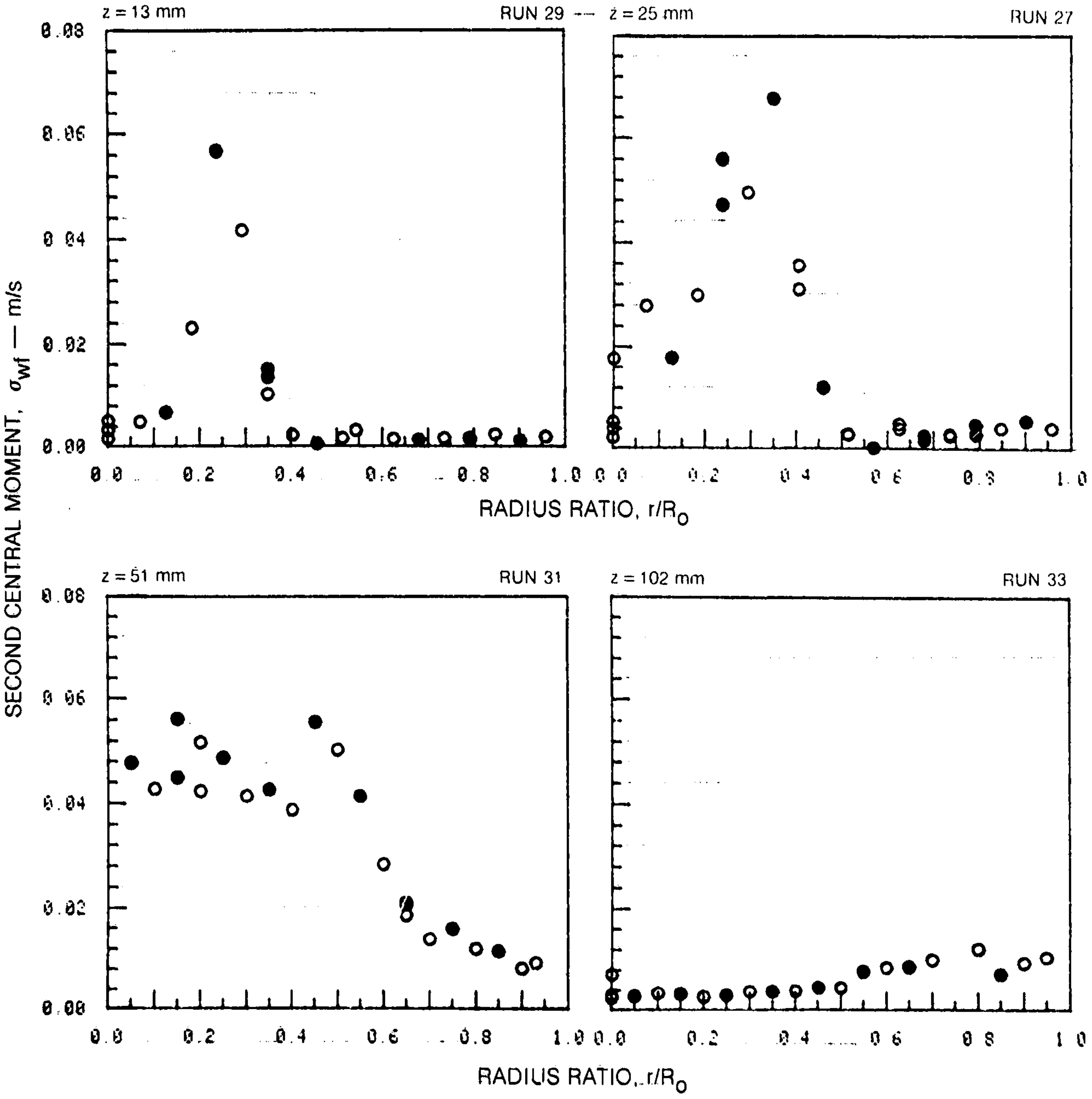

FIG. 67 (CONT.)

ORIGINAL PAGE IS
OF POOR QUALITY

SECOND CENTRAL MOMENT OF TURBULENT AZIMUTHAL MASS TRANSPORT RATE PROFILES

	HORIZONTAL TRAVERSE	VERTICAL TRAVERSE
OPEN SYMBOLS:	$\theta = 90°$	$\theta = 0°$
SOLID SYMBOLS:	$\theta = 270°$	$\theta = 180°$

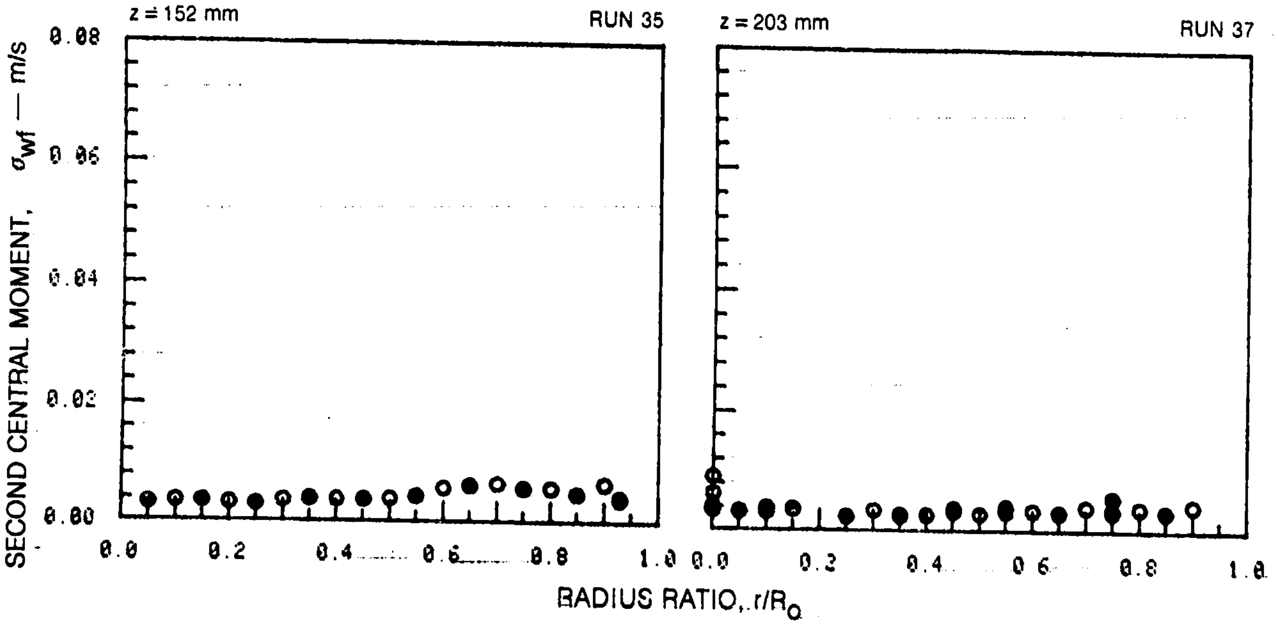

83-2-51-16B

ORIGINAL PAGE IS
OF POOR QUALITY

FIG. 68

SKEWNESS OF TURBULENT AZIMUTHAL MASS TRANSPORT RATE PROFILES

	HORIZONTAL TRAVERSE	VERTICAL TRAVERSE
OPEN SYMBOLS:	θ = 90°	θ = 0°
SOLID SYMBOLS:	θ = 270°	θ = 180°

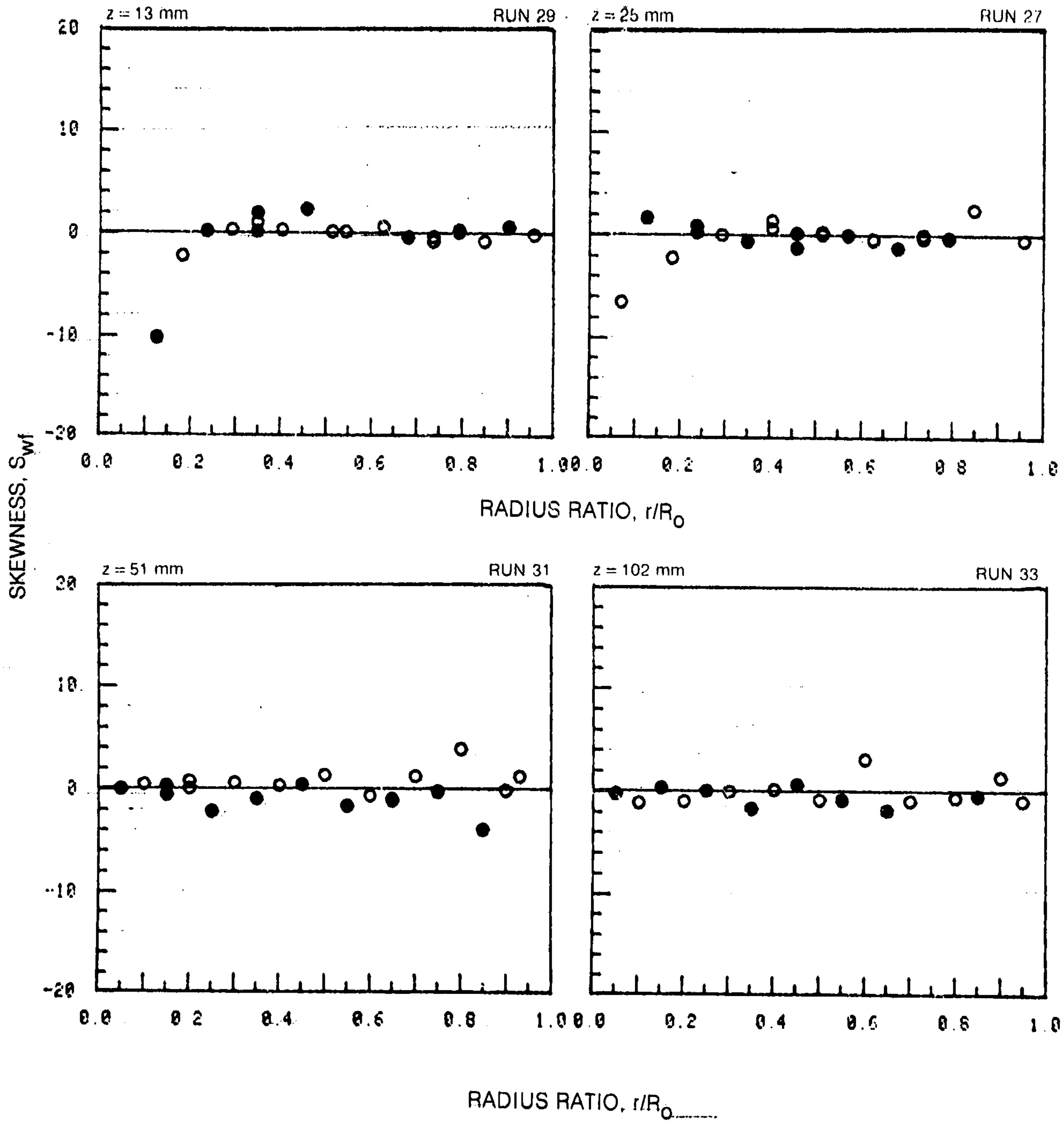

SKEWNESS OF TURBULENT AZIMUTHAL MASS TRANSPORT RATE PROFILES (CONT.)

	HORIZONTAL TRAVERSE	VERTICAL TRAVERSE
OPEN SYMBOLS:	θ = 90°	θ = 0°
SOLID SYMBOLS:	θ = 270°	θ = 180°

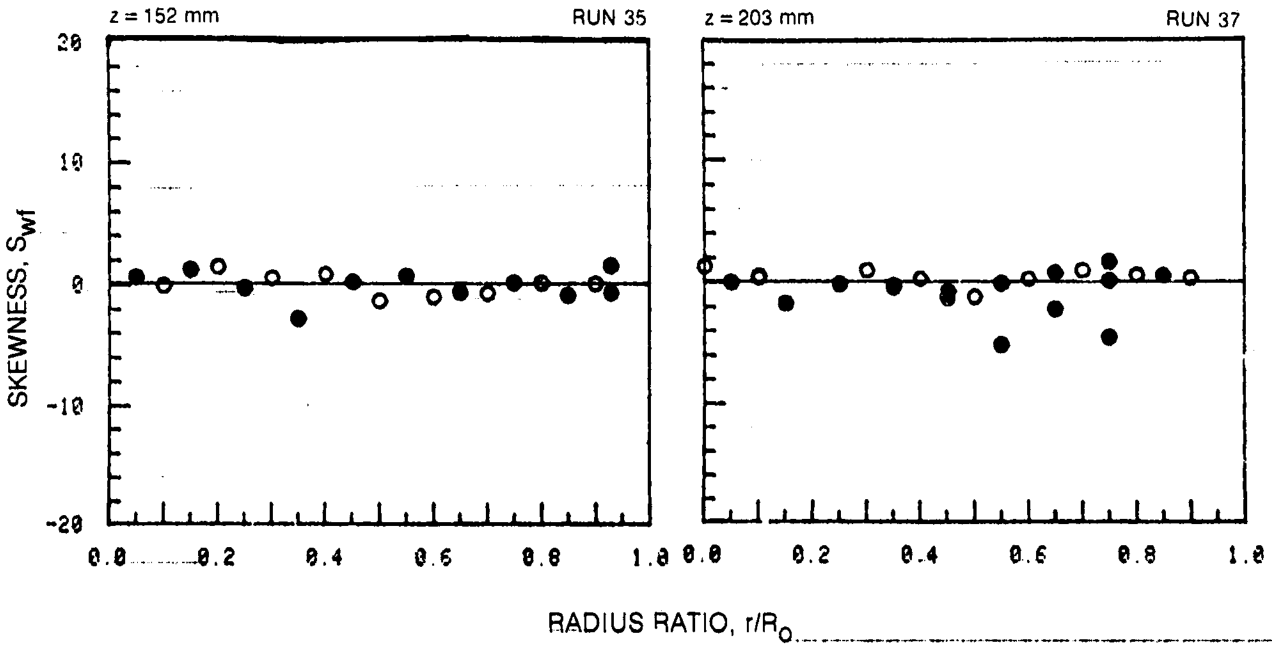

FIG. 69

KURTOSIS OF TURBULENT AZIMUTHAL MASS TRANSPORT RATE PROFILES

	HORIZONTAL TRAVERSE	VERTICAL TRAVERSE
OPEN SYMBOLS:	θ = 90°	θ = 0°
SOLID SYMBOLS:	θ = 270°	θ = 180°

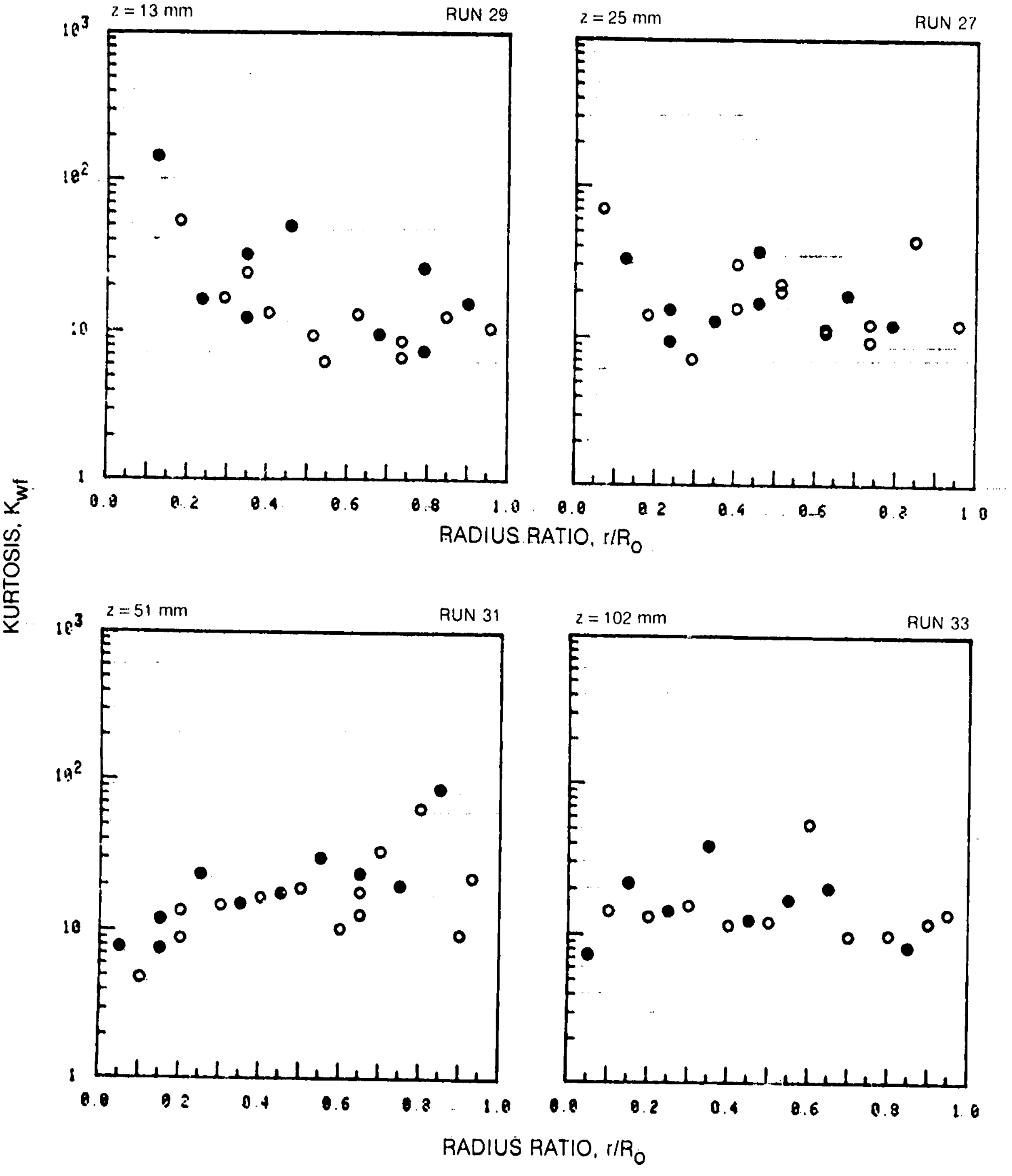

83-2-55-22A

FIG. 69 (CONT.)

KURTOSIS OF TURBULENT AZIMUTHAL MASS TRANSPORT RATE PROFILES (CONT.)

	HORIZONTAL TRAVERSE	VERTICAL TRAVERSE
OPEN SYMBOLS:	θ = 90°	θ = 0°
SOLID SYMBOLS:	θ = 270°	θ = 180°

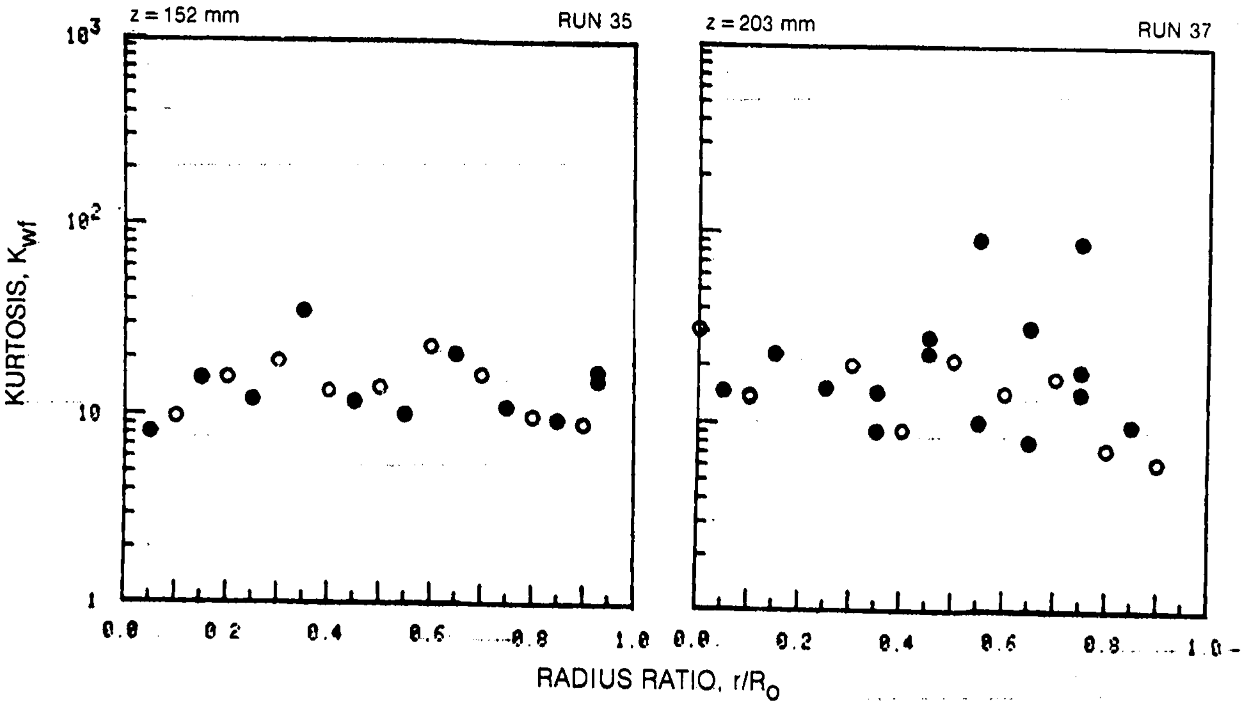

ORIGINAL PAGE IS
OF POOR QUALITY

FIG. 70

VISUALIZATION OF FLOW CONDITION 2 WITH SWIRL IN ANNULAR STREAM

$U_i = 0.27$ m/s $U_a = 1.66$ m/s

$Q_i = 3.1$ gpm $Q_a = 52.8$ gpm

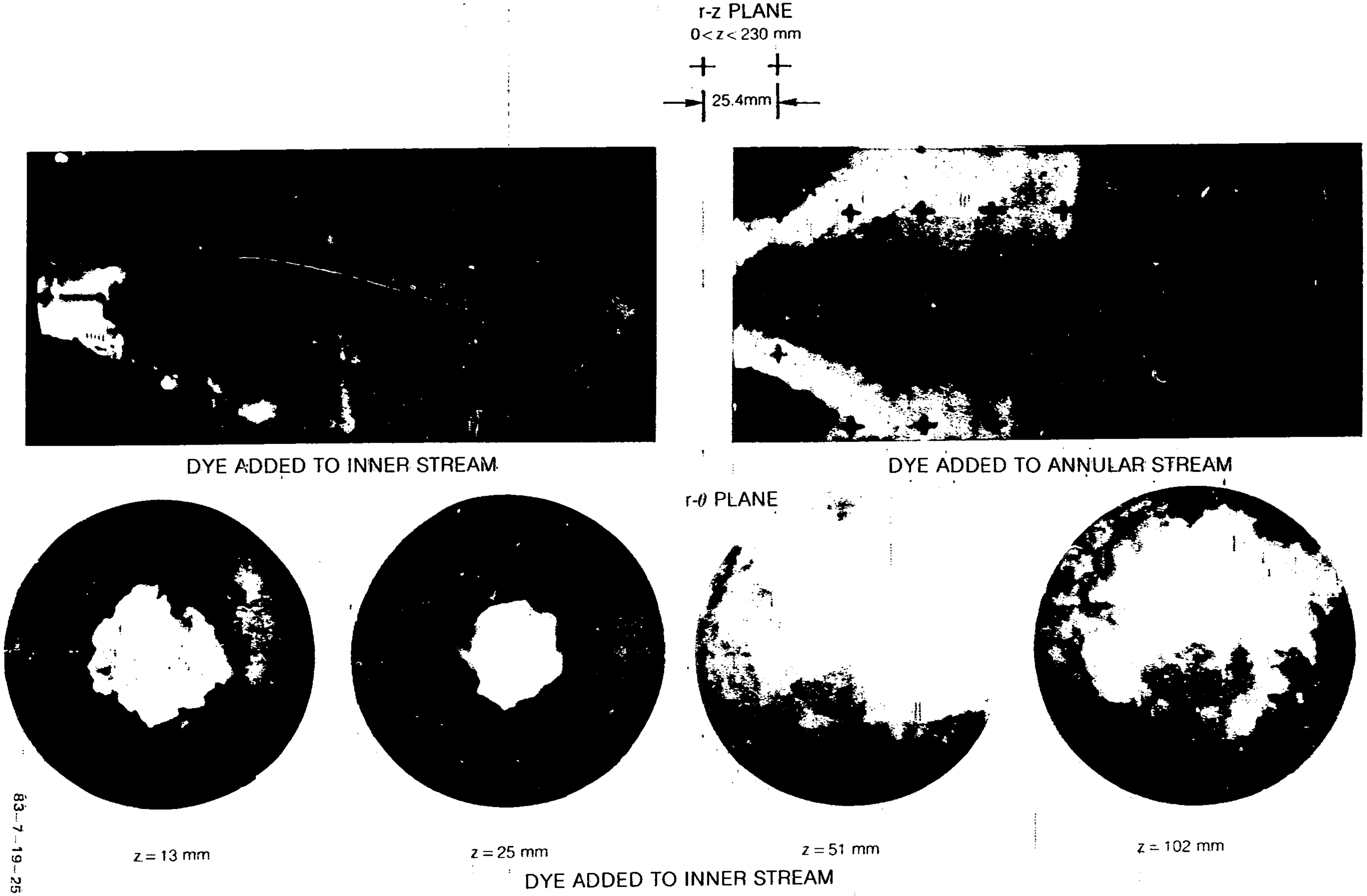
r-z PLANE
0 < z < 230 mm
25.4mm
DYE ADDED TO INNER STREAM
DYE ADDED TO ANNULAR STREAM
r-θ PLANE
z = 13 mm
z = 25 mm
z = 51 mm
z = 102 mm
DYE ADDED TO INNER STREAM

83-7-19-25

ORIGINAL PAGE IS
OF POOR QUALITY

FIG. 71

VISUALIZATION OF FLOW CONDITION 3 WITH SWIRL IN ANNULAR STREAM

$u_i = 2.08$ m/s $\quad u_a = 1.66$ m/s
$Q_i = 24.6$ gpm $\quad Q_a = 52.8$ gpm

r-z PLANE
$0 < z < 230$ mm

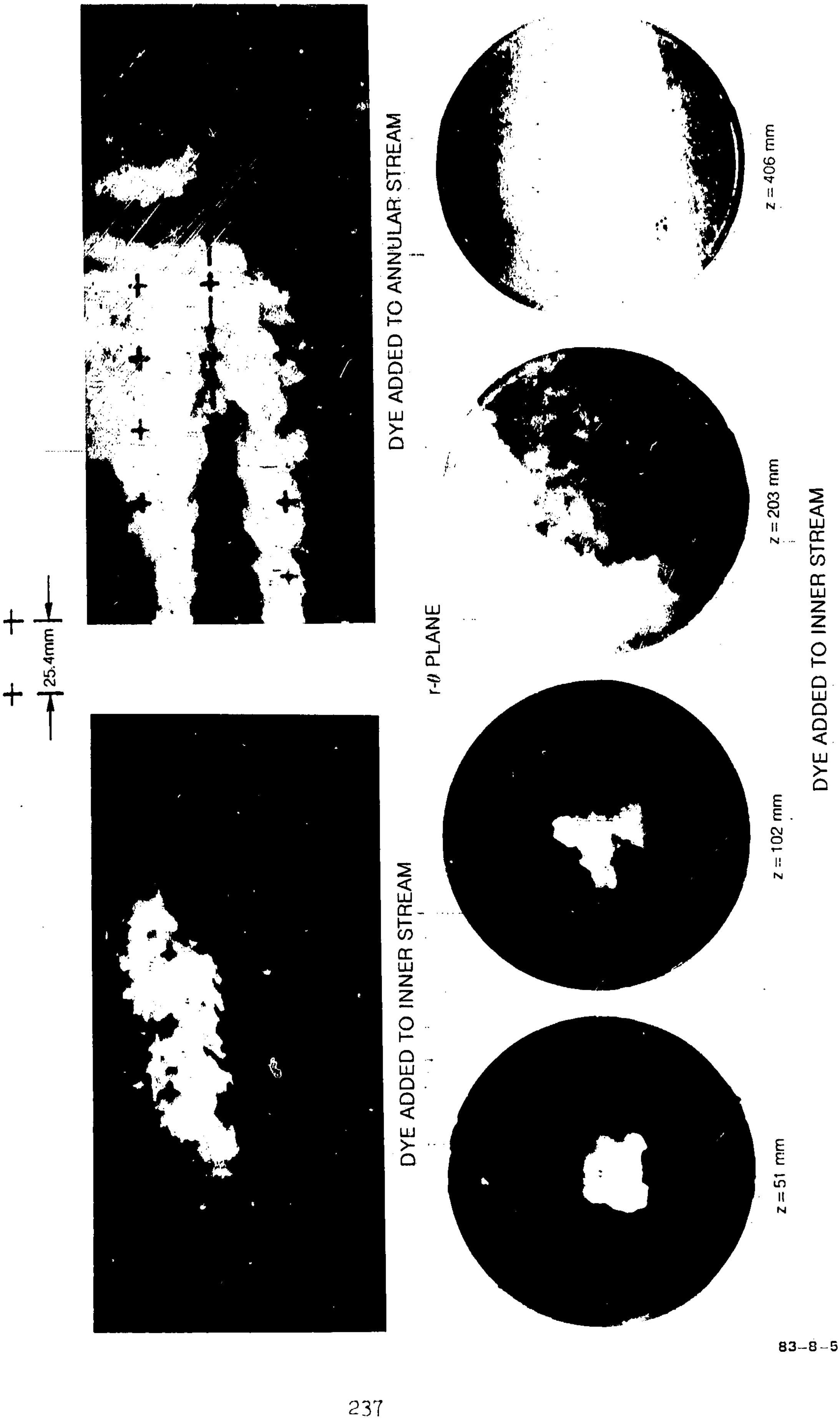
25.4mm
DYE ADDED TO INNER STREAM
DYE ADDED TO ANNULAR STREAM
r-θ PLANE
z = 51 mm
z = 102 mm
z = 203 mm
z = 406 mm
DYE ADDED TO INNER STREAM

83–8–5–29

FIG. 72

VISUALIZATION OF FLOW CONDITION 4 WITH SWIRL IN ANNULAR STREAM

$U_i = 0.94$ m/s $\quad U_a = 1.51$ m/s

$Q_i = 11.1$ gpm $\quad Q_a = 48.0$ gpm

r-z PLANE

$0 < z < 230$ mm

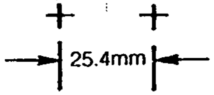

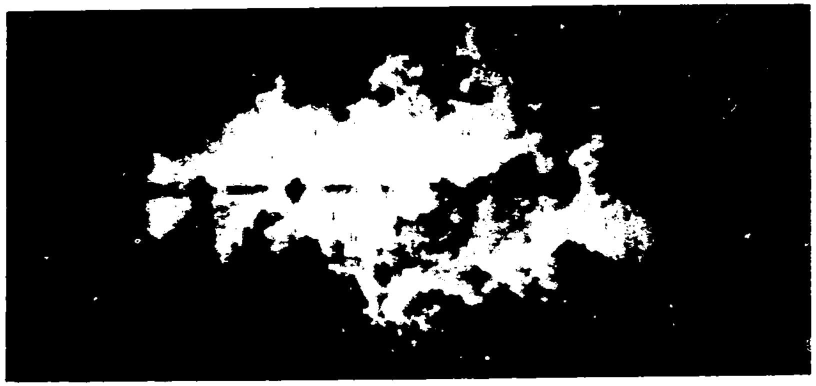

DYE ADDED TO INNER STREAM

r-θ PLANE

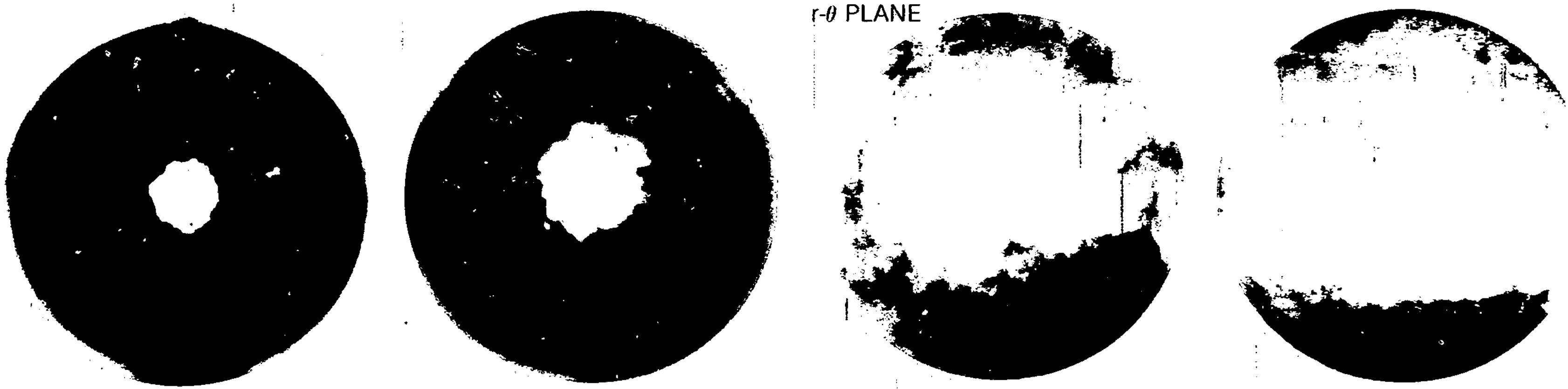

z = 25 mm

z = 51 mm

z = 102 mm

z = 203 mm

DYE ADDED TO INNER STREAM

83–8–5–27

VISUALIZATION OF FLOW CONDITION 5 WITH SWIRL IN ANNULAR STREAM

$U_i = 0.94$ m/s $U_a = 2.87$ m/s

$Q_i = 11.1$ gpm $Q_a = 94.8$ gpm

r-z PLANE

$0 < z < 230$ mm

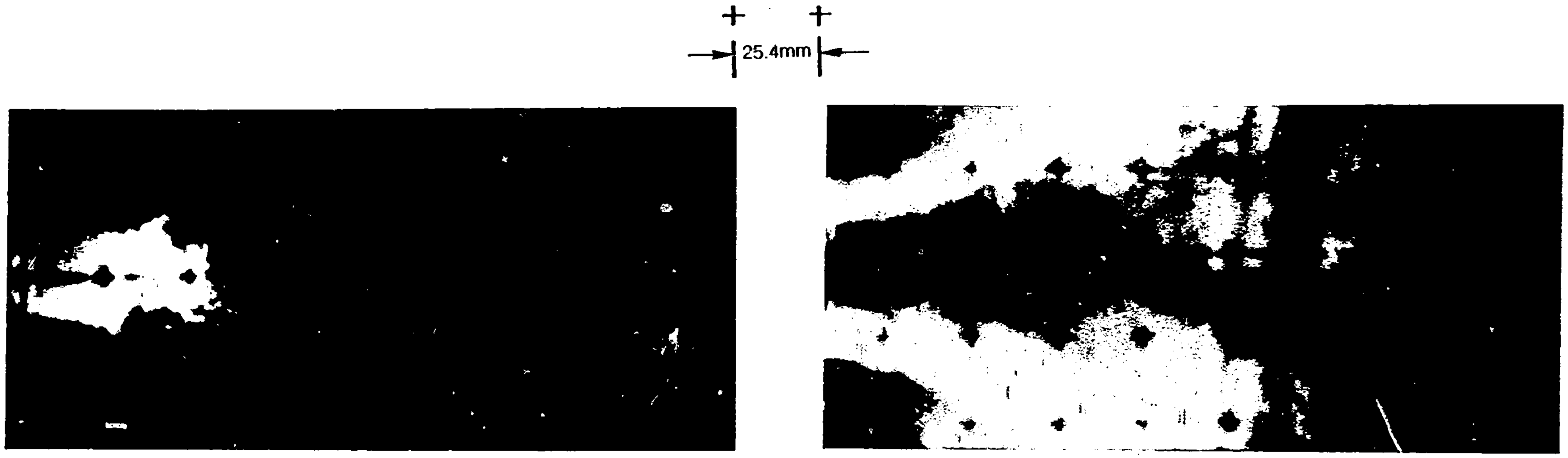

DYE ADDED TO INNER STREAM DYE ADDED TO ANNULAR STREAM

r-θ PLANE

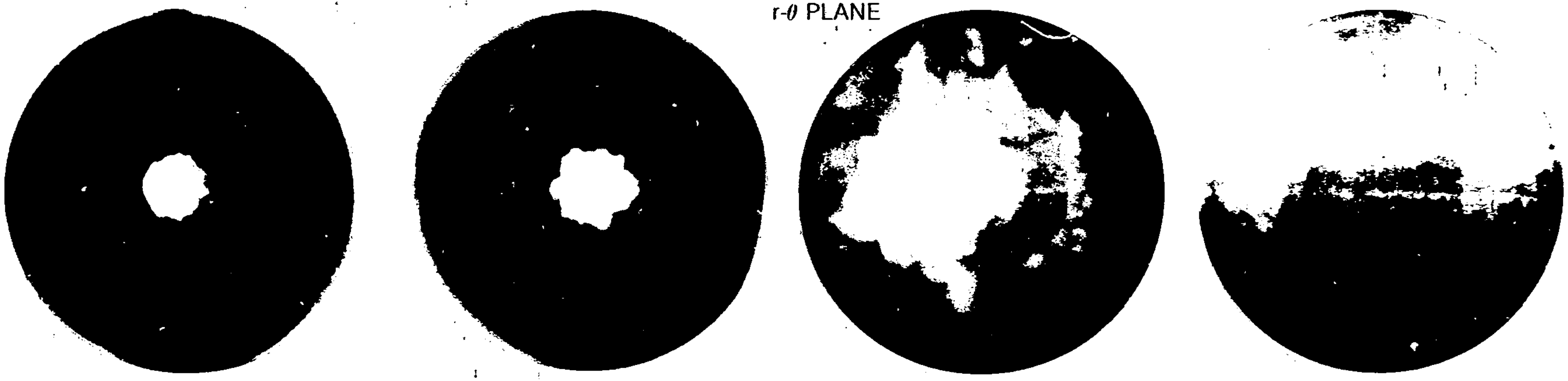

z = 13 mm z = 25 mm z = 51 mm z = 102 mm

DYE ADDED TO INNER STREAM

FIG. 73

ORIGINAL PAGE IS
OF POOR QUALITY

83–7–19–26

ORIGINAL PAGE IS
OF POOR QUALITY

FIG. 74

BLADE PASSAGE MEASUREMENTS

SWIRLER ORIENTATION

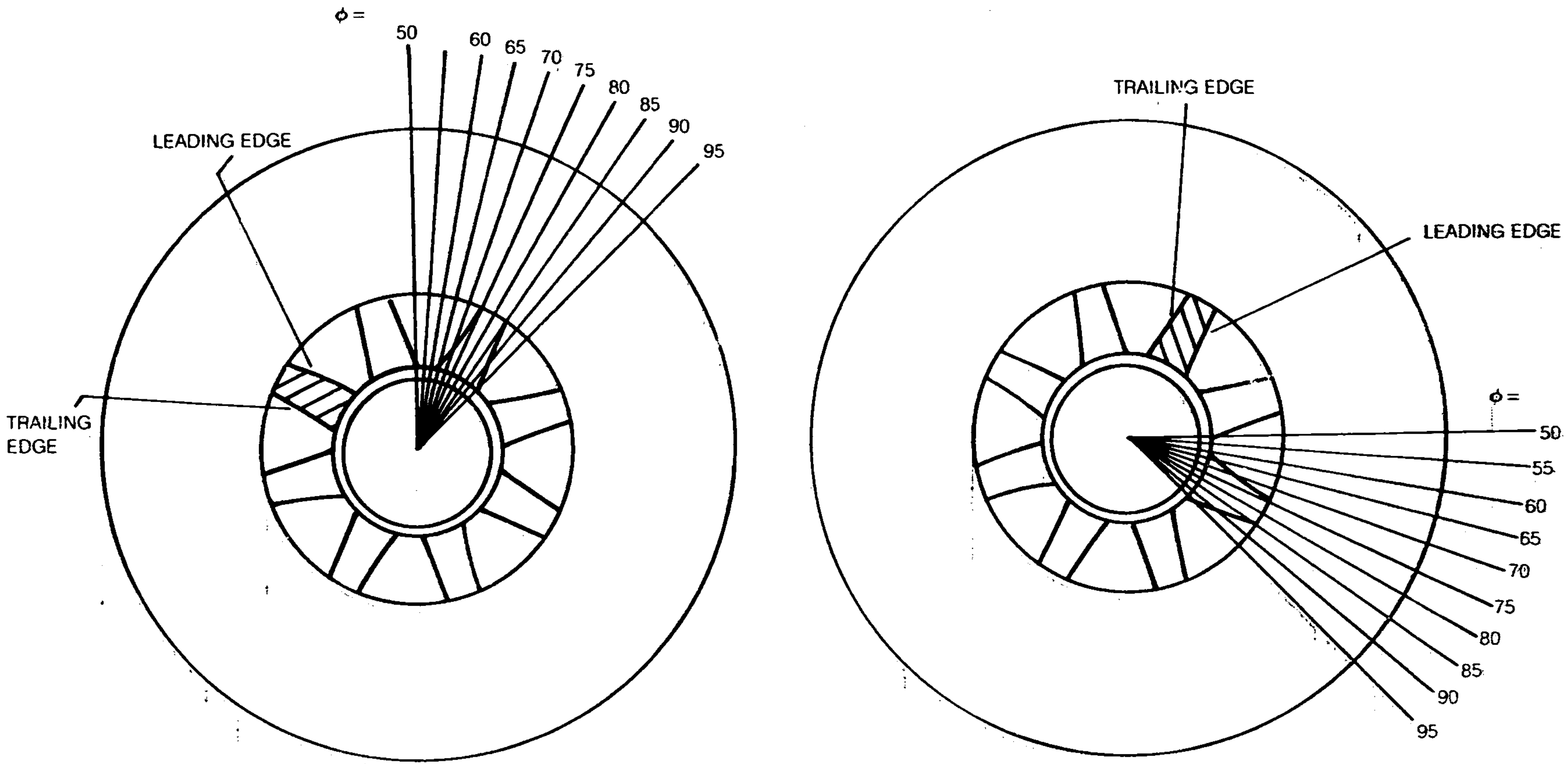

φ =
50
60
65
70
75
80
85
90
95
LEADING EDGE
TRAILING EDGE
TRAILING EDGE
LEADING EDGE
φ =
50
55
60
65
70
75
80
85
90
95

AXIAL/RADIAL VELOCITY MEASUREMENTS

AXIAL/AZIMUTHAL VELOCITY MEASUREMENTS

83-7-19-30

ORIGINAL PAGE IS
OF POOR QUALITY

MEAN AXIAL VELOCITY PROFILES

SWIRLER EXIT PLANE AT z = 0 mm DATA OBTAINED AT z = 5 mm SEE FIG. 74 FOR VANE ORIENTATION

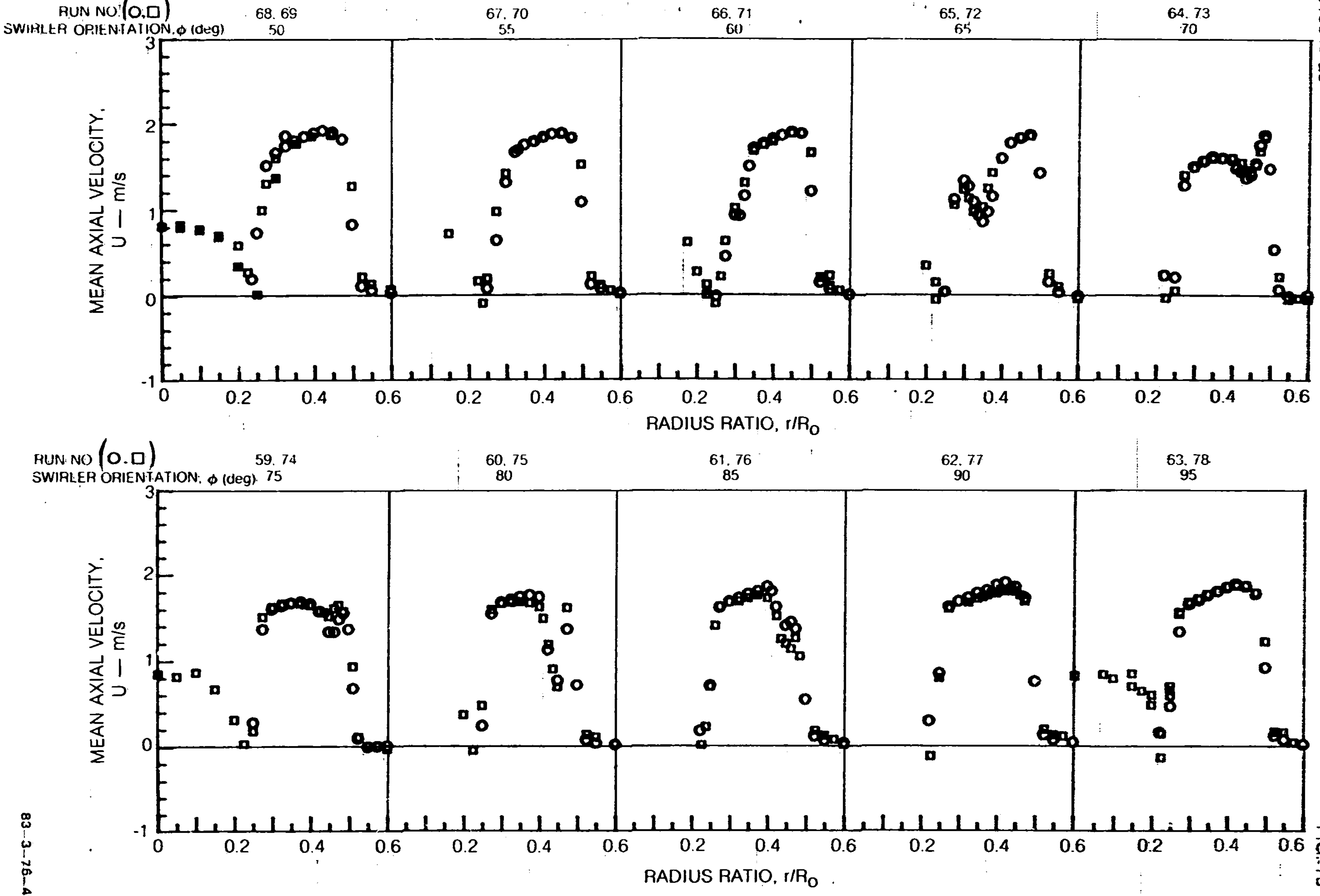

FIG. 75

83-3-76-42

ORIGINAL PAGE IS
OF POOR QUALITY

MEAN RADIAL VELOCITY PROFILES

SWIRLER EXIT PLANE AT $z = 0$ mm DATA OBTAINED AT $z = 5$ mm SEE FIG. 74 FOR VANE ORIENTATION

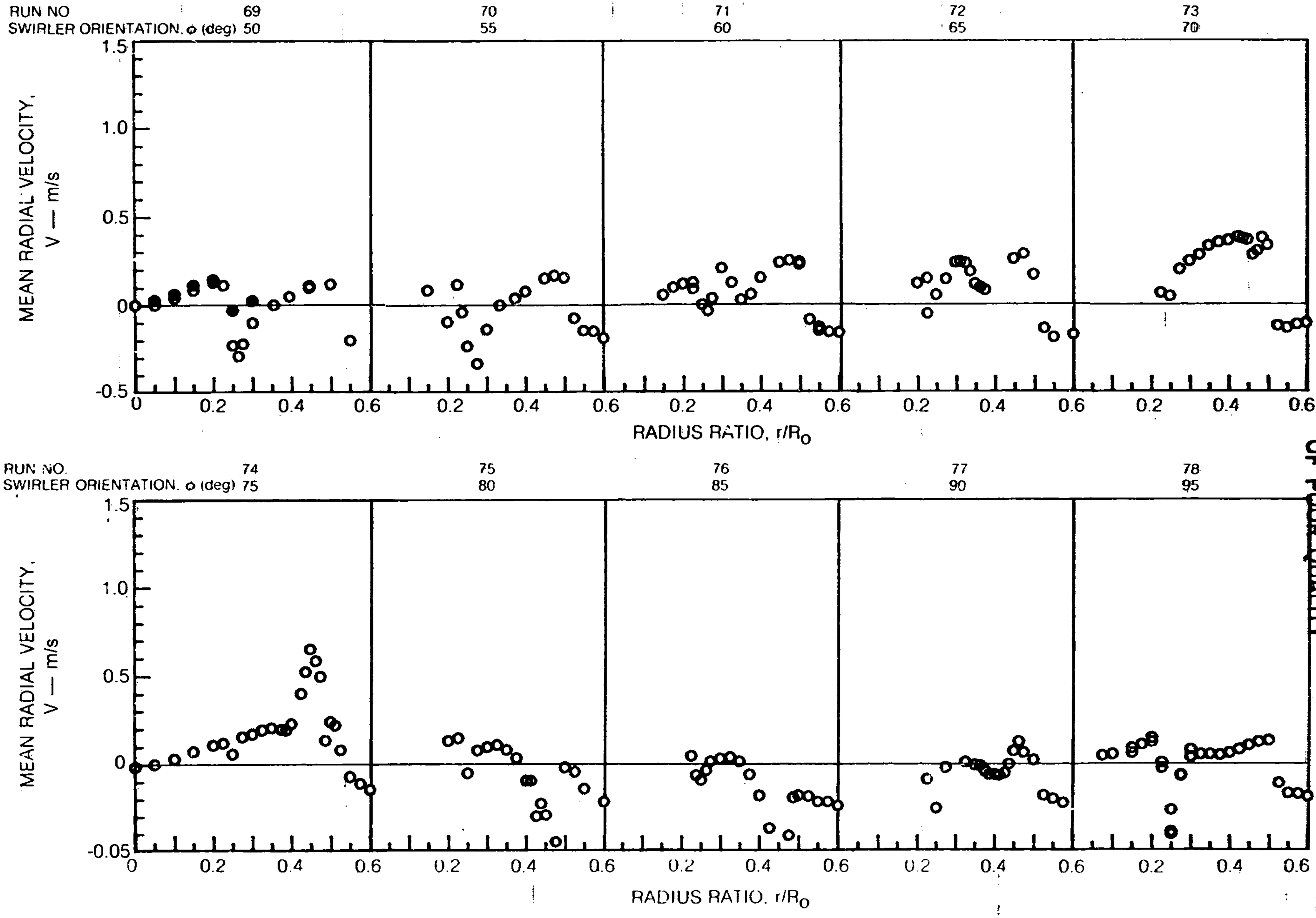

FIG. 76

83-3-76-50

ORIGINAL PAGE IS
OF POOR QUALITY

FIG. 77

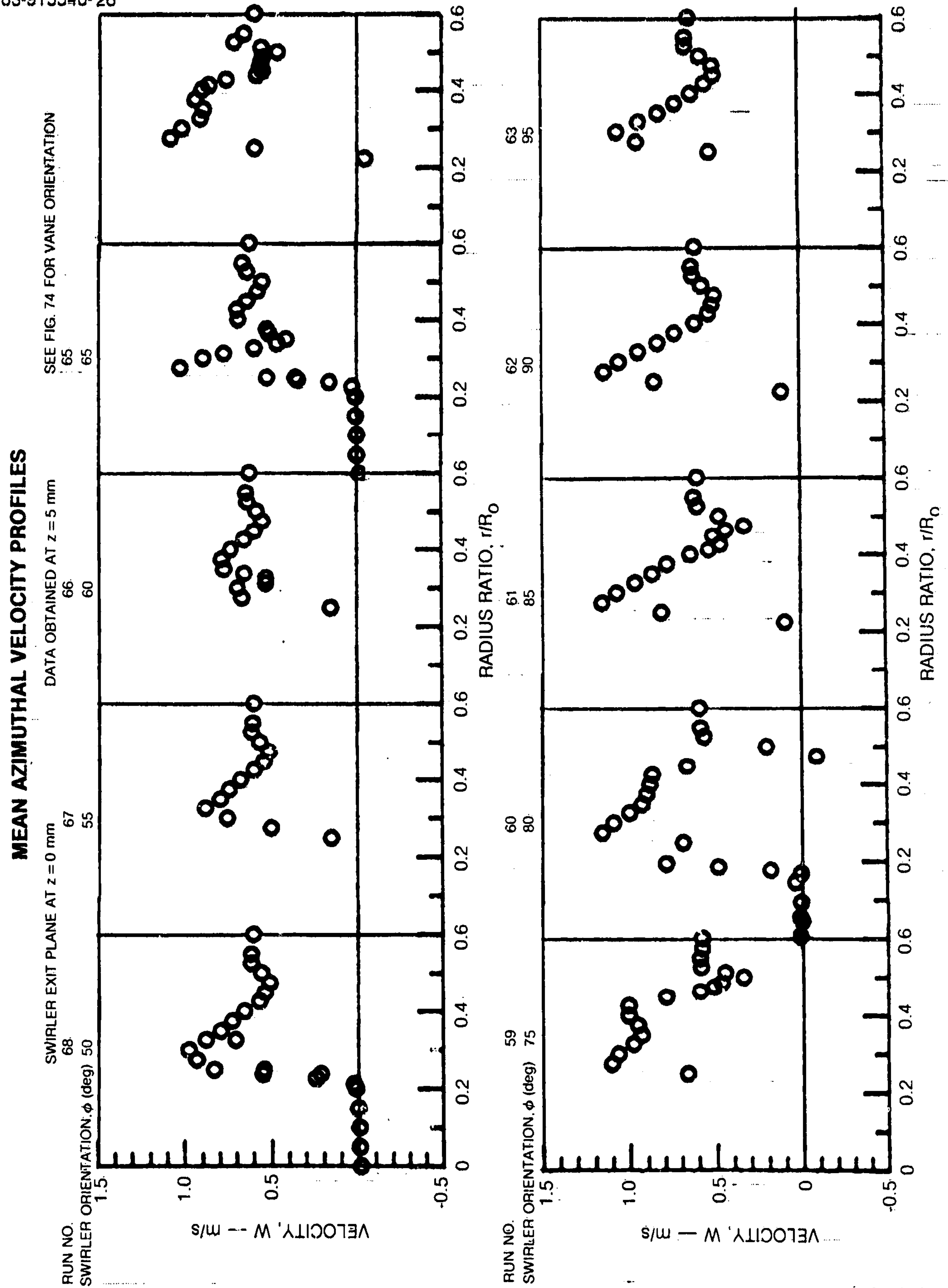
MEAN AZIMUTHAL VELOCITY PROFILES

83-3-50-4

ORIGINAL PAGE IS
OF POOR QUALITY

MEAN AXIAL VELOCITY PROFILES

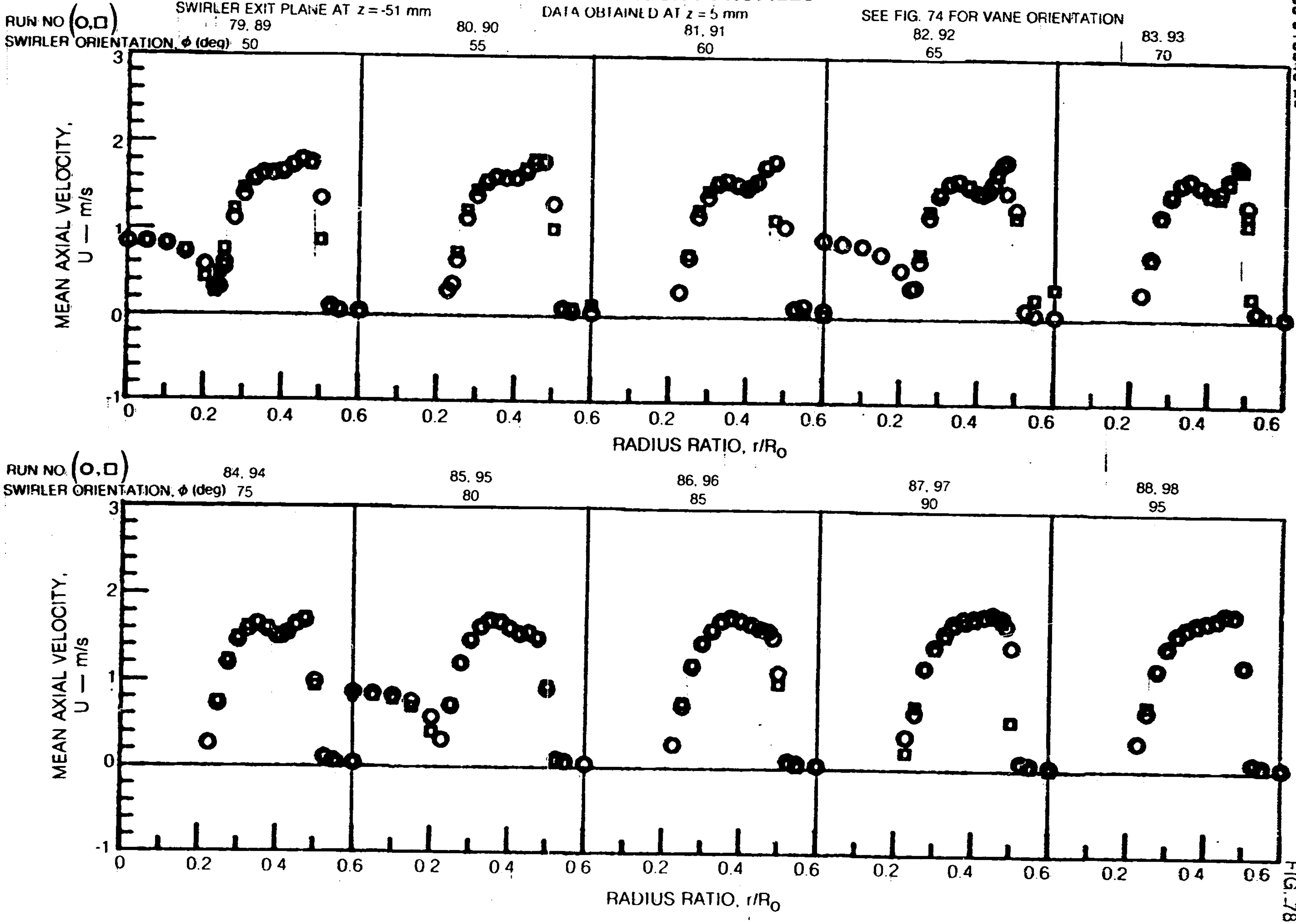

FIG. 78

ORIGINAL PAGE IS
OF POOR QUALITY

MEAN RADIAL VELOCITY PROFILES

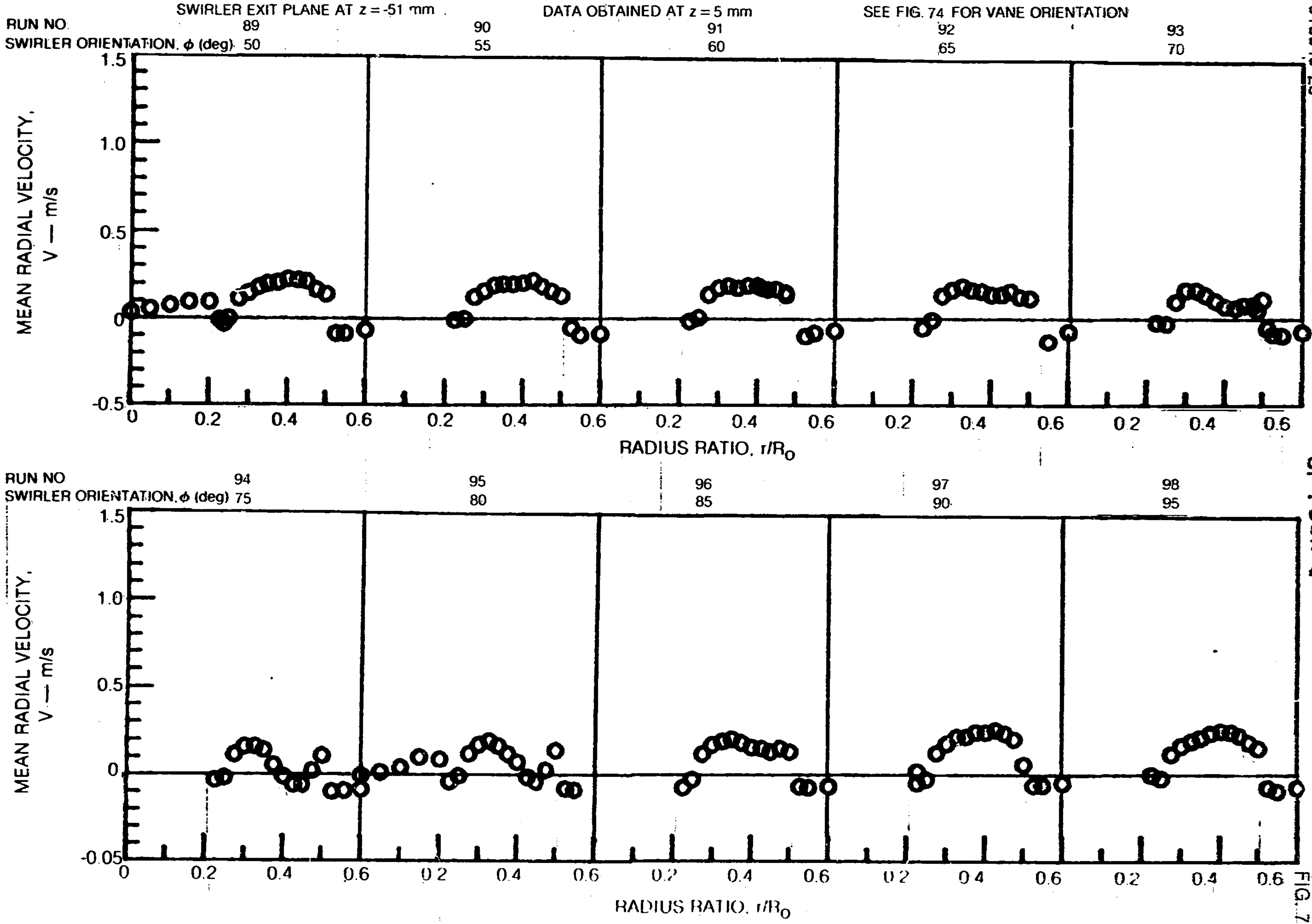

FIG. 79

83-7-19-16

MEAN AZIMUTHAL VELOCITY PROFILES

SWIRLER EXIT PLANE AT $z = -51$ mm

DATA OBTAINED AT $z = 5$ mm

SEE FIG. 74 FOR VANE ORIENTATION

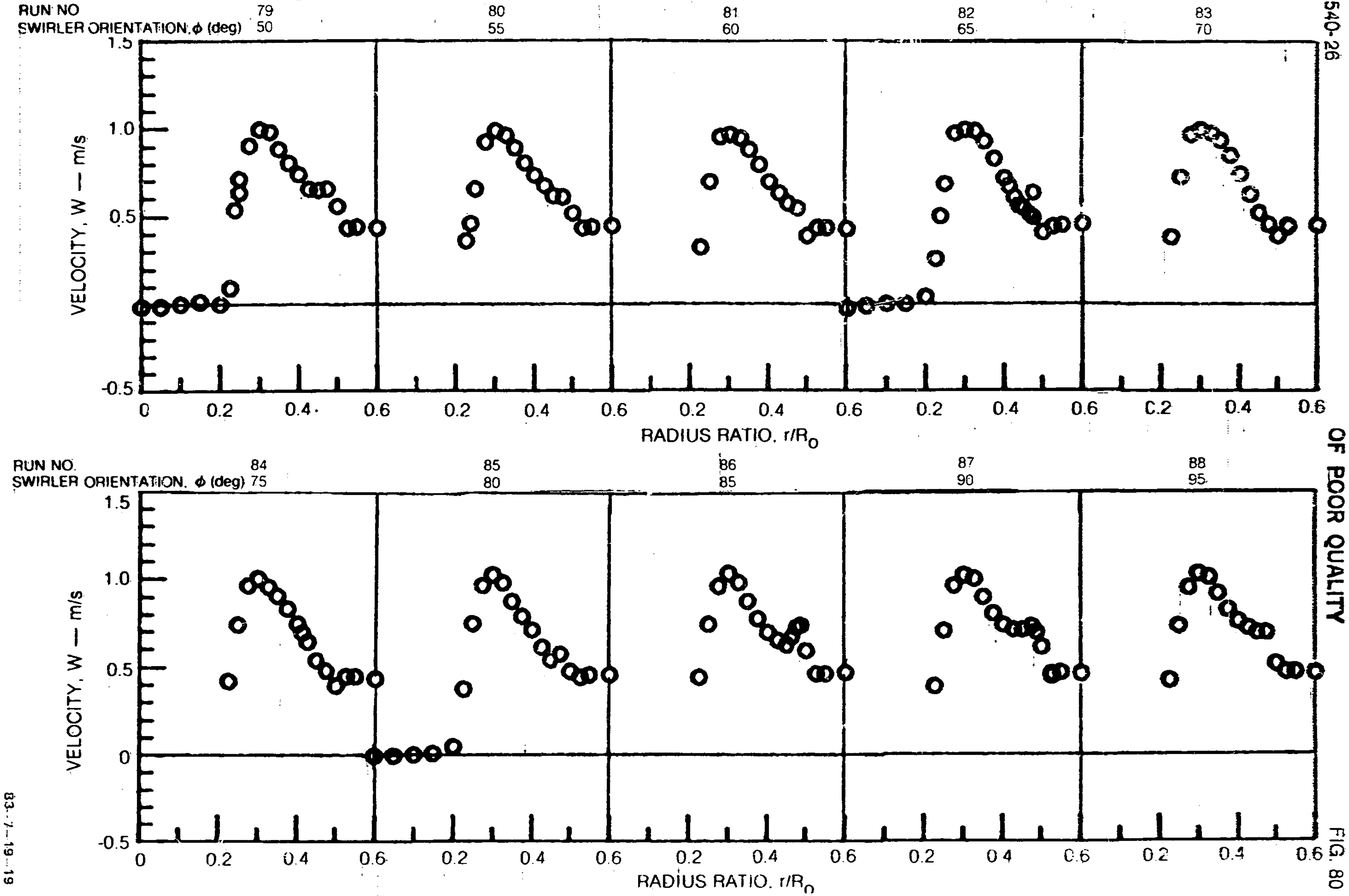

FIG. 80

83-7-19-19

ORIGINAL PAGE IS
OF POOR QUALITY

FLUCTUATING AXIAL VELOCITY PROFILES

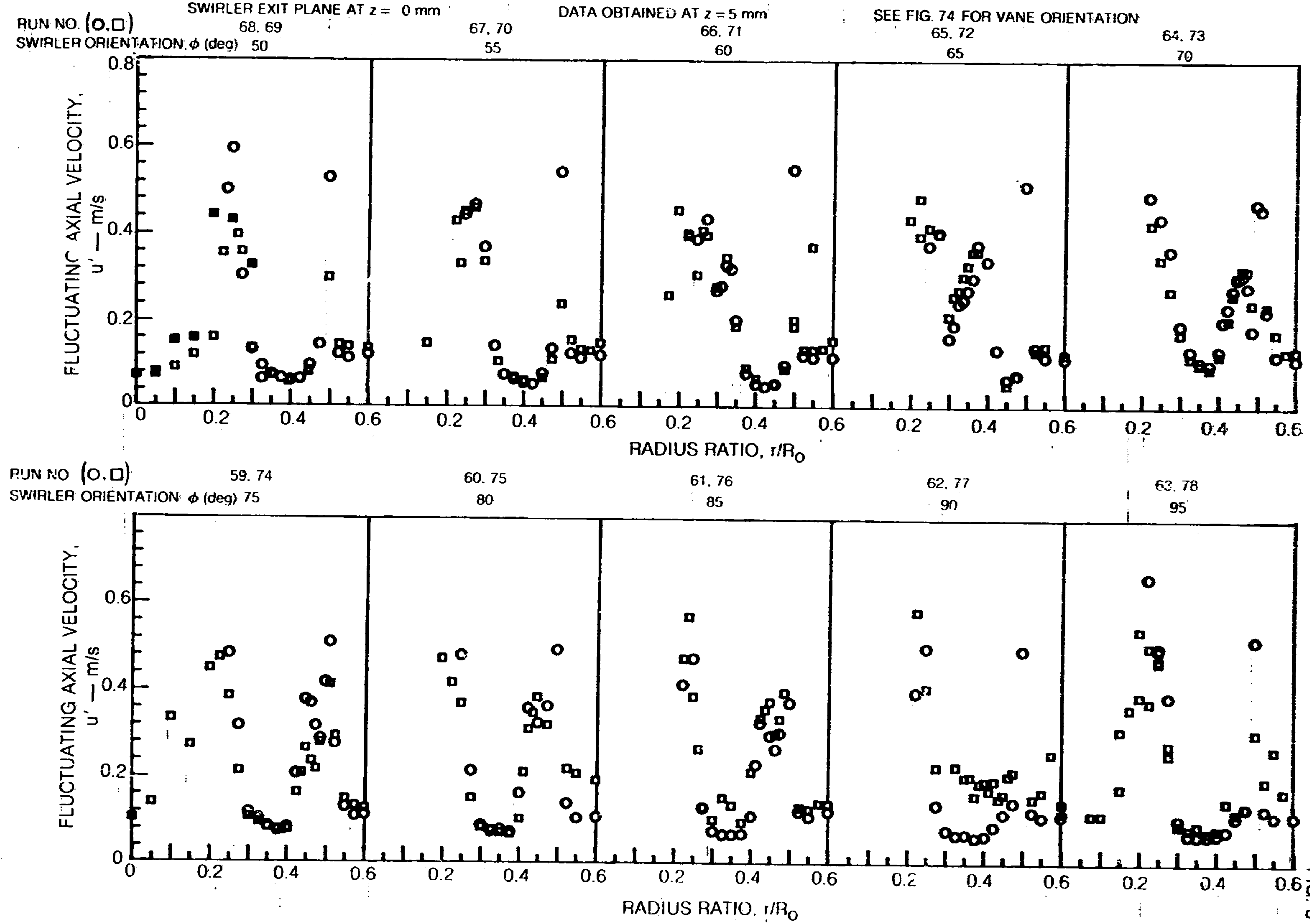

FIG. 81

83-3-76-43

ORIGINAL PAGE IS
OF POOR QUALITY

FLUCTUATING RADIAL VELOCITY PROFILES

SWIRLER EXIT PLANE AT z = 0 mm DATA OBTAINED AT z = 5 mm SEE FIG. 74 FOR VANE ORIENTATION

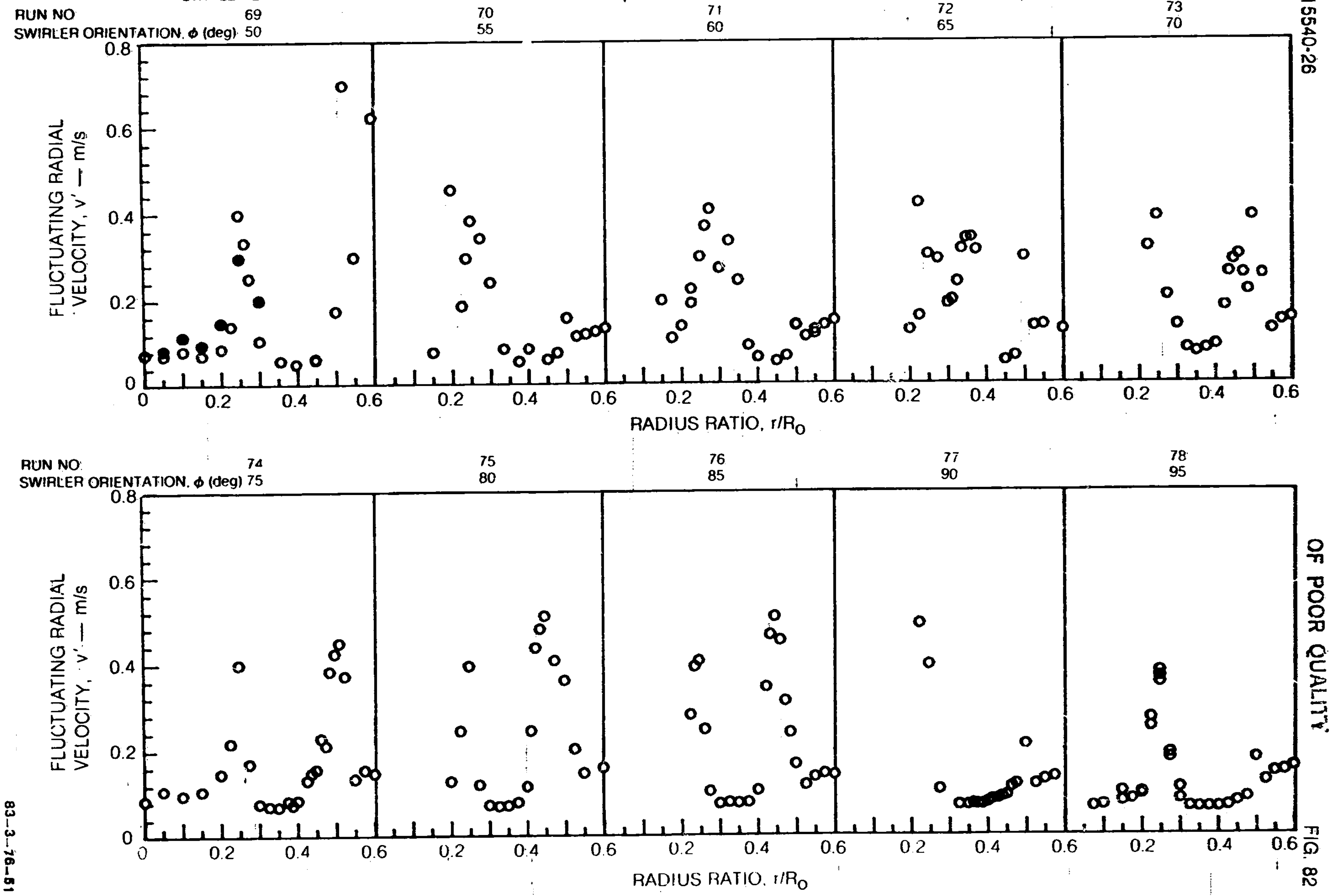

FIG. 82

83-3-76-51

FLUCTUATING AZIMUTHAL VELOCITY PROFILES

SWIRLER EXIT PLANE AT z = 0 mm DATA OBTAINED AT z = 5 mm SEE FIG. 74 FOR VANE ORIENTATION

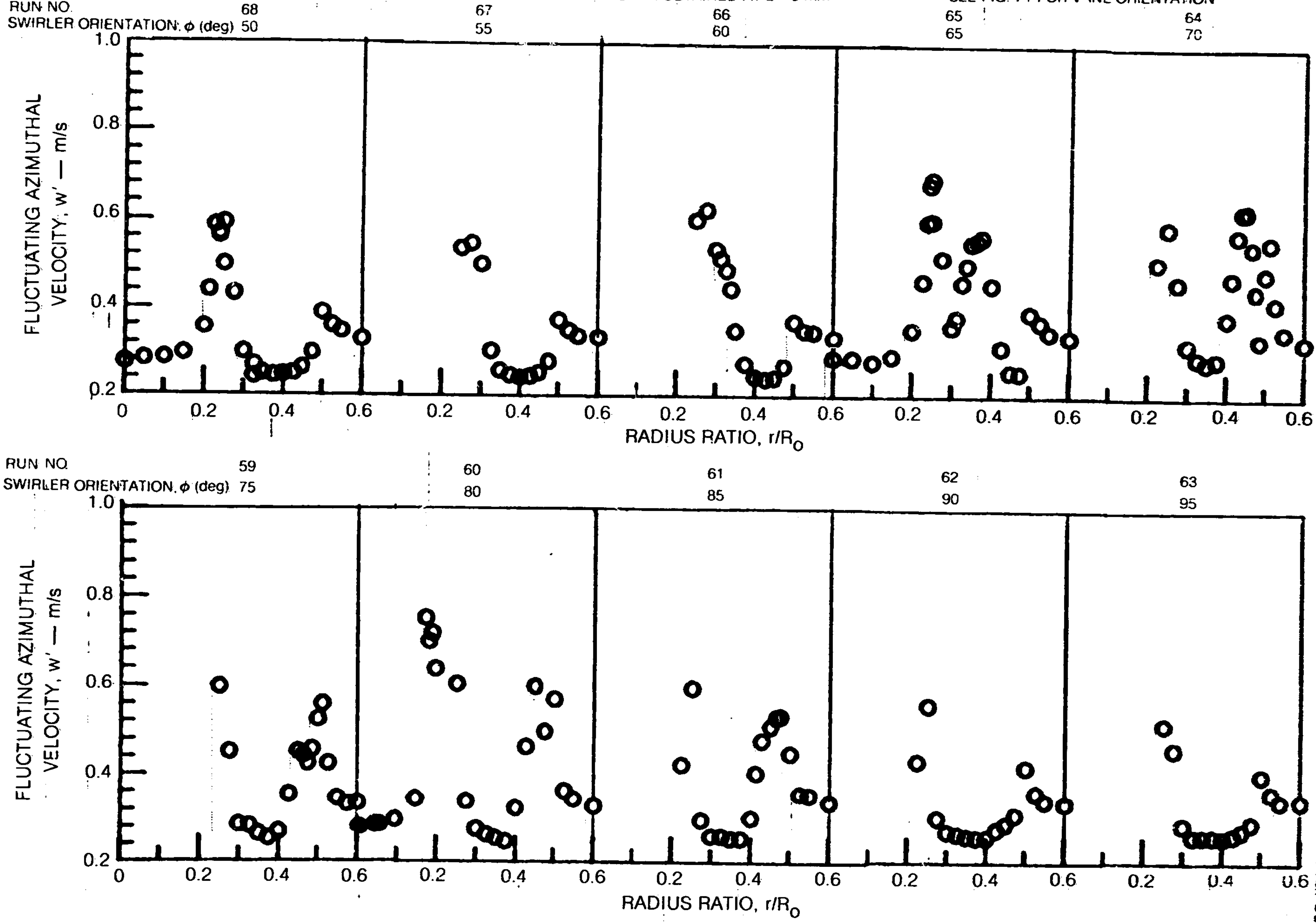

FIG. 83

83–7–19–22

ORIGINAL PAGE IS OF POOR QUALITY

FLUCTUATING AXIAL VELOCITY PROFILES

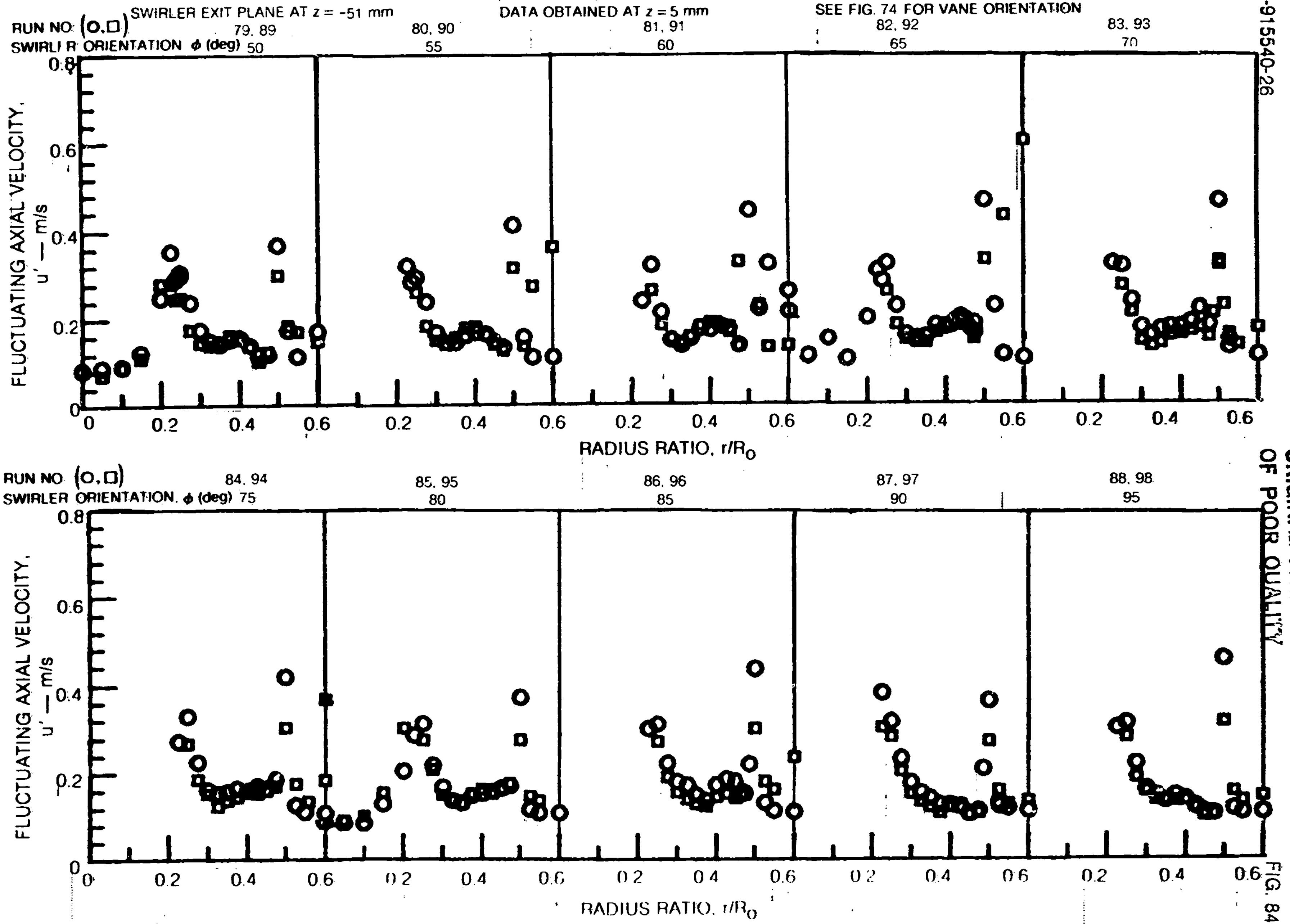

FIG. 84

83-7-19-14

FLUCTUATING RADIAL VELOCITY PROFILES

SWIRLER EXIT PLANE AT z = -51 mm DATA OBTAINED AT z = 5 mm SEE FIG. 74 FOR VANE ORIENTATION

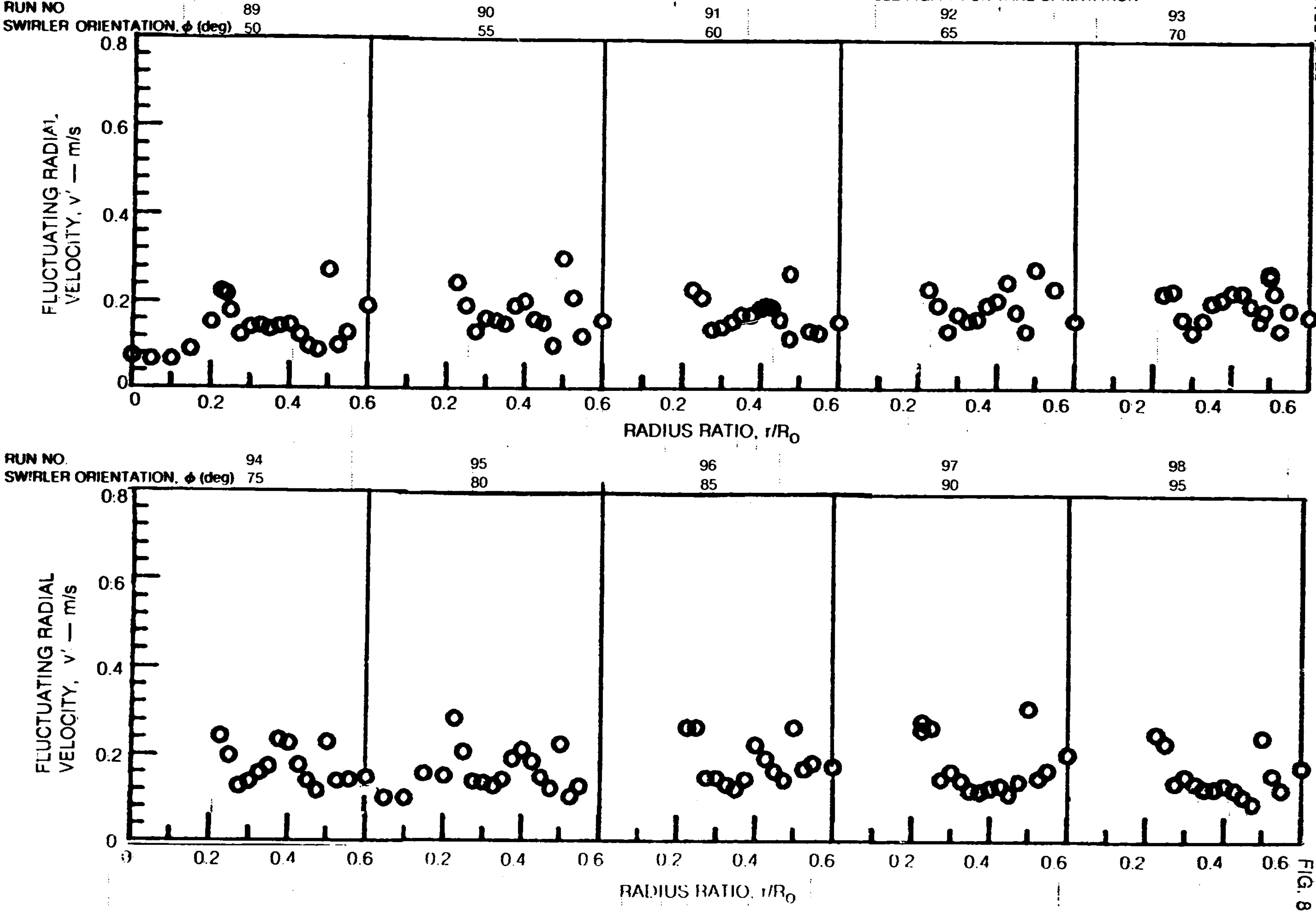

FIG. 85

83-7-19-15

FLUCTUATING AZIMUTHAL VELOCITY PROFILES

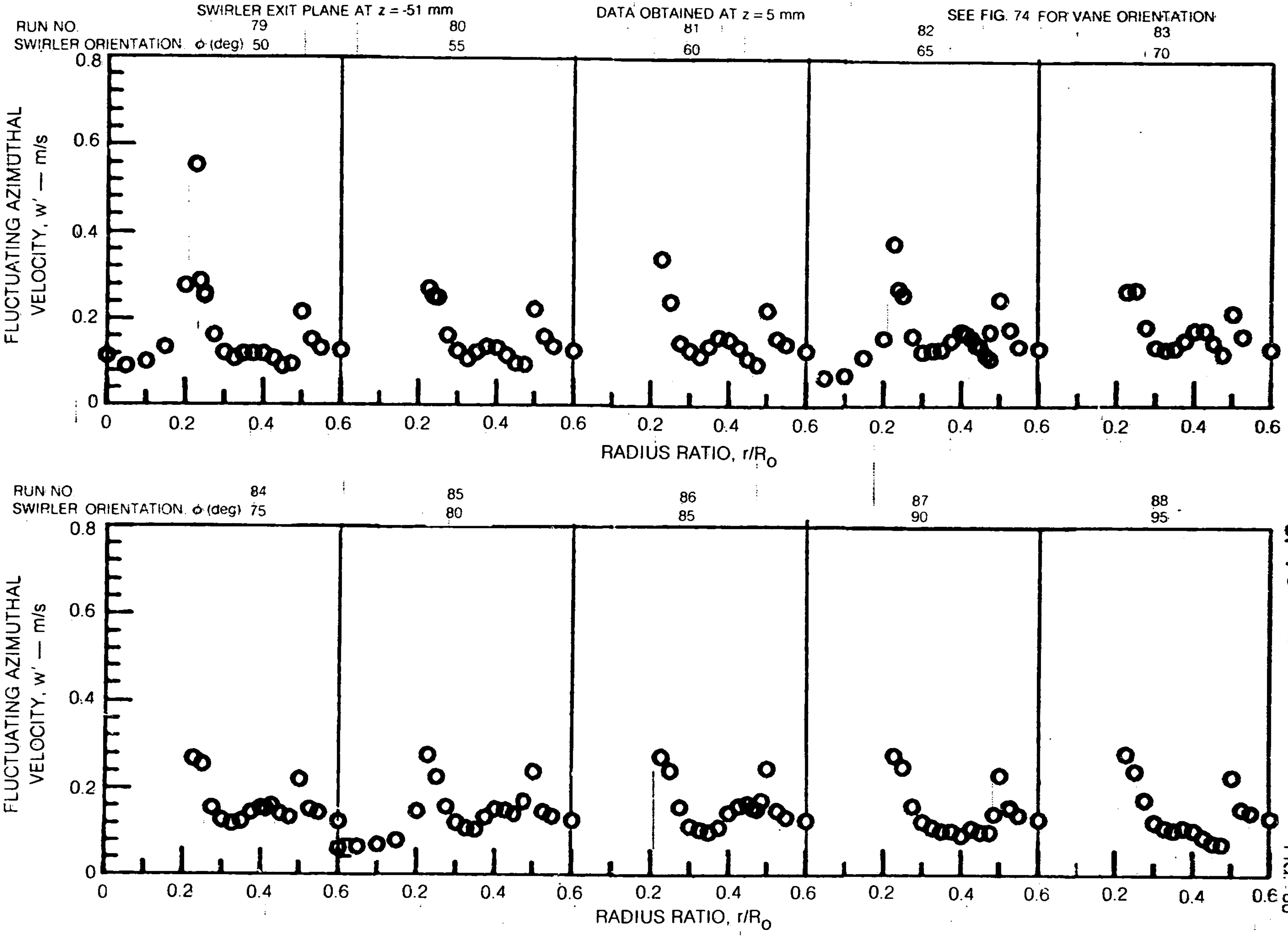

ORIGINAL PAGE IS OF POOR QUALITY

FIG. 86

83 7 19 21

ORIGINAL PAGE IS
OF POOR QUALITY

FIG. 87

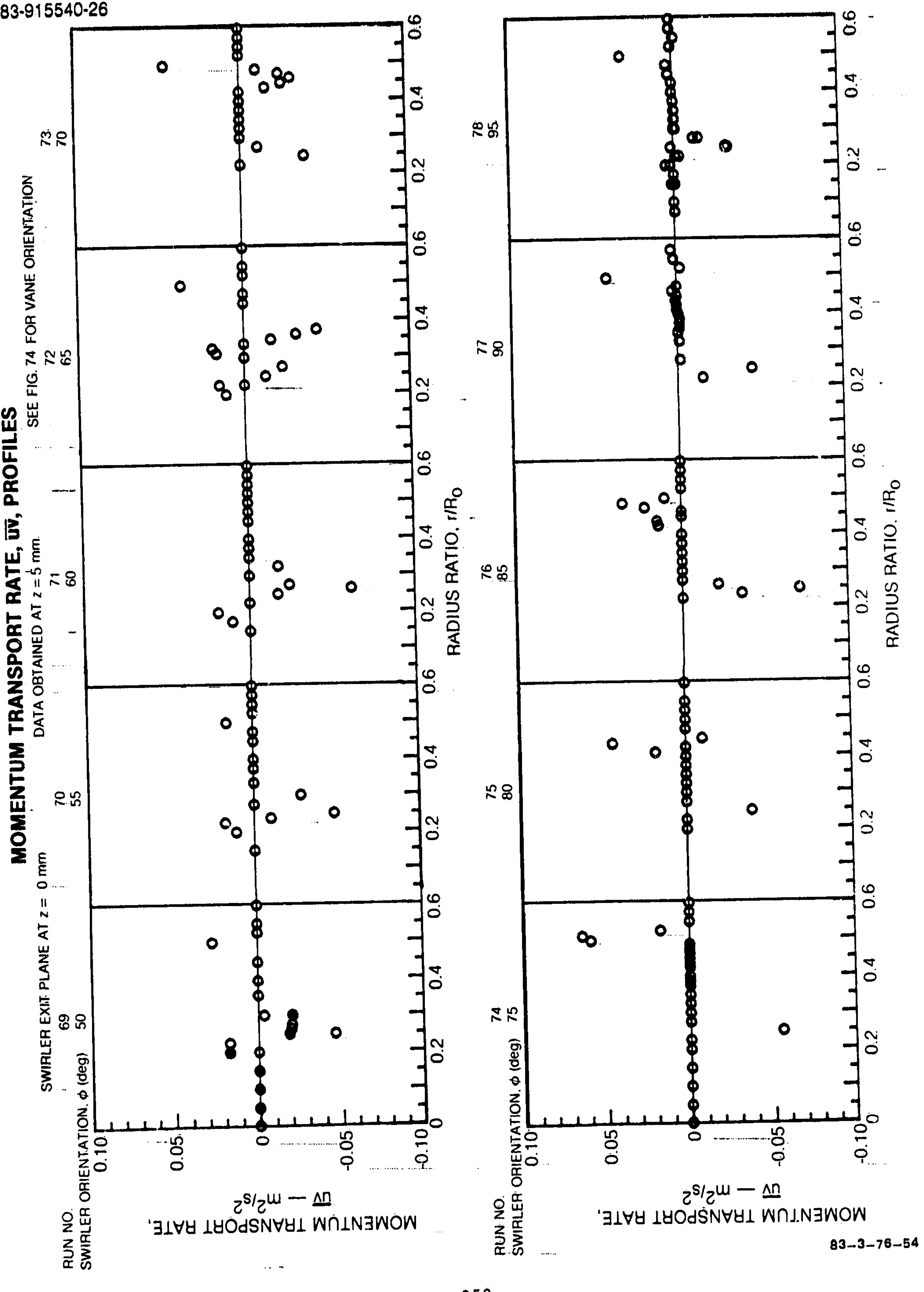

MOMENTUM TRANSPORT RATE, $\overline{uv}$, PROFILES

SWIRLER EXIT PLANE AT z = 0 mm DATA OBTAINED AT z = 5 mm

SEE FIG. 74 FOR VANE ORIENTATION

83-3-76-54

ORIGINAL PAGE IS OF POOR QUALITY

MOMENTUM TRANSPORT RATE, $\overline{uv}$, PROFILES

SWIRLER EXIT PLANE AT $z = -51$ mm DATA OBTAINED AT $z = 5$ mm SEE FIG. 74 FOR VANE ORIENTATION

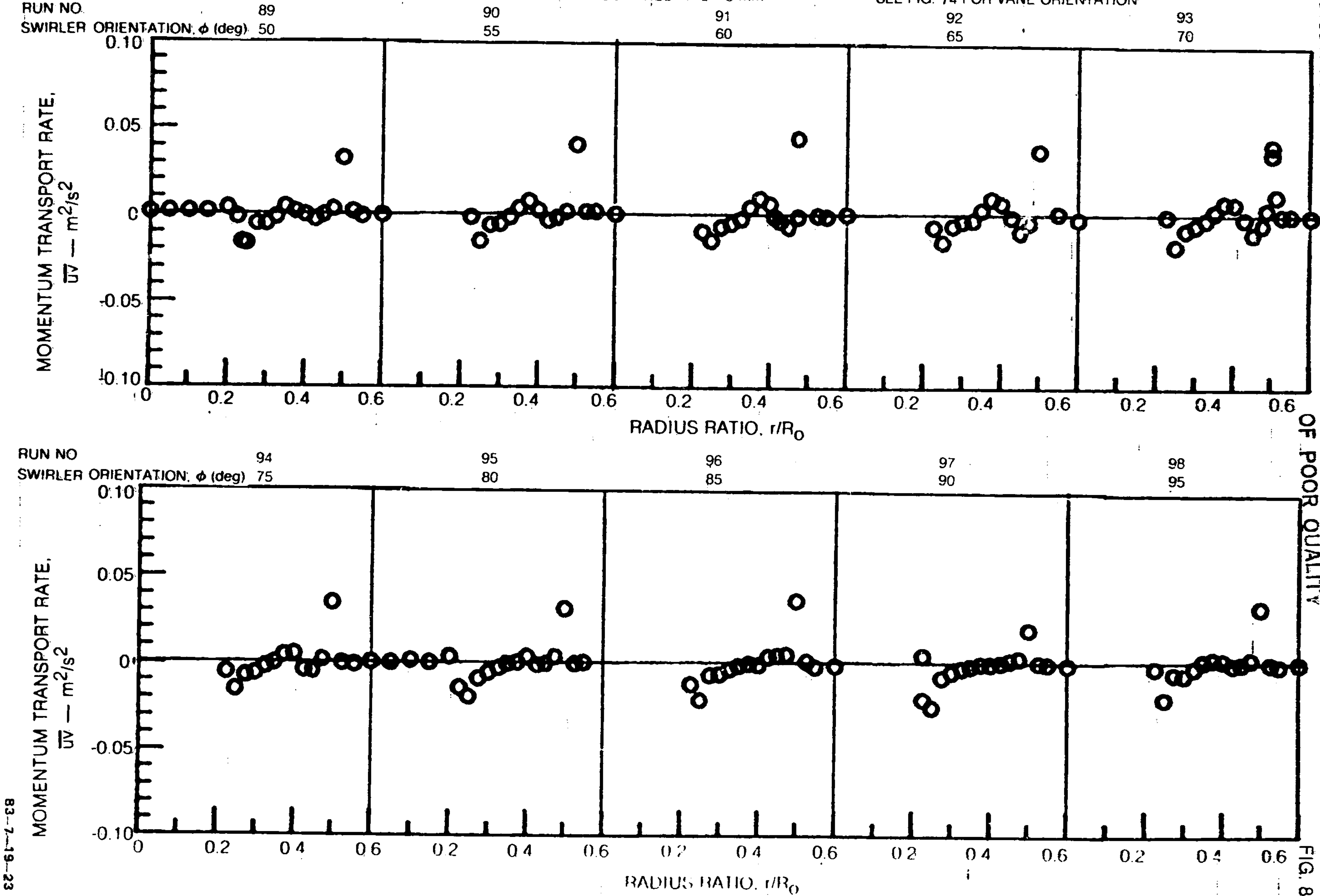

FIG. 88

83–7–19–23

ORIGINAL PAGE IS
OF POOR QUALITY

FIG. 89

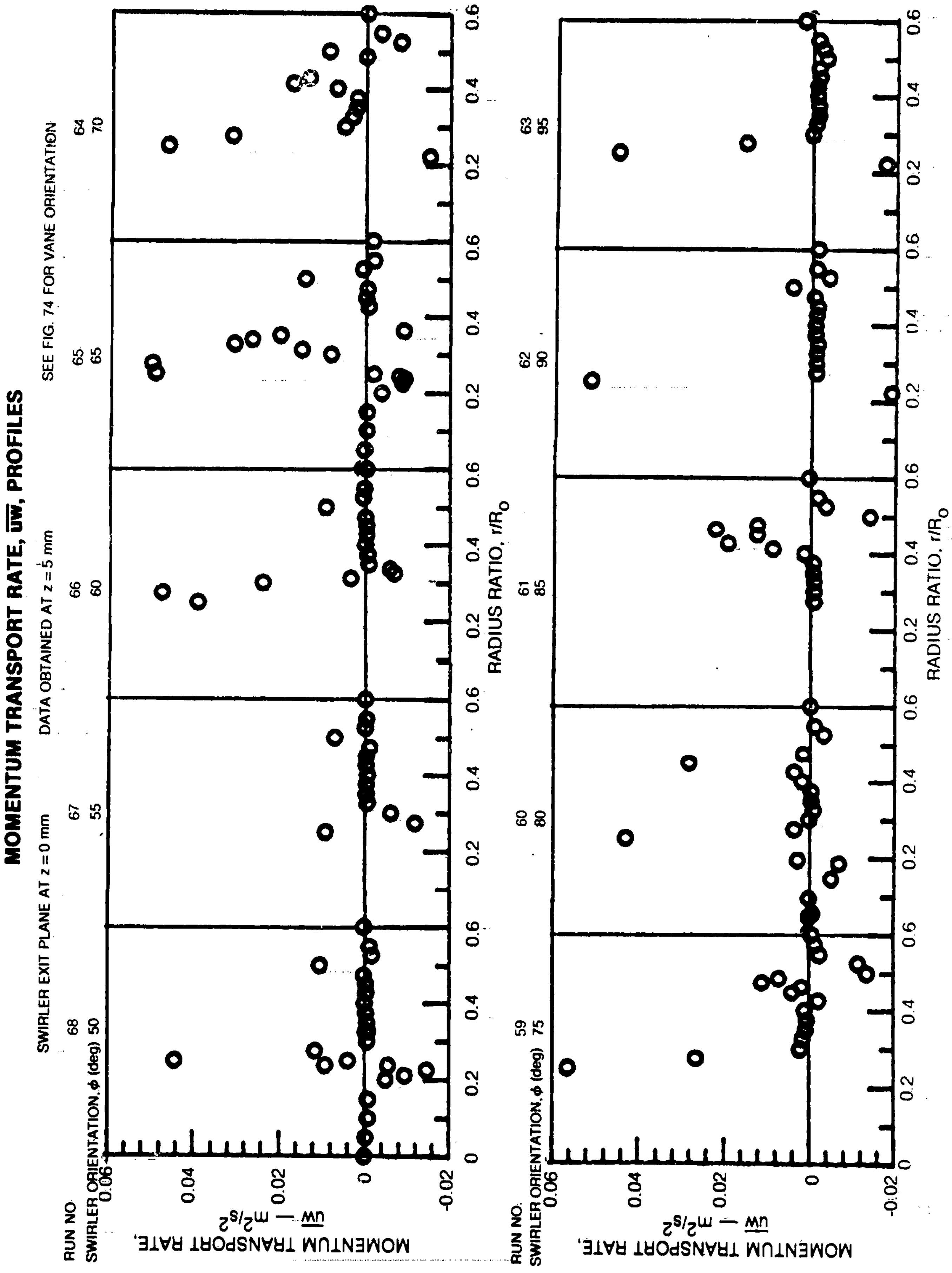

MOMENTUM TRANSPORT RATE, $\overline{uw}$, PROFILES

SWIRLER EXIT PLANE AT z = 0 mm

DATA OBTAINED AT z = 5 mm

SEE FIG. 74 FOR VANE ORIENTATION

83-3-76-37

ORIGINAL PAGE IS
OF POOR QUALITY

MOMENTUM TRANSPORT RATE, $\overline{uw}$, PROFILES

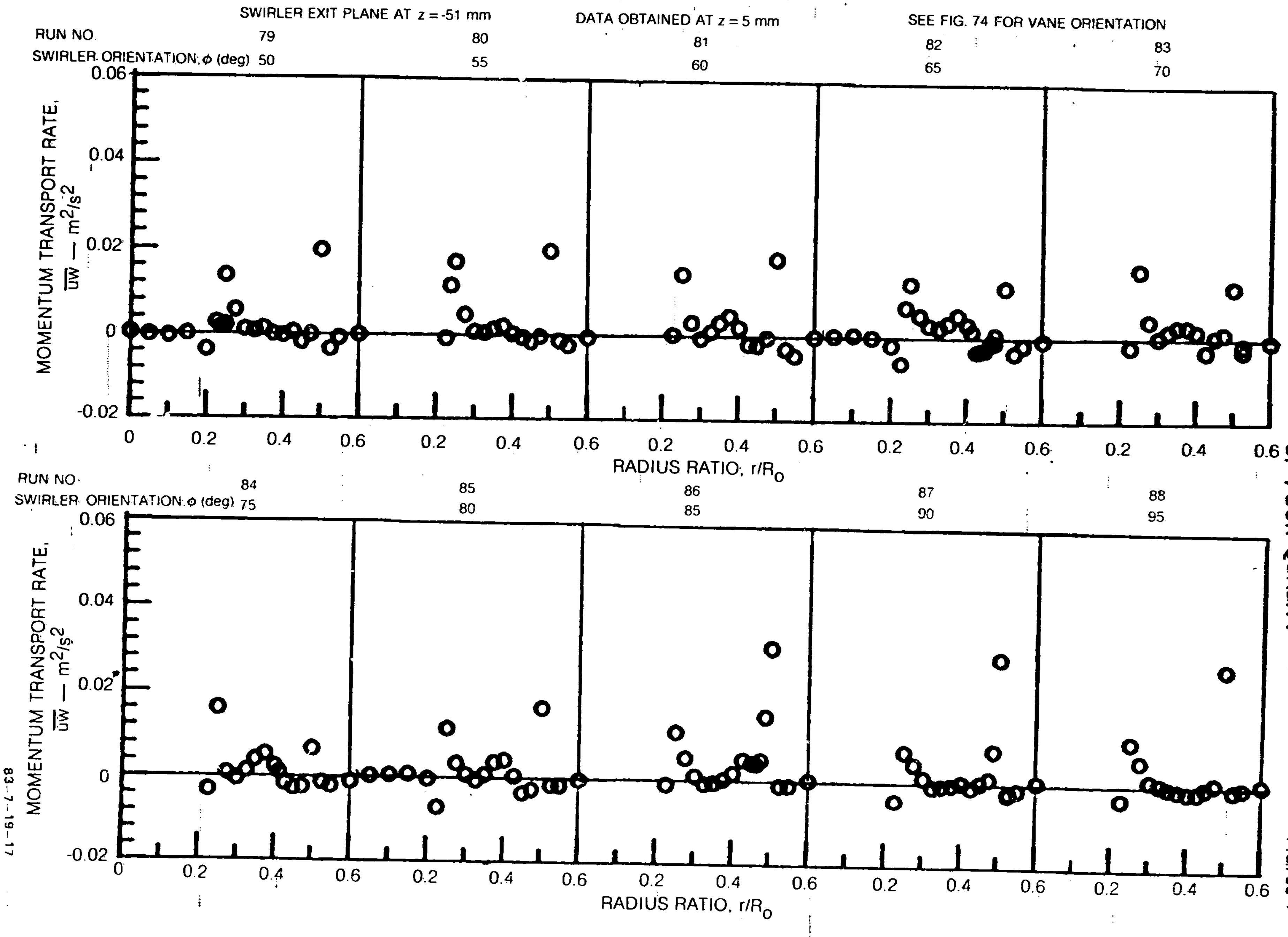

FIG. 90

83-7-19-17